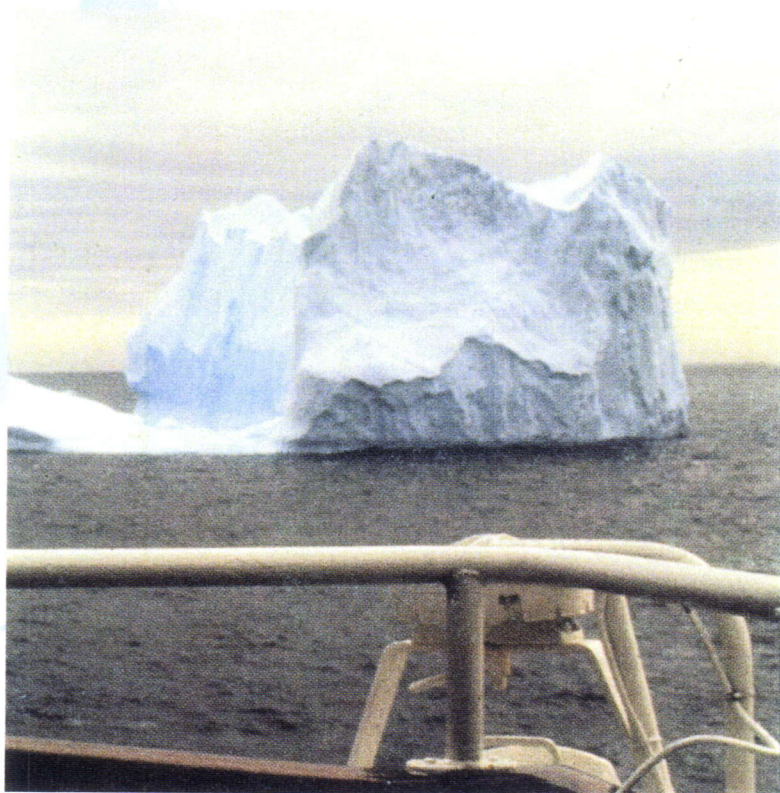


BELGIAN SCIENTIFIC RESEARCH PROGRAMME
ON THE ANTARCTIC
SCIENTIFIC RESULTS OF PHASE TWO
(10/1988 - 05/1992)
VOLUME I
**PLANKTON ECOLOGY
AND MARINE BIOGEOCHEMISTRY**

EDITED BY S. CASCHETTO



BELGIAN SCIENCE
POLICY OFFICE



BELGIAN SCIENTIFIC RESEARCH PROGRAMME ON THE ANTARCTIC

SCIENTIFIC RESULTS OF PHASE TWO (10/1988-05/1992)

VOLUME I

**PLANKTON ECOLOGY
AND MARINE BIOGEOCHEMISTRY**

EDITED BY S. CASCHETTO

BELGIAN SCIENCE POLICY OFFICE
1993

LEGAL NOTICE

Neither the Science Policy Office nor any person acting on behalf of the Office is responsible for the use which might be made of the following information.

No responsibility is assumed by the Publisher for any injury and/or damage to persons or property as a matter of products liability, negligence or otherwise, or from any use or operation of any methods, products, instructions or ideas contained in the material herein.

No part of this publication may be reproduced, stored in a retrieval system, or transmitted in any form or by any means, electronic, mechanical, photocopying, recording, or otherwise, without the prior written permission of the Publisher.

D/1993/1191/1

Published in 1993 by the
Belgian Science Policy Office.
Serial number ANTAR/93/4

FOREWORD

In 1985, the Belgian government decided to launch a research programme to give tangible form to Belgium's desire to make an active contribution towards the international scientific effort on the Antarctic. This programme was designed as a coordinated thematic action targeting scientific problems identified by the Antarctic Treaty System as top-level priorities in pursuance of two objectives: protection of the Antarctic environment and ecosystems, and the role played by Antarctica and the Southern Ocean in global climate mechanisms. Particular attention was given to the complementarity of the different research projects, all covering a period of three years.

Development of the Belgian research effort continued between 1988 and 1992 during the Second Phase of the Programme, following the same general strategy and options. In particular, the same four fields of research were retained: (i) Plankton Ecology, (ii) Marine Biogeochemistry, (iii) Marine Geophysics and (iv) Glaciology-Climatology.

This volume sets out the results of the research projects carried out during the Second Phase of the Programme, on Plankton Ecology and Marine Biogeochemistry.

The results of the research conducted in the other fields within the Programme are the subject of two separate volumes (Volume II: Marine Geophysics and Volume III: Glaciology-Climatology).

At present, Belgium's involvement in scientific research on the Antarctic is covered by the Third Phase of the Programme, which commenced in the summer of 1992.

CONTENTS

CARBON AND NITROGEN CYCLING THROUGH THE MICROBIAL NETWORK OF THE MARGINAL ICE ZONE OF THE SOUTHERN OCEAN WITH PARTICULAR EMPHASIS ON THE NORTHWESTERN WEDDELL SEA

Ch. Lancelot, S. Mathot, S. Becquevort, J.-M. Dandois and G. Billen

- Abstract1
 - Introduction3
 - Materials and methods7
 - Sea ice retreat and phytoplankton ice-edge bloom development15
 - Structure and functioning of the planktonic food web at the receding ice-edge31
 - The ecological model : description, formulation and parametrization51
 - Model results69
 - Conclusions and perspectives97
 - Acknowledgments101
 - References103
-

SEASONAL FLUCTUATION OF EXPORT AND RECYCLED PRODUCTION IN DIFFERENT SUBAREAS OF THE SOUTHERN OCEAN

L. Goeyens and F. Dehairs

- Abstract2
 - Introduction4
 - Material and methods8
 - Results18
 - Discussion26
 - Conclusions68
 - Acknowledgements70
 - References71
-

ECOTOXICOLOGY OF STABLE POLLUTANTS IN ANTARCTIC MARINE ECOSYSTEMS : MERCURY AND ORGANOCHLORINES

C. Joiris and L. Holsbeek

- Abstract1
 - Introduction2
 - Materials and methods2
 - Results and Discussion12
 - Conclusions29
 - References32
-

CO₂ AND O₂ IN ANTARCTIC MARINE ECOSYSTEMS

J.-M. Bouquegneau and C. Joiris

- Abstract1
 - Introduction2
 - Materials and methods2
 - Results3
 - Discussion11
 - Conclusion14
 - References15
-

BIOCHEMISTRY AND ECODYNAMICS OF ZOOPLANKTON OF THE SOUTHERN OCEAN

A. Goffart and J.-H. Hecq

- Abstract1
 - Introduction3
 - Weddell Sea4
 - EPOS leg 1 cruise : general objectives and work at sea4
 - Materials and methods5
 - Hydrodynamical context5
 - Results6
 - Ross Sea20
 - Vth ITALIANTARTIDE expedition : general objectives and work at sea ..20
 - Materials and methods21
 - General hydrology22
 - Results22
 - General conclusions48
 - Acknowledgements50
 - Bibliography51
-

CONTENTS OF VOLUME II
MARINE GEOPHYSICS

HIGH-RESOLUTION SEISMIC
INVESTIGATION OF THE EVOLUTION
(STRATIGRAPHY AND STRUCTURE) OF
THE CONTINENTAL MARGINS OF THE
EASTERN WEDDELL SEA AND OF THE
ANTARCTIC PENINSULA

M. De Batist, J.-P. Henriët, H. Miller, A.
Moons, B. Dennielou, N. Kaul, E. Maes,
W. Jokat, B. Schulze, G. Uenzelmann-
Neben, W. Versteeg and the GRAPE
TEAM (Geophysical Research of the
Antarctic Peninsula)

CONTENTS OF VOLUME III
GLACIOLOGY - CLIMATOLOGY

CHEMICAL AND ISOTOPIC
DISTRIBUTION IN ICE DUE TO WATER
FREEZING IN ANTARCTICA

R. Souchez and J.-L. Tison

NUMERICAL SIMULATIONS OF
WIND-DRIVEN FLOWS IN
THE ANTARCTIC COASTAL ZONES

M. Fettweis, C.-H. Yu and J. Berlamont

DEVELOPMENT OF A 3-DIMENSIONAL
MESO- γ PRIMITIVE EQUATIONS
MODEL : KATABATIC WINDS
SIMULATION IN THE AREA OF TERRA
NOVA BAY, ANTARCTICA

H. Gallée, G. Schayes and A. Berger

A NUMERICAL STUDY ON THE
RESPONSE OF THE ANTARCTIC ICE
SHEET TO CHANGES IN
ENVIRONMENTAL CONDITIONS

Ph. Huybrechts

ICE DYNAMICAL STUDIES IN THE SØR
RONDANE MOUNTAINS, DRONNING
MAUD LAND, EAST ANTARCTICA

F. Pattyn, H. Declair and Ph. Huybrechts

SEA ICE AND CIRCULATION IN
THE WEDDELL SEA

B. Petit and C. Demuth

RESEARCH CONTRACT ANTAR/II/05

**CARBON
AND NITROGEN
CYCLING THROUGH
THE MICROBIAL
NETWORK OF
THE MARGINAL ICE
ZONE OF THE
SOUTHERN OCEAN
WITH PARTICULAR
EMPHASIS ON
THE NORTHWESTERN
WEDDELL SEA**

Ch. Lancelot, S. Mathot,
S. Becquevort, J.-M. Dandois
and G. Billen

GROUPE DE MICROBIOLOGIE DES
MILIEUX AQUATIQUES

Université Libre de Bruxelles
Campus de la Plaine CP 221,
Bd du Triomphe
B-1050 Brussels, Belgium

TABLE OF CONTENTS

| | |
|--|------------|
| ABSTRACT | 1 |
| 1. INTRODUCTION | 3 |
| 2. MATERIALS AND METHODS | 7 |
| 2.1. Site description and field sampling | 7 |
| 2.2. Physical and optical measurements | 10 |
| 2.3. Chemical measurements | 11 |
| 2.4. Biomasses | 11 |
| 2.5. Biological activities | 13 |
| 3. SEA ICE RETREAT AND PHYTOPLANKTON ICE-EDGE BLOOM DEVELOPMENT | 15 |
| 3.1. Sea ice microbial communities and their impact on the water column at the time of ice melting | 15 |
| 3.2. Physical associated to sea ice retreat and phytoplankton ice-edge bloom initiation | 22 |
| 3.3. The role of trace metals | 28 |
| 4. STRUCTURE AND FUNCTIONING OF THE PLANKTONIC FOOD WEB AT THE RECEDING ICE-EDGE | 31 |
| 4.1. The complexe structure of the planktonic food-web | 31 |
| 4.2. The relative role of micro- and mesograzers in controlling phytoplankton activity in the northwestern Weddell Sea | 41 |
| 4.3. Food-web structure and krill distribution in the circumpolar marginal ice zone of the Southern Ocean : some scenarios | 45 |
| 5. THE ECOLOGICAL MODEL : DESCRIPTION, FORMULATION AND PARAMETRIZATION | 51 |
| 5.1. General structure of the ecological model | 51 |
| 5.2. The physical model | 55 |
| 5.3. The phytoplankton model | 55 |
| 5.4. The microbial loop model | 61 |
| 5.5. The inorganic nitrogen loop | 65 |
| 6. MODEL RESULTS | 69 |
| 6.1. Validation : the particular case of the northwestern Weddell Sea | 69 |
| 6.2. Sensitive analysis : factor controlling phytoplankton ice-edge blooms | 82 |
| 6.3. Applications | 90 |
| 7. CONCLUSIONS AND PERSPECTIVES | 97 |
| 8. ACKNOWLEDGMENTS | 101 |
| 9. REFERENCES | 103 |

ABSTRACT

Detailed biological measurements (phyto- and bacterioplankton biomass and activity and counting of two classes of protozooplankton) were carried out in the marginal ice zone of the northwestern Weddell Sea during sea ice retreat 1988 (EPOS expedition, Leg 2). These measurements clearly showed enhanced phyto-, bacterio- and protozooplankton production in the marginal ice zone, as compared to adjacent open sea and permanently ice-covered areas.

The combined analysis of available physical, chemical and biological observations indicated that the initiation of the phytoplankton bloom - dominated by nanoplanktonic species - was determined by physical processes operating in the marginal zone at the time of ice melting. The additional effects of grazing pressure by protozoa and deep mixing appeared responsible for a rather moderate phytoplankton biomass ($4 \mu\text{g Chl } a \text{ l}^{-1}$) with a relatively narrow geographical extent (100-150 km). The role of trace metals, in particular iron, was minor.

On the basis of these data, as well as of physical measurements related to the hydrodynamical stability of the water column, a coupled hydrodynamical-biological model describing the microbial network developing at the receding ice-edge of the circumpolar marginal ice zone of the Southern Ocean has been established. This model takes into account the various physical and biological controls exerted on phytoplankton development, and allows calculation of carbon and nitrogen circulation through the lower trophic levels of the pelagic ecosystem.

Carbon budget calculation thus reveals the quantitative importance of heterotrophic microorganisms in the fate of primary production : 88% of net primary production is assimilated by the microbial loop composed of bacteria, bacterivorous and herbivorous protozoa. These latter, ingesting as high as 61% of the primary production play a key role, both by linking krill and other mesozooplankton to microorganisms, and by regenerating ammonium. Total net microbial food web secondary production contributes 66% of the food resources available to krill and other mesozooplankton at the receding ice-edge. Ammonium released through the metabolic activity induces a shift from a nitrate-based primary production system in the ice-covered area to an ammonium-based one in the ice-free area. Similar budget calculated for the adjacent permanently open sea area magnifies the key role of protozoa, constituting as much as 88% of resource available to krill and other mesozooplankton.

Extrapolation of these calculations to the entire Southern Ocean area (bordered at the Antarctic Convergence), taking into account the seasonal variations of the sea ice cover, yields a value of 1.85 GT C for annual net primary production, increasing by a factor 3 the previous estimate proposed by El-Sayed (1984).

1. INTRODUCTION

Recognition of the important role played by the ocean in atmospheric cycles prompted closer examination of the role of organisms in these processes. A significant amount of atmospheric carbon dioxide is indeed susceptible to be fixed by surface waters and exported to the deep ocean after incorporation into the food-web, giving support to the concept of the biological pump. The efficiency of this pump depends on the complex functioning of the phytoplankton-based pelagic ecosystem. It is driven by solar irradiance and fueled by the supply of inorganic nutrients (nitrate, phosphate, silicate) originated from the deep ocean. In most marine areas, inorganic nutrients are exhausted by phytoplankton uptake during the growing season; the transport of carbon to deep waters is then controlled by the flux of inorganic nutrients to surface waters. In this case, the pump works at its maximum efficiency. In the Southern Ocean, however, relatively high concentrations of nitrate, phosphate and silicate are found in surface waters throughout the year. Yet phytoplankton biomass and primary production are lower than would be expected from inorganic nutrients availability. The pump therefore does not function at its maximal capacity. The Southern Ocean is thus a leading concern in oceanographic research not only as it relates to global biogeochemical cycles, but also as a potential site for intentional artificial enhancement of CO₂ flux into the ocean. Of particular interest within this context, is the identification of the factors controlling phytoplankton development and of the importance of the microbial loop in the surface layer. Indeed the timescale for the retention of photo-assimilated carbon in surface waters is dependent on biological and chemical transformations occurring in upper waters. Microbial activity produces dissolved organic carbon and returns inorganic carbon and nutrients through respiration and mineralisation whilst aggregate formation, faecal pellets production and vertical migration of large zooplankton speed up transfer of carbon to deep waters. In this regard, the concept of regenerated and new production is important as it introduces a distinction between the part of primary production which is recycled in the surface waters through rapid metabolism of heterotrophic microorganisms (grazers and bacteria) versus the part which escapes this rapid cycling and reaches the deep oceanic circulation and the benthos (Eppley & Peterson, 1979). New production is characteristically fueled by the winter standing stock of nitrates and sets up upper limits to export rates of organic matter from the surface layer; ammonium supports regenerated production that makes a negligible contribution to export to the deep ocean.

Several hypothesis have tempted to explain the paradox of high nutrients and low primary production in the Southern Ocean. To date, none has emerged as a widely admitted explanation.

The major role played by ice cover and the turbulence of the water column in controlling available light to phytoplankton and hence its development has been evidenced by numerous field data. It is now admitted that deep-mixed, ice-free areas are not exceptionally productive despite of very high nutrient concentrations, and are dominated by nanoplanktonic communities (El-Sayed, 1984; Smetacek *et al.*, 1990). On the other hand, many evidences (Smith & Nelson, 1986; Sullivan *et al.*, 1988; Comiso *et al.*, 1990) indicate that the circumpolar marginal ice zone is a region of enhanced primary production owing to the formation, at the time of ice melting, of a shallow vertically stable upper layer as a result of the production of meltwater and the subsequent seeding by actively growing sea ice microbes (Garrison *et al.*, 1987).

Yet phytoplankton biomass in these hydrodynamically stable areas remains generally low and surface nutrients, especially nitrate, remains well above depletion throughout the growing season (Hayes *et al.*, 1984). As alternatives, trace metals deficiency, in particular iron (Martin *et al.*, 1990), as well as grazing pressure by krill and other mesoplankton (Stretch *et al.*, 1988, Smetacek *et al.*, 1990) or protozoa (Hewes *et al.*, 1990) have been mentioned as potential chemical and biological factors controlling phytoplankton development in this area. These hypothesis are however not mutually exclusive and their importance may vary with location, time and environmental conditions.

As a matter of fact, ice-edge blooms exhibit consistently higher f ratio (the ratio of nitrate uptake to total inorganic nitrogen uptake) than ice-free communities (Smith & Nelson, 1990) suggesting that marginal ice zones are regions of greater export production. Contradictory, however, Hewes *et al.* (1985, 1990) and Garrison & Buck (1989) indicate that the pelagic food web of the marginal zone of the Weddell Sea is dominated by pico-, and nano-producers and micrograzers, suggesting that an important part of organic carbon and nitrogen is mineralised in the surface layer.

The control of phytoplankton ice-edge bloom development and the quantitative importance of the microbial loop were the main questions we addressed during the EPOS expedition (Leg 2), in the marginal ice zone of the northwestern Weddell Sea in spring 1988.

These objectives were approached through a detailed study of (i) the chemical, physical and biological processes associated with sea ice retreat and their controlling

factors; and (ii) the trophic relationships between dominant microorganisms, characterized by their size (pico-, nano-, micro-) and their trophic mode (auto-, heterotrophic).

A comprehensive analysis of the data collected during the EPOS expedition is presented here in order to (i) delineate the most important factors controlling phytoplankton ice-edge bloom development, (ii) evaluate the contribution of microbial secondary production and (iii) identify key organisms in regenerating inorganic nitrogen in upper surface waters of the investigated area. On this basis a predictive mathematical model of carbon and nitrogen circulation through the microbial network of the Antarctic food web is described and validated. By application to the marginal ice zone of the northwestern Weddell Sea, it makes possible to calculate a coherent budget of carbon and nitrogen cycling through the microbial network of the Antarctic food-web during the ice retreat period. This calculation provides an estimation of new production, of the quality of food available for krill ingestion, and of the exportation to the deep ocean layers.

2. MATERIALS AND METHODS

2.1 Site description and field sampling

The data set whereon this research is based was collected during the second leg of the European Polarstern Study (EPOS Leg 2) in the Scotia–Weddell Sea sector of the Southern Ocean, from November 22th 1988 to January 9th 1989. In this area located between the tip of the Antarctic Peninsula and the South Orkney Islands (Fig. 2.1), the open water of the Antarctic Circumpolar Current running in the Scotia Sea contacts the eastward flowing waters from the northern rim of the Weddell Gyre along a broad frontal zone. This boundary zone, with accompanying intense mesoscale activity, has been referred to as the Weddell–Scotia Confluence (WSC) by Gordon (1967). The hydrographical structure of the Confluence area is dominated by a sharp temperature gradient at its northern edge (the Scotia Front), extending from about 200 to 2500 meters. During late November, the Scotia Front was located between $57^{\circ}30'$ and 58° S; one month later, it was wider and had expanded southward to 59° S (Cederlöf *et al.*, 1989).

ANTAR
II/05

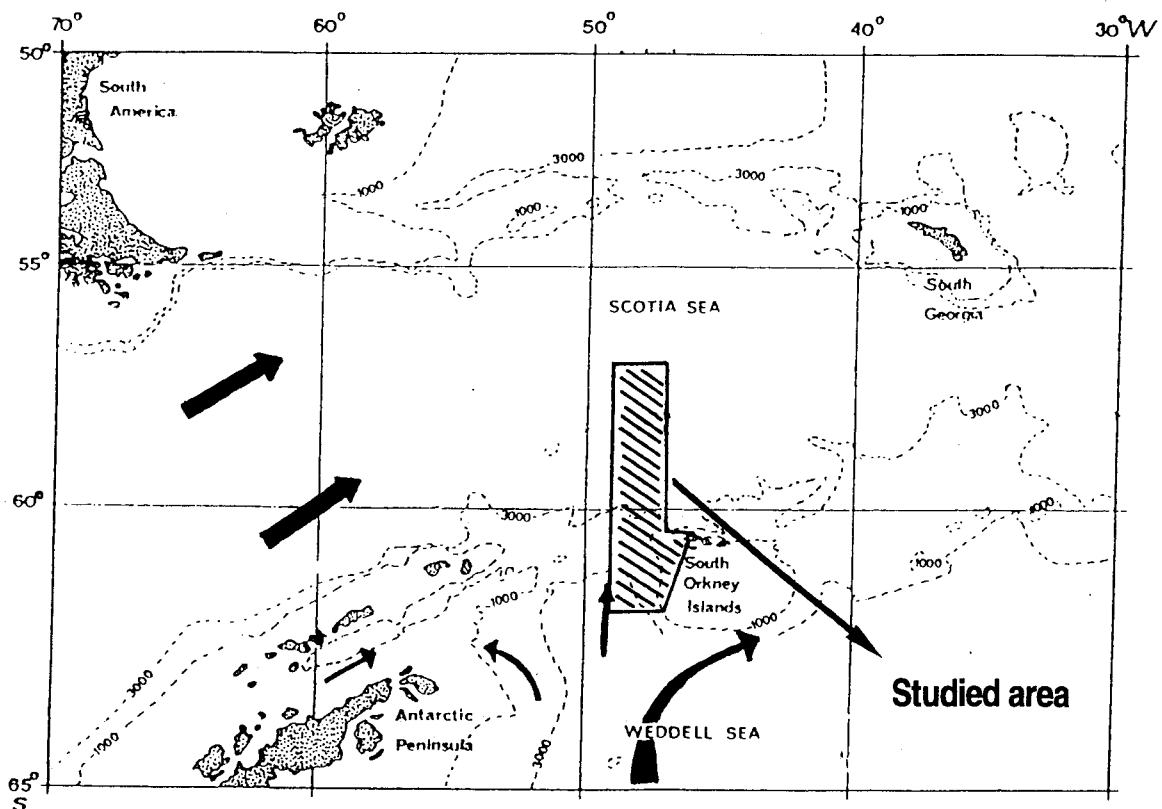


Figure 2.1 : Hydrodynamical characteristics of the studied area.

Superimposed to this frontal structure, seasonal sea ice covers this area up to latitude $58^{\circ} 30' S$ at its maximal extent. At the time of the cruise beginning, the process of ice melting has already started in this area since the end of October. Data collected in that part of the Weddell Sea during EPOS Leg 1 are therefore included in the present study. The whole data set thus refers to four North–South transects carried out along $49^{\circ} W$ (stations 100–113, 26–30 October; stations 143–153, 26–30 November; stations 172–179, 20–24 December; stations 182–194, 27–31 December) and two along $47^{\circ} W$ (stations 130–139, 11–13 November; stations 160–169, 13–17 December), between latitude $57^{\circ} S$ and $62^{\circ} S$ (Fig. 2.2). Precise coordinates and sampling conditions are described in details in Larsson (1990, EPOS Leg 1) and Veth *et al.* (1991, EPOS Leg 2).

Water column sampling: Sampling for physical, inorganic nutrients and chlorophyll *a* measurements was conducted at each half degree of latitude using a standard CTD rosette sampler equipped with 12 L Niskin bottles. Samples for biological activity measurements were collected within the upper mixed layer of annotated stations (see Fig. 2.2). Sampling for planktonic communities analysis (Chapter 4) was concentrated on two transects performed along the meridian $49^{\circ}W$ and $47^{\circ}W$ between $59^{\circ}S$ and $62^{\circ}S$ as well as two stations located at $59^{\circ}S$ (station 147) and $61^{\circ}S$ (station 151) which were visited several times during the cruise (see Fig. 2.2).

Ice sampling: Ice sampling was carried out randomly at three particular sites of the marginal ice zone of the northwestern Weddell Sea, namely stations 169, 178 and 194. According to the terminology proposed by Horner *et al.* (1988), three broad categories of microbial assemblage can be distinguished in the ice (Fig. 2.3) : surface assemblages which include infiltration assemblages at the snow–ice interface of floes as well as meltpool and tide crack microorganisms; interior assemblages (including brine channel and band assemblages) at depth within the ice; and bottom assemblages that develop in different types of ice near the ice–seawater interface. Whilst the two first groups of ice assemblages are frequently encountered in the pack ice of the northern Weddell Sea, the latter one is inconspicuous, being more typical of the land fast ice common in the Ross Sea (Horner, 1985). Thus samples from stations 169 and 194 are typical infiltration assemblages, whereas the brown coloured band sampled in the middle (60 to 80 cm from top of ice floe) of cores taken at station 178 presented the characteristics of a band assemblage.

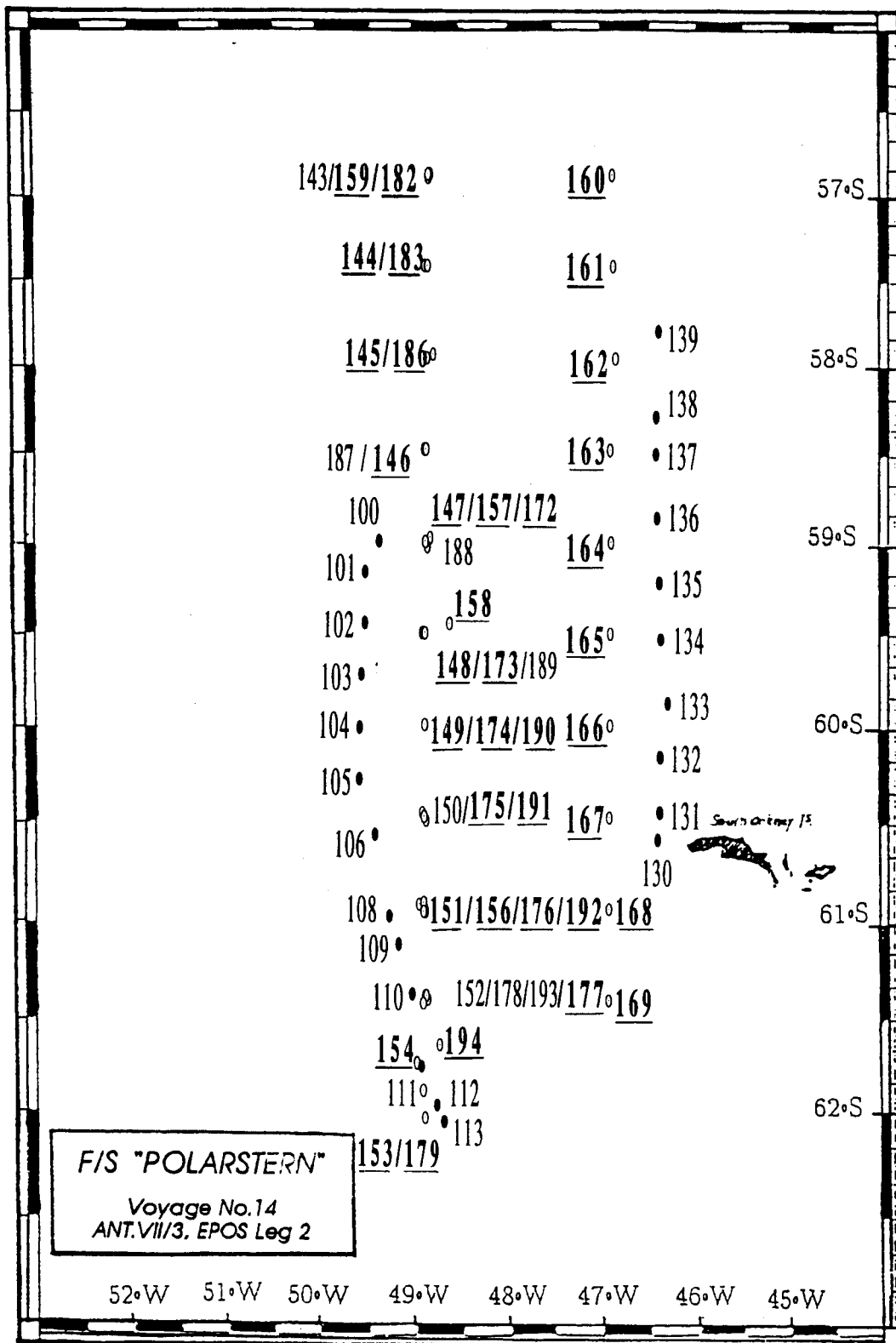


Figure 2.2 : Studied area and sampled stations (EPOS legs 1 and 2). Biological activity measurements at the annotated stations (for example 157).

To reduce osmotic shock (Garrison & Buck, 1986), ice samples were melted in GF/F, filtered sea water (1:20, v:v) in the dark prior to fixative addition or experimental study. For comparison between ice and water environments, samples of seawater were also collected directly under the ice floes.

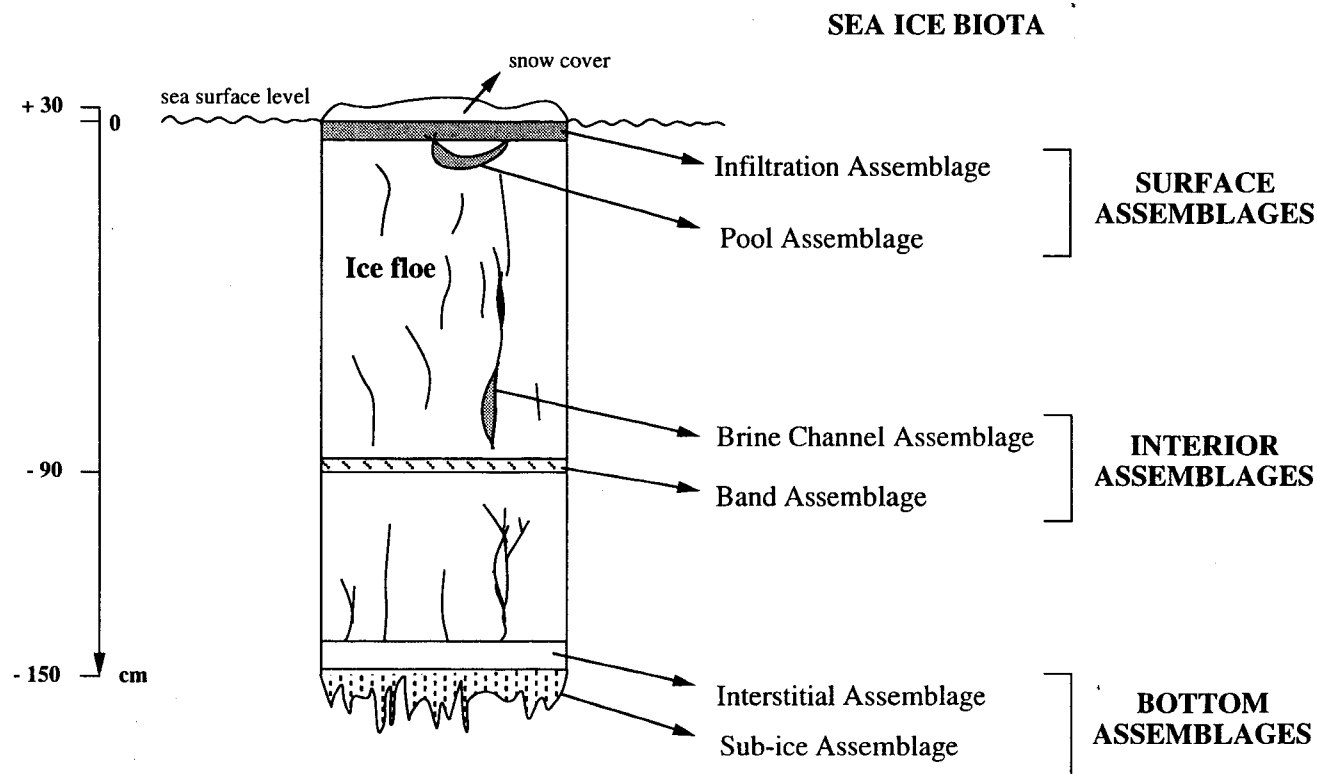


Figure 2.3 : Schematic representation of the kinds of algal assemblages found in sea ice (from Horner *et al.*, 1988).

2.2. Physical and optical measurements

Vertical profiles of salinity and temperature (EPOS–Leg 2 data report, 1989) were determined by use of a Neil Brown Mark IIIb CTD–profiler (EG & G Ocean Products). *In situ* temperature and salinity calibrations were conducted regularly during the cruise. Hydrographical data can be found in Larsson (1990, EPOS Leg 1) and Veth *et al.* (1991, EPOS Leg 2).

Incident Photosynthetically Available Radiation (PAR) was continuously measured by means of a cosine Li-Cor sensor set up on the upper deck of the ship. Subsurface light was calculated from the knowledge of ice coverage estimates (Lange & Eicken, 1989; van Franeker, 1989), using a mean of 0.15 and 0.95 for sea and snow-ice albedo respectively. Available light in the water column was calculated from the vertical light attenuation coefficient determined from light profiles measured by use of an underwater quantummeter (Magas & Svansson, 1989). The depth of the euphotic zone was determined at the 0.1 % level of incident surface light.

ANTAR
II/05

2.3. Chemical measurements

Nitrate + nitrite was determined with a Technicon Autoanalyzer II according to the method of Tréguer & Le Corre (1975). Calibration was carried out in the range of 20 to 40 $\mu\text{mol.N l}^{-1}$. Nitrate depletions were calculated from vertical distribution of nitrate concentration, and integrated down to the depth where nitrate reaches the winter value of 31.5 $\mu\text{mol.N l}^{-1}$ (see Goeyens *et al.*, 1991a for details). Ammonium concentrations were determined manually as described by Koroleff (1969 and 1976). Standardization was carried out between 0 and 3 $\mu\text{mol.N l}^{-1}$ (see Goeyens *et al.*, 1991b for details).

Chlorophyll *a* was determined by both spectrofluorometry (Neveux & Panouse, 1987) and spectrophotometry (Lorenzen, 1967).

2.4. Biomasses

Microbial biomasses were determined from the qualitative and quantitative analysis of auto- and heterotrophic microorganisms carried out with different microscopic techniques. Preservation solution, staining dye when required, and microscopy method specific to each taxonomic group (Taxon) considered are gathered in Table 2.I. Carbon biomass of each selected trophic group was calculated from biovolume measurement using the conversion factors listed in Table 2.II.

Table 2.I : Taxons, sampling treatment and microscopy analysis.

| Taxon | Sampling volume, ml | Preservation solution | Microscopic analysis |
|----------------------------------|----------------------------|---|--|
| Diatoms > 20µm Diatoms < 20µm | 50 – 100 10 – 20 | Glutardialdehyde-lugol (35 ⁰ / ₀₀ , v/v), (1% final conc.) | Inverted light microscopy (Utermöhl, 1958) |
| Flagellates | 10 – 20 | Glutardialdehyde (0.5% final conc.) | Epifluorescence microscopy after DAPI staining (Porter & Feig, 1980) |
| Ciliates | 50 – 100 | Glutardialdehyde-lugol (35 ⁰ / ₀₀ , v/v), (1% final conc.) | Inverted light microscopy (Utermöhl, 1958) |
| Bacteria | 2 – 5 | Formalin (2% final conc.) | Epifluorescence microscopy after DAPI staining (Porter & Feig, 1980) |

Table 2.II : Conversion factors for biomass estimate from biovolume measurement.

| Taxon | Carbon/Biovolume, pgC µm⁻³ | Reference |
|--------------|--|-----------------------|
| Diatoms | 0.11 | Edler, 1979 |
| Flagellates | 0.11 | Edler, 1979 |
| Ciliates | 0.08 | Beers & Stewart, 1970 |
| Bacteria | Biovolume dependent ratio* | Simon & Azam, 1989 |

$$*: \frac{\text{Carbon}}{\text{biovolume}} = \left[130 + 350 * e^{-\text{biovolume}/0.095} \right] * 10^{-3}$$

2.5. Biological activities

Phytoplankton: Daily integrated gross and net primary production and phytoplankton respiration were calculated, using the AQUAPHY set of equations (Lancelot *et al.*, 1989; Lancelot *et al.*, 1991), from data on phytoplankton ^{14}C assimilation rates in combination with the knowledge of daily light variations with depth.

Basically, the AQUAPHY model is based on the concept of reserve material storage by phytoplankton cells, according to the future requirements of their growth. The model considers thus phytoplankton cells as composed of monomeric precursors for macromolecule synthesis, of reserve products (lipids and polysaccharides), and of functional products (composed at 85% of proteins; Dorsey *et al.*, 1978), and assimilates protein synthesis to the measurement of *net* primary production, owing to the functional and structural nature of this cellular constituent. Photosynthesis directly, and storage products catabolism indirectly provide required energy and reductors for the biosynthesis of new cellular material as well as for the basal metabolic maintenance of the cell. So, the model explicitly calculates the **photosynthetic process (gross primary production)** – occurring only during the light period of a circadian day, and fueling the different pools of cellular metabolites – and the **phytoplankton growth process (net primary production)** reflected by the protein synthesis – continuing along the whole day, at the expense of reserve products accumulated by the phytoplankton cell during the light period. This model was chosen because it takes explicitly into account the interaction between phytoplankton physiology and the turbulent structure of its habitat, by describing the light history of the cells as reflected by the pool size of the storage products.

Experimental determination of the AQUAPHY parameters involved two kinds of tracer experiments conducted in parallel under simulated *in situ* conditions. For all these incubations, 250 to 700 ml seawater sample – which amount was chosen according to phytoplankton biomass – were incubated in transparent culture flasks with $\text{NaH}^{14}\text{CO}_3$ at a rate of $10 \mu\text{Ci}/100 \text{ ml}$ sample (Amersham, specific activity = 56 mCi mmol^{-1}). Photosynthetic parameters were calculated, using the Platt *et al.* (1985) equations, from short-term (4 hours) ^{14}C incubations performed at various light intensities at *in situ* temperature. Phytoplankton growth and respiration parameters were calculated, using the AQUAPHY equations through an isotopic model (Lancelot *et al.*, 1989), from data on long-term (24 hours) light-dark kinetics of ^{14}C assimilation into four pools of cellular constituents (lipids, small metabolites, polysaccharides and proteins).

Details on experimental procedure, biochemical fractionation and calculations are described in Lancelot & Mathot (1985), Lancelot *et al.* (1991a) and Mathot *et al.* (1992).

Microheterophs: Protozoan (mostly heterotrophic dinoflagellates and ciliates) grazing on algal cells was calculated from cell counts followed by carbon biomass calculation as described above, using the maximal hourly clearance rate of 10^5 body volume per protozoa determined by Björnson & Kuparinen (1991). In this calculation, only protozoa greater than $7 \mu\text{m}$ were considered as effective phytoplankton grazers; smaller heterotrophs were assumed to feed on bacteria.

Bacterial production rates were measured according to the ^3H -thymidine incorporation method of Fuhrman & Azam (1982). ^3H -thymidine was added at a final concentration of 10 nmol l^{-1} , a concentration shown saturating for the process of incorporation. The uptake of radioactivity in the cold TCA fraction was determined after 3–4 hours incubation. Empirical calibration with cell number increase in $0.2 \mu\text{m}$ filtered seawater reinoculated with $2 \mu\text{m}$ filtered seawater (the procedure of Riemann *et al.*, 1987) was carried out several times. The conversion factor found was $1.25 \cdot 10^9$ cells/nmol thymidine incorporated. Bacterial mortality was measured according to the method developed by Servais *et al.* (1985, 1989). Within this overall mortality rate, the part being attributed to grazing by nanoprotozoa was estimated by comparing the mortality rate of an unscreened sample to that of a $0.2 \mu\text{m}$ filtered sample membrane and poisoned with a colchicine–cycloheximide mixture.

Total ammonium remineralization by heterotrophic microorganisms was determined by isotope (^{15}N) dilution experiments. A detailed description of the methodology is given in Goeyens *et al.* (1991b). Ammonium regeneration by bacteria was calculated from bacterial growth rates using a carbon:nitrogen (w:w) ratio of 4 for the bacterial biomass as well as for its direct substrates. Ammonium regeneration by protozoa was calculated from grazing rates using a growth yield of 0.38 and carbon:nitrogen ratios of 4.5 and 5.6 for phytoplankton and protozoa respectively.

3. SEA ICE RETREAT AND PHYTOPLANKTON ICE-EDGE BLOOM DEVELOPMENT

ANTAR
II/05

Many evidences (Smith & Nelson, 1986; Sullivan *et al.*, 1988; Comiso *et al.*, 1990) indicate that the circumpolar marginal ice zone is a region of enhanced primary production owing to the formation, at the time of ice melting, of a shallow vertically stable upper layer as a result of the production of meltwater and the subsequent seeding by actively growing sea ice microbes (Garrison *et al.*, 1987). Their relative contribution in initiating phytoplankton ice-edge development in the marginal ice zone of the northwestern Weddell Sea is considered here below.

3.1. Sea ice microbial communities and their impact on the water column at the time of ice melting

Sea ice offers a set of physico-chemical conditions for microorganisms living in close association with it, either attached to ice crystal or suspended in the interstitial water between ice crystal (Horner, 1985). These microorganisms, originally planktonic or benthic, were incorporated within the ice during fall, at the time of frazil ice formation (Garrison *et al.*, 1983). Sea ice microalgae grow in early spring when incident light reaches sufficient levels, and are accompanied by the development of a microbial network composed of bacteria and various protozoa (Whitaker, 1977; Ackley *et al.*, 1979; Palmisano & Sullivan, 1983; Horner, 1985; Garrison & Buck, 1989; Garrison & Gowing, 1992; Sullivan, 1985; Kottmeier & Sullivan, 1987). When released from the ice upon melting, fate of these sea ice-associated microorganisms is variable : part is grazed by pelagic herbivores like krill (Marschall, 1988) and copepods (Fransz, 1988); part aggregates and settles down (Schnack *et al.*, 1985; von Bodungen *et al.*, 1986; Riebesell *et al.*, 1991) and part survives in the water column (Garrison & Buck, 1985). This latter part has been suggested to constitute an inoculum for phytoplankton ice-edge bloom development and associated secondary producers. The genesis of a phytoplankton ice-edge bloom through the release of living cells seeded into the water column depends however on the dilution factor related to the physical properties of the water column but also on the viability of the released microorganisms. Two approaches were developed to study the seeding capability of microalgae released in the northwestern Weddell Sea at the time of ice melting. One is based on the measurement of potential metabolic activities of released sea ice microalgae. The second approach, based on the direct comparison of microbial inhabitants of sea ice assemblages originating from various sea ice habitats and of adjacent surface waters,

will give an indirect estimate of the importance of sea ice microbial communities as inoculum for the ice-edge bloom development in this part of the circumpolar marginal ice zone of the Southern Ocean.

3.1.1. Potential photosynthetic activity of released sea-ice microalgae

The potential photosynthetic activity of sea ice microalgae released in the water column upon melting was measured through shipboard simulating seeding experiments under controlled conditions (Mathot *et al.*, 1991).

Comparison between photosynthetic parameters characteristic of sea ice communities collected at the snow ice interface (*infiltration assemblages*) and deeper within the ice (*band assemblages*) with those of phytoplankton communities sampled in the corresponding adjacent waters (Fig. 3.1, Table 3.I) indicates that infiltration layer microalgae are as efficient photosynthesizers as surface planktonic cells. These assemblages could then act as efficient inoculum when released in the water column. Microalgae released from band assemblages appear however less efficient, their photosynthetic capacity being lower by a 3.5 factor than that of local phytoplankton (Table 3.I). The relative importance of infiltration layer and band assemblages is however difficult to assess owing to the high spatial variability of the sea ice habitat (Eicken *et al.*, 1991). Accordingly, visual observation of the ice field of the northwestern Weddell Sea in 1988 evidenced high patchiness in the spatial distribution of algal-rich ice floes of strong brown or yellow coloration (the *brown ice*), these latter contrasting severely with the white algal-poor ice floes (Fig. 3.2). Following Horner (1985) however, ice assemblages encountered in the pack-ice of the northwestern Weddell Sea are mainly infiltration assemblages and to a lesser extent interior assemblages.

Table 3.I: Photosynthetic characteristics of the infiltration assemblage and the band assemblage (= vegetative cells only, with exclusion of the resting spores) from ice communities and of phytoplankton from the water column.

| | n | α | K_m | I_k |
|---------------|---|-----------------------|-------------------|---------------|
| Infiltr. Ass. | 2 | 0.00066 \pm 0.00007 | 0.049 \pm 0.003 | 75 \pm 12.8 |
| Band Ass. | 2 | 0.00018 \pm 0.00007 | 0.012 \pm 0.007 | 62 \pm 15.7 |
| Phytoplankton | 6 | 0.00042 \pm 0.00016 | 0.041 \pm 0.014 | 92 \pm 19 |

n = number of samples

α = photosynthetic efficiency [$h^{-1} (\mu E m^{-2} s^{-1})^{-1}$]

K_m = maximal specific rate of photosynthesis (h^{-1})

I_k = light adaptation parameter ($K_m/a : \mu E m^{-2} s^{-1}$)

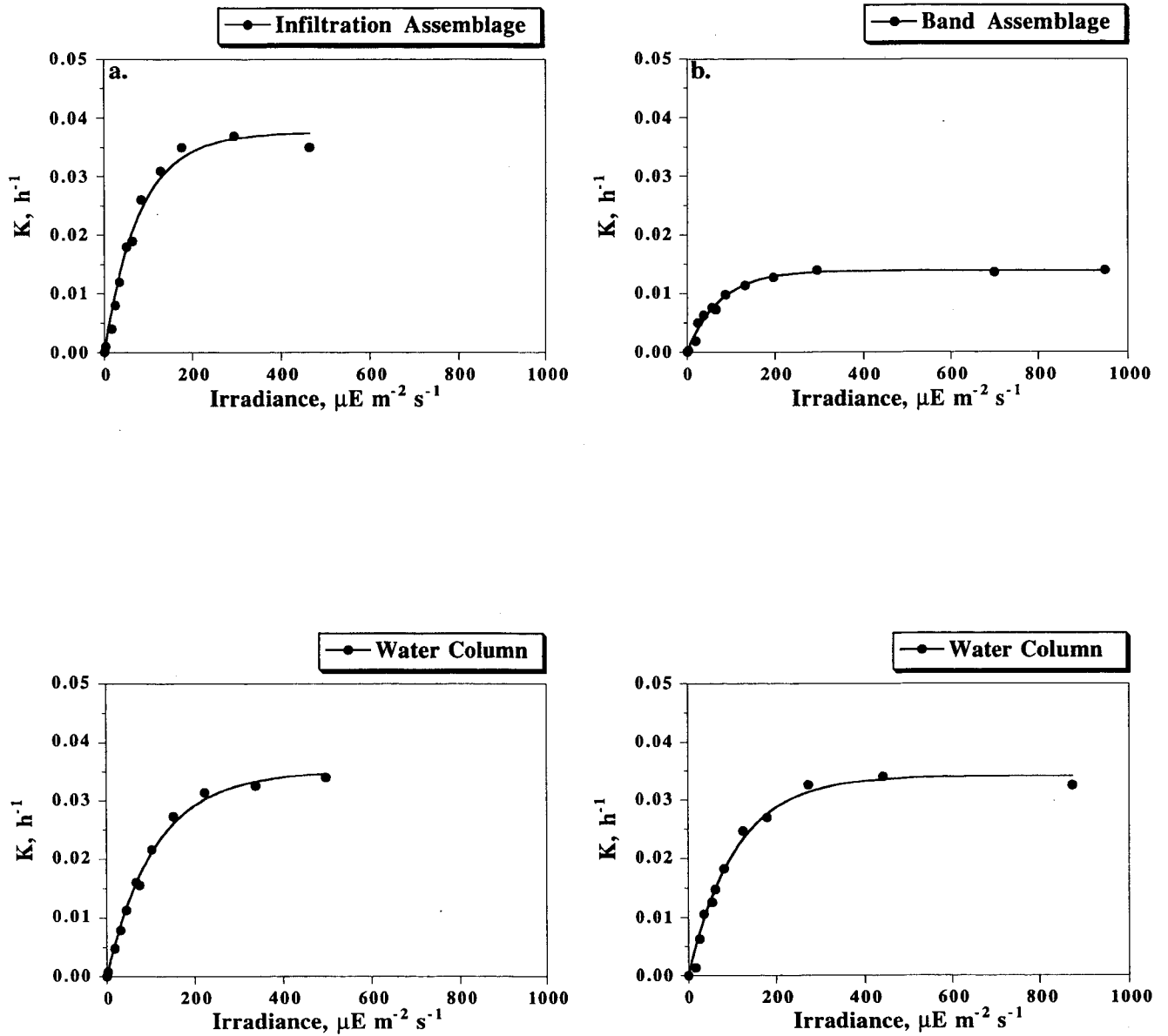


Figure 3.1 : Photosynthesis-irradiance relationship of surface layer phytoplankton and sea ice microalgae from the infiltration layer (a) and the interior layer (b).

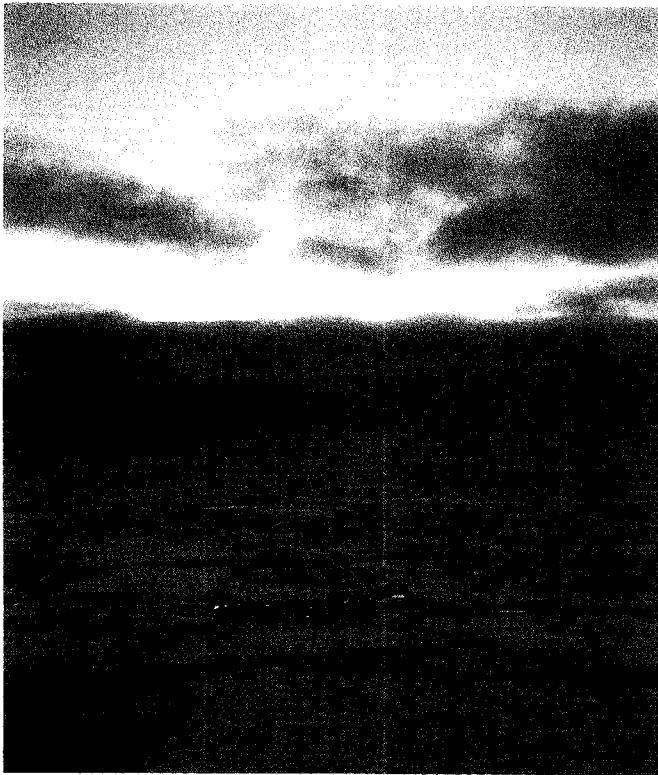
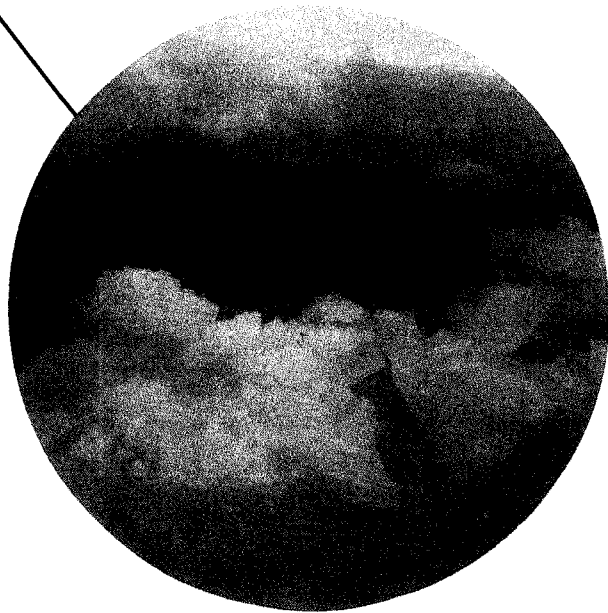
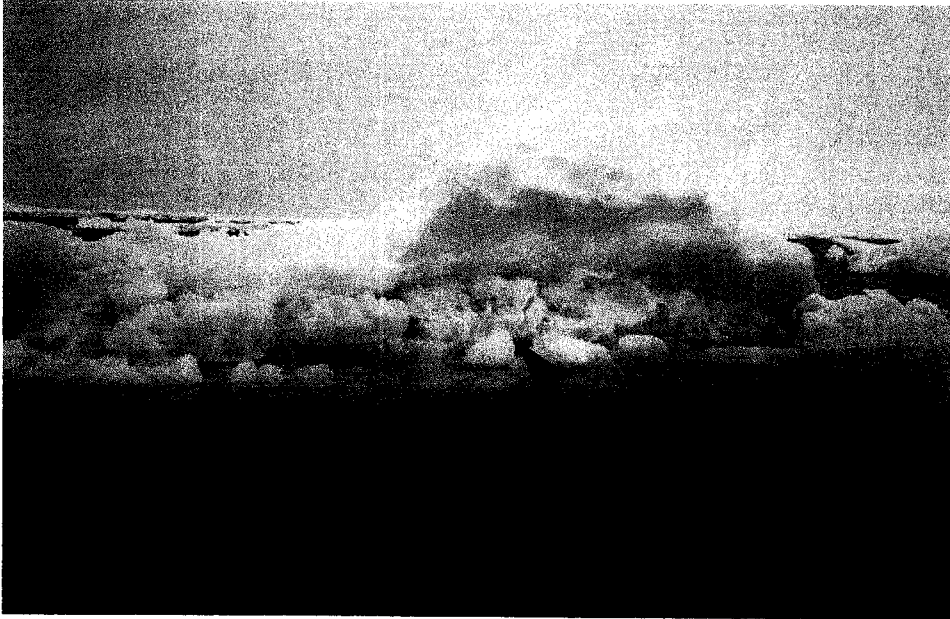


Figure 3.2 : Algal-rich ice floes of brown coloration (a), and white algal-poor ice floes (b) in the northwestern Weddell Sea (photographs by S. Mathot).

3.1.2. Sea ice microbial assemblages : complexity and patchiness

Microscopical analysis of sea ice infiltration layer and band assemblages randomly collected in the northwestern Weddell Sea revealed the existence of a complex microbial network composed of diatoms, autotrophic flagellates, bacterivorous and herbivorous protozoa and bacteria (Table 3.II). As a general trend, autotrophs contributed to a mean of 90 % (range : 76–96 %) of total microbial carbon, with little difference between assemblages from different sea ice habitats (Table 3.II). Bacterial biomass was relatively abundant contributing to 41 and 62 % of the total heterotrophic biomass in infiltration and band assemblages respectively. However, the taxonomic composition of both microalgae and protozoa varied greatly, according to the physical characteristics of the sea ice habitat. Whilst diatoms dominated dramatically the algal composition of all investigated ice areas (Table 3.II), the bulk of their biomass considerably differed from one sea ice habitat to another, with nano-sized *Nitzschia* sp. and micro-sized *Tropidoneis* sp. prevailing in infiltration assemblages, and micro-sized

Table 3.II : Composition of microorganisms in the sea ice & adjacent water column samples. Results expressed in % of total carbon biomass (autotrophs + heterotrophs). Diatoms R.S. = Resting Spores; Diatoms V.C. = Vegetative Cells; (-) = negligible.

| Taxon | Infiltr. Assembl. n = 4 | | Band Assemblage n = 2 | | Water Column n = 3 | |
|-------------------------------------|----------------------------|----------------|--------------------------|--------------|-----------------------|-----------------|
| | Range, | \bar{x} | Range, | \bar{x} | Range, | \bar{x} |
| Autotrophs | | | | | | |
| Diatoms R.S. | (-) | | 12-45 | 29±16.2 | (-) | |
| Diatoms V.C. | 65-93 | 77 ±8.7 | 50-63 | 56.5±6 | 11-15 | 13.4±1.6 |
| <i>Phaeocystis</i> col. | 0-3.3 | 1.2±1.2 | (-) | | (-) | |
| Dinoflagellates | 1-11 | 5.6±3.2 | 0-0.3 | 0.2±0.2 | 2-10 | 6.7±3.2 |
| Nanoflagellates | 3-13 | 6.9±4.3 | 0.2-1 | 0.6±0.4 | 38-50 | 43.6±4 |
| Aut. procaryotes (= cyanobact.?) | 0.1-1.8 | 0.9±0.6 | (-) | | (-) | |
| Total | 82-97 | 92±4.8 | 76-96 | 86±10 | 60-71 | 64±14.7 |
| Heterotrophs | | | | | | |
| Protozoa | | | | | | |
| . Ciliates | 0.1-2.4 | 0.9±0.7 | 1.4-2.9 | 2.2±0.8 | 1.9-3 | 2.5±0.4 |
| . Dinoflag. | 0.4-4.5 | 2.1±1.2 | 0-0.1 | 0.05±0.05 | 3.8-9 | 6.5±1.8 |
| . Nanoflag. | 0.2-3 | 1.6±0.7 | 0-0.6 | 0.3±0.3 | 7-12 | 9 ±2.1 |
| Bacteria | 1.3-11 | 3.8±3.5 | 1.3-22 | 12 ± 10.4 | 9-27 | 18.2±5.9 |
| Total | 3-18 | 8.3±4.9 | 4-24 | 14+10 | 29-40 | 36.3±4.9 |

Thalassiosira sp. and *Amphiprora* sp. in interior layers. Ciliates constituted the bulk of protozoa biomass of band assemblages. Within infiltration layer reversely, ciliates were scarce, whereas dinoflagellates and heterotrophic nanoflagellates contributed almost equally to protozoan biomass.

3.1.3. Fate of microbial assemblages at the time of ice melting : the role of krill

Contrasting with sea ice assemblages, microorganisms of adjacent surface waters were dominated by nano-sized microorganisms mainly autotrophic and heterotrophic flagellates, diatoms – mainly *Nitzschia* – representing a maximum of 15% of the total microbial biomass. Obviously the ice melting process in the northwestern Weddell sea gives rise to a shift from a diatom-dominated community in the ice environment to a nanoflagellate-dominated community in the water column (Fig. 3.3). This shift, in other respects not due to the inability of ice microorganisms to develop in sea water, has to be explained by an effective disappearance of ice microorganisms from the water column, either by grazing pressure or by sedimentation. The presence of numerous krill swimming around ice floes, scraping on concentrated sea ice assemblages (Cuzin-Roudy & Schnack, 1989) and the propensity of ice algae to aggregate formation followed by rapid sedimentation (Riebesell *et al.*, 1991) supports this assumption, so minimizing the contribution of ice algae to phytoplankton ice-edge development. Accordingly, a low seeding stock of $0.05 \mu\text{g Chl } a \text{ l}^{-1}$ was calculated by Lancelot *et al.* (1991a) from the empirical relationship between chlorophyll *a* concentrations in surface waters at the early beginning of ice melting and ice cover percentage (Fig. 3.4).

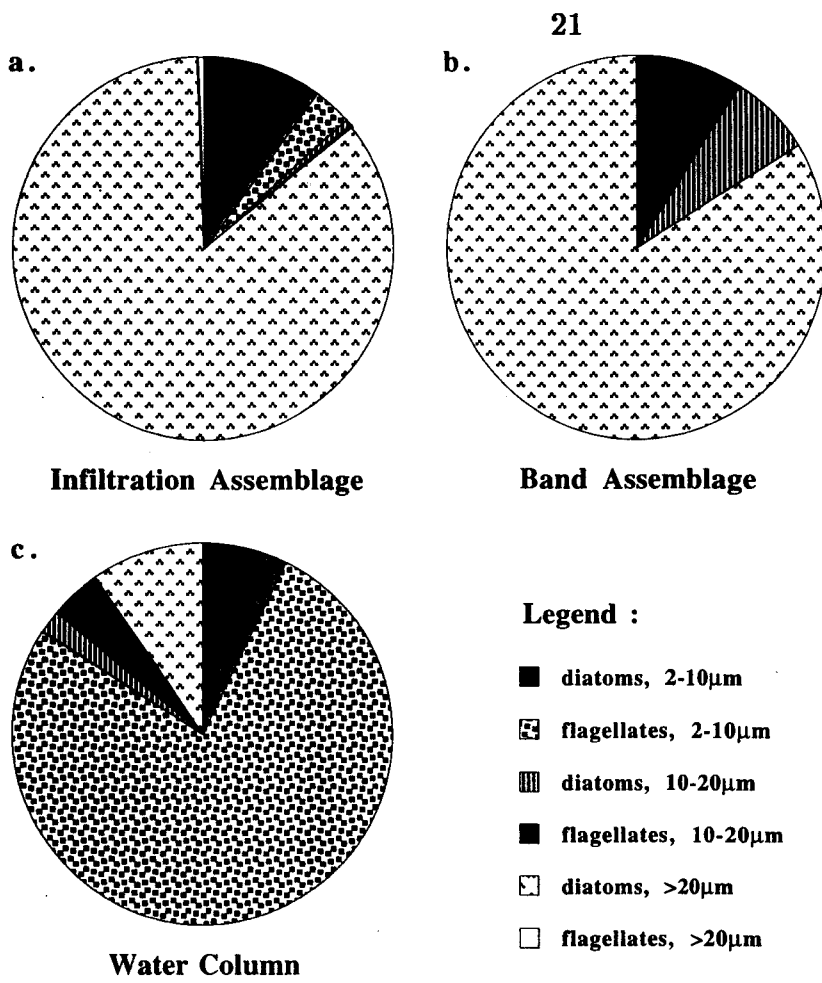


Figure 3.3 Distribution of autotrophic carbon biomass in three size classes with distinction between diatoms and flagellates typical of infiltration (a) and band (b) assemblages, and surface phytoplankton (c).

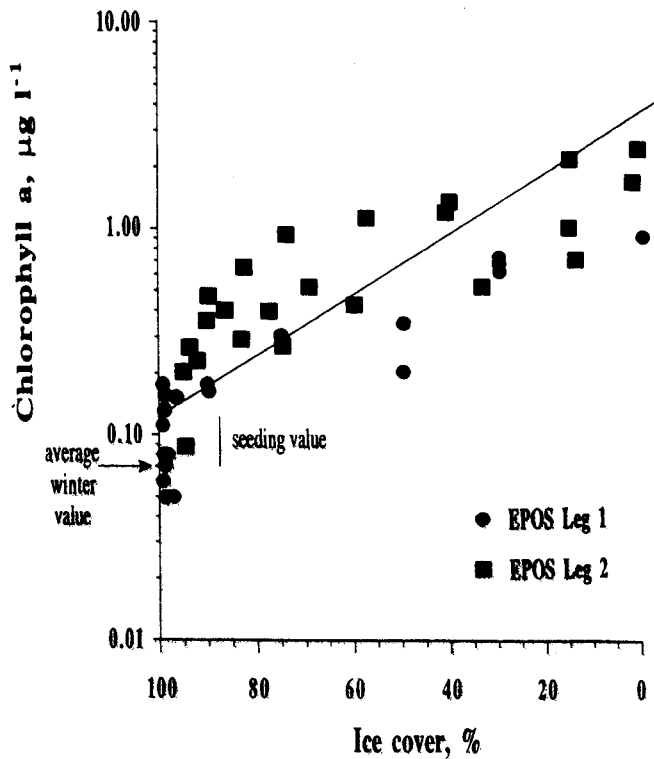


Figure 3.4 : Relationship between chlorophyll *a* concentration of surface waters and ice cover as measured in the marginal ice zone at the beginning of ice melting.

3.2. Physical processes associated to sea ice retreat and phytoplankton ice-edge bloom initiation

3.2.1. Phytoplankton bloom and the receding ice-edge

In 1988, the marginal ice zone around the 49° W meridian extended from latitude 58° 30' to 61° S, covering a distance of about 300 km. This zone is a dynamic frontal system which is not a sharply delimited line between the ice and the open ocean, but rather a wide transitional zone with large spatial (especially North-South) and temporal differences in its environmental properties. Figures 3.5 and 3.6 respectively show the spatio-temporal variation of ice cover (Fig.3.5) estimated by Lancelot *et al.* (1991b) in the studied sector during spring 1988, and the shift of the ice-edge further South (Fig.3.6). As seen on these figures, the process of ice retreat initiated in end October and completed in end December, proceeding at a mean rate of 5.5 km per day. Nevertheless, the ice-edge in this sector of the Weddell Sea does not retreat further south than 61° S because of a continuous supply of sea ice from the Weddell Gyre (Ackley, 1981). In agreement with previous observations (Comiso & Zwally, 1984), ice retreat did not occur at the same rate throughout the whole period, being minimal at the beginning (end October) and at the end (end December) of the process. During the period in between, intense ice melting occurred and sea ice retreat could cover distances as great as 9 km per day.

In close relationship with sea ice retreat, maximum chlorophyll *a* concentrations of about 4 $\mu\text{g l}^{-1}$ were systematically recorded close to the ice-edge, at a distance of about 50 km from its northern boundary (Fig. 3.6) and coincided with nitrate concentration minima (about 20 $\mu\text{mole l}^{-1}$). Moreover a 100 to 150 km-width belt of relatively elevated phytoplankton biomass (higher than 2 $\mu\text{g l}^{-1}$) was strongly associated with the receding ice-edge, moving in parallel with this latter (Fig. 3.6). On both sides of this region of enhanced primary production, mean chlorophyll *a* concentrations were very low (0.4 $\mu\text{g chl } a \text{ l}^{-1}$), reaching 1 $\mu\text{g l}^{-1}$ at a maximum.

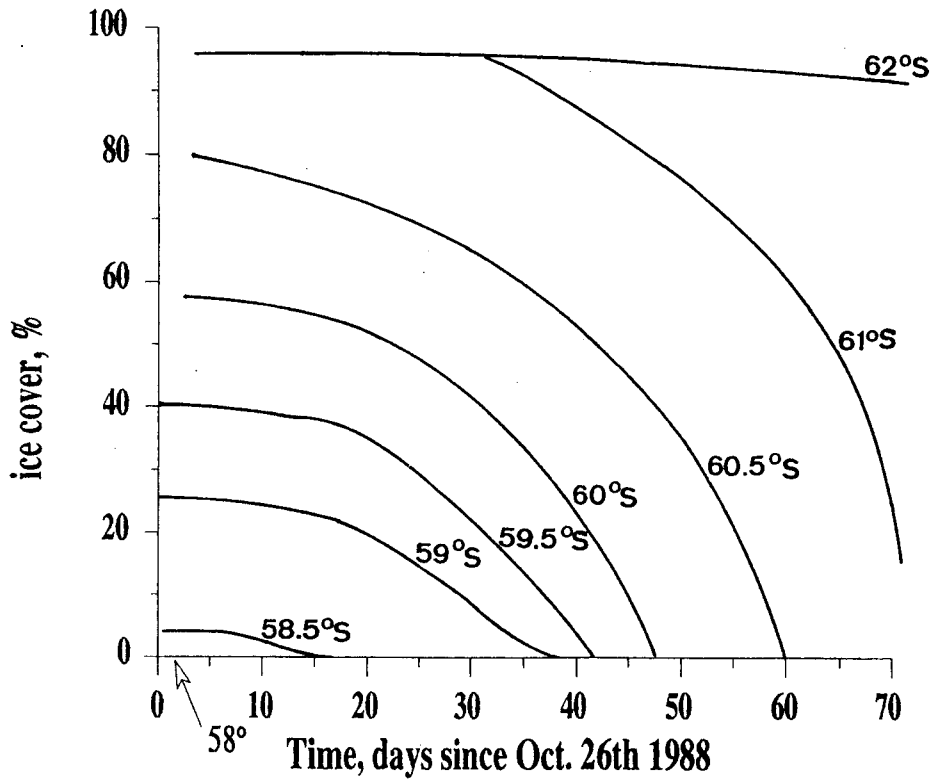
ANTAR
II/05

Figure 3.5 : Spatio-temporal evolution of ice cover around meridian 49° W during sea ice retreat 1988.

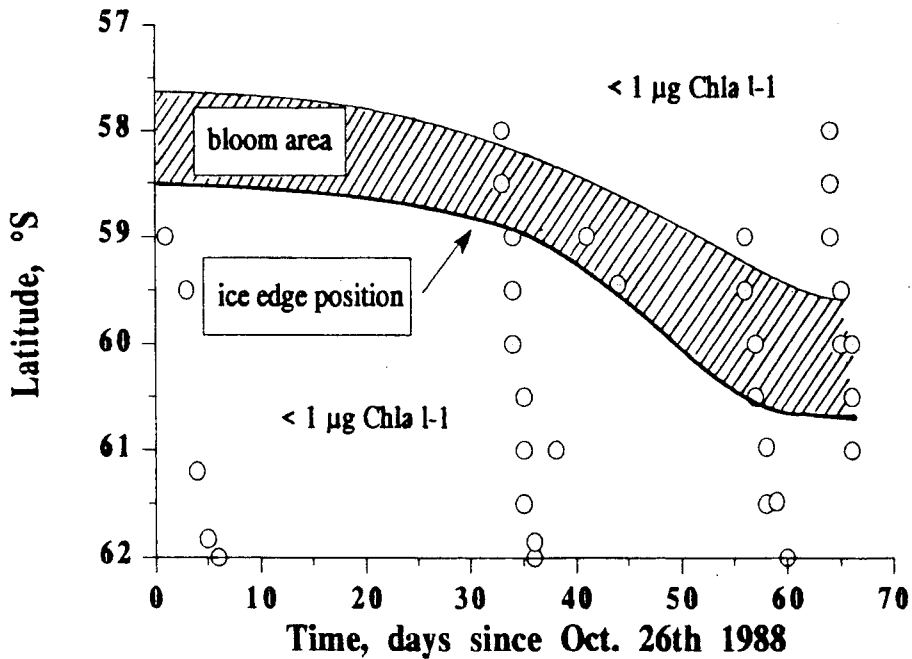


Figure 3.6 Sea ice retreat and related chlorophyll *a* spatio-temporal distribution. Sampling stations (□, EPOS Leg 1; O, EPOS Leg 2) and position of the ice-edge .

The strong relationship between the receding sea ice and phytoplankton bloom development is clearly evidenced by Fig. 3.7 that shows synoptic distribution of ice cover, averaged chlorophyll *a* concentrations over the upper wind mixed layer and nitrate depletions (the amount of nitrate removed from the water column by phytoplanktonic uptake during the ongoing growth season) observed or calculated over a one-month interval. During this period, sea ice retreated over a distance of 270 km (Fig. 3.7a). Accordingly, the peak of phytoplankton shifted from latitude 58° 30' S to 60° S (Fig. 3.7b), at a similar rate as the receding ice-edge (9 km day⁻¹ at this period of intense ice melting). Also, nitrate depletion (Fig. 3.7c) reached a maximum of 500 μM m⁻² that moved southward, closely following the sea ice retreat. More noteworthy is the similar feature of both phytoplankton blooms, in magnitude as well as in extent, suggesting that their controlling mechanisms are identical. Unexpected however is the moderate magnitude of spring bloom regarding the high ambient nutrient concentrations. The latter remained indeed well above depletion throughout the spring season (Goeyens *et al.*, 1991a; van Bennekom *et al.*, 1989). Such a low biological performance cannot be ascribed to low temperature stress on phytoplankton physiology, as photosynthetic and growth capacity at temperatures ranging from -1.8 to +2° C were of the same order of magnitude as those of temperate phytoplankton (Lancelot *et al.*, 1991a). Other factors likely prevent massive biomass development in this part of the circumpolar marginal ice zone. They are discussed in details in the following sections.

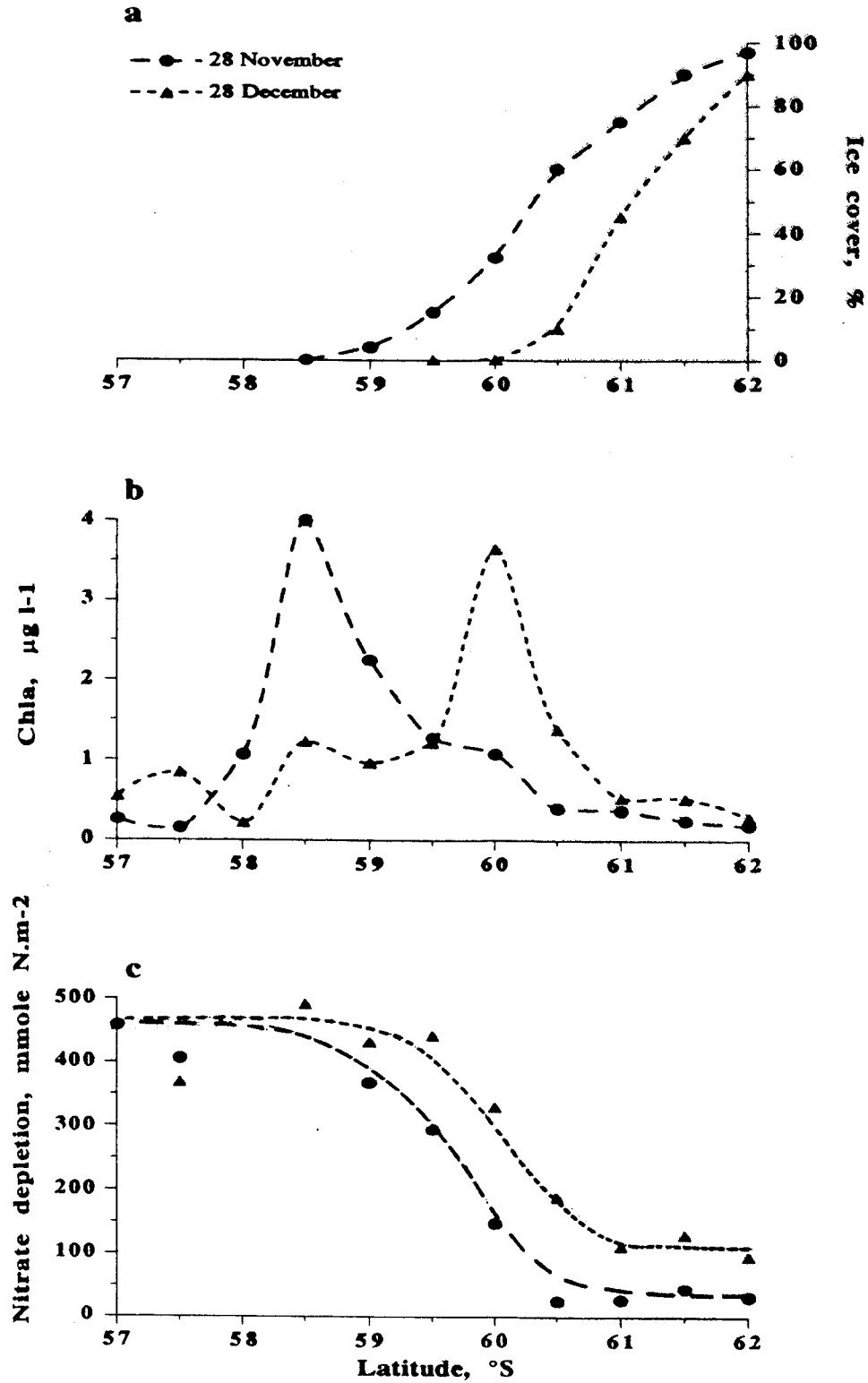


Figure 3.7 : Ice cover percentage (a), averaged chlorophyll *a* concentration over the upper mixed layer (b) and nitrate depletion (c) measured at one-month interval along the 49° W meridian.

3.2.2 The dual role of ice melting in phytoplankton initiation

Vertical stability caused by ice melting has been shown to be the necessary condition for phytoplankton ice-edge bloom initiation (Smith & Nelson, 1985; Sullivan *et al.*, 1988). The relationship between phytoplankton bloom development in the upper mixed layer and the density field of surface waters, as observed during the cross section in the marginal ice zone of early summer (Fig. 3.8), strongly suggest that vertical stability is a necessary but not sufficient condition to allow high biomass development. Indeed, the strong vertical stability of surface waters, created at about 20 % ice cover (Fig. 3.8), maintained itself in the recently ice-free area over a distance of about 250 km (close to the maximum winter sea ice extent around this meridian). On the contrary, corresponding chlorophyll *a* concentrations exhibited one order of magnitude variations around a sharp phytoplankton peak of $4 \mu\text{g l}^{-1}$ occurring at latitude 60° S (Fig. 3.8). Comparing this with average light in the upper mixed layer (this latter being calculated by taking into account the subsurface irradiance corrected for ice cover, the vertical light extinction coefficient and the depth of the wind mixed layer, see Fig. 3.8a) highlights the dual role of ice-melting in initiating phytoplankton bloom by providing optimal light conditions to phytoplankton cells owing to both the installation of a shallow vertically stable environment as well as the progressive removal of sea ice (Fig. 3.8). At ice coverage higher than 20 % however, phytoplankton development is prevented due to light limitation, despite relatively shallow upper mixed layers (Fig. 3.8a & b). In this ice covered area, environmental light is highly reduced by sea ice albedo to values well below than the light saturation level (I_k) of $100 \mu\text{E m}^{-2} \text{ s}^{-1}$ typical of phytoplankton cells growing in this sector of the Southern Ocean (Lancelot *et al.*, 1991a). Consequently, very low chlorophyll *a* concentrations (less than $0.5 \mu\text{g l}^{-1}$) are characteristic of these ice covered areas, apparently regardless the vertical stability (Fig. 3.8c).

In most marginal ice areas, the geographical extent of the bloom has been related to that of vertical stability, i.e. the persistence of optimal light conditions, whilst its decline has been attributed to dilution due to the northward degradation of the shallow upper mixed layer by either vertical or lateral processes (Smith & Nelson, 1985; Sullivan *et al.*, 1988; Mitchell & Holm-Hansen, 1991). Deepening of the upper mixed layer by decreasing average water column light to values lower than the phytoplankton light saturation level (Fig. 3.8) might well explain the low chlorophyll concentrations typical of the permanently ice-free area measured North of latitude 58° S. In the recently free of ice zone (between 58° and 60° S), on the contrary, vertical stability persisted seawards from the ice-edge, providing optimal light conditions to

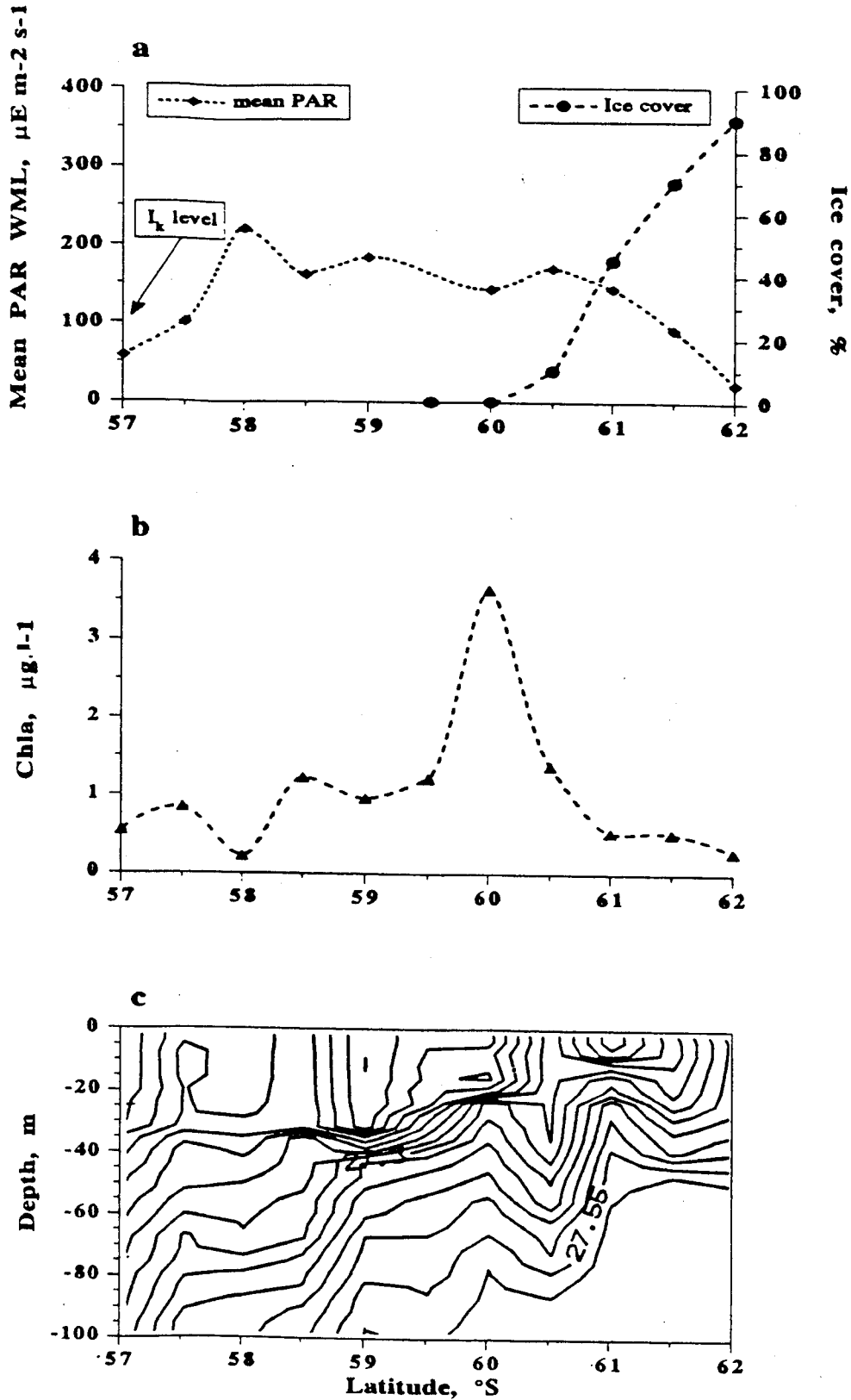


Figure 3.8 : Average light in the upper mixed layer (a), averaged chlorophyll *a* Concentration over the upper mixed layer (b) and density field (c) measured in end-December along the 49° W meridian.

phytoplankton cells (Fig.3.8). Northwards maintenance of vertical stability created in the marginal ice zone by sea ice melting is however a common phenomenon due to heating input (Veth *et al.*, 1992). In their comprehensive analysis of the physical processes contributing to the buoyancy flux in the marginal ice zone of the northwestern Weddell Sea during sea ice retreat 1988, these authors demonstrate that the total buoyancy flux is rather constant with the distance to the ice-edge, being mostly due to ice melting in the marginal ice zone and solar heating in the recently free of ice area. Consequently, similar wind mixed layers are expected in marginal ice zone and adjacent open areas under similar weather conditions. This means that the suboptimal performance of phytoplankton in the open ocean adjacent to the marginal ice zone, after an initial peak following the receding ice-edge, is not caused by turbulent mixing as is often assumed.

3.3. The role of trace metals

The hypothesis that Southern Ocean phytoplankton bloom is limited by deficiency of a trace metal, notably iron (Fe), was recently suggested by Martin & Fitzwater (1988) who extrapolated from bioassays conducted in a similar high nutrient region – the subarctic North Pacific Ocean (Martin & Fitzwater, 1988; Coale *et al.*, 1991). This iron limitation hypothesis for the Southern Ocean was tested in a suite of five experimental runs in different sub-areas of the studied sector of the marginal ice zone (de Baar *et al.*, 1990; Buma *et al.*, 1991). Despite a clear stimulation of growth in every single experiment due to Fe addition, the control bottles (no addition) also rapidly outgrew the levels of chlorophyll *a* in the field (Fig. 3.9). Firstly, this indicated the presence of enough dissolved Fe levels to sustain some growth, as later confirmed by seawater Fe concentrations exceeding 1 nM in the Weddell/Scotia Sea region and upstream Peninsula waters (Nolting *et al.*, 1991; Westerlund & Öhman, 1991; Martin *et al.*, 1990b). Secondly, the bottle effect of controls outgrowing the field was suggested to result from the exclusion of larger grazers (mesozooplankton, e.g. copepods, *Euphausia superba*, salps), allowing the accumulation of both phytoplankton (notably diatoms) and microzooplankton (Buma *et al.*, 1991). Experiments conducted one year later in the Ross Sea showed very similar trends in three out of four experiments, the fourth at the most offshore station more likely suggesting the sought after true Fe limitation (Martin *et al.*, 1990a). These results were interpreted to suggest that, despite observed Fe stimulation, the low phytoplankton stock in the Ross Sea is mostly controlled by loss terms (Dugdale & Wilkerson, 1990). However, in more offshore Antarctic waters, severe Fe limitation is still a valid hypothesis for testing, as

indicated by the results of the one offshore Ross Sea bottle experiment (Martin *et al.*, 1990b). Otherwise, assessments other than bottle enclosures are needed to provide unequivocal evidence for Fe limitation.

Summarizing it may safely be concluded that the Weddell–Scotia region of the EPOS study (as well as at least part of the Ross Sea) is not Fe limited *per se*. Other factors are likely responsible for the moderate ice–edge blooms here observed. Top down grazing control appears one of the more viable proposition, as low sedimentation rates of $0.005 - 0.03 \text{ d}^{-1}$ were actually calculated from sediment trap data (G. Cadée, pers. com., 1991). This hypothesis is examined in the following section.

ANTAR
II/05

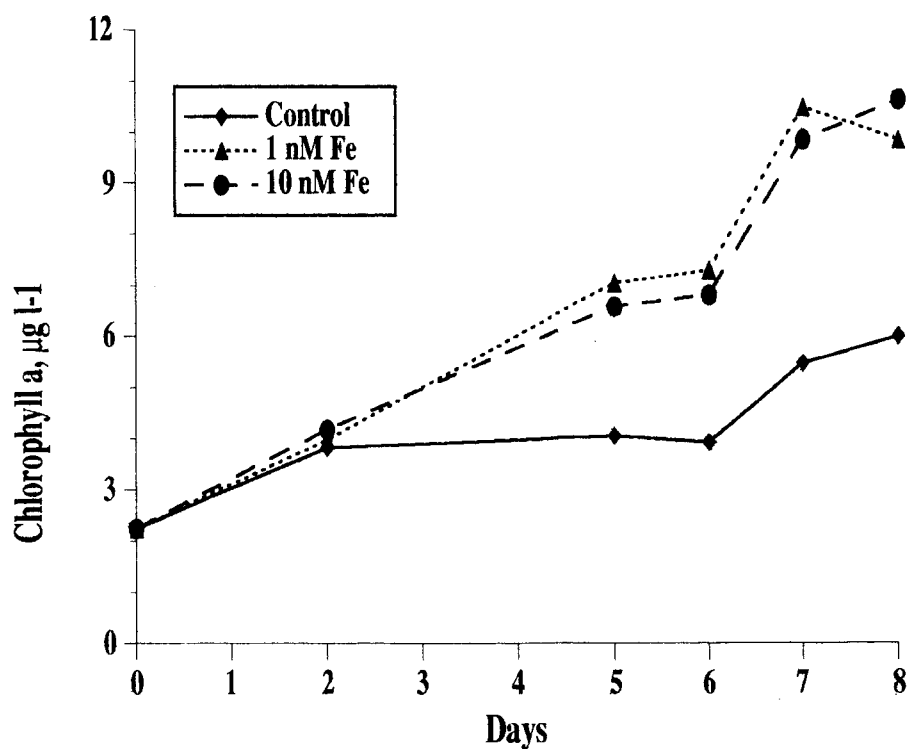


Figure 3.9 : Iron enrichment experiment carried out at latitude 59° S (after de Baar *et al.*, 1990).

4. STRUCTURE AND FUNCTIONING OF THE PLANKTONIC FOOD WEB AT THE RECEDING ICE-EDGE

ANTAR
II/05

4.1. The complex structure of the planktonic food-web

The development of phytoplankton blooms at the receding ice-edge is accompanied by the development of various heterotrophic organisms. The complex structure of the planktonic food web characteristic of the marginal ice zone (Fig. 4.1.) has been established on the basis of the identification of key planktonic organisms together with the analysis of their spatio-temporal variations as well as their mutual interactions.

4.1.1. Identification of key planktonic organisms

Auto- and heterotrophic microorganisms

Average carbon biomass distribution among the main taxonomic groups characterizing microbial communities of the marginal ice zone of the northwestern Weddell Sea is shown on Table 4.I. These taxons were chosen according to the size (nano-, micro-) and the trophic mode (phyto-, protozoo-, bacterioplankton). Within each trophic mode, additional taxons were considered on the basis of their relative abundance. This analysis revealed the dominance of nano-sized-microorganisms, both autotrophs and heterotrophs.

Phytoplankton biomass, ranging between 7.7 and 79.8 $\mu\text{gC l}^{-1}$ with a mean value of 25.7 $\mu\text{gC l}^{-1}$, constituted by far the bulk of the microbial biomass, contributing on an average to 65 % of the total microbial carbon (Table 4.I). Among autotrophs (mean carbon biomass = 25.7 $\mu\text{gC l}^{-1}$), the nanophytoplankton forms were the most important, representing 74 % of the total phytoplankton biomass with an average of 18.9 $\mu\text{gC l}^{-1}$. As a general trend, flagellates were shown to dominate the nanoplanktonic autotrophic community (87 %), whilst diatoms constituted the bulk of microphytoplankton (99 %). In one case however (station 147), when small *Chaetoceros* sp. were abundant, diatoms could significantly contribute to nanophytoplankton. Naked flagellates identified as *Prasinophyceae*, *Cryptophyceae* and *Prymnesiophyceae* were the dominant nanophytoplankters. Among these, *Cryptomonas* spp. (Fig. 4.2a) was by far the most important genus. Centric diatoms constituted the bulk of microphytoplankton, with *Corethron* sp., *Thalassiosira* sp. and *Rhizosolenia* sp. being the principal genus (Fig. 4.2b).

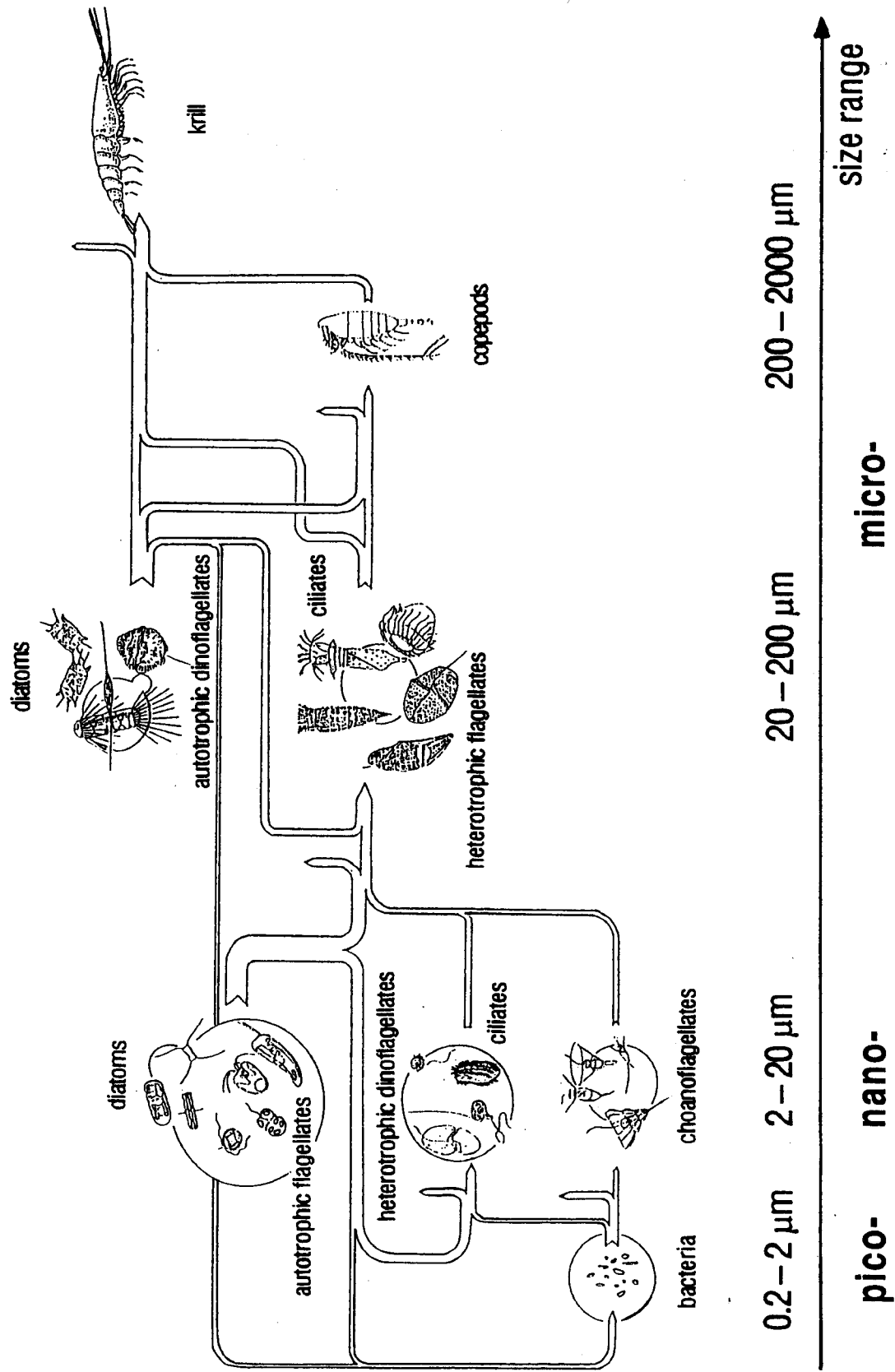


Figure 4.1 : Structure of the planktonic food web at the receding ice-edge of the northern Weddell Sea.

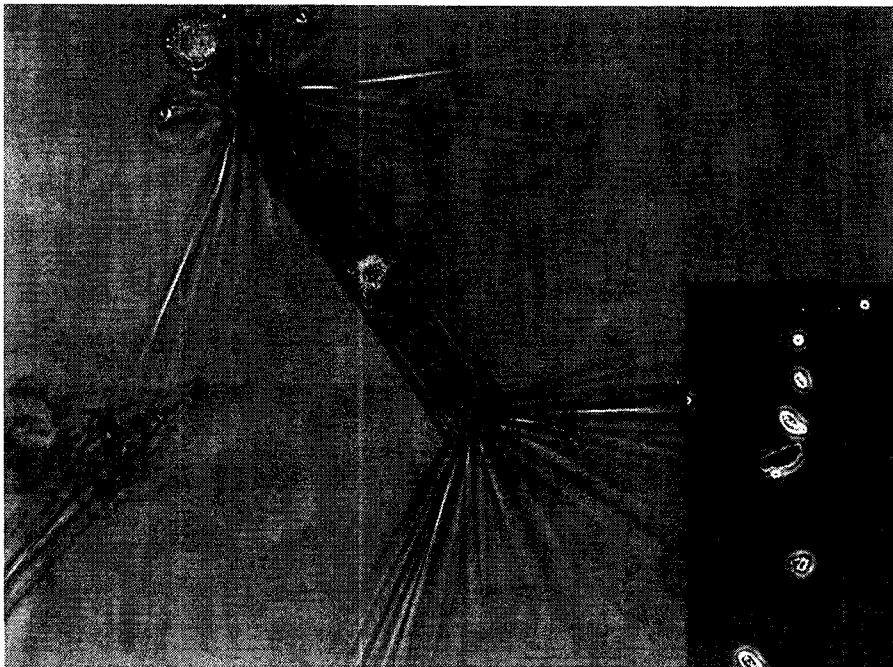
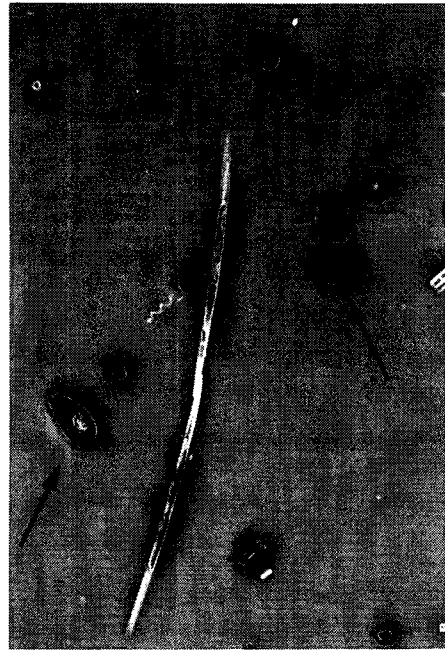
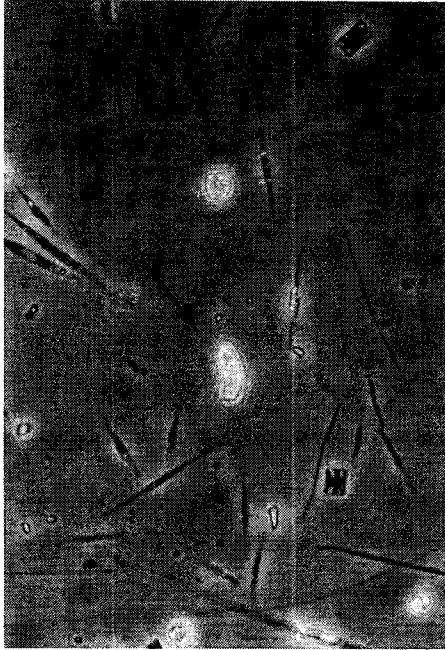
Table 4.I : Mean and extreme values of biomass for main microbial groups. Number of observations = 16. Units are $\mu\text{gC l}^{-1}$. Abbreviation : n.s. = not significative.

| Taxon | Nano-size, ($<20\mu\text{m}$) Mean (min. - max.) | Micro-size, ($>20\mu\text{m}$) Mean (min. - max.) | Total Mean (min. - max.) |
|--------------------------------|---|--|-------------------------------------|
| <u>Phytoplankton</u> | | | |
| Diatoms | 2.0 (0.1 - 18.6) | 6.7 (n.s. - 50.3) | 8.7 (0.1 - 68.9) |
| Dinoflagellates | 0.5 (0 - 2.1) | n.s. (0 - 0.5) | 0.5 (0 - 2.1) |
| Other flagellates | 16.4 (4.4 - 79.1) | 0.1 (0 - 2.0) | 16.5 (0.2 - 79.1) |
| <u>Total</u> | <u>18.9 (3.4 - 79.3)</u> | <u>6.8 (n.s. - 52.8)</u> | <u>25.7 (7.7 - 79.8)</u> |
| <u>Protozooplankton</u> | | | |
| Choanoflagellates | 0.1 (n.s. - 0.4) | - | 0.1 (0 - 0.7) |
| Dinoflagellates | 1.3 (0.3 - 3.4) | 1.3 (0 - 7.4) | 2.6 (0.7 - 7.7) |
| Other flagellates | 3.4 (0.3 - 20.3) | - | 3.4 (0.3 - 20.3) |
| Ciliates | 0.2 (0 - 1.0) | 1.6 (0.5 - 6.5) | 1.8 (0.5 - 6.7) |
| Amoeba | 1.2 (0 - 5.6) | - | 1.2 (0 - 5.6) |
| <u>Total</u> | <u>6.2 (0.7 - 27.6)</u> | <u>2.9 (0.5 - 11.2)</u> | <u>9.1 (1.8 - 29.2)</u> |
| <u>Bacterioplankton</u> | | | 4.2 (1.4 - 10.0) |

Among heterotrophs, protozooplankton was the most important in terms of biomass. Its mean biomass amounted to $9.1 \mu\text{gC l}^{-1}$, contributing to 23 % of the total microbial biomass. On an average, it represents 35 % of the phytoplankton biomass. Like phytoplankton, protozooplankton was dominated by nano-sized taxons, in which heterotrophic dinoflagellates and other heterotrophic flagellates contribute respectively to 29 and 37 % of the total nanoprotzooplankton biomass. The microzooplankton was composed of dinoflagellates and ciliates, these latter dominating at 55 % in biomass.

Bacterioplankton biomass varied around $4.6 \mu\text{gC l}^{-1}$, averaging 16 % of phytoplankton biomass. At one occasion, however, (station 147), a particularly high bacterial biomass of $10 \mu\text{gC l}^{-1}$ and 1.3 times greater than the phytoplanktonic standing stock was observed. This elevated bacterial biomass follows the passage of a krill swarm literally cleaning the water from its phytoplankton standing stock (Jacques & Panouse, 1991). Organic matter released through krill feeding activity might have thus stimulated bacterial growth.

a.



b.

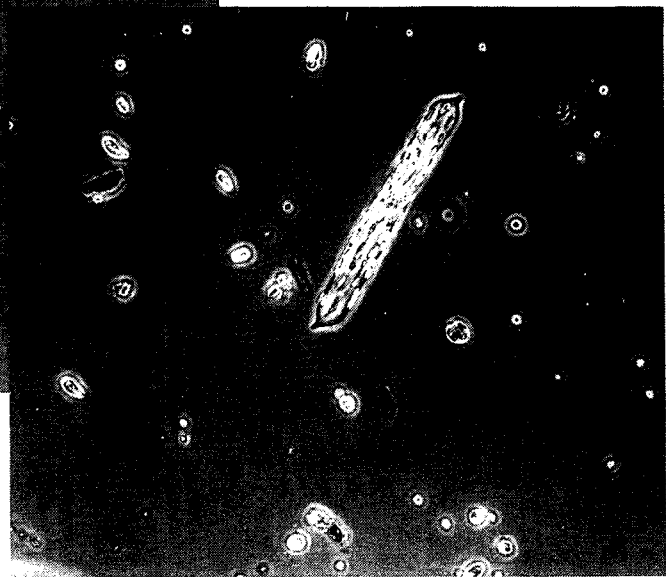


Figure 4.2 : Dominant phytoplankton species : (a) *Cryptomonas* spp.; (b) *Corethron* sp. and *Rhizosolenia* sp. (photographs by S. Mathot).

Mesozooplankton and krill

Oithona similis was the most abundant herbivorous copepod in the marginal ice zone of the northwestern Weddell Sea, the total biomass of which was however low in comparison with protozooplankton, varying between 0.5 and 13 $\mu\text{gC l}^{-1}$ (Fransz & Gonzalez, 1992). Higher copepod biomass reaching 50 $\mu\text{gC l}^{-1}$ was however recorded in the permanently open sea, North of the marginal ice zone.

The Antarctic krill *Euphausia superba*, one of the major components of mesozooplankton in the sea ice-associated area of the Southern Ocean (Hempel, 1985), leads a double life behavior : under-ice during winter, shifting to pelagic in summer (Smetacek *et al.*, 1990; Siegel *et al.*, 1990). By exploiting alternatively the sea ice algae and phytoplanktonic resources, krill might control the phytoplankton ice-edge bloom at different stages during the course of its development. Overwintering krill in the pack ice zone likely has a predominant role on phytoplankton ice-edge bloom initiation and magnitude, as it reduces the water column seeding by scraping the ice, especially when sea ice algae are released in the water column at the time of ice melting (Marschall, 1988; Stretch *et al.*, 1988; Smetacek *et al.*, 1990). High krill biomass (1–27 g m^{-2}) was recorded in the closed pack ice zone of the northwestern Weddell Sea in the early beginning of the ice melting process (Siegel *et al.*, 1990). These numbers underestimate however the existing krill standing stock, representing only organisms that could be sampled by trawls (Siegel *et al.*, 1990). Indeed, dense krill populations were effectively observed in the marginal ice zone, either evolving in the ridges resulting from piling ice floes (Bergström *et al.*, 1989, 1990) or washed onto the ice in the ship's wake (Cuzin-Roudy & Schalk, 1989).

High patchiness characterizes the distribution of krill swarms in their pelagic life, owing to their great mobility. During the 70 day-EPOS expedition, one single krill swarm was sampled, which biomass amounted 119 g m^{-2} (Schalk, 1990).

4.1.2. Trophic interactions at the receding ice-edge

The trophic interactions between the planktonic organisms of the marginal ice zone of the northern Weddell sea were determined indirectly from the analysis of the sequence of events occurring during the process of sea ice retreat, as deduced from the analysis of spatio-temporal variation of organisms biomass with regards to ice cover, and of the mutual interactions between auto- and heterotrophs established by correlation analysis between specific taxonomic groups.

The spatio-temporal variations of microorganisms (phytoplankton, bacteria and protozoa) and herbivorous copepods biomass averaged over the depth of the upper homogeneous surface layer (Fig 4.3, 4.4) clearly indicates that protozoa are the first heterotrophs to respond to phytoplankton ice-edge bloom. As shown on Fig.4.3, protozoan biomass closely follows phytoplankton biomass by increasing at the time of phytoplankton bloom. However, the high protozoan biomass reached at phytoplankton maximum maintains itself during the decline of the autotrophs, suggesting that these micrograzers do actively control phytoplankton development in this area of the Weddell Sea. Accordingly, a highly significant positive correlation ($r = 0.6$, $P < 0.005$; Table 4.II) relates the variations of phyto- and protozooplankton biomass.

Further investigation on trophic relationships between phytoplankton and protozoa was carried out through multiregression analysis of each dominant taxonomic group of either nano- or micro-sized protozooplankton on each different potential food resource (bacterioplankton, nano- or micro-sized phytoplankton, see Table 4.II). This statistical analysis indicated strong trophic interactions between food and consumers within the same size range, especially between heterotrophic nanoflagellates and nanophytoplankton and between heterotrophic dinoflagellates and microphytoplankton. This size overlapping of autotrophic food and herbivorous consumers is more evidenced by Fig. 4.5 that shows the size distributions of microbial (phytoplankton and protozoa) carbon biomass on a logarithmic scale of microorganism diameter for two typical patterns (Fig. 4.5a & 4.5b) of phytoplankton size distribution. Thus, the highly significant correlations existing between distinct taxonomic groups (Table 4.II) together with the overlapping of the peaks of both protozoan biomass and phytoplankton biomass (Fig. 4.5) show that the trophic organisation of the microbial community can be as complex as that presented on Fig.4.1. In this case indeed, the size ratio of about 1:10 between prey and predator suggested by Azam *et al.* (1983) does not hold, and the energy flux is thus not always oriented towards an increasing particle size as generally admitted.

Protozoa together with phytoplankton are in turn susceptible to be ingested by herbivorous copepods whose biomass, whilst maintained at low level in the area concerned by ice retreat, slightly increased in the recently free of ice area at the time of phytoplankton and protozoa biomass decline (Fig.4.3).

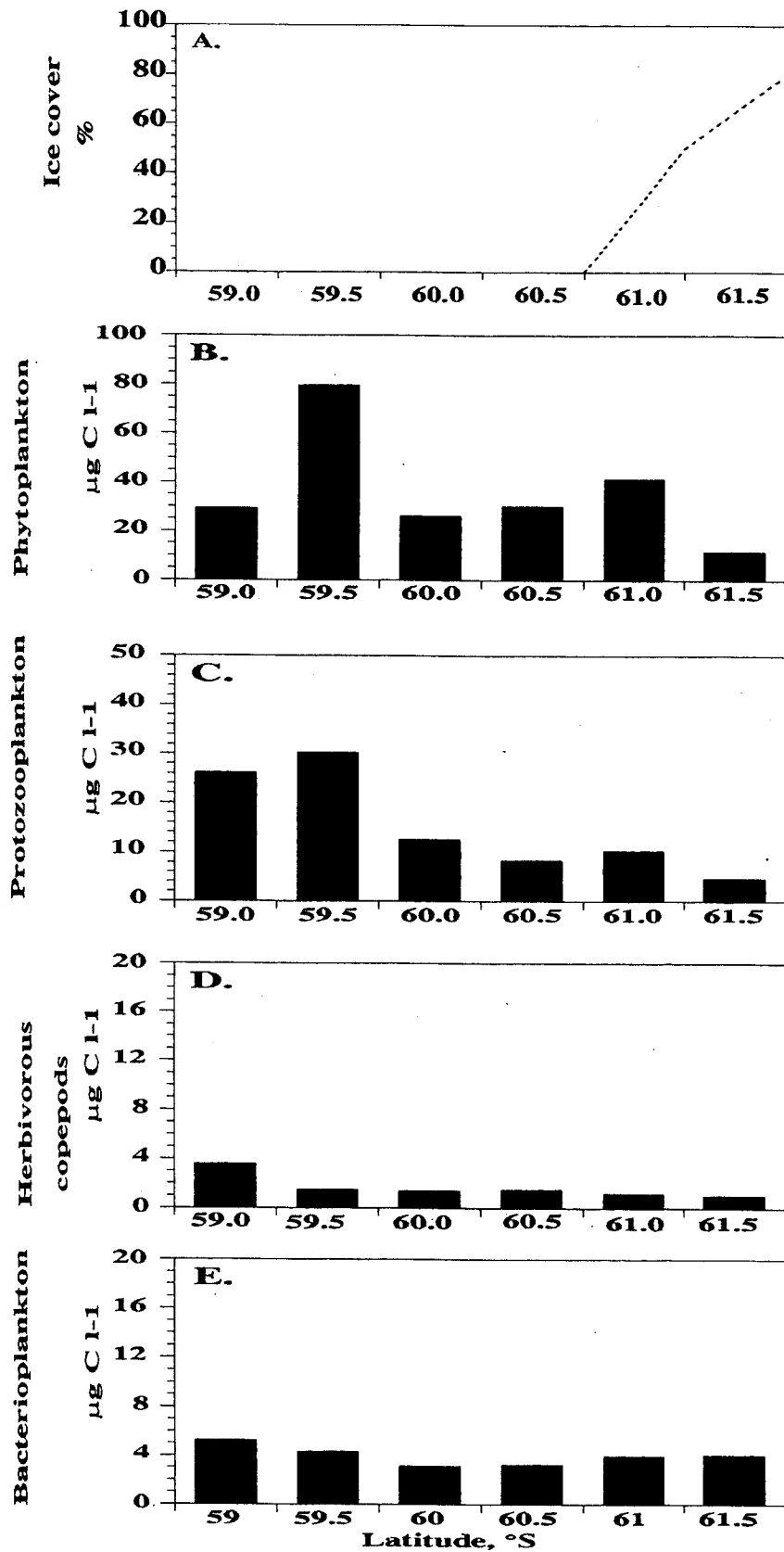


Figure 4.3 : Spatial variations of ice cover (a), phytoplankton (b), protozoa (c), herbivorous copepods (d) and bacterioplankton (e) carbon biomass along the meridian 49° W in end December 1988 (Transect 172–179, 20–24 Dec.).

meridian 49°W

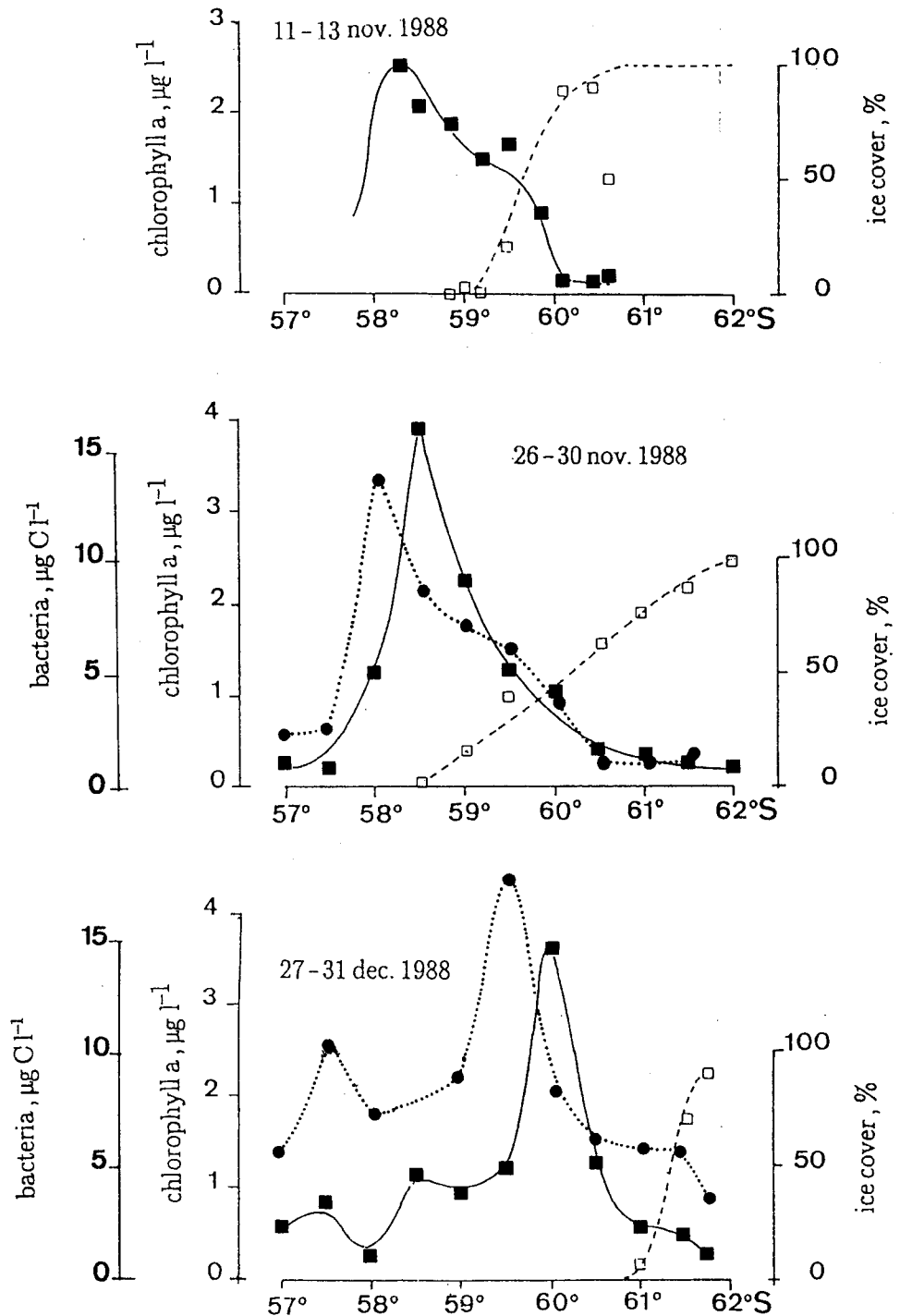


Figure 4.4 :

Spatio-temporal variation of phyto- (—) and bacterioplankton (●), and ice cover (□) along the meridian 49° W during spring 1988. Bacteria were not measured in early November.

Table 4.II : Correlation analysis between biomasses of selected taxonomic groups of microorganisms. Pearson's method followed by the Student test. Coefficients r and (P) are reported for the significant correlations (n.s. = not significant, i.e. $P > 0.05$).

| Food resource Consumer | Bacterio- plankton | Nanophyto- plankton | Microphyto- plankton | Total phyto- plankton |
|--------------------------------------|-----------------------|------------------------|-------------------------|--------------------------|
| <u>Bacterioplankton</u> | — | — | — | n.s. |
| <u>Nanoprotozooplankton</u> | | | | |
| Choanoflagellates | 0.86 *** | n.s. | n.s. | n.s. |
| Other flagellates | n.s. | 0.85 *** | n.s. | n.s. |
| Ciliates | 0.44 * | n.s. | n.s. | n.s. |
| Total | n.s. | 0.80 *** | n.s. | n.s. |
| <u>Microprotozooplankton</u> | | | | |
| Dinoflagellates | n.s. | n.s. | 0.84 *** | n.s. |
| Ciliates | n.s. | n.s. | 0.67 ** | n.s. |
| Total | n.s. | n.s. | 0.95 *** | 0.63 ** |
| <u>Total protozooplankton</u> | n.s. | 0.83 ** | n.s. | 0.68 ** |

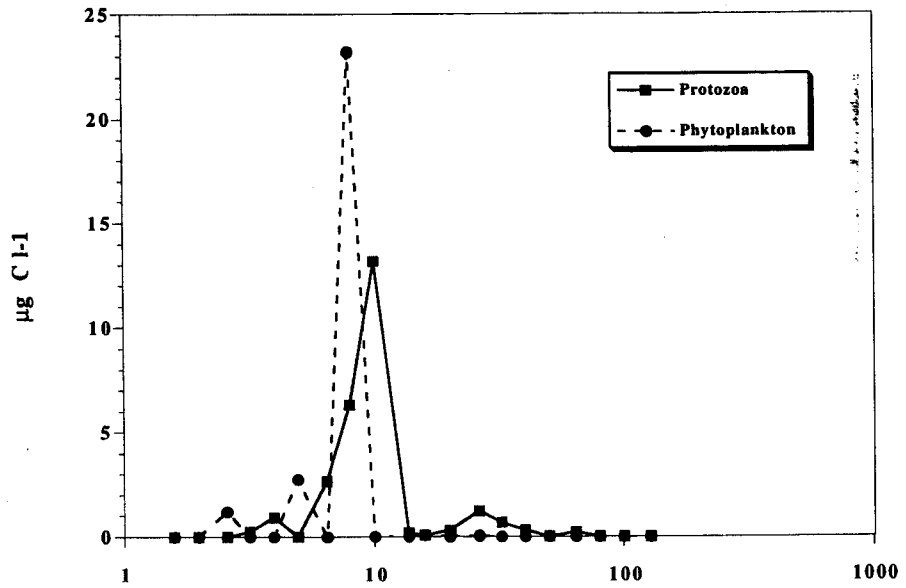
* : $P < 0.05$

** : $P < 0.005$

*** : $P < 0.0005$

On the other hand, no significant correlation was found between bacterial and phytoplanktonic biomasses (Table 4.II). Accordingly, the spatio-temporal evolution of chlorophyll a concentration and bacterial biomass (Fig. 4.4) clearly indicates a delay in the response of bacteria to phytoplankton development which follows the southward retreat of the ice-edge. Taking into account the rate of ice retreat, this delay can be estimated to about 10 days. This lag in the response of bacteria to phytoplankton development has been attributed to the macromolecular nature of the dissolved organic matter released from phytoplankton either by autolysis or sloppy feeding, which requires extracellular hydrolysis before being taken up (Billen & Becquevort, 1991). Among protozoa, only the filter-feeding ones, mainly the choanoflagellates and to a lesser extent nano-sized ciliates, should be active bacteria consumers according to the significant correlation relating these taxonomic groups to bacteria (Table 4.II).

a.



b.

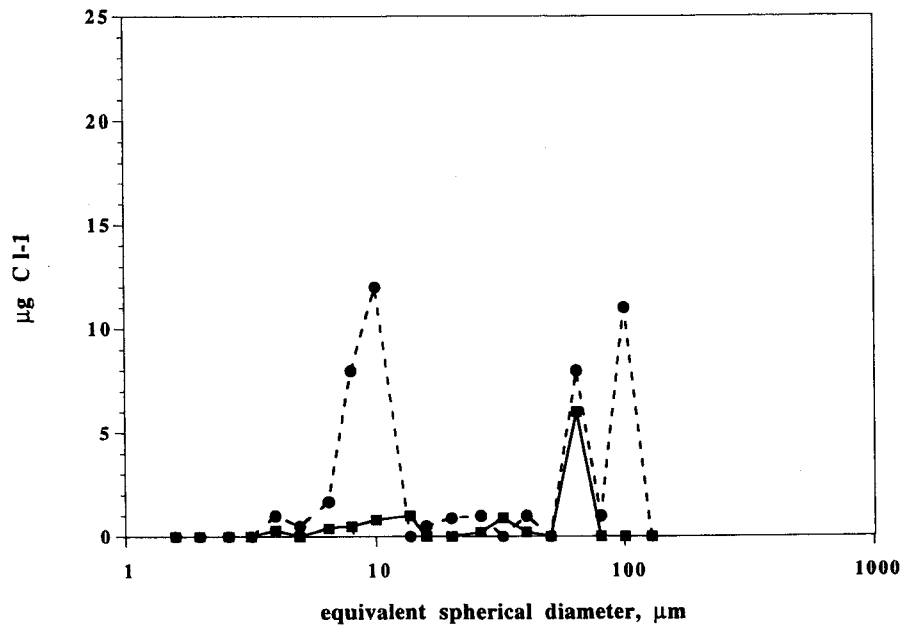


Figure 4.5 : Typical pattern of size distribution of phytoplankton and protozooplankton biomass.

4.2. The relative role of micro- and mesograzers in controlling phytoplankton activity in the northwestern Weddell Sea

4.2.1. The sustained grazing pressure exerted by protozoa and copepods and its implication for new to regenerated production ratio.

The relative role of herbivorous protozoa and copepods in controlling phytoplankton ice-edge bloom development was assessed by comparing calculated potential ingestion rates by these two grazers with daily integrated net primary production (Fig.4.6). This comparison strongly suggests that at least protozoa do actively control phytoplankton development at the receding ice-edge. Accordingly, potential ingestions higher than net primary production were occasionally calculated in the recently free-of-ice area. The role played by copepods on the other hand appears neglectable. Its food requirements should primarily be met by protozoa production in the recently free of ice area (Fig.4.6).

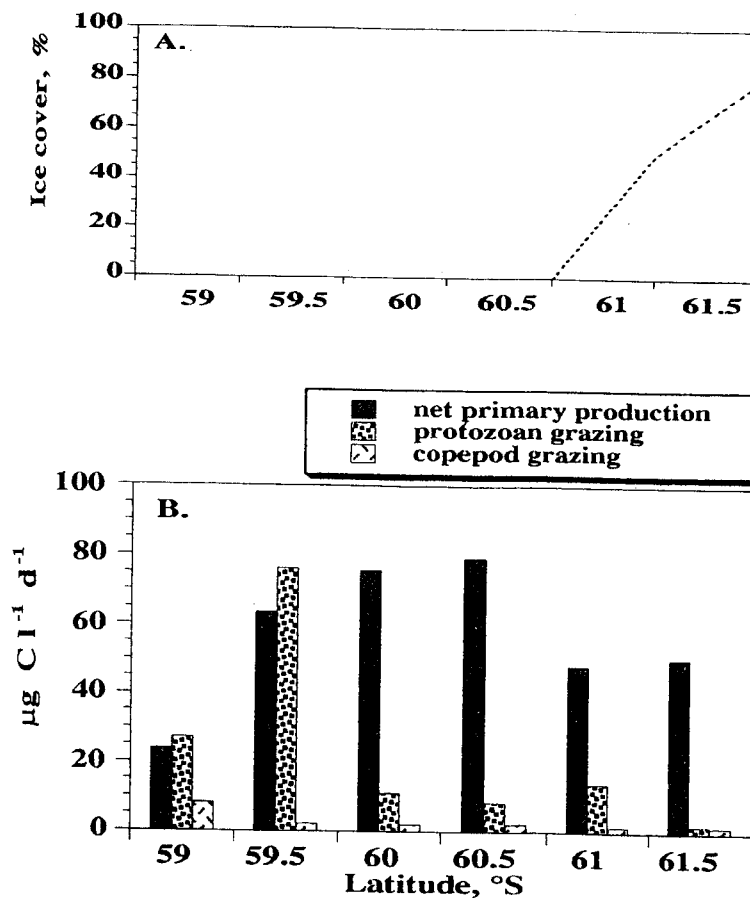
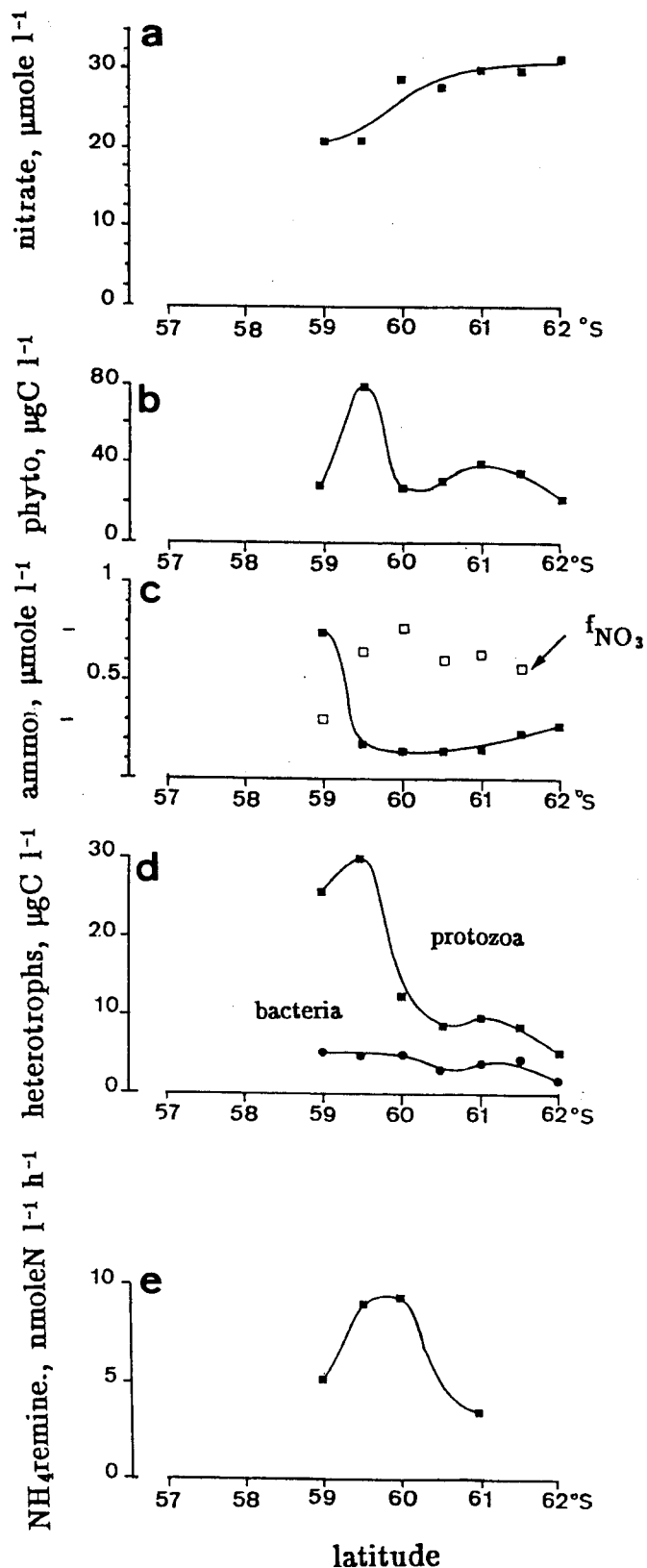


Figure 4.6 : Spatial variations of ice cover (a) and daily net primary production, protozoa and copepod grazing (b) along the meridian 49° W in end December 1988.

As a consequence of the high protozoa activity in the area concerned by ice retreat, ammonium concentration dramatically increases with the distance to the ice-edge (Fig.4.7). The balance of inorganic nitrogen forms available to phytoplankton is therefore modified in favor of ammonium, inducing a shift from a phytoplankton community preferably utilizing nitrate as nitrogen source to a predominance of ammonium-based primary producers. This is clearly evidenced by the sharp decrease of measured f_{NO_3} (the ratio between nitrate utilization and total nitrogen uptake by phytoplankton) with the distance to the ice-edge (Fig.4.7).

meridian 49°W
20–24 Dec.1988



ANTAR
II/05

Figure 4.7 :

Spatial variations of nitrate (a) and ammonium (c) concentration, of autotrophic (b) and heterotrophic (d) biomass, and of remineralization rate (e) along the meridian 49° W in end December 1988. Average values over the depth of the upper homogeneous layer.

4.2.2. The episodic role of krill

In the previous section, overwintering krill has been suggested to play a significant role in phytoplankton bloom initiation by grazing on sea-ice algae when released in the water column. In its pelagic life, krill, which is an excellent swimmer covering large distances, clears water column by grazing on meso- and microorganisms and controls the overall structure of the planktonic food-web. Such a krill passage was observed in the marginal ice zone of the northwestern Weddell sea during spring 1988. Its impact on the structure and functioning of the microbial network was dramatic. Phytoplankton and protozooplankton biomass was reduced to insignificant value. Chlorophyll *a* concentrations in particular (Fig. 4.8) were reduced from 2.5 to 0.3 $\mu\text{g l}^{-1}$ within less than 10 hours and the phytoplankton species composition shifted from a diatom- to a nanoflagellate-dominated community (Jacques & Panouse, 1991). Bacterial activity, on the other hand, was significantly enhanced due the increase of dissolved organic matter released by krill feeding activity.

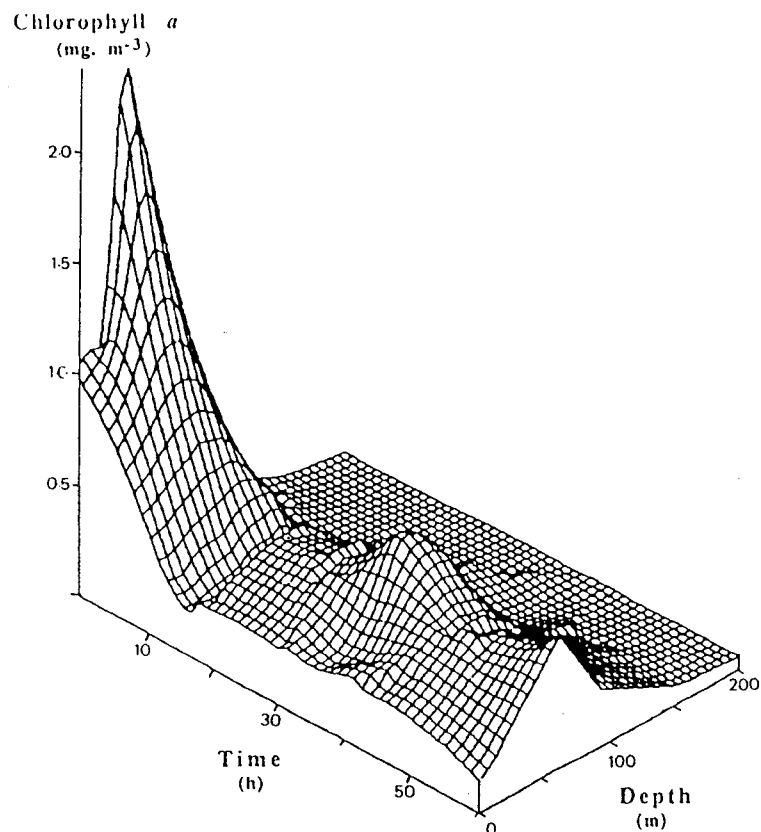


Figure 4.8 : Three-dimensional evolution of a diatom bloom at station 157 in the Weddell Sea (5th December 1988). The diatom bloom vanished in less than 10 h, probably grazed down by a krill swarm, and the phytoplankton community toppled towards a flagellate-dominated system (from Jacques & Panouse, 1991).

4.3. Food-web structure and krill distribution in the circumpolar marginal ice zone of the Southern Ocean : some scenarios

The comprehensive analysis of the structure and functioning of the food web at the receding ice-edge of the northwestern Weddell Sea outlines the key role played by krill in determining the local structure of the microbial network either as overwintering organism, by selectively eliminating micro-sized ice microorganisms released in the water column upon melting, and/or as mobile swarms in the free of ice areas by grazing on microorganisms and mesoplankton. Depending on the presence of active overwintering krill underneath the ice, the following microbial food web (Fig.4.9) are expected to prevail in the part of the Southern Ocean concerned by sea ice retreat :

In the absence of overwintering krill, sea ice diatoms and to a lesser extent *Phaeocystis* – the dominant component of sea ice biota (Horner, 1985; Mathot *et al.*, 1991) – seed surface waters at the time of ice melting. Fabulous ice-edge blooms dominated by large diatoms or *Phaeocystis* are therefore expected (Fig. 4.10a). Such blooms have been observed in the marginal ice zone of the Ross Sea, an area where krill density is more scarce (Marr, 1962), compared to the Weddell Sea.

In the presence of overwintering krill scraping on sea ice assemblages, sea ice diatom seeding is considerably reduced and ice-edge blooms are dominated by nanophytoplankton. At the same time, an efficient microbial network (Fig.4.10b) develops due to the concomitant development of protozoa probably originated from the sea ice biota (Garrison *et al.*, 1987; Mathot *et al.*, 1991). Resulting ice-edge blooms are relatively moderate.

Ice-free planktonic communities are regulated by episodic passage of krill swarms able to follow blooms spatially, thus grazing heavily on large diatoms, nanophytoplankton, protozoa and copepods (Fig.4.9). Resulting biomasses are very low, excepted bacteria (Fig.4.10b).

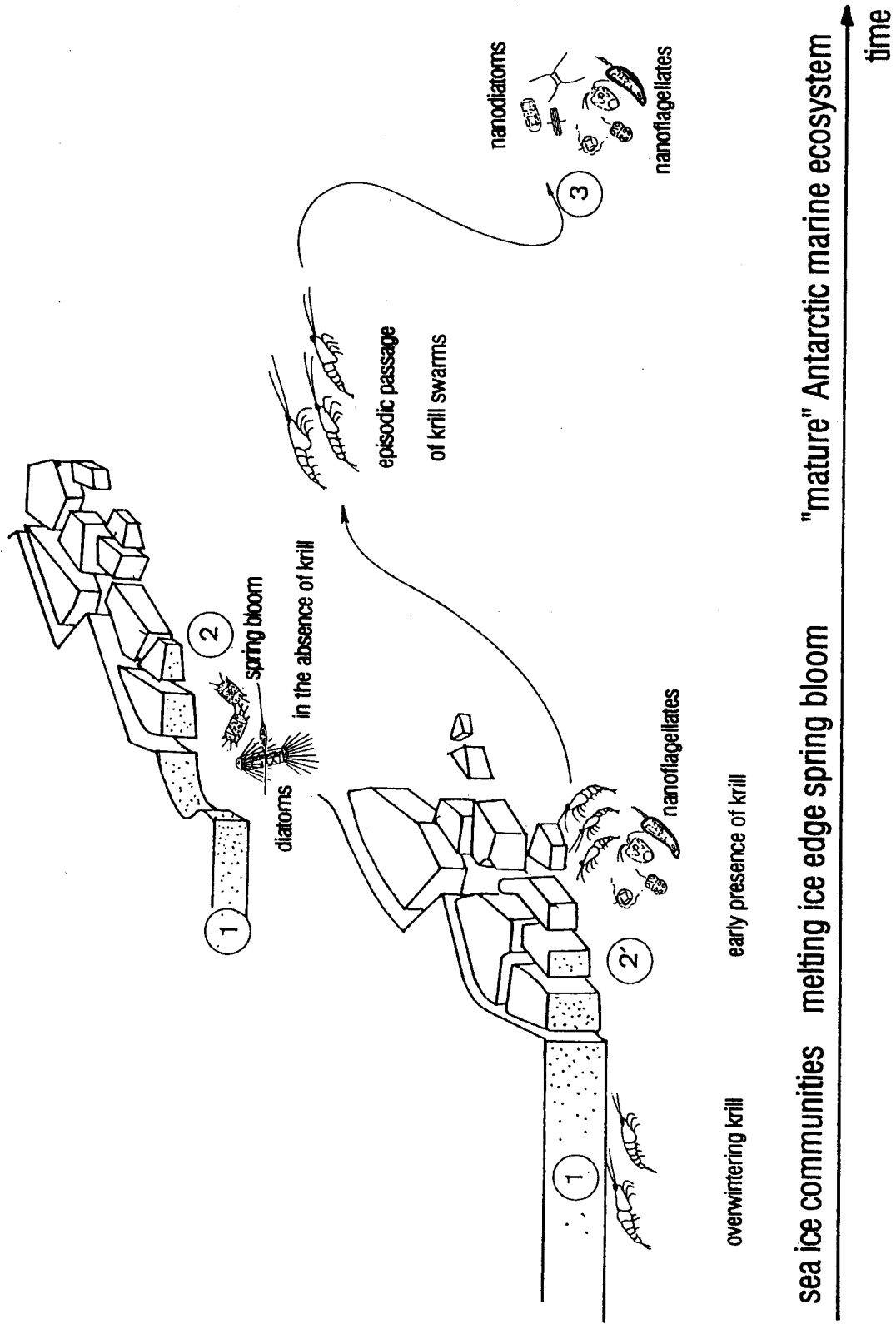
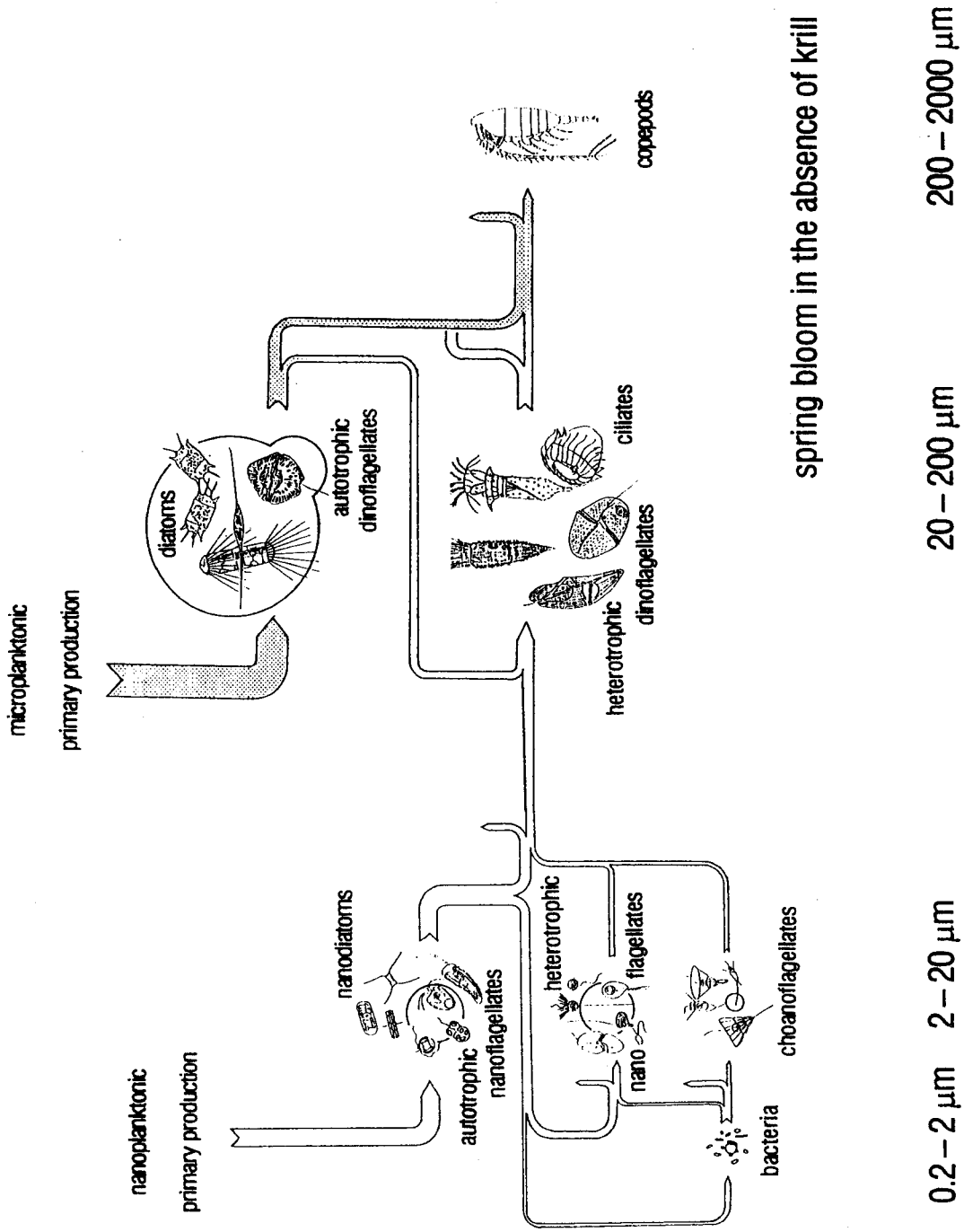


Figure 4.9 : Scenario relating spring and summer phytoplankton and the hypothetical annual cycle of krill suggested by Smetacek *et al.* (1990).

a.



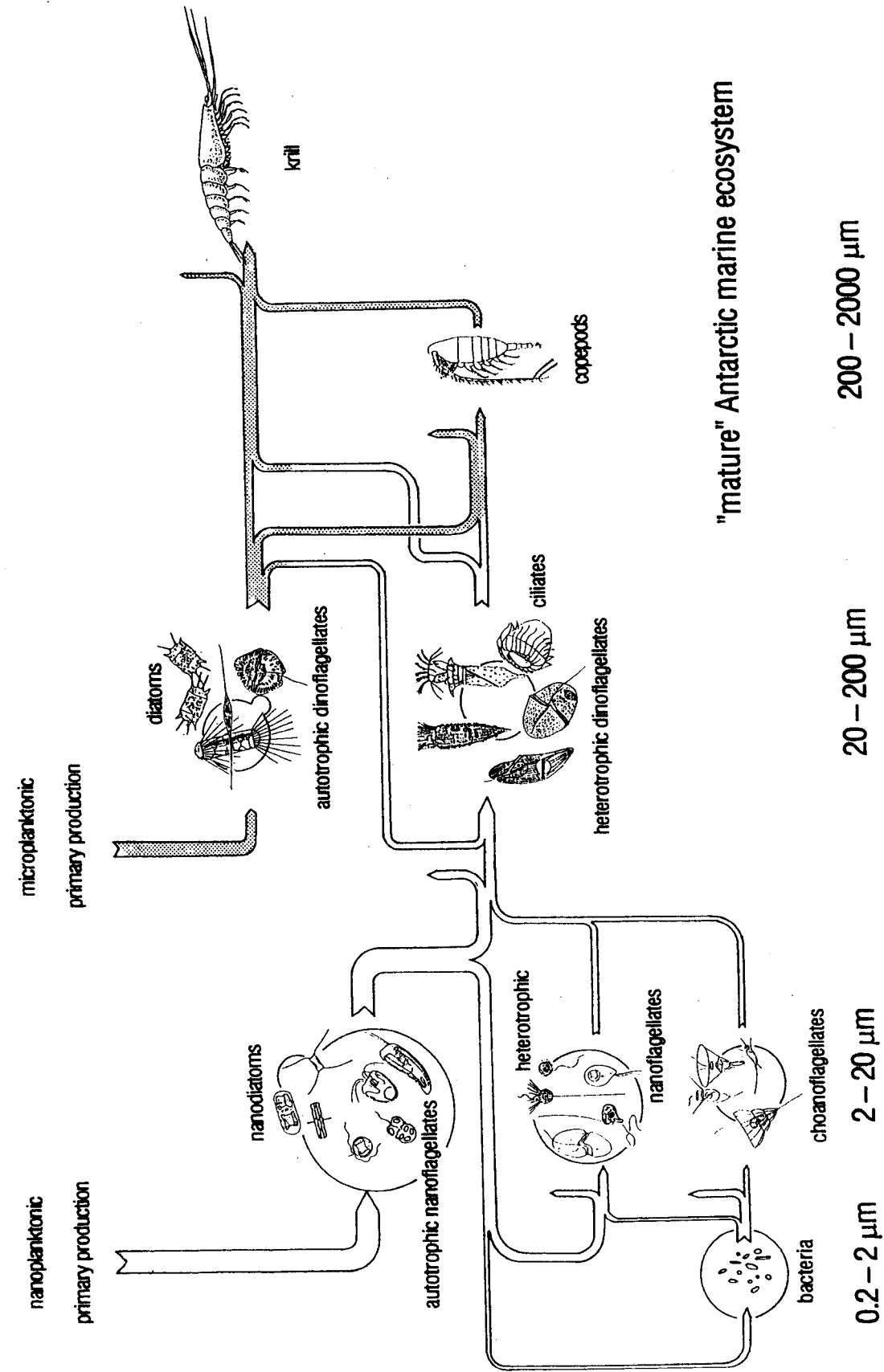


Figure 4.10 : Proposed structure of the Antarctic planktonic food web in the absence (a) and presence (b) of overwintering krill.



5. THE ECOLOGICAL MODEL : DESCRIPTION, FORMULATION AND PARAMETRIZATION

5.1. General structure of the ecological model

The general structure of the ecological model (Figure 5.1) has been established from the above analysis of the physical, chemical and biological events occurring in the marginal ice zone of the northwestern Weddell Sea at the time of ice melting. It is a two-layer 1D model composed of a well-mixed upper layer and a stratified deeper layer restricted to the euphotic depth (about 70 m in this area). No net horizontal advection is considered. This ecological model consists in a 1D hydrodynamical model calculating the thickness of the upper mixed layer from meteorological and ice cover observations coupled with a biological model composed of two submodules describing phytoplankton and microbial loop dynamics respectively. The model of phytoplankton growth calculates algal development using the output of the hydrodynamical model along with measured surface light as forcing variable, protozoan grazing as biological control and seeding as initial conditions. The model of microbial loop dynamics calculates bacterioplankton development using predicted temperature and dissolved organic matter calculated from predicted phytoplankton exudation and autolysis as forcing variables and grazing by small heteronano-flagellates as direct biological control. Both nitrate and ammonium are assimilated by phytoplankton whilst ammonium is occasionally taken up by bacteria according to the chemical composition of their substrates. Ammonium is regenerated through bacteria and bacterivorous and herbivorous protozoan activity. Losses by sedimentation calculated from sediment trap data (Cadée, pers. com.) are neglected due to their generally low value (0.005 to 0.03 d^{-1}) compared to grazing ($0.01 - 0.3 \text{ d}^{-1}$). Also trace elements, being not considered as limiting factor of phytoplankton development in this part of the circumpolar marginal ice zone (de Baar *et al.*, 1990; Buma *et al.*, 1991), are ignored by the model.

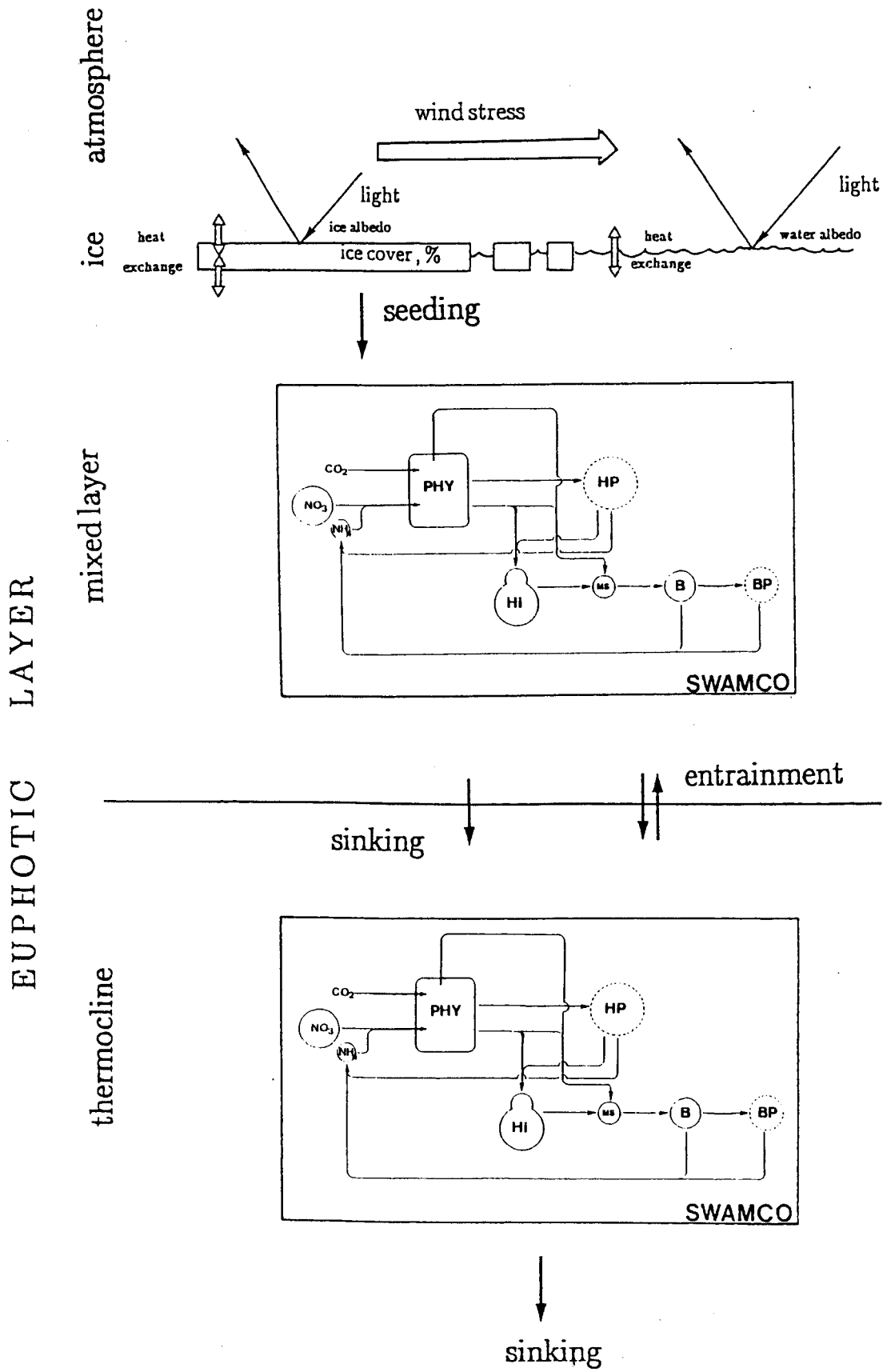


Figure 5.1 : Diagrammatic representation of the coupled hydrodynamical-biological model.

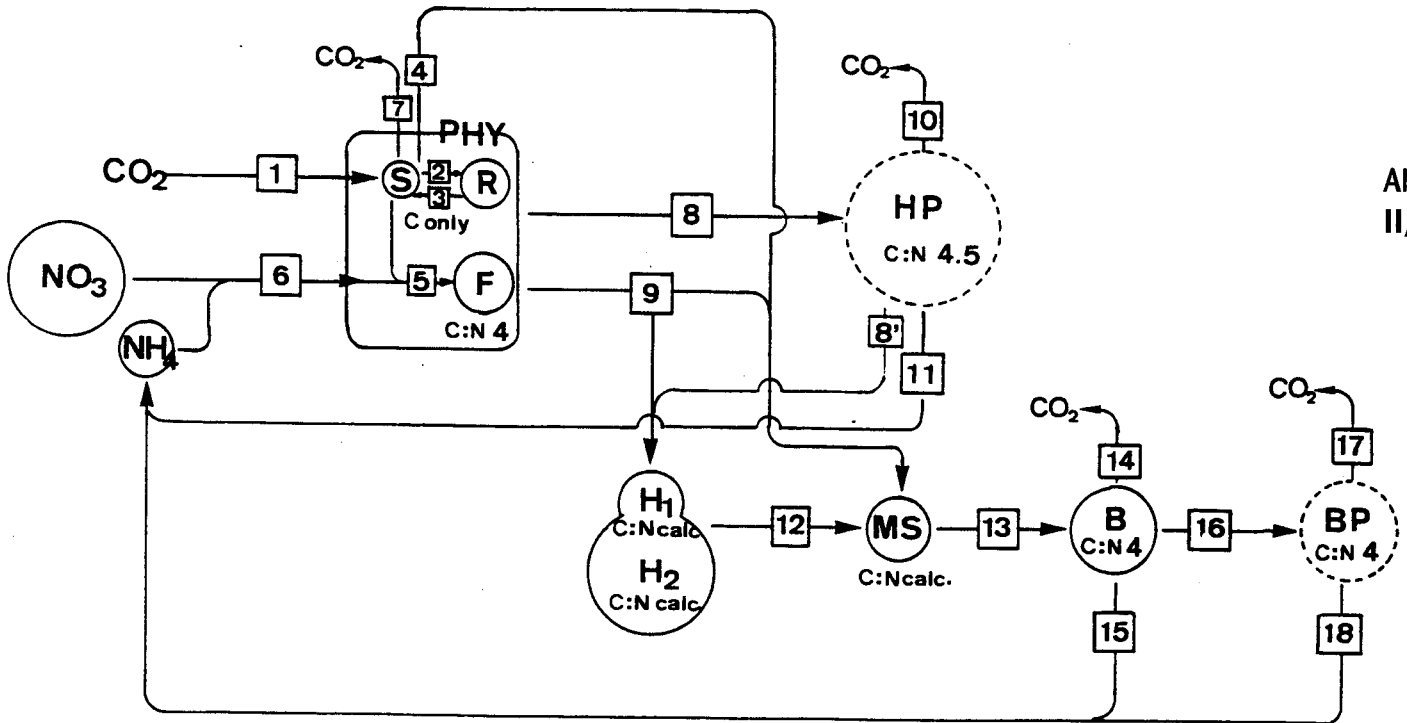


Figure 5.2 : Structure of the biological model SWAMCO. PHY = phytoplankton; HP = herbivorous protozoa; BP = bacterivorous protozoa.

State variables :

- NO₃ Nitrate ($\mu\text{gN l}^{-1}$)
 NH₄ Ammonium ($\mu\text{gN l}^{-1}$)
 F Functional cellular constituents of phytoplankton ($\mu\text{gC l}^{-1}$);
 invariant nitrogen:carbon (w:w) ratio $\text{NCF} = 0.28$
 R Cellular reserves of phytoplankton ($\mu\text{gC l}^{-1}$)
 S Small metabolites pool of phytoplankton ($\mu\text{gC l}^{-1}$)
 MS Dissolved organic matter of low molecular weight ($\mu\text{gC l}^{-1}$);
 variable nitrogen : carbon ratio
 H₁ Dissolved organic matter of high molecular weight with high biodegradability
 affinity ($\mu\text{gC l}^{-1}$); variable nitrogen : carbon ratio
 H₂ Dissolved organic matter of high molecular weight with low biodegradability
 affinity ($\mu\text{gC l}^{-1}$); variable nitrogen : carbon ration
 B Bacteria ($\mu\text{gC l}^{-1}$) invariant nitrogen : carbon (w:w) ratio $\text{NCB} = 0.25$

Processes :

- | | | | |
|----|-----------------------------------|----|--|
| 1 | Phytopl. photosynthesis | 10 | Herbivorous protozoa (HP) respiration |
| 2 | Phytopl. reserve synthesis | 11 | Ammonium regeneration by HP |
| 3 | Phytopl. reserve catabolism | 12 | Exoenzymatic hydrolysis of H ₁ , H ₂ |
| 4 | Phytoplankton exudation | 13 | Uptake of monomeric substrates by bacteria |
| 5 | Phytoplankton growth | 14 | Bacteria respiration |
| 6 | Inorganic nitrogen uptake | 15 | Ammonium regeneration by bacteria |
| 7 | Phytoplankton respiration | 16 | Bacterivorous protozoa (BP) grazing |
| 8 | Herbivorous protozoa (HP) grazing | 17 | Bacterivorous protozoa (BP) respiration |
| 8' | Sloppy feeding | 18 | Ammonium regeneration by BP |
| 9 | Phytoplankton autolysis | | |

The chemical and biological state variables of the model and the associated biological processes are described on Fig. 5.2. The differential equations describing changes in the main state variables of the model as the result of biological activity are gathered in table 5.1.

Table 5.1 : Differential equations of the biological model (without considering its coupling with the physical model).

Phytoplankton :

$$\begin{aligned} \frac{dF}{dt} &= \text{synthesis} - \text{grazing} - \text{autolysis} \\ \frac{dR}{dt} &= \text{synthesis} - \text{catabolism} - \text{grazing} - \text{autolysis} \\ \frac{dS}{dt} &= \text{synthesis} - \text{R\&F synthesis} + \text{R catabolism} - \text{exudation} - \text{respiration} - \\ &\quad \text{grazing} - \text{autolysis.} \end{aligned}$$

Microbial loop :

$$\begin{aligned} \frac{dH_{1,2}}{dt} &= \text{R\&F autolysis} - H_{1,2} \text{ exoenzymatic hydrolysis} \\ \frac{dMS}{dt} &= H_{1,2} \text{ exoenzymatic hydrolysis} - \text{bacteria uptake} + \text{phytoplankton} \\ &\quad \text{exudation} + \text{sloppy feeding} \\ \frac{dB}{dt} &= \text{growth} - \text{mortality} \end{aligned}$$

Inorganic nitrogen loop :

$$\begin{aligned} \frac{dNO_3}{dt} &= - \text{phytoplankton uptake} \\ \frac{dNH_4}{dt} &= - \text{phytoplankton uptake} - \text{bacteria uptake} + \text{bacteria regeneration} + \\ &\quad \text{herbivorous protozoa regeneration} + \text{bactivorous protozoa regeneration} \end{aligned}$$

5.2. The physical model

The model consists of a 1D turbulent hydrodynamical model that calculates the thickness of the wind mixed layer from the balance between the kinetic turbulent energy induced by the wind and the buoyancy input by surface heating and ice melting from the top and entrainment of heavy water from below. This model is an adaptation to polar waters of the 1D mixed-layer model developed by Denman (1973) for the open area and extended by van Aken (1984) with terms describing salt fluxes. The principal attributes and the mathematical formulation have been described in details in Veth (1991).

5.3. The phytoplankton model

Concept: The model of phytoplankton development (AQUAPHY model) considers one single phytoplankton taxonomic group characterized by three state variables : the functional and structural cellular components **F**, the internal reserves **R** and the monomers **S**. This model, based on the concept of energy storage theory developed by Cohen & Parnas (1976), was established in order to take into account the interaction between phytoplankton physiology and the turbulent structure of its habitat. It differs from most primary production models in that it explicitly distinguishes the photosynthetic process (*gross primary production*) – directly dependent on irradiance – from the process of phytoplankton growth (*net primary production*) – dependent on both ambient nutrient and energy availability related to the intracellular pool of storage products **R**. Cellular autolysis and protozoa grazing are the two phytoplankton mortality processes considered by the submodel.

Mathematical formulation: The following equations (see Fig. 5.2 and table 5.2 for symbols and units) are used for describing phytoplankton development :

$$\frac{dF}{dt} = sF - lF - gF \quad (1)$$

$$\frac{dS}{dt} = p - sR + cR - sF - e - r - lS - gS \quad (2)$$

$$\frac{dR}{dt} = sR - cR - lR - gR \quad (3)$$

In these equations :

- . The rate of phytoplankton growth sF is assumed to depend – when non limited by inorganic nutrients – on the internal pool of monomeric carbon precursors S following a Michaelis–Menten kinetics characterized by the constants μF_{\max} and K_S :

$$sF = \mu F_{\max} \frac{S}{S + K_S} F \quad (4)$$

- . The photosynthetic process p depends on irradiance I following a relationship described by Platt *et al.* (1980); it is characterized by three parameters normalized to biomass, the maximal photosynthetic capacity k_{\max} , the photosynthetic efficiency α and a description of the photoinhibition β :

$$p = k_{\max} [1 - \exp(-\alpha I / k_{\max})] \exp(-\beta I / k_{\max}) F \quad (5)$$

- . The synthesis of storage products sR is governed by the size of S following a Michaelis–Menten kinetic characterized by the constants ρ_{\max} and K_S :

$$sR = \rho_{\max} \frac{S'}{K_S + S'} F \quad (6)$$

where $S' = \frac{S}{F} - Q_S$

Q_S being the monomers cellular quotat.

- . The catabolism cR of storage products R is postulated to obey a first order kinetic characterized by the constant k_R :

$$cR = k_R R \quad (7)$$

- . The metabolic costs, in terms of a demand for ATP and reductors, are primarily met by cellular respiration r . This process is expressed by the sum of three terms, associated with maintenance processes, synthesis of new cellular material and motility respectively (Shuter, 1979) :

$$r = k_{1F} F + \xi sF + k_{2F} F \quad (8)$$

where k_{1F} and k_{2F} are first order constant and ξ a dimensionless constant assumed to vary according to the inorganic nitrogen source.

. The exudation process e , the rate of cell autolysis l and the phytoplankton mortality by herbivorous protozoan grazing g are described by first order kinetics :

$$e = \epsilon S \quad (9)$$

$$lR = k_L R; lS = k_L S; lF = k_L F \quad (10)$$

$$gR = k_G R; gS = k_G S; gF = k_G F \quad (11)$$

ANTAR
II/05

in which ϵ , k_L and k_G are first order constants.

Parameters : The physiological parameters of phytoplankton photosynthesis and growth have been determined by mathematical fitting of the experimental data relative to the photosynthesis versus light curve and light-dark kinetics measurement using the above equations. One example is given by Fig. 5.3.

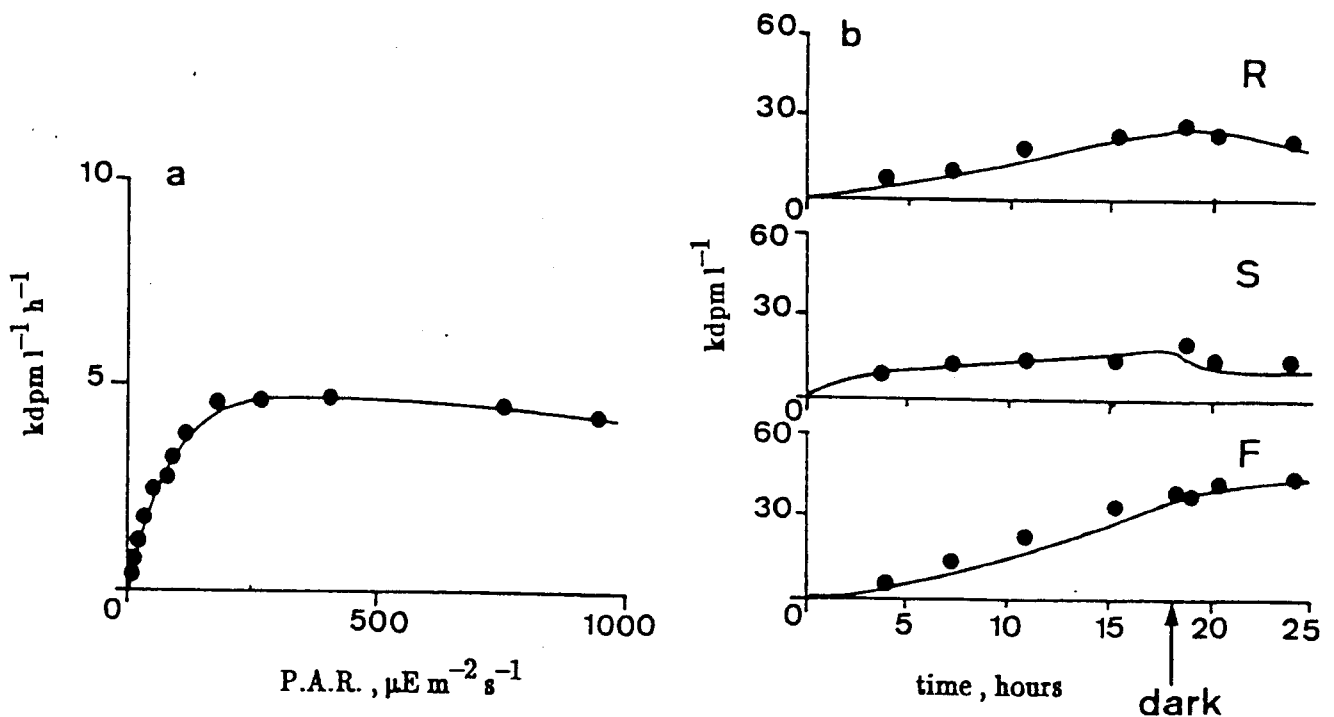


Figure 5.3 : Typical photosynthesis-light (a) and light-dark kinetics of ¹⁴C assimilation into cellular constituents (b) of ice-edge phytoplankton communities of the northern Weddell Sea. Station 169, 61°30'S - 47°W.

Values were normalized to functional biomass considering a carbon/chlorophyll *a* ratio of 25 as characteristic of the *in situ* phytoplankton communities. Maximal photosynthetic capacity k_{\max} (Fig. 5.5a), maximum specific growth rate $\mu_{F_{\max}}$ (Fig. 5.5b) and the light adaptation parameter I_k (Fig. 5.4), derived from Platt *et al.*'s equation vary within the range of those reported for antarctic phytoplankton (Tilzer *et al.*, 1986; Tilzer & Dubinsky, 1987). Our data combined with those similarly measured in the Prydz Bay area (Lancelot *et al.*, 1989) indicate however that the physiological parameters vary independently of temperature and available light (Fig. 5.4 and 5.5), suggesting that the dominant phytoplankton communities which succeed each other are the best adapted at each time to the environmental conditions. This long-term adaptation must be distinguished from the short-term dependence of photosynthetic activity on light and temperature described by Tilzer & Dubinsky (1987) which concerns only one single population at a given time. On basis of this, constant average values of physiological parameters (Table 5.2), characteristic of phytoplankton cells growing in the marginal ice zone of the Weddell Sea during spring 1988 have been chosen.

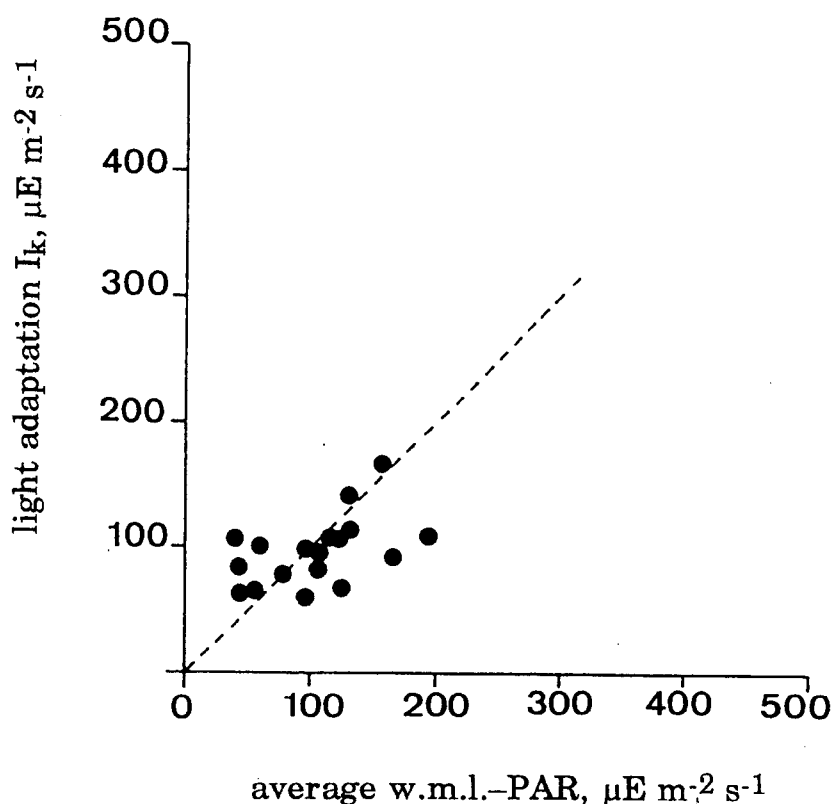


Figure 5.4 : Relationship between phytoplankton light adaptation I_k and average PAR in the upper mixed layer (dashed line shows 1/1 relationship).

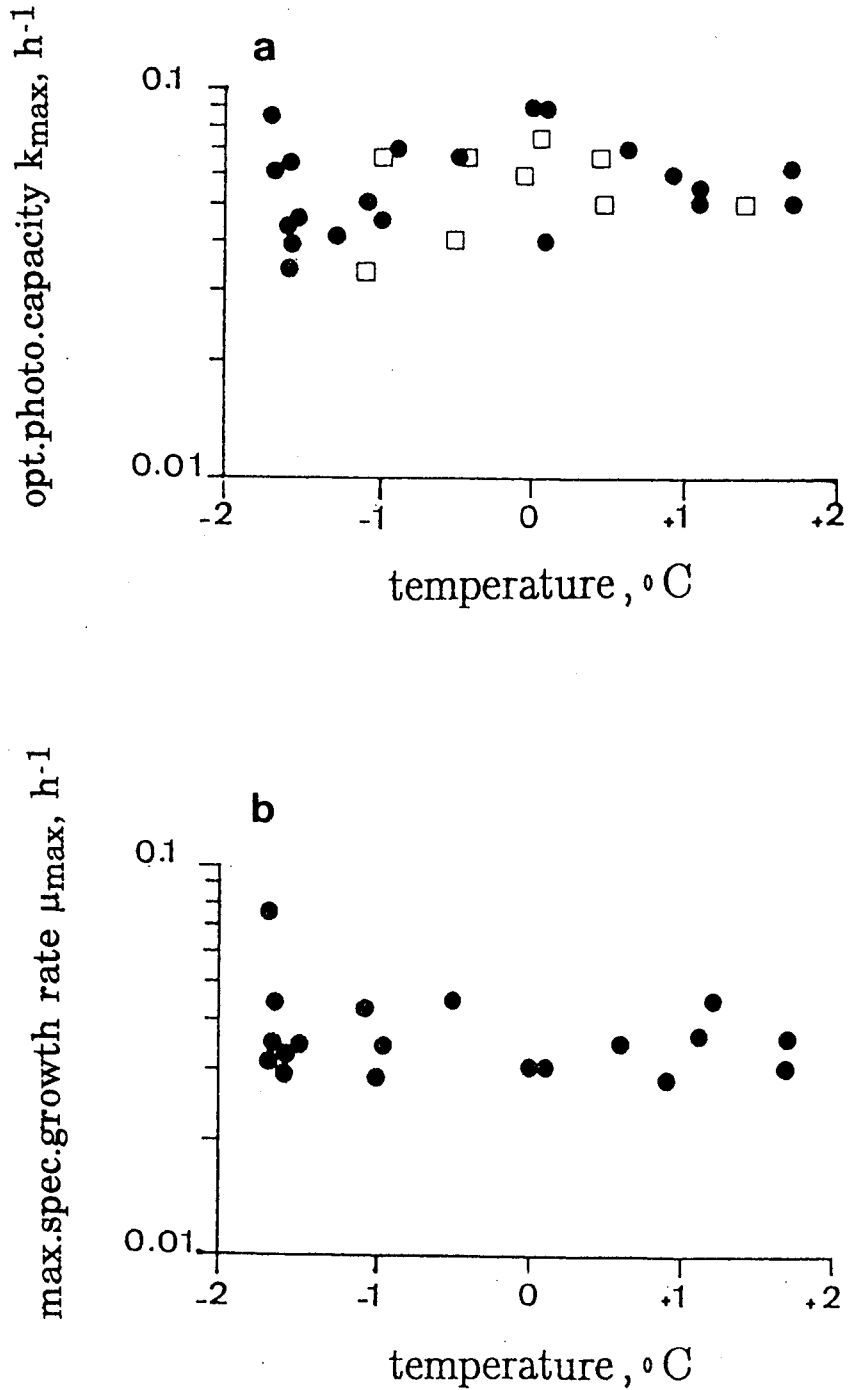
ANTAR
II/05

Figure 5.5 : Relationship between maximal photosynthetic capacity k_{max} (a) and maximum specific growth rate $\mu_{F_{max}}$ (b) and ambient temperature. (●): EPOS data; (□): Prydz Bay data (Lancelot *et al.*, 1989).

Phytoplankton cellular autolysis was assumed to be constant and proceeds at a rate of 0.002 h^{-1} according to Billen & Becquevort (1991). Herbivorous protozoan grazing has been considered as temperature dependent : the empirical linear regression relating specific grazing by herbivorous protozoa, as calculated from cell counts, to ambient temperature T is illustrated by Fig. 5.6. Its mathematical expression is the following :

$$kg = 0.004 T + 0.0075$$

For positive temperature however a constant rate of 0.01 h^{-1} was assumed.

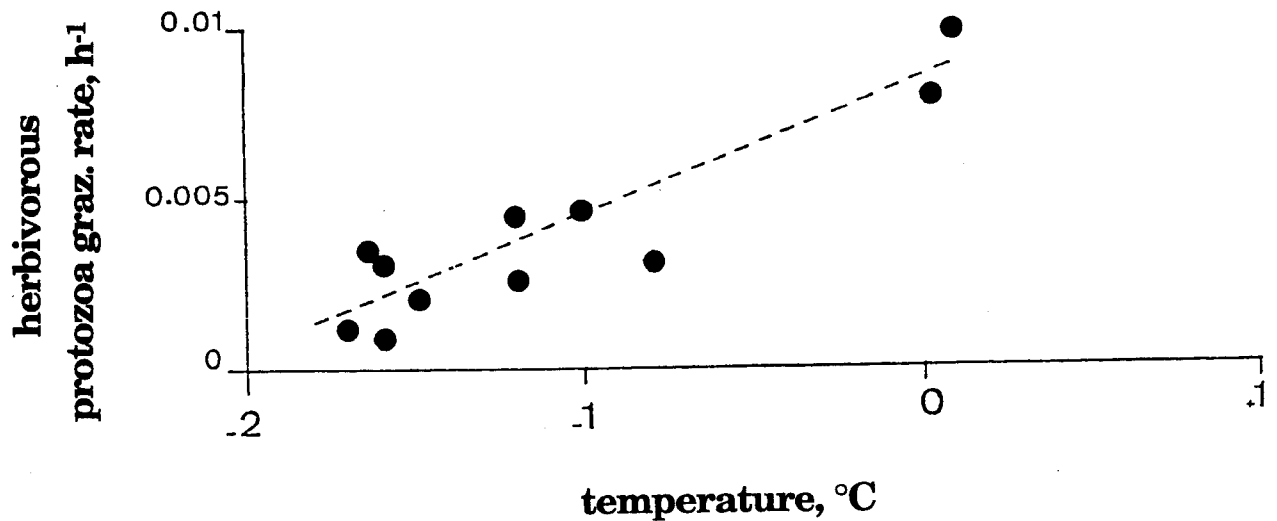


Figure 5.6 : Relationship between specific grazing rate of herbivorous protozoa on phytoplankton kg and ambient temperature.

5.4. The microbial loop model

Concept: The model of microbial loop dynamics (HSB model, Billen & Servais, 1989) considers one single bacterioplankton group B (including both free-living and attached bacteria on particles and aggregates) and 3 pools of dissolved organic substrates (monomers MS, rapidly biodegradable polymers H₁ and slowly biodegradable polymers H₂) for bacterioplankton development. Basically, bacterial growth is directly dependent on the concentration of monomeric substrates whilst most of the dissolved organic matter is in the form of macromolecules requiring extracellular hydrolysis. The model thus implies that the latter process is the limiting step of the whole process of organic matter degradation and bacterial growth (for experimental evidence, see Billen, 1991). The overall process of bacterioplankton mortality results from autolysis and grazing pressure by bacterivorous protozoa.

Mathematical formulation: The following set of equations (see table 5.2 for symbols and units) are used for describing microbial loop dynamics :

$$\frac{dH_1}{dt} = -eH_1 + Q(1R + 1F + slpR + slpF) \quad (12)$$

$$\frac{dH_2}{dt} = -eH_2 + (1 - Q)(1R + 1F + slpR + slpF) \quad (13)$$

$$\frac{dMS}{dt} = eH_1 + eH_2 - uptMS + \varepsilon S \quad (14)$$

$$\frac{dB}{dt} = Y_B uptMS - mB \quad (15)$$

In these equations :

- The extracellular hydrolysis eH_1 and eH_2 of biopolymers H₁ and H₂ – proportional to bacterial biomass B (Fontigny *et al.*, 1987) – obeys a Michaelis–Menten kinetics (Somville & Billen, 1983; Somville, 1984) characterized by specific parameters – $e_{i,max}$, K_{H_i} ($i = 1, 2$) – owing to the different susceptibilities to extracellular hydrolysis of H₁ and H₂ :

$$eH_i = e_{i,max} \frac{H_i}{K_{H_i} + H_i} B \quad (16)$$

Where $i = 1, 2$.

- Q is the part allocated to H₁ of macromolecules produced by phytoplankton autolysis and by sloppy feeding of herbivorous protozoa.

- . The sloppy feeding slP is assumed to represent a constant fraction J of herbivorous protozoa grazing.
- . The uptake of direct substrates $uptSM$ is assumed to obey an overall Michaelis-Menten kinetics (Parsons & Strickland, 1962; Wright & Hobbie, 1965) :

$$uptMS = b_{max} \frac{MS}{KMS + MS} B \quad (17)$$

where b_{max} and KMS are the maximum rate and half-saturation constant of substrate uptake by bacteria.

- . A constant fraction YB of the amount of substrates taken up is used for biomass production, the remaining part being respired (Servais, 1986).
- . The process of bacterial mortality mB is represented, as a first approximation, by a first order kinetics, characterized by the constant kBM :

$$mB = kBM B \quad (18)$$

Parameters : Most of the parameters involved in these equations have been determined from experiments conducted in the Weddell Sea (this study) and Prydz Bay area (Billen & Becquevort, 1991) :

- . The maximum uptake rate of MS by bacteria b_{max} is calculated as $\mu B_{max}/YB$. The maximum specific growth rate of bacteria μB_{max} (Fig. 5.7) clearly indicates suboptimal bacterial growth at temperature characteristic of the Southern Ocean (-2 to +2°C). Interestingly, this physiological response of bacteria to cold temperature strongly contrasts with phytoplankton cells that exhibit similar maximum specific growth rate in the Southern Ocean as in lower latitudes. The temperature dependency of μB_{max} (Fig. 5.7) is described by the following sigmoid relationship :

$$\mu B_{max} = \mu' B_{max} (T_{opt}) \left[0.1 + 0.9 \exp \left(- \left(\frac{T_{opt} - T}{dt} \right)^2 \right) \right]$$

with $\mu' B_{max}$ = μB_{max} value at optimal temperature (h^{-1}) i.e. $0.18 h^{-1}$
 T = ambient temperature ($^{\circ}C$)
 T_{opt} = optimal temperature ($^{\circ}C$) i.e. $18^{\circ}C$
 dt = sigmoid width ($^{\circ}C$) i.e. $7^{\circ}C$

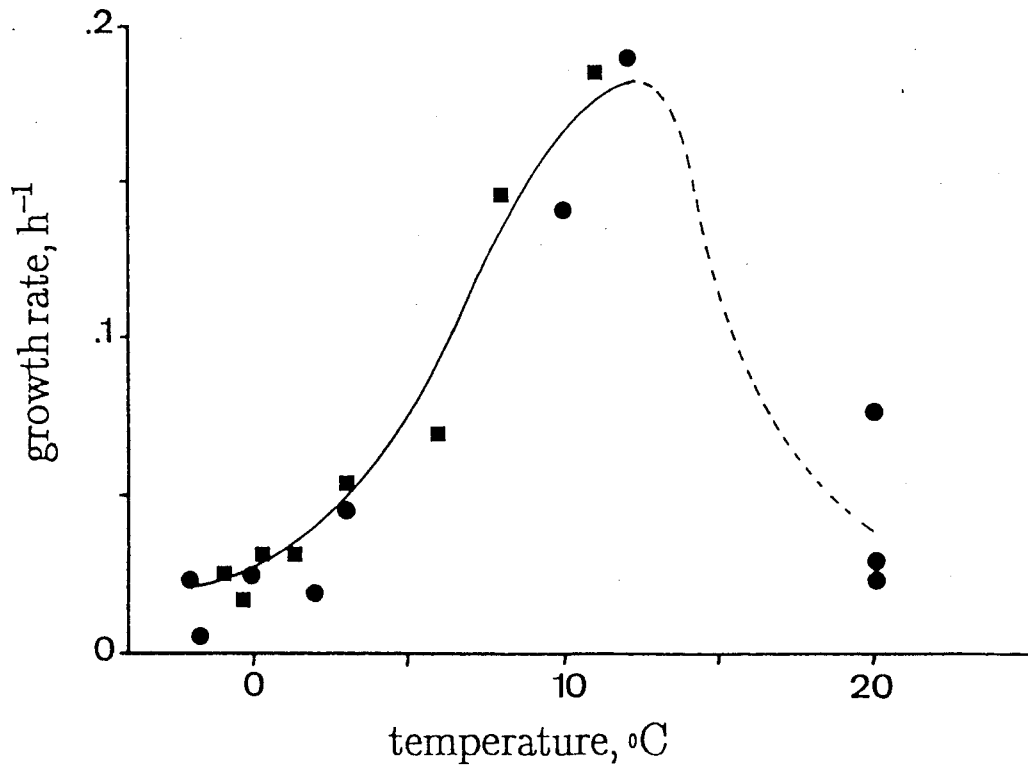


Figure 5.7 : Relationship between the maximum specific growth rate of bacteria $\mu_{B_{max}}$ and ambient temperature in the Weddell Sea (-) and in the Prydz Bay (●).

- . The value of Y_B , in the absence of nutrient limitation, is generally close to 0.3 (Servais *et al.*, 1987). K_{MS} is taken arbitrarily as 0.01 mgC.l^{-1} , as this parameter does not significantly influence the results of the calculations.
- . The parameters characterizing the rate of exoenzymatic hydrolysis of macromolecules from phytoplanktonic origin have been estimated on the basis of experiments in which the kinetics of bacterial degradation of a sonicated and filtered algal culture is measured after inoculation with a natural assemblage of bacteria (Servais, 1986; Billen, 1991). The same dependence to temperature (T) as described above for $\mu_{B_{max}}$ has been considered for $e_{1_{max}}$ and $e_{2_{max}}$.

$$e'_{1_{max}} = 0.75 \text{ h}^{-1}, \quad K_{H1} = 0.1 \text{ mgC.l}^{-1}$$

$$e'_{2_{max}} = 0.25 \text{ h}^{-1}, \quad K_{H2} = 2.5 \text{ mgC.l}^{-1}$$

- Measured rates of total bacterial mortality k_{BM} at *in situ* temperature vary between 0.002 and 0.005 h^{-1} (Fig. 5.8) with grazing by bacterivorous protozoa (size less than 7 μm) contributing for 22 to 100 % (Becquevort *et al.*, 1992). The following empirical linear regression relating specific mortality rate of bacteria to temperature T (Fig. 5.8) has been observed :

$$k_{BM} = 0.0005 T + 0.004$$

- The rate of H_i production through phytoplankton autolysis or protozoan sloppy feeding are the only adjustable parameters of the model. The former process was estimated to proceed at a rate of 0.002 h^{-1} whilst sloppy feeding by herbivorous protozoa was assumed to represent 10 % of the temperature-dependent grazing of herbivorous protozoa (Fig. 5.6). The model assumes in addition that the biopolymers of two classes of biodegradability (H_1 , H_2) are produced in a ratio 1:1 i.e., $Q = 0.5$.

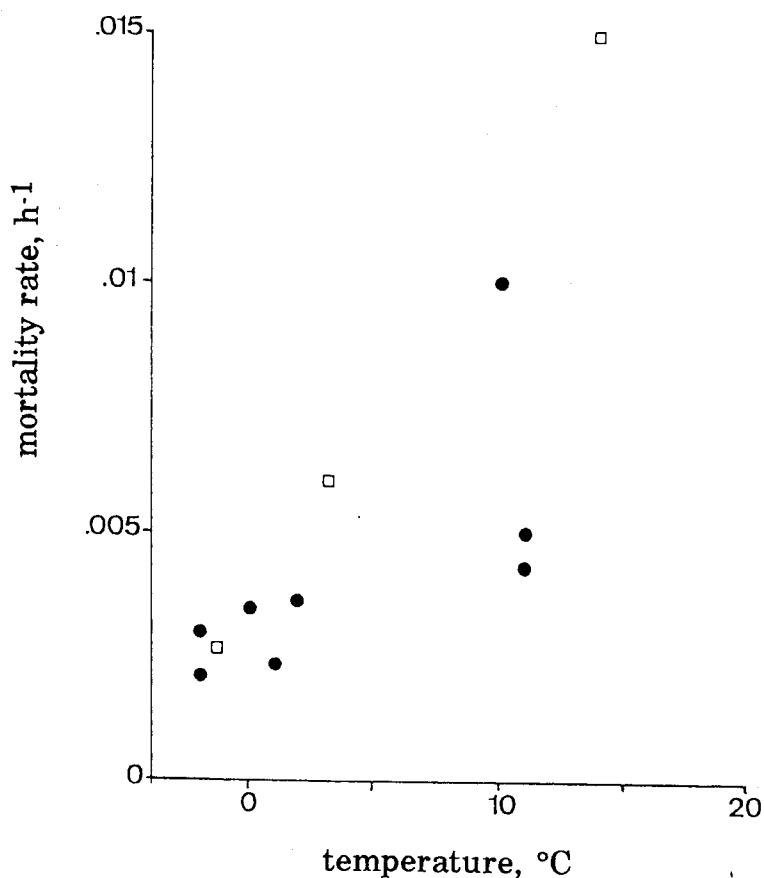


Figure 5.8 : Relationship between the specific mortality rate of bacteria and ambient temperature for natural assemblages. Weddell Sea (●) and Prydz Bay (□).

5.5. The inorganic nitrogen loop

Assumptions : Nitrate and ammonium are the inorganic nutrients considered by the model. Both nutrients, but ammonium preferably, are taken up by phytoplanktonic cells and assimilated into the functional constituents F (other phytoplankton constituents R and S are composed of carbon solely). Ammonium can be occasionally taken up by bacteria according to the nitrogen:carbon ratio of their substrate. Remineralized ammonium is released by bacteria, and bacterivorous and herbivorous protozoa as product of their metabolism. The quantitative importance of this regenerating processes is determined by the theoretical nitrogen:carbon ratio of these microorganisms in comparison with the nitrogen:carbon ratio of their respective substrate or food. Nitrification (biological oxidation of ammonium in nitrate), due to the lack of informations on the importance of this microbial process in the Southern Ocean, is neglected.

Mathematical formulation : On this basis, the following equations are used to describe the inorganic nitrogen loop :

$$\frac{dNO_3}{dt} = (-sF NCF) (1 - f_{NH_4}) \quad (19)$$

$$\frac{dNH_4}{dt} = (-sF NCF) f_{NH_4} + \text{uptMS} (NCMS - Y_B NCB) \quad (20)$$

$$+ mB (NCB - Y_{BP} NCBP) + (1 - J) gF (NCF - Y_{HP} NCHP)$$

In these equations :

- . NCF , $NCMS$, NCB , $NCBP$, $NCHP$ are the nitrogen:carbon (w:w) ratios of phytoplankton functional macromolecules, monomeric substrates, bacteria, bacterivorous and herbivorous protozoa respectively.
- . f_{NH_4} is the ratio of phytoplankton ammonium uptake to total inorganic nitrogen uptake.
- . Y_B , Y_{HP} , Y_{BP} are the growth efficiencies of bacteria, bacterivorous and herbivorous protozoa respectively.

Parameters : All parameters, except the nitrogen:carbon ratio of microorganisms for which theoretical values were chosen, have been determined experimentally :

- . Allocation of nitrogen uptake between NO_3 and NH_4 is calculated at any time by the model according to the empirical relationship relating the f_{NH_4} ratio to the relative ambient ammonium concentration (Fig. 5.9). This relationship has been established

from $^{15}\text{NO}_3$ and $^{15}\text{NH}_4$ uptake data performed during the EPOS expedition (Goeyens *et al.*, 1991a,b) and is mathematically described as follows :

$$f_{\text{NH}_4} = \gamma \frac{\text{NH}_4}{\text{N}_{\text{tot}}} + (1 - \gamma) \frac{\text{NH}_4}{\text{N}_{\text{tot}}}^{\delta}$$

with $\gamma = -0.21$; $\delta = 0.24$

- . Invariable NCF , NCB, NCBP, NCHP ratios of respectively 0.28, 0.25, 0.22 and 0.22 are considered whilst NCMS is calculated at any time by the model.
- . The value of 0.38 was estimated for protozoa growth efficiency YBP , YMP on the basis of microcosm experiments conducted under controlled conditions (Björnsen & Kuparinen, 1991).

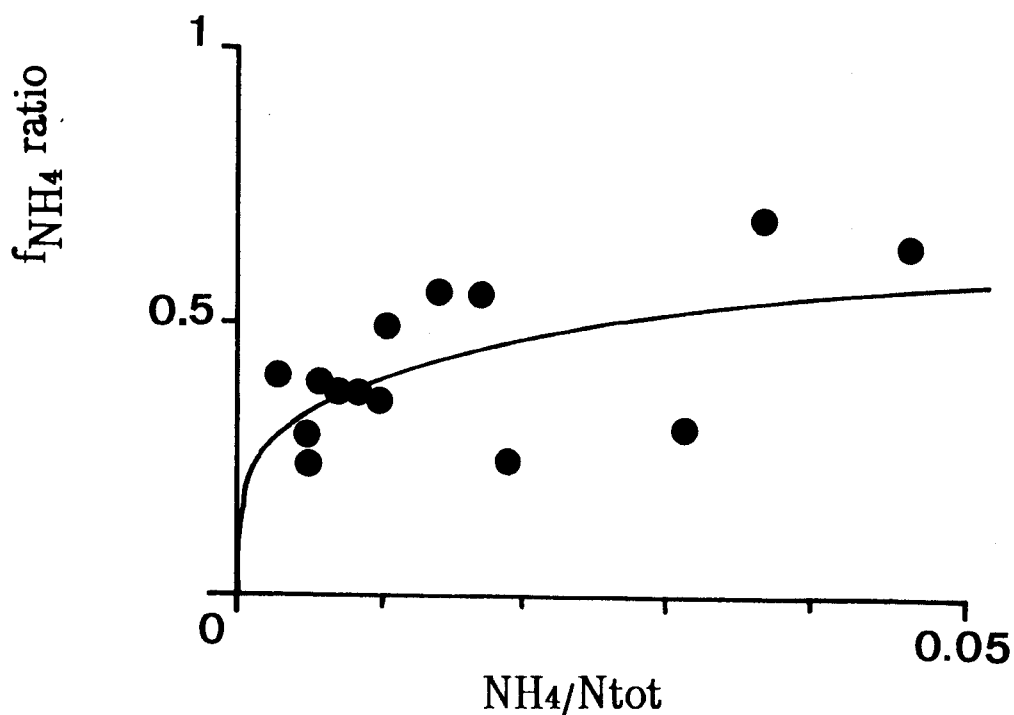


Figure 5.9 : Relationship between relative ammonium uptake by phytoplankton and relative ambient ammonium concentration.

Table 5.II : Physiological parameters characterizing ice-edge microbial communities.
(part 1)

| Parameters | | Units | ANTAR II/05 |
|---|---------|---|----------------|
| Phytoplankton : | | | |
| Photosynthetic efficiency (α) | 0.00065 | $\text{h}^{-1} (\mu\text{E m}^{-2} \text{sec}^{-1})^{-1}$ | |
| Optimal specific rate of photosynthesis (k_{max}) | 0.06 | h^{-1} | |
| Index of photoinhibition (β) | 0 | $\text{h}^{-1} (\mu\text{E m}^{-2} \text{sec}^{-1})^{-1}$ | |
| Maximal specific rate of R synthesis (ρ_{max}) | 0.06 | h^{-1} | |
| Constant of R catabolism (k_{R}) | 0.06 | h^{-1} | |
| Maximal specific rate of F synthesis (μ_{Fmax}) | 0.035 | h^{-1} | |
| Half-saturation constant of S assimilation (K_{S}) | 0.07 | dimensionless | |
| Cst of maintenance of basal metabolism ($k_{1\text{F}}$) | 0.0005 | h^{-1} | |
| Energetic costs for F synthesis (ξ) : | | | |
| ammonium source : | 0.32 | dimensionless | |
| nitrate source : | 0.70 | dimensionless | |
| Constant of motility ($k_{2\text{F}}$) | 0.0006 | h^{-1} | |
| Constant of exudation (ϵ) | 0.005 | h^{-1} | |
| Constant of cell autolysis (k_{L}) | 0.002 | h^{-1} | |
| Herbivorous protozoa : | | | |
| Constant of grazing (k_{G}) | | | |
| temperature (T) dependent : $k_{\text{G}} = 0.0086 + 0.004 T$ | | h^{-1} | |
| Growth efficiency (Y_{HP}) | 0.38 | dimensionless | |
| Constant of sloppy feeding (J) | 0.10 | dimensionless | |

Table 5.II : Physiological parameters characterizing ice-edge microbial communities.
(part 2)

| Parameters | | Units |
|--|------|---------------|
| Microbial loop : | | |
| Maximal specific growth rate of bacteria at optimal temperature ($\mu_{B_{max}}$) | 0.18 | h^{-1} |
| Half-saturation constant of MS uptake (K_{MS}) | 0.01 | $mgC\ l^{-1}$ |
| Maximal specific rate of H_1 hydrolyse $e_{1_{max}}$ at optimal temperature ($e_{1'_{max}}$) | 0.75 | h^{-1} |
| Half-saturation constant of H_1 hydrolysis (K_{H_1}) | 0.1 | $mgC\ l^{-1}$ |
| Maximal specific rate of H_2 hydrolysis $e_{2_{max}}$ at optimal temperature ($e_{2'_{max}}$) | 0.25 | h^{-1} |
| Half-saturation constant of H_2 hydrolysis (K_{H_2}) | 2.5 | $mgC\ l^{-1}$ |
| Constant of bacterial mortality (k_{BM}) temperature dependent : $k_{BM} = 0.0005 T + 0.0004$ | | h^{-1} |
| Growth efficiency of bacteria (Y_B) | 0.3 | dimensionless |
| Growth efficiency of bacterivorous protozoa (Y_{BP}) | 0.38 | dimensionless |

6. MODEL RESULTS

6.1. Validation : the particular case of the northwestern Weddell Sea

ANTAR
II/05

6.1.1. Calculation

The ecological model described in the previous section was run for latitudes 57°S to 62°S at meridian 49°W to simulate spring variations of inorganic nitrogen (nitrate and ammonium), phytoplankton, dissolved organic carbon and nitrogen (monomeric and polymeric) and bacteria concentrations in the marginal ice zone of the Scotia/Weddell Sea area during sea ice retreat 1988. The simulated period covered the EPOS expedition legs 1 & 2.

Local meteorological conditions (wind speed and solar radiation; Fig. 6.1), recorded incident P.A.R. and ice cover observations (van Franeker, 1989) are the forcing variables of the coupled physical-biological model. Initial values of the state variables (Table 6.I) are the concentrations measured at the very beginning of the cruise, i.e. when the ice melting process has not yet started. For phytoplankton, an initial Chl *a* concentration of 0.12 µg l⁻¹ was considered, corresponding to the addition of a seeding value of 0.05 µg Chl *a* l⁻¹ to a winter water column value of 0.07 (see Fig. 3.4).

Concentrations of the state variables were calculated at each half-degree of latitude in the area between 58 and 62°S during the 70 day-ice retreat period, by integration of equations 1-20 on the variations of light and temperature with time and on the depth up to the depth of the euphotic layer. The light absorption in the water column was assumed to obey the Beer-Lambert's law. The vertical light attenuation coefficient K_e was calculated by the model from predicted chlorophyll *a* concentration according to the empirical relationship described in Lancelot *et al.* (1991a) :

$$K_e = 0.054 \text{ Chl } a + 0.072$$

A two layer biological model was considered consisting of a homogeneous upper layer in which mixing was instantaneous and a stratified water column. Vertical and temporal step were 0.5m and 1h. Hourly values of the wind mixed layer depth and of temperature are provided by the physical model.

Table 6.I: Modelling the microbial network in the northwestern Weddell Sea : initial concentrations of the state variables.

| State variables | Concentrations | Units |
|----------------------------|----------------|---------------------|
| Inorganic nitrogen : | | |
| NH ₄ | 0.02 | μM |
| NO ₃ | 31.5 | μM |
| Phytoplankton : | | |
| Chlorophyll <i>a</i> | 0.12 | μg l ⁻¹ |
| F | 4 | μgC l ⁻¹ |
| R | 0.7 | μgC l ⁻¹ |
| S | 0.3 | μgC l ⁻¹ |
| Dissolved organic matter : | | |
| MS | 2.5 | μgC l ⁻¹ |
| H ₁ | 5 | μgC l ⁻¹ |
| H ₂ | 200 | μgC l ⁻¹ |
| Bacteria : | | |
| B | 1 | μgC l ⁻¹ |

6.1.2. Temporal variations

As an illustration of the physical, chemical and biological phenomenon operating within the marginal ice zone at the time of ice melting, Fig. 6.1–6.7 show temporal evolution of predicted physical, chemical and biological state variables and associated transformations or processes at latitude 59° 30' S during spring 1988. The 70-day simulated period at this latitude covers the whole ice melting process as well as a one-month ice-free period (Fig. 6.1) and thus well illustrates the entire sea ice retreat phenomenon, including the remnant effect of ice melting on the stability of ice-free surface waters (Veth *et al.*, 1992).

As a general trend, reasonable agreement is found between predictions and observations.

Short-term extreme wind fluctuations between 2 and 17 m s⁻¹ (as compared to an average value of 8 m s⁻¹) succeeded each other during the studied period at the given latitude (Fig. 6.1c). Solar radiation fluctuated similarly, giving rise to periods of sunny

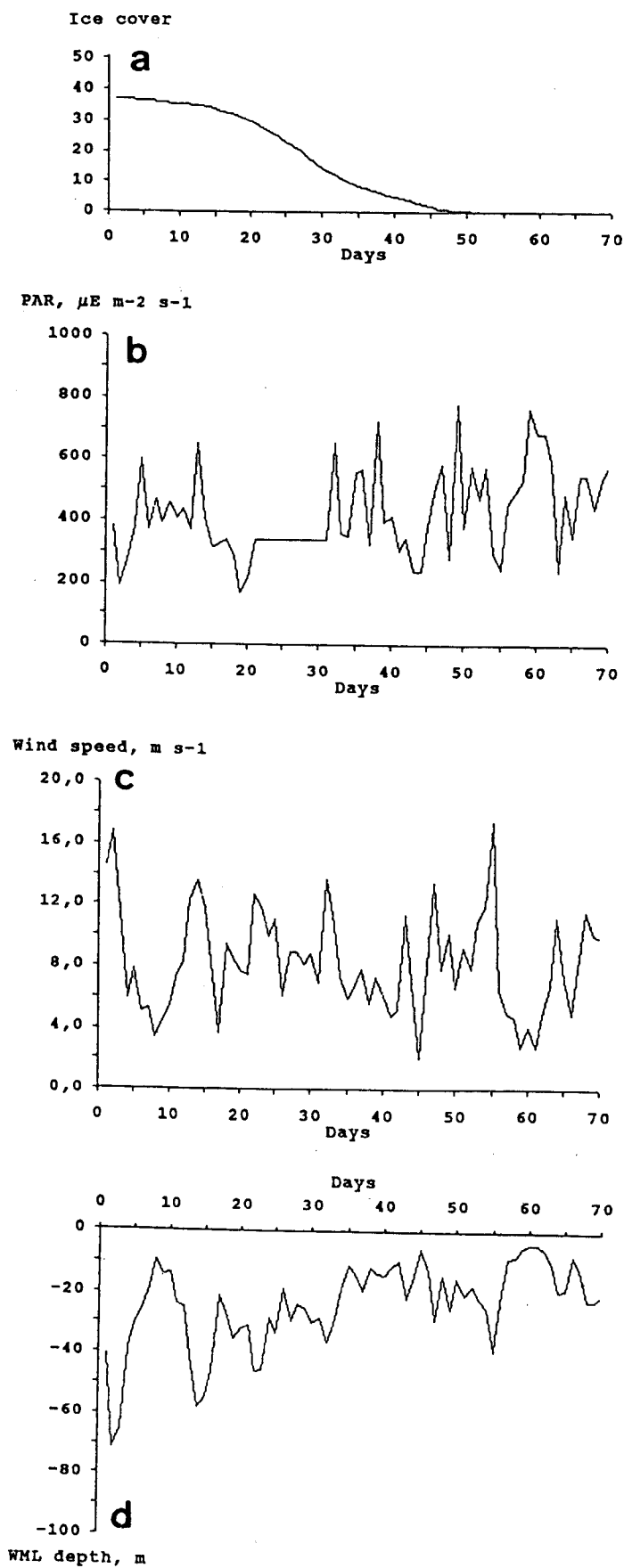


Figure 6.1 : Ice cover (a), global radiation (b), wind speed (c) and predicted upper mixed layer (d) at latitude $59^{\circ} 30' S$ during spring 1988.

days with low wind, or reversely, cloudy days with high wind. This has dramatical influence on the predicted depth of the upper mixed layer, which directly responds to diurnal fluctuations of wind speed and solar radiation (Fig. 6.1d), by varying between 4 and 70 m. The frequency, duration and strength of mixing events were particularly important during the ice-covered period characterized by an alternance of short-term shallow upper mixed layer (5 to 30 m) and deep vertical mixing (deeper than 50 m). Due to the high-friction coefficient of ice, the layer affected by transient wind events was on an average deeper within the ice covered period (70 m) than after ice melting (38 m), thus reducing to very low level the light available to phytoplankton circulating in upper layers covered by ice.

The key role played by vertical stability and ice cover in the onset of phytoplankton ice-edge development is evidenced by Fig. 6.2 and 6.3. The control of phytoplankton activity by surface light availability, on the one hand, is clearly shown on Fig. 6.2 which presents simulations of daily integrated photosynthesis and net primary production (Fig. 6.2b), and nitrate cumulative uptake by phytoplankton (Fig. 6.2c) when ice retreats from 40 % to 0 %. Predicted average net primary production is shown to vary between 200 (range : 50 – 300) and 750 (range : 400 – 1500) $\text{mgC m}^{-2} \text{d}^{-1}$, characteristic of high (> 20 %) and weak (< 20 %) ice coverage respectively, in agreement with previous field data in the marginal ice zone of the Weddell Sea (Smith & Nelson, 1986). Accordingly, cumulative nitrate uptake by phytoplankton increases exponentially at ice cover less than 20 % (Fig.6.2c).

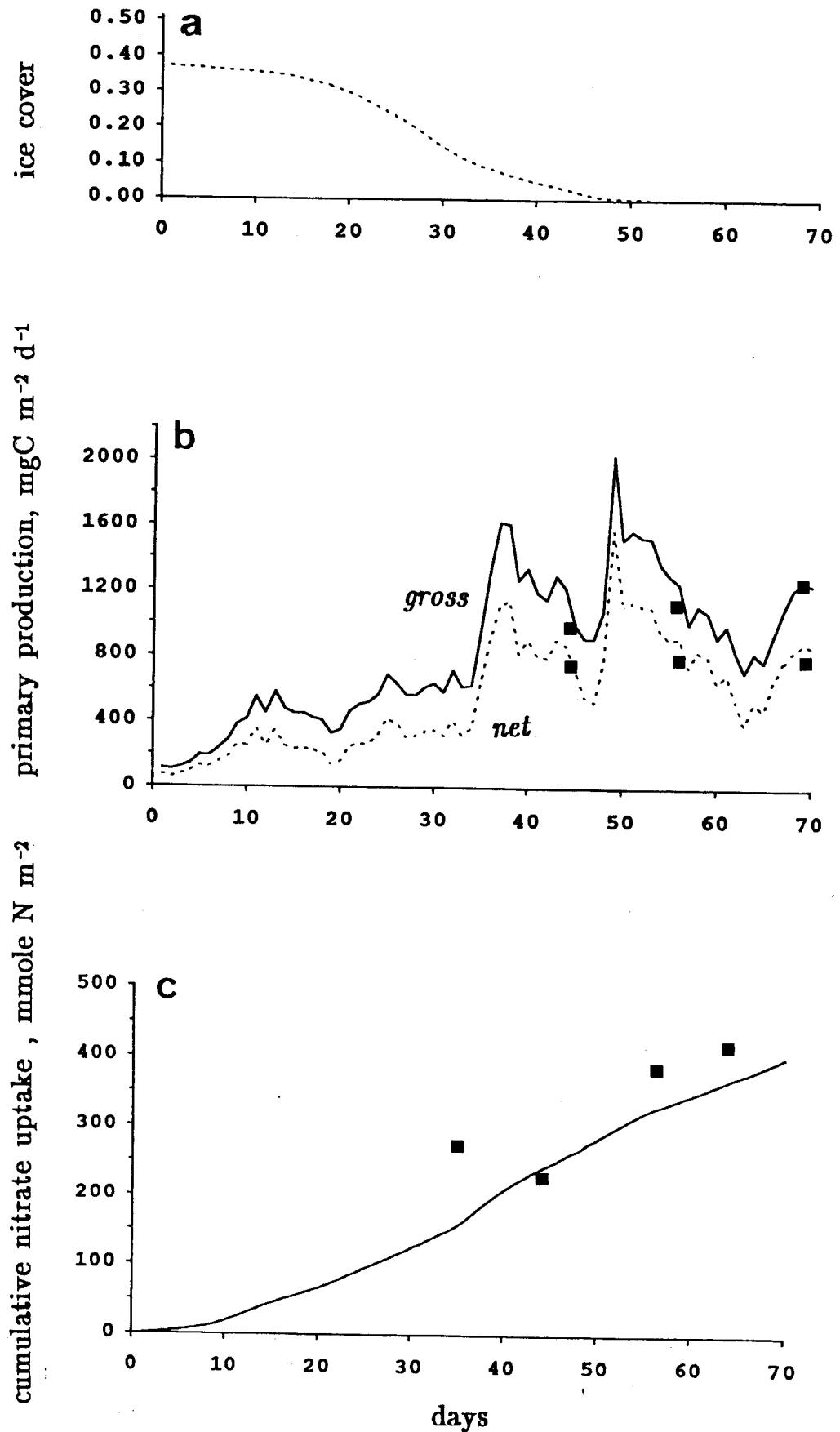
ANTAR
II/05

Figure 6.2 : Ice cover (a), predicted (lines) and measured (■) primary production (b) and cumulative nitrate uptake by phytoplankton (c) at latitude 59°30' S during spring 1988.

The additional influence of water column stability, on the other hand, can be seen on Fig. 6.3 showing the calculated variation of chlorophyll *a* concentration in the upper mixed layer during the same period. This simulation clearly suggests that vertical stability and ice cover less than 20 % are the conditions for the onset of an ice-edge phytoplankton bloom.

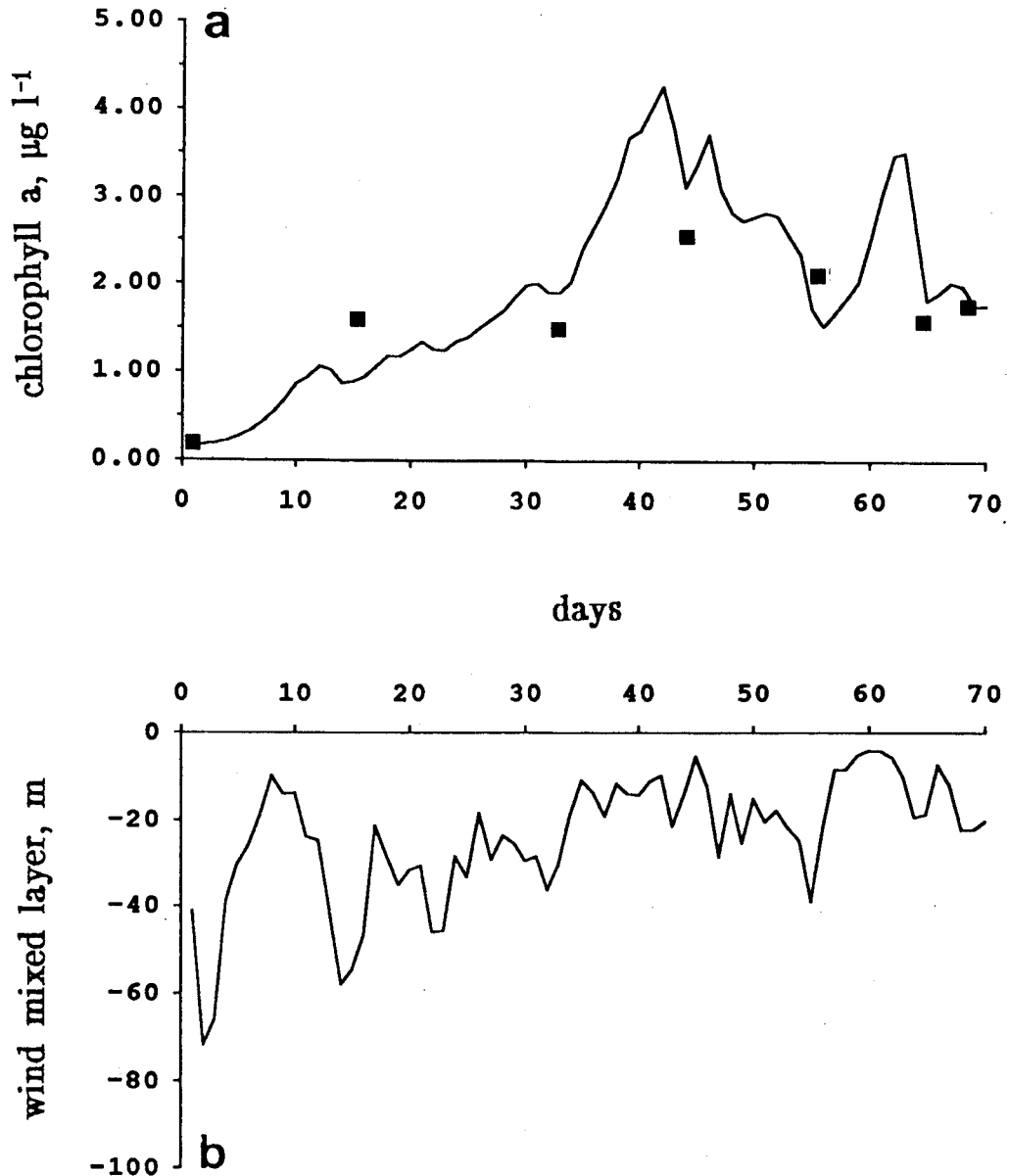


Figure 6.3 : Predicted (line) and observed (■) chlorophyll *a* concentrations in the upper mixed layer (a), and upper wind mixed layer depth (b) at latitude $59\ 30^{\circ}$ S during spring 1988.

The role played by protozoa grazing pressure on the control of ice-edge bloom magnitude and duration is evidenced by Fig. 6.4 that compares predicted net primary production and grazing pressure by herbivorous protozoa. Due to seawater temperature increase following ice melting and the concomitant increase of food resources, predicted grazing pressure reaches daily values close to or even higher than phytoplankton growth. In this latter case, an additional food resource supplied by bacteria and bacterivorous protozoa is thus required to sustain growth of herbivorous protozoa as shown by experimental data (section 4).

Accordingly, predicted bacterial daily production and biomass (Fig.6.5), whilst remaining at very low levels during the whole ice covered period, reach high values of $120 \text{ mgC m}^{-2} \text{ d}^{-1}$ and $20 \text{ } \mu\text{gC l}^{-1}$ respectively after the ice melting process. However, contrasting with grazing pressure of herbivorous protozoa that directly responds to phytoplankton biomass increase (Fig.6.4), a 20 day-delay between the peaks of phytoplankton and bacteria biomass is predicted by the model.

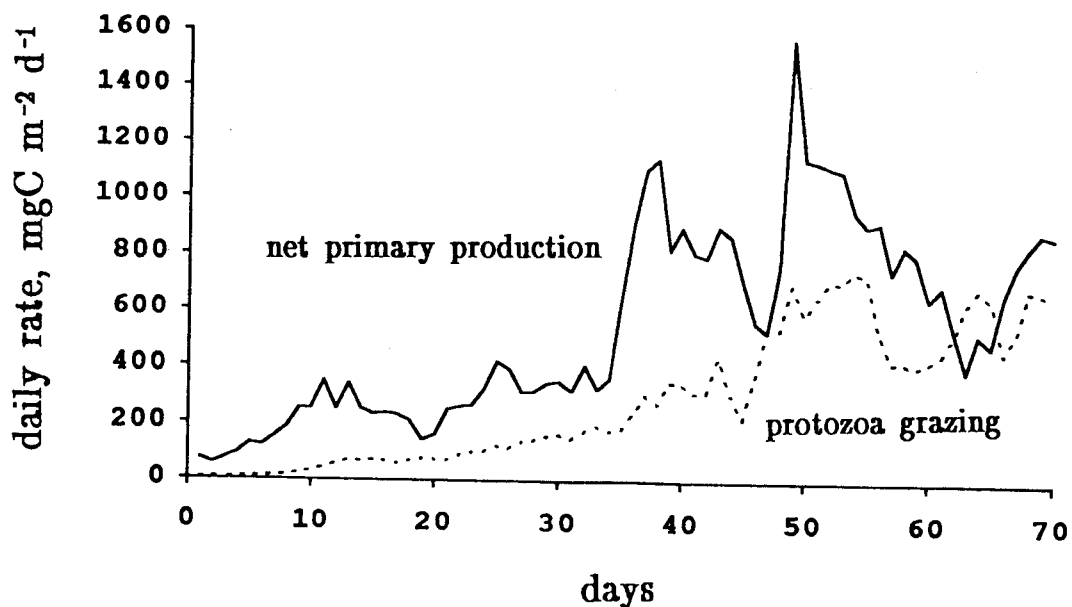


Figure 6.4 : Predicted daily primary production (solid line) and daily rates of protozoan grazing (dashed line) at latitude $59^{\circ} 30' \text{ S}$ during spring 1988.

Predicted ammonium concentration (Fig.6.6a), as a result of microheterotrophic activity (bacteria, bacterivorous and herbivorous protozoa) (Fig.6.7a), reaches concentrations higher than $1 \mu\text{M}$ after ice retreat. These elevated ammonium levels significantly reduce nitrate uptake by phytoplankton at the end of the simulated period (Fig.6.2c) as a consequence of phytoplankton preference for ammonium. This has dramatic influence on $f\text{N}_3$ ratio which decreases from 0.90 to 0.44 (Fig.6.6b), consistent with the observation that, in this area, the ice retreat phenomenon is accompanied by a shift from a dominant new production system towards a regenerated one.

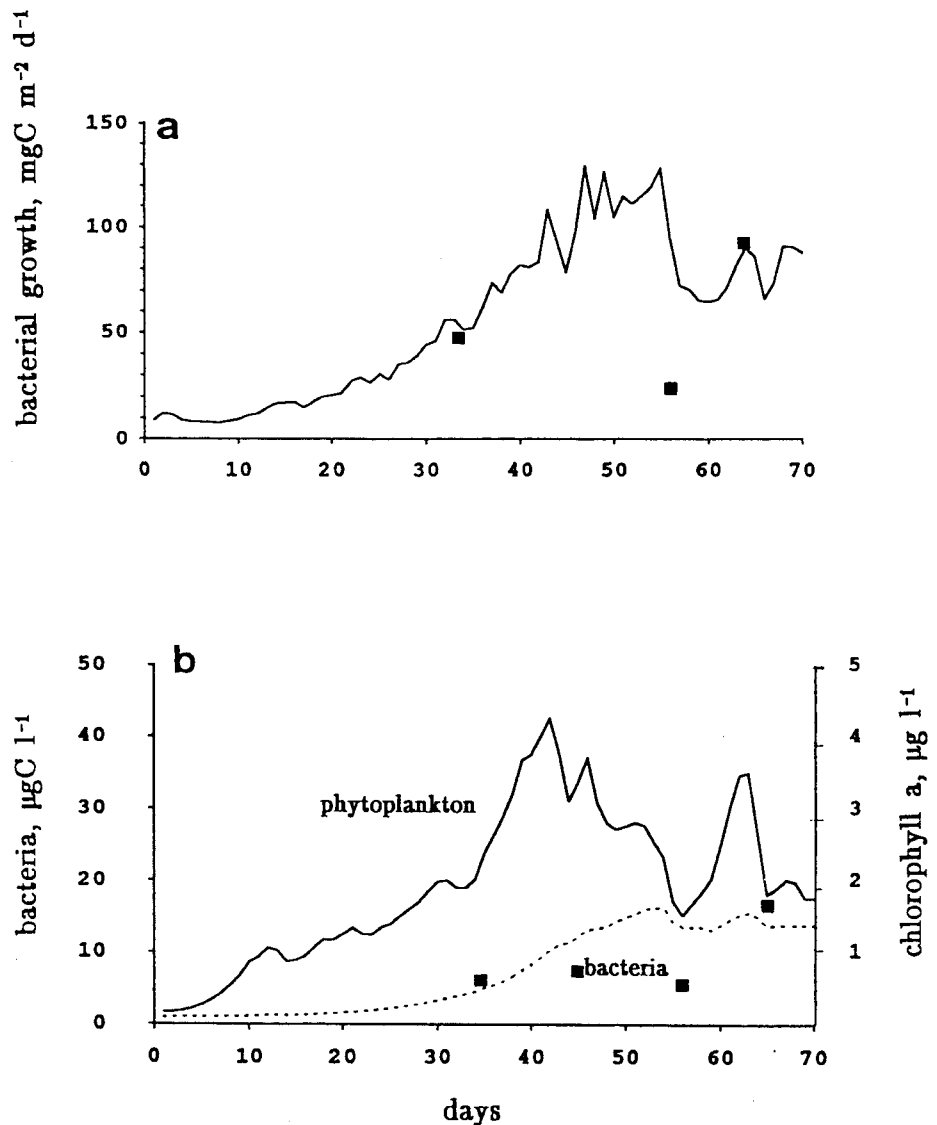


Figure 6.5 : Predicted (solid line) and measured (■) bacterial production (a), and predicted (dashed line) and measured (■) bacterial biomass compared with predicted phytoplanktonic biomass (solid line) (b) at latitude 59° S during spring 1988.

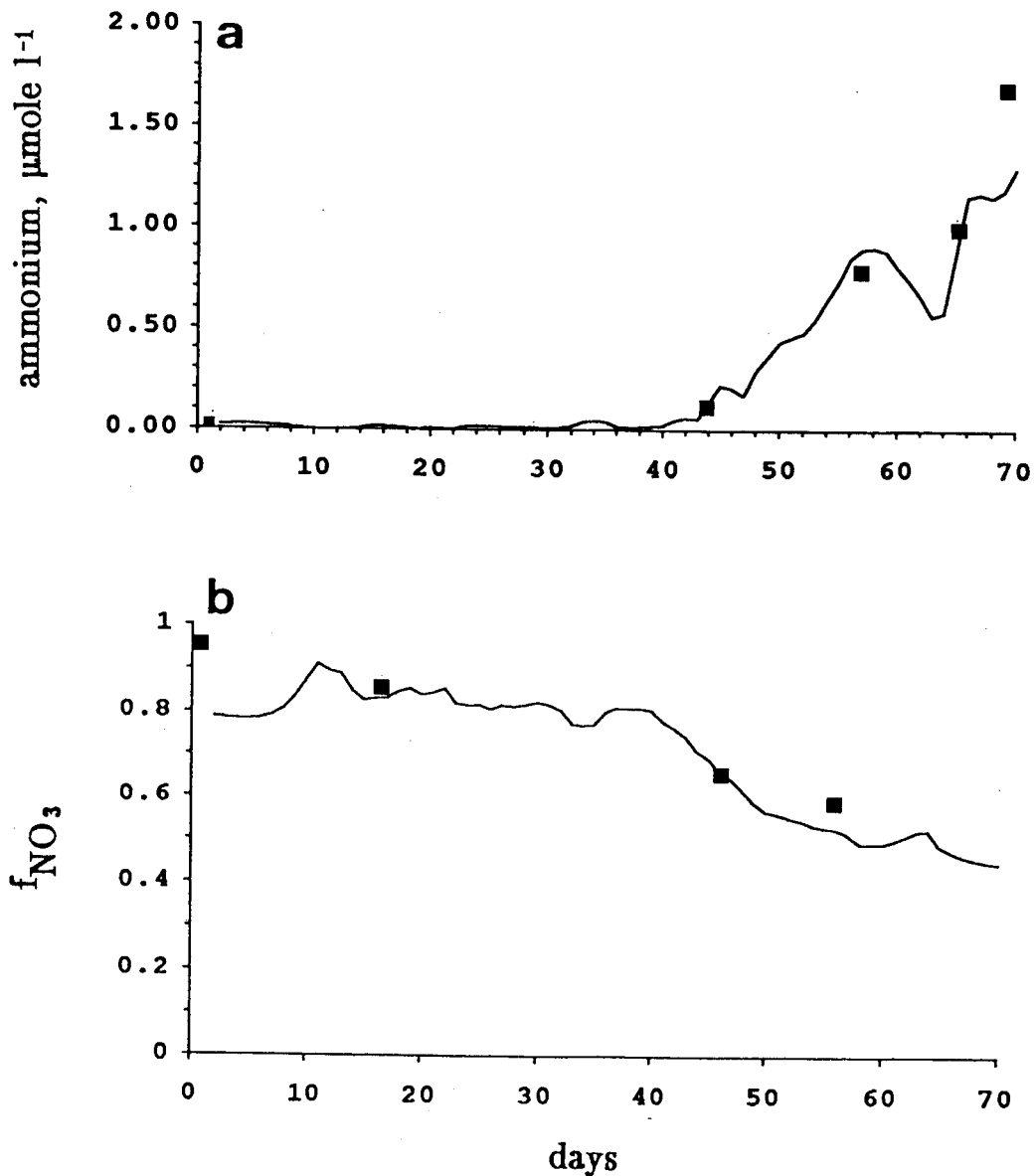
ANTAR
II/05

Figure 6.6 : Predicted (solid line) and measured (\blacksquare) ammonium concentration (a) and f_{NO_3} ratio (b) in the upper mixed layer at latitude $59^{\circ} 30' \text{ S}$ during spring 1988.

The respective role of herbivorous protozoa and bacteria in regenerating ammonia, illustrated by Fig. 6.7a, evidences the predominance of the former microorganisms during sea ice melting. After this period, however, predicted ammonium regeneration rate by bacteria due to bacterial activity reaches values close to that by herbivorous protozoa. Interestingly, the model predicts that ammonium regeneration through the only herbivorous protozoan activity could sustain almost entirely phytoplankton ammonium demand (Fig.6.7b). Predicted and observed accumulation of ammonium (Fig.6.6a) result therefore from the increase of bacterial activity following the decline of the phytoplankton ice-edge bloom.

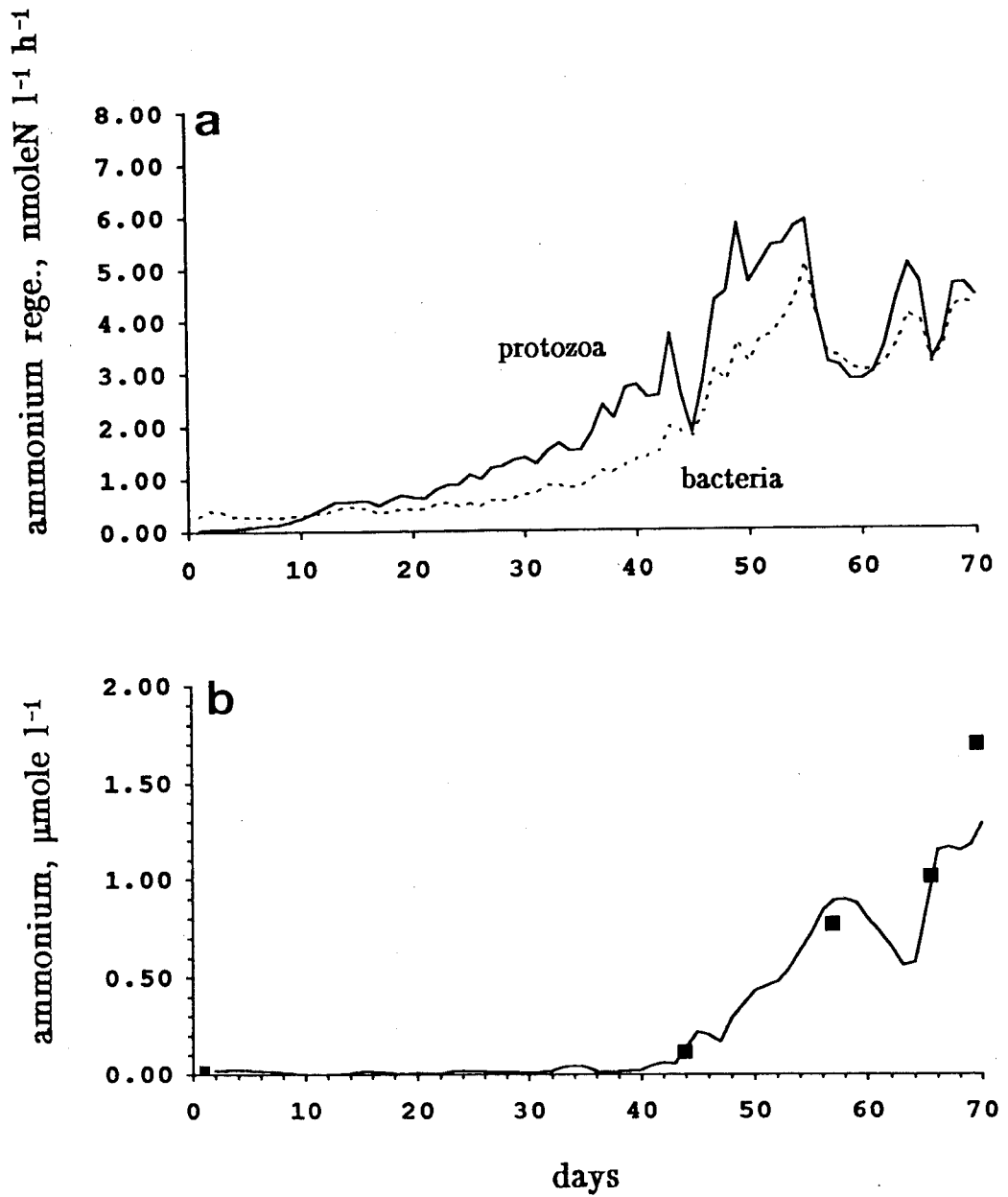


Figure 6.7 : Predicted (lines) and calculated (■) ammonium regeneration rates through bacterial and herbivorous protozoan activity (a) and ammonium concentration (b) at latitude $59^{\circ} 30' \text{ S}$ during spring 1988.

6.1.2. Spatio-temporal variations

The spatio-temporal variation of chlorophyll *a* (Fig.6.8a), bacteria (Fig.6.8b) and ammonium (Fig.6.8c) concentrations and nitrate depletion (Fig.6.8d), predicted during the sea ice retreat was drawn from model runs performed at each half-degree of latitude between 59 and 62° S. Agreement between prediction and observation is reasonably good excepted for bacterial biomass which predicted values in the recently ice-free area are significantly higher than observations.

For other variables, both the magnitude and the location of maxima at the ice-edge position and/or in the 100 km-band seawards from the ice-edge are well simulated. In particular the southward shift of maximum concentrations and biological activities with the receding ice-edge is clearly apparent from model simulations (Fig.6.8). At one occasion however (Fig.6.8a; lat.60°S, 20–24 Dec.), a strong discrepancy exists between predicted and measured chlorophyll *a* which is likely the consequence of a krill passage not taken into account by the model.

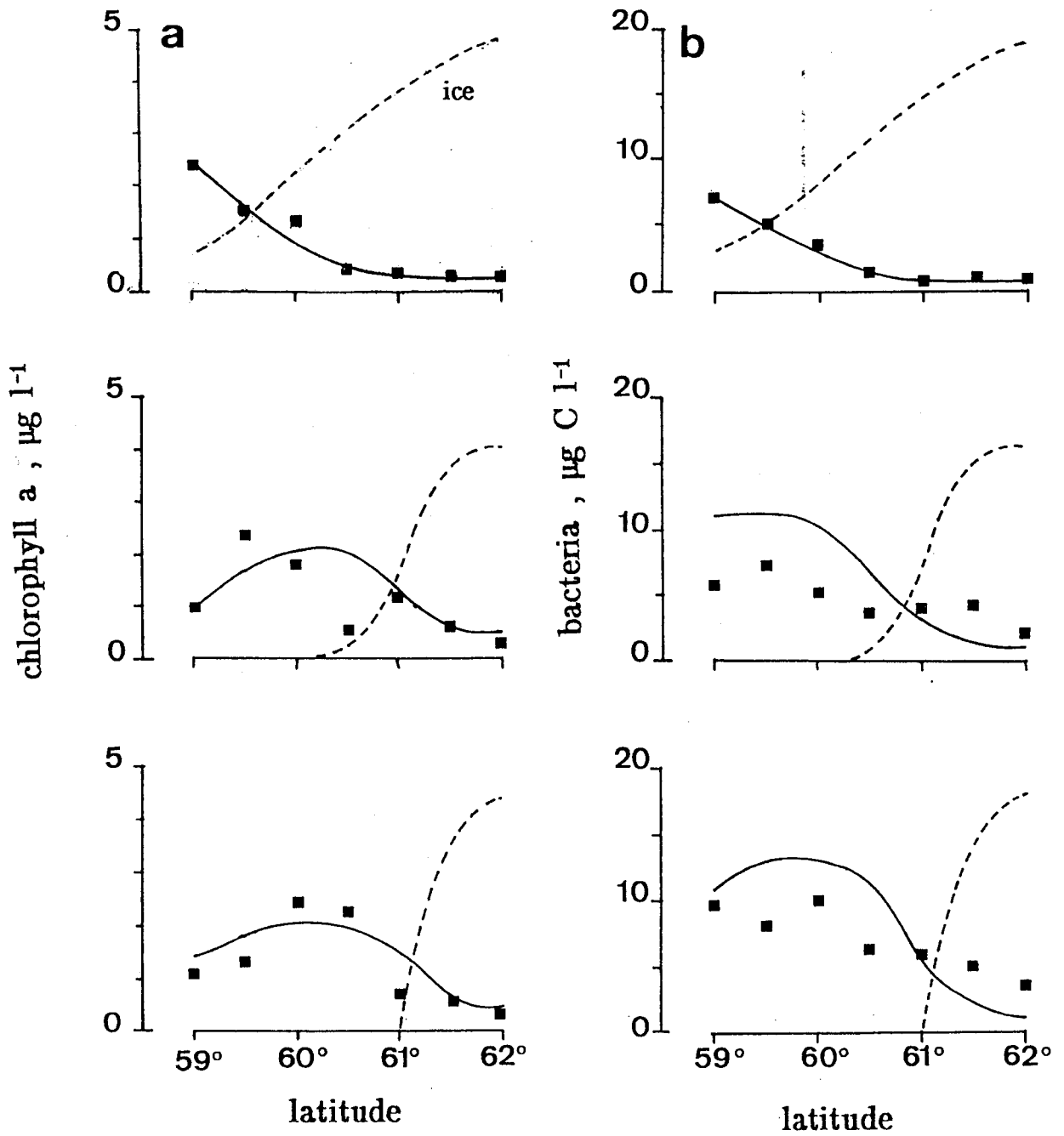


Figure 6.8ab : Predicted (solid line) and observed (\blacksquare) spatio-temporal variations of chlorophyll *a* (a) and bacterial (b) concentrations in the upper mixer layer in the northwestern Weddell Sea during sea ice retreat 1988. Ice retreat is represented on each graph as a dashed line.

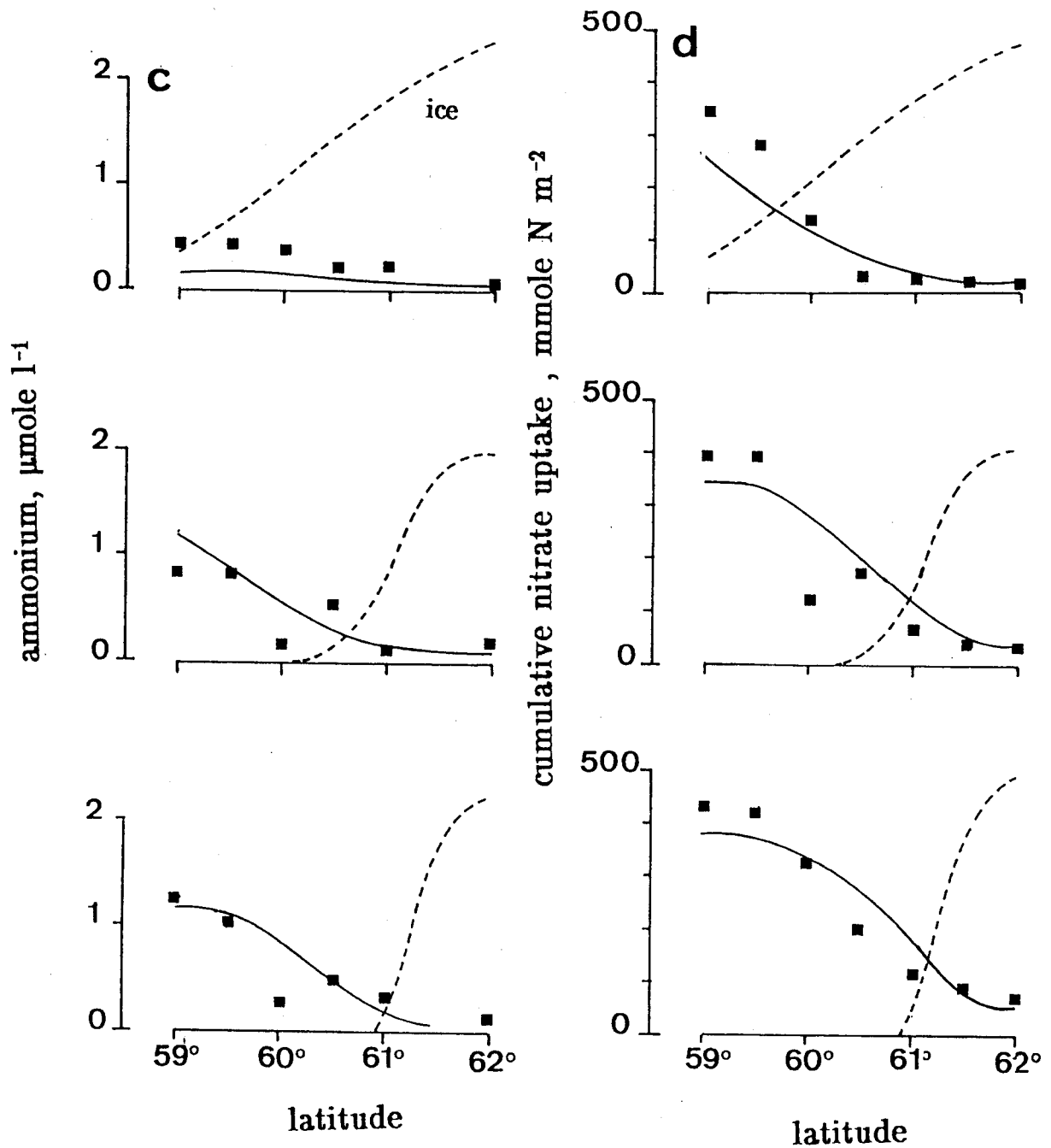


Figure 6.8cd : Predicted (solid line) and observed (■) spatio-temporal variations of ammonium concentrations in the upper mixed layer (c) and cumulative nitrate uptake by phytoplankton (d) in the northwestern Weddell Sea during sea ice retreat 1988. Ice retreat is represented on each graph as a dashed line.

6.2. Sensitivity analysis : factors controlling phytoplankton ice-edge blooms

The careful analysis of factors controlling phytoplankton bloom development in the marginal ice zone of the northwestern Weddell Sea, through both spatio-temporal examination of observations (sections 3 and 4) and model simulations (§ 6.1.2), suggests that ice-edge bloom initiation is mainly under control of physical processes determining the vertical stability of surface waters. Grazing pressure, on the other hand, actively controls both the magnitude and extent of the bloom, preventing occurrence of massive phytoplankton biomasses in this sector of the circumpolar marginal ice zone. Herbivorous protozoa exert a semi-continuous control on phytoplankton development whilst the role of krill is more episodic, owing to its life history. Krill acts on the height of the phytoplankton ice-edge bloom by determining sea ice algae seeding concentration of the water column and on the bloom development by grazing on phytoplankton patches during their migrations. The successive action of physical and biological factors limiting primary production might well explain the geographical location of phytoplankton blooms close to the retreating ice-edge. However, it is evident that these factors are not always exclusive, as shown for instance by the additional role played by physical processes like deep mixing on phytoplankton bloom magnitude through the vertical dilution of phytoplankton concentrations. To which extent physical and biological factors interact in generating and controlling phytoplankton blooms in the circumpolar marginal ice zone of the Southern Ocean was investigated through a sensitivity analysis of the coupled physical-biological model described here above applied at latitude $59^{\circ} 30' S$ within the marginal ice zone of the northwestern Weddell Sea during spring.

Meteorological conditions : Highly fluctuating weather conditions occurring at a scale sometimes less than one week are typical of the Southern Ocean (Deacon 1984). Accordingly, short-term extreme wind fluctuations between 2 and 17 m s^{-1} around an average value of 8 m s^{-1} succeeded to each other during the studied period at the given latitude (Fig. 6.1c). To which extent these episodic wind events affect sea ice-associated phytoplankton bloom development is depicted in Figs. 6.9. and 6.10. which compare the evolution of surface layer phytoplankton predicted for different weather scenarii. Comparison of simulations generated by local weather conditions and those averaged over the 70-day simulated period strongly suggests that during the ice-covered period, when light penetration is considerably reduced by sea ice albedo, current shallow upper layer events were insufficient for counterbalancing deep

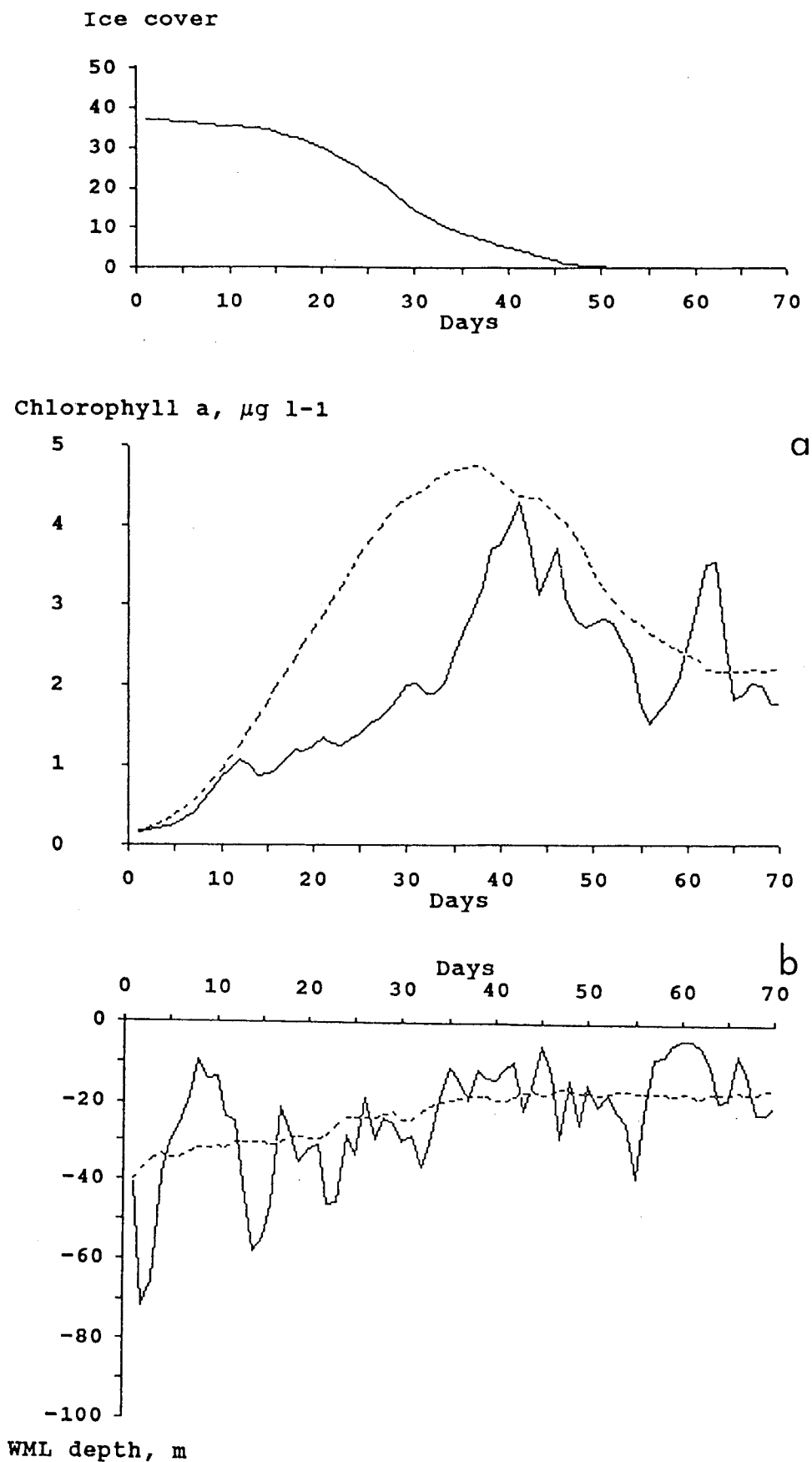
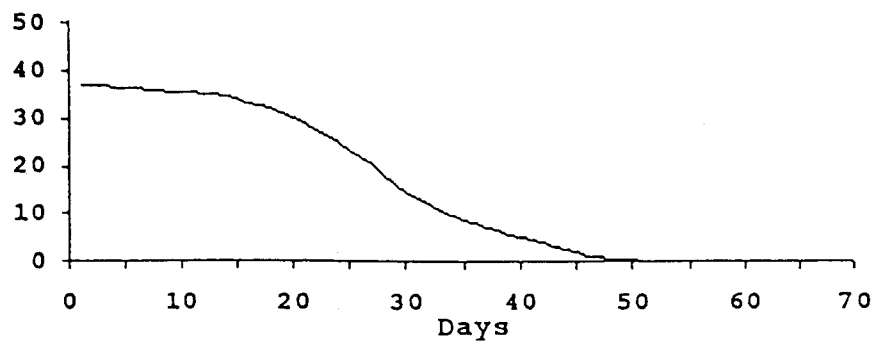
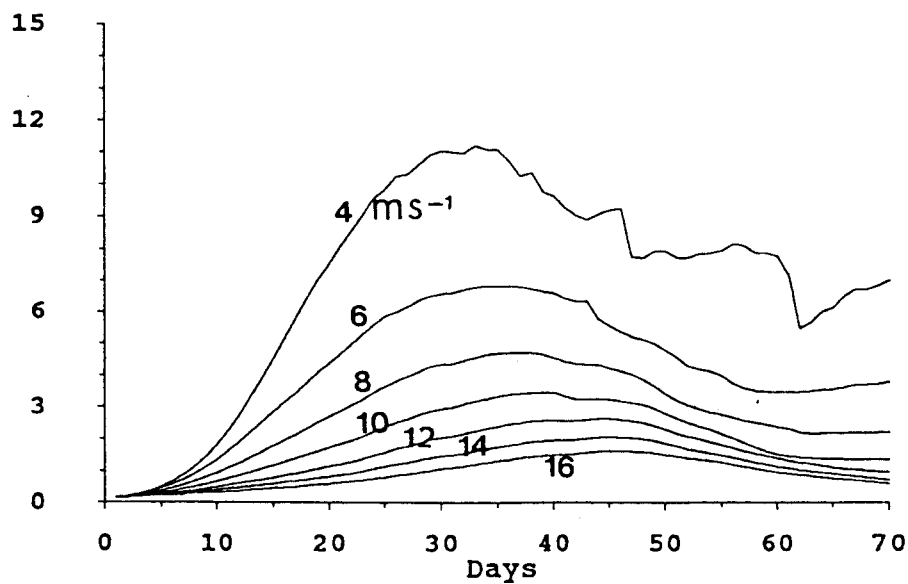


Figure 6.9 : Predicted chlorophyll *a* concentration (a) and upper mixed layer depth (b) at latitude $59^{\circ} 30' \text{ S}$ during the ice melting period under local (solid line) and averaged (dashed line) meteorological conditions.

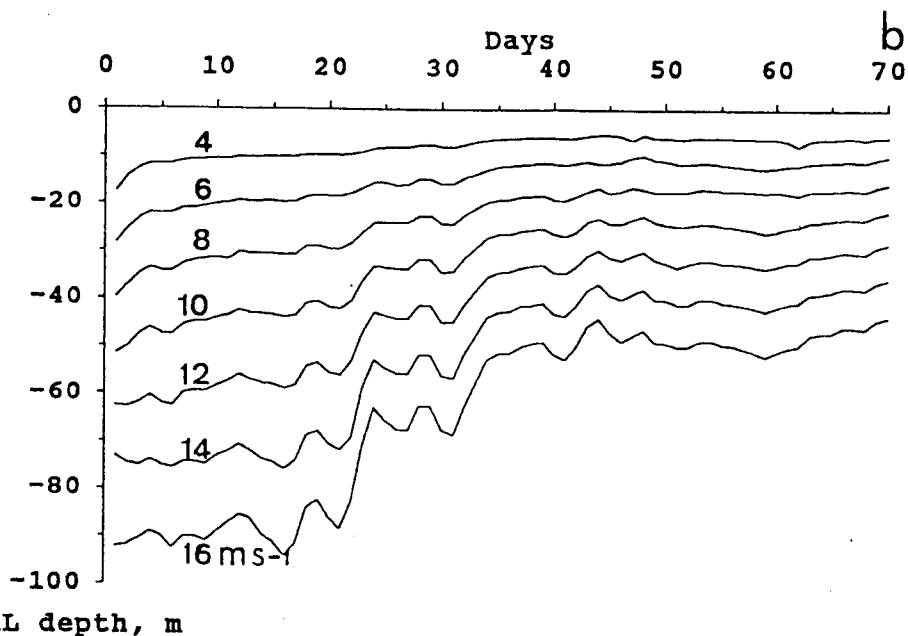
mixing which dilutes phytoplankton concentration in a lower mean irradiance environment. This is the consequence of the asymmetrical behavior of the wind mixed layer regarding deepening and shallowing. Indeed whilst phytoplankton dilution accompanies deep mixing, no concentration takes place during shallowing, with the result that a single deep mixing event has major consequence for phytoplankton bloom initiation. During EPOS expedition, in particular, the successive wind mixing events occurring during the ice-covered period considerably delays the exponential development of phytoplankton as well as its maximum level with respect to that predicted under constant averaged wind conditions (Fig. 6.9). On the other hand, very similar maximum chlorophyll *a* concentration of about $4.5 \mu\text{g l}^{-1}$ are predicted by both scenarios (Fig. 6.9).

The role of wind velocity on phytoplankton ice-edge bloom development and magnitude is evidenced by Fig. 6.10, which compares chlorophyll *a* concentrations predicted under various constant wind climates. These simulations show that, according to the wind speed, the phytoplankton peak appearance shifts with respect to ice cover, occurring between 0 and 20 % of this latter. More spectacular is the range of maximum phytoplankton concentration predicted, varying between 1.5 and $11 \mu\text{g Chl } a \text{ l}^{-1}$ (Fig. 6.10). Under constant wind of 14 m s^{-1} , however, no significant phytoplankton bloom is predicted.

Ice cover

ANTAR
II/05Chlorophyll a , $\mu\text{g l}^{-1}$ 

a



b

WML depth, m

Figure 6.10 : Predicted chlorophyll a concentration (a) and upper mixed layer depth (b) at latitude $59^{\circ} 30' \text{S}$ during the ice melting period under various constant wind speed.

Seeding: The role of seeding in generating phytoplankton ice-edge bloom was approached by comparing simulation runs with various initial concentrations of phytoplankton corresponding to realistic seeding concentrations. These latter were calculated from chlorophyll *a* concentrations measured in sea ice floes (Garrison *et al.*, 1986) diluted within the upper mixed layer at initial conditions, assuming an ice floe average diameter of 20 m at the time of melting (van Franeker, pers. com.) and a preferential peripheral distribution of sea ice communities. Simulations (Fig. 6.11) clearly show that seeding acts solely on the early development of phytoplankton during the ice covered period by allowing occurrence of sporadic minor blooms, the importance of which is related to weather conditions, without however affecting peak appearance and maxima reached by the ice-edge bloom.

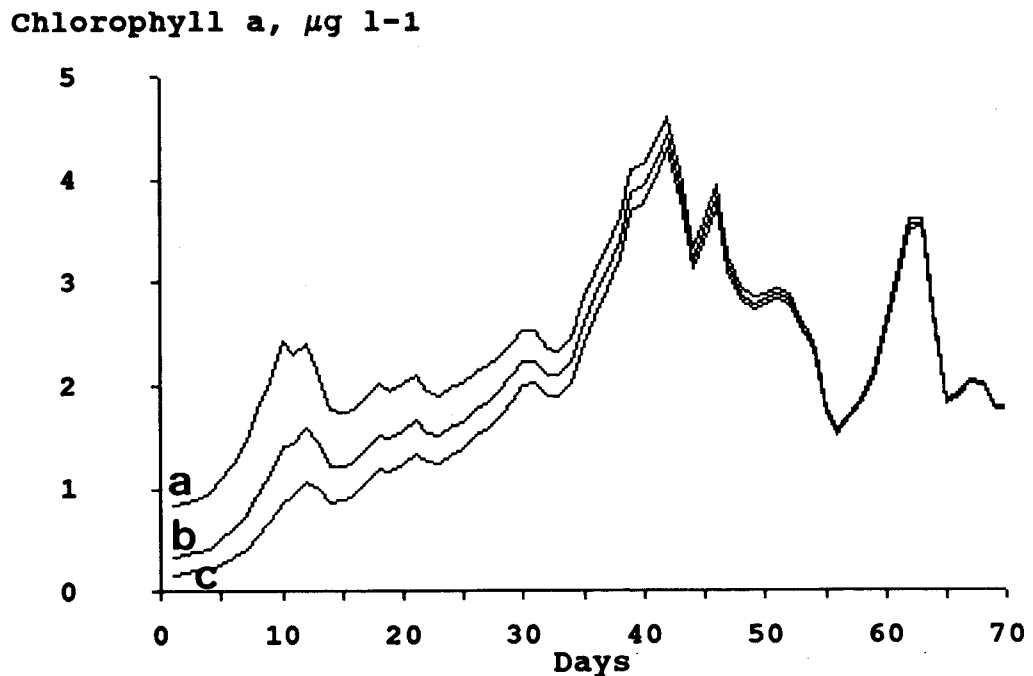


Figure 6.11 : Predicted chlorophyll *a* concentration at latitude 59 30° S during the ice melting period for various seeding scenarios of 0.8 (a), 0.4 (b), and 0.1 (c) $\mu\text{g Chl } a \text{ l}^{-1}$.

Grazing pressure : The role of protozoan grazing pressure in determining the level and magnitude of the ice-edge phytoplankton bloom on the other hand is outlined by analysing, especially after the ice melting period, predictions resulting from elimination of protozoan grazing pressure (Fig. 6.12). Whilst insignificant in the early development of phytoplankton, grazing pressure actively determines the maximum concentration of $7.5 \mu\text{g Chl } a \text{ l}^{-1}$ reached by the sea ice associated bloom which is 70 % up on eliminating grazing pressure (Fig. 6.12). Hence this concentration represents the maximum ice-edge phytoplankton biomass to be reached under local meteorological conditions. The ice-edge bloom extent on the other hand is clearly determined by the balance between phytoplankton losses due to grazing pressure and the persistence of optimal light conditions due to favorable wind conditions. Phytoplankton ice-edge decline is predicted under observed grazing pressure whilst bloom development persists when grazing is eliminated (Fig. 6.12).

ANTAR
II/05

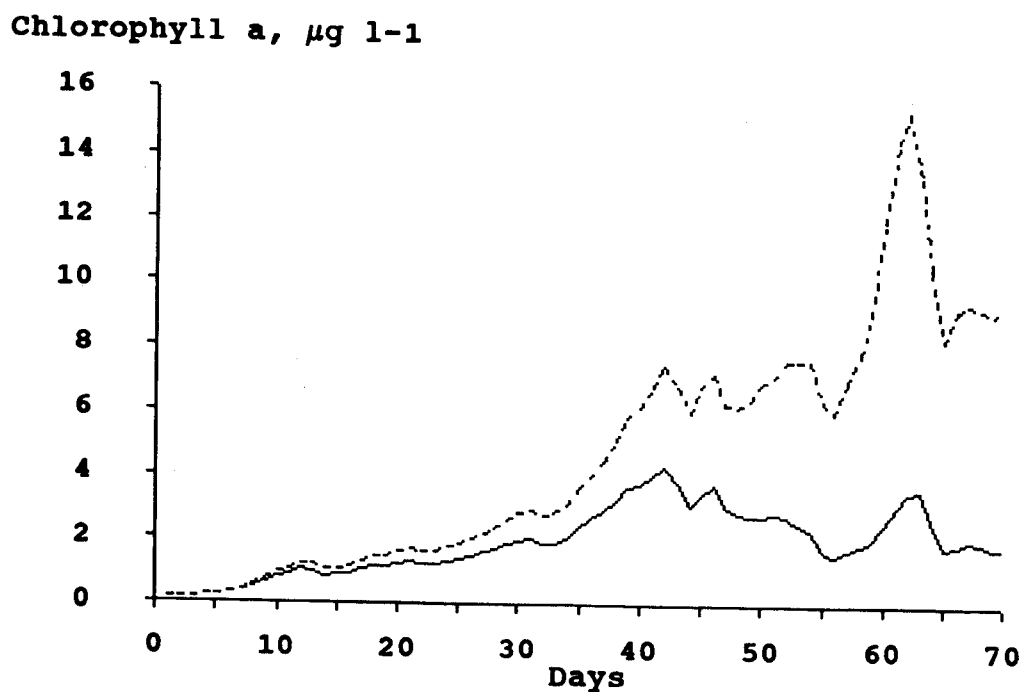


Figure 6.12 : Predicted chlorophyll *a* concentration at latitude $59^{\circ} 30' \text{ S}$ during the ice melting period under *in situ* grazing pressure by protozoa (solid line) and after protozoa elimination (dashed line).

Most scenarios predict a summer steady state phytoplankton concentration, the value of which greatly depending on weather conditions (Fig. 6.9 & 6.10) and grazing pressure (Fig. 6.12). The occurrence of secondary phytoplankton peaks during the ice-free period as predicted around day 20 by local weather conditions (Fig. 6.12) on the other hand, is clearly related to the amplitude and duration of wind mixing events. Indeed no summer development is predicted by constant wind scenarii (Fig. 6.10). The height of these secondary phytoplankton blooms is determined by both the grazing pressure and the persistence of vertical stability providing favorable light conditions to phytoplankton whilst their decline is mostly due to vertical dilution of phytoplankton into a lower mean irradiance field (Fig. 6.9).

Krill: The impact of krill passage on the development of sea ice associated phytoplankton bloom is determined by its occurrence with respect to phytoplankton development stage (Fig. 6.13). A single krill event occurring under the ice (Fig. 6.13a) has little influence on chlorophyll *a* bloom prediction associated to the ice melting process, reducing it to a mean value of 70 %, and no effect on secondary blooms resulting from stable wind mixing events. Reversely, a krill passage at the blooming stage eliminates the bloom and controls the magnitude of secondary summer peaks (Fig. 6.13b).

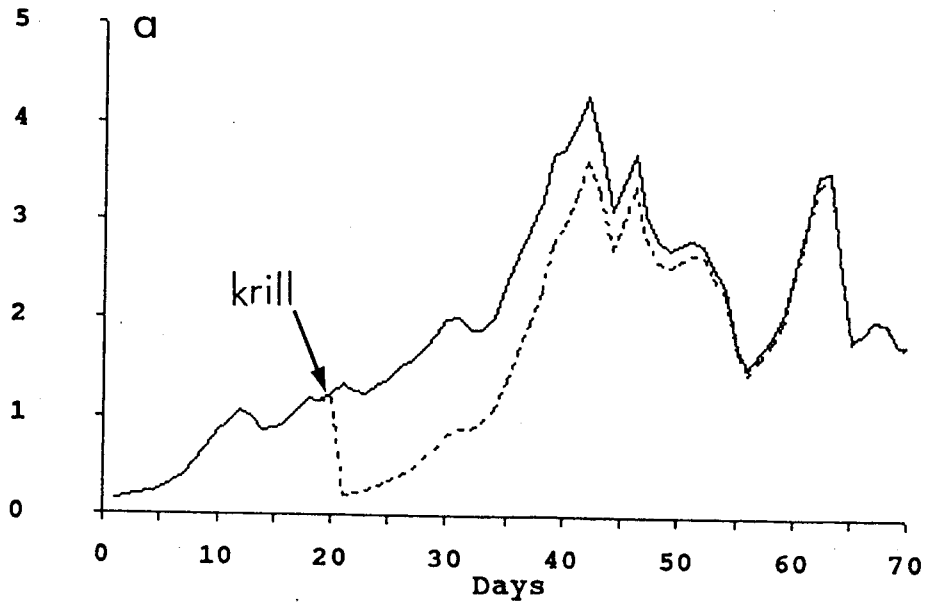
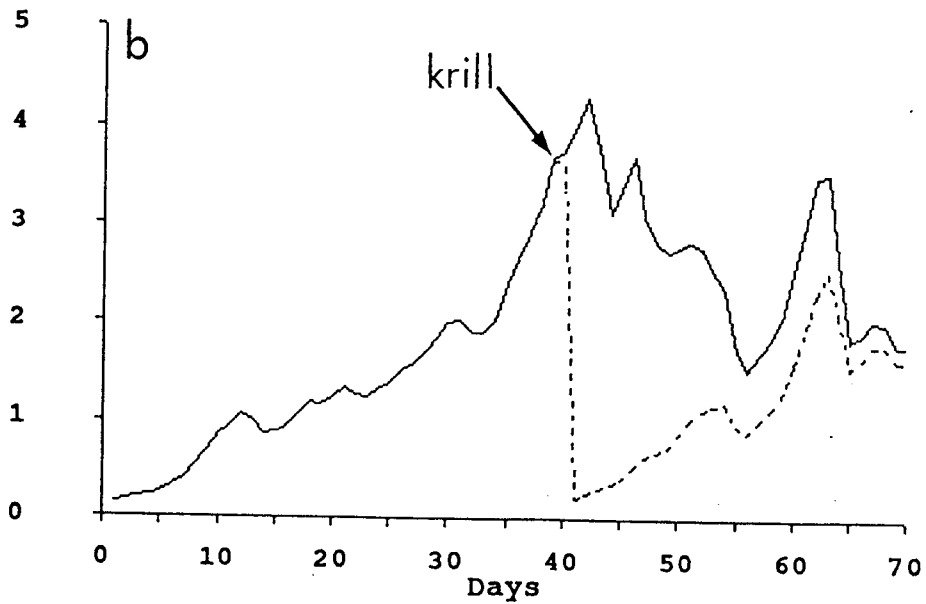
Chlorophyll a, $\mu\text{g l}^{-1}$ ANTAR
II/05Chlorophyll a, $\mu\text{g l}^{-1}$ 

Figure 6.13 : Predicted chlorophyll a concentration at latitude $59^{\circ} 30' \text{ S}$ during the ice melting period after krill passage at the initial (a) and blooming (b) stage of phytoplankton development.

6.3. Applications

6.3.1. Carbon and nitrogen budget of microbial activities during sea ice retreat : the particular case of the northwestern Weddell Sea

The budget of carbon and nitrogen cycling through the microbial network characteristic of the Weddell Sea marginal ice zone around the 49° W meridian has been calculated by integration over the ice-retreat period of biological activities predicted by the ecological model, in the area extended from latitude 58 30° S to 61° S. Results of these calculations expressed in gC m⁻² and gN m⁻² for the ice-retreat period (Table 6.II) are shown on Fig. 6.14.

This budget calculation indicates that a total of 33 gC m⁻² is produced by phytoplankton (net primary production) whilst 31 % (16 gC m⁻²) of the total photoassimilated C or gross primary production (50 gC m⁻²) is lost by respiration and 2 % (1 gC m⁻²) by exudation. 88 % of net primary production (29 gC m⁻²) is assimilated in the microbial food-web composed of bacterioplankton, bacterivorous and herbivorous protozoa. Total net microbial food-web secondary production amounts 8 gC m⁻² which represents an efficiency of about 25 %. This quantity added to the part of phytoplankton production not accounted by microbial loop consumption (4 gC m⁻²) gives a total amount of 12 gC m⁻². This amount represents the maximum predicted food resources available for krill and other zooplankton, provided by the marginal ice zone. This value fits reasonably well with local mesozooplankton demand estimated by Franz (pers. com.) at this period.

Organic production supported by nitrate represents 67 % (22 gC m⁻² or 5.2 gN m⁻²) of total net primary production (33 gC m⁻² or 7.6 gN m⁻²). This corresponds to a mean NO₃-based primary production or new production of 315 mgC m⁻² d⁻¹. This value is highly comparable to that of 400 mgC m⁻² d⁻¹ estimated in that part of the marginal ice zone of the Weddell Sea between meridian 41 and 37° W during spring 1983 by Smith & Nelson (1990) from scattered measurements of vertical profiles of ¹⁵NO₃ uptake multiplied by the Redfield carbon:nitrogen ratio. Ammonium production through herbivorous protozoan metabolism amounts 2.2 gN m⁻² which represents 61 % of total ammonium released by the microbial loop (3.6 gN m⁻²) and is almost balanced by phytoplankton ammonium demand (2.4 gN m⁻²). Total ammonium regenerated through the microbial loop is by far superior to ammonium uptake by phytoplankton, giving rise, in the absence of nitrification, to ammonium accumulation of 1.2 μM.

Table 6.II : Spring budget of microbial activities in the Scotia/Weddell Sea sector of the Southern Ocean.

ANTAR
II/05

| Processes | Marginal ice zone MIZ | Adjacent perma- nently Open Sea POOZ | Permanently ice-covered PICZ |
|--|--------------------------|--|------------------------------------|
| <i>PHYTOPLANKTON :</i> | | | |
| photosynthesis (gC m ⁻²) | 50 | 37 | 7 |
| excretion | 1 | 0.8 | 0.3 |
| respiration | 16 | 10.5 | 2.1 |
| net primary prod. : | | | |
| total (gC m ⁻²) | 33 | 25 | 4.2 |
| NO ₃ -based.(gC m ⁻²) | 22 | 14 | 3.2 |
| NH ₄ -based (gC m ⁻²) | 11 | 11 | 1 |
| fNO ₃ ratio | 0.66(0.39-0.79) | 0.57(0.46-0.78) | 0.75(0.69-0.79) |
| autolysis (gC m ⁻²) | 9 | 4.5 | 2 |
| <i>MICROHETEROTROPHS :</i> | | | |
| herbivorous protozoa (HP) | | | |
| grazing (gC m ⁻²) | 20 | 19.5 | 0.6 |
| bactivoros protozoa (BP) | | | |
| grazing (gC m ⁻²) | 1 | 0.5 | 0.2 |
| HP growth | 8 | 7.5 | 0.3 |
| DOC bacterial assimilation | 12 | 7.7 | 2.3 |
| bacterial growth | 3.5 | 2.3 | 0.7 |
| total NH ₄ regeneration (gN m ⁻²) | 3.6 | 2 | 0.5 |
| HP regeneration (gN m ⁻²) | 2.2 | 1.9 | 0.1 |
| Bact. & BP regeneration (gN m ⁻²) | 1.4 | 1.1 | 0.4 |
| <i>MAXIMUM FOOD AVAILABLE FOR KRILL AND ZOOPLANKTON</i> | | | |
| from phytoplankton (gC m ⁻²) | 4 | 1 | 1.5 |
| from microbial loop | 8 | 7.5 | 0.3 |

Comparing these results with similar calculations conducted in the adjacent permanently open (latitude 58° S) and ice-covered (latitude 62° S) zone as summarized on Table V1.2 well demonstrates that the marginal ice zone is a region of enhanced phytoplankton development at the time of ice melting. Net primary production associated with the process of ice retreat is about one order of magnitude and one third higher than in ice-covered areas limited by light availability and in the adjacent permanently ice-free area respectively. In this latter environment, however, model prediction indicates that high phytoplankton development is not so much prevented by light limitation mediated by deeper turbulent mixing (Lancelot *et al.*, 1993; Veth *et al.*, 1992), as often reported (Sullivan *et al.*, 1988), but rather by grazing pressure of herbivorous protozoa that increases with the advance of the season. As much as 94 % of primary production is indeed taken up by heterotrophic microorganisms, herbivorous protozoa for 78 %, leaving only 1 gC m⁻² to zooplankton and krill. 94 % (7.5 gC m⁻²) of food resources available to these latter (8.5 gC m⁻²) is then provided by microbial loop secondary production.

ANTAR
II/05

Comparing nitrogen budgets shows in addition that the ice-edge effect is even greater when new production is considered, indicating that substantially greater amounts of material are available for export from the marginal ice zone than from other Southern Ocean surface waters.

6.3.2. Ice-edge primary production of the Weddell Sea

Primary production associated to the receding ice-edge in the Weddell Sea has been estimated from extrapolation of the above budget to the region of the Weddell Sea area concerned by ice retreat. This calculation assumes that the food-web structure illustrated by Fig. 6.14 is representative of the marginal ice zone of the whole Weddell Sea, as supported by observations in other regions of the Weddell Sea (Hewes *et al.*, 1985, 1990; Garrison & Buck, 1989a, b). A mean superficie of 5.8 10⁶ km² was considered for the seasonal sea ice zone of the Weddell Sea (Smith & Nelson, 1986). This calculation yields a net ice-edge primary production of 192 10¹² gC, i.e. almost twice higher than the value estimated by Smith & Nelson (1986) from field primary productions and above sea ice zone superficie.

The geographical boundaries of the marginal ice zone, however, largely vary from year to year due to the variability in ice cover and concentration (Zwally *et al.*, 1983; Comiso & Zwally, 1989). During the period 1979–1986 in particular, the area of the

Weddell Sea concerned by ice retreat varied from 4.2 to 5.9 10^6 km² (Comiso & Zwally, 1989). On this basis, interannual variation of ice-edge associated primary production have been calculated for the Weddell Sea and are illustrated by Fig. 6.15. It shows that realistic interannual variation of sea ice extent in this sector of the Southern Ocean has a significant impact on ice-edge primary production.

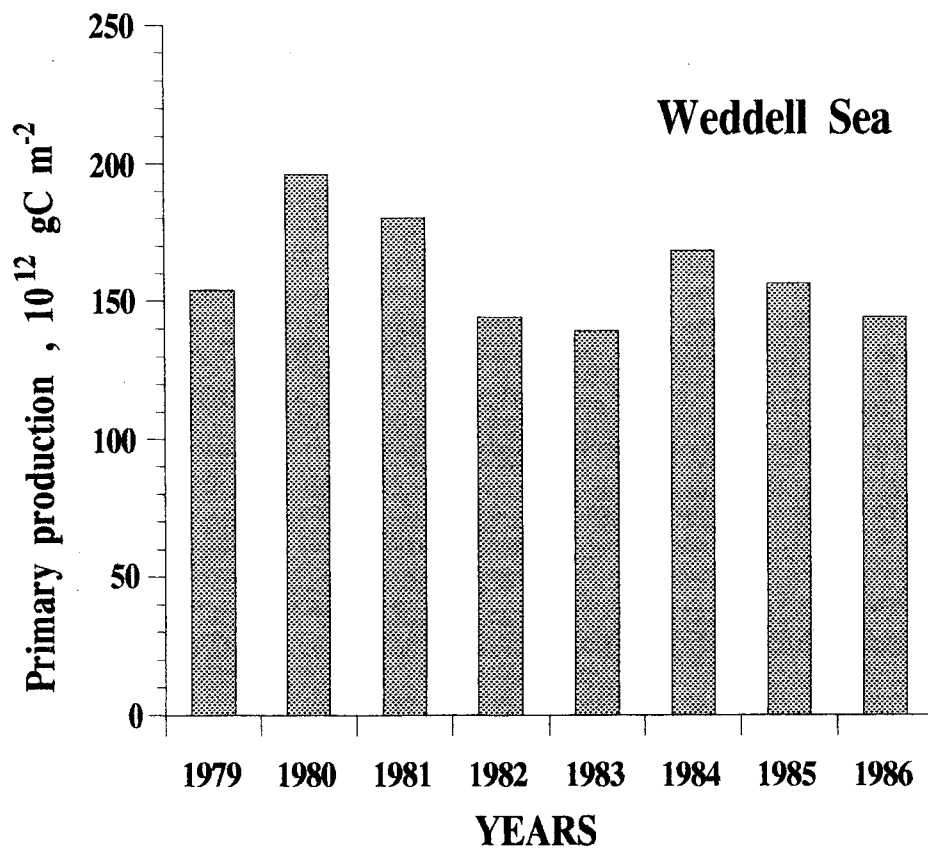


Figure 6.15 : Interannual variations of ice-edge primary production in the Weddell Sea for the period 1979–1986.

6.3.3. Annual primary production of the Southern Ocean

The presence in the Southern Ocean of seasonal sea ice which forms and melt according to the seasonal cycle strongly determines the pattern of primary production, making questionable any estimate of global primary production based on scattered local measurements as often reported in other oceanic areas. Application along the course of a seasonal cycle of the idealized ecological model developed in the previous section at the different latitudes of the Southern Ocean would allow realistic estimate of annual primary production in the Southern Ocean.

Providing the introduction of krill in the model, this is indeed the first model describing explicitly the interaction between the dynamics of sea ice retreat and the physiology of phytoplankton growth and mortality. Model runs over a seasonal cycle are actually prevented by lack of availability of meteorological data (the forcing variables of the model) time series and the inadequacy of existing meteorological models.

As an alternative, annual primary production of the Southern Ocean has been estimated by considering three different phytoplankton habitats, the permanently open ocean zone **POOZ**, the marginal ice zone **MIZ** and the permanently ice covered zone **PICZ**, the geographical limits and production of which vary according to the seasonal cycle. Total superficie of $38.1 \cdot 10^6 \text{ km}^2$ has been considered for the whole Southern Ocean, bordered by the Antarctic Convergence. Seasonal variation of phytoplankton habitat superficie has been calculated from monthly ice concentration contours established for the period 79–86 by Comiso & Zwally (1989) on the basis of polar microwave brightness temperature data collected by Nimbus-7 SMMR. For each sub-area, a monthly mean primary production has been considered (Table 6.III). Daily primary production typical of the growing season are those calculated by the model whilst autumn and winter values originated from a careful analysis of existing data (Mathot *et al.*, 1992). Result of this calculation, summarized on table 6.IV, evaluates to 1.85 GT the annual production of the Southern Ocean, increasing by a factor 3 the previous estimate by El Sayed (1984). Within this extreme environment, sea ice associated systems contribute for 30 % of the global primary production. Note that the calculations assume that the high protozoan grazing pressure observed in the Weddell Sea also applies in the whole circumpolar marginal ice zone. Recent data reporting occasional elevated phytoplankton biomass in the Ross Sea (Smith & Nelson, 1985; Tréguer *et al.*, 1991) and the Prydz Bay (Dehairs, pers. com.) contradict

however the above conclusion. On the other hand, grazing pressure by pelagic krill is not taken into account in the ice-free areas owing to the scarce knowledge on krill distribution. Contribution of sea ice associated areas to annual primary production as determined in the present report (Table 6.IV) constitutes thus a minimum estimate.

Table 6.III : Mean daily primary production in different areas of the Southern Ocean.

| Season | POOZ | MIZ | | PICZ | References |
|---|------|----------------|------------------|-------------------|--|
| | (1) | <15% IC (1) | 15-85% IC (1) | 85-100% IC (1) | |
| Growing season | | | | | |
| October | 180 | 160 | 85 | 30 | This model |
| November, December | | | | | |
| January, February | 300 | 470 | 300 | 60 | This model |
| Autumn | | | | | |
| March | 130 | | 130 | 30 | Smith & Nelson, 1990 |
| April, May | 100 | | 100 | 20 | Cota <i>et al.</i> , 1991 Cota <i>et al.</i> , 1991 |
| Winter | | | | | |
| June, July | 10 | | | 2 | Brightman & Smith, 1991 |
| ----- | | | | | |
| (1) mgC m ⁻² d ⁻¹ | | | | | |
| IC = ice cover | | | | | |

Table 6.IV : Annual primary production in the Southern Ocean.

| Area | Primary production 10 ¹² gC | |
|-------------------|--|------------|
| Open ocean | 1,293 | |
| Marginal ice zone | 507 | |
| Ice-covered area | 48 | |
| Total : | 1,850 | or 1.85 GT |

7. CONCLUSIONS AND PERSPECTIVES

The comprehensive analysis of the physical and chemical transformations and biological processes occurring in the marginal ice zone of the northwestern Weddell Sea at the time of ice retreat evidences the key role played by sea ice in determining the structure and functioning of the planktonic food web at the receding ice-edge. This role is twofold : (i) its structural characteristics provides a habitat for microorganisms and a refuge for overwintering krill and other mesozooplankton; (ii) the dynamics of its retreat and formation strongly influences the light conditions experienced by phytoplanktonic cells.

As a matter of evidence, the physical processes associated with ice retreat enhance the development of phytoplankton blooms at the receding ice-edge by providing phytoplankton cells with optimal light conditions owing to the formation of shallow vertically stable surface layer as a result of meltwater production.

The magnitude of the phytoplanktonic bloom is then regulated by the combined action of grazing pressure by protozoa, mesozooplankton and krill and meteorological conditions, these latter determining the vertical stability of surface waters. The relative importance of micro- and mesograzers in controlling phytoplankton ice-edge blooms, and hence the structure of the planktonic food-web, is determined both by the composition of sea-ice assemblages at the time of ice melting and the presence beneath the ice of overwintering krill and mesozooplankton. The former depends on the initial composition of sea-ice assemblages originating from planktonic and benthic auto- and heterotrophic microorganisms scavenged at the time of ice formation, the physico-chemical characteristics of the ice habitat and the environmental light conditions of early spring. Overwintering herbivorous underneath the ice, by grazing selectively on large phytoplankton like some diatoms and *Phaeocystis* colonies or their aggregates strongly determine the species composition of the seeded microbial population and hence the structure of the planktonic food-web developing at the receding ice-edge. In the presence of krill, a very efficient microbial network composed of nano-sized auto- and heterotrophs thus predominates and moderate phytoplankton ice-edge blooms are expected. On the contrary, in the absence of overwintering krill, large blooms dominated by micro-sized phytoplanktonic species should prevail.

The extent of the bloom in ice-free area is determined by local meteorological conditions, in particular the frequency and intensity of wind mixing events, and by passage of krill swarms. The impact of these latter on the structure of the planktonic food-web, whilst episodic, is dramatic as these grazers literally clear the water from phytoplankton, heterotrophic microorganisms and copepods. Only bacterial activity is enhanced after a krill event, owing to the release of organic matter resulting from the feeding activity of these grazers.

Thus, although the enhancement of ice-edge blooms by the physics associated to the process of ice melting is a general feature in the circumpolar marginal ice zone of the Southern Ocean, regional differences in the magnitude and extent of these blooms are however to be expected, depending on the geographical distribution of overwintering and pelagic krill. Our field experience as well as our literature knowledge suggest that large diatoms and *Phaeocystis* occur occasionally in the Ross Sea and Prydz Bay area whilst moderate ice-edge blooms of nanophytoplankton prevail in the Weddell Sea. In particular, our investigations in the marginal ice zone of the northwestern Weddell Sea revealed the existence in this area of a very efficient complex microbial network, with nano-sized protozoa grazing on phytoplankton and bacteria. Application in this area of a coupled hydrodynamical-biological model established on the basis of physical and biological processes measurements carried out during the EPOS cruise stress the quantitative importance of protozoa as regulator of ice-edge phytoplankton blooms, as link between krill and microorganisms and as important ammonium regenerator, inducing a shift from a nitrate- to a ammonium-based primary production system.

Taking all this into consideration, it becomes clear that the contribution of ice-edge blooms to the overall annual production of the Southern Ocean will be appraised by developing coupled hydrodynamical-biological models along the course of a seasonal cycle in different sub-regions of the circumpolar marginal ice zone of the Southern Ocean, chosen according to the physical characteristics and krill distribution. The general structure of this ecological model is illustrated by Fig. 7.1 that shows the seasonal cycle of sea ice and the coupling between the sea ice community (SIMCO) and planktonic (SWAMCO) biological model occurring in early spring and autumn. The former constitute the initial conditions of the SWAMCO model at the time of ice melting whilst the latter constitute the initial conditions of the SIMCO model at the time of ice formation. The ecological model of the microbial network developed in the

marginal ice zone constitutes a first step in this direction. Some limitation still prevents its successful application in every sub-region of the circumpolar marginal ice zone of the Southern Ocean. These limitations lie for instance in the inadequacy of the mathematical description of the grazing function, the consideration of one single phytoplankton compartment, and the lack of taking into account of krill. Further development of our research in the Southern Ocean will include the improvement of the existing model, with the development of two additional sub-models, describing respectively the metabolism of large phytoplankton species and protozooplankton and the consideration of the role of overwintering and pelagic krill.

ANTAR
II/05

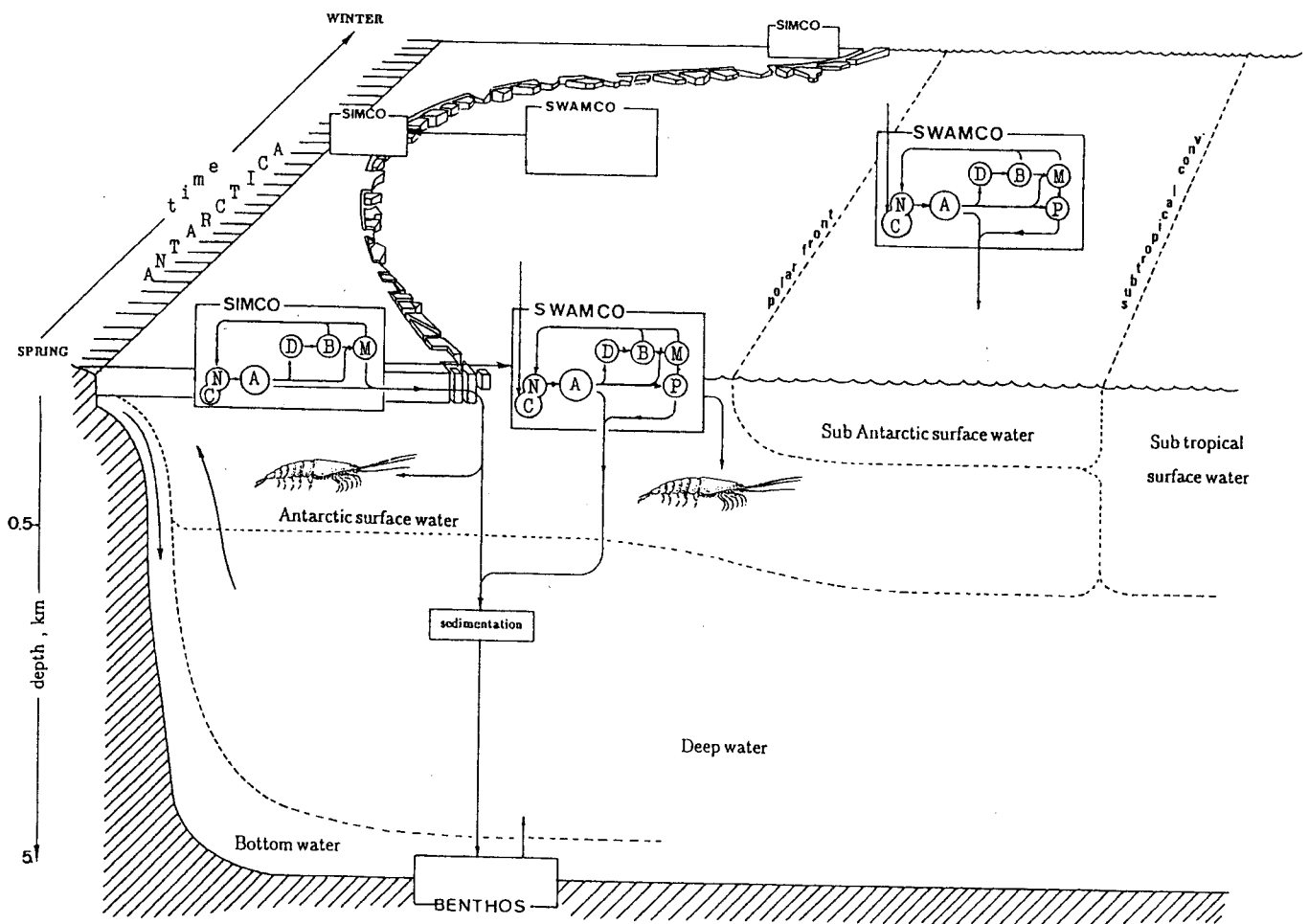


Figure 7.1 : Diagrammatic representation of the ecological model applied to the whole Southern Ocean along the course of a seasonal cycle.
SIMCO : model of sea ice microbial communities; **SWAMCO:** model of sea water microbial community. **C :** CO₂; **N :** inorganic nutrients; **A :** microalgae; **D :** dissolved organic matter; **B :** bacteria; **M :** micrograzers; **P :** particulate organic matter.



8. ACKNOWLEDGMENTS

This work is part of the Belgian Scientific Research Programme on Antarctica, funded by the Science Policy Office (Brussels, Belgium), under contract ANTAR/05.

ANTAR
II/05

All the data presented in this report were collected during the European venture EPOS on board of the German vessel RV POLARSTERN.

We take this opportunity to express our gratitude to the European Science Foundation and the Alfred Wegener Institut for allowing participation in EPOS and to thank the Captain and the crew of RV POLARSTERN for their helpful assistance during the work. We are especially grateful to Victor Smetacek and Kees Veth, respectively the Chief Scientist and Scientific Advisor of the Leg 2. The bright ideas and delightful personality of Victor, the organisations skill and comradeship of Kees contribute to the large success of this expedition.

The scientific concepts and ecological models we develop here are not only the fruit of the knowledge we gained from other studies in temperate aquatic environments, but mostly originate from scientific collaborations and discussions we had on board and during the different workshops and symposium that followed the expedition. We are especially grateful to Victor Smetacek. His impressive knowledge of polar biology, and his enthusiasm, greatly stimulated our understanding of the Antarctic pelagic ecosystem and the key role of krill. Also we thank Kees Veth for the physical development of the model and for the "credit" he gave to biological demands.

Our gratefulness to Peter Bjørnsen and Jorma Kuparinen who contributed to our knowledge of the protozoan grazing function and to Hein de Baar who puts some light on the iron problem.

Special thanks to our Belgian colleagues, Frank Dehairs and Leo Goeyens who took an active part in the formulation of the inorganic nitrogen loop.

Finally, all our thanks to our friends and colleagues of the EPOS Leg 2 expedition, each contributed in their individual unique way to the success of this expedition.

Last but not least, we thank Janine D'haenens for her assistance in the edition of this report.

9. REFERENCES

- Ackley, S.F., Buck, K.R. & Taguchi, S., 1979. Standing crop of algae in the sea ice of the Weddell Sea region. *Deep Sea Res.*, 26A : 269-282.
- Ackley, S.G., 1981. A review of sea-ice weather relationships in the Southern Hemisphere. In : *Sea level, ice and climate change*, Proceedings of the Canberra Symposium, IAHS Publ., 136 : 127-159.
- Becquevort, S., Mathot, S. & Lancelot, C., 1992. Interaction in the microbial community of the marginal ice zone of the northwestern Weddell Sea through size distribution analysis, *Polar Biol.*, 12 : 211-218.
- Beers, J.R. & Stewart, G.L., 1970. Numerical abundance and estimated biomass of microzooplankton. In : J.D.H. Strickland, ed., *The Ecology of the plankton of La Jolla, California, in the period April through September 1967*. Bull Scripps Inst. Oceanogr., 17 : 67-87.
- Bergström, B., Hempel, G., Hempel, I., Marschall, H.P., North, A., Siegel, B. & Strömberg, J.O., 1989. Antarctic krill (*Euphausia superba*). In : *The expedition Antarktis VII/1 and 2 (EPOS Leg 1) of RV "Polarstern" in 1988/1989. Reports on Polar Research*, Hempel I., ed., pp. 149-156.
- Bergström, B.I., Hempel, G., Marschall, H.P., North, A.W., Siegel V. & Strömberg, J.O., 1990. Spring distribution, size composition and behaviour of krill *Euphausia superba* in the western Weddell Sea. *Polar Rec.*, 26 : 85-89.
- Billen, G. & Fontigny, A., 1987. Dynamics of *Phaeocystis*-dominated spring bloom in Belgian coastal waters. II. Bacterioplankton dynamics. *Mar. Ecol. Progr. Ser.*, 37 : 249-257.
- Billen, G. & Servais, P., 1989. Modélisation des processus de dégradation de la matière organique en milieu aquatique. In : *Micro-organismes dans les écosystèmes océaniques*. Bianchi, M. et al., ed., pp 219-245, Masson, Paris.
- Billen, G., 1990. Delayed development of bacterioplankton with respect to phytoplankton : a clue for understanding their trophic relationships. *Arch. Hydbiol. Beih. Ergebn. Limnol.*, 114 : 415-429.
- Billen, G., 1991. Protein degradation in Aquatic Environments. In : *Microbial Enzymes in Aquatic Environments*, R. Chrost, ed., Springer Verlag, 7 : 123-143.
- Billen, G. & Becquevort, S., 1991. Phytoplankton-bacteria relationship in the Antarctic marine ecosystem. *Polar Res.* 10 : 245-253.
- Bjørnsen, P.K. & Kuparinen, J., 1991. Growth and herbivory by heterotrophic dinoflagellates in the Southern Ocean studied by microcosm experiments. *Mar. Biol.*, 109 : 397-405.
- Bölter, M. & Dawson, R., 1982. Heterotrophic utilization of biochemical compounds in Antarctic waters. *Neth.J.Sea Res.*, 16 : 315-332.
- Brightman, R.I. & Smith, W.O., Jr. 1989. Photosynthesis-irradiance relationships of Antarctic phytoplankton during austral winter. *Mar. Ecol. Progr. Ser.*, 53 : 143-151.

- Buma, A.G.J., de Baar, H., Nolting, R.F. & van Bennekom, A.J., 1991. Metal enrichment experiments in the Weddell-Scotia Seas : Effects of iron and manganese on various plankton communities, *Limnol. Oceanogr.*, 36 : 1865-1878.
- Cederlöf, U., Ober, S., Schmidt, R., Svansson, A. & Veth, C., 1989. Physics and chemistry : Hydrography. In : Hempel, I., Schalk, P.H. & Smetacek, V., ed. *Reports on Polar Research - The expedition ANTARKTIS VII/3 (EPOS Leg 2) of the RV "Polarstern" in 1988/89*, pp. 14-19.
- Coale, K.H., 1991. The effects of iron, manganese, copper and zinc enrichments on productivity and biomass in the Subarctic Pacific, *Limnol. Oceanogr.*, 36 : 1851-1864.
- Cohen, D. & Parnas, H., 1976. An optimal policy for the metabolism of storage materials in unicellular algae, *J. Theor. Biol.*, 56 : 1-18.
- Comiso, J.C. & Zwally, H.J., 1984. Concentration gradients and growth and decay characteristics of the seasonal sea ice cover, *J. Geophys. Res.*, 89 : 8081-8103.
- Comiso, J.C. & Zwally, H.J., 1989. Polar Microwave Brightness Temperatures from Nimbus-7 SMMR, *NASA Reference Publication 1223*, 82 p.
- Comiso, J.C., Maynard, N.G., Smith, W.O. & Sullivan, C.W., 1990. Satellite ocean color studies of Antarctic ice edges in summer and autumn, *J. Geophys. Res.*, C6 : 9481-9496.
- Cota, G.F., Kottmeier, S.T., Robinson, D.H., Smith, W.O. Jr & Sullivan, C.W., 1991. Bacterioplankton in the marginal ice zone of the Weddell Sea : biomass, production and metabolic activities during austral autumn. *Deep-Sea Res.*, 37(7) : 1145-1167.
- Cuzin-Roudy, J. & Schalk, P.H., 1989. Macrozooplankton - Biomass, development and activity. In : *The Expedition Antarktis VII/3 (EPOS LEG 2) of RV "Polarstern" in 1988/89, Reports on Polar Research*, Hempel, I., Schalk, P.H. & Smetacek, V., ed., pp. 146-159.
- Deacon, G., 1984. The Antarctic circumpolar ocean, *Studies in Polar Research*, Cambridge University Press, 180 p.
- de Baar, H., Buma, A.G.J., Nolting, R.F., Cadée, G.C., Jacques, G. & Tréguer, P., 1990. On iron limitation of the Southern Ocean : Experimental observations in the Weddell and Scotia Sea. *Mar. Ecol. Progr. Ser.*, 65 : 105-122.
- Denman, K.L., 1973. A time-dependent model of the upper ocean. *J. Phys. Ocean.*, 3 : 173-184.
- Dorsey, T.E., Mc Donald, P. & Roels, O.R., 1978. Measurements of phytoplankton protein content with the heated biuret-folin assay. *J. Phycol.*, 14 : 167-171.
- Dugdale, R.C. & Wilkerson, F.P., 1990. Iron addition experiments in the Antarctic, *Global Biochem. Cycles*, 4(1) : 13-19.
- Edler, L., 1979. Recommendations for marine biological studies in the Baltic Sea - Phytoplankton and Chlorophyll, *Baltic Marine Biologist*, 5 : 1-38.
- Eicken, H., Lange, M.A. & Dieckmann, G.S., 1991. Spatial variability of sea-ice properties in the northwestern Weddell Sea. *J. Geophys. Res.*, 96(C6) : 10603-10615.

- El-Sayed, S.Z., 1984. Productivity of the Antarctic waters : a reappraisal. In : *Marine Phytoplankton and productivity*, Holm-Hansen, O., Bolis, L. & Gilles, R., ed., Springer, Berlin, pp. 73-91.
- EPOS-Leg 2 (1991). Data report - Hydrography, Part 1 (second edition), NIOZ, Texel, The Netherlands.
- Eppley, R.W. & Peterson, B.J., 1979. Particulate organic flux and planktonic new production in the deep ocean, *Nature*, Lond., 282 : 677-680.
- Fontigny A., Billen G. & Vives Rego J., 1987. Some kinetics characteristics of exoproteolytic activity in coastal sea water. *Est.Coast.Mar.Sci.*, 25 : 127-134.
- Fransz, H.G., 1988. Vernal abundance, structure and development of epipelagic copepod populations of the Eastern Weddell Sea (Antarctica). *Polar Biol.*, 9 : 107-114.
- Fransz, H.G. & Gonzales, S.R., 1992. The spring-summer distribution, development and production of epipelagic copepod populations in the Weddell-Scotia Confluence, *EPOS Symposium Abstracts*, 103 pp.
- Fuhrman, J.A. & Azam, F., 1982. Thymidine incorporation area measure of heterotrophic bacterioplankton evaluation in marine surface waters : evaluation and field result. *Mar.Biol.*, 66 : 109-120.
- Garrison, D.L., Ackley, S.F. & Buck, K.R., 1983. A physical mechanism for establishing algal populations in frazil ice, *Nature*, Lond., 306 : 363-365.
- Garrison, D.L. & Buck, K.R., 1985. Sea-ice algal communities in the Weddell Sea : Species composition in ice and plankton assemblages, *Marine Biology of Polar Regions and Effects of Stress on Marine Organisms*, J.S. Gray & E. Christiansen, ed., J. Wiley & Sons Ltd.
- Garrison, D.L., Sullivan, C.W. & Ackley, S.F., 1986. Sea ice communities in Antarctica. *BioScience*, 36 : 243-249.
- Garrison, D.L., Buck, K.R. & Fryxell, G.A., 1987. Algal assemblages in Antarctic pack ice and in ice-edge plankton, *J. Phycol.*, 23 : 564-572.
- Garrison, D.L. & Buck, K.R., 1989a. Protozooplankton in the Weddell sea, Antarctica : Abundance and distribution in the ice-edge zone, *Polar Biol.*, 9 : 341-351.
- Garrison, D.L. & Buck, K.R., 1989b. The biota of antarctic pack ice in the Weddell Sea and Antarctic Peninsula regions, *Polar Biol.*, 10 : 211-219.
- Garrison, D.L. & Gowing, M.M., 1993. Protozooplankton. In : *Antarctic Microbiology* Friedmann, E.I., ed., in press.
- Goeyens, L., Sörensson, F., Tréguer, P., Morvan, J., Panouse, M. & Dehairs, F., 1991a. Spatiotemporal variability of inorganic nitrogen stocks and uptake fluxes in the Scotia-Weddell Confluence area during November and December 1988, *Mar. Ecol. Progr. Ser.*, 77(1) : 7-19.
- Goeyens, L., Tréguer, P., Lancelot, C., Mathot, S., Becquevort, S., Morvan, J., Dehairs, F. & Baeyens, W., 1991b. Ammonium regeneration in the Scotia-Weddell Confluence area during spring 1988. *Mar. Ecol. Progr. Ser.*, 78 : 241-252.

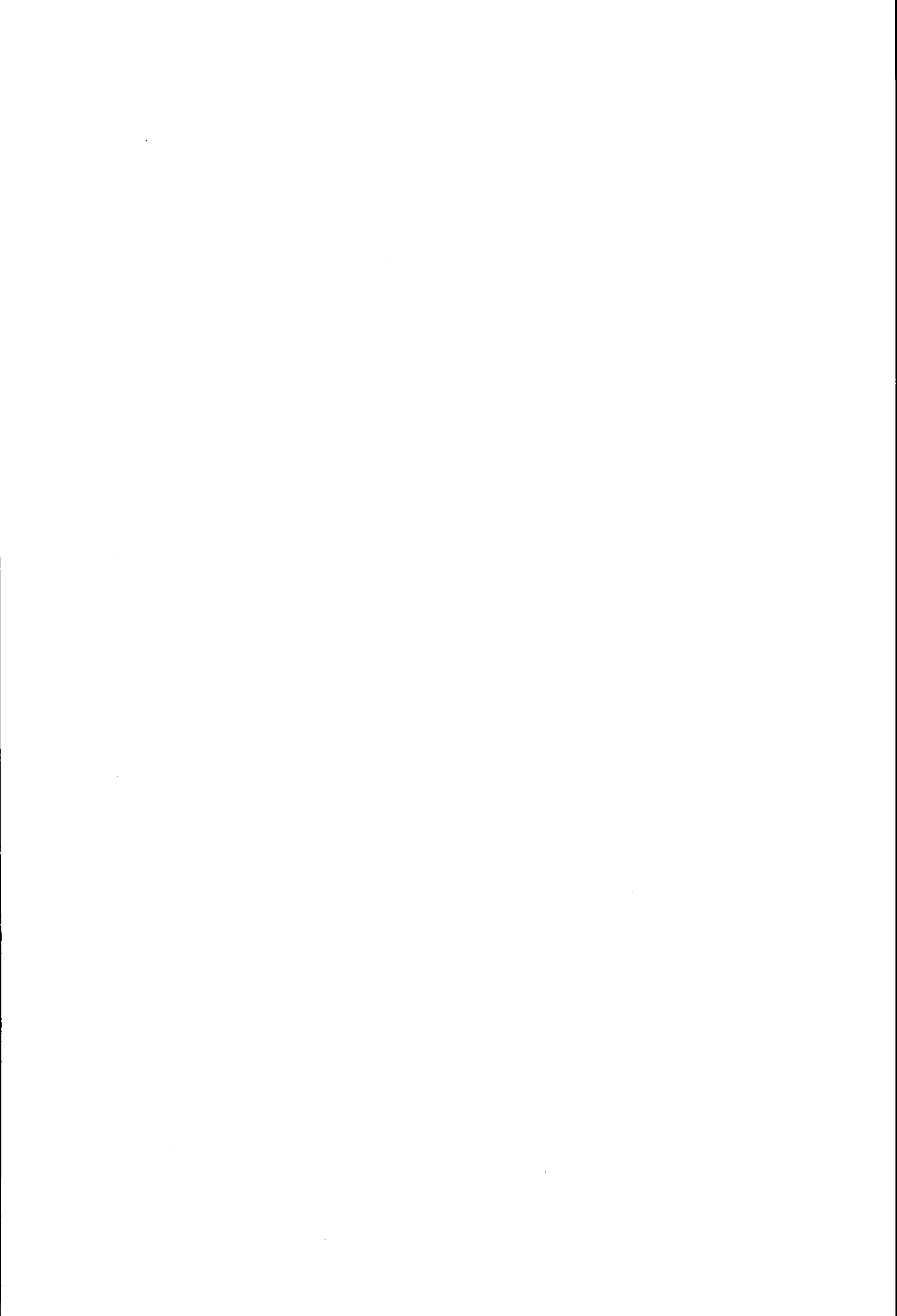
- Gordon, A.L., 1967. Structure of Antarctic waters between 20° W and 170° W. *Antarctic Map Folio Series*, Folio 6, V.C. Bushnell, ed., Amer. Geogr. Soc. pp 10.
- Hayes, P.K., Whitaker, T.M. & Fogg, G.E., 1984. The distribution and nutrient status of phytoplankton in the Southern Ocean between 20° and 70° W, *Polar Biol.* 3 : 153-165.
- Hempel, G., 1985. Antarctic marine food webs. In : *Antarctic Nutrient Cycles and Food Webs*, Siegfried, W.R., Condy, P.R. & Laws, R.M., ed., Springer Berlin Heidelberg New York, pp 266-270.
- Hewes, C.D., Holm-Hansen, O. & Sakshaug, R., 1985. Alternate carbon pathways at lower trophic levels in the Antarctic food web. In : *Antarctic nutrient cycles and food webs*, Siegfried, W.R., Condy, P.R. & Laws, R.M., ed., pp. 237-283.
- Hewes, C.D., Sakshaug, E., Reid, F.M. & Holm-Hansen, O., 1990. Microbial autotrophic and heterotrophic eucaryotes in Antarctic waters : Relationships between biomass and chlorophyll, adenosine triphosphate and particulate organic carbon, *Mar. Ecol. Progr. Ser.*, 63 : 27-35.
- Horner, R.A., 1985. Ecology of sea ice microalgae. In : *Sea Ice Biota*, Horner, R.A., ed., CRC Press, Boca Raton, pp. 83-103.
- Horner, R.A., Syvertsen, E.E., Thomas, D.P. & Lange, C., 1988. Proposed terminology and reporting units for sea ice algal assemblages. *Polar Biol.*, 8 : 249-253.
- Jacques, G. & Panouse, M., 1991. Biomass and composition of size fractionated phytoplankton in the Weddell Sea Confluence area, *Polar Biol.*, 11 : 315-328.
- Koroleff, F., 1969. Direct determination of ammonia in natural waters as indophenol blue. *Comm. Meet. int. Counc. Explor. Sea*, C.M.-ICES/C : 19-22.
- Koroleff, F., 1976. Determination of ammonia. In : Grasshof, K., ed., *Methods of seawater analysis*. Verlage Chemie, Weinheim, p. 126-133.
- Kottmeier, S.T. & Sullivan, C.W., 1987. Late winter primary production and bacterial production in sea ice and seawater west of the Antarctic Peninsula. *Mar. Ecol. Progr. Ser.* 36 : 287-298.
- Lancelot, C. & Mathot, S., 1985. Biochemical fractionation of primary production by phytoplankton in Belgian coastal waters during short- and long-term incubations with ¹⁴C-bicarbonate. I. Mixed diatom population. *Mar. Biol.*, 86(3) : 219-226.
- Lancelot, C., Billen, G. & Mathot, S., 1989. Ecophysiology of phytoplankton and bacterioplankton growth in the Southern Ocean. In : *Belgian Scientific Research Programme on Antarctica. Scientific Results of Phase One (Oct.85 - Jan.89)*. Vol.1 : *Plankton Ecology*, pp. 1-97.
- Lancelot, C., Veth, C. & Mathot, S., 1991a. Modelling ice-edge phytoplankton bloom in the Scotia-Weddell sea sector of the Southern Ocean during spring 1988. *J. Mar. Syst.*, 2 : 333-346.
- Lancelot, C., Billen, G., Veth, C., Becquevort, S. & Mathot, S., 1991b. Modelling carbon cycling through phytoplankton and microbes in the Scotia-Weddell Sea area during sea ice retreat; *Marine Chemistry*, 35(1-4) : 305-324.

- Lancelot, C., Mathot, S., Veth, C. & de Baar, H., 1993. Factors controlling phytoplankton ice-edge blooms in the marginal ice zone of the northwestern Weddell Sea during sea ice retreat 1988: field observations and mathematical modelling, *Polar Biol.*, 13 : 000-000.
- Lange, M.A. & Eicken, H., 1989. Sea ice conditions. In : *The Expedition Antarktis VII 1 and 2 (Epos I) of RV "Polarstern" in 1988/1989*. *Berichte zur Polarforschung*, Hempel, I., ed., pp. 55-63.
- Larsson, A.M., 1990. Hydrological, chemical and biological observations during EPOS 1. Distributed by Department of Oceanography, University of Gothenburg, Box 4038, S-400 40 Gothenburg, Sweden.
- Lorenzen, C.J., 1967. Determination of chlorophyll and phaeopigments: spectrophotometric equations, *Limnol. Oceanogr.*, 12 : 343-346.
- Magas, B. & Svansson, A., 1989. Optics. In : *The expedition Antarktis VII/3 (EPOS Leg 2) of RV "Polarstern" in 1988/1989*, *Berichte zur Polarforschung*, Hempel, I., Schalk, P.H. & Smetacek, V., ed., pp. 20-24.
- Marr, J.W.S., 1962. The natural history and geography of the Antarctic krill (*Euphausia superba* Dana). *Discovery Rep.* 32:33-464.
- Marschall, H.P., 1988. The overwintering strategy of Antarctic krill under the pack-ice of the Weddell Sea, *Polar Biol.*, 9 : 129-135.
- Martin, J.H. & Fitzwater, S.E., 1988. Iron deficiency limits phytoplankton growth in the north-east Pacific Subarctic, *Nature*, 331 : 341-343.
- Martin, J.H., Gordon, R.M. & Fitzwater, S.E., 1990a. Iron in Antarctic waters, *Nature*, 345 : 156-158.
- Martin, J.H., Fitzwater, S.E. & Gordon, R.M., 1990b. Iron deficiency limits phytoplankton growth in Antarctic waters, *Global Biogeochemical Cycles*, 4 : 5-12.
- Mathot, S., Becquevort, S. & Lancelot, C., 1991. Microbial communities from the sea ice and adjacent water column at the time of ice melting in the northwestern part of the Weddell Sea. *Polar Res.* 10 : 267-2755
- Mathot, S., Dandois, J.M. & Lancelot, C., 1992. Gross and net primary production in the Scotia-Weddell Sea sector of the Southern Ocean during spring 1988, *Polar Biol.*, 12 : 321-332.
- Mitchell, B.G. & Holm-Hansen, O., 1991. Observations and modelling of the Antarctic phytoplankton crop in relationship to mixing depth, *Deep Sea Res.*, 38(8/9A) : 981-1008.
- Neveux, J. & Panouse, M., 1987. Spectrofluometric determination of chlorophylls and phaeopigments, *Arch. für Hydrobiol.*, 109 : 567-581.
- Nolting, R.F., de Baar, H.J.W., van Bennekom, A.J. & Masson, A., 1991. Cadmium, copper and iron in the Scotia Sea, Weddell Sea and Weddell/Scotia Confluence (Antarctica), *Marine Chemistry*, 35 : 219-243.
- Palmisano, A.C. & Sullivan, C.W., 1983. Sea ice microbial communities (SIMCO). I. Distribution, abundance, and primary production of ice microalgae in Mc Murdo Sound, Antarctica in 1980, *Polar Biol.*, 2 : 171-177.

- Parsons, T.R. & Strickland, J.D.H., 1962. On the production of particulate organic carbon by heterotrophic processes in seawater, *Deep Sea Research*, 8 : 211-222.
- Platt, T., Gallegos, L.L. & Harrison, W.G., 1980. Photoinhibition of photosynthesis in natural assemblages of marine phytoplankton. *J. Mar. Res.*, 38 : 687-701.
- Porter, K.G. & Feig, Y.S., 1980. The use of DAPI for identifying and counting aquatic microflora. *Limnol.Oceanogr.*, 25(5) : 943-948.
- Riebesell, U., Schloss, I. & Smetacek, V., 1991. Aggregation of algae released from melting sea ice : Implication for seeding and sedimentation, *Polar Biol.*, 11 : 239-248.
- Riemann, B., Bjørnsen, P.K., Newell, S.Y. & Fallon, R.D., 1987. Calculation of bacterioplankton production from measurements of ³H-Thymidine incorporation. *Limn.Oceanogr.* 32 : 471-476.
- Schalk, P.H., 1990. Biology activity in the Antarctic zooplankton community, *Polar Biol.*, 10 : 405-411.
- Schnack, S.B., Smetacek, V.S., von Bodungen, B. & Stegmann, P., 1985. Utilization of phytoplankton by copepods in Antarctic Waters during spring. In : *Marine Biology of Polar Regions and Effects of Stress on Marine Organisms*, Gray, J.S. & Christiansen, M.E., ed., John Wiley & Sons Ltd, pp. 65-81.
- Servais, P., Billen, G. & Vives-Rego, J., 1985. Rate of bacterial mortality in aquatic environments. *Appl.Environ.Microbiol.* 49 : 1448-1455.
- Servais, P., 1986. Etude de la dégradation de la matière organique par les bactéries hétérotrophes en rivière. Développement d'une démarche méthodologique et application à la Meuse belge. Université Libre de Bruxelles. Faculté des Sciences. Thèse, 271 pp.
- Servais, P., Billen, G. & Hascoët, M.C., 1987. Determination of the biodegradable fraction of dissolved organic matters in waters, *Water Res.*, 21 : 445-450.
- Servais, P., Billen, G., Martinez, J. & Vives-Rego, J., 1989. Estimating bacterial mortality by the disappearance of ³H-labelled intracellular DNA. Technical validation and field measurements. *FEMS Microbiol. Ecology.*, 62 : 119-126.
- Shuter, B., 1979. A model of physiological adaptation in unicellular algae. *J. Theor. Biol.*, 78 : 519-552.
- Siegel, V., Bergström, B., Strömberg, J.O. & Schalk, P.H., 1990. Distribution, size frequencies and maturity stages of krill, *Euphausia superba*, in relation to sea-ice in the northern Weddell Sea. *Polar Biol.*, 10 : 549-557.
- Simon, M. & Azam, F., 1989. Protein content and protein synthesis rates of planktonic marine bacteria. *Mar. Ecol. Progr. Ser.*, 51 : 201-213.
- Smetacek, V., Scharek, R. & Nöthig, E.-M., 1990. Seasonal and regional variation in the pelagial and its relationship to the life history cycle of krill. In : *Antarctic Ecosystems : Ecological change and conservations*, Kerny, R. & Hempel, G., ed., Springer Verlag, Berlin Heidelberg, p.103-114.
- Smith, W.O.Jr & Nelson, D.M., 1985. Phytoplankton bloom produced by a receding ice-edge in the Ross Sea : Spatial coherence with the density field, *Science*, 227 : 163-165.

- Smith, W.O.Jr & Nelson, D.M., 1986. Importance of ice-edge phytoplankton blooms in the Southern Ocean., *Bioscience*, 36 : 251-257.
- Smith, W.O.Jr & Nelson, D.M., 1990. Phytoplankton growth and new production in the Weddell Sea marginal ice zone in the austral spring and autumn. *Limnol. Oceanogr.*, 35(4) : 809-821.
- Somville, M. & Billen, G., 1983. A method for determining exoproteolytic activity in natural waters. *Limnol. Oceanogr.*, 28 : 190-193.
- Somville, M., 1984. Measurement and study of substrate specificity of exoglucosidase activity in eutrophic water. *Appl. Environ. Microbiol.*, 48 : 1181-1185.
- Stretch, J.J., Hamner, P.P., Hamner, W.M., Michel, W.C., Cook, J. & Sullivan, C.W., 1988. Foraging behavior of Antarctic krill *Euphausia superba* on sea ice microalgae, *Mar. Ecol. Progr. Ser.*, 44 : 131-139.
- Sullivan, C.W., 1985. Sea ice bacteria : reciprocal interactions of the organisms and their environment. In : *Sea Ice Biota*, Horner, R.A., ed., CRC Press, Boca Raton, pp. 159-171.
- Sullivan, C.W., McClain, C.R., Comiso, J.C. & Smith, W.O.Jr, 1988. Phytoplankton standing crops within an Antarctic ice-edge assessed by satellite remote sensing. *J. Geophys. Res.*, 93(C10) : 12487-12498.
- Tilzer, M.M., Elbrächter, M., Gieskes, W.W. & Beese, B., 1986. Light-temperature interactions in the control of photosynthesis in Antarctic phytoplankton. *Polar Biol.* 5 : 105-111.
- Tilzer, M.M. & Dubinsky, Z., 1987. Effects of temperature and day length on the mass balance of Antarctic phytoplankton. *Polar Biol.*, 7 : 35-42.
- Tréguer, P. & Le Corre, P., 1975. Manuel d'analyses automatiques des sels nutritifs par Auto Analyser II Technicon, Université de Bretagne Occidentale, Brest.
- Utermöhl, H., 1958. Zur Vervollkommnung der quantitativen Phytoplankton - Methodik. *Mitt. int. Verein theor. angew. Limnol.*, 9 : 1-38.
- Van Aken, H.M., 1984. A one dimensional mixed-layer model for stratified Shelf Seas with tide and wind-induced mixing. *Dt. Hydrogr. Z.*, 37 : 1-27.
- van Bennekom, J., Estrada, M., Goeyens, L., Magas, B., Masson, A., Morvan, J., Tréguer, P., Svansson, A. & Veth, C., 1989. Distribution of nutrients in surface, subsurface and deep layers. In : *The Expedition Antarktis VII/3 (EPOS Leg 2) of RV "Polarstern" in 1988/1989*, Hempel, I., Schalk, P.H. & Smetacek, V., ed., *Ber. Polarforsch.*, pp 47-56.
- van Franeker, J.A., 1989. Sea ice conditions. In : *The Expedition Antarktis VII/3 (EPOS Leg 2) of RV "Polarstern" in 1988/89*, Hempel, I., Schalk, P.H. & Smetacek, V., ed., *Berichte Polarforschung*, pp. 10-13.
- Veth, C., 1991. The evolution of the upper water layer in the marginal ice zone, austral spring 1988, Scotia-Weddell Sea, *J. Mar. Syst.*, 2 : 451-464.
- Veth, C., Lancelot, C. & Ober, S., 1992. On processes determining the vertical stability of surface waters in the marginal ice zone of the north-western Weddell Sea and their relationship with phytoplankton bloom development. *Polar Biol.*, 12 : 237-243.

- von Bodungen, B., Smetacek, V.S., Tilzer, M.M. & Zeitzschel, B., 1986. Primary production and sedimentation during spring in the Antarctic Peninsula region, *Deep Sea Res.*, 33 : 177-194.
- Weber, L.H. & El-Sayed, S.Z., 1987. Contributions of the net, nano- and picoplankton to the phytoplankton standing crop and primary productivity in the Southern Ocean. *J. Plankton Res.*, 9(5) : 973-994.
- Westerlund, S. & Öhman, P., 1991. Iron in the water column of the Weddell Sea, *Marine Chemistry*, 35:199-217.
- Whitaker, T.M., 1977. Sea ice habitats of Signy Island (South Orkneys) and their primary productivity. In : Llano, G.A., ed., *Adaptations within Antarctic ecosystems*. Gulf Publ. Co., Houston, Texas, p. 75-82.
- Wright, R.T. & Hobbie, J.E., 1965. The uptake of organic solutes in lake water. *Limnol. Oceanogr.*, 10 : 22-28.
- Zwally, H.J., Parkinson, C.L. & Comiso, J.C., 1983. Variability of Antarctic sea ice and changes in carbon dioxide. *Science*, 220 : 1005-1012.





RESEARCH CONTRACT ANTAR/II/08

**SEASONAL
FLUCTUATION
OF EXPORT
AND RECYCLED
PRODUCTION
IN DIFFERENT
SUBAREAS OF THE
SOUTHERN OCEAN**

L. Goeyens and F. Dehairs

LABORATORIUM VOOR
ANALYTISCHE CHEMIE

Vrije Universiteit Brussel
Pleinlaan, 2
B-1050 Brussels, Belgium

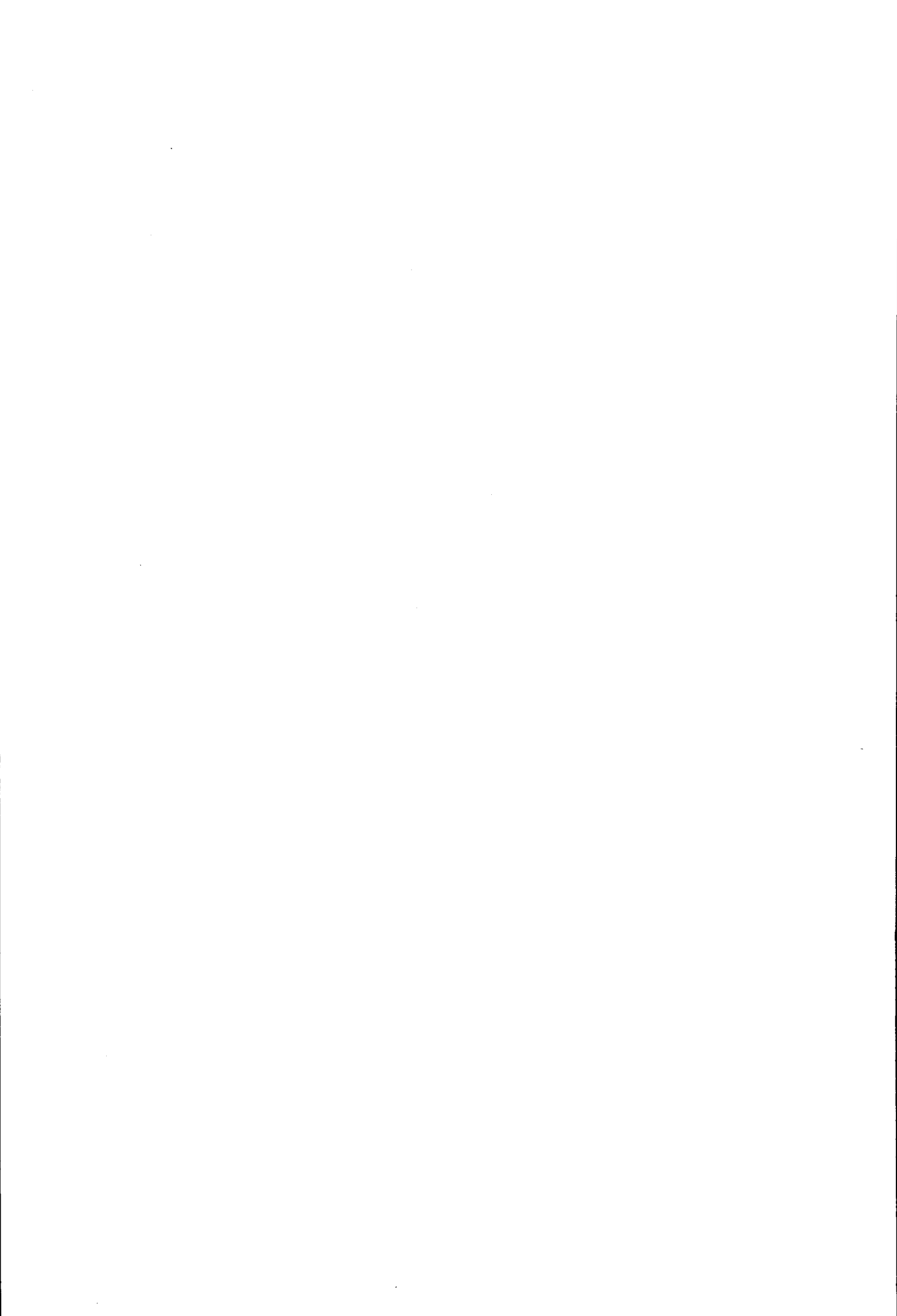


TABLE OF CONTENTS

| | |
|--|----|
| ABSTRACT | 2 |
| INTRODUCTION | 4 |
| MATERIAL AND METHODS | 8 |
| 1. Cruises | 8 |
| 2. Physical, chemical and biological parameters | 13 |
| 3. Biological activities | 15 |
| RESULTS | 18 |
| 1. Dissolved and particulate stocks | 18 |
| 2. Nitrate depletions and ammonium availabilities | 23 |
| 3. Organic carbon and nitrogen | 24 |
| 4. The biogenic Si fraction | 25 |
| DISCUSSION | 26 |
| 1. Distributions of nitrogenous nutrients in different areas of the Southern Ocean | 26 |
| 2. Suspended barite and particulate matter in Antarctic waters | 35 |
| 3. Ammonium build-up by heterotrophic remineralization | 41 |
| 4. Nitrate and ammonium uptake by autotrophic primary producers | 46 |
| 5. Barite and export production | 53 |
| 6. A scenario for the development of Southern Ocean blooms | 59 |
| CONCLUSIONS | 68 |
| ACKNOWLEDGEMENTS | 70 |
| REFERENCES | 71 |

ABSTRACT

As the role of the Southern Ocean in the global biogeochemical carbon cycle is nowadays a leading concern in oceanographic research, this study emphasizes the specific effects of nitrogenous nutrients on the origin, development and fate of primary production. The inherent consequences of nitrogen utilization by phytoplankton for the channelling of organic nitrogen towards in-situ regeneration or towards sedimentation are investigated.

Nitrate depletion, the indication of the over-all new production during the ongoing season, ranged from near zero values to very high values (over 1000 mmol N m⁻²). As a general trend nitrate depletions were lowest in the closed pack ice zones, while strongly enhanced nitrate removal was observed in the marginal ice zone of the Scotia-Weddell Confluence area and in the continental shelf zone near Amery Ice Shelf in Prydz Bay. For the former area the average nitrate depletion amounted to 345 mmol N m⁻², for the latter one it amounted to 570 mmol N m⁻². The onset of the new growth season was characterized by elevated nitrate uptake rates, lasting for relatively short periods in the early season only.

Subsequently, ammonium was regenerated mainly due to grazing but also due to bacterial degradation and started to accumulate in the upper layer of the water column. Especially in the marginal ice zone and in the vicinity of the ice edge, elevated ammonium concentrations of 2 μmol N l⁻¹ or more were measured and this resulted in considerable ammonium availabilities of >5%. The appearance of regenerated nitrogenous nutrients triggered a switch-over from predominantly new production towards increased importance of regenerated production.

The fraction of nitrate based primary production decreased but slightly during the growth season in areas which were largely covered by remnants of winter ice during austral summer; nitrate always contributed for ≥50% to primary production (average f-ratio ≥0.5). On the contrary, a drastic shift towards regenerated production was observed in the seasonally ice free zones in the vicinity of the ice edge and on the continental shelf. The f-ratios decreased to 0.30 in the Scotia-Weddell Confluence area and to 0.20 in the Prydz Bay shelf zone. These changes were mainly driven by the preference of phytoplankton for regenerated nitrogen, with the phytoplankton's community structure affecting the uptake regime to a minor

degree. It was observed that diatoms remained the dominant phytoplankton species in Prydz Bay even when f-ratios went down to 0.2. In open ocean areas, belonging to the Circumpolar Current system, such as the Scotia Sea and the off-shelf region of Prydz Bay, nitrate and ammonium uptake remained essentially of equal importance during the progressing season and only a reduced shift towards increased ammonium uptake was seen.

Export of primary production to subsurface waters (100 to 500 m depth region) was shown to be mimicked by the build-up of suspended barite stocks. This build-up was out of phase with the surface water processes but depended closely on the evolution of f-ratios in surface waters. Areas characterized by significant export towards mesopelagic depths were the open ocean systems of the Scotia Sea and the Circumpolar Current in the Indian Ocean's sector. These systems showed intermediate productivities. Excluding the impact by krill grazing, smallest export to subsurface layers, was observed in the marginal ice zone of the Scotia-Weddell Confluence and over the continental shelf in Prydz Bay. The latter regions demonstrated highest productivity as well as highest grazing pressure.

The results obtained during different Antarctic cruises provides clear evidence for a distinction between different Antarctic ecosystems. Intensive new production, characteristic for fertile zones bordering the retreating ice edge was mainly conveyed towards the regenerating microbial network. This was mirrored by enhanced ammonium availability and poor subsurface barite accumulation. On the other hand, the moderate to low primary production of open sea and close pack ice zones was available for export and only small amounts of the organic matter were remineralized in the upper layer.

Additionally, we propose a scaling function, based on the correlation between barite concentrations in the subsurface Ba-maximum layer and oxygen concentrations in the O₂-minimum layer observed for the Indian Ocean's sector. The equation provides a tool to estimate export of organic matter at any other Southern Ocean site starting with information on net barite accumulations over the season.

INTRODUCTION

Primary productivity in the Southern Ocean can vary widely depending on length of ice-free conditions and geographical location (Smith and Sakshaug 1990). Jacques (1991) differentiated between open ocean ecosystems and neritic areas, including the marginal ice zones. In the former environment, daily productivity is relatively small, but as a result of permanent or prolonged absence of ice, productivity can extend over a long period and thus result in a significant yearly averaged production. In the neritic and marginal ice zone environments, on the other hand, daily production can be intense, but lasts only for a relatively short period.

From the total amount of photosynthetically fixed carbon, the net production only carries a potential for material export out of the euphotic layer. Net production is defined as the difference between total carbon fixation and respiration. In order to assess the capacity of phytoplankton to support production at higher trophic levels and to understand the processes sequestering organic matter out of the pelagic food web the concepts "new production" and "regenerated production" were introduced. The difference is based on a partitioning of primary production according to the nitrogen source. Dugdale and Goering (1967) have defined all primary production associated with allochthonous nutrient inputs, primarily nitrate and dinitrogen, as new production. Otherwise, regenerated production results from the utilization of nitrogenous compounds, mainly ammonium and urea, which are regenerated in the euphotic layer. Indeed, since nitrification has exhausted all available ammonium, released during heterotrophic breakdown of organic matter from the previous seasons, deep ocean nitrogen is supplied to the phytoplankton as nitrate. This also implies that at the start of the season nitrate is the only available inorganic nitrogen form. If steady state conditions apply, this input of nitrate has to be balanced by an output of nitrogen from the surface layer, either associated with organisms and biogenic particles (Eppley and Peterson 1979, Eppley 1989), or with dissolved organic matter (Toggweiler 1989). It follows that sampling of the particle flux exiting the surface layer allows for the assessment of the fraction of new production carried by settling biogenic particles. This is called the export production. The missing fraction between new and export production is to be carried by dissolved organic matter. Its significance as a source for mineral

nutrient compounds in the deep sea, has been increasingly recognized in recent studies (Toggweiler 1989).

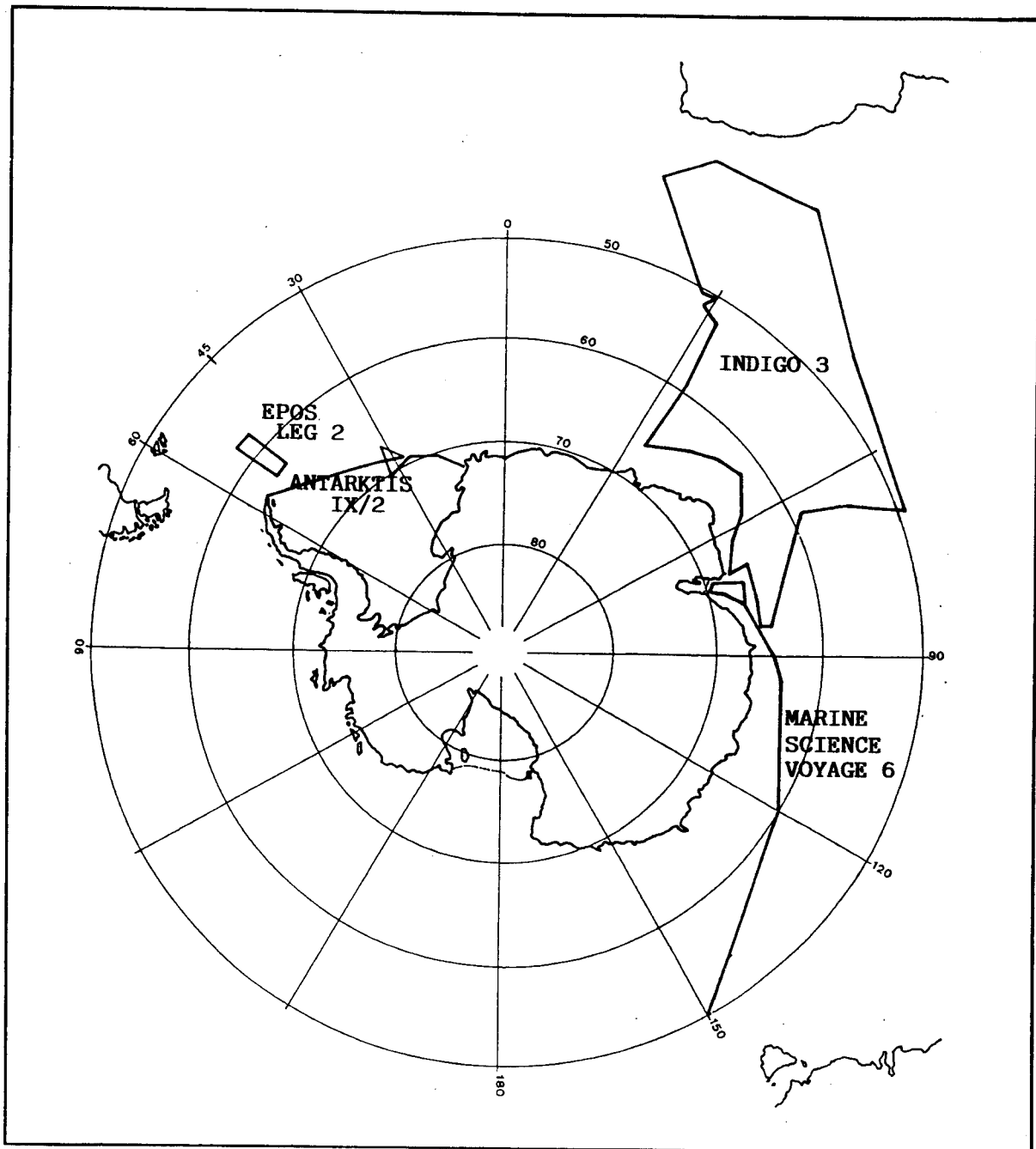
For the Southern Ocean ^{15}N nitrate uptake experiments suggest that new production remains often a very significant, if not the major fraction of total production (Smith and Nelson 1990), while most of the total primary production in other oceanic environments is thought to be regenerated production (Eppley and Peterson 1979, Harrison 1980).

Transfer of particulate biogenic matter out of the surface waters appears to be highly variable in the Southern Ocean both in time and space, as indicated by the data obtained from sediment trap deployments. For the Bransfield Strait for instance the sedimentation of biogenic matter shows strong seasonal fluctuations with a characteristic sharp spring maximum sustained by the settling of krill fecal pellets and very low sedimentation during the period of ice coverage (Wefer et al. 1990). On the other hand, particle flux at the northeastern boundary of the Weddell Sea (Maud Rise area) was observed to show less seasonal fluctuation and to be carried by aggregates (e.g. marine snow) and solitary particles (Wefer et al. 1990). Clearly, the Bransfield Strait situation reflects a typical loss system, where the major fraction of the spring diatom development is grazed and repacked as pellets for export downwards (Smetacek et al. 1990). The Maud Rise case possibly reflects a typical open ocean system of the Circumpolar Current, as described by Jacques (1991), where grazing pressure is low and where export consists of smaller particles. In this latter situation the observed yearly export is nevertheless significant, which is in agreement with observations that nitrate uptake in open ocean systems sustains a significant fraction of total production throughout the season (Goeyens et al. 1991). For small aggregates and solitary particles to have some significance in the material flux downwards, presence of skeletal parts, with higher densities than organic matter is probably essential. The Maud Rise site shows opal from diatoms to carry about 50% of the total flux (Wefer et al. 1990).

This is in agreement with the observation that diatom stocks remain relatively elevated during the season in the surface water of open ocean zones (Tréguer et al. 1991, Dehairs et al. 1992), while in marginal ice zones of the northern Weddell Sea diatom blooms appear as a transient event superimposed on the background nanoflagellate population (Smetacek et al. 1990). While extremely efficient as a mechanism for transport of biogenic matter to the deep sea, intense krill grazing and fecal pellet production is highly variable from site to site (Wefer et al. 1990,

Gonzales 1992) since it depends on krill swarm formation, which is known to occur preferentially in certain areas, such as the Antarctic Peninsula (Smetacek et al. 1990). It is probable that this represents the exceptional situation, with the settling of smaller protozoan and copepod pellets, aggregates and solitary particles being the more common picture. The efficiency of material transport to the deep ocean and the sediments will depend on the type of particles exported. Settling of large fecal pellet type particles provides for fast transport to deep water, while smaller aggregates and solitary particles sustain the material transport to intermediate depths. However, Southern Ocean diatoms were observed to reach the sediments as well while settling as solitary particles (for heavily silicified species) or incorporated in aggregates (Gersonde and Wefer 1987).

The aim of the present study is to contribute to a better understanding of seasonal and regional variabilities of new versus recycled production and to estimate export production in the Southern Ocean. In this study the term export production stands for the transfer of biogenic matter to intermediate depths (i.e. between approx. 100 and 600 m). For different environments (Figure 1), including the whole gradient from open ocean to closed pack-ice zone and the continental shelf, we studied the evolution of nitrate stocks, nitrate versus ammonium uptake rates and ammonium remineralization rates over the season. We also investigated the spatial variability in the composition of surface layer biogenic matter, to understand the effect of plankton composition on the nutrient uptake. The assessment of export fluxes to intermediate depths of the water column is based on estimates of microcrystalline barite accumulation in the subsurface layer and on an empirical scaling function, relating seasonal subsurface particulate Ba increase to subsurface oxygen utilization.



ANTAR
II/08

Figure 1 : Different subareas of the Southern Ocean,
studied during the INDIGO 3, EPOS LEG 2, ANATARKTIS IX/2
AND MARINE SCIENCE VOYAGE 6 cruises

MATERIAL AND METHODS

1. CRUISES

Data were collected during three different cruises : EPOS LEG 2 (1988 - 1989), from November 20 to January 7 in the Scotia-Weddell Confluence Area on board RV Polarstern; ANTARKTIS IX/2 (1990), from November 14 to December 30 in the Weddell Gyre on board RV Polarstern; and MARINE SCIENCE VOYAGE 6 (1991), from January 3 to March 20 in the Prydz Bay area on board RV Aurora Australis. Reference will also be made to results obtained during the earlier INDIGO 3 cruise (Dehairs and Goeyens 1989, Poisson et al. 1990) in the Indian sector of the Southern Ocean (Figure 2).

During EPOS LEG 2 (Figure 3) RV Polarstern followed four transects along 49° W and one along 47° W, all between 57° S and 62° S. The transects along 49° W are : W1 : stations 143 to 153 (November 26 to November 30), W2 : stations 154 to 159 (November 30 to December 12), W3: stations 172 to 179 (December 20 to December 24) and W4 : stations 182 to 194 (December 27 to December 31). The transect along 47° W is identified as transect E : stations 160 to 169 (December 13 to December 17).

The ANTARKTIS IX/2 cruise (Figure 4) provided a cross section of the Weddell Sea from Joinville Island at the tip of the Antarctic Peninsula to Kapp Norvegia.

Finally, MARINE SCIENCE VOYAGE 6 (Figure 5) combined a crossing of the Antarctic Convergence and Divergence between Tasmania and Prydz Bay and a narrow grid in the Prydz Bay off the shelf and on the shelf in the vicinity of Amery Ice Shelf.

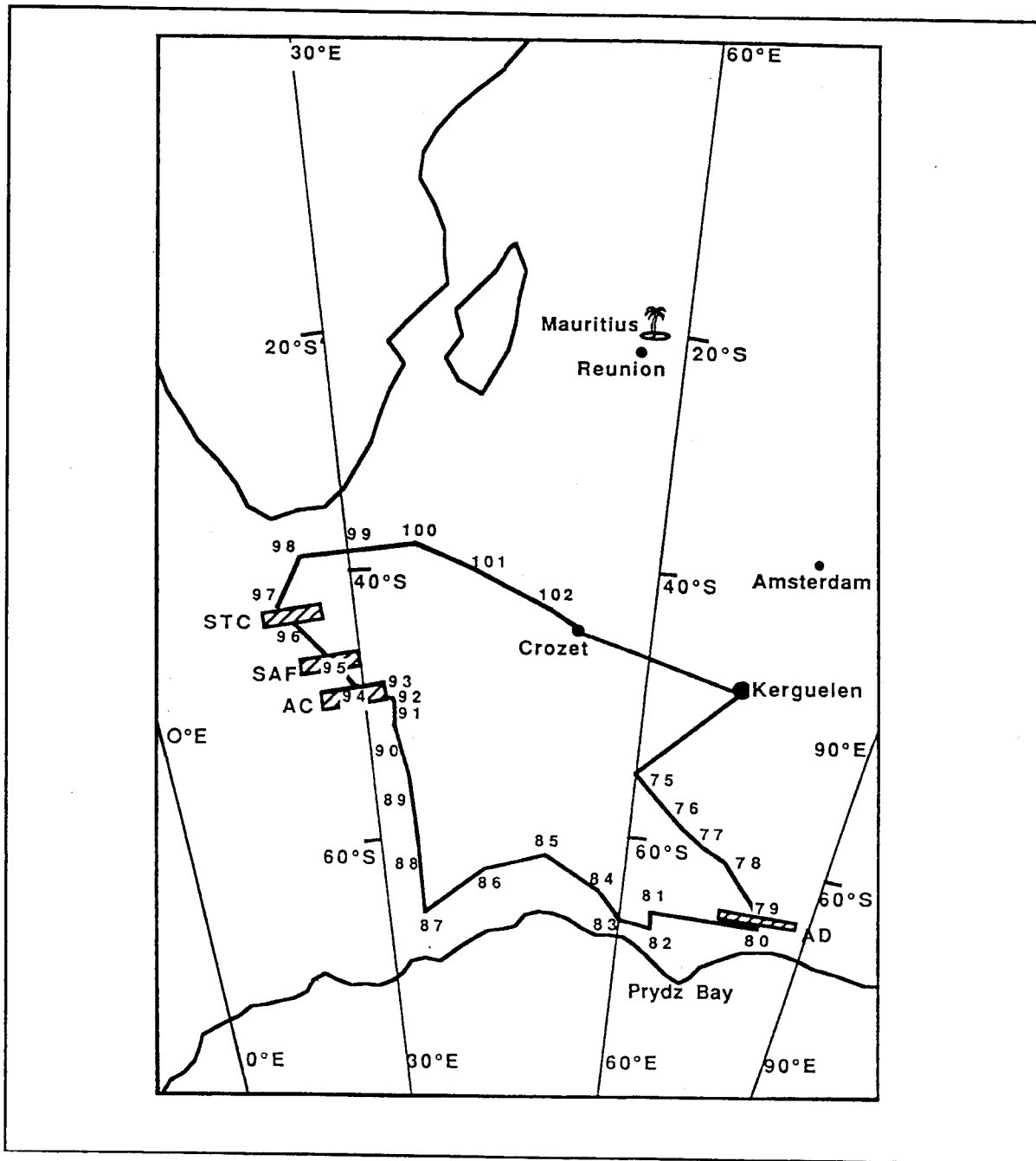


Figure 2 : Station positions during the INDIGO 3 cruise

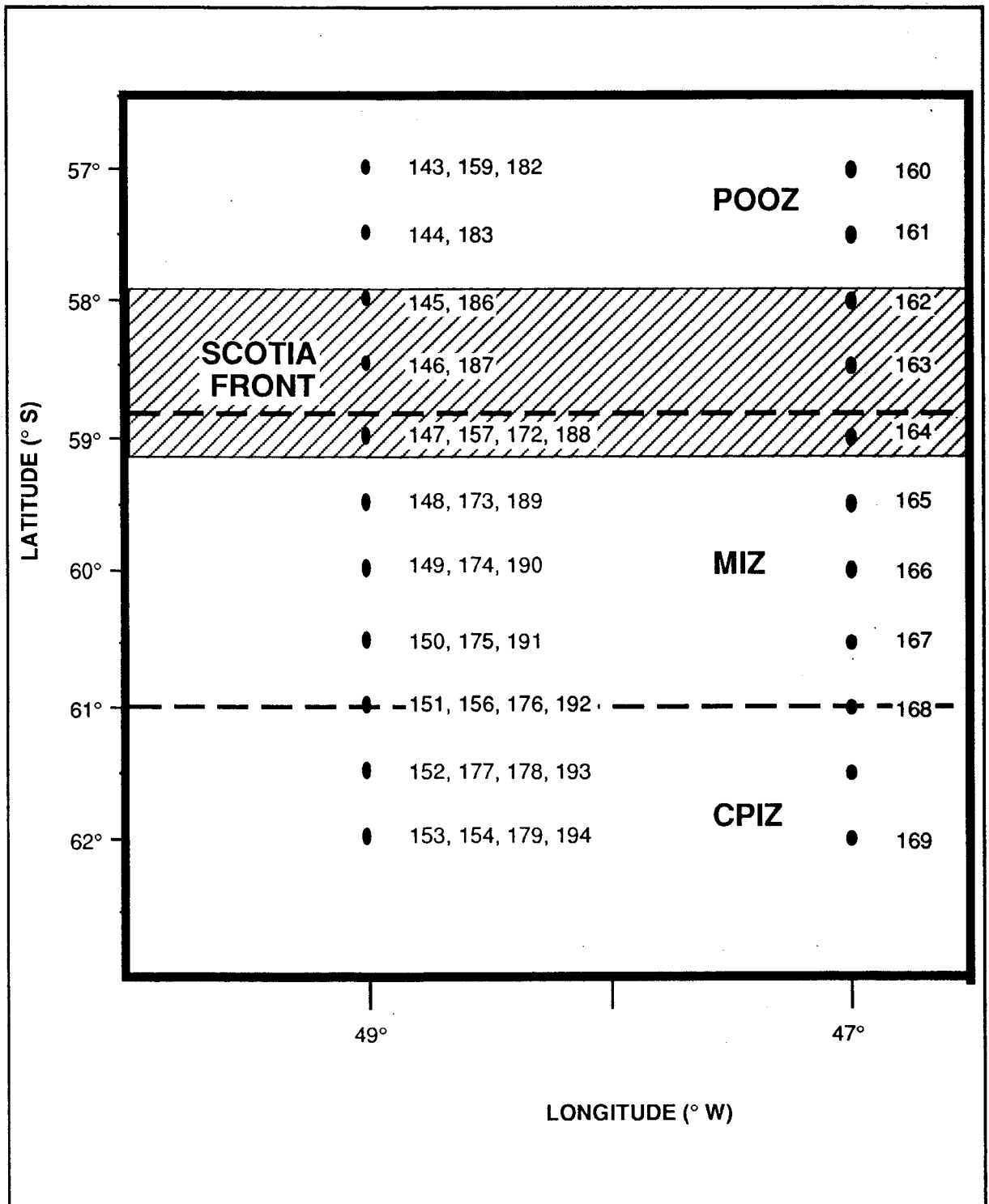


Figure 3 : Station positions during the EPOS LEG 2 cruise

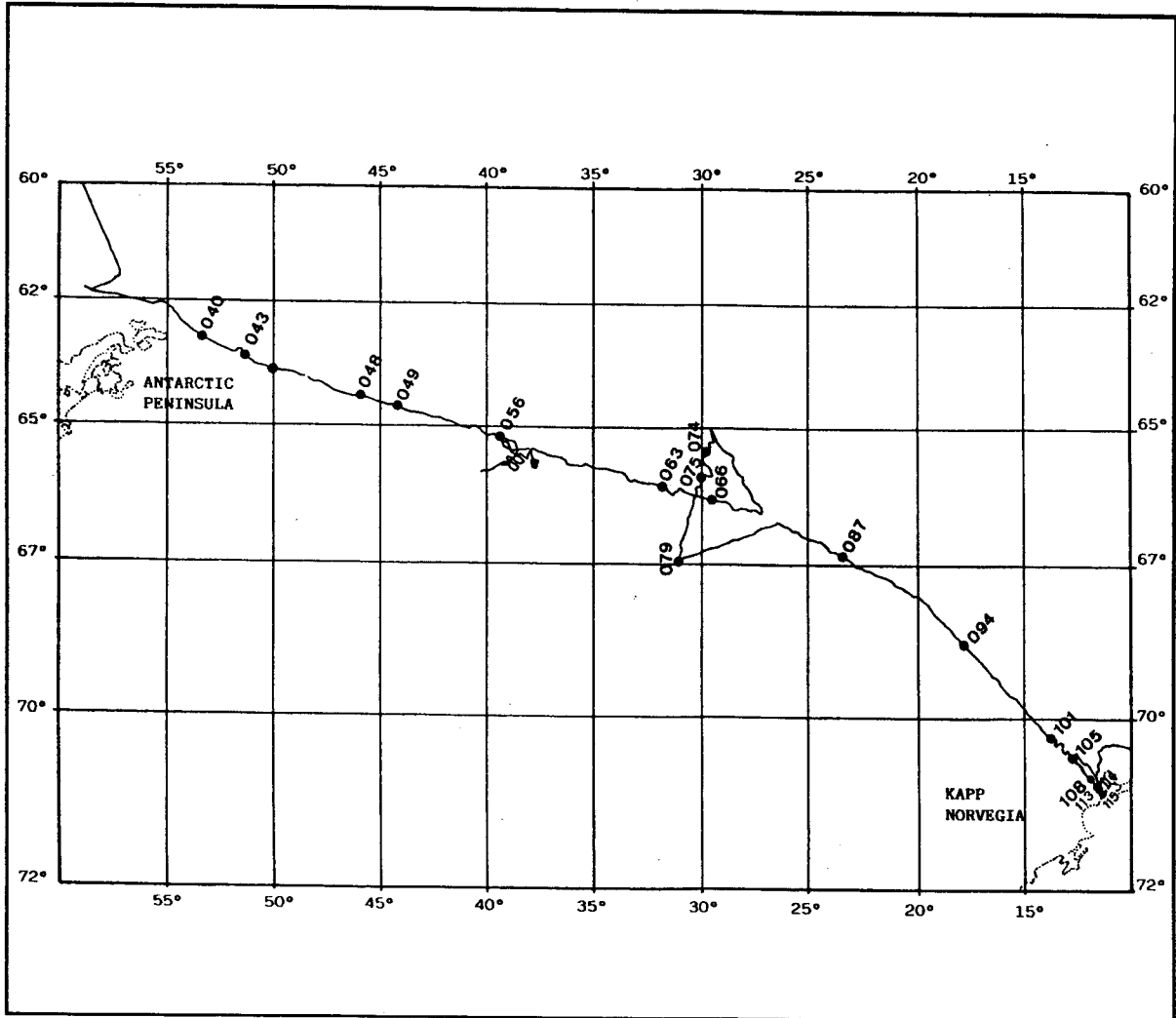
ANTAR
II/08

Figure 4 : Station positions during the ANTARKTIS IX/2 cruise

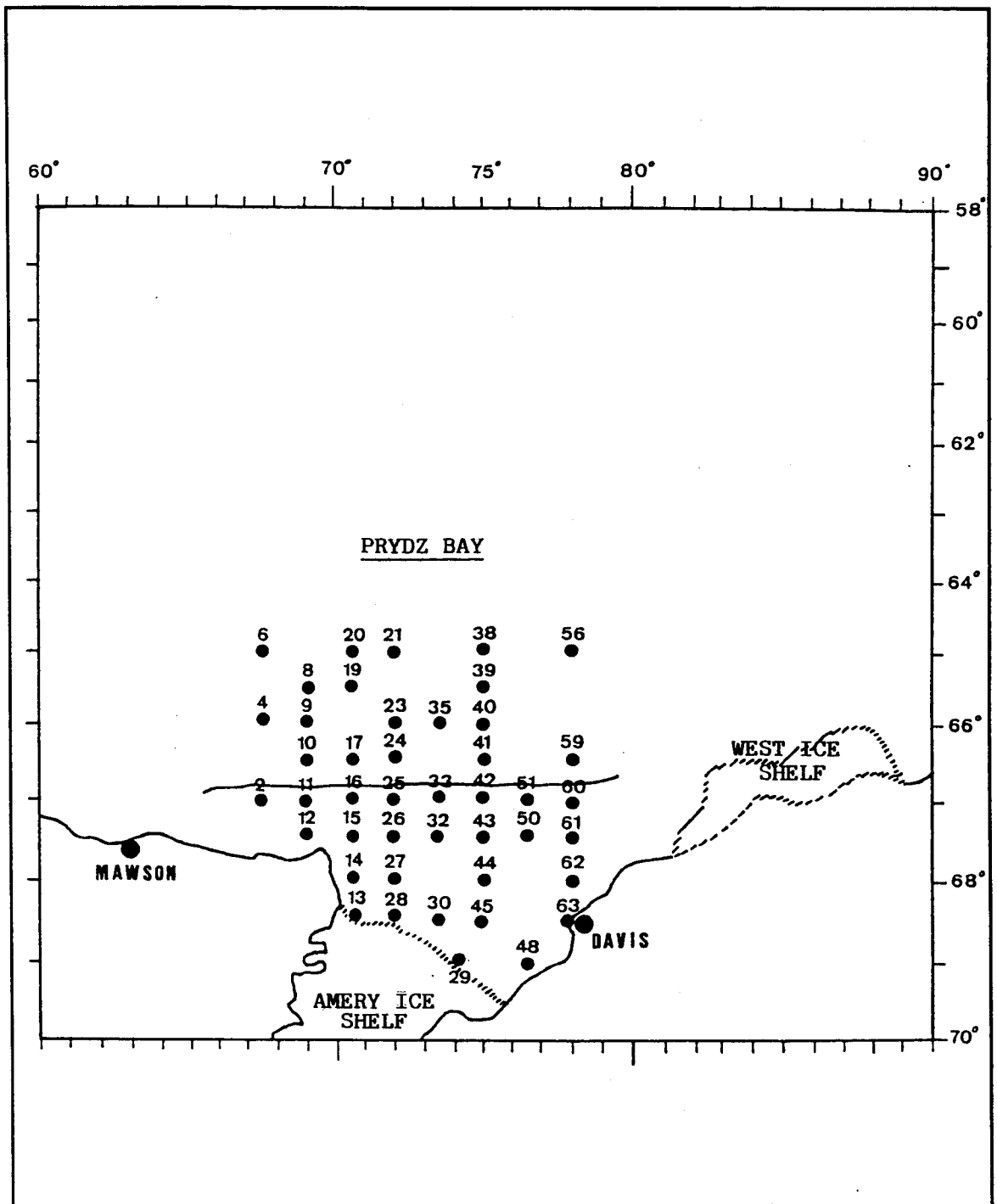


Figure 5 : Station positions during the MARINE SCIENCE VOYAGE 6 cruise

2. PHYSICAL, CHEMICAL AND BIOLOGICAL VARIABLES

In general, salinity, temperature, pressure, total alkalinity, oxygen, nutrient and chlorophyll concentrations were measured at every station and published in different cruise reports : INDIGO 3 (Poisson et al. 1990), EPOS LEG 2 (1991), ANTARKTIS IX/2 (Goeyens et al. 1991-c), and MARINE SCIENCE VOYAGE 6 (Tilbrook and Williams, ANARE report in preparation).

The samples for nutrient analyses were collected either from the 12 l Niskin bottles, mounted on the CTD rosette, or from 30 l Niskin bottles, used for total suspended matter filtration and for production - dissolution experiments. Nitrate plus nitrite was measured with a Technicon Autoanalyzer II according to the technique of Tréguer and Le Corre (1975). Millipore Milli-Q water was used as zero level; the calibration was carried out against 4 potassium nitrate standards in the range of 20 to 40 $\mu\text{mol N l}^{-1}$. During ANTARKTIS IX/2 and MARINE SCIENCE VOYAGE 6 nitrate analyses were respectively performed by J. Krest and A. Ross (Oregon State University) and by B. Tilbrook (CSIRO, Hobart). The samples for ammonium determination were immediately fixed by addition of the reagents and stored at ambient temperature for about 24 hours. Ammonium concentrations were determined manually, as described by Koroleff (1969). Freshly prepared Millipore Milli-Q water served as blank solution; standardization was carried out with two series of 5 ammonium sulphate standards ranging between 0 and 1 $\mu\text{mol N l}^{-1}$ and between 0 and 3 $\mu\text{mol N l}^{-1}$.

The sampling of total suspended matter (TSM) was carried out with 30 l Niskin bottles, fitted with teflon coated steel springs. Bottles were mounted on a hydrowire on a rosette. In general only the upper 500 m were investigated. Only during INDIGO 3 casts went down to 2000 m and at some stations even to the bottom. Suspended matter for POC and PN analysis was collected on precombusted (at 450°C) Whatman GF/F filters. During EPOS LEG 2 the filters were stored in deep-freezer until analysis in the home laboratory. At later cruises preference was given to drying of the loaded filters at 60° C and storage at ambient temperature in polystyrene petri dishes. POC and PN concentrations were analyzed with a Carlo Erba NA 1500 CN analyzer after carbonate elimination by HCl vapour during one hour. Acetanilide was used as standard compound. Detection limits, taken as three times the standard deviation of the blank average and assuming an average sample volume of 8 liter seawater, are for POC 0.03 $\mu\text{mol l}^{-1}$ and for PN 0.007 $\mu\text{mol l}^{-1}$.

I¹. M. Baumann and F. Brandini (Alfred Wegener Institute, Bremerhaven) analyzed the samples for POC and PN taken during ANTARKTIS IX/2.

For the determination of particulate Ba, Ca, Sr, Si, and Al concentrations ≥ 22 l of seawater were filtered. During INDIGO 3 and EPOS LEG 2 we used cellulose-ester membranes (Millipore : 47 mm \varnothing , 0.8 μm or 0.45 μm pore size). For the ANTARKTIS IX/2 and MARINE SCIENCE VOYAGE 6 cruises we used polycarbonate filters (Nuclepore : 47 mm \varnothing , 0.40 μm pore size). After filtration the filters were rinsed with approximately 20 ml of deionized water adjusted to pH 7, for carbonate particle preservation, and dried at 60°C. Samples were stored in polycarbonate petri dishes at ambient temperature. Several blank filters were treated similarly.

The collected particulate matter was brought into solution by alkaline fusion with LiBO_2 and redissolution of the fused sample in HNO_3 (Dehairs et al. , 1990; 1991). Final solutions were 0.5% in LiBO_2 and 4% in HNO_3 . As a result of this mineralization technique, the given particulate concentrations here represent total concentrations which include biogenic as well as lithogenic fractions. Ba, Ca, Sr and Al were determined by simultaneous and sequential Inductively Coupled Plasma Atomic Emission Spectrometry (Jobin-Yvon 48 and 38), using a concentric pneumatic glass nebulizer (Meinhard type C). The nebulizer argon flow was wetted with deionized water, to avoid clogging by salt crystallization in the nebulizer tip. Operating power is generally 1.8 kW. The argon flows are as follows: coolant, 19 l min^{-1} ; sample, 0.58 l min^{-1} ; auxiliary flow, 0.15 l min^{-1} . Si was determined by Electrothermal Atomic Absorption with Zeeman correction (Perkin Elmer 3030), using a thermal programme that included an ashing step at 1400°C and an atomization step with Ar-flow stop at 2650°C. Standards (Titrisol, Merck) were made up in a similar LiBO_2 / HNO_3 matrix as the samples. For Si, samples were diluted 20 to 100 times for the absorption signal to fit the linear part of the calibration curve. For MARINE SCIENCE VOYAGE 6 Si was measured by ICP-AES using the simultaneous JY-48 spectrometer. Considering filtrations of 22 liter of seawater, the detection limits, taken as 3 times the standard deviation on the average blank value, are : 0.011 nmol l⁻¹ for Ba; 0.025 nmol l⁻¹ for Sr; 0.4 nmol l⁻¹ for Al; 5.3 nmol l⁻¹ for Ca; and 10 nmol l⁻¹ for Si.

3. BIOLOGICAL ACTIVITIES

Total ammonium remineralization was determined with isotope (^{15}N) dilution experiments, carried out on seawater sampled with 30 l Niskin bottles. The seawater samples were confined in 2.75 l polycarbonate bottles (Nalgene), spiked with labelled ammonium (97% ^{15}N) and incubated for 24 hours at in situ temperature in the dark. Spike additions increased the ambient concentrations by $0.1 \mu\text{mol N.l}^{-1}$. Initial ammonium concentrations (immediately before and after spike addition) and final concentrations (at the end of the experiments) were measured. The ^{15}N atom percent of ammonium at the start of the experiment was calculated by application of the isotope dilution law. The final ^{15}N abundance of ammonium was determined by emission spectrometry, after isolation from the seawater matrix by an adapted diffusion method, and conversion into molecular nitrogen by the modified Dumas method (Fiedler and Proksch 1975). The emission spectrometric readings, obtained with a Jasco, Model NIA 1, N-15 Analyzer, are calibrated against certified standards (Goeyens et al. 1985) and against unenriched ammonium. The remineralization fluxes are calculated according to the modified linear differential equation model, introduced by Glibert et al. (1982-b). The remineralization rates obtained by the ^{15}N methodology were compared with independent estimates of ammonium production mediated by bacterioplankton and protozoa (Goeyens et al. 1991-b). These results are based on measurements of biovolumes and carbon metabolism, performed by C. Lancelot, S. Becquevort and S. Mathot (Université Libre de Bruxelles).

From the differences between real and fitted values of the standard ammonium concentrations we conclude that the deviation for concentrations between 0 and $1 \mu\text{mol N l}^{-1}$ amounts maximally to 2%, whereas it is 0.4% for concentrations exceeding $1 \mu\text{mol N l}^{-1}$. For the calculated ^{15}N abundances this results in an estimated maximal coefficient of variation of 29%. Reproducibility tests for the emission spectrometric readings, on the other hand, showed that for the measured ^{15}N abundances the coefficients of variation never exceeded 2%. The resulting errors for the remineralization rate range, therefore, between 5 and 30%, with errors larger than 10% occurring when the samples showed high ammonium concentrations.

During EPOS LEG 2 experiments for the study of nitrogen uptake rates were carried out as follows : the incubations for the study of nitrogen uptake rates were

started immediately after adding ^{15}N labelled nitrate or ammonium (99% atom ^{15}N) to the samples in 4 l polycarbonate bottles. Spike additions increased the concentrations by about 10%. All bottles were incubated for 24 hours at 0°C , with a 16h : 8h light : dark cycle. Incident radiation was $100\ \mu\text{E m}^{-2}\ \text{s}^{-1}$. The particulate material in the samples was collected onto precombusted Whatman GF/F glass fiber filters. The particulate nitrogen was converted to N_2 by a Dumas combustion method, according to Kristiansen and Paasche (1982). The $^{14}\text{N}/^{15}\text{N}$ ratio was measured by emission spectrometry with a Statron NOI-5 ^{15}N Analyzer. F. Sörensson (University of Göteborg) took care of these measurements. During ANTARKTIS IX/2 surface samples were incubated in natural irradiance conditions inside a plexiglass on-deck incubator for 24 hours. Comparison of data obtained from ^{15}N incubations with independently obtained primary production data (^{14}C incubations carried out in an on-deck incubator) prove very good agreement (Goeyens et al. 1991-a). During MARINE SCIENCE VOYAGE 6 incubations were carried out in a room thermostated at 1°C . We determined the incorporation of ^{15}N in particulate matter with the Jasco, Model NIA 1, N-15 Analyzer, as described for the remineralization experiments. The content of particulate carbon and nitrogen was determined using a Carlo Erba CN analyzer.

Nitrate uptake rates were calculated using the classic formulas for ^{15}N incorporation (Dugdale and Goering 1967, Harrison 1983). For ammonium uptake, a process inherently related with ammonium regeneration, the earlier mentioned model of Glibert et al. (1982-b) was used. The relative contributions of new and regenerated nitrogen to primary production are estimated by the f-ratio (Eppley and Peterson 1979, Eppley 1981) :

$$\text{f-ratio} = \frac{\rho_{\text{NO}_3}}{\rho_{\text{NO}_3} + \rho_{\text{NH}_4}}$$

No other forms of recycled nitrogen, such as urea and other organic compounds, were included.

McCarthy et al. (1977) introduced a relative preference index (RPI) as a more comprehensive way of describing the nitrogen utilization relative to the nitrogen availability. The RPI for a given nutrient N_i is defined as:

$$\text{RPI} = \frac{\frac{\rho_{N_i}}{\rho_{N_1} + \rho_{N_2} + \dots + \rho_{N_i}}}{\frac{N_i}{N_1 + N_2 + \dots + N_3}},$$

where ρ_{N_i} is the absolute uptake rate and N_i the concentration of the i^{th} nutrient.

RESULTS

1. DISSOLVED AND PARTICULATE STOCKS

Our comparison of the different subareas in the Southern Ocean is primarily based on differences in nitrogen availability. Therefore, we considered the nitrate and ammonium pools present in the upper layer of the water column. Since at almost every sampling position largely more than 90% of the chlorophyll was present in the upper 75 m, we decided to define the integrated quantities of nitrate and ammonium in these upper 75 m as the respective nutrient stocks available for phytoplankton nutrition. In the result's tables depth-weighted averages of the nitrogen stocks are given in $\mu\text{mol N l}^{-1}$.

In an analogical way, the surface water stocks of POC and PN, as well as those of particulate Ba, Ca, Sr, Si and Al are presented as depth-weighted averages of the integrated amount present in the upper 75 m. POC and PN are expressed as $\mu\text{mol l}^{-1}$; for particulate Ba, Ca, Sr, Si and Al the units are respectively : pmol l^{-1} , nmol l^{-1} , nmol l^{-1} , $\mu\text{mol l}^{-1}$ and nmol l^{-1} .

The collected results of the EPOS LEG 2 and ANTARKTIS IX/2 cruises are summarized in Tables I and II; for the MARINE SCIENCE VOYAGE 6 cruise the data of the different stations for vertical and for horizontal profilings are separated into Tables III and IV.

"P_{Ba,1}" represents depth-weighted average concentrations for a depth interval of 350 m in the depth region of the subsurface Ba maximum (i.e. between 100 and 500 m). "P_{Ba,2}" represents the depth-weighted average value for the upper 75 m. For EPOS LEG 2 transect W3 (December 20 to 24) no subsurface Ba data are given since only the upper 300 m of the water column were sampled.

Table I : collected results of the EPOS LEG 2 cruise (1988). Latitude and longitude are in °S and °W respectively; nitrate and ammonium stocks are given in $\mu\text{mol l}^{-1}$; POC and PN stocks are in $\mu\text{mol l}^{-1}$; PBa stocks are in pmol l^{-1} ; PCa, PSr and PAI stocks are in nmol l^{-1} ; and PSi stocks are in $\mu\text{mol l}^{-1}$

| station | lat. | long. | NO3 | NH4 | POC | PN | PBa ₁ | PBa ₂ | PCa | PSr | PSi | PAI |
|---|------|-------|------|-----|------|-----|------------------|------------------|-----|------|------|-----|
| Transect W1, November 26 to 30 | | | | | | | | | | | | |
| 143 | 57.0 | 49.0 | 26.8 | 0.3 | 7.6 | 1.3 | 252 | 66 | 237 | 0.92 | 0.76 | 7.1 |
| 144 | 57.5 | 49.0 | 27.3 | 0.5 | | | | | | | | |
| 145 | 58.0 | 49.0 | 29.6 | 0.2 | 11.0 | 2.1 | 138 | 41 | 19 | 0.11 | 0.42 | 8.4 |
| 146 | 58.5 | 49.0 | 19.8 | 0.6 | | | | | | | | |
| 147 | 59.0 | 49.0 | 27.9 | 0.9 | 15.9 | 2.8 | 145 | 164 | 34 | 0.40 | 1.73 | 6.0 |
| 148 | 59.5 | 49.0 | 27.6 | 1.0 | | | | | | | | |
| 149 | 60.0 | 49.0 | 29.6 | 0.6 | 7.3 | 1.2 | 133 | 46 | 27 | 0.24 | 0.43 | 4.0 |
| 150 | 60.5 | 49.0 | 31.3 | 0.2 | | | | | | | | |
| 151 | 61.0 | 49.0 | 31.2 | 0.2 | | | 143 | 15 | 10 | 0.07 | 0.11 | 1.1 |
| 152 | 61.5 | 49.0 | 31.0 | 0.3 | | | | | | | | |
| 153 | 62.0 | 49.0 | 31.4 | 0.2 | 2.8 | 0.5 | 129 | 17 | 9 | 0.07 | 0.05 | 1.1 |
| Transect W2, November 30 to December 12 | | | | | | | | | | | | |
| 154 | 62.0 | 49.0 | 31.6 | 0.2 | | | | | | | | |
| 156 | 61.0 | 49.0 | 31.8 | 0.1 | 4.5 | 0.7 | 158 | 21 | 5 | 0.09 | 0.14 | 0.7 |
| 157 | 59.0 | 49.0 | 26.7 | 2.0 | 5.2 | 1.1 | 90 | 18 | 10 | 0.13 | 0.45 | 0.9 |
| 158 | 59.4 | 48.6 | 28.8 | 0.9 | 11.7 | 2.3 | 87 | 110 | 6 | 0.18 | 0.40 | 6.9 |
| 159 | 57.0 | 49.0 | 27.6 | 0.4 | 4.4 | 0.8 | 247 | 47 | 25 | 0.09 | 0.51 | 2.5 |
| Transect E, December 13 to 17 | | | | | | | | | | | | |
| 160 | 57.0 | 47.0 | 28.9 | 0.3 | 2.7 | 0.7 | 98 | 37 | 89 | 0.28 | 0.29 | 2.6 |
| 161 | 57.5 | 47.0 | 27.7 | 0.5 | | | | | | | | |
| 162 | 58.0 | 47.0 | 27.4 | 0.5 | 2.5 | 0.6 | 156 | 37 | 44 | 0.12 | 0.12 | 2.5 |
| 163 | 58.5 | 47.0 | 27.9 | 0.6 | | | | | | | | |
| 164 | 59.0 | 47.0 | 25.5 | 0.8 | 6.9 | 1.6 | 80 | 107 | 12 | 0.02 | 0.16 | 2.1 |
| 165 | 59.5 | 47.0 | 26.3 | 1.6 | | | | | | | | |
| 166 | 60.0 | 47.0 | 28.3 | 0.6 | 3.5 | 0.9 | 115 | 1012 | 13 | 0.02 | 0.21 | 5.1 |
| 167 | 60.5 | 47.0 | 28.8 | 0.4 | | | | | | | | |
| 168 | 61.0 | 47.0 | 29.3 | 0.6 | 4.8 | 0.9 | 157 | 29 | 17 | 0.18 | 0.14 | 8.6 |
| 169 | 61.5 | 47.0 | 29.4 | 0.3 | 4.6 | 1.0 | 124 | 61 | 13 | 0.16 | 0.17 | 2.3 |
| Transect W3, December 20 to 24 | | | | | | | | | | | | |
| 172 | 59.0 | 49.0 | 23.4 | 1.5 | 10.6 | 1.8 | | 71 | 26 | 0.29 | 0.25 | 6.6 |
| 173 | 59.5 | 49.0 | 25.8 | 0.8 | 11.1 | 2.0 | | 44 | 40 | 0.39 | 0.20 | 3.5 |
| 174 | 60.0 | 49.0 | 31.4 | 0.5 | 7.0 | 1.0 | | 39 | 26 | 0.29 | 0.19 | 3.1 |
| 175 | 60.5 | 49.0 | 29.8 | 0.3 | 4.6 | 0.6 | | 34 | 15 | 0.07 | 0.23 | 1.4 |
| 176 | 61.0 | 49.0 | 31.1 | 0.2 | 5.6 | 0.9 | | 49 | 62 | 0.16 | 0.43 | 4.3 |
| 177 | 61.5 | 49.0 | 29.9 | 0.2 | 4.1 | 0.8 | | 26 | 19 | 0.14 | 0.18 | 0.2 |
| 178 | 61.5 | 49.0 | 32.2 | 0.2 | | | | | | | | |
| 179 | 62.0 | 49.0 | 31.0 | 0.3 | 2.0 | 0.4 | | 33 | 9 | 0.09 | 0.26 | 5.7 |
| Transect W4, December 27 to 31 | | | | | | | | | | | | |
| 182 | 57.0 | 49.0 | 27.8 | 0.3 | 8.0 | 1.3 | 315 | 93 | 222 | 0.92 | 2.94 | 5.2 |
| 183 | 57.5 | 49.0 | 26.8 | 0.7 | | | | | | | | |
| 186 | 58.0 | 49.0 | 28.4 | 0.3 | 4.0 | 0.9 | 205 | 7 | 10 | 0.05 | 0.37 | 1.0 |
| 187 | 58.5 | 49.0 | 24.5 | 0.8 | | | | | | | | |
| 188 | 59.0 | 49.0 | 25.0 | 1.4 | 1.8 | 0.4 | 190 | 22 | 20 | 0.08 | 0.12 | 2.4 |
| 189 | 59.5 | 49.0 | 27.1 | 1.0 | | | | | | | | |
| 190 | 60.0 | 49.0 | 27.1 | 0.6 | 5.1 | 1.0 | 100 | 14 | 6 | 0.09 | 0.08 | 1.7 |
| 191 | 60.5 | 49.0 | 29.0 | 0.5 | | | | | | | | |
| 192 | 61.0 | 19.0 | 30.0 | 0.3 | 5.2 | 0.9 | 110 | 7 | 8 | 0.02 | 0.13 | 1.1 |
| 193 | 61.5 | 49.0 | 29.7 | 0.3 | | | | | | | | |
| 194 | 61.7 | 49.0 | 30.6 | 0.3 | 3.5 | 0.4 | 52 | 36 | 18 | 0.13 | 0.13 | 1.8 |

ANTAR
II/08

Table II : collected results of the ANTARKTIS IX/2 cruise (1990). Latitude and longitude are in °S and °W respectively; nitrate and ammonium stocks are given in $\mu\text{mol l}^{-1}$; POC and PN stocks are in $\mu\text{mol l}^{-1}$; PBa stocks are in pmol l^{-1} ; PCa, PSr and PAI stocks are in nmol l^{-1} ; and PSi stocks are in $\mu\text{mol l}^{-1}$

| station | lat. | long. | NO3 | NH4 | POC | PN | PBa,1 | PBa,2 | PCa | PSr | PSi | PAI |
|---------|------|-------|------|-----|-----|-----|-------|-------|-----|------|------|------|
| 40 | 63.3 | 53.4 | 29.4 | 0.3 | 1.1 | 0.3 | | | | | | |
| 43 | 63.6 | 51.4 | 29.9 | 0.0 | 0.9 | 0.1 | | | | | | |
| 45 | 63.8 | 50.0 | 31.3 | 0.1 | 1.7 | 0.2 | | | | | | |
| 48 | 64.4 | 45.8 | 29.7 | 0.1 | 2.3 | 0.2 | | | | | | |
| 49 | 64.4 | 44.2 | 29.2 | 0.1 | 2.7 | 0.2 | 296 | 111 | <5 | 0.04 | 0.31 | 35. |
| 56 | 65.3 | 39.3 | 29.2 | 0.2 | 2.4 | 0.3 | | | | | | |
| 63 | 66.1 | 31.8 | 27.5 | 0.2 | 2.2 | 0.3 | | | | | | |
| 66 | 66.4 | 29.5 | 28.3 | 0.1 | 2.7 | 0.3 | 143 | 62 | 15 | 0.07 | 0.74 | 14.4 |
| 74 | 65.5 | 29.8 | 28.4 | 0.2 | 3.6 | 0.4 | 351 | 102 | <5 | 1.95 | 0.44 | 8.8 |
| 75 | 66.0 | 30.1 | 28.2 | 0.3 | 3.3 | 0.4 | | | | | | |
| 79 | 67.5 | 31.1 | 29.2 | 0.1 | 3.7 | 0.4 | 283 | 15 | <5 | 0.07 | 0.40 | 4.3 |
| 87 | 67.4 | 23.3 | 29.4 | 0.2 | 2.1 | 0.1 | 332 | 82 | <5 | 0.05 | 0.50 | 18.4 |
| 94 | 68.8 | 17.9 | 29.4 | 0.3 | 2.4 | 0.1 | | | | | | |
| 97 | 69.9 | 15.7 | 30.0 | | 2.3 | 0.3 | | | | | | |
| 101 | 70.3 | 13.7 | 29.8 | 0.1 | 1.9 | 0.2 | | | | | | |
| 105 | 70.6 | 12.7 | 30.5 | 0.0 | 2.4 | 0.3 | | | | | | |
| 108 | 71.0 | 11.8 | 29.9 | 0.1 | 2.0 | 0.2 | | | | | | |
| 113 | 71.0 | 11.7 | 30.2 | 0.1 | 2.9 | 0.3 | 129 | 169 | 6 | 0.05 | 0.08 | 9.4 |
| 114 | 71.0 | 11.6 | 30.1 | 0.2 | 3.4 | 0.4 | | | | | | |
| 115 | 71.1 | 11.4 | 30.4 | 0.3 | 2.7 | 0.3 | | | | | | |

Table III: collected results of the MARINE SCIENCE VOYAGE 6 cruise (1991). Latitude and longitude are in °S and °W respectively; nitrate and ammonium stocks are given in $\mu\text{mol l}^{-1}$; POC and PN stocks are in $\mu\text{mol l}^{-1}$; PBa stocks are in pmol l^{-1} ; PCa, PSr and PAI stocks are in nmol l^{-1} ; and PSi stocks are in $\mu\text{mol l}^{-1}$

| station | lat. | long. | NO3 | NH4 | POC | PN | PBa,1 | PBa,2 | PCa | PSr | PSi | PAI |
|--------------------|------|-------|------|-----|------|-----|-------|-------|-----|------|------|------|
| On shelf stations | | | | | | | | | | | | |
| 2 | 67.0 | 67.5 | 28.2 | 0.8 | 4.2 | 0.5 | 324 | 40 | 32 | 0.51 | 0.87 | 2.4 |
| 11 | 67.0 | 69.0 | 29.2 | 0.6 | | | | | | | | |
| 12 | 67.5 | 69.0 | 21.7 | 0.7 | | | | | | | | |
| 13 | 68.5 | 70.5 | 11.4 | 2.3 | 24.4 | 3.8 | 148 | 236 | 140 | 0.36 | 3.88 | 9.8 |
| 14 | 68.0 | 70.5 | 21.3 | 1.0 | | | | | | | | |
| 15 | 67.5 | 70.5 | 23.2 | 1.6 | | | | | | | | |
| 16 | 67.0 | 70.5 | 25.2 | 0.5 | 7.9 | 1.2 | 141 | 104 | 25 | 0.47 | 1.16 | 3.8 |
| 25 | 67.0 | 73.0 | 27.9 | 0.4 | | | | | | | | |
| 26 | 67.5 | 73.0 | 25.1 | 0.6 | | | | | | | | |
| 27 | 68.0 | 73.0 | 22.3 | 0.6 | 28.8 | 5.0 | 146 | 167 | 119 | 0.98 | 6.16 | 8.2 |
| 28 | 68.5 | 73.0 | 17.7 | 1.8 | | | | | | | | |
| 29 | 69.0 | 74.3 | 19.1 | 1.6 | 19.8 | 3.5 | 139 | 111 | 61 | 0.82 | 3.05 | 1.3 |
| 30 | 68.5 | 73.5 | 19.9 | 1.8 | | | | | | | | |
| 32 | 67.5 | 73.5 | 21.1 | 0.7 | 20.8 | 3.2 | 149 | 33 | 35 | 0.74 | 1.56 | 1.4 |
| 33 | 67.0 | 73.5 | 26.1 | 0.3 | | | | | | | | |
| 42 | 67.0 | 75.0 | 24.5 | 0.4 | | | | | | | | |
| 43 | 67.5 | 75.0 | 23.0 | 0.5 | | | | | | | | |
| 44 | 68.0 | 75.0 | 21.6 | 1.6 | 19.7 | 3.3 | 132 | 56 | 75 | 8.86 | 2.73 | 3.7 |
| 45 | 68.5 | 75.0 | 19.8 | 2.4 | | | | | | | | |
| 48 | 68.5 | 76.5 | 22.8 | 2.0 | 12.8 | 1.9 | 140 | 110 | 72 | 0.97 | 2.01 | 16.7 |
| 50 | 67.5 | 76.5 | 23.9 | 1.0 | | | | | | | | |
| 51 | 67.0 | 76.5 | 25.8 | 0.5 | 18.4 | 2.7 | 206 | 243 | 108 | 1.99 | 4.01 | 6.3 |
| 60 | 67.0 | 78.0 | 26.7 | 0.8 | | | | | | | | |
| 61 | 67.5 | 78.0 | 25.4 | 1.0 | | | | | | | | |
| 62 | 68.0 | 78.0 | 24.4 | 0.7 | 14.4 | 2.2 | 144 | 156 | 74 | 0.91 | 2.01 | 4.9 |
| 63 | 68.5 | 78.0 | 18.6 | 1.1 | | | | | | | | |
| Off shelf stations | | | | | | | | | | | | |
| 4 | 66.0 | 67.5 | 30.1 | 0.3 | | | | | | | | |
| 6 | 65.0 | 67.5 | 30.2 | 0.1 | 3.5 | 0.6 | 255 | 126 | 24 | 0.40 | 1.13 | 1.3 |
| 8 | 65.5 | 69.0 | 30.0 | 0.2 | 3.6 | 0.6 | 267 | 76 | 15 | 0.21 | 1.30 | 1.9 |
| 9 | 66.0 | 69.0 | 29.3 | 0.4 | | | | | | | | |
| 10 | 66.5 | 69.0 | 29.8 | 0.5 | 3.9 | 0.7 | 253 | 114 | 67 | 0.71 | 0.58 | 4.7 |
| 17 | 66.5 | 70.5 | 29.5 | 0.4 | | | | | | | | |
| 19 | 65.5 | 70.5 | 29.0 | 0.1 | | | | | | | | |
| 20 | 65.0 | 70.5 | 29.4 | 0.0 | | | | | | | | |
| 21 | 65.0 | 73.0 | 29.3 | 0.2 | 4.2 | 0.7 | 264 | 62 | 21 | 0.42 | 0.90 | 1.3 |
| 23 | 66.0 | 73.0 | 28.5 | 0.1 | | | | | | | | |
| 24 | 66.5 | 73.0 | 29.2 | 0.2 | 5.5 | 1.0 | 192 | 100 | 63 | 0.49 | 1.10 | 3.3 |
| 35 | 66.0 | 73.5 | 28.4 | 0.2 | 6.4 | 1.0 | 237 | 76 | 33 | 0.59 | 1.14 | 2.7 |
| 38 | 65.0 | 75.0 | 27.9 | 0.3 | 5.2 | 0.9 | 222 | 110 | 29 | 0.53 | 1.06 | 3.5 |
| 39 | 65.5 | 75.0 | 28.5 | 0.2 | | | | | | | | |
| 40 | 66.0 | 75.0 | 28.3 | 0.3 | | | | | | | | |
| 41 | 66.5 | 75.0 | 27.3 | 0.9 | 6.2 | 1.0 | 205 | 39 | 18 | 0.35 | 0.93 | 1.3 |
| 56 | 65.0 | 78.0 | 28.6 | 0.2 | 3.6 | 0.7 | 304 | 136 | 54 | 0.64 | 0.73 | 4.5 |
| 59 | 66.5 | 78.0 | 25.9 | 0.4 | | | | | | | | |

ANTAR
II/08

Table IV : collected results of the horizontal profilings sampled during the MARINE SCIENCE VOYAGE 6 cruise (1991). Latitude and longitude are in °S and °W respectively; POC and PN stocks are given in $\mu\text{mol l}^{-1}$; PBa stocks are in pmol l^{-1} ; PCa, PSr and PAI stocks are in nmol l^{-1} ; and PSi stocks are in $\mu\text{mol l}^{-1}$

| station | lat. | long. | POC | PN | PBa ₂ | PCa | PSr | PSi | PAI |
|---------|------|-------|------|------|------------------|-----|------|------|------|
| A | 47.8 | 140.1 | 7.8 | 1.1 | 386 | 97 | 0.51 | 0.46 | 11.1 |
| B | 48.7 | 139.6 | 5.7 | 0.9 | 114 | 181 | 1.24 | 0.65 | 18.3 |
| C | 49.7 | 136.6 | 5.8 | 0.9 | 151 | 333 | 2.03 | 0.73 | 11.8 |
| D | 50.3 | 135.3 | 7.4 | 1.0 | 177 | 336 | 1.69 | 0.61 | 16.0 |
| E | 50.9 | 134.0 | 4.6 | 0.6 | 187 | 301 | 1.95 | 0.47 | 13.9 |
| F | 51.8 | 132.3 | 6.2 | 0.9 | 109 | 398 | 2.61 | 1.25 | 22.1 |
| G | 52.4 | 131.5 | 6.2 | 1.0 | 171 | 342 | 1.84 | 1.90 | 23.3 |
| H | 53.2 | 129.7 | 4.9 | 0.7 | 77 | 330 | 1.19 | 0.98 | 15.9 |
| I | 54.3 | 127.4 | 6.1 | 0.8 | 319 | 378 | 1.67 | 1.35 | 27.2 |
| J | 55.2 | 125.5 | 7.3 | 1.0 | 93 | 148 | 1.05 | 1.48 | 16.6 |
| K | 56.3 | 123.1 | 6.6 | 1.0 | 85 | 186 | 1.23 | 1.25 | 15.1 |
| L | 57.3 | 120.7 | 6.3 | 0.8 | 344 | 204 | 1.09 | 1.46 | 30.6 |
| M | 58.2 | 118.8 | 5.3 | 0.8 | 162 | 379 | 2.97 | 2.94 | 25.7 |
| N | 59.3 | 116.1 | 4.0 | 0.6 | 50 | 147 | 0.93 | 0.67 | 12.2 |
| O | 59.9 | 112.3 | 7.5 | 1.2 | 164 | 220 | 0.92 | 1.48 | 19.4 |
| P | 60.3 | 109.6 | 4.4 | 0.7 | 71 | 101 | 0.66 | 0.94 | 15.3 |
| Q | 60.8 | 106.8 | 7.7 | 1.2 | 69 | 299 | 2.18 | 2.68 | 15.7 |
| R | 61.6 | 102.6 | 8.8 | 1.5 | 57 | 120 | 0.86 | 1.78 | 12.2 |
| S | 62.1 | 99.9 | 8.7 | 1.5 | 129 | 132 | 1.02 | 3.38 | 29.2 |
| T | 62.6 | 96.9 | 11.1 | 1.8 | 220 | 119 | 0.96 | 4.16 | 49.0 |
| U | 63.3 | 92.0 | 8.7 | 1.6 | 201 | 386 | 3.10 | 2.55 | 51.2 |
| V | 63.3 | 89.1 | 13.1 | 2.0 | 348 | 78 | 0.77 | 2.22 | 52.0 |
| W | 63.3 | 85.3 | 6.9 | 1.04 | 106 | 168 | 1.20 | 0.98 | 24.3 |
| X | 63.7 | 81.6 | 8.3 | 1.3 | 111 | 79 | 1.32 | 2.94 | 39.2 |
| Y | 64.9 | 80.3 | 8.5 | 1.3 | 138 | 113 | 1.05 | 2.63 | 42.4 |
| Z | 66.2 | 78.7 | 13.8 | 2.2 | 70 | 33 | 0.25 | 0.84 | 20.4 |
| 12/3 | 61.0 | 96.1 | 2.4 | 0.4 | 60 | 38 | 0.68 | 0.74 | 3.8 |
| 13/3 | 58.6 | 104.7 | 4.4 | 0.7 | 338 | 179 | 1.28 | 1.34 | 21.0 |
| 14/3 | 56.2 | 112.6 | 2.6 | 0.5 | 364 | 50 | 1.12 | 1.04 | 8.7 |
| 15/3 | 53.6 | 120.1 | 1.9 | 0.4 | 582 | 175 | 2.19 | 0.56 | 10.5 |

2. NITRATE DEPLETIONS AND AMMONIUM AVAILABILITIES

A conservative estimate of the seasonal productivity consists in calculating the nitrate depletion. Summer stratification in the Southern Ocean is characterized by seasonally warmed and less saline surface water overlying the remnant of the winter mixed layer marked by a temperature minimum. This layer is called the winter water. Differences between the winter nitrate concentration (the concentration in the temperature minimum layer) and the concentrations in the surface layer are defined as depletions (Le Corre and Minas 1983, Jennings et al. 1984). The term "depletion" signifies in this context the amount of nitrate removed from the water column during the ongoing growth season and leads to an estimate of seasonal phytoplankton productivity. It is used in the same sense as by Jennings et al. (1984) and must be distinguished from the notion of very low concentrations, limiting phytoplankton growth. However, for temperature minimum layers within the euphotic zone this approach can underestimate the nitrate depletion. Therefore, we based our calculations on the nitrate concentration in the temperature minimum layer or in the layer beneath the euphotic zone.

For important differences between nitrate concentrations in winter and at the moment of sampling the depletion can be biased by gradient-induced diffusion. We estimated this vertical flux by :

$$\text{Flux} = K \times \frac{\Delta \text{NO}_3}{\Delta \text{depth}}$$

Assuming a mean coefficient of diffusion (K) of $0.5 \text{ cm}^2 \text{ s}^{-1}$ (Gordon et al. 1984) and considering a duration of the productive season at the sampling moment of about 100 days, the underestimation of the nitrate depletions amounts to less than 10 %. Since this is a very maximum value, no corrections for diffusive fluxes are introduced (Goeyens et al. 1991-a).

We often observed enhanced ammonium concentrations at stations characterized by large nitrate depletions. Increases in ammonium stock, together with decreased nitrate stocks, alter considerably the inorganic nitrogen supply to phytoplankton. Nutrient signatures are represented by the ammonium availability, the proportional molar fraction of ammonium in the dissolved inorganic nitrogen pool:

$$\text{NH}_4 \text{ availability} = \frac{\text{NH}_4 \text{ stock}}{\text{NH}_4 \text{ stock} + \text{NO}_3 \text{ stock}} \times 100.$$

3. ORGANIC CARBON AND NITROGEN

The elemental ratios (POC : PN) were similar to those of compositionally normal phytoplankton, not at all or minimally biased by detrital matter. The observed regression of POC versus PN for the Scotia Weddell Confluence samples (EPOS LEG 2) is :

$$\text{POC} = -0.02 + 5.61 \text{ PN, with } R^2 = 0.94$$

and for the Prydz Bay area (MARINE SCIENCE VOYAGE 6) the obtained regression is :

$$\text{POC} = 0.20 + 5.94 \text{ PN, with } R^2 = 0.99.$$

These equations concern all samples taken in the upper 500 to 600 m. For the transects between Antarctica and Tasmania (MARINE SCIENCE VOYAGE 6), during which only surface waters were sampled (- 10m), we obtained :

$$\text{POC} = 0.41 + 6.03 \text{ PN, with } R^2 = 0.97.$$

This low POC : PN ratio, observed throughout suggests that most of the organic material present was fresh, or living. To check this, we compared measured total POC values with estimates of POC carried by living cells. This approach was only possible for the EPOS LEG 2 expedition, for which countings and volume estimations are available for autotrophic and heterotrophic cells (Becquevort et al. 1992). POC estimates based on cell counts were performed for the near surface samples (-10 m) and only for stations South of the Scotia Front. The obtained regression is :

$$\text{POC}_{\text{cells}} = -0.8 + 0.44 \text{ POC}_{\text{total}} , \text{ with } R^2 = 0.77.$$

The observed correlation is reasonably good, considering the potential variability induced by differences in time of sampling for cell counts and for elemental analysis of TSM, but a problem arises due to the small slope value: $\text{POC}_{\text{cells}} / \text{POC}_{\text{total}} = 0.44$. This difference between calculated and measured POC values can be explained by a combined effect of changes in cell volume, due to shrinkage during sample preparation for cell counts, and presence of detrital POC. Shrinkage effect for the type of fixative (glutaraldehyde + lugol) used by Becquevort et al. (1992) is reported to vary between 38 and 76 % of living cell volume for protozoa

and between 60 and 85% for autotrophic cells (Choi and Stoecker 1989). Carbon will be underestimated by the same factors. With on average 74% of plankton carbon being carried by autotrophs and 26 % by heterotrophs, we calculate that the total shrinkage effect could reduce cell-carbon values to between 54 % (i.e. $0.74 \times 0.6 + 0.26 \times 0.38 = 0.54$) and 83 % (i.e. $0.74 \times 0.85 + 0.26 \times 0.76 = 0.83$) of the original value with no shrinkage effect. From these values we calculate that detrital POC could account for between 19% (i.e. $1 - 0.44 / 0.54$; maximum shrinkage effect) and 47 % (i.e. $1 - 0.44 / 0.82$; minimum shrinkage effect) of total POC.

ANTAR
II/08

4. THE BIOGENIC SI FRACTION

Van Bennekom et al. (1991) observed an average Al/Si atomic ratio of 6×10^{-4} in diatom frustules sampled as net-phytoplankton. This ratio is similar to the one we observe for true open ocean stations in the Indian Ocean's sector of the Circumpolar Current (Al/Si atomic ratio = 4×10^{-4} ; from the data in Poisson et al. 1990). Assuming that Al and Si are carried only by crustal material (aluminosilicates) and diatoms, we calculated the biogenic Si fraction (Bio-Si) using the total Al and Si concentrations and the Al/Si ratios in the diatoms (Al/Si atomic ratio = 4×10^{-4}) and in the crustal component (Al/Si atomic ratio = 0.3; Bowen 1979) applying the following equation:

$$\text{Bio-Si} = \text{Si}_{\text{sample}} - (\text{Si/Al})_{\text{crust}} \times \text{Al}_{\text{crust}}$$

For the upper 75 m of the water column for all areas sampled we observed that the biogenic Si fraction represents ≥ 94 % of total Si. For the deeper water column (between 70 and 500 m) the lithogenic Si fraction is generally more important and can approach 60 % for the Scotia-Weddell Confluence area. Over the Prydz Bay shelf, however, the lithogenic fraction does not exceed 30 %, despite the shallow water column with depths generally not exceeding 500m.

DISCUSSION

1. DISTRIBUTION OF NITROGENOUS NUTRIENTS IN DIFFERENT AREAS OF THE SOUTHERN OCEAN

Subregions in the Southern Ocean.

The extreme diversities in phytoplankton assemblages and dynamics led to a distinction between different habitats of the Southern Ocean. The northernmost border of the winter ice extension (approximately 58° S) separates the Permanently Open Ocean Zone (POOZ) from the Seasonally Ice Covered Zone (SICZ). In a recent publication Jacques (1991) described the open ocean ecosystem and the "neritic" provinces with substantial ice coverage during summer. The former, though partially covered with ice during winter, is a totally ice free zone in summer. It is characterized as a mainly oligotrophic system in spite of its high inorganic nutrient load. Phytoplankton biomass and daily primary production are always low; on average they amount to respectively $<0.3 \text{ mg chl-a m}^{-3}$ and to $<0.30 \text{ g C m}^{-2} \text{ d}^{-1}$ (Jacques 1989). Oxidized nitrogen is the most significant nutrient for primary production; for the Indian Ocean's sector Collos and Slawyk (1986) have reported f-ratios >0.8 . The ecosystem of "neritic" provinces, on the other hand, shows considerably larger yearly-averaged productions and more pronounced transitions from new to regenerated production, sensu Dugdale and Goering (1967).

In the SICZ the hydrographical conditions of the water column vary from a stratified system in predominantly ice-covered areas and near ice edges to a well mixed system at the border of the POOZ. The retreating ice edge exhibits intense blooms of phytoplankton, culminating in larger amounts of biogenic material ($>4 \text{ mg chl-a m}^{-3}$) for short periods of time and inducing the highest nutrient depletions measured in the Antarctic area (Jennings et al. 1984, Smith and Nelson 1986). In areas adjoining the POOZ as well as in regions with heavy ice cover substantially less nutrient depletion occurs and phytoplankton standing stocks do in general never exceed $4 \text{ mg chl-a m}^{-3}$. Mathot et al. (1992) quantified subregional variability in the zone of seasonal ice retreat of the Scotia-Weddell Confluence area. Average values for net primary production in the open sea zone, in the almost completely ice covered zone and in the intermediate marginal ice zone amount respectively to 0.55, 0.24 and $0.97 \text{ g C m}^{-2} \text{ d}^{-1}$. In order to document the important variability in the SICZ we distinguish : (1) the Open Ocean Zone (OOZ), where winter ice melts

completely during austral spring and summer; (2) the Marginal Ice Zone (MIZ) or the transition area between the OoZ and the ice covered area; (3) the Coastal and Continental Shelf Zone (CCSZ), a shallow area in the neighbourhood of the Antarctic continent and surrounding islands, and (4) the Closed Pack Ice Zone (CPIZ) characterized by considerable amounts of ice remaining during austral summer (Figure 6). While plankton dynamics in the different subsystems are discussed by Lancelot et al. (1989) and Tréguer et al. (1992), in the present study we highlight mainly on dissolved inorganic nitrogen distributions in each of these compartments and on their relation with biogenic suspended matter.

ANTAR
II/08

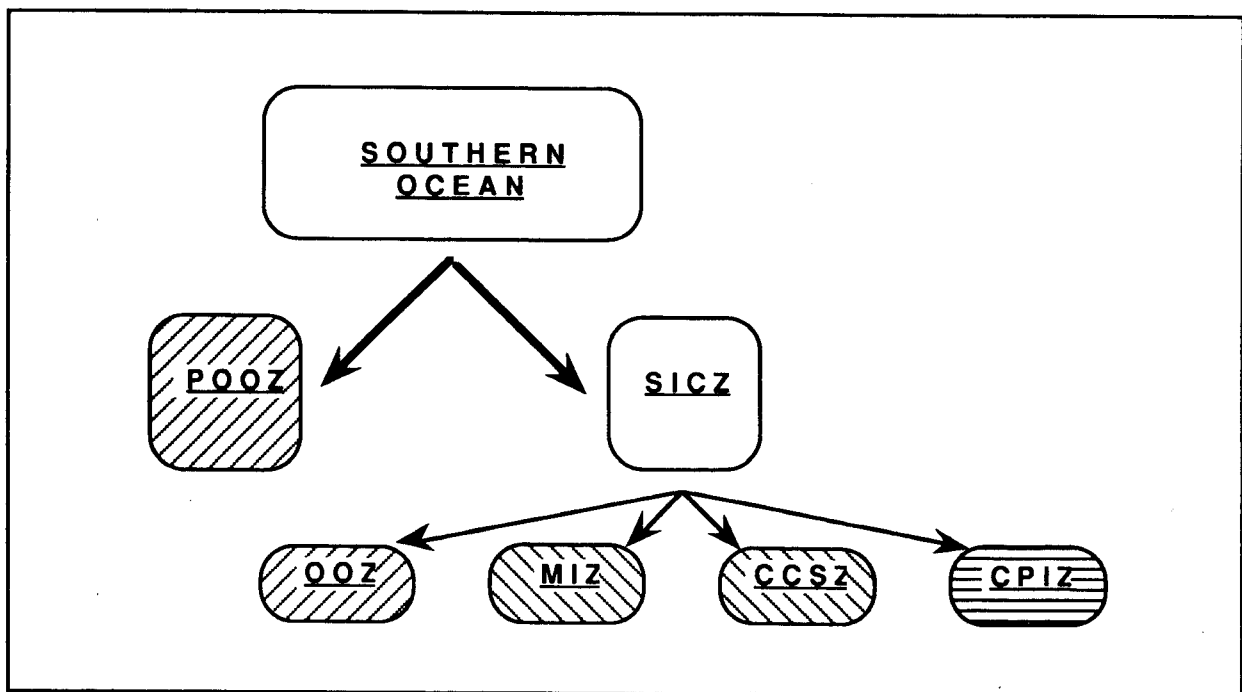


Figure 6: The different subareas in the Southern Ocean. Boxes with similar cross hatching represent areas with similar properties

Dissolved inorganic nitrogen in Antarctic waters. The high surface water nutrient concentrations are a striking feature of the Southern Ocean; in the region South of the Polar Front the surface nutrient concentrations remain high during the growth season. Throughout the year surface nitrate concentrations in the different sectors of this ocean exhibit a slight positive gradient, varying from about $20 \mu\text{mol N l}^{-1}$ at the Antarctic Convergence to concentrations between 25 and $30 \mu\text{mol N l}^{-1}$ at

the Antarctic Divergence (Sharp 1983, Jones et al. 1990). Severe reductions of the nitrate pool are rather unusual. Nevertheless, concentrations $<10 \mu\text{mol N l}^{-1}$ have been measured near the ice edge in Ross Sea, Weddell Sea and Prydz Bay. Sommer and Stabel (1986) measured extremely low concentrations of 2.2 and $4.2 \mu\text{mol N l}^{-1}$ in Drake Passage during spring 1984. Also during the MARINE SCIENCE VOYAGE 6 cruise in the Prydz Bay area (January to March 1991) surface concentrations as low as $2.8 \mu\text{mol N l}^{-1}$ were measured. In the Southern Ocean the dissolved inorganic nitrogen pool is mainly nitrate, with ammonium representing only 2 to 10 %. However, several investigations in the Indian Ocean's sector (Slawyk 1979, Le Jehan and Tréguer 1983, Probyn and Painting 1985), in the Ross Sea (Biggs 1982, El-Sayed et al. 1983, Nelson and Smith 1986), and the Weddell Sea and the Scotia Sea (Olson 1980, Glibert et al. 1982a, Rönner et al. 1983, Koike et al. 1986) emphasize the seasonal importance of ammonium. Especially during late spring and summer ammonium concentrations can increase to $2 \mu\text{mol N l}^{-1}$ and more. Our measurements in the Scotia-Weddell Confluence area (EPOS LEG 2) and in the Prydz Bay area (MARINE SCIENCE VOYAGE 6) confirm these very high values.

The permanently open ocean zone.

Many of the areas we sampled during the different cruises are covered by ice during austral winter. However, the northernmost areas sampled in the Indian Ocean's sector (INDIGO 3) and the Scotia-Weddell Confluence (EPOS LEG 2) are typical for the POOZ. The data for inorganic nitrogen distributions are summarized in Table V.

The Scotia Sea stations, studied during EPOS LEG 2, reflect a typical early spring situation (November and December 1988). The average surface nitrate concentration amounts to $27 \pm 1 \mu\text{mol N l}^{-1}$ and the depth-weighted average nitrate and ammonium concentrations for the upper 75 m of the water column are respectively 28 ± 1 and $0.4 \pm 0.1 \mu\text{mol N l}^{-1}$. The ammonium availability is 1.5 ± 0.5 %. Ammonium availability is increasing with progress of the growth season as illustrated by the case of EPOS LEG 2 station 183 (transect W4), sampled at the end of the study (December 27, 1988), for which an ammonium availability of 2.7 % was measured. This station also showed a marked ammonium maximum of $0.99 \mu\text{mol N l}^{-1}$ at the bottom of the euphotic layer. The INDIGO 3 stations represent a late spring and early summer situation (January and February). Average surface nitrate concentration is $25 \pm 1 \mu\text{mol N l}^{-1}$ and depth-weighted average nitrate

content for the upper 75 m is $25.2 \pm 0.4 \mu\text{mol N l}^{-1}$. INDIGO 3 ammonium concentrations were determined with autoanalyzer techniques and therefore questionable. They are not discussed here.

Table V : Nitrogen signature in POOZ ecosystems sampled at the northernmost stations of the INDIGO 3 and EPOS LEG 2 cruises. Nutrient concentrations and stocks are in $\mu\text{mol N l}^{-1}$; ammonium availabilities are in percent of total dissolved inorganic nitrogen

| station | surface NO_3 | NO_3 stock | NH_4 stock | NH_4 availability |
|-------------------|-----------------------|---------------------|---------------------|----------------------------|
| INDIGO 3 | | | | |
| 75 | 26.6 | 24.9 | | |
| 89 | 24.3 | 25.8 | | |
| 90 | 24.1 | 25.0 | | |
| 94 | 24.0 | 25.0 | | |
| EPOS LEG 2 | | | | |
| 143 | 26.8 | 26.8 | 0.3 | 1.2 |
| 144 | 27.1 | 27.3 | 0.5 | 1.7 |
| 145 | 27.7 | 29.6 | 0.2 | 0.8 |
| 159 | 26.2 | 27.6 | 0.4 | 1.4 |
| 160 | 27.5 | 28.9 | 0.3 | 1.1 |
| 161 | 27.1 | 27.7 | 0.5 | 1.8 |
| 162 | 26.9 | 27.4 | 0.5 | 1.7 |
| 182 | 26.4 | 27.8 | 0.3 | 1.2 |
| 183 | 24.8 | 26.8 | 0.7 | 2.7 |
| 186 | 27.0 | 28.4 | 0.3 | 1.1 |

ANTAR
II/08

The seasonally ice covered zone.

For all SICZ stations sampled during the four cruises a highly variable nitrogen signature is noted. Surface nitrate concentrations vary from a minimum of 2.8 to a maximum of $32 \mu\text{mol N l}^{-1}$. Ammonium, on the other hand, represents from 0 to 16.9 % of the total inorganic nitrogen pool in the upper layer. This large variability in nitrate and ammonium stocks agrees well with the observed diversity within the SICZ system. However, the picture becomes clearer when considering the OOZ, MIZ, CCSZ and CPIZ regions separately. The first region is illustrated by the southernmost INDIGO 3 stations and the off-shelf stations sampled during MARINE SCIENCE VOYAGE 6 (Table VI). Surface nitrate concentrations vary between 20 and $28 \mu\text{mol N l}^{-1}$, with an average value of $26 \pm 2 \mu\text{mol N l}^{-1}$. The nitrogen stocks (expressed as depth-weighted average concentrations), available to primary producers in the upper 75m, are respectively $28 \pm 2 \mu\text{mol N l}^{-1}$ for nitrate and $0.3 \pm$

0.2 $\mu\text{mol N l}^{-1}$ for ammonium, with ammonium representing approximately 1 % of the inorganic nitrogen stock. These data indicate that there is no clear distinction between the POOZ and OOOZ areas in the Circumpolar Current. This is in agreement with the definition of the open ocean ecosystem as given by Jacques (1991).

Table VI : Nitrogen signature in OOOZ ecosystems sampled during the INDIGO 3 and MARINE SCIENCE VOYAGE 6 cruises in the Circumpolar Current. Nutrient concentrations and stocks are in $\mu\text{mol N l}^{-1}$; ammonium availabilities are in percent of total dissolved inorganic nitrogen; nitrate depletions are in mmol N m^{-2}

| station | surface NO_3 | NO_3 stock | NH_4 stock | NH_4 availability | NO_3 depletion |
|--------------|-----------------------|---------------------|---------------------|----------------------------|-------------------------|
| INDIGO 3 | | | | | |
| 76 | 24.9 | 25.0 | | | 247 |
| 77 | 25.6 | 26.1 | | | 253 |
| 78 | 20.7 | 23.4 | | | 495 |
| 79 | 22.9 | 25.2 | | | 355 |
| 80 | 20.1 | 25.5 | | | 297 |
| 81 | 26.4 | 27.7 | | | 216 |
| 82 | 25.5 | 26.3 | | | 289 |
| 83 | 25.0 | 26.4 | | | 197 |
| 84 | 27.1 | 27.5 | | | 197 |
| 86 | 25.9 | 25.5 | | | 274 |
| 87 | 25.7 | 27.0 | | | 183 |
| 88 | 24.0 | 24.3 | | | 289 |
| MAR SCI VO 6 | | | | | |
| 4 | 28.4 | 30.1 | 0.3 | 1.1 | 101 |
| 6 | 28.4 | 30.2 | 0.1 | 0.4 | 124 |
| 8 | 28.2 | 30.0 | 0.2 | 0.7 | 125 |
| 9 | 27.4 | 29.3 | 0.4 | 1.4 | 166 |
| 10 | 27.9 | 29.8 | 0.5 | 1.5 | 72 |
| 17 | 26.9 | 29.5 | 0.4 | 1.3 | 150 |
| 19 | 27.6 | 29.0 | 0.1 | 0.2 | 154 |
| 20 | 27.7 | 29.4 | 0.0 | 0.2 | 121 |
| 21 | 28.0 | 29.3 | 0.2 | 0.5 | 134 |
| 23 | 27.4 | 28.5 | 0.1 | 0.5 | 226 |
| 24 | 27.0 | 29.2 | 0.2 | 0.6 | 139 |
| 35 | 26.9 | 28.4 | 0.2 | 0.6 | 142 |
| 38 | 25.7 | 27.9 | 0.3 | 1.0 | 299 |
| 39 | 25.3 | 28.5 | 0.2 | 0.7 | 271 |
| 40 | 25.7 | 28.3 | 0.3 | 1.0 | 252 |
| 41 | 23.0 | 27.3 | 0.9 | 3.0 | 299 |
| 56 | 26.6 | 28.6 | 0.2 | 0.8 | 216 |

The MIZ areas, where ice coverage, ice retreat and subsequent water column stabilization significantly affect the productivity in surface water, contrast strongly with the OOZ ecosystem. Marginal ice zones and areas near the shelf edge (CCSZ) can show marked nitrate depletion and enhanced ammonium availability, indicating high productivity. For the Scotia-Weddell Confluence area, studied during EPOS LEG 2, typical MIZ stations were found between 59° S and 61° S (Table VII). MARINE SCIENCE VOYAGE 6 stations near the edge of Amery Ice Shelf (CCSZ) showed a very similar and even more extreme situation (Table VIII). In the CPIZ, on the contrary, these features are significantly less pronounced. Almost all stations sampled during the ANT IX/2 cruise and the southermost stations of EPOS LEG 2 are typical of the CPIZ (Table IX).

ANTAR
II/08

Table VII : Nitrogen signature of a typical MIZ ecosystem sampled in the Scotia Weddell Confluence area during the EPOS LEG 2 cruise. Nutrient concentrations and stocks are in $\mu\text{mol N l}^{-1}$; ammonium availabilities are in percent of total dissolved inorganic nitrogen; nitrate depletions are in mmol N m^{-2}

| station | surface NO ₃ | NO ₃ stock | NH ₄ stock | NH ₄ availability | NO ₃ depletion | |
|---------|-------------------------|-----------------------|-----------------------|------------------------------|---------------------------|-----|
| W1 | 146 | 19.6 | 19.8 | 0.6 | 2.9 | 815 |
| | 147 | 23.7 | 27.9 | 0.9 | 3.0 | 292 |
| | 148 | 25.1 | 27.6 | 1.0 | 3.6 | 312 |
| | 149 | 26.7 | 29.6 | 0.6 | 2.1 | 150 |
| W2 | 157 | 23.0 | 26.7 | 2.0 | 6.9 | 424 |
| | 158 | 25.9 | 28.8 | 0.9 | 3.2 | 216 |
| E | 164 | 21.9 | 25.5 | 0.8 | 3.2 | 452 |
| | 165 | 23.3 | 26.3 | 1.6 | 5.9 | 396 |
| | 166 | 26.4 | 28.3 | 0.6 | 1.9 | 260 |
| | 167 | 25.3 | 28.8 | 0.4 | 1.3 | 188 |
| W3 | 172 | 20.6 | 23.4 | 1.5 | 6.2 | 586 |
| | 173 | 20.2 | 25.8 | 0.8 | 2.9 | 490 |
| | 174 | 29.2 | 31.4 | 0.5 | 1.6 | 83 |
| | 175 | 28.0 | 29.8 | 0.3 | 1.0 | 180 |
| W4 | 188 | 19.1 | 25.0 | 1.4 | 5.1 | 496 |
| | 189 | 19.8 | 27.1 | 1.0 | 3.6 | 352 |
| | 190 | 20.2 | 27.1 | 0.7 | 2.3 | 331 |
| | 191 | 26.1 | 29.0 | 0.5 | 1.6 | 188 |

The EPOS LEG 2 stations, situated between 59° S and 61° S, illustrate a spring situation in the MIZ. Surface nitrate concentrations vary from 19 to 29 $\mu\text{mol N l}^{-1}$. The lowest values reflect a greater maturity of the season, whereas the highest ones indicate that conditions are still very close to a winter situation. These low

surface concentrations and decreased nitrate stocks in the upper layer are reflected in the high nitrate depletions. The total quantities, removed during the ongoing growth season, amount on average to 345 mmol N m⁻², with a minimal value of 83 and a maximum of 815 mmol N m⁻². These same stations also show significant increases in ammonium concentration. Depth-weighted average ammonium concentrations for the upper 75 m are $0.9 \pm 0.5 \mu\text{mol N l}^{-1}$. Consequently, enhanced ammonium availabilities were found, ranging between 1.0 % and 6.2 %. During the EPOS LEG 2 cruise a maximal depth-weighted average ammonium concentration of $2.0 \mu\text{mol N l}^{-1}$ was measured for the upper 75 m at station 157 (59° S - 49° W).

Table VIII : Nitrogen signature in a typical CCSZ ecosystem sampled in Prydz Bay during the MARINE SCIENCE VOYAGE 6 cruise. Nutrient concentrations and stocks are in $\mu\text{mol N l}^{-1}$; ammonium availabilities are in percent of total dissolved inorganic nitrogen; nitrate depletions are in mmol N m⁻²

| station | surface NO ₃ | NO ₃ stock | NH ₄ stock | NH ₄ availability | NO ₃ depletion |
|---------|-------------------------|-----------------------|-----------------------|------------------------------|---------------------------|
| 2 | 26.7 | 28.2 | 0.8 | 2.6 | 166 |
| 11 | 25.3 | 29.2 | 0.6 | 2.0 | 128 |
| 12 | 19.1 | 21.7 | 0.7 | 3.2 | 638 |
| 13 | 4.7 | 11.4 | 2.3 | 16.9 | 1487 |
| 14 | 9.7 | 21.3 | 1.0 | 4.6 | 711 |
| 15 | 12.9 | 23.2 | 1.6 | 6.4 | 583 |
| 16 | 14.8 | 25.2 | 0.5 | 1.8 | 425 |
| 25 | 24.0 | 27.9 | 0.4 | 1.4 | 181 |
| 26 | 14.3 | 25.1 | 0.6 | 2.3 | 395 |
| 27 | 12.0 | 22.3 | 0.6 | 2.6 | 616 |
| 28 | 2.8 | 17.7 | 1.8 | 9.2 | 984 |
| 29 | 6.6 | 19.1 | 1.6 | 7.8 | 856 |
| 30 | 7.5 | 19.9 | 1.8 | 8.4 | 556 |
| 32 | 17.1 | 21.1 | 0.7 | 3.1 | 730 |
| 33 | 25.8 | 26.1 | 0.3 | 1.2 | 405 |
| 42 | 21.6 | 24.5 | 0.4 | 1.4 | 530 |
| 43 | 17.8 | 23.0 | 0.5 | 2.2 | 660 |
| 44 | 13.1 | 21.6 | 1.6 | 7.0 | 474 |
| 45 | 11.2 | 19.8 | 2.4 | 10.6 | 857 |
| 48 | 13.2 | 22.8 | 2.0 | 7.9 | 702 |
| 50 | 15.9 | 23.9 | 1.0 | 4.0 | 546 |
| 51 | 21.5 | 25.8 | 0.5 | 1.9 | 425 |
| 59 | 19.0 | 25.9 | 0.4 | 1.5 | 404 |
| 60 | 16.0 | 26.7 | 0.8 | 2.8 | 305 |
| 61 | 14.8 | 25.4 | 1.0 | 4.0 | 424 |
| 62 | 17.6 | 24.4 | 0.7 | 2.9 | 441 |
| 63 | 14.8 | 18.6 | 1.1 | 5.4 | 765 |

Table IX : Nitrogen signature in CPIZ ecosystems sampled during the EPOS LEG 2 and ANTARKTIS IX/2 cruises. Nutrient concentrations and stocks are in $\mu\text{mol N l}^{-1}$; ammonium availabilities are in percent of total dissolved inorganic nitrogen; nitrate depletions are in mmol N m^{-2}

| station | surface NO_3 | NO_3 stock | NH_4 stock | NH_4 availability | NO_3 depletion | |
|------------|-----------------------|---------------------|---------------------|----------------------------|-------------------------|-----|
| EPOS LEG 2 | | | | | | |
| W1 | 152 | 30.8 | 31.0 | 0.3 | 0.8 | 43 |
| | 153 | 31.1 | 31.4 | 0.2 | 0.7 | 11 |
| W2 | 154 | 32.0 | 31.6 | 0.2 | 0.5 | 6 |
| E | 168 | 26.9 | 29.3 | 0.6 | 2.0 | 145 |
| | 169 | 28.3 | 29.4 | 0.3 | 1.1 | 155 |
| W3 | 176 | 29.5 | 31.1 | 0.2 | 0.6 | 86 |
| | 177 | 28.9 | 29.9 | 0.2 | 0.8 | 163 |
| | 178 | 31.3 | 32.2 | 0.2 | 0.7 | 6 |
| | 179 | 30.6 | 31.0 | 0.3 | 0.8 | 39 |
| W4 | 192 | 27.7 | 30.0 | 0.3 | 1.0 | 112 |
| | 193 | 28.9 | 29.7 | 0.3 | 0.8 | 135 |
| | 194 | 30.0 | 30.6 | 0.3 | 0.9 | 69 |
| ANT IX/2 | | | | | | |
| | 40 | 29.3 | 29.5 | 0.1 | 0.4 | 106 |
| | 43 | 30.0 | 29.9 | 0.0 | 0.0 | 12 |
| | 45 | 31.3 | 31.3 | 0.1 | 0.2 | 9 |
| | 48 | 29.6 | 29.7 | 0.1 | 0.4 | 7 |
| | 49 | 29.2 | 29.2 | 0.1 | 0.4 | 13 |
| | 56 | 28.8 | 29.2 | 0.2 | 0.8 | 34 |
| | 63 | 27.6 | 27.5 | 0.2 | 0.8 | 10 |
| | 66 | 28.1 | 28.3 | 0.1 | 0.4 | 23 |
| | 74 | 28.6 | 28.4 | 0.2 | 0.6 | 32 |
| | 75 | 28.1 | 28.2 | 0.3 | 0.9 | 18 |
| | 79 | 28.9 | 29.2 | 0.1 | 0.4 | 56 |
| | 87 | 29.3 | 29.4 | 0.2 | 0.8 | 51 |
| | 94 | 29.4 | 29.4 | 0.3 | 1.0 | 32 |
| | 101 | 29.8 | 29.8 | 0.1 | 0.3 | 47 |
| | 105 | 30.6 | 30.5 | 0.0 | 0.0 | 14 |
| | 108 | 30.0 | 29.9 | 0.1 | 0.2 | 0 |
| | 113 | 30.3 | 30.2 | 0.1 | 0.3 | 9 |
| | 114 | 30.2 | 30.1 | 0.2 | 0.7 | 16 |
| | 115 | 30.5 | 30.4 | 0.3 | 1.1 | 0 |

ANTAR
II/08

The CCSZ stations, studied in January and February during the Prydz Bay cruise, are even more depleted in nitrate. Surface values for these stations vary between 3 and $19 \mu\text{mol N l}^{-1}$. The considerable nitrate removal and correspondingly high standing stocks of plankton (see Table III), represent an early summer situation in this area. An average nitrate depletion of $570 \pm 281 \text{ mmol N m}^{-2}$ characterizes this

region with a few peak values of 850 mmol N m⁻² and more. As observed for the MIZ, the CCSZ stations showed relatively high ammonium stocks with a depth-weighted average concentration of $1.0 \pm 0.6 \mu\text{mol N l}^{-1}$. A maximum value of $2.4 \mu\text{mol N l}^{-1}$ was observed at station 45 (68.5° S - 76.5° E). This resulted in high ammonium availabilities, with the maximum value being 16.9 % of the total dissolved inorganic nitrogen pool. On average the ammonium availability was $5 \pm 4 \%$.

At the typical CPIZ stations, sampled during EPOS LEG 2 and ANT IX/2 the picture is completely different. Surface nitrate concentrations during spring amount on average to $30 \pm 1 \mu\text{mol N l}^{-1}$, with a minimum value of 26.1 and a maximum of $32.0 \mu\text{mol N l}^{-1}$. The high nitrate stocks (mean depth-weighted average nitrate concentrations in the upper 75 m are $30 \pm 1 \mu\text{mol N l}^{-1}$) and correspondingly low depletions indicate poor productivity in the water column. Likewise, ammonium stocks and availabilities in the water column are low. Compared to the MIZ (EPOS LEG 2) and to the CCSZ (MARINE SCIENCE VOYAGE 6) the ammonium stocks are about five times smaller and hardly represent 1% of the total inorganic nitrogen pool in the CPIZ.

Table X summarizes the distinct nitrogen features for the different subareas of the Southern Ocean.

Table X : mean nitrogen signature in the different subareas of the Southern Ocean. Nutrient concentrations and stocks are in $\mu\text{mol N l}^{-1}$; ammonium availabilities are in percent of total dissolved inorganic nitrogen; nitrate depletions are in mmol N m^{-2}

| Area | Surface NO ₃ | NO ₃ stock | NH ₄ stock | NH ₄ availability | NO ₃ depletion |
|------|-------------------------|-----------------------|-----------------------|------------------------------|---------------------------|
| POOZ | 26 ± 1 | 27 ± 1 | 0.4 ± 0.1 | 1.5 ± 0.5 | |
| OOZ | 26 ± 2 | 28 ± 2 | 0.3 ± 0.2 | 0.9 ± 0.7 | 217 ± 90 |
| MIZ | 24 ± 3 | 27 ± 3 | 0.9 ± 0.5 | 3 ± 2 | 345 ± 181 |
| CCSZ | 16 ± 6 | 23 ± 4 | 1.0 ± 0.6 | 5 ± 4 | 570 ± 281 |
| CPIZ | 30 ± 1 | 30 ± 1 | 0.2 ± 0.1 | 0.6 ± 0.4 | 47 ± 50 |

2. SUSPENDED BARITE AND BIOGENIC PARTICULATE MATTER IN ANTARCTIC WATERS.

Micro-crystalline barite (BaSO_4) is the major carrier of Ba in oceanic suspended matter (Dehairs et al. 1980). This barite appears to precipitate within aggregates of biogenic detritus where conditions of BaSO_4 saturation develop. During the settling of the aggregates out of the euphotic layer, heterotrophic oxidation of the organic detritus results in the breakdown of the carrier aggregate and release of the discrete barite crystals into the water column (Stroobants et al. 1991). This overall process explains the occurrence of the characteristic Ba/barite maximum in the 100 to 500 m depth region and the relationship between barite content and biological activity in the euphotic layer, observed in the World's Ocean (Dehairs et al. 1980, 1990 and 1991; Bishop 1988 and 1989).

The regional variability of surface water suspended matter composition, based on the data in Tables I to IV and in Table XI, which repeats essential information of the earlier INDIGO 3 cruise, is summarized in Table XII. The data represent averages \pm 1 sigma, per cruise and per subregion. For Ba we also give the values for the subsurface waters where the Ba maximum is located.

Table XI : composition of suspended matter for samples collected in POOZ and OOZ ecosystems during the INDIGO 3 cruise; PBa concentrations are in pmol l^{-1} ; PCa, PSr and PAI concentrations are in nmol l^{-1} ; and PSi concentrations are in $\mu\text{mol l}^{-1}$

| station | lat. | long. | PBa ₁ | PBa ₂ | PCa | PSr | PSi | PAI |
|---------|------|-------|------------------|------------------|-----|------|------|------|
| 75 | 56.5 | 63.2 | 445 | 151 | 103 | 1.46 | 0.92 | 10.2 |
| 76 | 59.5 | 69.9 | 399 | 257 | 200 | 3.27 | 1.18 | 1.3 |
| 78 | 61.8 | 76.3 | 437 | 1364 | 284 | 5.53 | 9.40 | 4.4 |
| 79 | 64.2 | 84.0 | 253 | 4443 | 355 | 3.57 | 2.39 | 5.5 |
| 81 | 66.0 | 67.3 | 223 | 88 | 132 | 1.15 | 0.63 | 1.3 |
| 84 | 64.5 | 58.0 | 188 | 56 | 62 | 0.38 | 0.19 | 0.5 |
| 86 | 63.8 | 42.0 | 366 | 101 | 178 | 1.55 | 1.00 | |
| 87 | 65.2 | 32.0 | 247 | 76 | 61 | 0.67 | 0.68 | 1.6 |
| 88 | 61.0 | 32.3 | 378 | 269 | 206 | 2.47 | 0.23 | 2.1 |
| 89 | 57.0 | 31.7 | 375 | 76 | 159 | 1.98 | 1.57 | 1.3 |
| 90 | 53.0 | 31.2 | 392 | 217 | 137 | 1.77 | 1.79 | 1.1 |
| 94 | 50.6 | 27.0 | 190 | 208 | 175 | 1.94 | 0.81 | 1.8 |

The POOZ is documented by the INDIGO 3 stations 75, 89, 90, 94; the EPOS LEG 2 Scotia Sea stations 143, 145, 159, 160, 162, 182, 186 and the MARINE SCIENCE

VOYAGE 6 transects between Tasmania and Prydz Bay. The latter data set represents only surface water (-10m) concentrations.

Concentrations of Si, Ca, Sr are generally high relative to the other regions. The average concentration of total Si is close to $1 \mu\text{mol l}^{-1}$. Indian Ocean's sector values are consistently high in Si, while Scotia Sea samples show much larger variability. The average concentration for Ca is $>100 \text{ nmol l}^{-1}$, with Scotia Sea samples showing the largest variability. Average Ba (surface water) and Sr concentrations are respectively in excess of 85 pmol l^{-1} and 0.85 nmol l^{-1} . For POC and PN the average concentrations are respectively close to 6 and $1 \mu\text{mol l}^{-1}$. Subsurface Ba is high with an average value of 287 pmol l^{-1} .

The Ooz is documented by the INDIGO 3 stations 76, 78, 79, 81, 86, 87, 88; MARINE SCIENCE VOYAGE 6 stations 2, 6, 8, 10, 21, 24, 35, 38, 41, 51, 56, G and transects.

The situation is very similar to the one observed for the POOZ. Average total Si is high, between 1 and $2 \mu\text{mol l}^{-1}$. Average Ca and Sr for the INDIGO 3 stations and the transects are respectively in excess of 150 nmol l^{-1} and 1.2 nmol l^{-1} .

For the off-shelf stations in the Prydz Bay area (MARINE SCIENCE VOYAGE 6), however, the average concentrations are lower (Ca, Sr respectively 40 and 0.6 nmol l^{-1}). Average surface Ba values are $\geq 100 \text{ pmol l}^{-1}$. Subsurface Ba is high and similar to the value for the POOZ. POC and PN also are similar to the values for POOZ. However, for the transects slightly higher averages (POC: $7.6 \mu\text{mol l}^{-1}$ and PN: $1.2 \mu\text{mol l}^{-1}$) are observed. The particulate Ba profiles for MARINE SCIENCE VOYAGE 6 are similar to those observed 4 years earlier in the same region, during INDIGO 3.

The CCSZ is documented by the Prydz Bay shelf stations 13, 16, 27, 29, 32, 44, 48, 62 sampled during the MARINE SCIENCE VOYAGE 6 cruise.

For Ba (surface water), Ca and Sr the situation is similar to the one observed for POOZ and Ooz. Average total Si is significantly higher ($2.8 \mu\text{mol l}^{-1}$) than observed for POOZ and Ooz. The same holds for average POC ($16.5 \mu\text{mol l}^{-1}$) and PN ($3.0 \mu\text{mol l}^{-1}$). Average subsurface Ba concentrations, on the contrary, are lower (120 pmol l^{-1}) than in POOZ and Ooz. In fact, average Si, POC and PN values are the highest observed for the different Southern Ocean subsystems.

Table XII : Average suspended matter composition in the different subareas of the Southern Ocean; between brackets : 1 sigma values; values marked with an asterisk represent averages without data for INDIGO 3 stations 78 and 79

| Region Expedition | POC $\mu\text{mol l}^{-1}$ | PON $\mu\text{mol/l}$ | Ba deep pmol l^{-1} | Ba surf pmol l^{-1} | Ca nmol l^{-1} | Sr nmol l^{-1} | Tot-Si $\mu\text{mol l}^{-1}$ | Bio-Si % | Al nmol l^{-1} |
|-----------------------------------|----------------------------|-----------------------|------------------------------|------------------------------|-------------------------|-------------------------|-------------------------------|----------|-------------------------|
| POOZ | | | | | | | | | |
| • EP2; I3 | 5.8 (3.2) | 1.1 (0.5) | 287 (136) | 89 (69) | 111 (90) | 0.88 (0.77) | 0.96 (0.20) | 94 | 3.7 (3.3) |
| • Mar.Sci. Transects (50°30-57°S) | 5.3 (1.8) | 0.8 (0.2) | - | 240 (173) | 262 (110) | 1.68 (0.49) | 1.01 (0.42) | 95 | 16.9 (5.9) |
| OOZ | | | | | | | | | |
| • I3 | - | - | 311 (94) | 141* (96) | 140* (66) | 1.58* (0.11) | 0.65* (0.40) | 96 | 2.4 (1.8) |
| • Mar.Sci. | 5.9 (4.3) | 0.9 (0.9) | 248 (41) | 102 (57) | 42 (11) | 0.62 (0.47) | 1.25 (0.94) | 99 | 3.0 (1.6) |
| • Mar.Sci. Transects (> 57°S) | 7.6 (3.1) | 1.2 (0.5) | - | 155 (103) | 164 (106) | 1.25 (0.78) | 1.98 (1.05) | 96 | 27.3 (14.7) |
| • Overall | - | - | 275 (73) | 116* (73) | 77* (65) | 0.96* (0.26) | 1.04* (0.83) | | 2.8 (1.7) |
| CCSZ | | | | | | | | | |
| • Mar. Sci. | 18.6 (6.7) | 3.0 (1.2) | 142 (6) | 122 (65) | 75 (39) | 0.75 (0.25) | 2.82 (1.60) | 99 | 6.2 (5.2) |
| MIZ | | | | | | | | | |
| • EP2 | 7.6 (4.0) | 1.4 (0.7) | 118 (37) | 64 (46) | 20 (11) | 0.18 (0.14) | 0.37 (0.46) | 95 | 3.6 (2.1) |
| CPIZ | | | | | | | | | |
| • EP2 | 4.1 (1.2) | 0.7 (0.2) | 119 (37) | 30 (9) | 18 (17) | 1.14 (0.01) | 0.18 (11) | 96 | 2.9 (2.7) |
| • ANT/IX | 2.4 (0.7) | 0.3 (0.1) | 256 (106) | 90 (52) | 4 (6) | 0.07 (0.01) | 0.41 (0.22) | 80 | 15.1 (10.9) |
| • Overall | 3.0 (1.2) | 0.4 (0.3) | - | 52 (44) | 13 (15) | 0.10 (0.01) | 0.27 (0.19) | | 7.8 (9.1) |

ANTAR
II/08

The high Si concentrations observed for on-shelf and off-shelf stations in the Prydz Bay area are in agreement with observations on phytoplankton composition, showing consistent diatom predominance (H. Marchant, personal communication).

The MIZ is documented by the EPOS LEG 2 stations 147, 149, 157, 158, 164, 166, 172, 173, 174, 175, 188, 190.

Ba (surface) and Ca, Sr, Si concentrations are significantly lower than observed for POOZ, OOZ and CCSZ. This is in agreement with observed phytoplankton predominance by naked nanoflagellates in this area (Jacques and Panouse, 1991; Becquevort et al. 1992; I. Schloss and M. Estrada, personal communication). However, the case of EPOS LEG 2 station 147 (transect W1; late November) is peculiar. At this station Si was high ($1.73 \mu\text{mol l}^{-1}$) in agreement with diatom abundance in the phytoplankton (Jacques and Panouse 1991). However, intense grazing by krill in early December eliminated the diatoms and induced nanoflagellate take-over of the phytoplankton population. Subsurface Ba is also low (average concentration 120 pmol l^{-1}). However, POC and PN with average values respectively of 7.6 and $1.4 \mu\text{mol l}^{-1}$ are higher than observed for POOZ and OOZ.

The CPIZ region is documented by the EPOS LEG 2 stations 151, 153, 156, 168, 169, 176, 177, 178, 179, 192, 194 and all stations of ANTARKTIS IX/2.

Surface water Ba, Ca, Sr, Si, POC, PN concentrations are the lowest observed for the different areas studied. For the EPOS LEG 2 stations, average subsurface Ba, although slightly larger than for the MIZ, is low compared to POOZ and OOZ. However, for the central Weddell Sea (ANTARKTIS IX/2 stations), subsurface Ba is high with concentrations similar to those of the OOZ and POOZ in the Indian Ocean sector. This is difficult to understand in view of the extremely low productivities and biomasses present in the surface waters, but it is possible that in this case the subsurface Ba reflects the export production of the previous season (see below section 5).

Strong concentration gradients for Ca, Sr, Si and also subsurface Ba are observed between Scotia Sea and Confluence, through the Scotia Front boundary separating the OOZ (Scotia Sea) from the MIZ (Confluence proper) (Dehairs et al. 1992).

The higher Ca concentrations observed in the Scotia Sea, relative to the area South of the Scotia Front, reflect the latitudinal distribution of different coccolithophorid species. The heavily calcified *Emiliana huxleyi* was abundant in the Scotia Sea and its distribution was restricted to this area (Buma et al. 1989; H. Thomsen and J. Larsen, personal communication). Similar observations were done by McIntyre and Bé (1967), who showed for the Atlantic sector that the 2°C

isotherm represented the southern boundary of the distribution of this coccolithophorid. This isotherm coincides approximately with the Scotia Front, South of which only weakly calcified coccolithophorid flagellates occur (H. Thomsen and J. Larsen, personal communication).

In general, the different subsystems of the Indian Ocean's sector and the Scotia Sea behave similarly, with higher concentrations of biogenic elements (Si, Ca, Sr) associated with skeletal material. It also appears that highest subsurface Ba concentrations occur in the POOZ and OOOZ areas of the Circumpolar Current. The high biogenic Si contents in the POOZ and OOOZ regions of the Circumpolar Current indicate that diatoms remain the dominant phytoplankton group during the season. This is confirmed by the data for cell counts also indicating diatom dominance in the phytoplankton of these areas (Alder et al. 1989, Jacques and Panouse 1991, I. Schloss, M. Estrada and H. Marchant, personal communication). Thus, presence of diatoms might appear as an important factor for the build-up of significant subsurface Ba/barite concentrations, as suggested earlier by Bishop (1988). However, two observations indicate that diatom presence does not necessarily result in the build-up of a subsurface Ba/barite maximum.

First, in the Confluence area (MIZ) during EPOS LEG 2 the diatom bloom which induced the large nitrate depletion observed in this area disappeared as a result of intense grazing during a krill event (Jacques and Panouse 1989, Gonzales 1992). After the diatom disappearance, nano- and picoplankton developed and the system switched from dominance of new production to dominance of regenerated production (see below section 3). Despite an original high diatom biomass no significant subsurface Ba/barite maximum developed.

Second, in the continental shelf region of Prydz Bay (CCSZ) during MARINE SCIENCE VOYAGE 6 diatoms were the dominant phytoplankton group throughout January and March (H. Marchant, personal communication), in agreement with the very high concentrations of particulate Si in surface waters (Average Si = $2.82 \mu\text{mol l}^{-1}$ with $\geq 99\%$ of this amount present as biogenic Si; Table XII). Over the shelf region, close to Amery Ice Shelf, the nitrate depletions and particulate Si reached the highest values we ever observed in the Southern Ocean (station 28: nitrate concentration at -15m = $2.8 \mu\text{mol l}^{-1}$; station 27: particulate Si concentration at -15m = $11.8 \mu\text{mol l}^{-1}$). This intense diatom bloom did not result in significant subsurface Ba/barite stocks.

How can we explain these apparent conflicting observations ? Different possible processes that could account for these observations are discussed later in section 5. It is possible, however, that duration of the growth season is of importance. The Ooz of the Indian sector and the Scotia Sea is characterized by longer phytoplankton growth periods, as a result of year round ice free conditions; or relatively long lasting ice-free summer periods. Productivities are not very high but continue over long time scales (Jacques 1991). On the contrary, for the MIZ in the Confluence area the diatom bloom was very intense but lasted only for a relatively short period (i.e. probably <1 month) as a result of krill grazing. For the Prydz Bay shelf productivity was also very intense as witnessed by the large nitrate depletions and the very high biomasses reflected by the Si and POC concentrations. For the Confluence area intense krill grazing, during the krill event, may have eliminated conditions for plankton aggregation and barite precipitation (Dehairs et al. 1992). Prydz Bay is characterized by the short residence time of its shelf waters (Smith et al., 1984). Therefore, fast export of locally produced detrital biogenic material to the off-shelf region may explain the absence of a significant subsurface Ba/barite build-up over the Prydz Bay shelf.

It thus appears that a phase lag exists between the occurrence of processes in surface water (production, accumulation) and their expression in subsurface layers. It is only for situations where surface water processes last during a sufficiently long period (probably several months), that significant Ba/barite standing stocks will build-up and reflect export production. This appears to be the typical situation in the Ooz and POoz. In these regions no intense grazing events followed by pulses of fecal pellet fluxes occur, as observed in the Confluence area (Gonzales, 1992) and the Bransfield Strait (Wefer et al. 1990). It is likely that in the POoz and Ooz regions export is carried essentially through solitary particles and aggregates of biogenic detritus which, compared to the fecal pellets, settle more slowly through the water column and represent the suitable environment for barite precipitation. This type of vertical transport might be represented by the sediment trap fluxes for Maud Rise, in the northeastern Weddell Sea (Wefer et al. 1990) which underpin the importance of solitary particles and aggregates and show much less seasonal fluctuations compared to neritic areas like the Bransfield Strait (Wefer et al. 1990) and Kapp Norvegia (Bathmann et al. 1991).

3. AMMONIUM BUILD-UP BY HETEROPTROPHIC REMINERALIZATION

The understanding of the nitrogen patterns in the upper layer of the Southern Ocean requires the consideration of the chemical and biological fluxes during the growth season. Kamykowski and Zentara (1985) point out that the water South of the Subtropical Convergence exhibits a potential for nitrate excess at silicate depletion. They observed that the greatest excess occurs at the Antarctic Convergence and declines towards the Antarctic continent. Further South, over the continental shelf, nitrate excess changes into an excess of silicate, as observed in Ross Sea (see also Nelson and Smith 1986) and Weddell Sea (Kamykowski and Zentara 1985). This nitrogen signature suggests the importance of nitrogen recycling, mainly ammonification, for phytoplankton growth and its apparent decrease with increasing latitude. The importance of remineralization in the upper 100 m of the Southern Ocean water column is confirmed by several other authors (Biggs 1982, Le Jehan and Tréguer 1983, Koike et al. 1986). In a more exhaustive study on spatial and temporal variability of nutrients in the Southern Ocean Kamykowski and Zentara (1989) stress that the utilization of nitrate and ammonium by phytoplankton is nearly equal in the region extending from the coast of Antarctica to the Antarctic Divergence, whereas ammonium is likely to be the dominant nitrogen source between the Divergence and the Polar Front. For the Scotia-Weddell Confluence area the importance of ammonium is predominant around 60° S, the latitude of the northernmost winter ice extension. In the ensuing paragraphs we will refine this view by a more detailed information on the f-ratios in the different subareas of the Southern Ocean and on the role of ammonium in phytoplankton nutrition.

For the World's Ocean the largest fraction of the inorganic nitrogen pool is accounted for by the thermodynamically stable nitrate form. In the Southern Ocean, however, ammonium also can account for a significant fraction of the total pool. Especially in spring and early summer the MIZ and CCSZ are characterized by large ammonium stocks, representing up to 16.9 % of the dissolved inorganic nitrogen in the upper layer (Tables VIII and IX). Data on ammonium distributions and related remineralization processes in the Scotia-Weddell Confluence area during sea ice retreat in 1988 (EPOS LEG 2) provide evidence for important ammonium remineralization by heterotrophic microorganisms in the MIZ. In contrast, remineralization rates were small in the adjacent POOZ and CPIZ areas (Goeyens et al. 1991-b).

In literature enhanced biomasses of different trophic levels are reported for the MIZ (Garrison et al. 1986, Ross and Quetin 1986, Smith and Nelson 1986). Observations during the EPOS LEG 2 also indicate the presence of larger numbers of organisms at different trophic levels in the MIZ (Schalk 1990, Billen and Becquevort 1991, Jacques and Panouse 1991, Becquevort et al. 1992). In the euphotic zone of Antarctic waters extensive grazing on pico- and nanoplankton by nano- and microheterotrophs can take place and this heterotrophic microbial process is to be considered as a major fraction of the MIZ production (Smetacek et al. 1990, Lancelot et al. 1991). Distribution data for microheterotrophs (<200 μm) presented by Becquevort et al. (1992) for EPOS LEG 2, indicate that the largest biomasses occur consistently in the MIZ. In comparison with the POOZ and the CPIZ, the biomass carried by microheterotrophs in the MIZ is about one order of magnitude larger. In general nano- and picoplanktonic organisms represent the largest fraction within the heterotrophic community, with biomasses ranging from 70% to 90% of the total microheterotroph biomass (Becquevort et al. 1992). Moreover, it is observed that the protozoan community, dominated by dinoflagellates, develops almost simultaneously with the phytoplankton, while bacterial activity is slightly delayed (Becquevort et al. 1992).

Presence of high ammonium stocks, as well as enhanced quantities of microheterotrophs in the Scotia-Weddell Confluence area (EPOS LEG 2), suggest high remineralization rates. This is confirmed by the rates of ammonium remineralization by micrograzers and bacteria (Table XIII), as obtained from ^{15}N dilution experiments and also as estimated from measured biomasses and carbon metabolism (Goeyens et al. 1991-b). The experimental results for the POOZ and the CPIZ indicate mean remineralization rates of $2 \text{ nmol N l}^{-1} \text{ h}^{-1}$. Moreover, no significant variation in remineralization rate was observed in these regions during the whole period of investigation. A completely different time-course was observed in the MIZ, where remineralization rates are a factor of 2 to 8 higher. For the MIZ the data in Table XIII also show decreasing remineralization rates with time: transect W2 (early December), $16 \text{ nmol N l}^{-1} \text{ h}^{-1}$; transect W3 (second half of December), $8 \text{ nmol N l}^{-1} \text{ h}^{-1}$ (= average of three values) and transect W4 (late December), $5.2 \text{ nmol N l}^{-1} \text{ h}^{-1}$. The MIZ data of transect W3 reveal that the remineralization process can predominantly result from protozoan activity (Stations 172 and 173) rather than from bacterial activity. However, for Station 157 (transect W2; $59^\circ \text{ S} - 49^\circ \text{ W}$), characterized by the krill event, bacterial activity is very high and protozoan activity

extremely small (Table XIII). This suggests that the krill swarm, has grazed on autotrophic as well as on heterotrophic prey organisms, and has generated huge amounts of organic substrates triggering the bacterial activity.

Table XIII : Remineralization rates measured during EPOS LEG 2 in the Scotia-Weddell confluence area

| Area | Station | Remineralization rate ($\text{nmol N l}^{-1} \text{h}^{-1}$), obtained from | | |
|------|------------------|--|--|----------|
| | | ^{15}N dilution experiments | microbial biomass and activity measurements | |
| | | | Bacteria | Protozoa |
| POOZ | 159 (W1, 57°S) | 2.1 | nd | nd |
| | 182 (W4, 57°S) | 2.5 | nd | nd |
| MIZ | 157 (W2, 57°S) | 16 | 17.8 | 0.1 |
| | 172 (W3, 57°S) | 5 | 1 | 3.1 |
| | 173 (W3, 57.5°S) | 9 | 1 | 8 |
| | 174 (W3, 58°S) | 9 | 1.2 | 0.7 |
| | 190 (W4, 58°S) | 5.2 | 2.5 | 1.3 |
| CPIZ | 156 (W2, 61°S) | 1.7 | 0.9 | 0.3 |
| | 176 (W3, 61°S) | 3.5 | 0.6 | 1.6 |
| | 192 (W4, 61°S) | 2.1 | nd | nd |

nd : no data available

ANTAR
II/08

EPOS LEG 2 mesozooplankton data show that lowest biomasses are found under the pack ice, whereas considerably higher values occur close to and in the MIZ (Schalk 1990). The reported maximal zooplankton biomasses amount to 30 gww m^{-2} in the MIZ and to 24 gww m^{-2} in the ice covered area. The krill biomass measured during the same expedition varied between 0.2 and 45 gww m^{-2} , with only Station 157 being characterized by an exceptionally dense krill swarm of 400 gww m^{-2} . When taking into account the maximal zooplankton biomass of 30 gww m^{-2} , caught in a vertical haul from a depth of 400 m , it is calculated that the zooplanktonic contribution to the ammonium input does not exceed $0.12 \text{ nmol N l}^{-1} \text{h}^{-1}$. This production rate is obtained by using the ammonium excretion rate for

mixed zooplankton of $1.6 \mu\text{mol N g}^{-1}\text{ww h}^{-1}$, given by Biggs (1982). As the considered biomass, caught at 59°S during transect W1, is the highest for the studied area, the corresponding excretion rate is considered as an absolute maximum. The calculated rates of ammonium excretion by krill, obtained from observed krill stocks and from the excretion formula described by Johnson et al. (1984) range generally from 0.001 to $0.08 \text{ nmol N l}^{-1} \text{ h}^{-1}$. Only at the krill-rich Station (157, W2) about $0.45 \text{ nmol N l}^{-1} \text{ h}^{-1}$ is produced by the swarm. As none of the other stations exhibited dense krill swarms like the one observed at Station 157, the ammonium excretion by krill is estimated to amount maximally to $0.08 \text{ nmol N l}^{-1} \text{ h}^{-1}$ for the studied area. It results that the combined rate of ammonium production by krill and zooplankton amounts to less than $0.2 \text{ nmol N l}^{-1} \text{ h}^{-1}$. When compared to bacterial and microzooplankton activities (Table XIII), mesozooplankton activity clearly contributes only to a minor degree in the overall ammonium regeneration process, a conclusion that is in good agreement with previous results (Biggs 1982, Biggs et al. 1985).

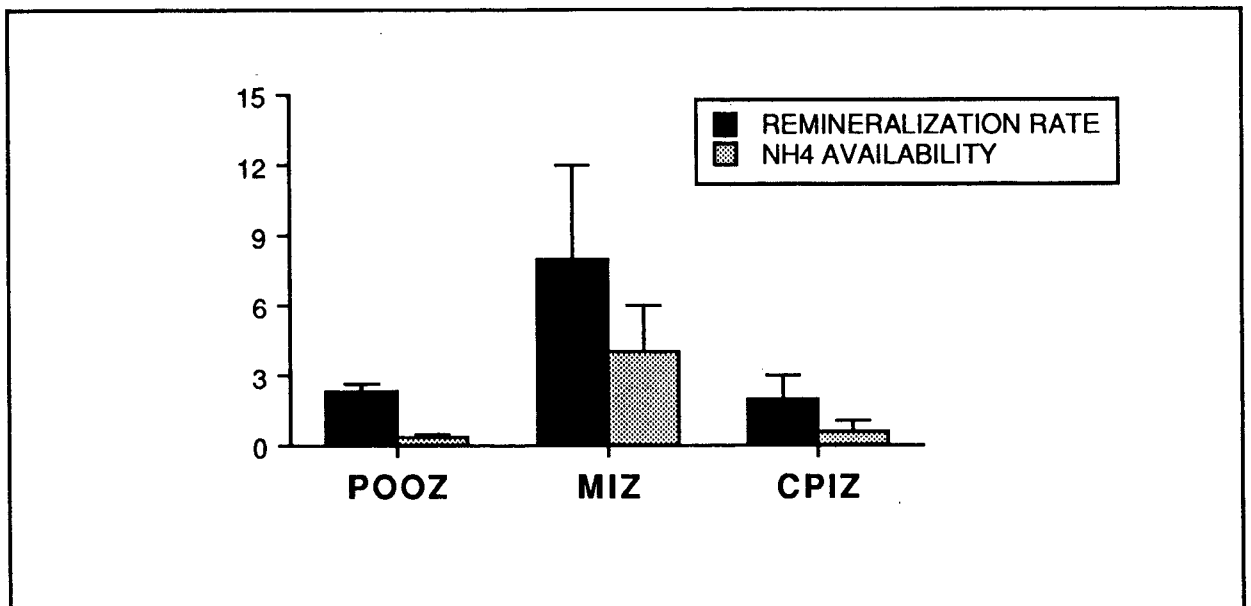


Figure 7 : mean remineralization rates ($\text{nmol N l}^{-1} \text{ h}^{-1}$) and ammonium availabilities (%), measured in the different subareas of the Southern Ocean during the EPOS LEG 2 cruise

In the area studied during EPOS LEG 2 the regional variability of the ammonium remineralization processes results in differences in ammonium build-up (Figure 7)

and availability (Figure 7). Means of depth-weighted average ammonium concentrations amount to 0.4, 0.9 and 0.2 $\mu\text{mol N l}^{-1}$ in the POOZ, MIZ and CPIZ respectively. The ammonium availabilities in the euphotic layer amount to 0.4, 4 and 0.2 % and the ammonium remineralization rates to 2.3, 8 and 2 $\text{nmol N l}^{-1} \text{h}^{-1}$ in the POOZ, MIZ and CPIZ respectively.

4. NITRATE AND AMMONIUM UPTAKE BY AUTOTROPHIC PRIMARY PRODUCERS

Different studies on nitrogen assimilation in the Southern Ocean have revealed that phytoplankton meets a large part of its nitrogenous needs by taking up ammonium despite high ambient concentrations of nitrate (Table XIV). Ammonium represents generally less than 10 % of the inorganic nitrogen stock available to phytoplankton. Exceptionally high stocks are uncommon, but were found however (Koike et al 1986, Verlencar et al 1990). We found >10 % of the dissolved inorganic nitrogen stock to be ammonium at MIZ and ice edge stations during EPOS LEG 2 and MARINE SCIENCE VOYAGE 6 (Tables VIII and IX).

Investigations in the Indian Ocean's sector during austral summer indicate a large predominance of nitrate uptake (mean f-ratio = 0.87; Table XIV). In the Scotia Sea, on the contrary, ammonium uptake rates are similar or slightly in excess of nitrate uptake rates for 4 different studies carried out at different moments of the growth season. Furthermore, the f-ratios show a progressive decrease between September and February, in parallel with an increasing ammonium availability (Table XIV). Seasonally ice covered areas, well documented by studies in the Scotia-Weddell area, are characterized by a marked shift from high f-ratios at the beginning of the growth season to much lower ratios at the end of the season and by increasing ammonium pools when the season is progressing. This agrees well with observations elsewhere in the CCSZ. Probyn and Painting (1985) found that reduced nitrogen (ammonium plus ureum) supplied on average 58% of the phytoplankton nitrogen requirements in an area off the coast between Cape Ann and Mawson (Indian Ocean's sector). Since their data reflect the surface water nitrogen assimilation only, average new production for the entire euphotic zone is probably lower. These observations are consistent with findings for two other studies in the Ross Sea, where considerably lower f-ratios indicated greater utilization of reduced nitrogen (Olson 1980, Nelson and Smith 1986). However, Smith and Nelson (1990) report nitrate was the major source of inorganic nitrogen taken up by phytoplankton in the MIZ of the Weddell Sea, where the integrated f-ratios for the euphotic zone average respectively 0.52 for austral spring investigations (November 1983) and 0.72 for austral fall (March 1986). And also at the western Ross Sea ice edge these higher f-ratios were observed (Nelson and Smith 1986). Calculated relative preference indices for ammonium indicate, nevertheless, that ammonium is nearly always the preferred nitrogen form for phytoplankton growth as well in polar as in temperate regions (Smith and Harrison 1991).

Table XIV : f-ratios and ammonium availabilities in the Southern Ocean

| Area | Season | f-ratio | NH ₄ availability | Reference |
|---------------------|------------------------|---------|------------------------------|---|
| POOZ | | | | |
| Scotia Sea | September-October 1978 | 0.54 | 1.2 | Olson (1980) |
| Scotia Sea | November-December 1988 | 0.47 | 1.2 | Goeyens et al. (1991) |
| Scotia Sea | January-February 1981 | 0.11 | 5.9 | Rönner et al. (1983) |
| Scotia Sea | February-March 1979 | 0.40 | 4.4 | Glibert et al. (1982) |
| Indian Ocean | January -February 1985 | | 2.8 | Verlencar et al. (1990) |
| Indian Ocean | March 1977 | | 3.4 | Slawyk (1979) |
| Indian Ocean | March 1980 | 0.87 | 2.2 | Collos and slawyk (1986) |
| SICZ | | | | |
| Scotia-Weddell Area | September-October 1978 | 0.48 | 0.9 | Olson (1980) |
| Scotia-Weddell Area | September-October 1988 | 0.97 | | Kristiansen et al. (1992) |
| Scotia-Weddell Area | November 1983 | 0.52 | | Smith and Nelson (1990) |
| Scotia-Weddell Area | November-December 1988 | 0.56 | 2.6 | Goeyens et al (1991) |
| Scotia-Weddell Area | January-February 1981 | 0.19 | 5.1 | Rönner et al. (1983) |
| Scotia-Weddell Area | February-March 1979 | 0.37 | 3.7 | Glibert et al. (1982) |
| Scotia-Weddell Area | March 1981 | 0.16 | 8.5 | Koike et al. (1986) |
| Bransfield Strait | March 1981 | | | Koike et al. (1986) |
| Weddell Sea | March 1986 | 0.72 | | Smith and Nelson (1990) Nelson et al. (1989) |
| Indian Ocean | January-February 1985 | | 3.5 | Verlencar et al. (1990) |
| Indian Ocean | March-April 1984 | 0.58 | 1.6 | Probyn and Painting (1985) |
| Ross Sea | December-January 1977 | 0.40 | 1.0 | Olson (1980) El-Sayed et al. (1983) |
| Ross Sea | January-February 1983 | 0.41 | | Nelson and Smith (1986) |

ANTAR
II/08

In addition, accumulating evidences suggest that the amount of regenerated production, the dominant size class and the dominant species within the phytoplankton community are linked. Several observations (von Bröckel 1981 and 1985, Probyn and Painting 1985, Nelson and Smith 1986, Jacques and Panouse 1991) describe the importance of picoplanktonic and nanoplanktonic (<20 µm) forms for primary production. According to Hewes et al. (1990) nanophytoplanktonic forms dominate in areas with low chlorophyll concentrations (<1 µg l⁻¹) and increases in biomass result from enhanced microphytoplankton presences. However, during the EPOS LEG 2 cruise the predominance of nanophytoplanktonic forms was also obvious at stations with high chlorophyll contents (Becquevort et al. 1992). Especially transects W3 and W4 were

characterized by a phytoplankton community in the chlorophyll maximum that consisted largely of flagellates (Becquevort et al. 1992, I. Schloss and M. Estrada personal communication). Other authors observed phytoplankton communities consisting mainly of diatoms. Nelson and Smith (1986) for instance emphasize that for an intense diatom bloom, associated with a receding ice edge in the western Ross Sea, nitrate uptake rates were high enough to satisfy approximately 65% of the phytoplankton nitrogen demand. This apparent variability of nitrate versus ammonium uptake can possibly be interpreted in terms of growth season maturity, with the succession of a diatom dominated bloom to a flagellate dominated bloom during the season (see also Holm-Hansen 1985, Koike et al. 1986), but also in terms of geographical and/or topographical variability (von Bodungen et al. 1986).

We studied the assimilatory fluxes at the first trophic level and their variability in relation to nutrient and biomass distributions in the Scotia-Weddell area (EPOS LEG 2) using (1) a conservative approach, based on the mathematical treatment of nitrate depletions sensu Le Corre and Minas (1983) and Jennings et al. (1984) and (2) the ^{15}N methodology. Integrated amounts of nitrate removed from the water column between the previous winter and the sampling moment refer specifically to new production (Dugdale and Goering 1967) during the productive period. During the different transects (W1 to W4) in the Scotia-Weddell Confluence, maximal depletions were found in the MIZ extending between $58^{\circ}30'$ S and $60^{\circ}30'$ S, with an average value of $345 \pm 181 \text{ mmol N m}^{-2}$. In the POOZ, north of the MIZ, average nitrate depletion was $149 \pm 56 \text{ mmol N m}^{-2}$ and in the CPIZ, to the South, average nitrate depletion was $77 \pm 53 \text{ mmol N m}^{-2}$. Furthermore, for latitudes where nitrate depletions were highest, we observed considerable subsurface ammonium concentrations and ammonium availabilities (Tables VI, VIII and X). The presence of ammonium in the upper layer is affected by physical processes, such as advection and diffusion, but mainly by biological processes. Besides being assimilated by autotrophs as a nitrogen source ammonium is an important reaction product in the remineralization process and it is the substrate for bacterial nitrification in deeper waters. In the euphotic layer nitrification rates have consistently been found to be negligible (Olson 1981, Ward et al. 1982, Enoksson 1986).

Elevated nitrate depletions and uptake rates do not signify absence of ammonium assimilation. Both nitrogen sources, nitrate as well as ammonium, are important in phytoplankton nutrition and are taken up simultaneously. As a general trend f-ratios

are reduced when ammonium concentrations increase (Smith and Harrison 1991), but the effect is variable and usually does not lead to a complete inhibition (Dortch 1990). The uptake rates (Table XV) show relatively small variability in the POOZ and CPIZ. In the former region the f-ratio decreases from 0.51 to 0.45 indicating a change to slight preponderance of ammonium uptake between November and December. In the southernmost CPIZ nitrate uptake prevails as the f-ratios vary between 0.56 and 0.74. In the MIZ, on the contrary, the variability in f-ratio is more drastic than in either the POOZ or CPIZ. The highest measured f-ratio amounts to 0.83, the lowest one to 0.30. Very significant is the fast transition from a value of 0.77 in late November (Station 147) towards values of 0.30 (Station 157) and 0.31 (Station 172) in December.

ANTAR
II/08

Table XV : wind mixed layer integrated uptake rates for nitrate and ammonium in the Weddell-Scotia Confluence area (EPOS LEG 2)

| station | NO ₃ uptake rate (nmol N.l ⁻¹ .d ⁻¹) | NH ₄ uptake rate (nmol N.l ⁻¹ .d ⁻¹) | total N uptake (nmol N.l ⁻¹ .d ⁻¹) | f-ratio |
|---------|---|---|--|---------|
| POOZ | | | | |
| 143 | 38 | 37 | 75 | 0.51 |
| 159 | 27 | 33 | 60 | 0.45 |
| 160 | 24 | 29 | 53 | 0.45 |
| MIZ | | | | |
| 147 | 361 | 110 | 471 | 0.77 |
| 157 | 20 | 47 | 67 | 0.30 |
| 158 | 280 | 97 | 377 | 0.74 |
| 164 | 76 | 133 | 209 | 0.36 |
| 172 | 60 | 135 | 195 | 0.31 |
| 173 | 247 | 132 | 379 | 0.65 |
| 174 | 318 | 101 | 419 | 0.78 |
| 175 | 198 | 134 | 332 | 0.60 |
| CPIZ | | | | |
| 151 | 64 | 38 | 102 | 0.63 |
| 156 | 73 | 47 | 120 | 0.61 |
| 176 | 211 | 76 | 287 | 0.74 |
| 177 | 61 | 47 | 108 | 0.56 |

A comparison of the values for nitrate depletion and the measured nitrogen uptake rates at the different stations can be used to describe the ecosystem's phytoplankton production over the season. Our mathematical approach and data interpretation is based on values for the wind mixed layer, since no nitrogen uptake data at greater depths are available (Goeyens et al. 1991-a). Nelson et al. (1987) state that quantitative estimates of the effects of ice edge blooms on nutrient

depletion, primary productivity and sediment accumulation, all depend upon assumptions of the bloom's duration. The integrated nitrate depletion constitutes the minimal amount removed from the water by biological processes, mainly assimilation by phytoplankton. Since a correct estimation of the bloom's start is very difficult, the translation of nitrate depletions into average uptake rates for nitrate is very inexact. The other way round, one can estimate the duration of the nitrate uptake process by using nitrate depletion data and measured nitrate uptake rates, assuming constancy of uptake rate since the onset of the growth season, and compare the calculated length of season with the time elapsed since the area was still ice covered. The greatest ice cover gradient moved southward at a speed of approximately 1° latitude per month along 49° W in the Scotia and Weddell Seas during EPOS LEG 2 (Lancelot et al. 1991). It can thus be deduced that the study area was ice free one to two months before sampling. In other words, the durations of nitrate uptake, calculated as the depletion divided by the uptake rate, can never exceed 60 days if they are to be considered realistic. Otherwise the assumption of constant uptake has to be rejected. Table XVI summarizes the calculated durations based on nitrate depletions and nitrate uptake rates integrated over the wind mixed layer for EPOS LEG 2. For the MIZ the values fall into two well separated groups; one with an acceptable value for the season's duration as compared to the maximal time of ice retreat, the second one with completely unrealistic values. The first group, with calculated durations of less than two months shows an average duration of 14 days, varying from 4 to 21 days, which is very plausible compared to the time necessary for ice melting. The other group shows calculated durations which are an order of magnitude larger (average =160 days; range between 66 and 447 days).

A remarkable agreement exists between realistic estimates of nitrate uptake duration and f-ratios in favour of nitrate assimilation. On the other hand, for those stations where production is based on reduced nitrogen uptake, the calculated nitrate uptake durations give unrealistic estimates, indicating that at these stations the nitrate uptake rates have been much higher earlier in the season. These relations and also the observed transition from new to regenerated production at the northern boundary of the MIZ (Stations 147, 157, 172, 59° S), show how a prevailing new production shifts into a prevailing regenerated one during December in this area.

Different authors have described the Antarctic system is preferentially based on regenerated production (Olson 1980, Glibert 1982, Rönner et al. 1983, Holm-Hansen 1985, Probyn and Painting 1985). This study suggests that, during spring, the MIZ ecosystem evolves from a first phase where new production predominates into a second one dominated by regenerated production.

Table XVI : Estimation of bloom season 's duration from nitrate depletions and corresponding nitrate uptake rates during EPOS LEG 2

ANTAR
II/08

| station | integrated NO ₃ uptake (mmol N.m ⁻² .d ⁻¹) | integrated NO ₃ depletion (mmol N.m ⁻²) | duration (d) |
|---------|--|--|-----------------|
| POOZ | | | |
| 143 | 1.22 | 80 | 66 |
| 159 | 0.36 | 46 | 128 |
| 160 | 0.53 | 49 | 92 |
| MIZ | | | |
| 147 | 5.78 | 121 | 21 |
| 157 | 0.30 | 134 | 447 |
| 158 | 3.57 | 74 | 21 |
| 164 | 2.51 | 313 | 125 |
| 172 | 2.16 | 408 | 189 |
| 173 | 4.45 | 319 | 71 |
| 174 | 4.45 | 32 | 7 |
| 175 | 1.58 | 28 | 18 |
| CPIZ | | | |
| 151 | 0.83 | 13 | 16 |
| 156 | 1.10 | 4 | 4 |
| 176 | 3.38 | 22 | 7 |
| 177 | 0.31 | 6 | 21 |

The nitrogen uptake regime of the CPIZ, as studied during EPOS LEG 2, shows much less variability. This feature was confirmed by data obtained during the ANTARKTIS IX/2 cruise in spring 1990, showing consistent preponderance of nitrate uptake at all stations located between 62.5° S and 71° S (f-ratios ranging between 0.50 and 0.82; average value = 0.7; Table XVII).

Based on the nitrate depletions and the nitrate uptake rates, we calculated the maximal duration of the growth season is less than 1 month. This seems very realistic, but it must be stressed that stations 63, 75 and 94 in the central Weddell Sea (ANT IX/2) show a significantly lower f-ratio, indicating that these stations are

characterized by a more advanced seasonal maturity. Furthermore, the ammonium availabilities are also higher in this area.

Table XVII : nitrogen uptake rates during the ANTARKTIS IX/2 cruise in the CPIZ

| station | nitrate uptake rate (nmol N l ⁻¹ d ⁻¹) | ammonium uptake rate (nmol N l ⁻¹ d ⁻¹) | f-ratio | growth season's duration (d) | ammonium availability (%) |
|---------|--|---|---------|---------------------------------|------------------------------|
| 40 | 50.8 | 11.2 | 0.82 | 30 | 0.7 |
| 45 | 8.8 | 2.5 | 0.78 | 11 | 0.2 |
| 48 | 6.6 | 4.0 | 0.62 | 30 | 0.4 |
| 56 | 30.8 | 7.1 | 0.81 | 29 | 0.8 |
| 63 | 18.7 | 10.0 | 0.65 | 16 | 0.8 |
| 75 | 21.6 | 21.2 | 0.50 | 19 | 0.9 |
| 94 | 6.8 | 5.9 | 0.53 | 29 | 1.0 |
| 108 | 21.0 | 7.3 | 0.74 | 10 | 0.2 |
| 114 | 21.5 | 7.9 | 0.73 | 9 | 0.7 |

Some preliminary results of the MARINE SCIENCE VOYAGE 6 expedition illustrate a different nitrogen uptake behaviour of the Prydz Bay phytoplankton (Table XVIII). Two stations located in the vicinity of the shelf break (2 and 16) exhibit relatively low uptake rates, whereas two on-shelf stations (29 and 48) are characterized by enhanced uptake rates (one order of magnitude higher). The average f-ratio of 0.44 (maximal value = 0.66 and minimal value = 0.21) signifies a slightly higher importance of ammonium utilization. Nevertheless, for station 29 the f-ratio amounts to 0.21, the lowest value we ever measured. This nitrogen regime corresponds with a warm surface layer (0.18° C) or a greater season's progress. This limited number of data indicates already how important regenerated production became for the CCSZ ecosystem after an initial and short period of preponderant nitrate uptake. The nitrate depletion at station 29 amounts to 856 mmol N m⁻², what indicates that at the season's onset nitrate uptake was significantly higher than the measured 36 nmol N l⁻¹ d⁻¹.

Table XVIII : nitrogen uptake rates during the MARINE SCIENCE VOYAGE 6 cruise in the CCSZ

| station | nitrate uptake rate (nmol N l ⁻¹ d ⁻¹) | ammonium uptake rate (nmol N l ⁻¹ d ⁻¹) | f-ratio |
|---------|--|---|---------|
| 2 | 37.1 | 19.3 | 0.66 |
| 16 | 18.0 | 27.3 | 0.40 |
| 29 | 35.8 | 139.1 | 0.21 |
| 48 | 90.7 | 86.2 | 0.51 |

5. BARITE AND EXPORT PRODUCTION

Subsurface Ba/barite maximum, O₂ minimum and nitrate depletion

For the Indian Ocean's sector sampled during INDIGO 3 we observed the subsurface Ba/barite accumulation to coincide with the oxygen minimum (a typical profile is shown in Figure 8) and the amount of Ba/barite in the subsurface maximum to anti-correlate with the oxygen content in the O₂-minimum (Dehairs et al. 1990).

ANTAR
II/08

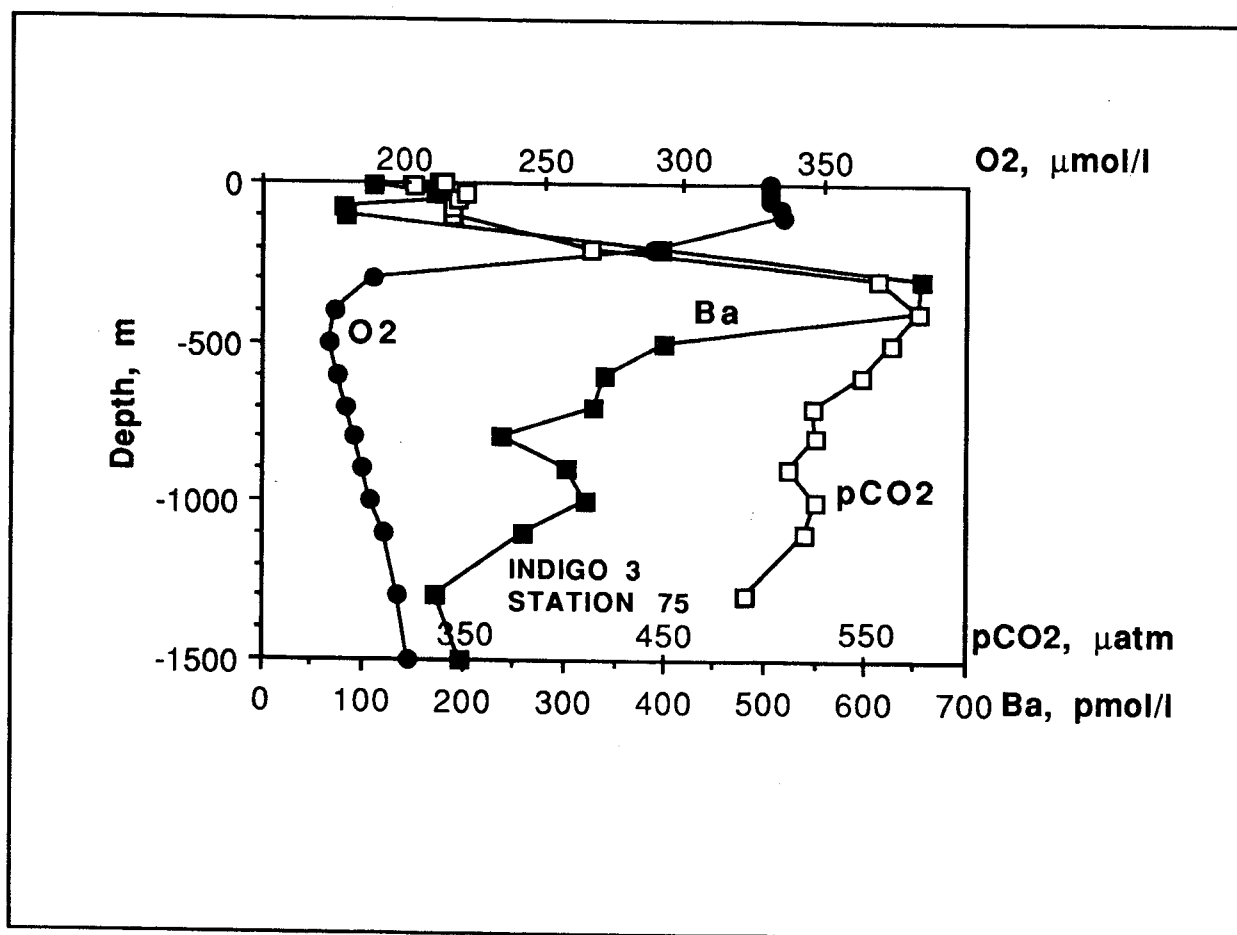


Figure 8: Vertical profile of particulate Ba at INDIGO 3 station 75. Also shown are the profiles of dissolved O₂ and pCO₂

Furthermore, the evolution of oxygen in the O₂-minimum and nitrate in the nitrate maximum, which occurs in the same depth region, follows Redfield's O₂ / N ratio (135 / 15 = 9): O₂ = -9.65 (NO₃) + 9980, with R² = 0.757, and therefore emphasizes the role of respiration processes in controlling oxygen in the O₂-minimum. We calculated earlier that the observed oxygen decrease in the O₂-minimum between

consecutive stations, downstream in the general Circumpolar Current, is compatible with existing data on production and export for the Circumpolar Ocean (Dehairs et al. 1990).

This conclusion could not be verified for the Scotia-Weddell Confluence area, sampled during EPOS LEG 2, due to the lack of sufficient oxygen data and the complexity of water circulation in the Confluence area. However, the off-shelf stations of the Prydz Bay area, sampled during MARINE SCIENCE VOYAGE 6, do follow the general trend of subsurface Ba/barite increase with oxygen decrease in the O₂-minimum, observed for the INDIGO 3 stations (see Figure 10, below).

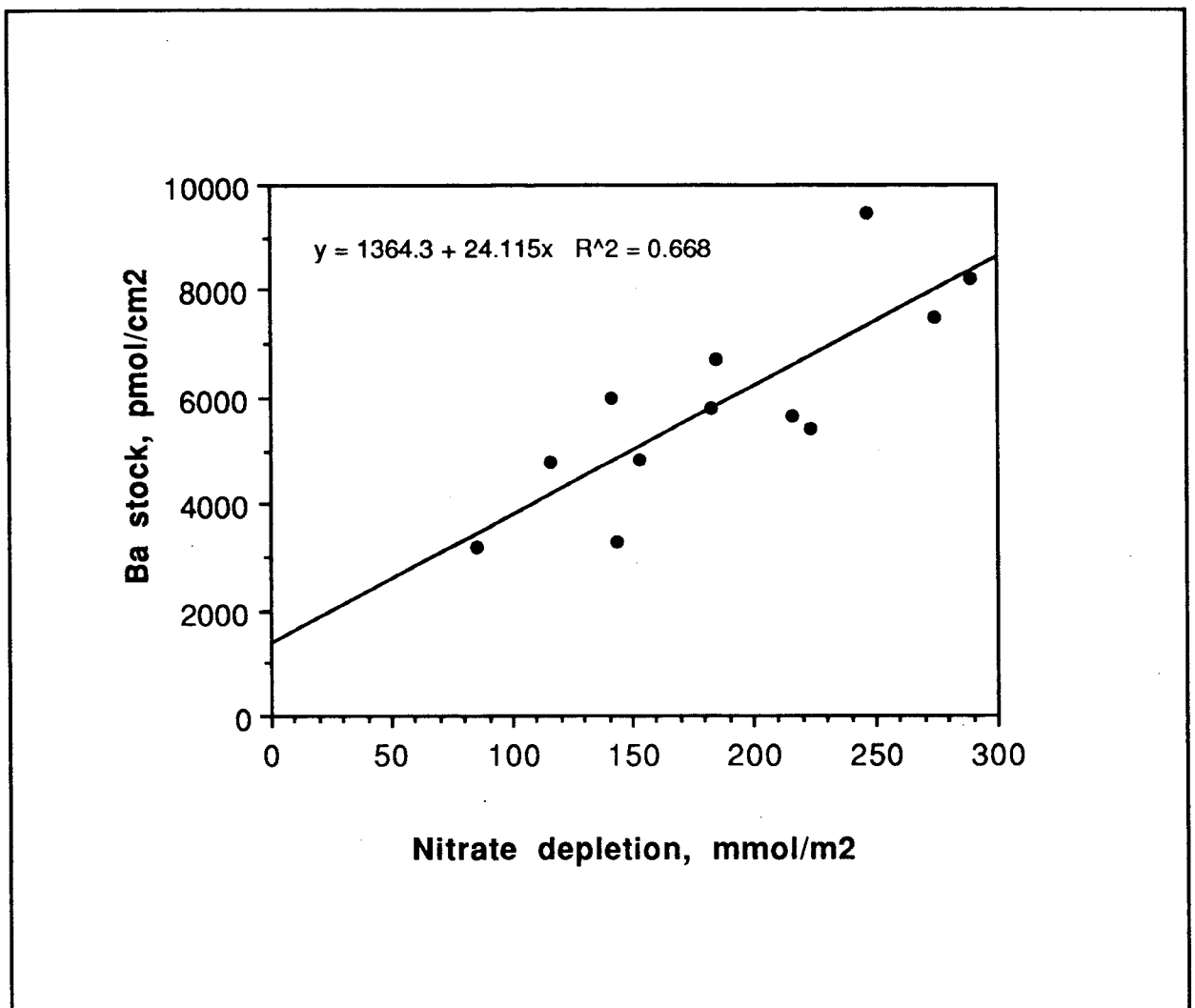


Figure 9: Subsurface particulate Ba stock (pmol cm⁻²) versus nitrate depletion (mmol m⁻²) for O₂Z stations sampled during INDIGO 3 and EPOS LEG 2.

Moreover, we observed that subsurface Ba/barite correlated closely with nitrate depletion for the OOZ stations of the Scotia Sea and the Indian Ocean's sector (Figure 9).

However, for MIZ stations in the Scotia-Weddell Confluence and CCSZ stations on the Prydz Bay shelf, the considerable nitrate depletions are not reflected in high subsurface Ba/barite stocks (data not indicated in Figure 9). The observed correlation suggests for the OOZ that nitrogen, assimilated as nitrate, was transferred to subsurface layers, while this was not (yet) the case for the MIZ and the CCSZ. Several processes could explain this absence of export signal in the MIZ and the CCSZ.

First, it is probable that the time elapsed since the season's onset is too short and that export has not yet occurred to a significant degree. In that case, nitrate-nitrogen should still reside mainly in surface water pools of particulate organic matter and dissolved organic matter. For the very early season this is indeed the case, with about half of the nitrate depletion being localized in the particulate nitrogen pool (see below section 6).

Second, MIZ and CCSZ are systems evolving towards predominance of recycled production over new production as indicated by the low *f*-ratios attained with progressing season (see Table XV and Table XVIII). In this case original nitrate uptake was channeled into retention systems, as recognized earlier for Southern Ocean ecosystems by Smetacek et al. (1990). It is interesting that for Prydz Bay this is achieved under maintained predominance of diatoms in the phytoplankton community.

Third, the material exported is transferred elsewhere and local subsurface waters are bypassed. For the MIZ in the Scotia-Weddell Confluence we have already described the disappearance of the diatoms by intense krill grazing. In that case export is accounted for by krill biomass increase and fecal pellet transfer to deep water (i.e. below the upper 500 m we investigated). For the CCSZ it can be argued that the short residence time of the water above the Prydz Bay shelf impedes significant accumulation and degradation of organic matter exported to local subsurface waters. Indeed, residence time of water over the Prydz Bay shelf is only about 1 month due to fast flushing of the shelf by a cyclonic gyre (Smith et al. 1984).

Usefulness of the barite tracer for estimating export production

For the Indian Ocean's sector, sampled during INDIGO 3, and the off-shelf Prydz Bay stations, sampled during MARINE SCIENCE VOYAGE 6, we observe a correlation between the Ba/barite maximum and the oxygen minimum (Figure 10). This correlation is shown for the Ba stock, integrated over a 200 m depth interval in the Ba maximum region, versus the oxygen stock integrated over 200 m in the O₂-minimum region. The setting of this depth interval at 200m is somewhat arbitrary, but it generally represents the maximum distance over which the O₂-minimum is resolved.

The observed Ba/O₂ regression is:

$$\text{Ba} = 164240 \times 10^{-3.524 \times 10^{-4}} (\text{O}_2) ; \text{ with } R^2 = 0.89.$$

We will assume that this correlation applies universally. Thus we can calculate the oxygen consumption corresponding to the "net" Ba stock in a 200 m depth interval centered on the Ba-maximum for any other profile. Using the Redfield O₂/C ratio of 135/100 we express the O₂ consumed as POC exported to the subsurface since the start of the season. A critical step in this approach resides in the choice of the value for the background Ba signal which has to be subtracted from the overall signal in order to obtain the net increase of Ba since the start of the season. From a close observation of the numerous Ba profiles, we have acquired for the Southern Ocean, we can conclude that in absence of any significant subsurface Ba maximum the residual Ba concentration down to 500 m is about 125 pmol l⁻¹. Integrated over a depth interval of 200 m this concentration represents a background Ba stock of 2500 pmol cm⁻².

In Table XIX we show the calculated values for export of the production to the subsurface depth region for the OOZ, MIZ and CPIZ regions of the Scotia Weddell Confluence area (EPOS LEG 2). It must be stressed that the approach outlined above can be subject to large errors for both MIZ and CPIZ, since in these cases the net Ba signal is small compared to the background signal. Corresponding seasonal gross primary productions (GPP) in Table XIX are calculated by considering an average f-ratio for each area deduced from Table XV. The ratio of this calculated GPP for the season over the daily production rate, obtained for the different regions of the Confluence area (Mathot et al. 1992) , gives an estimate of the season's duration. This calculated season's duration should be realistic for the proposed approach to be valid. In this approach we assume, of course, that the daily production rates given by Mathot et al. (1992) are representative for the whole

season. For the OoZ the calculated season's duration is about 6 months. When compared with the durations based on the nitrate depletions and the nitrate uptake rates (Table XV) the present values are 2 to 3 times higher, except when compared with the value for station 159, which indicates a long season's duration of 4 months.

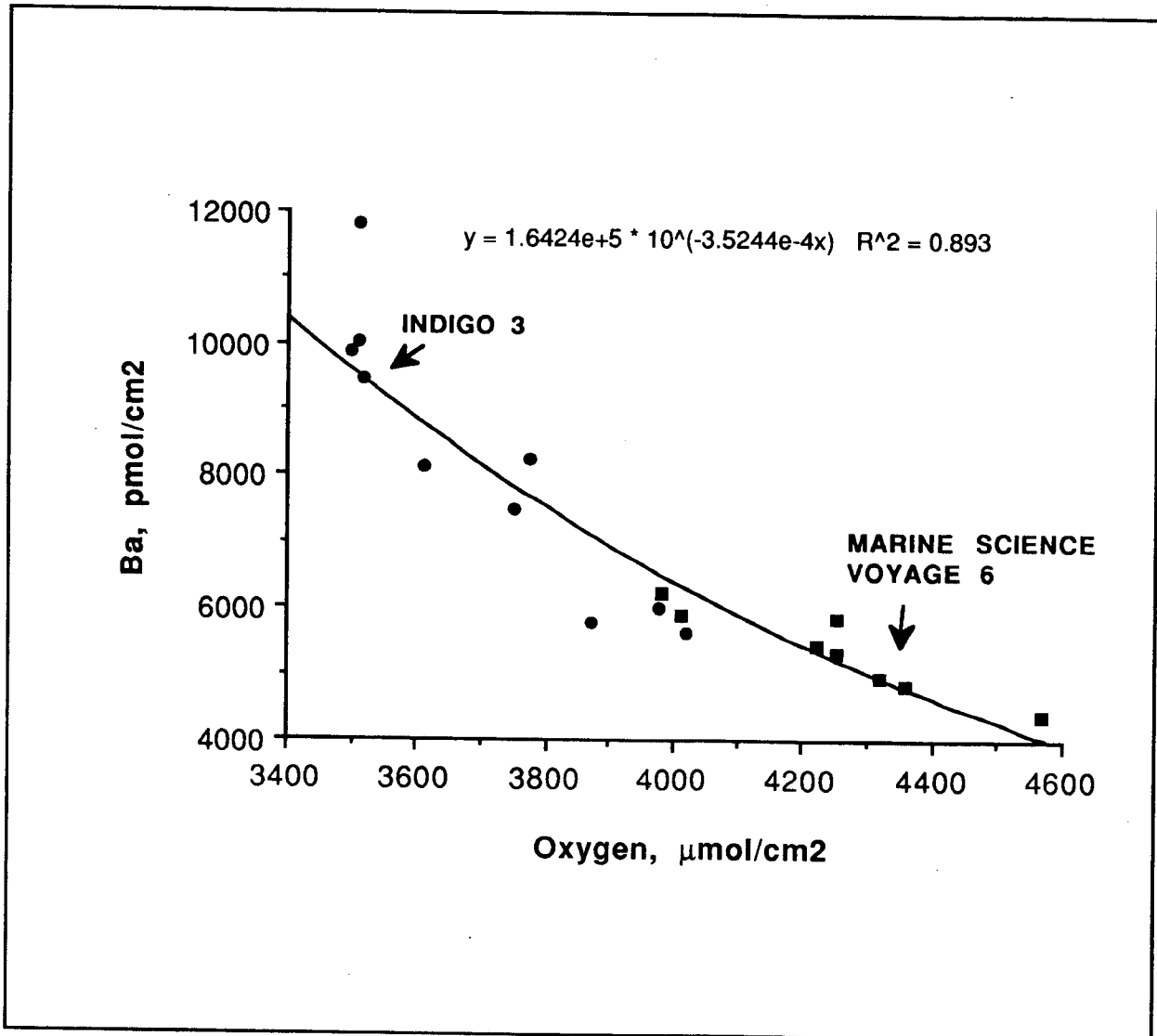


Figure 10: stocks of particulate barium (pmol cm⁻²) in the subsurface layer versus stocks of dissolved oxygen (μmol cm⁻²) in the oxygen minimum layer.

Table XIX: Comparison between seasonal gross primary production (GPP°) calculated using the observed net stocks of Ba in the subsurface Ba maximum with measured production rates based on ^{14}C incorporation, in the Scotia-Weddell Confluence area (GPP^* ; Mathot et al., 1992). Δ 's denote net changes. Coefficients used are : $O_2/POC = 1.35$; f-ratios as in Table XV.

| Area | ΔBa stock $pmol\ cm^{-2}$ | ΔO_2 stock $\mu mol\ cm^{-2}$ | ΔPOC stock $\mu mol\ cm^{-2}$ | POC exp $mg\ m^{-2}$ | f-ratio | GPP° $mg\ m^{-2}$ | GPP^* $mg\ m^{-2}\ d^{-1}$ | Season days |
|------|--------------------------------------|--|--|-------------------------|---------|-------------------------------|---------------------------------|----------------|
| OOZ | 2550 | 866 | 641 | 76,980 | 0.5 | 153,960 | 870 | 177 |
| MIZ | 300 | 140 | 104 | 12,440 | 0.3 | 41,480 | 1520 | 27 |
| CPIZ | 560 | 249 | 184 | 22,130 | 0.7 | 31,620 | 420 | 75 |

For the MIZ the calculated duration in Table XIX is similar to the estimates based on nitrate depletions and nitrate uptake rates (Table XVI), but only for the case of high f-ratios (>0.5). For the CPIZ it is higher by up to a factor 10. In this latter case it is probable that the ice-algae community exports part of its organic matter stock to the subsurface water column. The GPP by the ice algae community is not included in the value given by Mathot et al. (1992) for the CPIZ and therefore calculation of the season's duration for the CPIZ makes not much sense.

From the above we can nevertheless conclude that subsurface barite accumulation appears to trace export production reasonably well. This export production appears to be essentially a function of the season's duration and the relative importance of new versus recycled production. Highest values are observed for the OOZ where the season has lasted longest, and new production maintains approximately a 50% contribution to total production over the season.

6. A SCENARIO FOR THE DEVELOPMENT OF SOUTHERN OCEAN BLOOMS

In the MIZ of the Scotia-Weddell area (EPOS LEG 2) ammonium regeneration was more intensive than in the adjacent POOZ and CPIZ, where ammonium production in the mixed layer was limited. This resulted in a different ammonium build-up and availability in these three subzones (Figure 7). The average ammonium stocks amounted respectively to 46, 91 and 22 mmol N m⁻² in the POOZ, MIZ and CPIZ.

It has been shown previously by Smith and Nelson (1990) that Antarctic phytoplankton has the ability to increase its rate of ammonium uptake when the availability of ammonium is increased. On the other hand, it is known for temperate regions (Wheeler and Kokkinnakis 1990), and also for Antarctic systems (Smith and Nelson 1990), that nitrate uptake is reduced at elevated ammonium levels. Both these considerations are in agreement with the observed shift from predominant new production towards predominant regenerated production in the MIZ during the EPOS LEG 2 study, and with the relatively slight decrease of the f-ratio in both the POOZ and the CPIZ (Goeyens et al. 1991-a). Indeed, the f-ratios obtained for repeated uptake measurements in the MIZ (EPOS LEG 2, between 59° S and at 59°30' S) show a maximal decrease from 0.77 at the beginning of the cruise to 0.30 at the end. On the other hand, much less variation is observed for the POOZ as well as for the CPIZ. The former is characterized by an average f-ratio of 0.47, whereas for the latter the average f-ratio amounts to 0.62 (Figure 11). These observations give evidence for the increasing importance of ammonium generation by microbial heterotrophic activity with seasonal progress, but in the MIZ the transition towards ammonium based production is more drastic. Since nitrate is never negligible for phytoplankton nutrition, the original concept that regenerating systems consist of autotrophs assimilating recycled nutrients produced by the heterotrophs after the nitrate pool was exhausted, does not hold. The lowest measured nitrate concentrations are never limiting primary production and the lowest measured f-ratios exceed largely those for temperate regions given by Eppley (1989). It thus appears that the shift towards ammonium uptake is mainly driven by phytoplankton preference after an increase of the ammonium availability due to heterotrophic activity. In the POOZ and the CPIZ the increase of ammonium availability is less pronounced and induces but a gradual and limited decrease of the f-ratio.

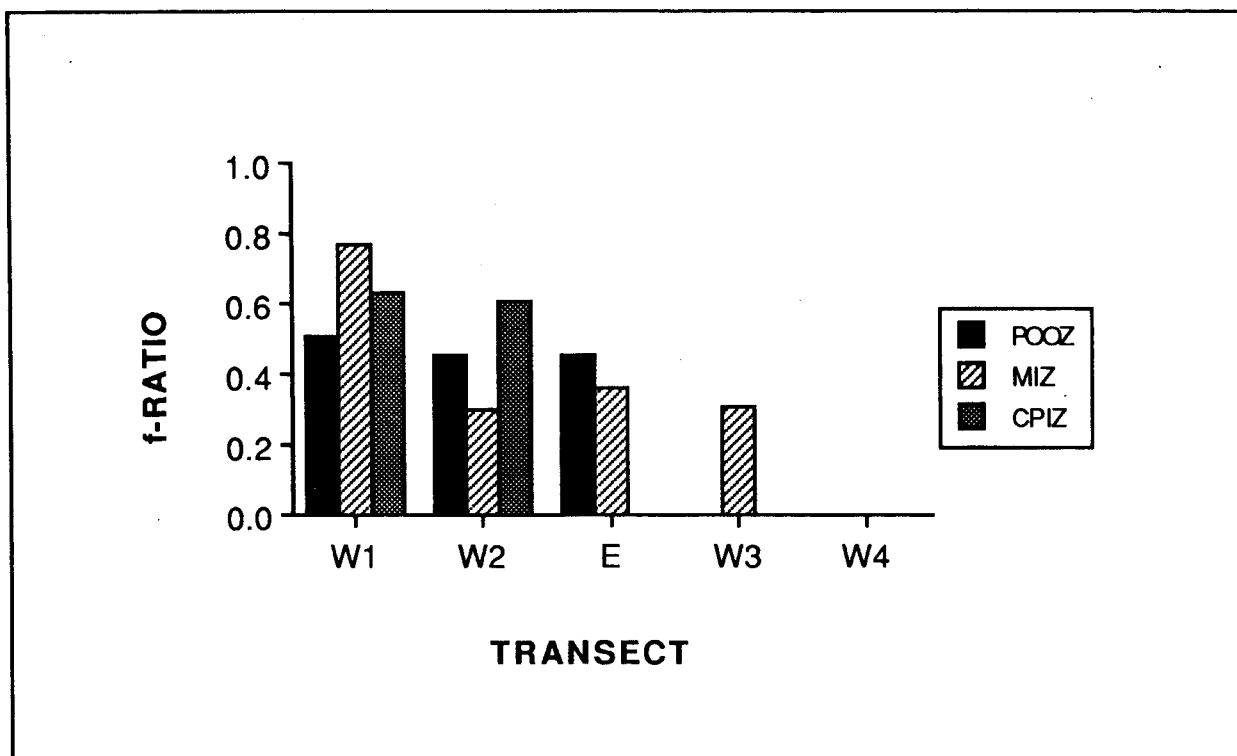
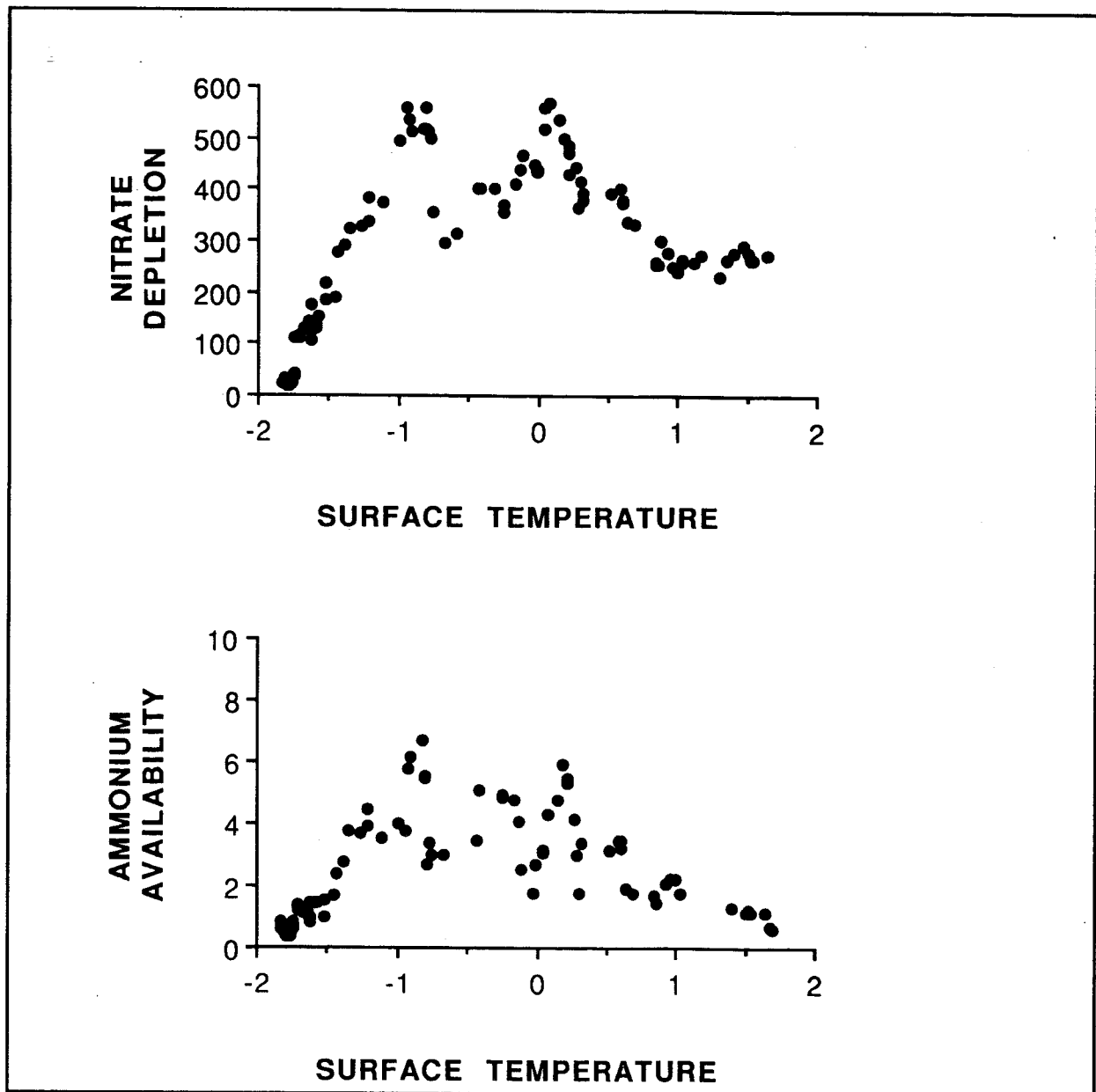


Figure 11 : seasonal time-course of f-ratios in the POOZ, MIZ and CPIZ studied during the EPOS LEG2 cruise

Without considering geographical position of the stations and calendar date of sampling, we arranged our data in a sequence reflecting the growth season's maturity by sorting them in ascending order of surface water temperature. This approach is based on an original idea of C. Veth (personal communication, and Veth 1991) and it is only used to gain insight in the general trends exhibited by parameters as nitrate depletion, ammonium availability and particulate stocks. These different parameters obtained for the different regions of the Southern Ocean are combined and represented by their smoothed values (smoothing width = 5).

The graphs of nitrate depletions and of ammonium availability versus surface temperature give very similar pictures (Figure 12). Both parameters show a steep and almost linear increase from zero to a maximal value within a temperature range from -1.8°C (the coldest temperature of the water during winter) to approximately -0.8°C . From Figure 12 it is observed that nitrate depletion reaches a (smoothed) maximum of 600 mmol N m^{-2} . Ammonium availability reaches a (smoothed) maximum of 6%. The striking agreement between both these parameters during the initial phase of the season (i.e. between -1.8 and -0.8°C) led us to consider this



ANTAR
II/08

Figure 12 : variability in nitrate depletion (mmol N m^{-2}) and variability in ammonium availability (%) with increasing surface temperature ($^{\circ}\text{C}$)

period, corresponding with a surface water heating of 1°C , separately. From the EPOS LEG 2 data set (EPOS LEG 2, 1992), during which several geographical locations were repeatedly sampled during the months of November and December, we learned that such a 1°C temperature increase of surface water occurred in about 15 days. The linear relations for nitrate depletions, ammonium stocks as well as particulate nitrogen stocks versus increasing surface water temperature are as follows :

nitrate depletion = $958.9 + 510.4 \text{ temperature}$ ($R = 0.92$),

ammonium stock = $267.7 + 144.7 \text{ temperature}$ ($R = 0.90$), and

particulate nitrogen = $389.7 + 205.3 \text{ temperature}$ ($R = 0.83$).

The nitrogen balance for this initial phase of the season shows that about two thirds of the nitrate removed from the water during this period are converted into the particulate nitrogen and ammonium pools. The remaining third must be accounted for by the stock of dissolved organic matter and the export of particulate material from the upper layer. The simultaneous decrease of the nitrate and increase of the ammonium pools indicate significant regeneration and suggest the presence of a considerable pool of dissolved organic nitrogen in the surface water. Since we have not analysed for dissolved organic nitrogen an estimate of its magnitude is not possible here.

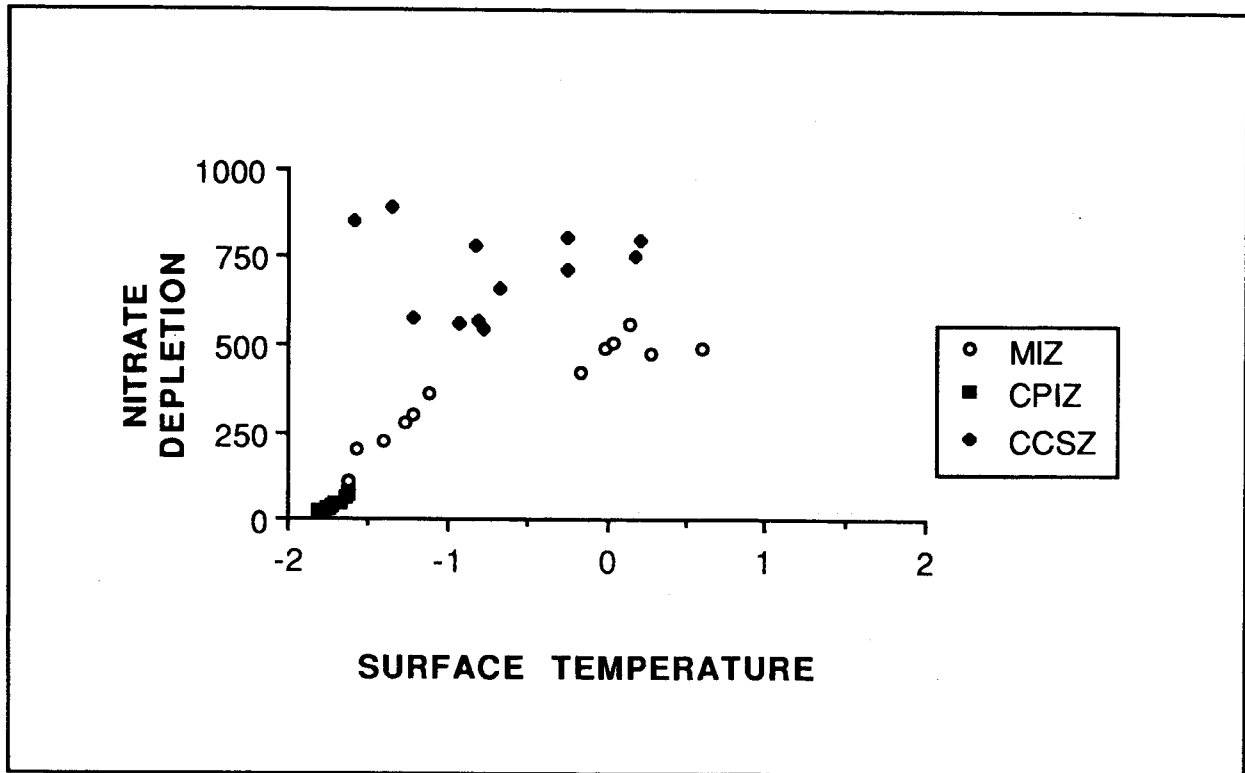
The second phase of the growth season shows considerably more scatter. As a general trend nitrate depletion and ammonium availability show a progressive decline when temperature rises above 1° C . The observed minimum in the temperature range between -0.8° C and 0° complicates the overall pattern. This minimum is mainly carried by data points from the on-shelf Prydz Bay area. We believe the specific character of topography and water mass circulation in the Prydz Bay area may be responsible for this peculiar behaviour.

The PN pool also shows a clear general trend towards decreasing concentrations after the initial surge phase.

Since it is likely that regional variability exists in compositional change of the algal communities and predation efficiency of herbivorous plankton during the growth season we studied the different Southern Ocean subareas separately.

In Figure 13 the nitrate depletion versus temperature plot is shown for the CPIZ, MIZ and CCSZ separately. It becomes clear that the rate of nitrate removal during the early phase is highest in the CCSZ, where ice coverage disappears very quickly with spring warming, while in the MIZ and especially in the CPIZ, where some ice remains throughout the year, nitrate depletion rates are considerably smaller. Furthermore, it is observed that the nitrate depletions level off at different maximum values, as discussed earlier. The steep increase in nitrate depletion during the early season is paralleled by a steep increase in PN concentration (Figure 14). The measured PN maxima vary largely, however, for each zone : in the CPIZ

maxima never exceed $1 \mu\text{mol N l}^{-1}$, whereas in the MIZ and CCSZ concentrations of $3 \mu\text{mol N l}^{-1}$ and more were measured.



ANTAR
II/08

Figure 13 : nitrate depletion (mmol N m^{-2}) versus surface water temperature ($^{\circ}\text{C}$) in the MIZ, CPIZ and CCSZ

After the early phase, characterized by a fast nitrate assimilation leading to enhanced particulate nitrogen stocks, ammonium regeneration by heterotrophic activity and ammonium assimilation by autotrophs become the significant processes controlling the nitrogen flux. This is obvious from the graph representing f-ratio versus surface temperature (Figure 15). For the CPIZ, f-ratios are somewhat scattered and fluctuate between 0.8 and 0.5, with lowest f-ratios consistently coinciding with highest ammonium availabilities. This coincidence of low f-ratio with high ammonium availability is also observed in the MIZ and the CCSZ. For the MIZ stations a drastic decrease in f-ratio from 0.8 to 0.3 was observed at the end of the surge phase (i.e. about three weeks after the growth season started). Similarly for the CCSZ, our preliminary results of the Prydz Bay study show that the f-ratio decreased from 0.51 (surface temperature = -0.922°C) to 0.21 when the surface temperature had reached more than 0.2°C .

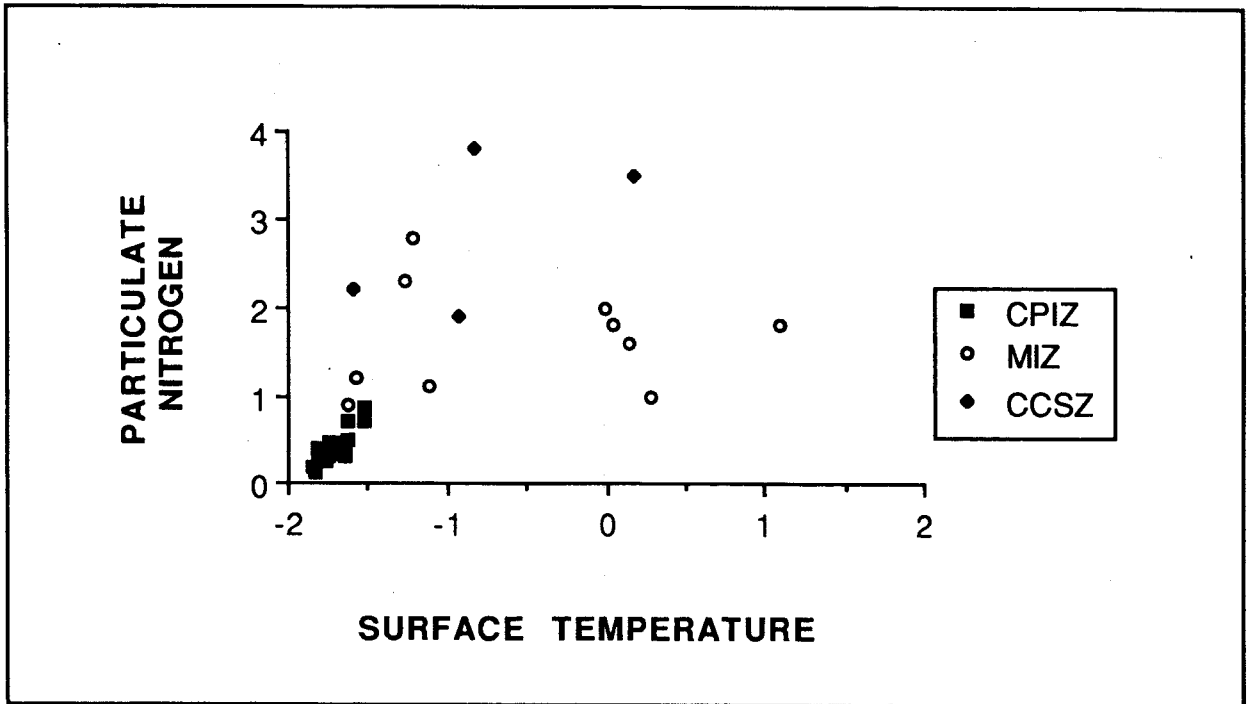


Figure 14 : evolution of the depth weighted averages for particulate nitrogen stock ($\mu\text{mol N l}^{-1}$) versus the surface water temperature ($^{\circ}\text{C}$)

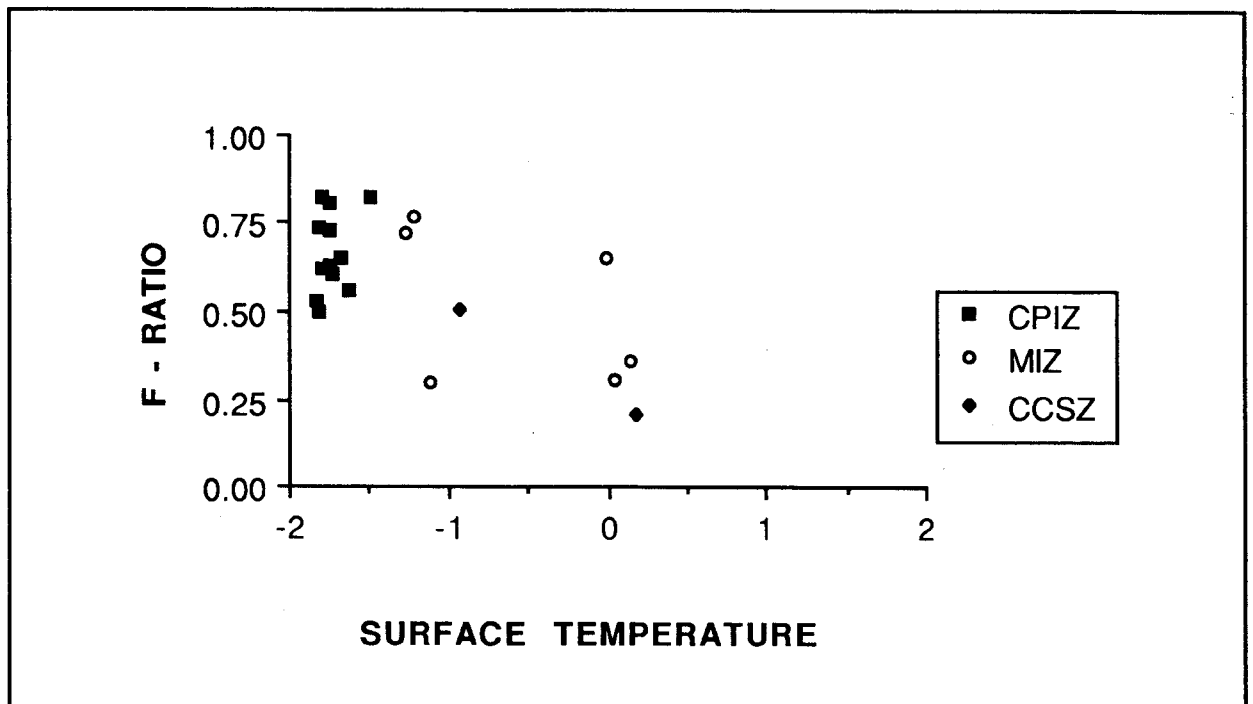


Figure 15 : evolution of the f-ratios versus surface water temperature ($^{\circ}\text{C}$)

In the Scotia-Weddell area, we observed that microzooplankton was more important than bacterioplankton in controlling the ammonium regeneration (Table XIII). Nevertheless, after the krill event (EPOS LEG 2, station 157), bacterially mediated ammonium regeneration was shown to be the main ammonium source. The krill swarm clearly induced the drastic PN decrease and it triggered enhanced ammonium regeneration. Passages of krill swarms happen at the event scale but have obviously a determining role in the life cycle of phytoplankton living near and in ice covered areas. Repeated samplings in the MIZ of the Weddell Scotia Confluence area revealed a permanent absence of diatoms after the krill swarm passed. Diatoms were replaced by a flagellate dominated bloom, with chlorophyll a concentrations reaching nearly 2 mg m^{-3} . A less pronounced but similar picture exists for the CPIZ. M. Baumann (personal communication) found decreased numbers of diatoms in areas characterized by lower f-ratios. This picture is completely different from the observations in the Prydz Bay region, where diatoms remained dominant (H. Marchant, personal communication) when f-ratios decreased to low values with progress of the season. In this latter case the clear switch in importance of nitrogen source, is not accompanied by a compositional change of the phytoplankton assemblage.

The situation is different for the subsurface expression of the exported production. In early season (i.e. between -1.8°C and $+1^\circ \text{C}$) the subsurface particulate Ba content appears to fluctuate around some background level (Figure 16). When temperature exceeds 1°C we observe clear trends for increased particulate Ba stocks in the subsurface waters. Thus, the subsurface mineralization of part of the season's production, indicated by the barite accumulation, only becomes apparent when the phytoplankton development is already declining in surface waters. It is possible that the complete mineralization of the organic matter exported to the subsurface region is achieved only in the coming winter. This is suggested by the Ba data for ANTARKTIS IX/2, showing for the central Weddell Sea significant subsurface stocks (Table III) and absence of significant phytoplankton development in local surface waters. It is possible that in this case the subsurface Ba signal reflects the export intensity of the previous season. The accumulation of barite in the subsurface region possibly results from (1) a preponderant advective transport and not from gravitational settling, controlling the redistribution of released barite (Dehairs et al. 1980), and (2) the increased residence time of the watermass in this central area of the Weddell Gyre (E. Fahrbach, personal communication).

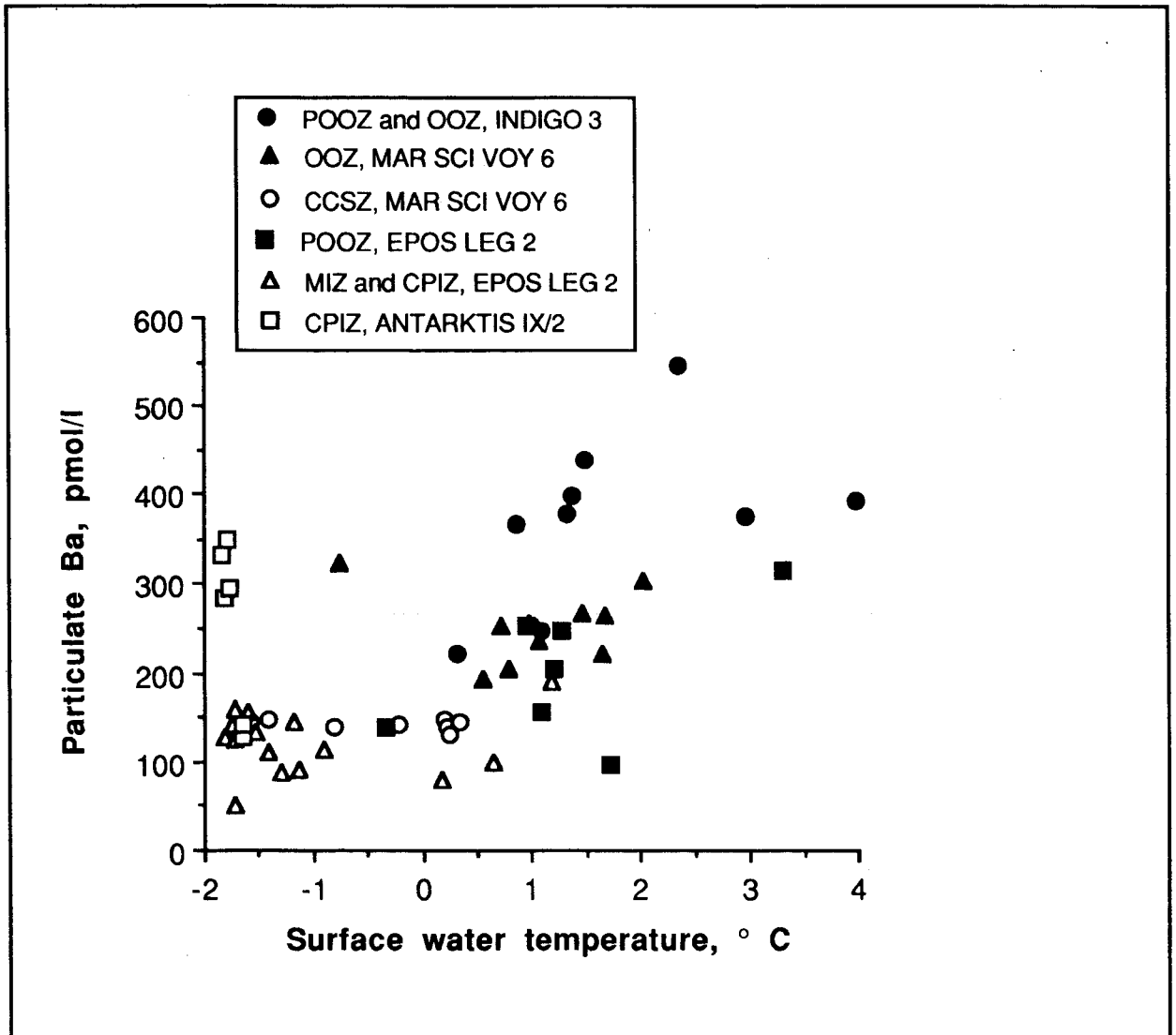


Figure 16 : Particulate Ba (pmol l^{-1}) versus the surface water temperature ($^{\circ}\text{C}$) for all data obtained during four cruises.

Judged from Figure 16, production of subsurface barite should occur in all different subregions considered, if residence time of the subsurface waters is long enough to allow for transport and accumulation of organic matter in subsurface layers and its heterotrophic oxidation.

However, caution is required when considering Figure 16. Indeed, using the evolution of temperature rise as an indication of time is valid only for environments which all evolved from a similar original winter situation. This is certainly not the case for all environments shown in here, since they do not all evolve through the

whole temperature range shown. Furthermore, a certain "memory effect" between successive seasons is possible as suggested by the ANTARKTIS IX/2 data, for which high subsurface Ba stocks indicate export of organic matter to have occurred, although the temperature of the surface waters is still very low. In this case the Ba signal is likely to have been carried over from the previous season.

Therefore, we must be careful and not consider time is the only factor determining the presence or absence of subsurface signals for export production. We can not exclude the impact of the type of production occurring in surface waters (i.e. new versus regenerated production). Indeed, in the temperature range between -1°C and 0°C , where lowest subsurface Ba values occur, we observed preference for ammonium uptake and subsequent reduced export towards subsurface waters. For the samples in this temperature range (mainly MIZ and CCSZ samples) it is probable that even with time no subsurface Ba maximum will develop.

CONCLUSIONS

The Southern Ocean is an extremely diverse ecosystem, characterized by very low temperatures, seasonal or permanent ice coverage and extreme seasonal variability in light regime. The variability in this vast reservoir led us to distinguish five subareas with marked differences in nitrogenous nutrient signature, biogenic element distributions and plankton dynamics.

The observed evolutions in nitrate depletion and in f-ratio allow for the description of a general nitrogen flux pattern. At the start of the growth season phytoplankton exclusively assimilates nitrate. The faster the ice cover melts the higher the nitrate depletion rate and the larger the PN stock in the euphotic layer. The amounts of nitrate removed from the upper layer vary considerably in the different subareas. The MIZ and CCSZ are characterized by huge nitrate depletions, exceeding the ones measured in the CPIZ by at least one order of magnitude. In the OOZ, as well as in the POOZ, an intermediate situation prevails. After a short early phase, the ammonium availability increases and autotrophic organisms switch from new to regenerated production. The measured ammonium availabilities show the same trend as the nitrate depletions : very high values in the MIZ and CCSZ, very low values in the CPIZ and intermediate ones in the OOZ. The increasing importance of regenerated nutrients in primary production is mainly driven by phytoplankton preference after remineralization processes supplied more and more ammonium. Nevertheless, the nitrate pool never becomes exhausted and nitrate assimilation still contributes for about one third of the total inorganic nitrogen uptake. This scenario with initial and very high uptake of nitrate, followed by a drastic change after the ammonium availability increased is clearly confirmed by the MIZ study (EPOS LEG 2) and the CCSZ study (MARINE SCIENCE VOYAGE 6) and to a lesser degree by the results of the CPIZ study (EPOS LEG 2 and ANTARKTIS IX/2). In literature it is often emphasized that regenerated production is characteristic for nano- and picosized phytoplankton mainly consisting of flagellates. While nanoflagellates became indeed the predominant phytoplankton group in the Scotia-Weddell Confluence area, large diatoms remained predominant in the Prydz Bay area.

For the MIZ and CCSZ regions it is likely that the initial growth surge, sustained by nitrate uptake, triggered the fast development of the grazers (mainly micrograzers

for the MIZ; micrograzers and copepods for the CCSZ). This resulted in high ammonium production rates and the phytoplankton switched from nitrate to ammonium assimilation. This reflects a typical retention system, sensu Peinert et al. (1989), with reduced export to subsurface layers and extremely low build-up of subsurface barite stocks. The phytoplankton community structure does not necessarily change as a result of this change in production type, as indicated by maintained diatom dominance in Prydz Bay. However, if krill, the typical K-strategist comes on stage, the phytoplankton composition can completely change as a result of the very high grazing pressure.

ANTAR
II/08

In the other subregions (POOZ, OOOZ, CPIZ) no intense blooms develop and as a result no significant grazing develops. Therefore, production of ammonium is not as large as observed for MIZ and CCSZ and nitrate contribution in phytoplankton nutrition remains relatively high (f-ratios ≥ 0.5). These systems have export to the subsurface layers, as witnessed by the build-up of barite stocks and the decrease of oxygen in subsurface waters. The export is carried by aggregates and solitary particles since grazing is kept low. This picture fits the export system described by Peinert et al. (1989).

The main question is then why do these intense blooms develop in specific areas, such as the MIZ and the CCSZ ? Is it ice melting and ensuing stabilization of the water column with the installation of a shallow mixed layer, or does the enhanced presence of trace elements such as Fe have an effect ? That Fe might have an impact is suggested by elevated subsurface concentrations of lithogenic compounds (reflected in the presence of Al) in the Confluence area (Dehairs et al., 1992) and the inner shelf area of Prydz Bay.

In situations with significant export it is shown that its magnitude is reflected in the seasonal build-up of subsurface barite and consumption of oxygen. Net changes in suspended barite stocks can therefore be used to estimate export production to subsurface waters.

We emphasize that export towards the subsurface depths is significant in regions where grazing pressure (except when exerted by krill) is minimal. These are not the regions characterized as retention systems, where high productivities induce enhanced grazing pressure.

ACKNOWLEDGEMENTS

This research would not have been possible without the logistical assistance of the Alfred Wegener Institute, the Australian Antarctic Division and Terres Australes et Antarctiques Françaises and without the efficient help of the crew members of RV "Marion Dufresne", RV "Polarstern" and RV "Aurora Australis". The research conducted in the framework of EPOS LEG 2 was sponsored partly by the European Science Foundation. We are particularly grateful to A. Poisson, V. Smetacek, E. Fahrbach, H. Marchant and R. Williams, scientific officers of the different cruises we participated in, for having integrated us in their research teams.

We acknowledge the assistance and help of : N. Stroobants for preparation of EPOS LEG 2 suspended matter samples; O. Raguenu, for sample preparation and ICP-AES analysis of the ANTARKTIS IX / 2 suspended matter samples; M. Elskens for ammonium analysis and 15-N incubation experiments during the MARINE SCIENCE VOYAGE 6 cruise; O. Colette for sample preparation and ICP-AES analyses of the MARINE SCIENCE VOYAGE 6 suspended matter samples; A. Vandenhoudt for the ET-AAS analysis of Si in total suspended matter samples of the EPOS LEG 2 and ANTARKTIS IX / 2 cruises. Access to the ICP-AES instrumentation at the Geological Survey of Belgium was made possible by the late Dr. H. Neybergh.

F. Dehairs is Research Associate at the National Fund for Scientific Research, Belgium.

REFERENCES

- Alder, V., Cuzin-Roudy, J., Fransz, G., Granelli, E., Larsen, J., Rabbani, M. and Thomsen, H. 1989. Macro- and micrograzing effects on phytoplankton communities. In : The expedition Antarktis VII/03 (EPOS LEG 2) of RV "Polarstern" in 1988/89. Hempel, I., Schalk, P. H. and Smetacek V. (Eds.). *Berichte zur Polarforschung* 65, Bremerhaven : 123-130.
- Bathmann, U., Fischer, G., Müller, P. J. and Gerdes, D. 1991. Short-term variations in particulate matter sedimentation off Kapp Norvegia, Weddell Sea, Antarctica : relation to water mass advection, ice cover, plankton biomass and feeding activity. *Polar Biol.* 11 : 185 - 195.
- Becquevort, S., Mathot, S. and Lancelot C. 1992. Interactions in the microbial community of the marginal ice zone of the Northwestern Weddell Sea through size distribution analysis. *Polar Biol.* 12 : 267 - 275.
- Biggs, D. C. 1982. Zooplankton excretion and ammonium cycling in near surface waters of the Southern Ocean. I. Ross Sea, austral summer, 1977 - 1978. *Polar Biol.* 1 : 55 - 67.
- Biggs, D. C., Amos, A. F. and Holm-Hansen, O. 1985. Oceanic studies of epi-pelagic ammonium distributions : the Ross Sea ammonium flux experiment. In : Antarctic nutrient cycles and food webs. Siegfried, W. R., Condy, P. R. and Laws, R. M. (Eds.). Springer-Verlag, Berlin : 93 - 103.
- Billen, G. and Becquevort, S. 1991. Phytoplankton-bacteria relationship in the Antarctic marine ecosystem. *Polar Res.* 10 : 245 - 253.
- Bishop, J. K. B. 1988. The barite-opal-organic carbon association in oceanic particulate matter. *Nature* 332 : 341-343.
- Bishop, J. K. B. 1989. Regional extremes in particulate matter composition and flux: Effects on the chemistry of the ocean interior. In : Productivity of the Oceans: Present and Past, Dahlem Workshop Reports, Life Science Research Report 44. Berger, W.H., Smetacek, V.S., and Wefer, G. (Eds.). John. Wiley, New York : 117-137.
- Botazzi, E. M., Schreiber, B. and Bowen, V. T. 1971. Acantharia in the Atlantic Ocean, their abundance and preservation. *Limnol. Oceanogr.* 16 : 677-684.

- Bowen, H. J. M. 1979. Environmental Chemistry of the Elements. Academic Press, London, 333 p.
- Buma, A., Estrada, M., Larsen, J., Riebesell, U., Schloss, I. and Thomsen, H. A. 1989. Unicellular organisms studied alive using photographic and video techniques In : The expedition Antarktis VII/03 (EPOS LEG 2) of RV "Polarstern" in 1988/89. Hempel, I., Schalk, P. H. and Smetacek V. (Eds.). Berichte zur Polarforschung 65, Bremerhaven : 102 - 110.
- Choi, J. W. and Stoecker, D. K. 1989. Effects of fixation on cell volume of marine planktonic protozoan. Appl. Environ. Microbiol. 55 : 1761 - 1765.
- Collos, Y. and Slawyk, G. 1986. ^{13}C and ^{15}N uptake by marine phytoplankton - uptake ratios and the contribution of nitrate to the productivity of Antarctic waters (Indian Ocean sector). Deep-Sea Res. 33 : 1093 - 1051.
- Dehairs, F., Chesselet, R. and Jedwab, J. 1980. Discrete suspended particles of barite and the barium cycle in the open ocean. Earth Planet. Sci. Lett. 49, 528 - 550.
- Dehairs, F. and Goeyens, L. 1989. The biogeochemistry of barium in the Southern Ocean. In : Antarctica, Volume II, Marine Geochemistry, Caschetto S. (ed.), Prime Minister's Services, Science Policy Office, Brussels, pp 100.
- Dehairs, F., Goeyens, L., Stroobants, N., Bernard, P., Goyet, C., Poisson, A. and Chesselet, R. 1990. On suspended barite and the oxygen-minimum in the Southern Ocean. Global Biogeochem. Cycles 4 : 85-102.
- Dehairs, F., Goeyens, L., Stroobants, N. and Mathot, S. 1992. Elemental composition of suspended matter in the Scotia-Weddell Confluence area during spring and summer 1988 (EPOS LEG 2). Polar Biol. 12 : 25 - 33.
- Dehairs, F., Stroobants, N. and Goeyens, L. 1991. Suspended barite as a tracer of biological activity in the Southern Ocean, Mar. Chem. 35 : 399 - 410.
- Dortch, Q. 1990. The interaction between ammonium and nitrate uptake in phytoplankton. Mar. Ecol. Prog. Ser. 61 : 183 - 201.
- Dugdale, R. C. and Goering, J. J. 1967. Uptake of new and regenerated forms of nitrogen in primary productivity. Limnol. Oceanogr. 12 : 196 - 206.

- El-Sayed, S. Z., Biggs, D. C. and Holm-Hansen, O. 1983. Phytoplankton standing crop, primary productivity, and near-surface nitrogenous nutrient fields in the Ross Sea, Antarctica. *Deep-Sea Res.* 30 : 871 - 886.
- Enoksson, V. 1986. Nitrification rates in the Baltic Sea : Comparison of three isotope techniques. *Appl. Environ. Microbiol.* 51 : 244 - 250.
- Eppley, R. W. 1981. Autotrophic production of particulate matter. In : *Analysis of Marine Ecosystems*. Longhurst, A. R. (Ed.). Academic Press, London : 343 - 361
- Eppley, R. W. 1989. New production : history, methods, problems. In : *Productivity of the Oceans: Present and Past*, Dahlem Workshop Reports, Life Science Research Report 44. Berger, W.H., Smetacek, V.S., and Wefer, G. (Eds.). John Wiley, New York : 85 - 97.
- Eppley, R. W. and Peterson, B. J. 1979. Particulate organic flux and planktonic new production in the deep ocean. *Nature* 282 : 677 - 680.
- EPOS LEG 2, 1991 EPOS LEG 2 data report hydrography, part 1, second version. Netherlands Institute for Sea Research, Texel.
- Fiedler, R. and Proksch, G. 1975. The determination of nitrogen-15 by emission and mass spectrometry in biochemical analysis : a review. *Anal. Chim. Acta* 78 : 1 - 62
- Garrison, D. L., Sullivan, C. W. and Ackley, S. F. 1986. Sea ice microbial communities In Antarctica. *Bioscience* 36 : 243 - 250.
- Gersonde, R. and Wefer, G. 1987. Sedimentation of biogenic silicious particles in Antarctic waters from the Atlantic sector. *Mar. Paleontol.* 11 : 311 - 332.
- Glibert, P. M., Biggs, D. C. and McCarthy, J. J. 1982-a. Utilization of ammonium and nitrate during austral summer in the Scotia Sea. *Deep-Sea Res.* 29 : 837 - 850.
- Glibert, P. M., Lipschultz, F., McCarthy, J. J. and Altabet, M. A. 1982-b. Isotope dilution methods of uptake and remineralization of ammonium by marine plankton. *Limnol. Oceanogr.* 27 : 639 - 650.
- Goeyens, L., Farbach, E., Behmann, T., Hinrichsen, H., Krest, J., Ross, A. and Wisotski, A. 1991-c. Summer Weddell Gyre Study, Data Report No 1. Alfred Wegener Institute for Polar and Marine Research, Bremerhaven.

- Goeyens, L., Sörensson, F., Tréguer, P., Morvan, J., Panouse, M. and Dehairs, F. 1991-a. Spatiotemporal variability of inorganic nitrogen stocks and assimilatory fluxes in the Scotia-Weddell Confluence area. *Mar. Ecol. Prog. Ser.* 77 : 7 - 19.
- Goeyens, L. G., Stichelbaut, L. W., Post, E. J. and Baeyens, W. F. 1985. Preparation method for solid samples with low nitrogen content for spectrometric nitrogen-15 analysis. *Analyst* 110 : 135 - 139.
- Goeyens, L., Tréguer, P., Lancelot, C., Mathot, S., Becquevort, S., Morvan, J., Dehairs, F. and Baeyens, W. 1991-b. Ammonium regeneration in the Scotia-Weddell Confluence area during spring 1988. *Mar. Ecol. Prog. Ser.* 78 : 241 - 252.
- Gonzales, H. E. 1992. The distribution and abundance of fecal pellets in the Scotia and Weddell Seas (Antarctica) and their role in the particle flux. *Polar Biol.* 12 : 81 - 91.
- Gordon, A. L., Chen, C. T. A. and Metcalf, W. G. 1984. Winter mixed layer entrainment of Weddell deep water. *J. Geophys. Res.* 89 : 637 - 640.
- Harrison, W. G. 1980. Nutrient regeneration and primary production in the sea. In : *Primary productivity in the sea*. P. G. Falkowski (Ed.). Plenum Press, New York : 433 - 460.
- Harrison, W. G. 1983. Use of isotopes. In : *Nitrogen in the Marine Environment*. Carpenter, E. J. and Capone, D. G. (Eds.). Academic Press, New York : 763 - 807.
- Hewes, C. D., Sakshaug, E., Reid, F. M. H. and Holm-Hansen, O. 1990. Microbial autotrophic and heterotrophic eucaryotes in Antarctic waters : relationships between biomass and chlorophyll, adenosine triphosphate and particulate carbon. *Mar. Ecol. Prog. Ser.* 63 : 27 - 35.
- Holm-Hansen, O. 1985. Nutrient cycles in antarctic marine ecosystems. In : *Antarctic nutrient cycles and food webs*. Siegfried, W. R., Condy, P. R., Laws, R. M. (Eds.). Springer Verlag, Berlin : 6 - 10.
- Jacques, G. 1989. Primary production in the open Antarctic Ocean during the austral summer. A review. *Vie Milieu* 39 : 1 - 17.
- Jacques, G. 1991. Is the concept new production - regenerated production valid for the Southern Ocean? *Mar. Chem.* 35 : 273 - 286.

- Jacques, G. and M. Panouse, 1989. Phytoplankton, protozooplankton and bacterioplankton. In : The expedition Antarktis VII/03 (EPOS LEG 2) of RV "Polarstern" in 1988/89. Hempel, I., Schalk, P. H. and Smetacek V. (Eds.). Berichte zur Polarforschung 65, Bremerhaven : 61-67.
- Jacques, G. and Panouse, M. 1991. Biomass and composition of size fractionated phytoplankton in the Weddell-Scotia Confluence area. Polar Biol. 11 : 315 - 328.
- Jennings, J. C., Gordon, L. I. and Nelson, D. M. 1984. Nutrient depletion indicates high primary productivity in the Weddell Sea. Nature 309 : 51 - 54.
- Johnson, M. A., Macaulay, M. C. and Biggs, D. C. 1984. Respiration and excretion within a mass aggregation of euphausia superba : implications for krill distribution. J. Crust. Biol. 4 : 174 - 184.
- Jones, E. P., Nelson, D. M. and Tréguer, P. 1990. Chemical oceanography of the Arctic and Antarctic Ocean. In : Polar Oceanography. Smith, W. O. Jr (Ed.). Academic Press, San Diego : 407 - 476.
- Kamykowski, D. and Zentara, S. J. 1985. Nitrate and silicic acid in the world ocean : patterns and processes. Mar. Ecol. Prog. Ser. 26 : 47 - 59.
- Kamykowski, D. and Zentara, S. J. 1989. Circumpolar plant nutrient covariation in the Southern Ocean : patterns and processes. Mar. Ecol. Prog. Ser. 58 : 101 - 111.
- Koike, I., Holm-Hansen, O. and Biggs, D. C. 1986. Inorganic nitrogen metabolism by Antarctic phytoplankton with special reference to nitrogen cycling. Mar. Ecol. Prog. Ser. 30 : 105 - 116.
- Koroleff, F. 1969. Direct determination of ammonia in natural waters as indophenol blue. Inter. Cons. Explor. Sea, C. M. 1969 : C, 19 - 22.
- Kristiansen, S. and Paasche, E. 1982. Preparation of ¹⁵N labelled phytoplankton samples for optical emission spectrometry. Limnol. Oceanogr. 27 : 373 - 375.
- Kristiansen, S., Syvertsen, E. E. and Farbrot, T. 1992. Nitrogen uptake in the Weddell Sea during late winter and early spring. Polar Biol. 12 : 245 - 251.
- Lancelot, C., Billen, G., Becquevort, S., Mathot, S. and Veth, C. 1991. Modelling carbon cycling through phytoplankton and microbes in the Scotia-Weddell Sea area during ice retreat. Mar. Chem. 35 : 305 - 319.

- Lancelot, C, Billen, G. and Mathot, S. 1989. Ecophysiology of phyto- and bacterioplankton growth in the Southern Ocean. In : Antarctica, Volume I, Plankton Ecology. Caschetto, S. (Ed.). Prime Minister's Services, Science Policy Office, Brussels : 1 - 97.
- Le Corre, P. and Minas, H. J. 1983. Distribution et évolution des éléments nutritifs dans le secteur indien de l' Océan Antarctique en fin de période estivale. *Oceanol. Acta* 6 : 365 - 381.
- Le Jehan, S. and Tréguer, P. 1983. Uptake and regeneration $\Delta\text{Si}/\Delta\text{N}/\Delta\text{P}$ ratios in the Indian sector of the Southern Ocean. Originality of the biological cycle of silicon. *Polar Biol.* 2 : 127 - 136.
- McCarthy J. J., Taylor W.R. and Taft J.L. 1977. Nitrogenous nutrition of the plankton in the Chesapeake Bay. Nutrient availability and phytoplankton preferences. *Limnology and Oceanography* 22 : 996 - 1011.
- Mathot, S., Dandois, J-M. and Lancelot, C. 1992. Gross and net primary production in the Scotia-Weddell Sea sector of the Southern Ocean during spring 1988. *Polar Biol.* 12 : 321 - 332.
- McIntyre, A. and Bé, A. W. H. 1967. Modern Coccolithophoridae of the Atlantic Ocean - I. Placoliths and Cyrtoliths. *Deep-Sea Res.* 14 : 561 - 597.
- Nelson, D. M. and Smith, W. O. Jr. 1986. Phytoplankton bloom dynamics of the western Ross Sea ice edge - II. Mesoscale cycling of nitrogen and silicon. *Deep-Sea Res.* 33 : 1389 - 1412.
- Nelson, D. M., Smith, W. O. Jr., Gordon, L. I. and Huber, B. A. 1987. Spring distributions of density, nutrients, and phytoplankton biomass in the ice edge zone of the Weddell-Scotia Sea. *J. Geophys. Res.* 92 : 7181 - 7190.
- Nelson, D. M., Smith, W. O. Jr., Muench, R. D., Gordon, L. I., Sullivan, C. W. and Husby, D. M. 1989. Particulate matter and nutrient distributions in the ice-edge zone of the weddell Sea : relationship to hydrography during late summer. *Deep-Sea Res.* 36 : 191 - 209.
- Olson, R. J. 1980. Nitrate and ammonium uptake in Antarctic waters. *Limnol. Oceanogr.* 25 : 1064 - 1074.
- Olson, R. J. 1981. ^{15}N tracer studies of the primary nitrite maximum. *J. Mar. Res.* 39 : 203 - 226.

- Peinert, R., Bodungen von, B. and Smetacek, V. C. 1989. Food web structure and loss rate. In : Productivity of the Oceans: Present and Past, Dahlem Workshop Reports, Life Science Research Report 44. Berger, W.H., Smetacek, V.S., and Wefer, G. (Eds.). John. Wiley, New York : 35 - 48.
- Poisson, A., Schauer, B. and Brunet, C. 1990. Les Rapports des campagnes à la mer, MD 53/INDIGO 3 à bord du "Marion Dufresne", 3 janvier- 27 février 1987. Les Publications de la Mission de Recherche des Terres Australes et Antarctiques Françaises, No 87-01, Fascicule 2, 269 p.
- Probyn, T. A. and Painting, S. J. 1985. Nitrogen uptake by size-fractionated phytoplankton populations in Antarctic surface waters. *Limnol. Oceanogr.* 30 : 1327 - 1332.
- Rønner, U., Sörensson, F. and Holm-Hansen, O. 1983. Nitrogen assimilation by phytoplankton in the Scotia Sea. *Polar Biol.* 2 : 137 - 147.
- Ross, R. M. and Quetin, L. B. 1986. How productive are Antarctic krill? *Bioscience* 36 : 264 - 269.
- Schalk, P. H. 1990. Biological activity in the Antarctic zooplankton community. *Polar Biol.* 10 : 405 - 411.
- Sharp, J. H. 1983. Distribution of inorganic and organic nitrogen in the sea. In : Nitrogen in the Marine Environment. Carpenter, E. J. and Capone, D. G. (Eds.). Academic Press, New York : 1 - 35.
- Slawyk, G. 1979. ^{13}C and ^{15}N uptake by phytoplankton in the Antarctic upwelling area : results from the Antiprod I cruise in the Indian Ocean sector. *Aust. J. Mar. Freshwater Res.* 30 : 431 - 438.
- Smetacek, V., Scharek, R. and Nöthig, E.-M. 1990. Seasonal and regional variation in the pelagial and its relationship to the life history cycle of krill. In : Antarctic Ecosystems, ecological change and conservation. Kerry, K. R. and Hempel, G. (Eds.). Springer-verlag, Berlin : 103 - 114.
- Smith, N. R., Zhaoqian, D., Kerry, K. R. and Wright, S. 1984. Water masses and circulation in the region of Prydz Bay, Antarctica. *Deep-Sea Res.* 31 : 1121-1147.
- Smith, W. O. Jr. and Harrison, W. G. 1991. New production in polar regions : the role of environmental controls. *Deep-Sea Res.* 38 : 1463 - 1479.

- Smith, W. O. Jr. and Nelson, D. M. 1986. Importance of ice edge phytoplankton production in the Southern Ocean. *Bioscience* 36 : 251 - 257.
- Smith, W. O. Jr. and Nelson, D. M. 1990. Phytoplankton growth and new production in the Weddell Sea MIZ in the austral spring and autumn. *Limnol. Oceanogr.* 35 : 809 - 821.
- Smith, W. O. Jr. and Sakshaug, E. 1990. Polar phytoplankton. In : *Polar Oceanography*. Smith, W. O. Jr. (Ed.). Academic Press, San Diego, p. 477 - 526.
- Smith, N. R., Zhaoqian, D., Kerry, K. R. and Wright, S. 1984. Water masses and circulation in the region of Prydz Bay, Antarctica. *Deep-Sea Res.* 31 : 1121-1147.
- Sommer, U. and Stabel, H. H. 1986. Near surface nutrient and phytoplankton distribution in the Drake Passage during early december. *Polar Biol.* 6 : 107 - 110.
- Stroobants, N., Dehairs, F., Goeyens, L., Vanderheijden, N. and Van Grieken, R. 1991. Barite formation in the Southern Ocean water column. *Mar. Chem.* 35 : 411 - 421.
- Toggweiler, J. R. 1989. Is the downward dissolved organic matter (DOM) flux important in the carbon transport. In : *Productivity of the Oceans: Present and Past, Dahlem Workshop Reports, Life Science Research Report 44*. Berger, W.H., Smetacek, V.S., and Wefer, G. (Eds.). John. Wiley, New York : 65-84.
- Tréguer, P., and Jacques, G. V. 1992. Dynamics of nutrients and phytoplankton, and fluxes of carbon, nitrogen and silicon in the Antarctic Ocean. *Polar Biol.* 12 : 149 - 162.
- Tréguer, P. and Le Corre, P. 1975. *Manuel d' analyses automatiques des sels nutritifs par AutoAnalyser II Technicon*. Université de Bretagne Occidentale, Brest.
- Tréguer, P., Lindner, L., Van Bennekom, A. J., Leynaert, A., Panouse, M. and Jacques, G. 1991. Production of biogenic silica in the Weddell-Scotia seas measured with ^{32}S . *Limnol. Oceanogr.* 26 : 1217 - 1227.
- van Bennekom, A. J., Buma, A. and Nolting, R. F. 1991. Dissolved aluminium in the Weddell-Scotia Confluence and effect of Al on the dissolution kinetics of biogenic silica. *Mar. Chem.* 35 : 412 - 423.

- Verlencar, X. N., Somasunder, K. and Qasim, S. Z. 1990. Regeneration of nutrients and biological productivity in Antarctic waters. *Mar. Ecol. Prog. Ser.* 61 : 41 - 59.
- Veth, C. 1991. The evolution of the upper water layer in the marginal ice zone, austral spring 1988, Scotia-Weddell Sea. *J. Mar. Systems* 2 : 451 - 464.
- von Bodungen, B., Smetacek, V. S., Tilzer, M. M. and Zeitschel, B. 1986. Primary production and sedimentation during spring in the Antarctic Peninsula region, *Deep-Sea Res.* 33 : 177 - 194.
- von Bröckel, K. 1981. The importance of nanoplankton within the pelagic antarctic ecosystem. *Kieler Meeresforsch.* 5 : 61 - 67.
- von Bröckel, K. 1985. Primary production data for the southwestern Weddell Sea. *Polar Biol.* 4 : 75 - 80.
- Ward, B. B., Olson, R. J. and Perry, M. J. 1982. Microbial nitrification rates in the primary nitrite maximum off Southern California. *Deep-Sea Res.* 29 : 247 - 255.
- Wefer, G., Fischer, G., Fütterer, D. K., Gersonde, R., Honjo, S. and Ostermann, D. 1990. Particle sedimentation and productivity in Antarctic waters of the Atlantic sector. In : *Geological history of the Polar Oceans : Arctic versus Antarctic*. Bleil, U. and Thiede, J. (Eds.). Kluwer Academic Publishers, Amsterdam : 363-379.
- Wheeler, P. A. and Kokkinnakis, S. A. 1990. Ammonium recycling limits nitrate use in the oceanic subarctic Pacific. *Limnol. Oceanogr.* 35 : 1267 - 1278.



RESEARCH CONTRACT ANTAR/II/07
(part A)

**ECOTOXICOLOGY OF
STABLE POLLUTANTS
IN ANTARCTIC MARINE
ECOSYSTEMS :
MERCURY AND
ORGANOCHLORINES**

C. Joiris and L. Holsbeek

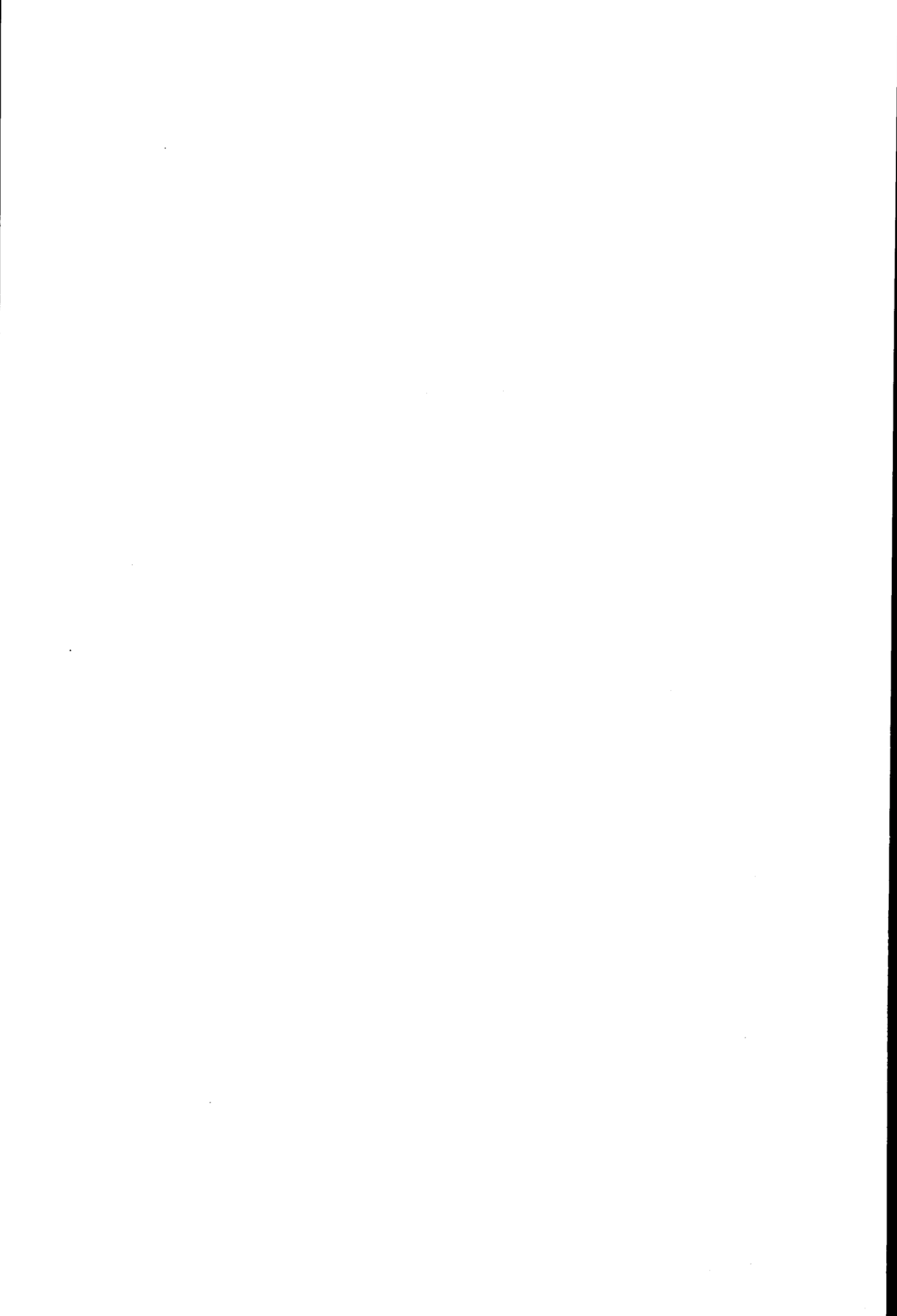
LABORATORIUM VOOR
ECOTOXICOLOGIE

Vrije Universiteit Brussel
Pleinlaan, 2
B-1050 Brussels, Belgium



Content.

| | |
|---|----|
| Abstract. | 1 |
| Introduction. | 2 |
| Materials and methods. | 2 |
| Results and discussion: | 12 |
| 1. Mercury in suspended particulate matter. | 15 |
| 2. Mercury in fish. | 17 |
| 3. Mercury in seabirds. | 15 |
| 4. Organochlorines in suspended particulate matter. | 22 |
| 5. Organochlorines in seabirds. | 28 |
| Conclusions. | 29 |
| References. | 32 |



ABSTRACT.

The ecotoxicological study of marine ecosystems concerns the determination of the concentration and transfer mechanisms of stable pollutants in the main biological compartments. In the Antarctic, data were gathered on heavy metals: total and organic (methyl) mercury, and organochlorines: pesticides and PCBs.

Contamination of phytoplankton (suspended particular matter) is high when expressed on fresh (or dry) weight basis and reaches values as high as in the heavily polluted North Sea. In order to determine and compare the contamination at the ecosystem level, it is however necessary to express the same data in other units, namely per volume of seawater, since particulate matter is directly contaminated from the water through adsorption, absorption and partition on the lipids. It appears then that the Antarctic marine systems are about six times less contaminated than the North Sea. The high concentrations per weight unit are resulting from much lower biomasses in the Antarctic: the total load of basically water insoluble residues is almost entirely distributed on less particles, leading to a higher load per particle.

This relatively high contamination by mercury and organochlorines is also more recent than in Western Europe and North America, where their utilization was controlled or banned from the seventies on, while they are still used on a large scale in southern developing countries. A high DDT to DDE ratio provides a typical example of this phenomenon.

This situation: relatively low ecosystem load, high concentration on the particulate matter, allows to detect the main transfer mechanisms of the contaminants to the higher trophic levels: if the higher trophic levels, e.g. fish, were mainly indirectly contaminated through their food, high levels of mercury and organochlorines were to be expected. The obtained results show, on the contrary, that contamination levels are much lower than in the North Sea. This clearly shows the importance of direct contamination from the water to the fish, a confirmation of experimental data. Seabirds being indirectly contaminated from this fish, also present low levels of pollutants, compared with North Sea data.

INTRODUCTION.

The aim of this study is to determine the contamination levels of marine Antarctic ecosystems by stable pollutants: heavy metals (mercury: total and methyl Hg) and organochlorines (PCBs and pesticides). Two main arguments lead to the study of polar regions from this point of view:

- they tend to represent "no contamination levels" for polluting residues, or at least should present concentrations as close as possible to the natural ones (in the case of organochlorines, zero). Especially the Antarctic is often proposed, with its extremely limited, local and recent human impact. Some data however indicate that Antarctic ecosystems are significantly contaminated by organochlorines (DDTs) from the 1960's on (Sladen *et al.*, 1966; Tatton and Ruzicka, 1967; Risebrough *et al.*, 1976). So that another hypothesis must be taken into account. Antarctica is contaminated from various sources in the southern hemisphere, mainly through the atmosphere. Its contamination could be increasing and of more recent origin than in northern zones, where organochlorine pesticides were banned around 1970 and PCBs around 1990, while their utilization is still high and increasing in developing countries.

- because of their very different ecological structure and functioning, their study can bring important improvement in the understanding of the mechanisms of accumulation and transfer of stable pollutants, in comparison with northern systems already studied in some details. In our case, we will more especially compare with our data obtained by using the same techniques in the heavily polluted area of the North Sea and Scheldt estuary.

This ecological approach concerns the main biological compartments: phytoplankton (in fact suspended particulate matter collected by continuous centrifugation), zooplankton, fish and seabirds.

MATERIALS AND METHODS.

Particulate matter was sampled by continuous centrifugation; the water was pumped under the hull of the ship, at a depth of about 12 m. The Alfa-Laval centrifuge had a debit of about 10 m³ per day and its rotation speed was 1500 tours per minute. Samples were collected every 24 hours, in order to obtain enough material for analysis (from 50 mg dry weight on). All samples were collected within the "EPOS box", from October 18 till November 16, 1988 (leg 1) and from November 26, 1988 till January 4, 1989 (leg 2): between 58° and 63.5° S, and between 45° and 54° W (approximately between Elephant Island, at the tip of the Peninsula, and Signy Island, Southern Orkneys).

Fish samples were provided from two sources:

- January - February 1991, Prydz Bay, cruise AAMBER 90/91 (Australian Antarctic Division);
- Alfred Wegener Institute, Bremerhaven: existing deepfrozen samples (Weddell Sea, 1989).

Seabirds samples were collected at two occasions:

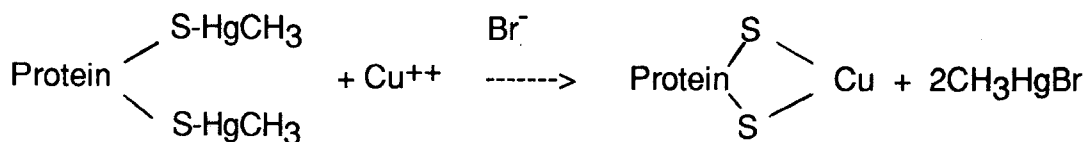
- during the ANT VIII/ 6 cruise of RV Polarstern in the African sector of the Southern Ocean, March-April 1990 (VUB). This series allows to study and compare the different tissues of a same animal, but few birds only are concerned.
- in the Weddell Sea in 1986, seabirds were shot in the frame of a study on their diet (stomach content: Ainley *et al.*, 1991); liver samples were kept and later analyzed in our laboratory. This series concerns more seabirds, but one tissue only was collected: liver.

ANTAR
II/07
A

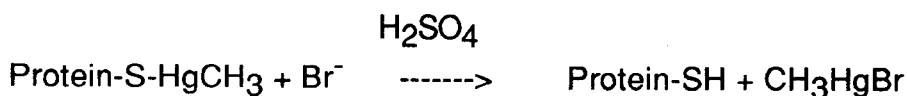
Total mercury concentration was determined by specific atomic absorption spectrometry (MAS 50 Mercury Analyzer from Perkin-Elmer) with external standardization.

Methylmercury concentration was determined by gas chromatography. It is not only present under the CH_3HgX form, but can also appear bound to protein thiol groups. In that case a treatment of the protein fraction is necessary in order to extract all the of methylmercury. For this purpose, the lyophilized sample is treated with NaBr and CuSO_4 in a sulfuric medium:

Extraction. The CuSO_4 helps to release the CH_3Hg bound to the thiol groups by the following reaction:



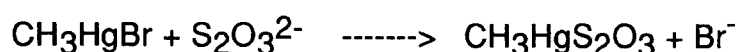
the NaBr builds up a very stable complex with methylmercury in a sulfuric medium following the reaction:



The complex formed with the NaBr is extracted by toluene. The inorganic mercury (HgX), that can be present simultaneously, is not extracted by this process despite its slight solubility in toluene, due to its strong tendency to make ion-complexes with the halogenures following the reaction:



Purification. The methylmercury is then extracted from the toluene with a thiosulphate hydroalcoholic solution that solubilises it by building up a very specific thiomethylmercury complex following the reaction:



This treatment enables the elimination of the lipids and of other liposoluble compounds that could disturb the chromatographic analysis. The complex is finally reconverted in bromure and re-extracted in toluene.

Analysis. The solution is analyzed with a liquid gas chromatograph Shimadzu GC-14A with an electron-capture detector. The column is a wide bore capillary borosilicate glass column SP 1000 (length 30 m). The complex is degraded during the analysis and the methylmercury is detected. The CH₃HgBr and CH₃HgCl injections give the same peak with the same retention time.

Internal standard. Before the chromatographic injection, we add 200 ml of a 1-octanol solution in order to detect any error on the 1 µl - on column - injection.

External standard. A solution of CH₃HgCl (2.26 µg/ml) is used as external standard.

Worked standard and yield. The yield is the fraction of methylated mercury left after treatment of the samples; treatment of a Standard solution along with the samples (Worked Standard) helps us to determine the loss of Hg and the actual yield.

The theoretical yield (=63.5%) is determined as follows:

| | | | |
|--|---------------|--------------------|----------------|
| * after first extraction: (6 ml added, 5 ml toluene kept) | yield: | 5/6 | |
| | | to 2nd extraction: | 1/6 |
| * after 2nd extraction 1/6 (6 ml added, 5 ml toluene kept) | yield: | 5/6 + (1/6 x 5/7) | = 40/42 |
| | loss: | 1/6 x 2/7 | = 2/42 |
| * after purification 40/42 (4.5 ml thiosulph. added, 3 ml kept) | yield: | 40/42 x 3/4.5 | = 240/378 |
| | | | = 63.5% |

In order to evaluate the actual yield, the value for the Worked Standard (1 μ l injected) is compared with the value for the Standard solution before treatment. This actual yield should be equal to the theoretical yield ($\pm 5\%$). Comparing the actual and the theoretical yields ensures us that the treatment of the sample was carried out correctly. When actual and theoretical yield are equal, the value/area for the Worked Standard solution will be used to calculate all final concentrations. Doing so, we compensate for the 36.5% loss of Hg along the treatment of the samples:

$$\text{conc. sample injected} = \frac{\text{area sample} \times \text{conc. Standard } \mu\text{g/ml}}{\text{area Standard}} \times \frac{100}{63.5}$$

equals

$$\text{conc. sample injected} = \frac{\text{area sample} \times \text{conc. Standard } \mu\text{g/ml}}{\text{area Worked Standard}}$$

ANTAR
II/07
A

Detection limits and error. We put the absolute detection limit for the Shimadzu GC on **0.00004** μg MeHg which corresponds with an area of 70000 on the chromatographe. Measurements beyond this value are either 0 (no peak) or between 0 and 70000 and consequently marked as 'trace'.

The median detection limit for the whole method (median sample weight 1.3 g dw, all Hg dissolved in 2 ml toluene) is then calculated to be **0.09** μg Hg/g dw.

Test for a matrix effect. A test was conducted to check for the possibility of any unexpected interaction between methylmercury and the sample in which it was analyzed (the matrix). Such an interaction could reduce the accuracy of measurements. One tissue sample (*Esox lucius*- muscle) was divided into five parts. Sample 1 was prepared for analysis as usual. Known quantities of methylmercury were added to samples 2 through 5 before they were prepared for analysis. The results of analysis for all five samples are reported in table 1. Medians of the measurements of each sample are reported in the last column.

As expected, concentrations measured increase in a linear fashion with the quantity of methylmercury added. Figure 1 describes this relationship graphically. The slope of the regression line is 1.3, which seems sufficiently close to the ideal slope (of 1.0) to consider a matrix effect negligible for methylmercury measurements.

Table 1: Results of the test for a matrix effect in methylmercury measurements.

| sample number | $\mu\text{g MeHg}$ added | $\mu\text{g MeHg}$ / g fw | <i>n</i> | median $\mu\text{g MeHg}$ / g fw |
|---------------|--------------------------|---------------------------|----------|----------------------------------|
| 1 | 0.00 | 0.54 | 1 | 0.54 |
| 2 | 0.23 | 0.58 0.63 0.69 | | |
| 3 | 0.68 | 0.65 | 4 | 0.64 |
| 4 | 1.13 | 1.19 | 1 | 1.19 |
| | | 2.06 2.01 | | |
| 5 | 2.26 | 2.06 | 3 | 2.06 |
| | | 3.10 3.67 | 2 | 3.38 |

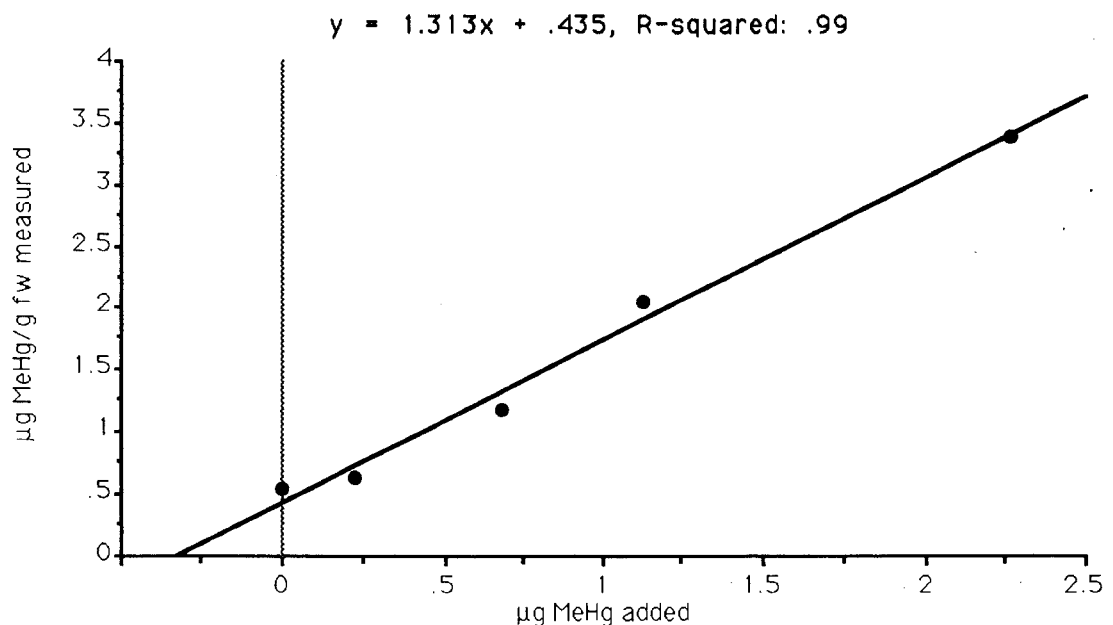


Figure 1: Linear regression between measured methylmercury and added methylmercury.

Determination of organochlorines: PCBs and pesticides.

Extraction and clean-up.

- a sample of 1 to 20 g fresh weight is homogenized after addition of water-free Na_2SO_4 in order to obtain a completely pulverized and waterfree powder;
- lipophilic compounds are extracted with 100 ml hexane for a period of 10 hours (Soxhlet extraction). The hexane is evaporated, the extracted lipids are weighed and redissolved in 5 ml hexane.

Clean-up is done in florisil column (the exact quantity of florisil is determined after standardization). The organochlorine compounds are separated by two successive elutions: 1) 100 ml of hexane and 2) 100 ml of hexane-ether 1/1.

PCBs and DDE are determined in the first elution; the other organochlorine residues in the second one.

Determination. The organochlorine residues are determined with gas-liquid chromatography (Packard Instruments model 437), capillary column, electron capture detection, Shimadzu CR 1A integrator, automatic injection LS607, temperature programme.

Technical procedure. Injection: splitless with injectorflush after 0.5 min (50 ml N₂/min); injection volume: 1 µl; injector temperature 250°C; carrier gas 0.6 bar N₂; bypass 20 ml/min N₂; column: fused silica CPSil 8CB (25 m length; 0.22 mm diameter; 0.12 µm film/thickness); oven temperature programme:

| first elution: | second elution: |
|----------------------|-----------------------|
| 90°C: 2 min | 90°C :2min |
| 90°- 180°C: 20°C/min | 90 - 180°C:20°C/min |
| 180 - 190°C: 2°C/min | 180 - 190°C:2°C/min |
| 190 - 220°C: 2°C/min | 190°C :10 min |
| 220 - 270°C: 4°C/min | 190 - 220°C: 4°C/ min |
| 270°C: 10 min. | 220 - 270°C: 5°C/ min |
| | 270°C:15 min. |

PCBs are recognized on the chromatograms as a standard mixture Aroclor 1254 (13 peaks were used) and as 9 individual congeners (see further).

Identification. The identification of PCB residues is based on the utilization of two types of standardization: firstly by comparing with the standard Aroclor 1254 mixture (close to the PCB pattern found in marine samples), and secondly by comparing with nine of the most "classical" PCB congeners, namely IUPAC nrs 28, 52, 101, 118, 138, 153, 170, 180 and 194, in order of increasing chlorine content (Fig. 2). The chromatograms of the first elution show peaks comparable to the standard mixtures, although more highly chlorinated PCBs are present in the sample than in the 1254 mixture. Such a difference could be explained by the long distance from the sources of PCBs, more highly chlorinated congeners being slightly more stable than the less chlorinated ones.

Quantification. The quantitative evaluation of PCBs constitutes a complex problem, even if most publications do not mention it and tend to avoid the discussion. The first approach makes use of external standardization with an Aroclor 1254 mixture:

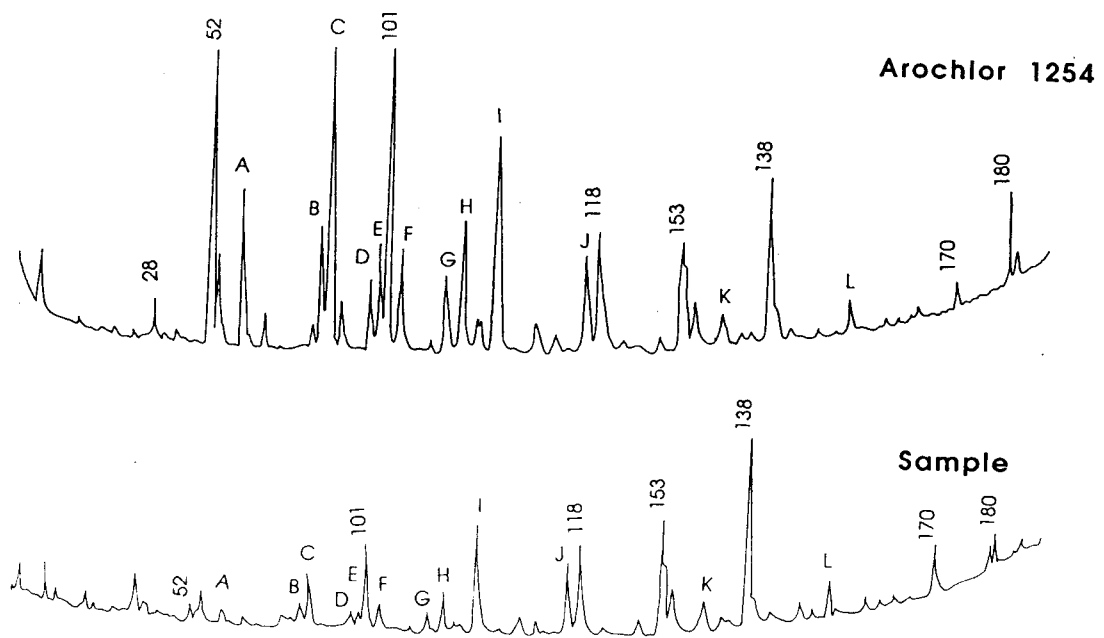


Figure 2: Chromatograms of PCBs in particulate matter and of the standard mixture Arochlor 1254 (13 peaks: A-L), and nine individual congeners (28-194).

this "total" PCB concentration is calculated on the basis of 13 out of the detected peaks. Separate congeners can also be used in a second approach: the sum of the 9 selected congeners provides an underestimated total PCB load; in our Antarctic samples these congeners account for about 33 percent of the "total" PCBs for particulate matter and 31 % for netplankton (Table 2): no major qualitative difference could be detected between the two compartments. The relative contribution of the individual congeners to the sum of all congeners was also compared between both compartments (Table 2): for the congeners 101 to 170, the differences are relatively small (the levels of the other congeners are too low to be considered here). These results, reflecting a similarity in PCB pattern in the two compartments, allow comparison on the basis of "total" PCBs expressed as Arochlor 1254. Figure 3 provides a graphical confirmation of these values and shows the strong correlation between the sum of 9 congeners and "total" PCBs, as well as between individual congeners and "total" PCBs, both in particulate matter (Fig. 3 a) and in netplankton (Fig. 3 b).

Further in the discussion, we will consider the concentration of "total" PCBs expressed as Arochlor 1254, considering that it still provides, within a compartment, a reliable basis for comparison. It also allows comparison with older data (obtained from packed column analysis).

Table 2: Relative contribution of five individual congeners to the sum of nine congeners in particulate matter, netplankton and the standard mixture Aroclor 1254 (expressed in %).

| Congener (IUPAC nr) | Particulate matter | | Netplankton | | Aroclor 1254 |
|---------------------------|--------------------|-------|----------------|-------|-----------------|
| | mean (n=35) | stdev | mean (n=14) | stdev | |
| 101 | 17 | 7 | 17 | 6 | 26 |
| 118 | 15 | 8 | 15 | 5 | 18 |
| 138 | 30 | 8 | 18 | 6 | 18 |
| 153 | 15 | 6 | 12 | 5 | 12 |
| 170 | 9 | 5 | 7 | 2 | 3 |

ANTAR
II/07
A

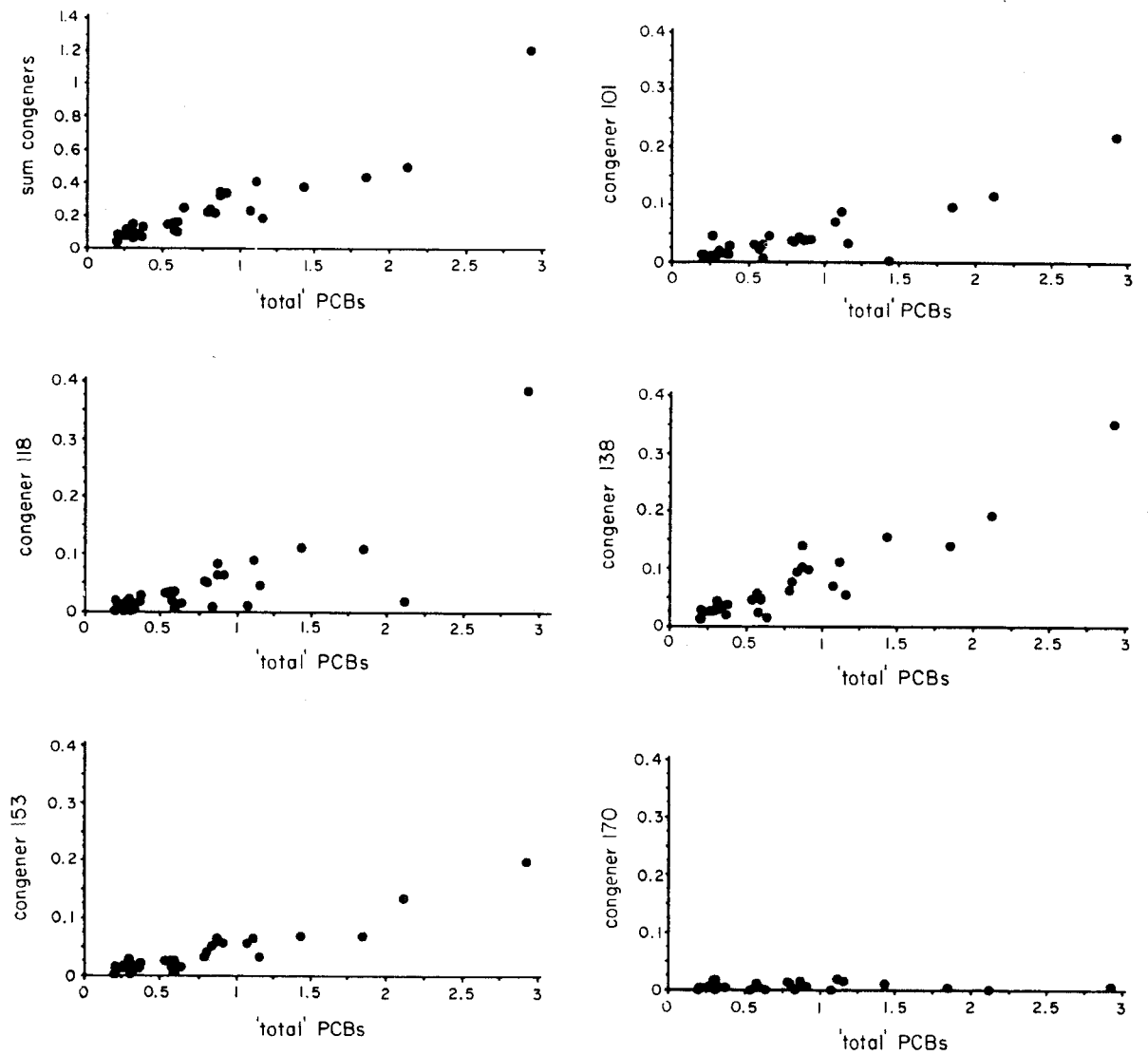


Figure 3a: Correlation between the sum of nine congeners, and individual congeners, and "total" PCBs (as Aroclor 1254) in particulate matter ($\mu\text{g}/\text{g}$ dry weight).

ANTAR
II/07
A

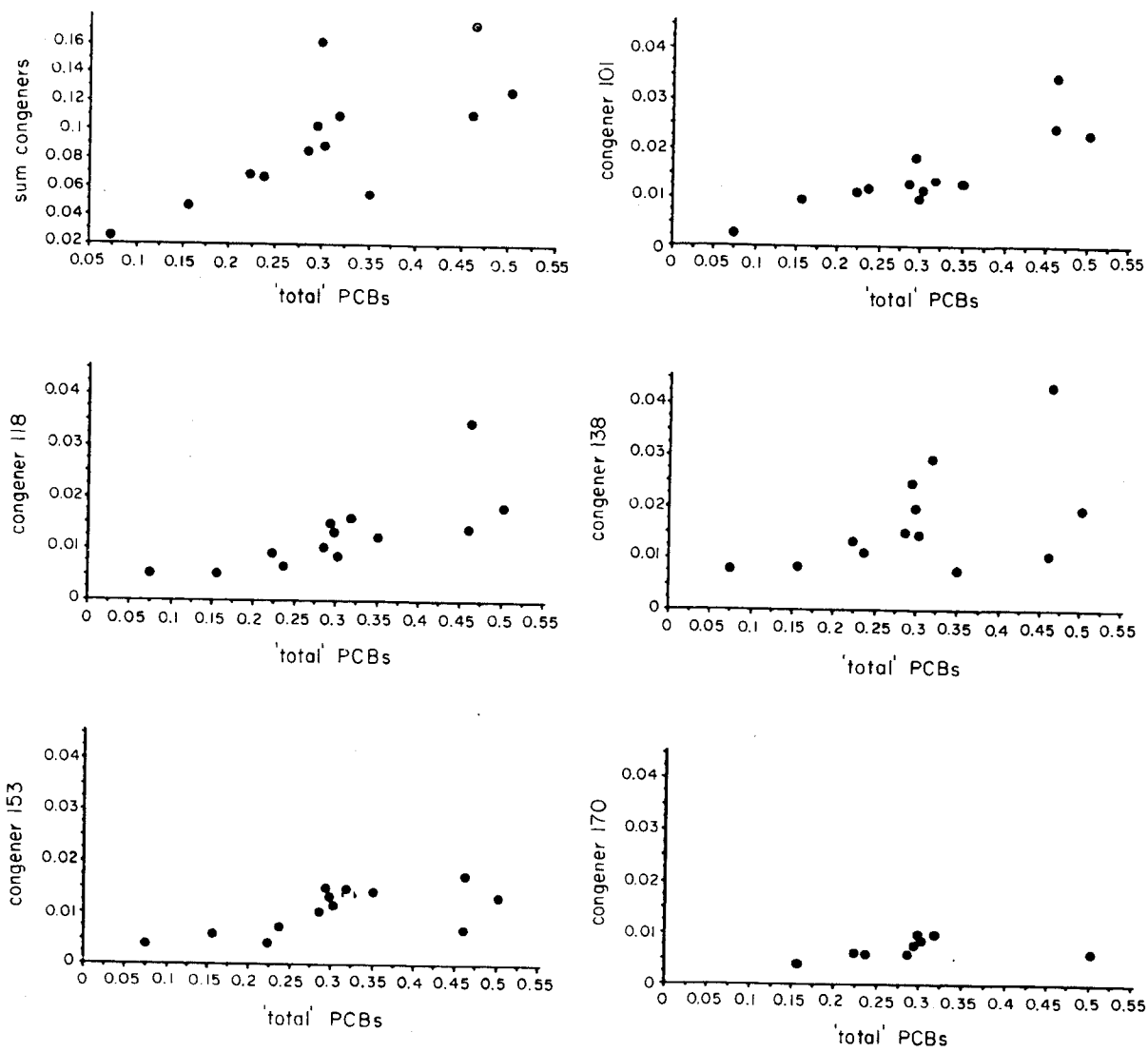


Figure 3b: Correlation between the sum of nine congeners, and individual congeners, and "total" PCBs (as Aroclor 1254) in netplankton ($\mu\text{g/g}$ dry weight).

RESULTS AND DISCUSSION.

1. MERCURY in SUSPENDED PARTICULATE MATTER.

Total mercury content was determined in suspended particulate matter (mainly phytoplankton) collected by continuous centrifugation in the northern Weddell Sea during the legs 1 and 2 of the EPOS 1 cruise of the icebreaking RV Polarstern, from October 16, 1988 to January 4, 1989. No geographical variation was detected; the mean concentration was 0.8 $\mu\text{g Hg/g}$ dry weight and the median value 0.5 $\mu\text{g Hg/g dw}$ ($n=27$). Expressed per seawater volume, this corresponds to a mean level of 0.4 $\mu\text{g Hg/m}^3$. On this basis, the main conclusion is that the Antarctic ecosystem is 7 times less contaminated than the temperate, heavily polluted North Sea. Because of a 10 times lower amount of particulate matter per volume in the Antarctic, however, the Hg levels per weight unit are of the same order of magnitude, or even higher, than in the North Sea.

A synopsis of the results (Table 3) shows no geographical difference in total mercury levels in the whole area, nor between open water and ice-covered zones, nor between the different ice-covered zones (Outer Marginal Ice Zone OMIZ, Inner Marginal Ice Zone IMIZ, Closed Pack Ice CPI). The mean value of mercury contamination for 27 samples is 0.79 $\mu\text{g Hg/g}$ dry weight (1.06 during leg 1 and 0.37 for leg 2) and the median 0.54 $\mu\text{g Hg/g}$ dry weight (0.70 for leg 1 and 0.23 for leg 2).

It is however essential to also express the data as total load per seawater volume ($\mu\text{g/m}^3$), in order to allow a meaningful comparison with other regions. Based on measurements of total and organic carbon in the centrifuge samples, on one hand, and in a given volume of water by filtration, on the other hand, a mean factor of 0.55 g dry weight/ m^3 was determined, and a mean concentration of 0.43 $\mu\text{g Hg/m}^3$ calculated (median: 0.30).

A clear effect of the particulate matter concentration on its mercury content could be detected when expressing the contamination as a function of the amount of particulate matter collected during 24 hours: by a constant debit, this amount is directly dependant on the particulate matter concentration (Figure 4).

Conclusions.

The contamination of Antarctic suspended particulate matter, mainly phytoplankton, by mercury is relatively high: 0.5 $\mu\text{g Hg/g}$ dry weight ("ppm"), median value. This is

of the same order of magnitude, or even higher, than in the heavily polluted North Sea, with levels of 0.14 to 0.55 (Anonymous, 1983), 0.16 (Decadt *in* Bouquegneau Table 3: Total mercury content of suspended particulate matter from the northern Weddell Sea.

| cruise | | zone (*) | sample | total Hg | |
|--------------------|-------|-----------|------------|-----------------------------|-------------|
| EPOS 1 | nr | | weight | $\mu\text{g} / \text{g dw}$ | |
| | | | mg dw (**) | | |
| leg 1 | 1 | OW+OMIZ | 71 | 1.85 | |
| | 2 | IMIZ | 117 | 0.79 | |
| | 3 | CPI | 152 | 0.70 | |
| | 4 | CPI | 40 | 1.19 | |
| | 5 | CPI | 19 | 3.37 | |
| | 6 | CPI | 170 | 0.42 | |
| | 7 | IMIZ | 163 | 0.44 | |
| | 8 | OW+OMIZ | 193 | 0.54 | |
| | 9 | OMIZ | 194 | 0.73 | |
| | 10 | OMIZ+IMIZ | 21 | 2.22 | |
| | 11 | CPI | 58 | 0.93 | |
| | 12 | CPI | 186 | 0.55 | |
| | 13 | CPI | 73 | 0.70 | |
| | 19 | IMIZ+OMIZ | 215 | 0.48 | |
| | 20 | OMIZ+OW | 215 | 0.32 | |
| | 22 | IMIZ | 32 | 2.13 | |
| | 23 | OW | 79 | 0.56 | |
| | leg 2 | 1 | OW | 290 | 0.18 |
| | | 2 | OW+OMIZ | 123 | 0.20 |
| | | 3 | IMIZ+CPI | 149 | 0.26 |
| | | 4 | IMIZ+CPI | 166 | 0.65 |
| | | 5 | OW | 153 | 0.14 |
| | | 6 | OW | 285 | 0.31 |
| 8 | | OMIZ+OW | 225 | 0.11 | |
| 10 | | OW | 263 | 0.31 | |
| 12 | | OW | 242 | 0.15 | |
| 13 | | OW | 118 | 1.69 | |
| mean | | | | 0.79 | |
| standard deviation | | | | 0.79 | |
| median | | | | 0.54 | |

* OW: open water; OMIZ: outer marginal ice zone (<3 tenths ice cover); IMIZ: inner marginal ice zone (3 to 8); CPI: closed pack ice (>8).

** mg dry weight/ 24 hours centrifugation.

ANTAR
II/07
A

and Joiris, 1988) and $0.14 \mu\text{g Hg/g dw}$ (Van Alsenoy *et al.*, 1989). This apparently paradoxical conclusion (one expects Antarctica to be much less contaminated than the North Sea) is due to the fact that the amount of particulate matter (phytoplankton) per water volume is about 10 times lower in the Antarctic. The total load per seawater volume however, is low in Antarctica ($0.4 \mu\text{g Hg/m}^3$) compared with the North Sea ($2.2 \mu\text{g Hg/m}^3$).

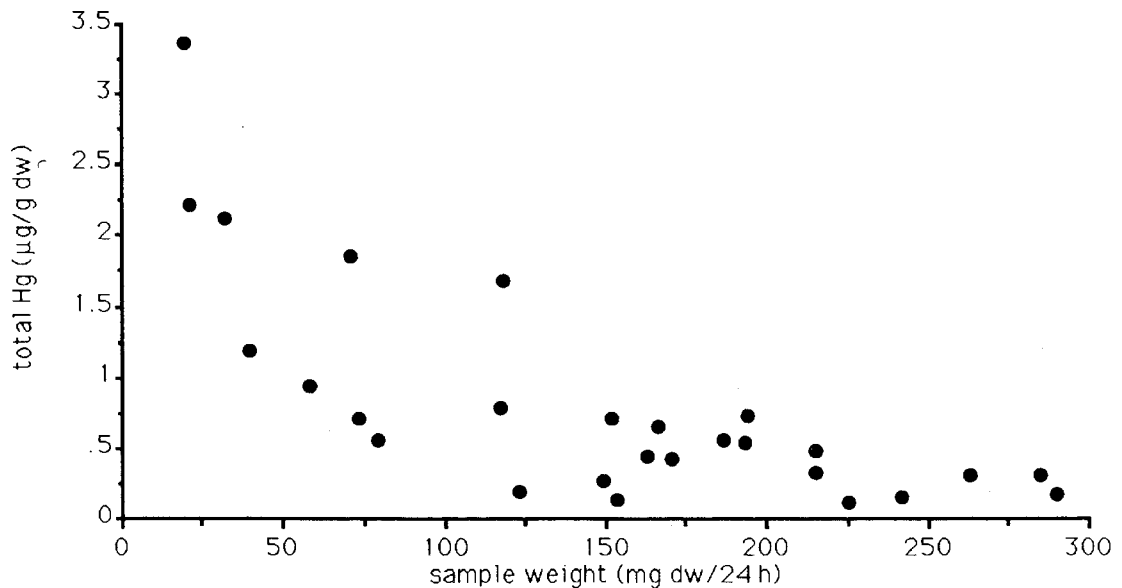


Figure 4: Total mercury content of particulate matter ($\mu\text{g Hg/g dry weight}$) as a function of organic matter concentration, expressed as the amount of matter collected by continuous centrifugation during 24 hours (mg dry weight).

In order to compare contaminations in different zones or periods, it is thus useless to only use information on the concentration of stable pollutants expressed on a weight basis. It is necessary to identify the basic contamination mechanism and to normalize the data. This normalization varies with the systems involved and can concern e.g. organic matter content for PCBs in sediments, lipid content for organochlorines in different fish species, diet composition for organochlorines in raptors, age and sex for organochlorines in cetaceans, etc.

In the case of particulate matter directly contaminated from the water through adsorption mechanisms, eventually completed by absorption and partition, the results should be normalized and expressed per seawater volume, taking into account the amount of particulate matter present in seawater. The dependence of mercury contamination on the amount of particulate matter (Figure 4) was already

noticed for PCBs in the North Sea (Delbeke and Joiris, 1988) and is typical for contaminants with low water solubility (t.i. with high octanol/ water partition coefficient): the lower the amount of particulate matter per seawater volume, the higher their contamination expressed on a weight basis. Within our series of data (Table 3), the lower contamination observed during EPOS leg 2 is to be understood by the increasing amount of particulate matter due to the growth of phytoplankton.

The general conclusion is that the Antarctic ecosystem is 5 to 6 times less contaminated by mercury than the North Sea on a seawater volume basis, but that its lower amount of particulate matter causes a higher contamination per weight unit. With the practical consequence that Antarctic particulate matter can actually be more contaminated and that organisms feeding on this particulate matter might become more contaminated than similar organisms from temperate, heavily polluted regions like the North Sea.

Comparable conclusions were drawn from the study of organochlorines contamination of particulate matter in Antarctica: the PCB load, expressed per seawater volume, was 5 times lower than in the North Sea, but the PCB concentration per dry weight almost twice higher (Joiris and Overloop, 1991).

2. MERCURY in FISH.

Total Hg levels were determined in Antarctic fish. Due to the small size of most of the fishes, we could not study and compare the concentrations in different tissues: values are given for muscle or complete fish mainly (Table 4).

For each species, results are rather reproducible, with standard deviations clearly lower than the mean values. It is therefore possible to compare between species, and to detect specific differences: the most contaminated one are *Bathylagus antarcticus*, with a mean of $0.54 \mu\text{g} \Sigma \text{Hg/ g dry weight}$ (maximal value of 0.78) and *Pagothenia hansonii* with a mean of 0.51 and a maximum of 0.94 (3 samples only). The other species seem to show comparable low concentration of 0.1 to $0.2 \mu\text{g} \Sigma \text{Hg/ g dw}$.

Levels of methyl mercury (MeHg) show very similar trends, so that MeHg values expressed as % of the total are rather constant at about 50% and higher.

Contamination levels are relatively low: we obtained a mean value of $1.5 \mu\text{g} \Sigma \text{Hg/ g dw}$ in the North Sea. The Antarctic fish are thus 3 and 10 times less contaminated, respectively. One must however take into account that North Sea fish have a larger size than the Antarctic ones. Since Hg contamination is increasing with age (with length) by fish, the difference of contamination of both systems is probably lower than the factors 3 and 10 mentioned. This conclusion is

fitting in the general constation that Antarctic marine ecosystems are about 6 times less contaminated than the North Sea at the phytoplankton level, both for Hg and for organochlorines when data are expressed per volume of water), but that the low biomasses in the Antarctic cause higher contamination per weight unit.

Table 4: Total and methyl mercury levels in Antarctic fish.

| species | <i>n</i> | | μg Σ Hg/g dw | μg MeHg/g dw | Me/ Σ Hg % |
|--|----------|---------|--------------------------------------|----------------------------|----------------------|
| <i>Electrona antarctica</i> | 11 | mean | 0.22 | 0.11 | 57 |
| | | st.dev. | 0.11 | 0.03 | |
| <i>Bathylagus antarcticus</i> | 11 | mean | 0.54 | 0.29 | 57 |
| | | st.dev. | 0.23 | 0.11 | |
| <i>Trematomus lepidorhinus</i> | 8 | mean | 0.12 | | |
| | | st.dev. | 0.03 | | |
| <i>Notothenia kempfi</i> | 2 | mean | 0.17 | 0.17 | 100 |
| | | st.dev. | 0.03 | 0.01 | |
| <i>Cryodraco antarcticus</i> | 2 | mean | 0.19 | 0.09 | 48 |
| | | st.dev. | 0.03 | 0.03 | |
| <i>Pleuragramma antarcticum</i> juvenile (AAMBER 90/91) | 2 | mean | 0.11 | — | — |
| | | st.dev. | 0.02 | — | |
| <i>Pleuragramma antarcticum</i> adult (AWI 1989) | 11 | mean | 0.11 | 0.05 | 48 |
| | | st.dev. | 0.05 | 0.04 | |
| <i>Chaenodraco wilsoni</i> | 3 | mean | 0.09 | 0.04 | 43 |
| | | st.dev. | 0.01 | 0.03 | |
| <i>Pagothenia hansonii</i> | 3 | mean | 0.51 | 0.49 | 79 |
| | | st.dev. | 0.38 | 0.55 | |
| <i>Chionodraco hamatus</i> | 2 | mean | 0.18 | — | — |
| | | st.dev. | 0.01 | — | |

3. MERCURY in SEABIRDS.

1. Comparison of the different tissues (Table 5).

In general, the ratio between liver and muscle, and kidney and muscle contaminations can be considered as normal with values of 1.2 and 2.3

respectively. The obvious exceptions are the Kerguelen Petrel (91/3) and an Antarctic Petrel (91/6) with ratios of 16 and 4 respectively. These very high values (especially the first one) and high liver concentrations (9 and 1 $\mu\text{g } \Sigma\text{Hg/g dw}$) probably reflect the existence of a recent, acute contamination. Such acute cases, however, probably depend on a remobilization of liposoluble residues like organochlorines or methyl mercury after physiological stress and utilization of own fat reserves. MeHg concentrations are however not very high here: one must envisage another possibility, namely the eventual existence of a slow mineralization process leading, for the oldest animals, to such a high liver accumulation of anorganic Hg that it becomes toxic. Such a phenomenon was studied in some details in cetaceans from the North Sea, where a mineralization of MeHg lead to an important liver concentration of anorganic Hg, only partially detoxified by selenium (thiemanite) and metallothioneins. By similarity, the same hypothesis might be proposed for seabirds, but still needs confirmation.

The observation that MeHg concentrations are much more stable among the different samples fits into the scheme of accumulation and mineralization with increasing age.

A comparison with North Sea data, with median values of 0.1 to 0.7 for the muscle of different species and 0.8 to 2 for the liver, reflects contaminations of the same order of magnitude

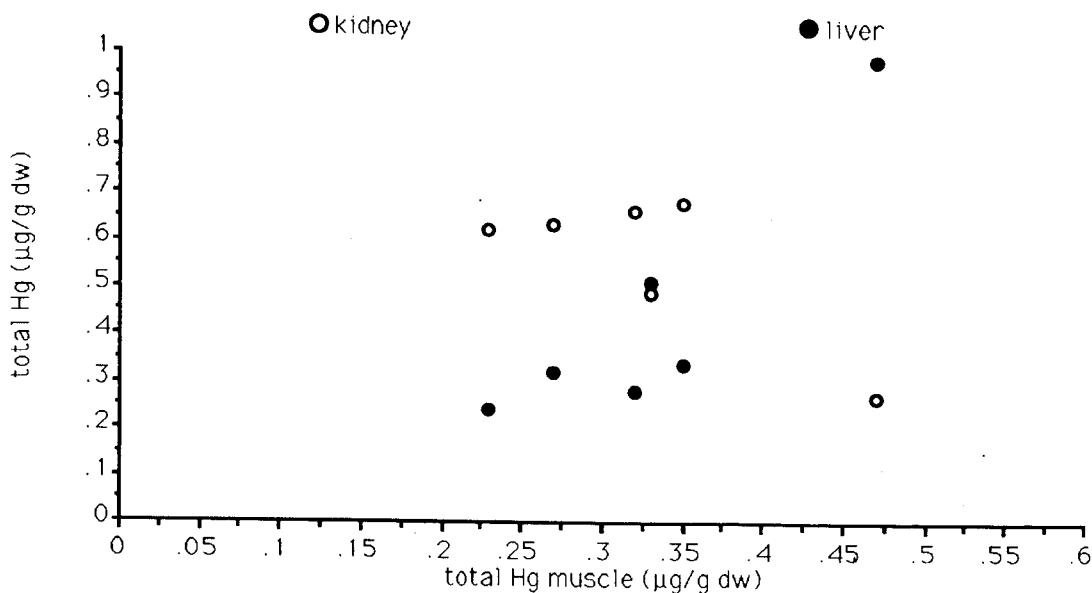


Figure 5: Hg concentration in Antarctic seabirds: total Hg in kidney and liver as a function of muscle concentration.

Table 5: Total and methyl mercury in different tissues of Antarctic seabirds.

| Species | muscle | <i>n</i> | liver | <i>n</i> | liver/ muscle | kidney | <i>n</i> | kidney/ muscle |
|--------------------------------|--------|----------|-------|----------|------------------|--------|----------|-------------------|
| Σ Hg (μg/g dw) | | | | | | | | |
| <i>Puffinus griseus</i> | 0,32 | 3 | 0,3 | 4 | 1,01 | 0,65 | 4 | 2,1 |
| <i>Thalassoica antarctica</i> | 0,34 | 3 | 0,7 | 3 | 2,36 | 0,51 | 3 | 1,5 |
| <i>Pterodroma brevirostris</i> | 0,55 | 1 | 9,0 | 1 | 16,3 | 5,76 | 1 | 10,5 |
| median | 0,33 | | 0,4 | | 1,2 | 0,65 | | 2,3 |
| mean | 0,33 | | 0,4 | | 1,6 | 0,60 | | 1,9 |
| st. dev. | 0,08 | | 0,3 | | 1,4 | 0,16 | | 0,5 |
| MeHg (μg/g dw) | | | | | | | | |
| <i>Puffinus griseus</i> | 0,13 | 4 | 0,3 | 4 | 2,7 | 0,34 | 4 | 2,5 |
| <i>Thalassoica antarctica</i> | 0,13 | 3 | 0,4 | 4 | 3,3 | 0,34 | 4 | 3,2 |
| <i>Pterodroma brevirostris</i> | 0,39 | 1 | 1,3 | 1 | 3,4 | 0,78 | 1 | 2,0 |
| median | 0,14 | | 0,3 | | 3,0 | 0,35 | | 2,5 |
| mean | 0,13 | | 0,3 | | 2,8 | 0,34 | | 2,7 |
| st. dev. | 0,02 | | 0,1 | | 1,2 | 0,10 | | 0,7 |

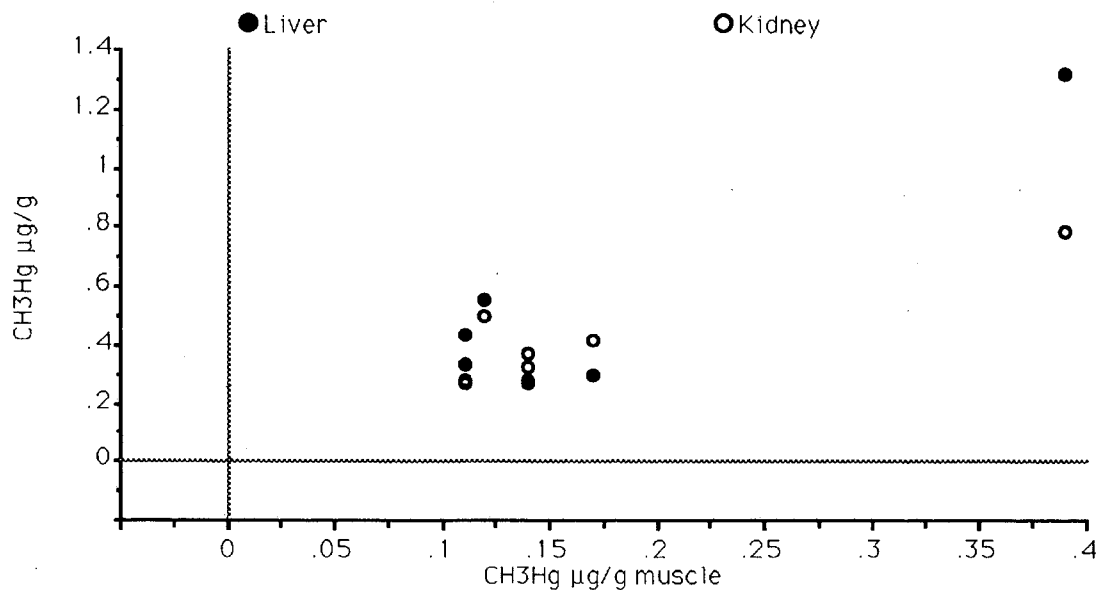


Figure 6: Hg concentration in Antarctic seabirds: MeHg in kidney and liver as a function of muscle concentration.

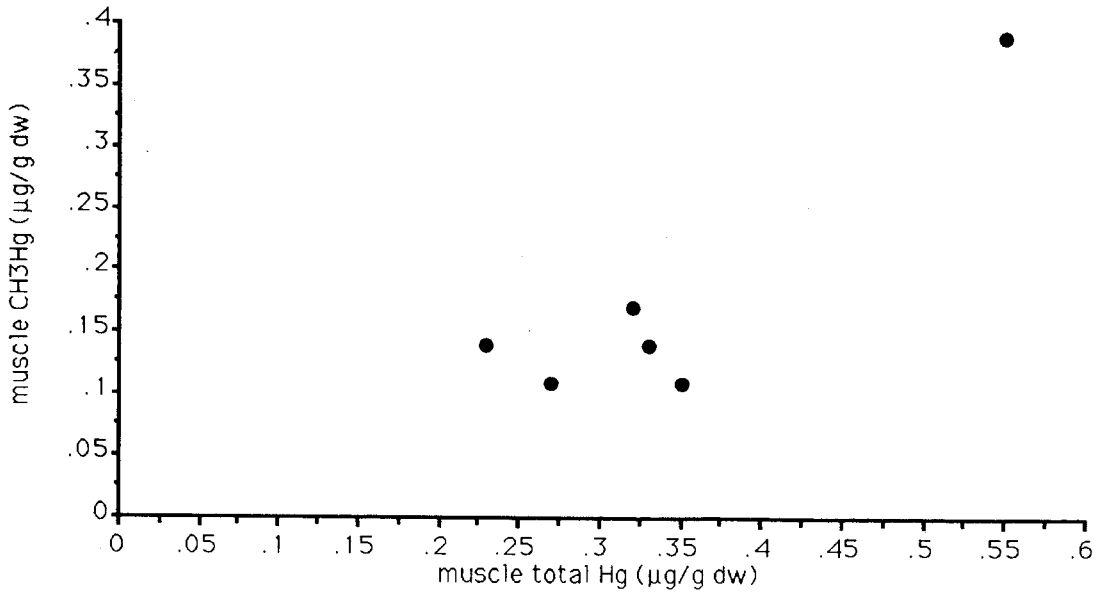


Figure 7: Hg concentration in Antarctic seabirds: MeHg as a function of total Hg in muscle.

ANTAR
II/07
A

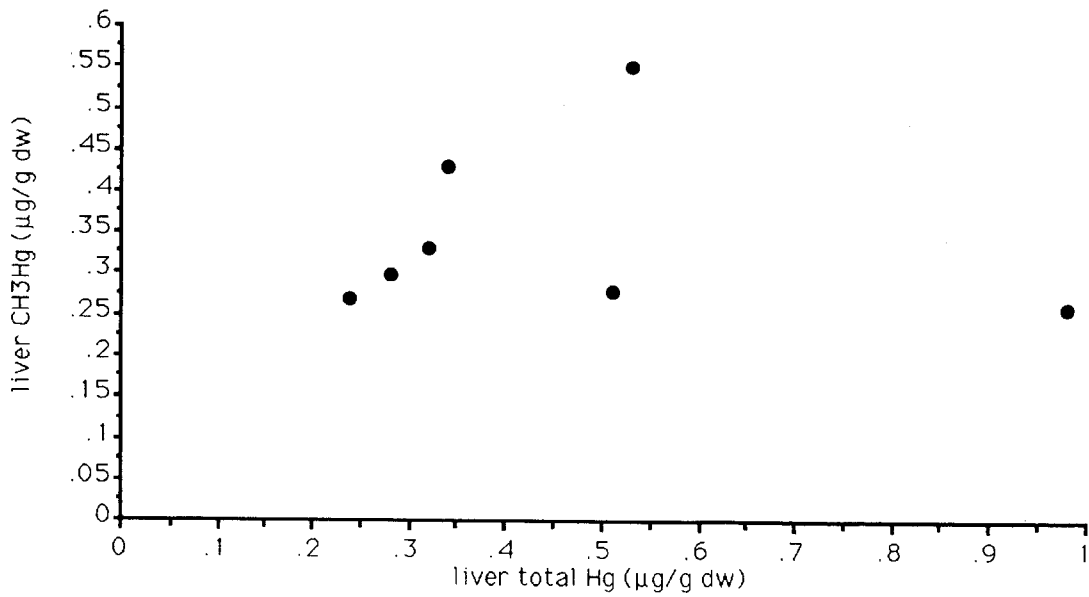


Figure 8: Hg concentration in Antarctic seabirds: MeHg as a function of total Hg in the liver.

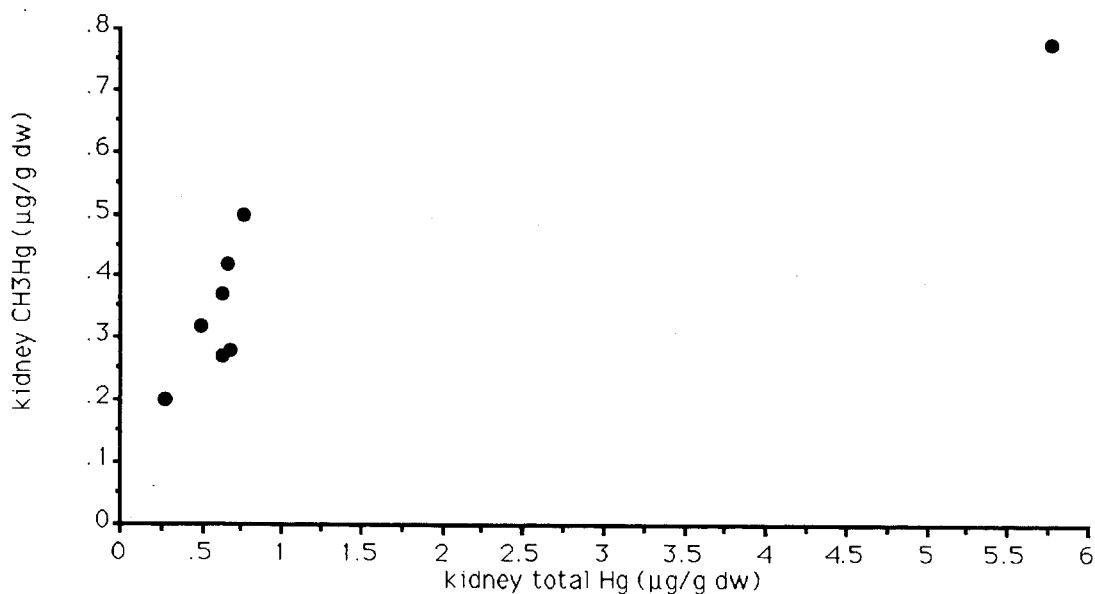


Figure 9: Hg concentration in Antarctic seabirds: MeHg as a function of total Hg in the kidney.

2. Comparison of the different species.

A first discussion of the results (Table 6) shows a mean contamination of 2.63 µg/g dry weight, all species included (n=45). If the very highly contaminated Giant Petrel is excluded, this mean becomes 1.43. It is however much better to use median values, the distribution of the data being, as always, not normal: the contamination by total Hg is **0.85 µg Hg g⁻¹ dw** (n=44).

This represents a relatively high contamination in the Antarctic, since the figures are only 6 times lower than in seabirds from the heavily polluted North Sea (*Larus ridibundus* has a mean liver contamination of 1.9, *Uria aalge* 9.5 and *Rissa tridactyla* 4.5). Such observations, however, fit into previous results obtained on particulate matter and zooplankton, in the North Sea and the Antarctic: the whole pollution was about 6 times lower in the Antarctic than in the North Sea, but the low biomass (particulate matter concentration) in the Antarctic caused a contamination, expressed as a concentration (e.g. µg g⁻¹ dry weight), as high in both systems. The same conclusion was drawn for Hg and for organochlorine residues (Bouquegneau and Joiris, 1987; Delbeke 1984; Delbeke and Joiris, 1988; Delbeke *et al.*, 1990; Joiris and Holsbeek, submitted; Joiris and Overloop, submitted; Joiris

et al., in prep.). The high contamination of Antarctic cetaceans (e.g. Abarnou *et al.*, 1986) can be explained the same way.

Levels of methyl mercury clearly show less variations: the median value is **0.35 $\mu\text{g MeHg g}^{-1}$ dw** (n=15), with min 0.13 and max 0.58. As a consequence, the much higher variations of total Hg, not reflected in parallel variations of MeHg, strongly influence the proportion of MeHg to total Hg: the higher the total contamination in liver, the lower the MeHg to total Hg ratio. The low total Hg values correspond to more than 80 % MeHg; for the highest Σ Hg levels, less than 10 % is MeHg. In similarity with results obtained on dolphins (Joiris *et al.*, 1991), one may propose the hypothesis that (Antarctic) seabirds accumulate Σ Hg as a function of age, and slowly mineralize MeHg, so that the oldest birds show very high levels of mineral Hg in the liver. Age determination clearly becomes an important factor in such studies.

These results should, from the ecological point of view, be discussed as a function of the diet of the seabirds: it is generally accepted that most of them are krill consumers, but this conclusion is mainly dependant on data obtained at the colony, from adults feeding their chicks. A recent study (Ainley *et al.*, 1991) concerning birds shot at sea, however showed the great importance of fish in the "at sea" diet of most of Antarctic seabirds - and our study concern the same individuals.

ANTAR
II/07
A

Table 6: Mercury contamination of Antarctic seabirds (liver; mean value).

| Species | | Σ Hg $\mu\text{g/}$ | | | MeH | |
|-----------------------|--------------------------------|----------------------------|-------------|----|-----------------|----|
| | | g fw | g dw | n | $\mu\text{g/g}$ | n |
| | | | | | dw | |
| Southern Giant Petrel | <i>Macronectus giganteus</i> | 18.6 | 53 | 1 | | |
| Antarctic Petrel | <i>Thalassoica antarctica</i> | 0.45 | 1.44 | 11 | 0.25 | 6 |
| Cape Pigeon | <i>Daption capense</i> | 1.02 | 3.14 | 6 | | |
| Blue Petrel | <i>Halobaena caerulea</i> | 0.43 | 1.30 | 2 | | |
| Southern Fulmar | <i>Fulmarus glacialisoides</i> | 0.37 | 1.16 | 7 | 0.39 | 3 |
| Prion | <i>Pachyptila desolata</i> | 0.27 | 0.83 | 6 | | |
| Kerguelen Petrel | <i>Pterodroma brevirostris</i> | 0.8 | 2.43 | 1 | | |
| Σ Petrels | | 0.51 | 1.44 | 33 | 0.30 | 9 |
| Wilson's Storm-Petrel | <i>Oceanites oceanicus</i> | 0.32 | 0.98 | 5 | | |
| Arctic Tern | <i>Sterna paradisaea</i> | 0.22 | 0.62 | 6 | 0.38 | 3 |
| mean | all | 0.87 | 2.63 | 45 | | |
| | all - Macronectes | 0.46 | 1.43 | 44 | 0.35 | 15 |
| median | | | 0.85 | 45 | 0.35 | 15 |

4. PCBs and ORGANOCHLORINE PESTICIDES in PHYTO- and ZOOPLANKTON.

From January 3 to February 27, 1987, we participated in the INDIGO 3 cruise of the French R.V. Marion Dufresne in the Indian sector of the Southern Ocean from latitude 38 to 67°S and from longitude 18 to 84°E.

Samples from the lower trophic levels (phyto- and zooplankton) were taken and analyzed for organochlorine residue (PCBs and pesticides) content. The quantitative and qualitative aspects of determining the type of PCB mixture are first discussed, stressing the need to standardize the expression of data.

The PCB concentration in particulate matter (mainly phytoplankton) appears to be high and similar to that of temperate zones: 0.74 µg/g dry weight. In order to interpret such results correctly at the ecosystem level, however, it is necessary to standardize by expressing them in other units such as per lipid weight and per volume of seawater. When contamination is expressed per water volume, it is more constant than per dry weight, and seven times lower (1.2 µg/m³) than in northern temperate zones (8.8 µg/m³ in the North Sea). The Antarctic ecosystems are thus less contaminated than temperate ones -- as expected - but the very low phytoplankton biomasses present cause high PCB levels per unit of biomass. These results confirm the necessity of using different systems of units in order to correctly express the contamination levels and to identify the main mechanisms responsible for the accumulation of stable pollutants.

PCB levels in netplankton samples (mainly zooplankton) are comparable with phytoplankton on a dry weight basis (0.7 µg/m³), lower on a lipid weight basis (5.8 µg/g lw for netplankton, 16.3 for particulate matter) and are much higher per seawater volume (27.2 µg/m³ for netplankton, 1.2 for particulate matter).

Netplankton contamination is comparable in the Antarctic (0.35 µg/g dw) and the North Sea (0.70): this is due to the fact that zooplankton is indirectly contaminated and that its food (primarily phytoplankton) has equally high contamination, on a dry weight basis, in both ecosystems.

The presence of other organochlorines: lindane, heptachlor epoxide, dieldrin, DDE and DDT was noticed in various samples at levels varying between low, trace, or not detectable. The high DDT/ DDE ratio reflects the more recent origin of Antarctic organochlorines.

The main water masses were identified from their physico-chemical and biological parameters (water temperature, salinity, dissolved oxygen, chlorophyll); the main

frontal systems were positioned as follows, from North to South: Subtropical Convergence between 41°S and 43°S; less pronounced Subantarctic Front at 47°S and Antarctic Convergence or Polar Front at 50°S and very clear Antarctic Divergence at 66°S (Goffart and Hecq; Joiris and Overloop *in* Poisson and Caschetto, 1989).

Particulate matter (mainly phytoplankton) was sampled by pumping water under the water surface and continuous centrifugation for a period of about 24 hours in order to obtain sufficient material for determination of PCBs and pesticides. This process resulted in 37 samples (Fig. 9).

Netplankton samples were obtained with a 200 µm mesh size net towed horizontally for a period of 20 minutes at 2 knots at every station (see Fig. 10).

PCBs.

Geographical comparison.

1. Particulate matter.

In order to attempt to elucidate the main transfer mechanism, the PCB concentrations have to be expressed in different systems of units (see introduction). Three major zones are compared: Subtropical, Antarctic "Proper" (the Antarctic zone, between the Convergence and the Divergence) and South of the Divergence. On a dry weight basis, a slightly higher contamination level seems to appear in the subtropical zone: 1.4 µg PCB/ g dry weight compared with 0.7 in the two other zones (see Fig. 12, table 7). When the data are expressed per volume seawater, by multiplying the PCB level per unit of biomass by the amount of biomass present per volume seawater, (Fig. 13, table 6), however, no difference appears to exist between the three zones: PCB concentration is 1.2 µg/ m³ mean value for the whole region. These observations are confirmed by application of the non-parametric test of Kruskal-Wallis: no significant difference was detected between zones, but the H value is much lower for the results expressed per m³, which reflects the greater homogeneity of this series.

In comparison with the North Sea ecosystem (Table 7), the results indicate a comparable PCB level expressed per dry weight: the observed difference was not significant at the 0.05 level in a Mann-Whitney test. Per volume water, the contamination of the Antarctic samples is less variable than in the other units (see Figs. 12 & 13, Table 7) and lower than in the North Sea. These findings reflect again the fact that the most important mechanism for particulate matter contamination are adsorption, absorption and partition.

As a whole (per volume seawater), Antarctica is less contaminated than temperate regions - as expected - but the lower biomass levels cause a high PCB concentration per unit of biomass.

Table 7: Total PCB concentration of particulate matter expressed as Aroclor 1254 in different units (dry weight: dw; lipid weight: lw; per volume of seawater: m³) for the different zones (mean, standard deviation, *n*: number of samples).

| PCBs Zone | ng/gdw | | | µg/glw | | | µg/m ³ | | |
|----------------------|--------|----------|-------|--------|----------|-------|-------------------|----------|-------|
| | mean | <i>n</i> | stdev | mean | <i>n</i> | stdev | mean | <i>n</i> | stdev |
| Subtropical | 1433 | 4 | 994 | 24.6 | 4 | 16.6 | 1.24 | 3 | 0.76 |
| Antarctic "proper" * | 677 | 23 | 522 | 15 | 26 | 11.2 | 1.19 | 17 | 0.68 |
| South Divergence | 678 | 2 | 544 | 10 | 2 | 4.1 | 1.08 | 2 | - |
| Kerguelen ** | 356 | 3 | 257 | 20.7 | 3 | 4.9 | - | - | - |
| Mean | 741 | 32 | 617 | 16.3 | 35 | 11.6 | 1.18 | 22 | 0.66 |
| North Sea *** | 675 | 20 | - | 118 | 20 | - | 8.8 | 20 | - |

* Between Convergence and Divergence

** Very coastal samples from the Bays of Rhodes and Port aux Français

*** Delbeke and Joiris, 1988.

2. Netplankton.

Netplankton, sampled with a 200 µm mesh size net, consisted mainly of zooplankton,

but sometimes included phytoplankton; one sample consisting of pure krill *Euphausia superba* (station 86).

No difference appeared when comparing PCB concentrations on a dry weight basis in the three zones (table 8): 0.37 µg/ g dry weight, mean value for the whole region, 0.37 for the Subtropical zone, 0.38 for the Antarctic proper, and 0.30 South of the Divergence. Expressed per volume seawater, differences appear however between the three major zones: 0.01 for the Subtropical region; 0.04 for the Antarctic Proper and 0.001 µg/ m³ South of the Divergence, with a mean value for the whole region of 0.03 µg/ m³. A Kruskal-Wallis test confirmed that no significant difference between zones could be detected.

The PCB levels are of the same order of magnitude in the Antarctic netplankton and the North Sea zooplankton on a dry weight basis (table 8), and no significant difference appeared in a Mann-Whitney test.

Comparison of the PCB levels in particulate matter and netplankton.

The PCB levels in netplankton and particulate matter (Tables 7 & 8) are comparable on a dry weight basis (0.35 $\mu\text{g/g}$ dw for netplankton NP, 0.74 for particulate matter PM or 0.64 without taking into account the high values from the sub-tropical zone); they are higher in particulate matter on a fat weight basis (16.3 $\mu\text{g/g}$ lw in PM, 5.8 in NP), indicating a higher lipid content of netplankton. Per seawater volume, the difference between particulate matter and netplankton contaminations is still more marked (1.2 $\mu\text{g/m}^3$ in PM, 27.2 in NP), reflecting the higher abundance of particulate matter than netplankton in Antarctic waters. As stated earlier, the higher homogeneity of results expressed per seawater volume in particulate matter than in netplankton (to be noticed at the level of the ratio between standard deviation and mean) reflects the differences in contamination mechanisms: direct contamination for particulate matter (adsorption, absorption and partition on the lipids), indirect contamination for zooplankton (through the food, i.e. primarily phytoplankton).

ANTAR
II/07
A

Table 8: Total PCB contamination of netplankton

| PCBs Zone | ng/g dw | | | $\mu\text{g/g}$ lw | | | $\mu\text{g/m}^3$ | | |
|----------------------|---------|----|-------|--------------------|----|-------|-------------------|----|-------|
| | mean | n | stdev | mean | n | stdev | mean | n | stdev |
| Subtropical | 370 | 3 | 114 | 6.2 | 3 | 1.2 | 10.7 | 3 | 7 |
| Antarctic "proper" * | 381 | 10 | 332 | 6.0 | 10 | 2.4 | 38.0 | 7 | 62 |
| South Divergence | 30 | 1 | - | 3.0 | 1 | 4.1 | 1.0 | 1 | - |
| Mean | 354 | 14 | 295 | 5.8 | 14 | 2.2 | 27.2 | 11 | 50.3 |
| North Sea ** | 700 | 20 | - | 7.0 | 20 | - | 0.02 | 20 | - |

* Between Convergence and Divergence

** zooplankton (Delbeke and Joiris, 1988).

Organochlorine pesticides.

The level of organochlorine pesticides in netplankton was generally low, and in many samples just above the detection limit (trace) or not detected at all. The following pesticides were present in most samples: lindane with average values of 19 ng/g dry weight and 343 ng/g lipid weight, heptachlor epoxide 27 and 342, and dieldrin 9 and 153. Heptachlor and aldrin were not detected (table 9). No geographical difference was noticed.

DDT and DDE were present as traces only or were not detected at all in particulate matter. 50% of the netplankton samples contained very low concentrations of DDT and DDE, with an average of 4 ng DDT/ g dw and 7 ng DDE/ g dw. The DDT to DDE ratio provides usefull information on the age of the residues, since DDT is slowly metabolized into the more stable DDE. In our results, it had a mean value of 2.55 and varied between 0 (DDE present, DDT not detected) and 8, within a small series of 6 positive samples. Such findings are confirmed by the analyses of Antarctic seabirds (Lukowski, 1978b, 1983a, 1983b) and dolphins (Abarnou *et al.*, 1986), with DDT to DDE ratios ranging up to 10. In North Sea plankton samples, DDT was never detected: this clear difference reflects the recent use of DDT in southern countries, while in Europe it was significantly reduced or stopped in the seventies.

In particulate matter, most of the results were present as trace or not detected: this is why they are not reported here.

Table 9: Organochlorine pesticides in Antarctic netplankton (nd: not detected).

| Pesticide | n | ng/g dw | | ng/g lw | |
|--------------------|----|---------|-------|---------|-------|
| | | mean | stdev | mean | stdev |
| lindane | 11 | 19 | 4 | 340 | 7 |
| heptachlor | 11 | nd | | nd | |
| heptachlor epoxide | 11 | 27 | 10 | 340 | 60 |
| dieldrin | 9 | 9 | 2 | 153 | 20 |
| aldrin | 9 | nd | | nd | |
| pp'-DDT | 6 | 4 | 2 | 99 | 30 |
| pp'-DDE | 9 | 7 | 5 | 115 | 60 |

Conclusions.

The PCB contamination of particulate matter (sampled by continuous centrifugation and consisting mainly of phytoplankton) is of the same order of magnitude in the Antarctic waters as in the North Sea when expressed as a concentration per dry weight. One expects however Antarctic ecosystems to be much less contaminated than temperate ones, especially the heavily polluted North Sea, since the direct local contamination is extremely limited and the stable pollutants have to be imported from adjacent inhabited zones. In order to understand these high levels, one must consider the contamination mechanisms and express the results in

different unit systems: per volume of seawater, the PCB level is seven times lower in the Antarctic than in the North Sea. This is the figure to be used in order to compare the contamination of different zones. Due to the basic contamination mechanisms of particulate matter -- adsorption, absorption and partition - and due to the much lower biomass present in the Antarctic, similar levels are however reached per unit of biomass. The fact that the contamination expressed per fat weight is lower in Antarctic particulate matter, reflects its higher lipid content. This leads to the paradoxical consequence that, even if the Antarctic ecosystem is six times less contaminated by PCBs than the North Sea, its biological components might be as contaminated -- or even more contaminated - than in the North Sea.

At the zooplankton level, indeed, the PCB contamination of the Antarctic and the North Sea ecosystems are comparable.

The presence of organochlorine pesticides: lindane, heptachlor epoxide, dieldrin, DDE and DDT was noticed in various samples at levels varying between traces and low concentration or were not detected. The high DDT/ DDE ratio reflects the recent origin of Antarctic organochlorines: in the North Sea ecosystems, no DDT is detected.

Since the use of organochlorines is still increasing in the southern hemisphere while it is strongly limited or forbidden in northern countries, one must expect still increasing levels in the Antarctic. This suggests an urgent need to improve our knowledge of the levels and the fate of stable pollutants in the southern regions, and more especially in the Antarctic.

5. PCBs and ORGANOCHLORINE PESTICIDES in SEABIRDS.

Organochlorines concentrations were determined in the same seabirds, collected in March-April 1990 on board the RV Polarstern (see Hg in seabirds, page 15).

Levels were generally low (table 10): aldrin, dieldrin, lindane, heptachlor and heptachlor epoxyde were below our detection limit. Residues of the DDT group were determined in most of the samples; the high DDT to DDE ratios reflect the existence of recent contaminations, as already noted in suspended particular matter. A similar pattern of low concentrations was found for PCBs: the concentration of "total" PCBs never exceeds $0.2\mu\text{g/g}$ dw, in muscle nor in liver. The individual congeners 101, 118, 153 and 138 were often detected, but only as traces (table 11).

ANTAR
II/07
A

CONCLUSION.

The contamination of phytoplankton (suspended particulate matter) both by PCBs and by total mercury is higher than expected, a reflection of the existence of important sources of contamination in the southern hemisphere reaching the Antarctic marine ecosystems through atmospheric transport. At the ecosystem level, the loads are about six times lower than in the North Sea. Due to the lower biomass present in the Antarctic, however, and the direct contamination of particulate matter from the water (adsorption, absorption and partition on the lipids), concentrations expressed per weight unit are as high in Antarctica as in the North Sea.

This high concentration of Hg and PCBs could cause a high contamination of the higher trophic levels, if indirect contamination through the food were the main contamination mechanism for fish. Since this is not the case (contamination of fish is low, compared with North Sea levels), one must on the contrary conclude that direct contamination of fish plays an important role. These field observations confirm conclusions obtained in the laboratory after exposure to low PCB concentrations (Zhu *et al.*, 1992). By comparing the Antarctic and North Sea ecosystems, indeed, one can detect the relative importance of direct and indirect uptakes in nature: in case of indirect contamination, one expects comparable contamination levels in both ecosystems, since the concentrations are of the same level in particulate matter. In case of direct contamination from the water, on the contrary, one expects six times lower concentrations in Antarctic fish, since the ecosystem - and thus the water - contamination is six times lower than in the North Sea. This is why, the contamination of fish being six times lower in Antarctica, we concluded to the existence of an important direct contamination mechanism.

Seabirds' contamination is of course indirect. Since their food (fish) is less contaminated in the Antarctic, it is normal to determine lower levels in the seabirds as well.

From the practical point of view, however, one must take into account that contamination is recent and still increasing in the Antarctic, while it is older and probably stabilized or decreasing in northern industrialized regions like Western Europe and North America.

Table 10: Organochlorine pesticides in Antarctic birds

| nr. | species | tissue | Lindane µg/g dw | Heptachlor µg/g dw | Hept.Epox µg/g dw | Aldrin µg/g dw | Dieldrin µg/g dw | pp'DDE µg/g dw | pp'DDD µg/g dw | pp'DDT µg/g dw |
|-----|------------------|------------|--------------------|-----------------------|----------------------|-------------------|---------------------|-------------------|-------------------|-------------------|
| 1 | Sooty Shearwater | muscle | n.d. | n.d. | n.d. | n.d. | n.d. | n.d. | n.d. | n.d. |
| | | liver | n.d. | n.d. | n.d. | n.d. | n.d. | n.d. | n.d. | trace |
| 2 | Sooty Shearwater | muscle | n.d. | n.d. | n.d. | n.d. | n.d. | n.d. | n.d. | 0.14 |
| | | liver | n.d. | n.d. | n.d. | n.d. | n.d. | n.d. | n.d. | n.d. |
| 4 | Sooty Shearwater | muscle | n.d. | n.d. | n.d. | n.d. | n.d. | n.d. | n.d. | 0.44 |
| | | liver | n.d. | n.d. | n.d. | n.d. | n.d. | n.d. | n.d. | 0.25 |
| 5 | Sooty Shearwater | muscle | n.d. | n.d. | n.d. | n.d. | n.d. | n.d. | n.d. | 0.20 |
| | | liver | n.d. | n.d. | n.d. | n.d. | n.d. | n.d. | n.d. | 0.27 |
| 6 | Antarctic Petrel | liver | n.d. | n.d. | n.d. | n.d. | n.d. | n.d. | n.d. | 0.50 |
| 7 | Antarctic Petrel | muscle | n.d. | n.d. | n.d. | n.d. | n.d. | 0.005 | n.d. | 0.42 |
| | | liver | n.d. | n.d. | n.d. | n.d. | n.d. | 0.005 | n.d. | 0.61 |
| 8 | Antarctic Petrel | muscle | n.d. | n.d. | n.d. | n.d. | n.d. | 0.012 | n.d. | 0.35 |
| | | liver | n.d. | n.d. | n.d. | n.d. | n.d. | 0.010 | n.d. | 0.37 |
| 3 | Kerguelen Petrel | muscle | n.d. | n.d. | n.d. | n.d. | n.d. | 0.008 | trace | 0.27 |
| | | liver | n.d. | n.d. | n.d. | n.d. | n.d. | 0.006 | trace | 0.36 |
| | | trace | < 0.01 | < 0.002 | < 0.02 | < 0.002 | < 0.02 | < 0.004 | < 0.05 | < 0.07 |
| | | det. limit | 0.01 | 0.001 | 0.01 | 0.001 | 0.01 | 0.002 | 0.03 | 0.04 |

ANTAR
II/07
A

Table 11: PCBs in Antarctic birds

| nr. | species | tissue | Σ CB µg/g dw | Σ28-194 µg/g dw | CB 28 µg/g dw | CB 52 µg/g dw | CB 101 µg/g dw | CB 118 µg/g dw | CB 153 µg/g dw | CB 138 µg/g dw | CB 180 µg/g dw | CB 170 µg/g dw | CB 194 µg/g dw |
|-----|------------------|-----------|-----------------|--------------------|------------------|------------------|-------------------|-------------------|-------------------|-------------------|-------------------|-------------------|-------------------|
| 1 | Sooty Shearwater | muscle | n.d. | n.d. | n.d. | n.d. | n.d. | n.d. | n.d. | n.d. | n.d. | n.d. | n.d. |
| | | liver | n.d. | n.d. | n.d. | n.d. | n.d. | n.d. | n.d. | n.d. | n.d. | n.d. | n.d. |
| 2 | Sooty Shearwater | muscle | n.d. | n.d. | n.d. | n.d. | n.d. | n.d. | n.d. | n.d. | n.d. | n.d. | n.d. |
| | | liver | n.d. | n.d. | n.d. | n.d. | n.d. | n.d. | n.d. | n.d. | n.d. | n.d. | n.d. |
| 4 | Sooty Shearwater | muscle | < 0.033 | < 0.009 | n.d. | n.d. | n.d. | n.d. | n.d. | trace | n.d. | n.d. | n.d. |
| | | liver | n.d. | n.d. | n.d. | n.d. | n.d. | n.d. | n.d. | n.d. | n.d. | n.d. | n.d. |
| 5 | Sooty Shearwater | muscle | n.d. | n.d. | n.d. | n.d. | n.d. | n.d. | n.d. | n.d. | n.d. | n.d. | n.d. |
| | | liver | < 0.077 | < 0.015 | n.d. | n.d. | n.d. | n.d. | trace | trace | n.d. | n.d. | n.d. |
| 6 | Antarctic Petrel | liver | < 0.232 | < 0.064 | n.d. | n.d. | 0.017 | 0.019 | trace | 0.021 | n.d. | n.d. | n.d. |
| 7 | Antarctic Petrel | muscle | n.d. | n.d. | n.d. | n.d. | n.d. | n.d. | n.d. | n.d. | n.d. | n.d. | n.d. |
| | | liver | n.d. | n.d. | n.d. | n.d. | n.d. | n.d. | n.d. | n.d. | n.d. | n.d. | n.d. |
| 8 | Antarctic Petrel | muscle | < 0.082 | < 0.019 | n.d. | n.d. | trace | n.d. | trace | trace | n.d. | n.d. | n.d. |
| | | liver | < 0.086 | < 0.026 | n.d. | n.d. | trace | 0.010 | n.d. | trace | n.d. | n.d. | n.d. |
| 3 | Kerguelen Petrel | muscle | < 0.116 | < 0.026 | n.d. | n.d. | n.d. | 0.010 | trace | trace | n.d. | n.d. | n.d. |
| | | liver | n.d. | n.d. | n.d. | n.d. | n.d. | n.d. | n.d. | n.d. | n.d. | n.d. | n.d. |
| | | trace | < 0.015 | < 0.009 | < 0.007 | < 0.007 | < 0.007 | < 0.007 | < 0.006 | < 0.009 | < 0.009 | < 0.008 | < 0.025 |
| | | det.limit | 0.008 | 0.004 | 0.003 | 0.004 | 0.004 | 0.004 | 0.003 | 0.005 | 0.005 | 0.004 | 0.013 |

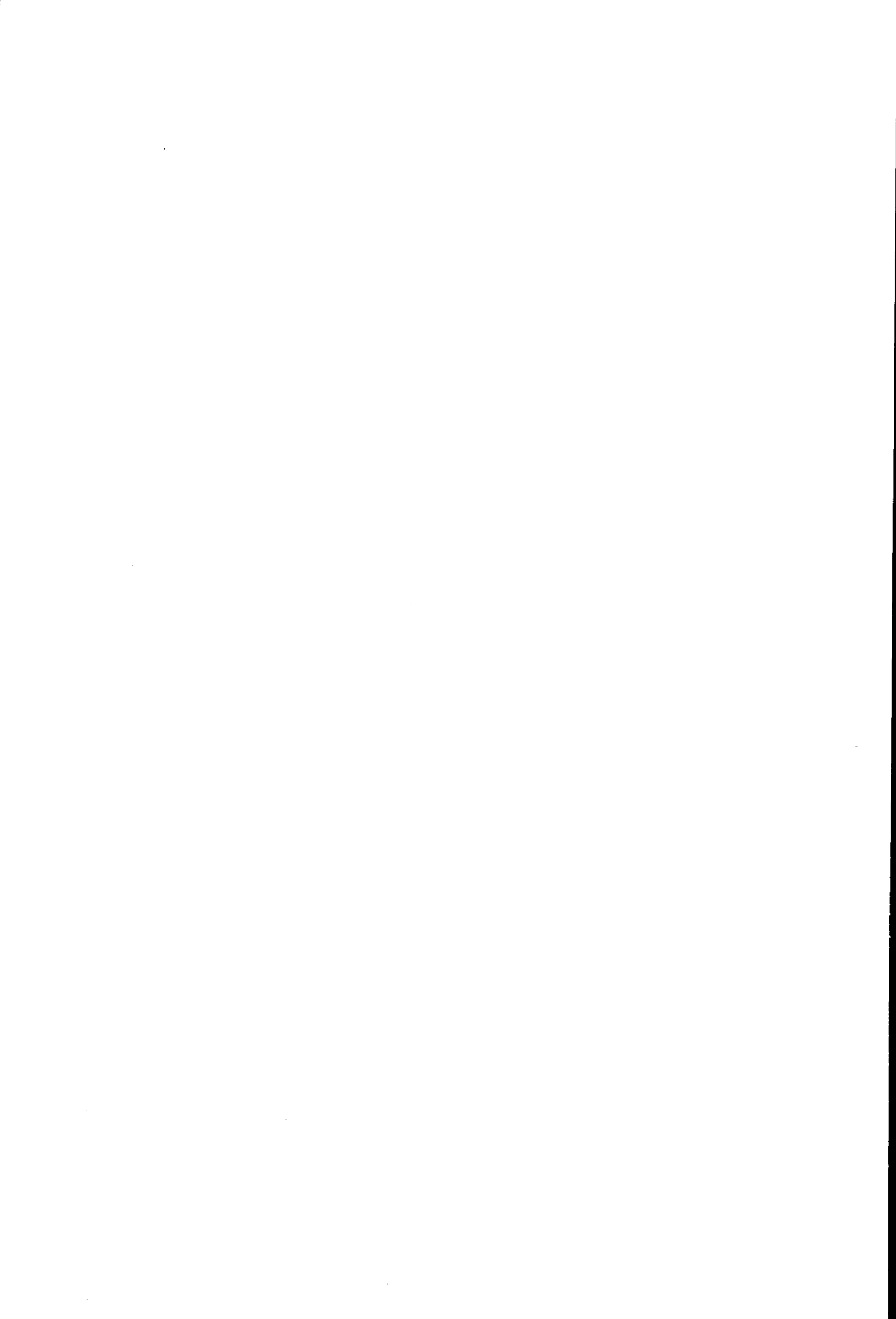
References.

- Abarnou, A., Robineau, D. and Michel, P. 1986. Contamination par les organochlorés des dauphins de Commerson des îles Kerguelen. *Oceanol. Acta*, 9, 19-29.
- Ainley, D.G., Fraser, W.R., Smith, W.O.Jr., Hopins, T.L. and Torres, J.J. 1991. The structure of upper level pelagic food webs in the Antarctic: effect of phytoplankton distribution. *J. Marine Systems*. In press.
- Anonymous, 1983. Metalen in boorkernen en oppervlaktesedimenten van de Noordzee. *Waterkundig Laboratorium Delft*. Internal Report.
- Bouquegneau, J.M. and Joiris, C. 1988. The fate of stable pollutants - heavy metals and organochlorines - in marine organisms. *Adv. in Compar. and Environ. Physio.*, 2, 219-247.
- Bouquegneau, J.M., Joiris, C. and Delbeke, K. 1985. Marine ecotoxicology: Field and laboratory approaches, 368-379. In: *Progress in Belgian Oceanographic Research*. R. Van Grieken and R. Wollast (Eds). Brussels. 479 pp.
- Courtney, W.A.M. and Langston W.J. 1981. Organochlorines in Antarctic Marine systems. *Br. Antarct. S. Bull.*, 53, 225-262.
- Delbeke, K. and Joiris, C. 1985. Ecotoxicology of organochlorine residues in Marine ecosystems, 358-367. In: *Progress in Belgian Oceanographic Research*. R. Van Grieken and R. Wollast (Eds). Brussels. 479 pp.
- Delbeke, K. and Joiris, C., 1988. Accumulation mechanisms and geographical distribution of PCBs in the North Sea. *Océanis*, 14: 399-410.
- Delbeke, K., Joiris, C.R. and Bossicart, M., 1990. Organochlorines in different fractions of sediments and in different planktonic compartments of the Belgian continental shelf and the Scheldt estuary. *Environmental Pollution*, 66: 325-349.
- Delbeke, K., Joiris, C. and Decadt, G. 1984. Mercury contamination of the Belgian avifauna, 1970-1981. *Env. Poll. (series B)*, 7, 205-221.
- Duinker, J.C., Knap, A.H., Binkley, K.C., Van Dam, G.H., Darrel-Rew, A. and Hillebrand, M.T.J. 1988. Method to represent the qualitative and quantitative characteristics of PCB mixtures. *Mar. Poll. Bull.*, 19, 74-79.
- Hidaka, H., Tanabe, S., Kawano, M and Tatsukawa, R. 1984. Fate of DDTs, PCBs and chlordane compounds in the Antarctic Marine ecosystem. In : Proceedings of the Sixth Symposium on Polar Biology. T. Hoshiai and M. Fukuchi (Eds) *Memoirs of Nat. Inst. Polar Res.*, special issue No 32.
- Hidaka, H. and Tatsukawa, R. 1983. Environmental Pollution of chlorinated Hydrocarbons around Syowa station. *Antarctic Rec.*, 80: 14-29.

- Joiris, C., G. Billen, C. Lancelot, MH. Daro, JP. Mommaerts, A. Bertels, M. Bossicart, J. Nijs and JH. Hecq. 1982. A budget of carbon cycling in the Belgian coastal zone: relative roles of zooplankton, bacterioplankton and benthos in the utilization of primary production. *Neth. J. Sea Res.*, 16, 260-275.
- Joiris, C., J.M. Bouqueneau, K. Delbeke and W. Overloop. 1987. Contamination by stable pollutants (organochlorines and heavy metals) of a common dolphin *Delphinus delphis* found dying in Belgium. *Europ. Cetacean Soc. Newsl.*, 1, 30-31.
- Joiris, C.R. and Holsbeek, L. 1991. Mercury in suspended particulate matter from the northern Weddell Sea, Antarctica. Submitted.
- Joiris, C.R., Holsbeek, L., Bouqueneau, JM. and Bossicart, M. 1991. Mercury contamination of the harbour porpoise *Phocoena phocoena* and other cetaceans from the North Sea and the Kattegat. *Water, Air and Soil Pollution*, 56, 283-293.
- Joiris, C.R., Liang, W., Holsbeek, L. and Bossicart, M. 1992. Mercury contamination of North Sea seabirds. In prep.
- Joiris, C.R. and Overloop, W., 1991. PCBs and organochlorine pesticides in phytoplankton and zooplankton from the Indian sector of the Antarctic Ocean. *Antarctic Sc.*, 3: 371-377.
- Lukowski, A.B. 1978a. DDT and its metabolites in Antarctic krill (*Euphausia superba* Dana) from South Atlantic. *Pol. Arch. Hydrobiol.*, 25, 663-668.
- Lukowski, A.B. 1978b. DDT and its metabolites in Antarctic birds. *Pol. Arch. Hydrobiol.*, 25, 729-737.
- Lukowski, A.B. 1983a. DDT residues in the tissues and eggs of three of penguins from breeding colonies at Admiraty Bay (King Georges Island, South Shetland Islands). *Pol. Polar Res.*, 59 4, 129-134.
- Lukowski, A.B. 1983b. DDT and its metabolites in the tissues and eggs of migrating Antarctic seabirds from the regions of the South Shetland Islands. *Pol. Polar Res.*, 4, 135-141.
- Poisson, A. et Caschetto, S. Eds. 1989. Les rapports des campagnes à la mer: MD 53/ Indigo 3 à bord du "Marion Dufresne" 3 janvier - 27 février 1987. No 87.01. 102 pps.
- Risebrough, R.W., Walker II, W., Schmidt, T.T., deLappe, B.W. and Connors, C.W. 1976. *Nature*, 264, 738.
- Sladen, W.J.L., Menzie, C. M. and Reichel, W.L., 1966. DDT residues in Adélie Penguins and crabeater seals from Antarctica. *Nature*, 210: 671- 673.

- Subramanian, B.R., Tanabe, S., Hidaka, H. and Tatsukawa, R. 1983. DDTs and PCBs isomers and congeners in Antarctic Fish. *Arch. Environm. Contam. Toxicol.*, 12, 621-626.
- Tanabe, S., Tatsukawa, R., Kawano, M. and Hidaka, H. 1982. Global distribution and atmospheric transport of chlorinated Hydrocarbons HCH (BHC) isomers and DDT compounds in the Western Pacific, Eastern Indian and Antarctic Oceans. *J. Oceanogr. Soc. Japan*, 38, 137-148.
- Tanabe, S., Hidaka, H. and Tatsukawa, R. 1983. PCBs and chlorinated hydrocarbons pesticides in Antarctic atmosphere and hydroshere. *Chemosphere*, 12, 277-288.
- Tatsukawa, R. and Tanabe, S. 1983. Geochemical and biochemical behaviour of the open ocean environment. In: *Proceedings PCB Seminar Scheveningen*, The Hague, The Netherlands, Sept. 28-30.
- Tatton, O'G. and Ruzicka, J.H.A., 1967. Organochlorine pesticides in Antarctica. *Nature*, 215: 346-348.
- Van Alsenoy, V., Van Put, A., Bernard, P. and Van Grieken, R., 1989. Chemical characterization of suspensions and sediments in the North Sea and Scheldt estuary. In: G. Pichot (Editor), *Progress in Belgian Oceanographic Research 1989*: 351-368.
- Zhu, L., Bouquegneau, JM., Delbeke, K. and Joiris, C. 1992. PCBs uptake and elimination kinetics in guppy *Poecilia reticulata*. Submitted.

ANTAR
II/07
A



RESEARCH CONTRACT ANTAR/II/07
(part B)

**CO₂ AND O₂
IN ANTARCTIC
MARINE
ECOSYSTEMS**

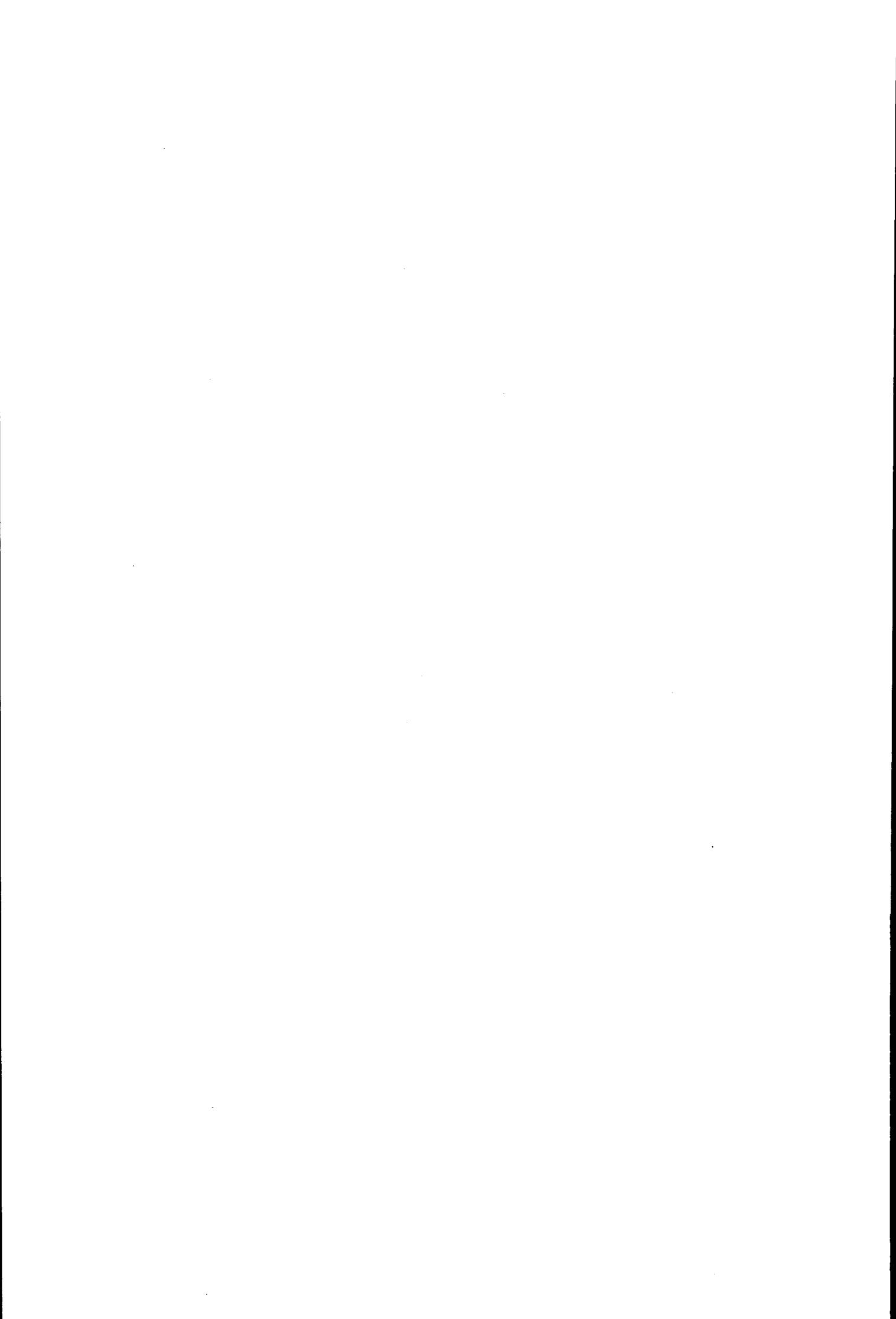
J.-M. Bouquegneau*
and C. Joiris**

* SERVICE D'OCÉANOLOGIE

Université de Liège
B-4000 Liège Sart Tilman B6,
Belgium

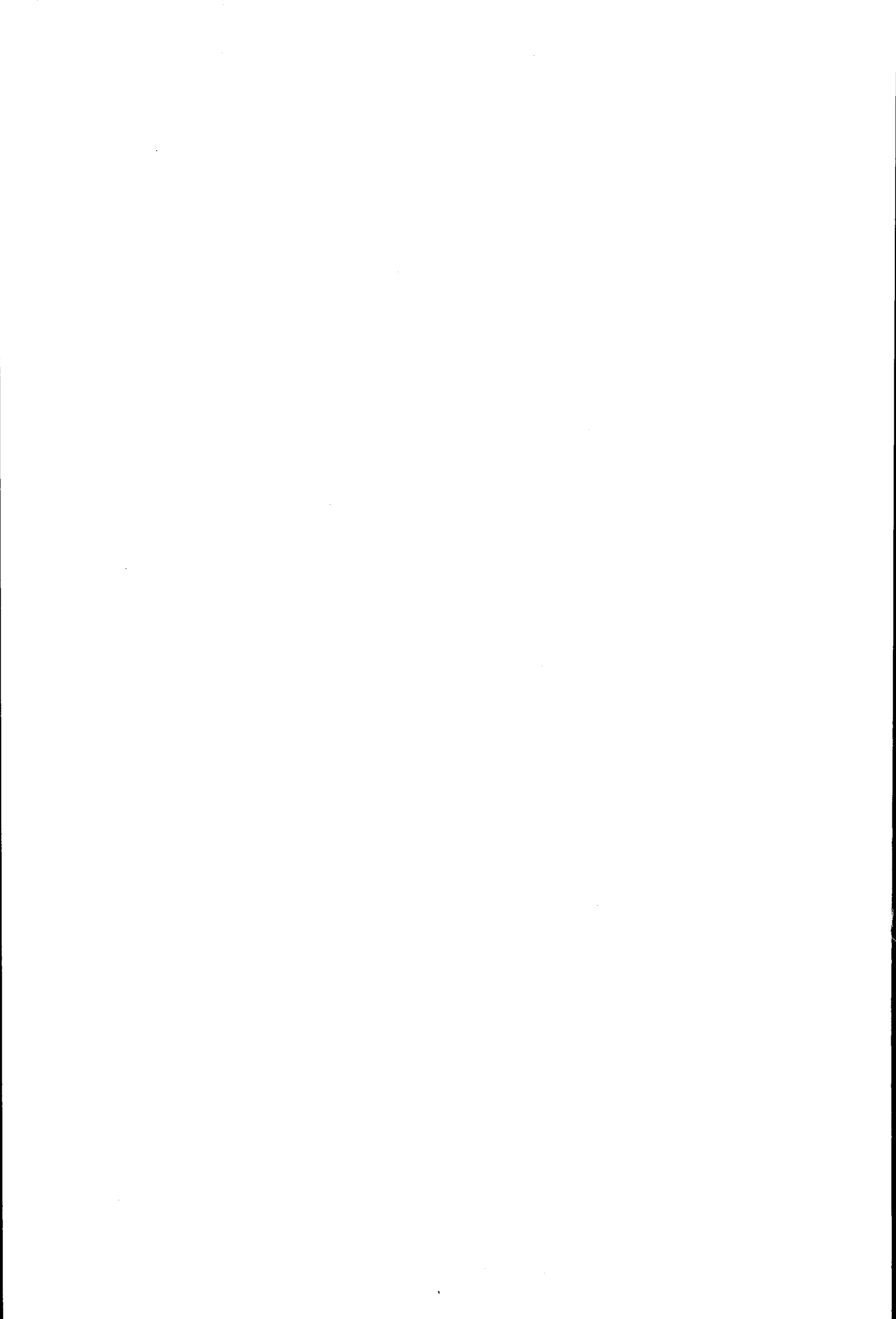
** LABORATORIUM VOOR
ECOTOXICOLOGIE

Vrije Universiteit Brussel
Pleinlaan, 2
B-1050 Brussels, Belgium



Content.

| | |
|-------------------------------|-----------|
| Abstract. | 1 |
| Introduction. | 2 |
| Materials and methods. | 2 |
| Results. | 3 |
| Discussion. | 11 |
| Conclusion. | 14 |
| References. | 15 |



INFLUENCE of PHYSICAL and BIOLOGICAL PROCESSES on the CONCENTRATION of O₂ and CO₂ in the ICE-COVERED WEDDELL SEA in the SPRING of 1988.

(JM. Bouquegneau, WWC. Gieskes, GW. Kraay and AM. Larsson).

Abstract.

In October and November 1988, photosynthetic oxygen production at the ice edge in the northwestern Weddell Sea was far in excess of plankton community respiration; the net oxygen evolution rate that was measured was high enough to explain the oxygen saturation values that were recorded. However in the ice-covered area to the south, respiration dominated - a cause of the low oxygen concentration recorded in that region as important as upwelling of oxygen -poor water. The oxygen production and consumption rates of the plankton were compatible with carbon dioxide concentrations registered at the ice edge underneath the pack-ice: one mole of oxygen for each mole of carbon dioxide, as expected on the basis of the 1 to 1 ratio in the simplest photosynthesis-respiration equations. The relation between photosynthetic oxygen evolution and carbon dioxide consumption on the one hand, and heterotrophic consumption and release on the other, underline the importance of the activity of the microbial ecosystem (phytoplankton and microheterotrophs) in determining the concentration of these gases in both the ice-free and ice-covered Southern Ocean.

ANTAR
II/07
B

Introduction.

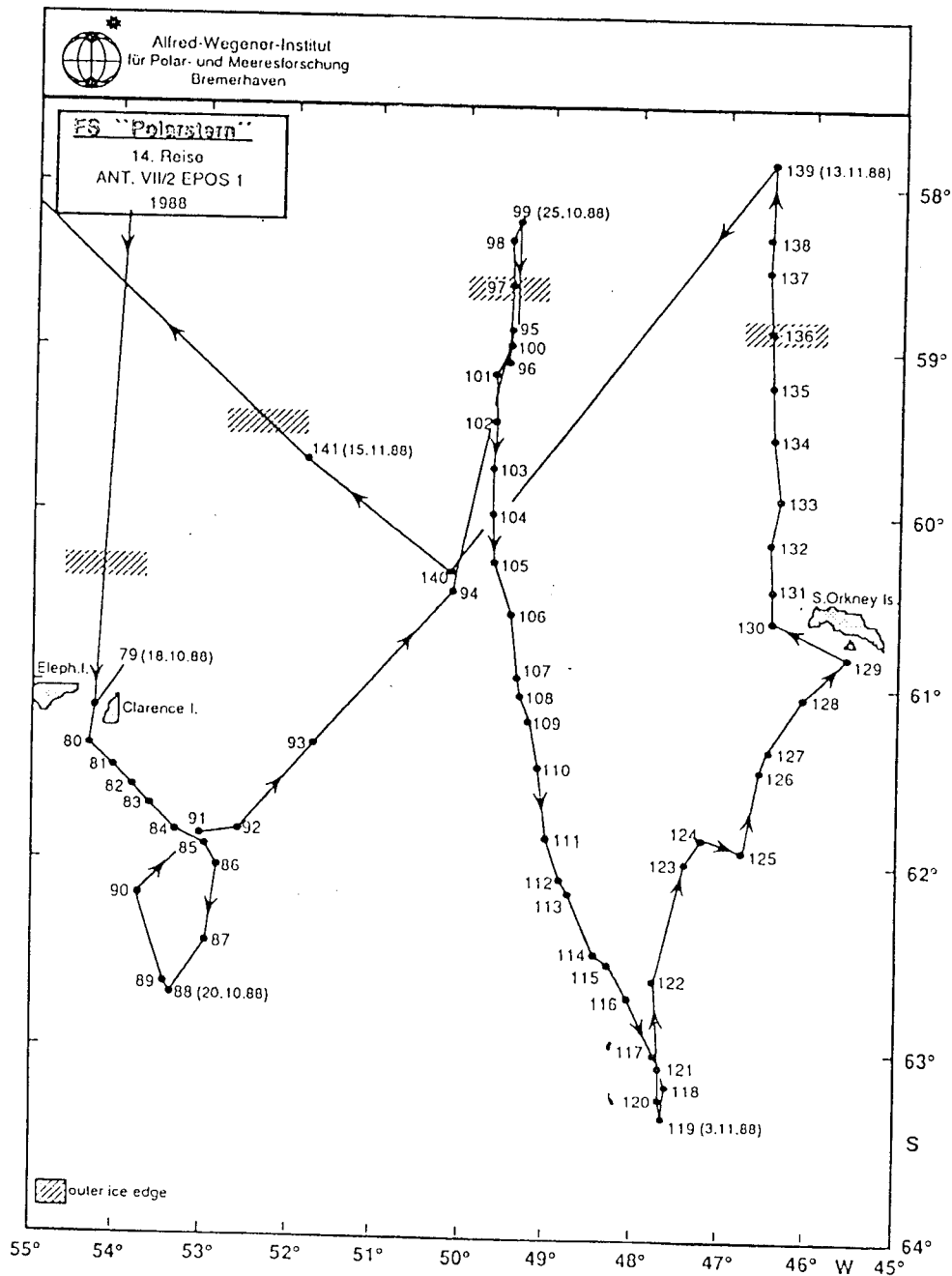
In the ice-covered region of the Southern Ocean around Antarctica, heterotrophic activity of plankton has been found to be significant, both underneath sea ice and under ice shelves (Azam *et al.*, 1979; Lipps *et al.*, 1979; Rivkin and Putt, 1987). Thus, biological activity can be held responsible for the low oxygen saturation values that are normally recorded there. On the other hand, Gordon *et al.* (1984) suggested that physical processes alone, namely upwelling of oxygen-poor warm deep water, may explain the low oxygen saturation values under the ice cover of Southern Ocean seas such as the Weddell Sea. These controversial statements regarding the relative importance of biotic *versus* abiotic factors determining the concentration of oxygen must be reconciled in view of recent interest in the role of the ocean in the recycling of atmospheric gases, including carbon dioxide, the concentration of which is also, just like oxygen, governed both by biological and physical oceanographic processes.

We got the opportunity to investigate the influence of these processes on the concentration of both O₂ and CO₂ in Antarctic waters during a cruise of RV "Polarstern", a ship with ice breaking facilities that can penetrate far into the pack-ice zone. The EPOS 1, leg 1, expedition was planned for October and November 1988. In this period of the year, a phytoplankton bloom should be expected along the marginal ice edge (Jennings *et al.*, 1984; Marra and Boardman, 1984; Smith and Nelson, 1986; Jacques, 1989), while microbial activity in the ice-covered region to the south should be restricted mainly to the underside of the ice (Marra *et al.*, 1982; Grossi *et al.*, 1984; Kottmeier *et al.*, 1985; Garrison *et al.*, 1986). This provides the ideal situation to determine the regional and temporal oxygen and carbon dioxide distribution, both known to be affected by biological processes (photosynthesis and respiration) and physical factors (mixing, temperature, and gas exchange at the air-water interface). It was our purpose to estimate the relative importance of these factors on the O₂ and CO₂ contents of the water in the area, which can be considered a region representative for the whole Southern Ocean.

Materials and Methods.

Figure 1 shows the itinerary of EPOS 1 leg 1, with the position of the outer ice edge. The third section (from station 99 to station 119) and the fourth

Figure 1: Itinerary of EPOS 1. Section III starts from station 99 to 119. Section IV starts from station 119 to 139.



ANTAR
II/07
B

section (from station 119 to station 139) have been investigated for this study.

mouth Winkler bottles and then titrated according to the Winkler method modified by Carritt and Carpenter (1966); in our method, the titration end point is detected photometrically (Tijssen, 1979; Williams and Jenkinson, 1982). The precision was estimated to be $0.013 \text{ ml O}_2 \cdot \text{l}^{-1}$ ($0.58 \mu\text{M}$). Oxygen saturation values were calculated according to the formula of Weiss (1970).

pH was determined with the probe conceived by Distèche (1959, 1962) to be used under pressure. The precision of the measurement is 0.01 pH unit and the stability of the electrochemical cell allows the detection of 0.001 pH unit variations. Calibration of the pH-meter was done by titrating standard phosphate solutions ($\text{Na}_3\text{PO}_4 + \text{NaCl}$ added to reach a salinity of 35.00 psu). Details of the method have been presented by Frankignoulle and Distèche (1984).

Total alkalinity was determined by the Gran titration method (1952). Results are corrected to take into account fluorides and sulfates, as suggested by Hansson and Jagner (1973). The accuracy, established using standard carbonate, is 0.2 %. Total inorganic carbon concentration was calculated as proposed by Millero (1979), using dissociation constants for carbonic and boric acids determined on the N.B.S.-scale (Hansson, 1973; Mehrbach *et al.*, 1973).

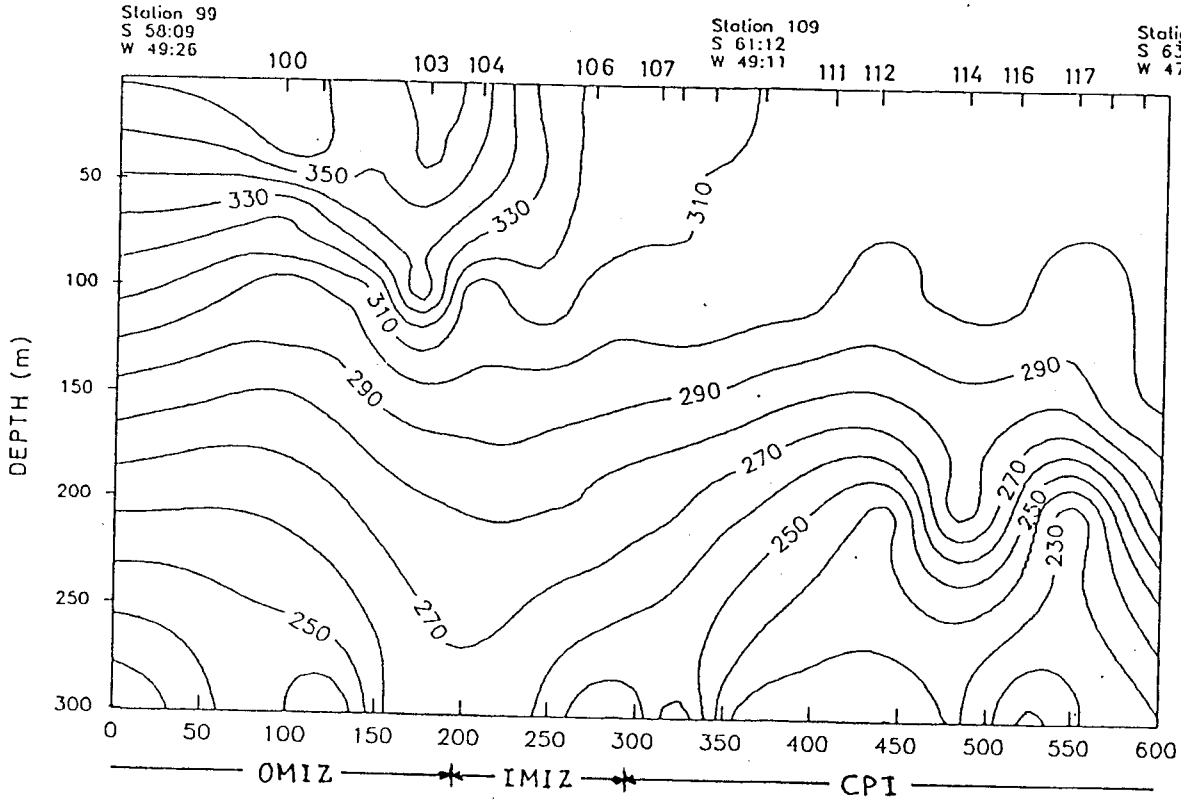
Results.

The oxygen distribution for sections II and IV (see fig. 1) is presented in figure 2. The pattern was similar on both sections, in accordance with the hydrography (see Larsson *et al.*, 1990). In the surface water, the oxygen concentration decreased towards the south from a maximum of $380 \mu\text{M}$ (103 % of full saturation) in the ice-free zone north of the marginal ice edge, to a minimum of $300 \mu\text{M}$ (79 %) in the ice covered area to the south.

In the mixed layer below the sea ice (cf Wakatsuchi, 1982; 1983), the oxygen concentration average was $310 \mu\text{M}$ (82 %). This is about $50 \mu\text{M}$ below full saturation at this temperature. In the marginal ice zone, this mean was $340 \mu\text{M}$ (90 %) and in the open water zone, it was $355 \mu\text{M}$ (95 %). In deeper water below 200 m, oxygen concentration were lower than $270 \mu\text{M}$ (75 %). This was true both in the open water area and in the ice zone. The mean for the water between 200 and 300 m was $250 \mu\text{M}$ (68 %).

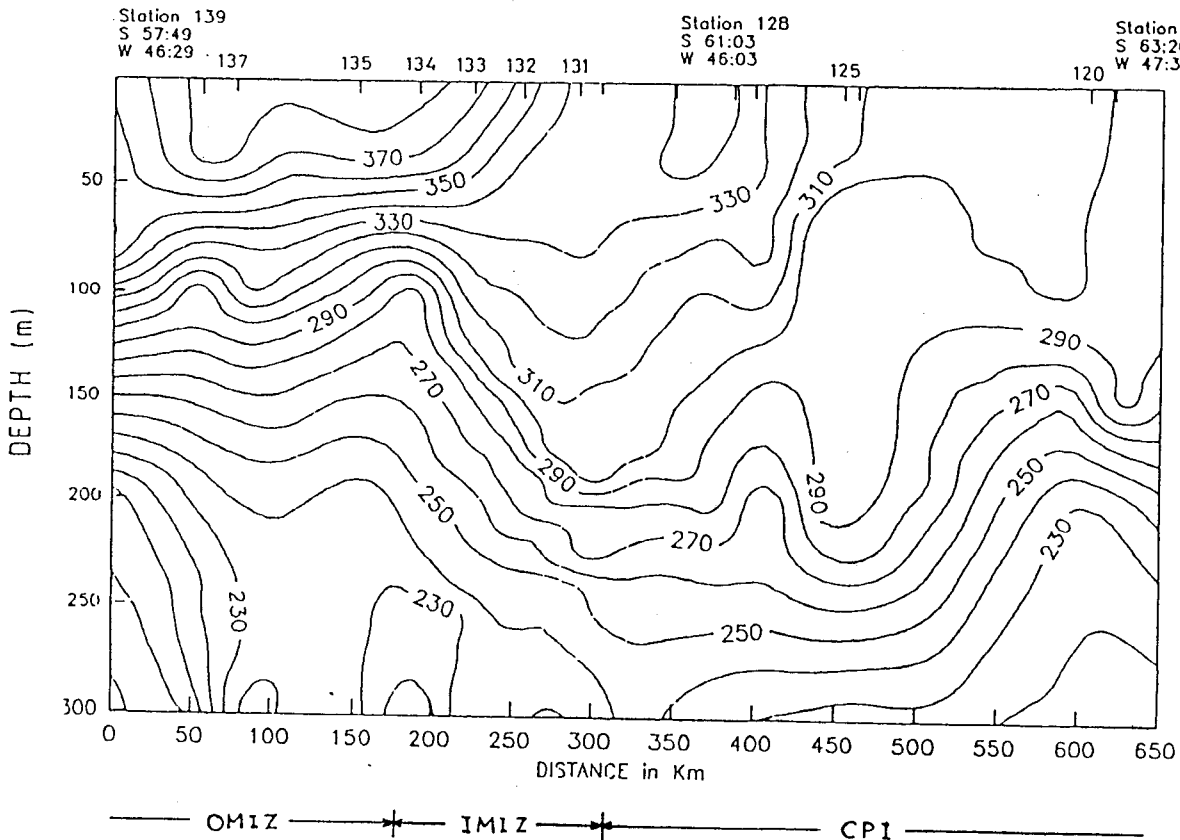
Figure 2: Oxygen diagrams along transects II and IV: $\mu\text{M/l}$. OMIZ = outer marginal ice zone; IMIZ = inner marginal ice zone; CPI = closed pack ice.

SECTION 3 STATIONS 99-119, OXYGEN IN MIKROMOLAR



ANTAR
II/07
B

SECTION 4 STATIONS 139-119, O₂ Mikromolar



The temperature variations (figure 3) show a cold surface layer of -1.8°C under the ice and increasing surface temperatures towards the north, to -0.07°C outside the ice edge. At great depths under the ice, temperature increased to $+0.2^{\circ}\text{C}$ at 300 m. In the outer ice edge zone, the isolines for temperature were almost vertical beneath 150 m, with warm water tongues coming up from deeper layers giving rapid temperature changes from -1.0 to $+0.6^{\circ}\text{C}$.

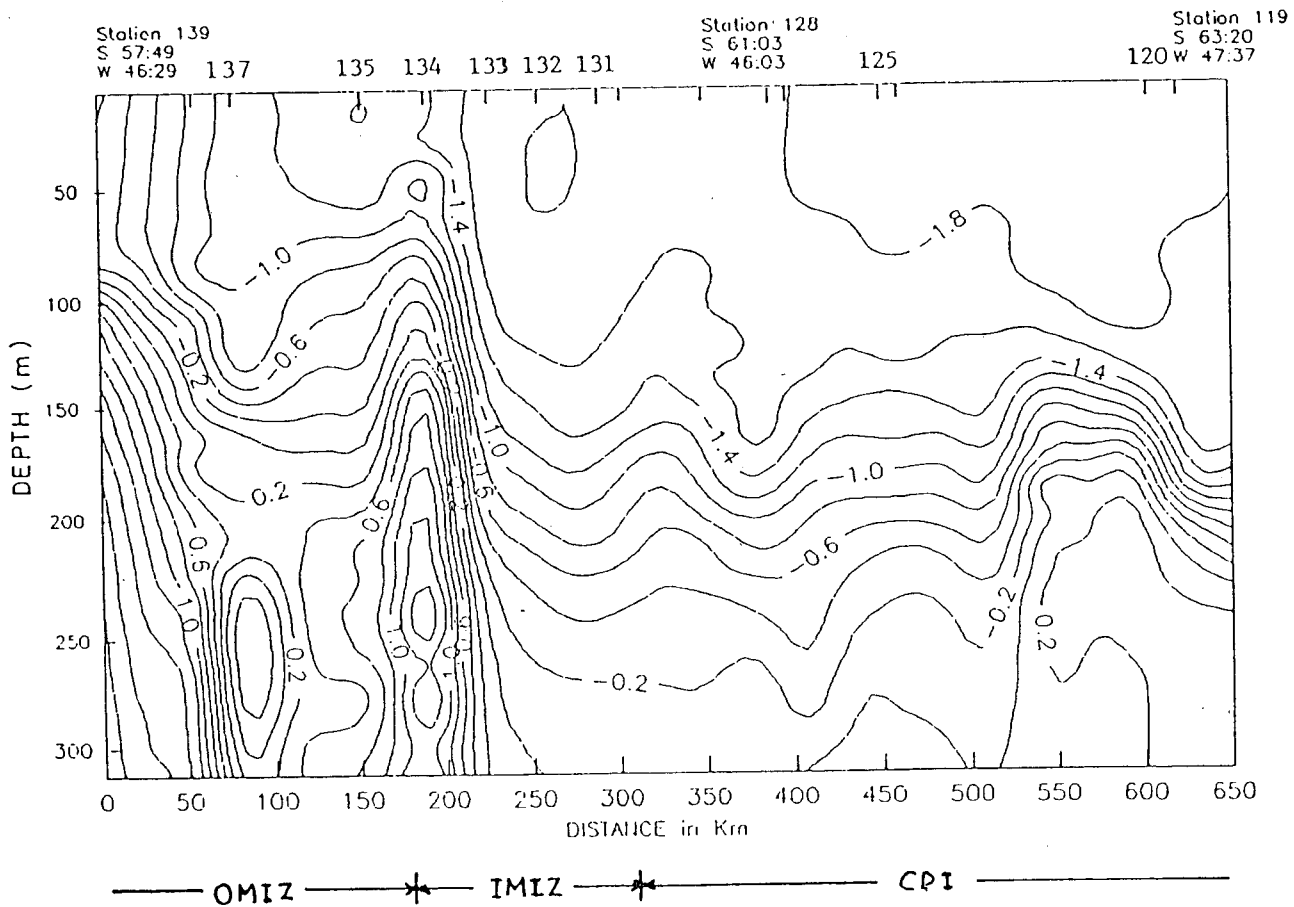


Figure 3: Temperature diagram along transect IV: $^{\circ}\text{C}$.

Figure 4 shows the variations of total alkalinity along section IV. Alkalinity increased with depth. Lowest values were encountered near the surface, at the sea-ice edge. At 60 °S, a vertical more alkaline water tongue nearly reached the surface. Figure 5 shows the variations of pH which, in contrast with alkalinity, decreased with depth at the marginal ice zone (latitude 59 - 60 °S), while it remained rather constant under the pack-ice. However, a clear horizontal gradient of increase can be seen from the south to the north in the surface layer.

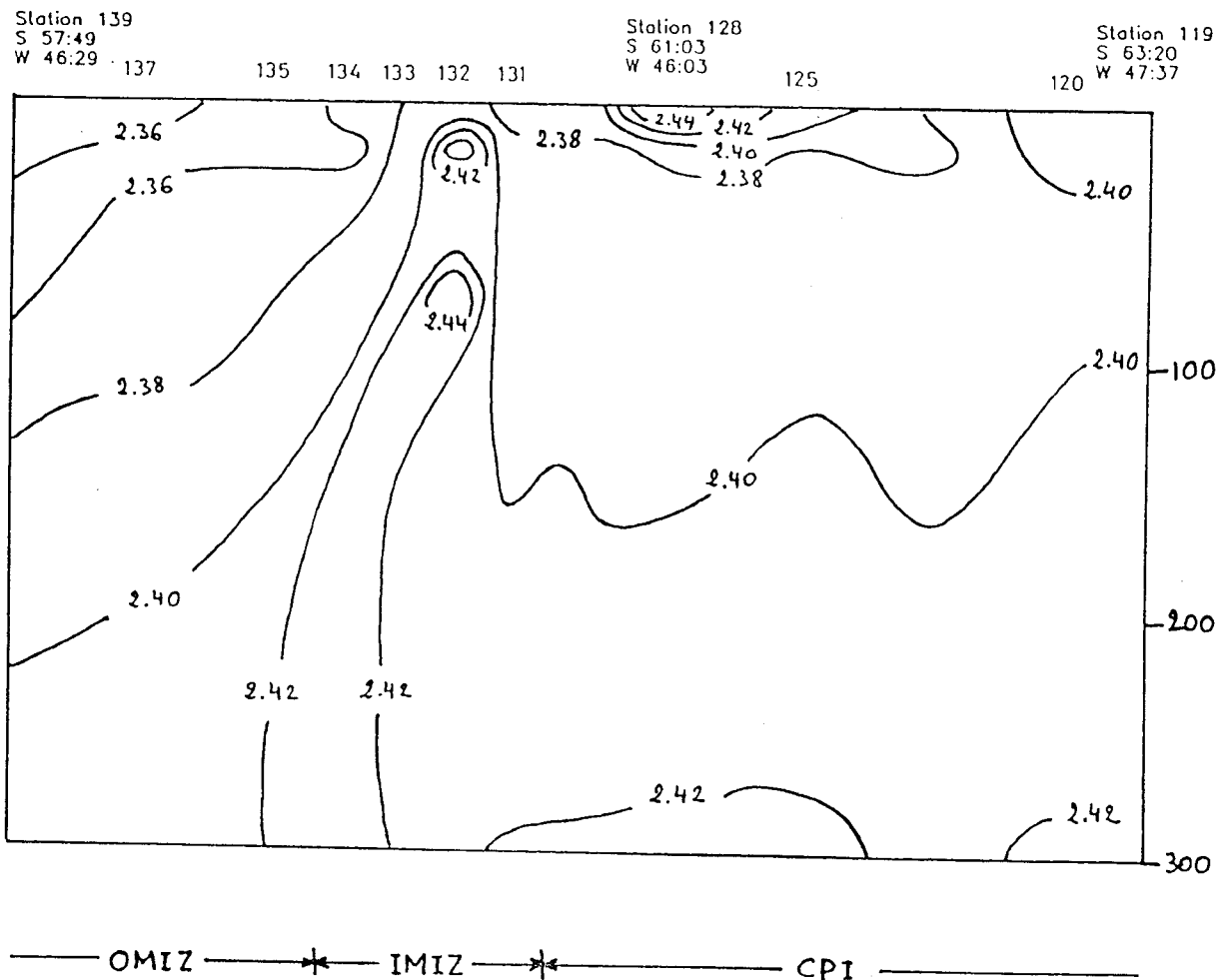


Figure 4: Total alkalinity diagram along transect IV: mEq/l.

Total dissolved inorganic concentrations were calculated from the data presented in figures 4 and 5, and are reported in figure 6. Here again, an important gradient of decrease from the pack-ice zone to the open sea was detected all along the section in the surface layer, but only under the pack-ice in deeper waters (from 100 - 300 m). A vertical gradient was observed at the ice edge and in open sea, but not beneath the pack-ice.

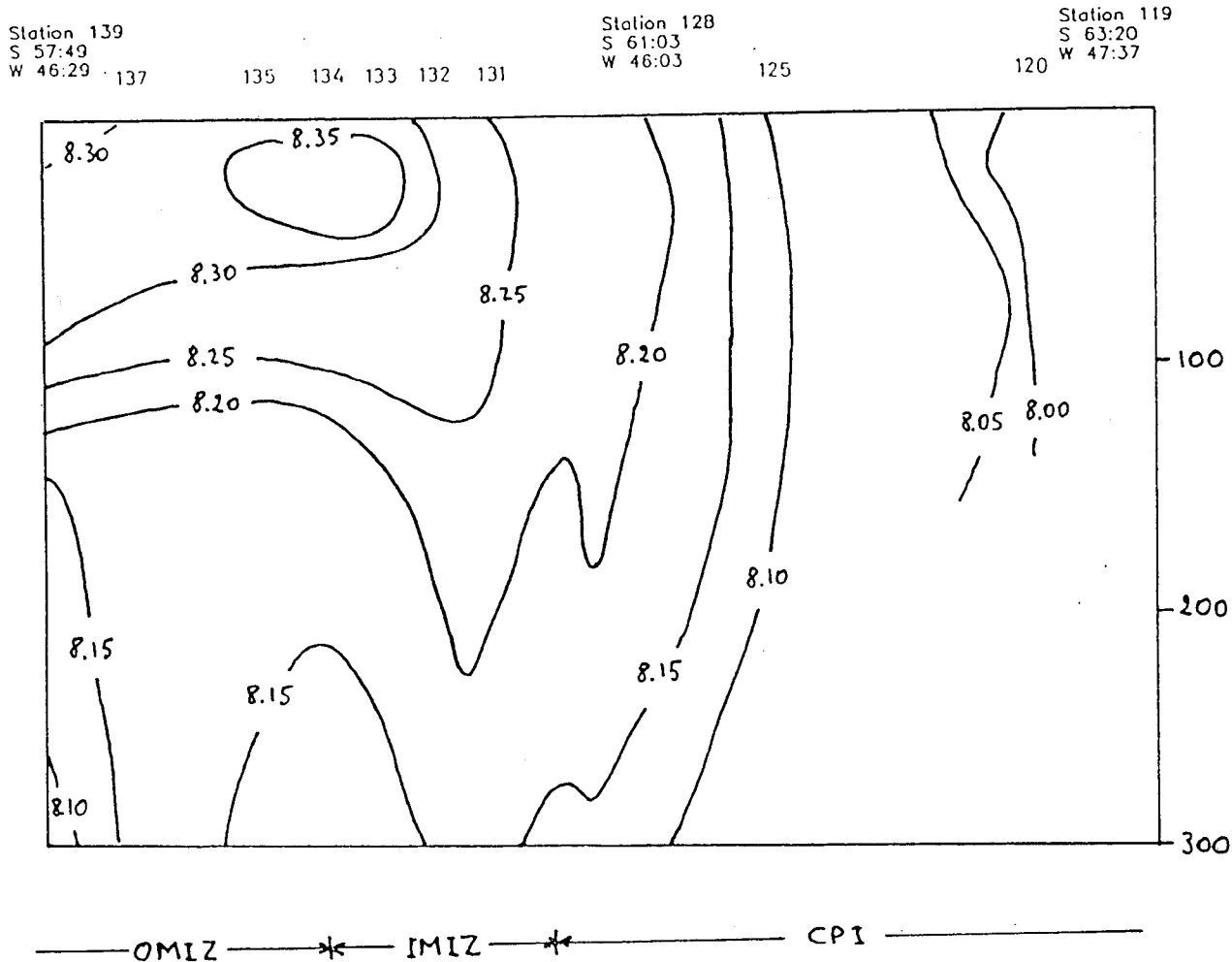


Figure 5: pH diagram along transect IV.

In table 1, we summarize our measurements of oxygen change in the water during incubations in "light" and in "dark" bottles. Net production values result from gross oxygen production (light minus dark values at the end of the incubation) minus respiration (decrease of oxygen during dark incubation). Notice that these net productions merely represent potential primary production at stations in the pack-ice zone: the plankton population living in this region was transferred from the darkness under the ice, where no photosynthesis could possibly take place, to the light in the incubator on board.

Table 1: Primary production and consumption of oxygen measured by the light-and-day bottle method. Values are means of the oxygen produced under incubator irradiances of 860, 380 and 190 $\mu\text{E m}^{-2} \text{s}^{-1}$ during incubations of 8-9 hrs. Chlorophyll values by courtesy of G. Dieckmann and E.M. Nöthig.

| Station | gross prod. $\text{mmol m}^{-3} \text{h}^{-1}$ (light-dark) | net prod. $\text{mmol m}^{-3} \text{h}^{-1}$ (light -initial) | Chl.a mg m^{-3} | respiration $\text{mmol m}^{-3} (24\text{h})^{-1}$ | oxygen & satu -ration |
|---------|---|--|-----------------------------|---|-----------------------------|
| 100 a | 0.243 | 0.195 | 0.59 | 1.15 | 95 |
| 104 | 0.148 | 0.123 | 0.17 | 0.55 | 94 |
| 113 | 0.040 | 0.038 | 0.14 | 0.14 | 81 |
| 117 | 0.054 | 0.045 | 0.05 | 0.05 | 81 |
| 112 | 0.038 | 0.013 | 0.07 | 0.61 | 80 |
| 115 | 0.066 | 0.060 | 0.08 | 0.08 | 80 |
| 124 | 0.065 | 0.052 | 0.16 | 0.30 | 79 |
| 126 | 0.050 | 0.050 | 0.17 | 0.00 | 87 |
| 131 | 0.042 | 0.042 | 0.06 | 0.00 | 88 |
| 135 | 0.602 | 0.472 | 1.60 | 3.12 | 102 |
| 136 | 0.548 | 0.488 | 1.80 | 1.44 | 101 |
| 137 | 0.537 | 0.403 | 2.00 | 4.08 | 99 |
| 139 | 0.353 | 0.328 | 0.90 | 0.60 | 99 |
| 140 | 0.044 | 0.009 | 0.27 | 0.84 | 86 |

ANTAR
II/07
B

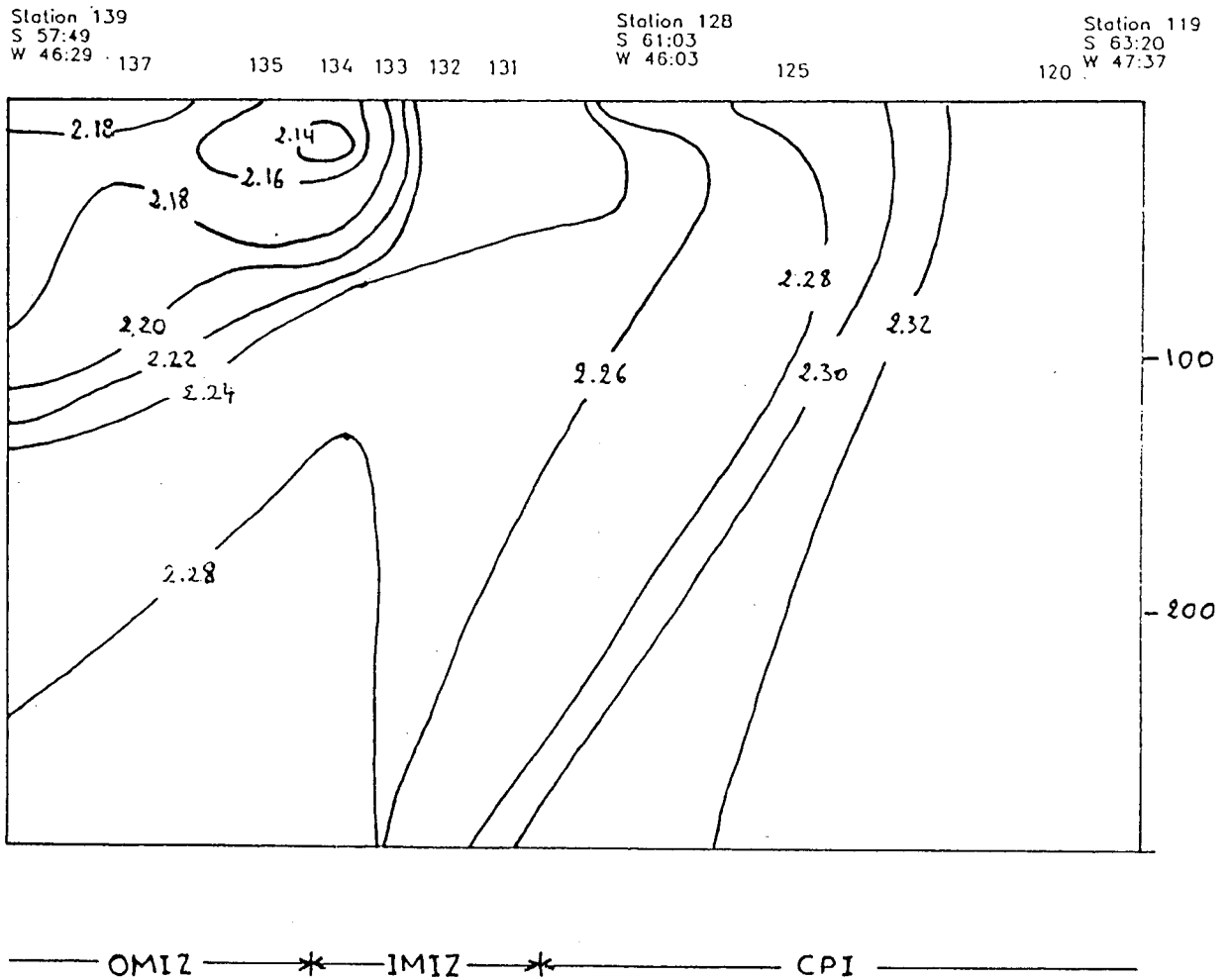


Figure 6: Total dissolved inorganic carbon diagram along transect IV: mmol/l.

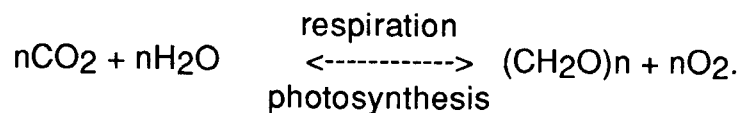
It can be seen (Table 1) that in most of the area, primary production was extremely low. We were unable to determine significant diurnal variations of CO_2 or O_2 in the water because of this low activity, and most probably also due to water mass variability. However, the precision of our highly sensitive oxygen measurement technique was so great that in spite of low values, we were able to find a significant correlation between the amount of carbon fixed (^{14}C method; data by courtesy of M. Tilzer and R. Heusel) and the photosynthetic oxygen increase during incubations. Mean (potential) phytoplankton production at all stations with sea-ice cover was only $0.06 \text{ mmol O}_2 \text{ m}^{-3} \text{ h}^{-1}$. At the northern open water stations, net oxygen production was much higher (up to $0.49 \text{ mmol O}_2 \text{ m}^{-3} \text{ h}^{-1}$), in line with the much higher Chl a values in this area: $0.5 \mu\text{g}$ per liter, versus less than 0.05 in the water underneath the ice in the survey region of 61°S (see Larsson *et al.*, 1990).

Respiration (initial oxygen concentration in the bottles minus the dark bottle value at the end of incubation) was low everywhere (Table 1). Assuming that the respiration rate remains equal throughout the day and the night, we can extrapolate respiration rates during the incubation period to respiration during 24 hrs. The mean value of respiration was $0.29 \text{ mmol O}_2 \cdot \text{m}^{-3} \cdot (24 \text{ hrs})^{-1}$ at all stations in the sea-ice zone and $2.3 \text{ mmol O}_2 \cdot \text{m}^{-3} \cdot (24 \text{ hrs})^{-1}$ in the bloom area just north of the ice edge. Notice that as much as 90 % of the whole survey area was covered by ice and snow. Therefore, only 10 % of the oxygen evolution (assuming a day length of 14 hours: $14 \text{ times } 0.063 \text{ mmol} \cdot \text{m}^{-3} \cdot \text{h}^{-1} = 0.882 \text{ mmol O}_2 \cdot \text{m}^{-3} \cdot \text{d}^{-1}$) in the ice-covered zone was actually released, i.e. 10 % of $0.882 = 0.09 \text{ mmol} \cdot \text{m}^{-3} \cdot \text{d}^{-1}$. This is much less than the respiration (oxygen consumption in the bottles) that we registered: $0.29 \text{ mmol O}_2 \cdot \text{m}^{-3} \cdot (24 \text{ hrs})^{-1}$.

Discussion.

The considerable O_2 and pH variation from north to south cannot simply be related to temperature and salinity effects. In the case of pH, the variation was 0.35 pH unit, while the maximal temperature variation of only $2 \text{ }^\circ\text{C}$, detected along the same transect, would only account for a 0.025 pH unit variation. When considering oxygen, similar conclusions can be drawn: at 100 % saturation, the differences between maximal and minimal O_2 concentrations would be $20 \text{ mmol} \cdot \text{m}^{-3}$, while the observed variation reached $180 \text{ mmol} \cdot \text{m}^{-3}$.

To estimate the relative importance of biological and physical processes, the effects of photosynthesis and respiration have to be compared with transport of O_2 and CO_2 by turbulent movements and by intrusion from the atmosphere. If biological activity (photosynthesis and heterotrophic respiration in the pelagic system) alone is responsible for O_2 and CO_2 variations, we would expect a ratio of about 1 between oxygen and carbon dioxide when



In figure 7, we present the relation between both concentrations along the whole section. From this figure, we can calculate a ratio O_2/CO_2 (molar) of 0.5 at the ice-covered stations, indicating that not only heterotrophic processes cause the lowering of oxygen concentrations and increase of the CO_2 concentrations. In the algal bloom to the north, in the marginal ice edge

zone, the ratio was nearly 1:1 (082), which implies that in that region, biological activity dominated all processes that determine O_2 and CO_2 concentrations.

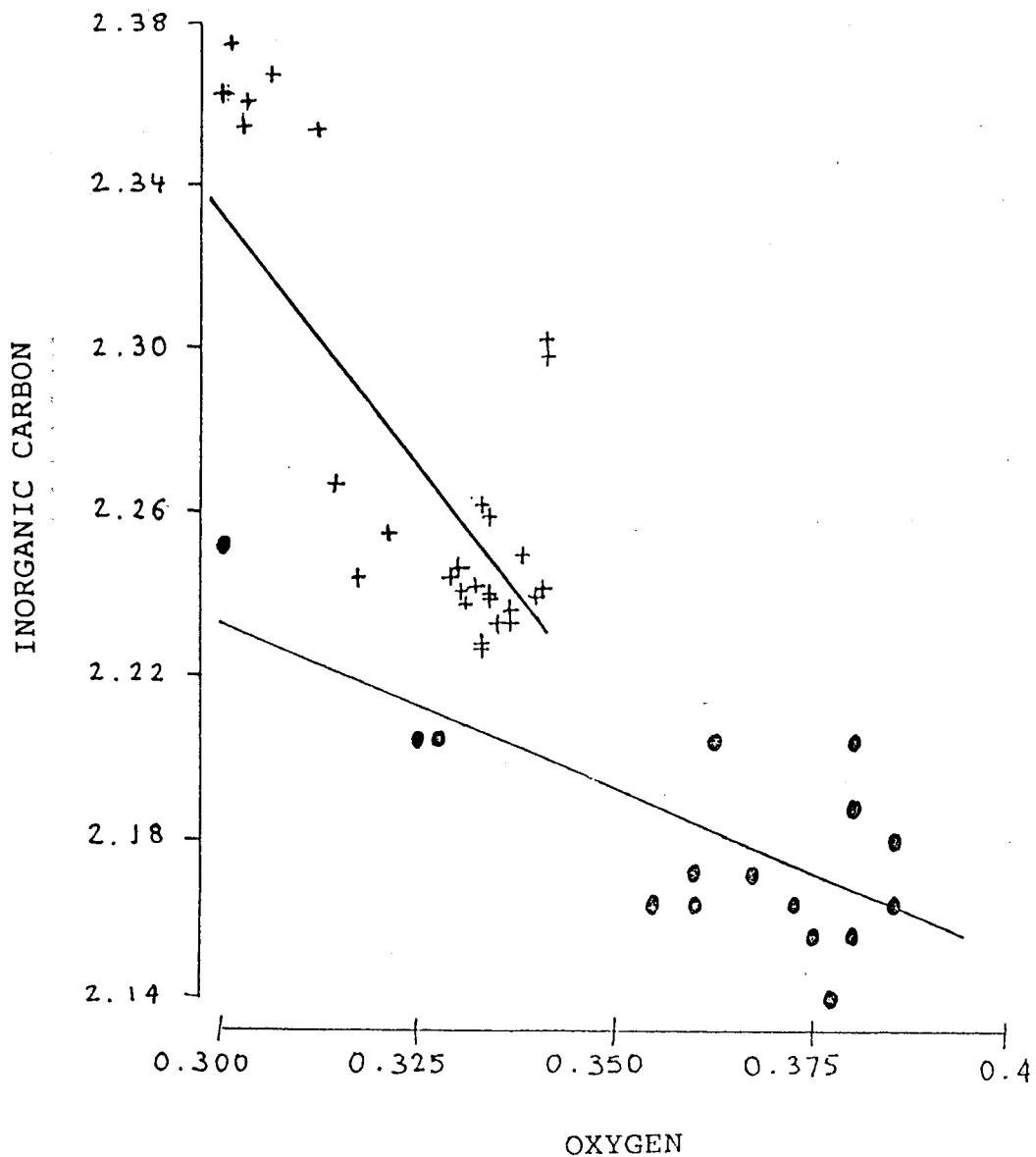


Figure 7: Linear regression between CO_2 and O_2 concentrations (mmol/l) in the water between the surface and 80 m depth.

+ : pack ice (stations 120 - 132) $n = 28$, slope : -2.25, $r = -0.706$
 o : ice edge bloom (stations 134 - 139) $n = 16$, slope : -0.82, $r = -0.736$

If respiration only would account for the relatively low oxygen concentrations under the ice, we can easily calculate how long it would take to go from 100 % O₂ saturation values to the 80 % registered underneath the ice cover. In this southern region, mean heterotrophic consumption of oxygen in the "dark" bottles that were incubated was 0.29 mmol.m⁻³.(24 hrs)⁻¹. This means that no less than 6 months of respiration would be required to reach the 80 % saturation value. Before we took our samples, the residence time of the water in darkness (under the ice, in the austral winter) may have been 6 months, but as we have argued above, the 0.5 ratio between O₂ and CO₂ concentrations under the ice (south of 61 °S) suggests that other phenomena than biological activity alone are of equal importance to account for the observed variations in O₂ and CO₂. It is well known that upwelling occurs in this zone (see e.g. Gordon and Huber, 1984; Gordon, 1988). This kind of upwelling is also visible in our figures 3 and 4. In fact, alkalinity (Fig 4) which in this case, can be considered as independent of biological activity and CO₂ air-water exchanges (see e.g. Frankignoulle and Bouquegneau, 1990), can be used as an indicator of water mass movements. In the ice-covered area, upwellings of deep warm water should in fact bring at the surface layer oxygen poor water.

The effect of this upwelling can be estimated in a T vs O₂- diagram (Figure 8). As well as in a TS- diagram, all possible combinations between Warm Deep Water and Surface Water lie along the strait mixing line between the water masses (e.g. Weiss, 1979). However, due to consumption during the mixing processes, this line was curved in ice-covered areas. The curvature indicates that the magnitude of the consumption was 20-30 mmol O₂.m⁻³.

On the other hand, in the marginal ice zone, where a phytoplankton bloom was found, we can calculate that the oxygen saturation encountered could be reached within a week by photosynthetic oxygen production alone. The primary production here was up to 0.49 mmol O₂.m⁻³.h⁻¹, or about 7 mmol.m⁻³.day⁻¹ (10 hours); minus respiration (which goes on for 24 hours), this is a net production of 4 mmol. From 80 to 100 % saturation is 68 mmol.m⁻³, so it would last 2 weeks to reach the saturation values that were registered (slightly above 100 %) purely on the basis of the phytoplankton's photosynthetic activity. Under windy conditions, exchange with the air may be around 30 mmol O₂. m⁻².(24 hours)⁻¹, i.e. over a 60 m depth range, 0.5 mmol O₂.m⁻³.d⁻¹. Apparently, primary production was far higher (roughly 10 times) than oxygen exchange with the air. This also supports the idea of the

preponderance of biological activity in determining the oxygen concentration in the surface layer of the marginal ice edge zone.

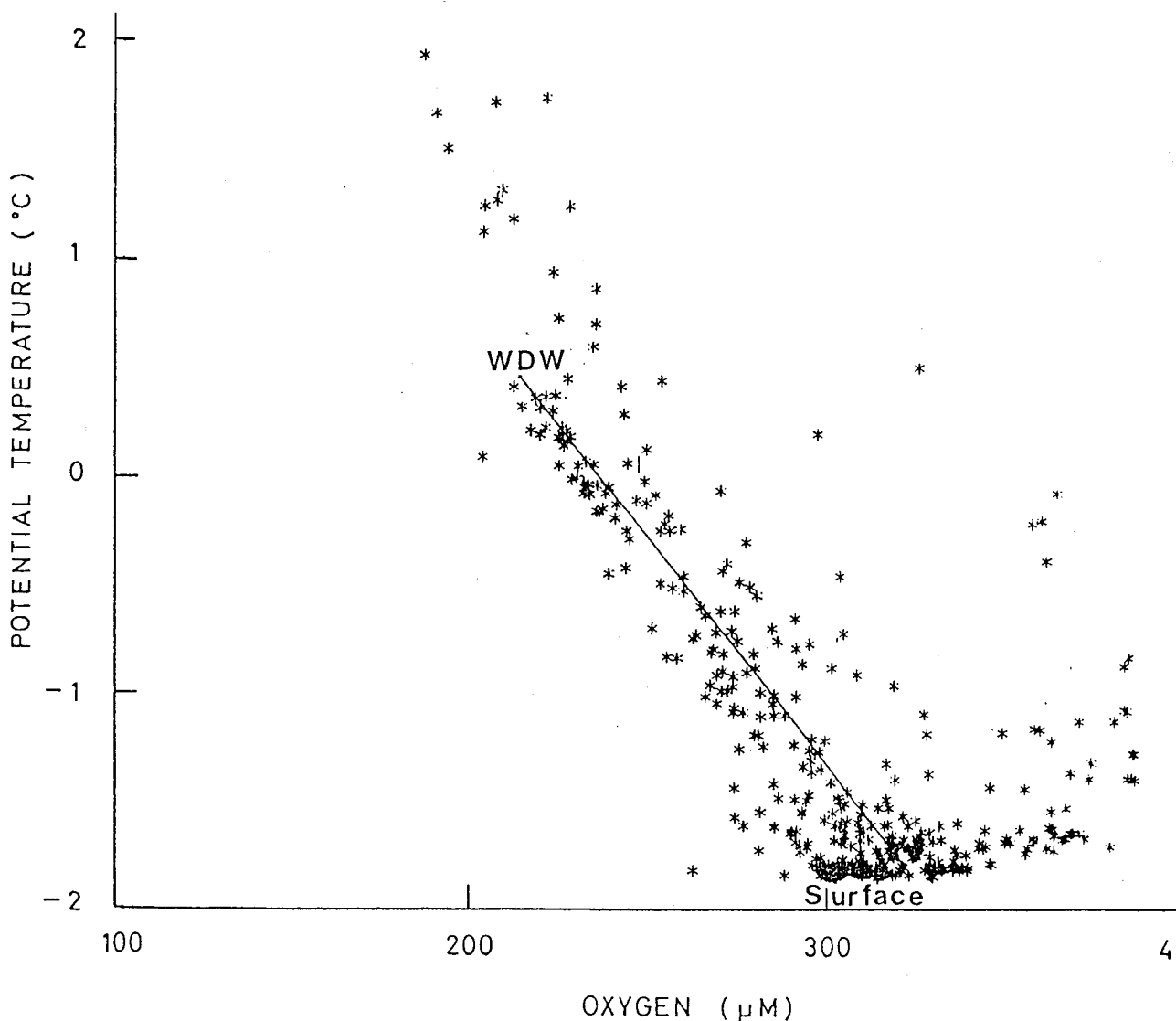


Figure 8: Potential temperature - oxygen for transects II and IV. A straight line representing the sub-surface mixing between Warm Deep Water and Surface Water has been fitted to the points.

Conclusion.

We conclude that in the ice-covered region of the survey area, biological activity may be as important as physical processes in determining the concentration of O_2 and CO_2 that we observed there. In the northern part of the surveyed region, however, at the marginal ice edge and just north of it, photosynthetic activity was the most important factor controlling O_2 and CO_2 levels recorded there.

References.

- Azam, F., JR. Beers, L. Campbell, AF. Carlucci, O. Holm-Homson, FMH. Reid and DM.Karl. 1979. Occurrence and metabolic activity of organisms under the Ross Ice Shelf, Antarctica, at station J9. *Science*, 203: 451-453.
- Carit, DE. and JH. Carpenter. 1966. Comparison and evaluation of currently employed modifications of the Winkler method for determining dissolved oxygen in sea water. NASCO report. *J. mar. Res.*, 24: 286-318.
- Distèche, A. 1959. pH measurements with a glass electrode withstanding 1500 kg/cm² hydrostratic pressure. *Rev. Sci. Instr.*, 30: 474-478.
- Distèche, A. 1962. Electrochemical measurements with a glass electrode at high pressure. *J. Electrochem. Soc.*, 109: 1084-1092.
- Frankignoulle, M. and JM. Bouquegneau. 1990. Upwelling characterization in Calvi Bay by means of the total alkalinity. *Bull. Soc. roy. Sc. Lg.*, 59: 89-96.
- Frankignoulle, M. and A. Distèche. 1984. CO₂ chemistry in the water column above a *Posidonia oceanica* seagrass bed and related air-sea exchanges. *Oceanol. Acta*, 7: 209-217.
- Garrison, DL., CW. Sullivan and SW. Ackley. 1986. Sea ice microbial community studies in the Antarctic. *BioSci.*, 36: 243-250.
- Gordon, AL. 1988. The Soutern Ocean and global climate. *Océanis*, 31: 39-46.
- Gordon, AL., CTA. Chen and WG. Metcalf. 1984. Winter mixed layer entrainment of Weddell deep water. *J. Geophys. Res.*, 89: 637-640.
- Gordon, AL. and BA. Huber. 1984. Thermohaline stratification below the Southern Ocean sea ice. *J. Geophys. Res.*, 89: 641-648.
- Gran, G. 1952. Determination of the equivalence point in potentiometric titrations. Part II. *Int. Congress of Anal. Chem.*, 77: 661-671.
- Grossi, SM., ST. Kottmeier and CW. Sullivan. 1984. Sea ice microbial communities. III. Seasonal abundance of microalgae and associated bacteria, Mc Murdo Sound, Antarctica. *Microb. Ecol.*, 10: 231-242.
- Hansson, I. 1973. A new set of pH scales and standard buffers for seawater. *Deep Sea Res.*, 25: 140-147.
- Hansson, I. and D. Jagner. 1973. Evaluation of the accuracy of Gran plots by means of computer calcualtions. *Anal. et Chim. Acta*, 65: 363-373.
- Jacques, G. 1989. Primary production in the open Antarctic Ocean during the austral summer. A review. *Vie & Milieu*, 39: 1-17.

- Jennings, JC., LI. Gordon and DM. Nelson. 1984. Nutrient depletion indicates high primary productivity in the Weddell Sea. *Nature*, 309: 51-54.
- Kottmeier, ST., MA. Miller, MP. Lizoffe, LL. Craft, B. Gulliksen and CW. Sullivan. 1985. Ecology of sea ice microbial communities (SIMCO) during the 1984 winter to summer transition in Mc Murdo Sound, Antarctica. *Antarct. J. U.S.*, 20: 128-130.
- Larsson, AM., PI. Sehlstedt, F. Bianchi, F. Cioce, G. Socal, EM. Nöthig, G. Dieckmann and JM. Bouquegneau. 1990. Hydrographical, chemical and biological observations during the European Polarstern Study - EPOS, leg 1 - 11 october to 19 November 1988 with RV Polarstern. A-M. Larsson, ed. Dpt of Oceanography, University of Gothenburg, Sweden.
- Lipps, JR. TE. Rona and TE. Deaca. 1979. Life below the Ross Ice Shelf, Antarctica. *Science*, 203: 447-449.
- Marra, J., LH. Brckle and HW. Docklow. 1982. Sea ice and water column plankton distributions in the Weddell Sea in late winter. *Antarc. J. US.*, 17: 111-112.
- Marra, J. and DC. Bardman. 1984. Late winter chlorophyll a distribution in the Weddell Sea. *Mar. Ecol. Prog. Ser.*, 19: 197-205.
- Mehrback, C., CH. Culberson, JE. Hawley and RM. Pytkowicz. 1973. Measurements of the apparent dissociation constants of carbonic acid in seawater at atmospheric pressure. *Limnol. Oceano.*, 18: 897-907.
- Millero, FJ. 1979. The thermodynamics of the carbonate system in seawater. *Geochim. Cosmochim. Acta*, 43: 1651-1661.
- Rivkin, RB. and M. Putt. 1987. Heterotrophy and photoheterotrophy by Antarctic microalgae: light- dependent incorporation of amino acids and glucose. *J. Phycol.*, 23: 442-452.
- Smith, WO. and DM. Nelson. 1986. Importance of ice-edge phytoplankton production in the Southern Ocean. *BioSci.*, 36: 25-257.
- Tijssen, SB. 1979. Diurnal oxygen rhythm and primary production in the mixed layer of the Atlantic Ocean at 20 °N. *Neth. J. Sea Res.*, 13: 79-84.
- Wakatsuchi, M. 1983. Brine exclusion process from growing sea ice. *Contr. Inst. Low Temp. Sci.*, A33:29-65.
- Wakatsuchi, M. 1982. Seasonal variations in water structure and fast ice near Syowa Station, Antarctica, in 1976. *Antarc. Rec.*, 74: 85-108.
- Weiss, RF. 1970. The solubility of nitrogen, oxygen and argon in water and sea water. *Deep-Sea Res.*, 17: 721-735.

Weiss, RF. HG. Ostlund and H. Craig. 1979. Geochemical studies in the Weddell Sea. *Deep-Sea Res.*, 26A: 1093-1120.

Williams PJ. LeB. and NW Jenkinson. 1982. A transportable microprocessor-controlled precise Winkler titration suitable for field station and shipboard use. *Limnol. Oceanol.*, 27: 576-584.

ANTAR
II/07
B



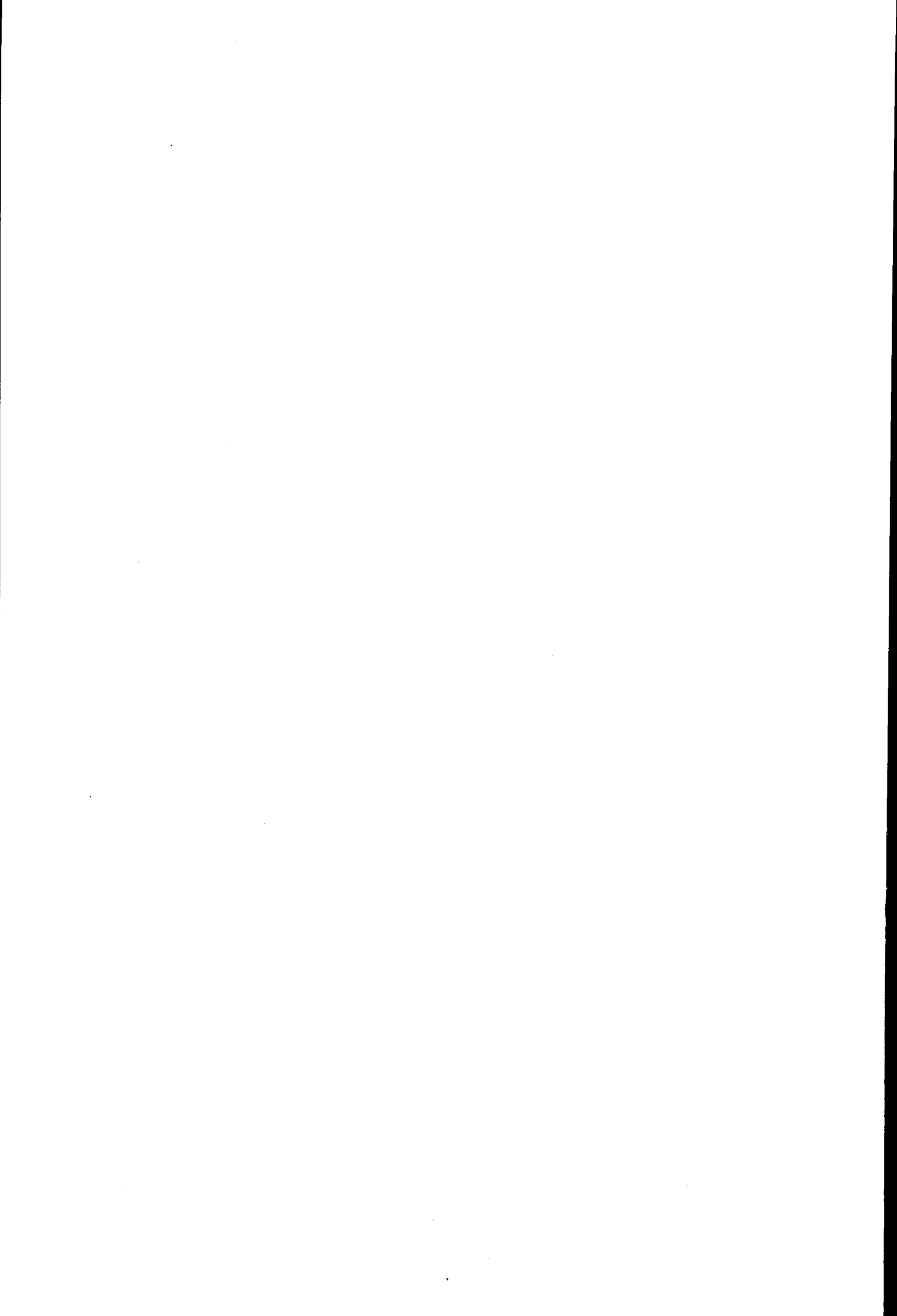
RESEARCH CONTRACT ANTAR/II/06

**BIOCHEMISTRY
AND ECODYNAMICS
OF ZOOPLANKTON
OF THE
SOUTHERN OCEAN**

A. Goffart and J.-H. Hecq

UNITÉ D'ECOHYDRODYNAMIQUE

Université de Liège
Institut de Physique B5
B-4000 Liège Sart Tilman, Belgium



CONTENTS

| | |
|--|----|
| ABSTRACT..... | 1 |
| 1. INTRODUCTION..... | 3 |
| 2. WEDDELL SEA..... | 4 |
| 2.1 EPOS leg 1 cruise: general objectives and work at sea..... | 4 |
| 2.2 Materials and methods..... | 5 |
| 2.3 Hydrodynamical context..... | 5 |
| 2.4 Results..... | 6 |
| 2.4.1 Hydrological characteristics and sea ice conditions..... | 6 |
| a. Horizontal pattern of water masses..... | 6 |
| b. Vertical structure of water column..... | 7 |
| 2.4.2 Latitudinal distribution of nutrients and phytoplankton..... | 8 |
| a. Horizontal distribution..... | 8 |
| b. Vertical distribution..... | 8 |
| 2.4.3 Latitudinal distribution of zooplankton..... | 12 |
| 2.4.4 Lipid contents and fatty acids composition of zooplankton..... | 12 |
| 2.4.5 Discussion..... | 15 |
| 3. ROSS SEA..... | 20 |
| 3.1 Vth ITALIANTARTIDE expedition: general objectives and work at sea..... | 20 |
| 3.2 Materials and methods..... | 21 |
| 3.3 General hydrology..... | 22 |
| 3.4 Results..... | 22 |
| 3.4.1 Sea ice conditions..... | 22 |
| 3.4.2 Hydrological characteristics..... | 22 |
| a. Latitudinal transect (stations 2 to 19)..... | 22 |
| b. Ross Sea continental slope section (stations 13 to 16)..... | 25 |
| c. Offshore - inshore transect at 75°S (stations 19 to 25)..... | 26 |
| 3.4.3 Distribution of nutrients..... | 28 |
| a. Latitudinal section (stations 2 to 19)..... | 28 |
| b. Ross Sea continental slope section (stations 13 to 16)..... | 28 |
| c. Offshore - inshore transect at 75°S (stations 19 to 25)..... | 31 |
| 3.4.4 Surface distribution of phytoplankton..... | 31 |
| 3.4.5 HPLC characterization of phytoplankton..... | 33 |
| 3.4.6 Fatty acids composition of phytoplankton..... | 35 |

| | |
|---|----|
| 3.4.7 Zooplankton distribution..... | 40 |
| a. Area of the Antarctic Convergence | 40 |
| b. Ross Sea continental slope section (stations 13 to 16) | 40 |
| 3.4.8 General distribution of Krill | 43 |
| 3.4.9 Discussion | 45 |
| | |
| 4. GENERAL CONCLUSIONS..... | 48 |
| | |
| 5. ACKNOWLEDGEMENTS..... | 50 |
| | |
| 6. BIBLIOGRAPHY..... | 51 |

ABSTRACT

The goal of the study was to determine how the distribution and biochemical speciation of planktonic production is controlled by abiotic parameters of the environment, like ice-melting, pack-ice retreat, vertical stratification and various mesoscale frontal system.

The factors affecting planktonic spring blooms at the level of the ice edge and of the adjacent open waters were particularly emphasized, both in the Weddell Sea and in the Ross Sea. Lipids and liposoluble pigments of plankton and krill have been especially used as biotracers.

The interpretation of the whole set of data collected during EPOS leg 1 in the Weddell Sea showed that in early spring (October-November 1988), the vertical stratification and horizontal distribution of water masses control the main development of phytoplankton blooms, restricted to the ice edge. However, the paucity of zooplankton abundance and its minimal lipid content, probably due to the overwintering and complete exhaustion of lipid reserves, contradicted the idea of general lipid richness in Antarctic zooplankton.

Observations on samples performed from November 1989 to February 1990 during the Vth ITALIANTARTIDE expedition in the Pacific sector of the Southern Ocean and in the Ross Sea confirmed that the most important factors regulating the Antarctic pelagic food chain are physical processes operating within the circumpolar marginal ice zone during the ice melting period. In the southern Ross Sea, during the spring, the waters diluted by the melting of the Ross ice shelf develop an extensive diatom bloom, characterized by very high chlorophyll levels, reaching maximum values of 187.64 mg/m² when integrated from the surface to 150 meters. Because nutrients depletion indicates a long and intense period of production, such blooms might be expected to contribute substantially to the global productivity of the Ross Sea. As a typical characteristic of the Ross Sea, the ice free surface is propagating from South to North, with an increase of the water surface exposed to the sunlight. The diversity of water column characteristics seems due to specific local constraints more than to diversity of ecosystems.

The most original results obtained during these cruises are that fatty acids composition and liposoluble pigments of phytoplankton detected by HPLC seem to depend essentially on the time after the waters become ice free. Moreover, phaeophorbids and ammonia concentrations in the water column, which are reliable tracers of zooplankton activity, follow a similar distribution pattern as that of zooplankton nutritional activity. In addition, the vertical distribution of zooplankton and krill influence highly the

distribution of all planktonic organic material in the water column and the recycling mechanisms, occurring in euphotic zone or in the deeper layers.

1. INTRODUCTION

Previous studies driven at macroscale in the Indian sector of the Southern Ocean (Goffart and Hecq, 1989) have confirmed the idea that the most important factors regulating the Antarctic pelagic food chain are hydrodynamical processes which strongly influence the distribution and productivity of planktonic organisms.

Between the Subtropical Convergence and the Antarctic Divergence, the spatial structure of high chlorophyll *a* concentrations is bound up with the main frontal systems having the characteristics of a convergence and, in the Antarctic Surface Water, with the areas of increased stability (Goffart and Hecq, 1989). Moreover, it seems that in summer, the stabilization of the upper layers of the water column due to the retreat of the constantly melting ice-edge may induce successive phytoplanktonic and zooplanktonic blooms, from North to South. A patchy distribution of the different trophic levels is observed, with, northwards, old zooplanktonic populations and southwards, young phytoplankton. In these conditions, zooplankton communities, exposed to an environment with sharp peaks in the food available and long period of diet, respond by marked propensity to convert food into lipid stores (Hecq *et al.*, 1981; Hagen 1988; Falk-Petersen, 1990).

As a consequence, an accurate knowledge of the physical processes controlling the primary productivity and the ecodynamics of zooplankton is required.

Our general purpose was to determine the mechanisms of distribution and biochemical speciation of planktonic production as a function of abiotic parameters of the environment, with a view to determining the evolution of the lipid content of zooplankton and krill. The final objective was to establish a conceptual model modelize all these phenomena in order to evaluate the nutritional quality of the pelagic food web (lipid content).

We focused mainly on the study at mesoscale of the ice edge and of the adjacent open water, where the development of spring blooms of phytoplankton was expected, both in the Weddell Sea and in the Ross Sea.

2. WEDDELL SEA

2.1 EPOS leg 1 cruise: general objectives and work at sea

Leg 1 of the EPOS programme was carried out on board of the R.V. "Polarstern" from Rio Grande (Brazil) to Punta Arenas (Chile) from October 11 to November 19, 1988. In the Weddell Sea, studies focused on the sea ice and its northern edge during the period of early ice melting and retreat. Long transects in and out of the sea ice were planned to sample the three major zones representative of the Southern Ocean ecosystems: the open water, the seasonal sea ice zone and the permanent pack ice (figure 1).

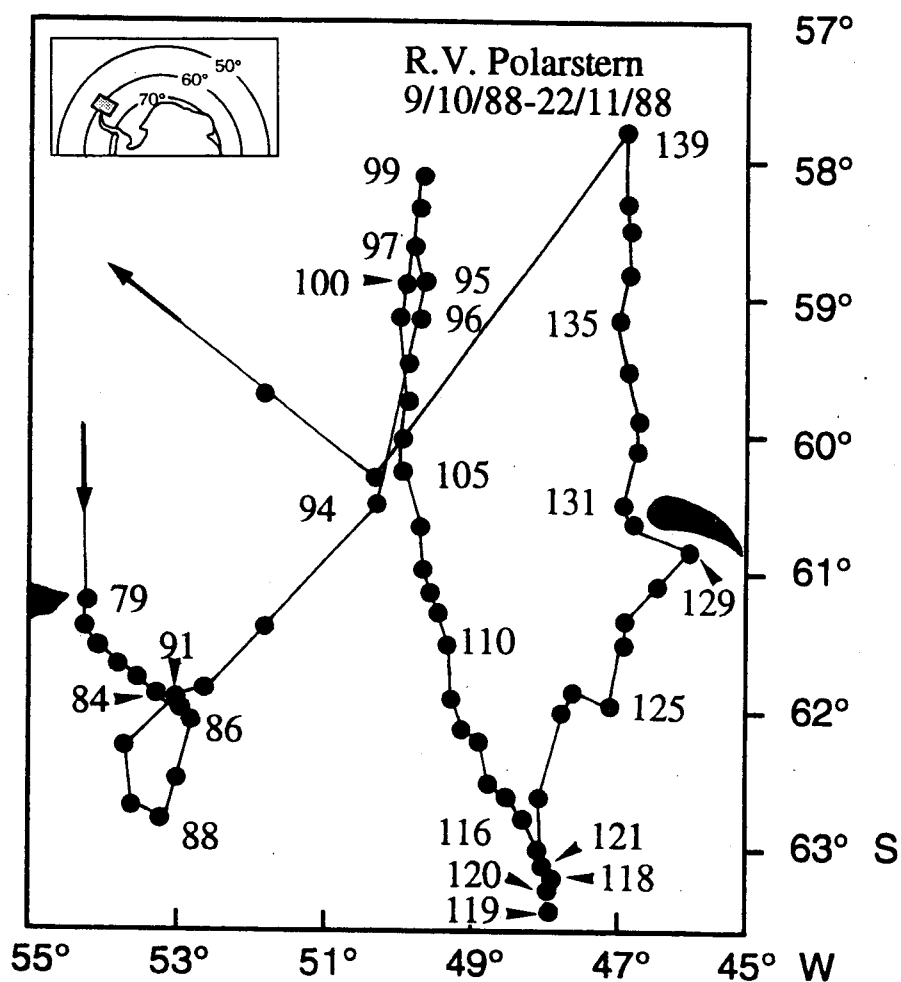


Figure 1: EPOS leg 1 cruise track.

Data discussed in this report were mainly collected between 63°21'S 47°40'W (station 119; November 3, 1988) and 57°50'S 46°29'W (station 139; November 13, 1988). They represent a typical situation. A total number of 450 samples of phytoplankton and 23 vertical hauls of zooplankton were collected.

2.2 Materials and methods

At each station, CTD measurements were carried out with a Neil Brown Mark III sonde by A.M. Larsson and P.I. Sehlstedt. Nitrate and silicate were analyzed on board by a Technicon II Autoanalyser by F. Bianchi team. The different contributions are collected in Larsson (1990).

During the whole cruise, continuous subsurface profiles of *in vivo* fluorescence were recorded using a Turner 111 fluorimeter. At the vertical stations, *in vivo* fluorescence and HPLC chlorophyll *a* measurements were carried out at 10 depths between 0 and 200 meters. HPLC procedure is described in Hecq *et al.* (1992).

Vertical hauls of net zooplankton were performed by means of a Bongo net in the pack ice area, at the ice edge and in the open water. A standard fishing depth was from 300 meters to the surface (mesh size was 300 microns). Based on main taxa, samples were roughly sorted on board and immediately freeze-dried. Lipid content of each sample was analyzed in Liège using the sulfophosphovanillin method (Barnes and Blackstock, 1973). Fatty acids were separated and quantified by Gas Liquid Chromatography, according to Hecq and Goffart (1984).

2.3 Hydrodynamical context

In the Weddell Sea, cold water of the westerly transport due to East Wind Drift runs close to the continent and circulates around in a clockwise manner (Everson, 1976), forming the Weddell Gyre (figure 2).

At the northern limit of the Weddell Sea, the Weddell-Scotia Confluence is a frontal system separating the northern branch of the Weddell Gyre and the eastward flowing waters of the Circumpolar Current (West Wind Drift). The hydrological structure of the Confluence area is dominated by the Scotia front, a sharp temperature gradient extending from about 200 to 2.500 meters. South of the Scotia front, a dynamic and highly variable transition zone consists of meso-scale water masses and eddies originating from occasional transfer of warm deep Circumpolar Water through the Scotia front (Cederlöf *et al.*, 1989).

According to Gordon *et al.* (1982), in the Atlantic sector of the Southern Ocean, the Weddell-Scotia Confluence and the Antarctic Divergence overlap.

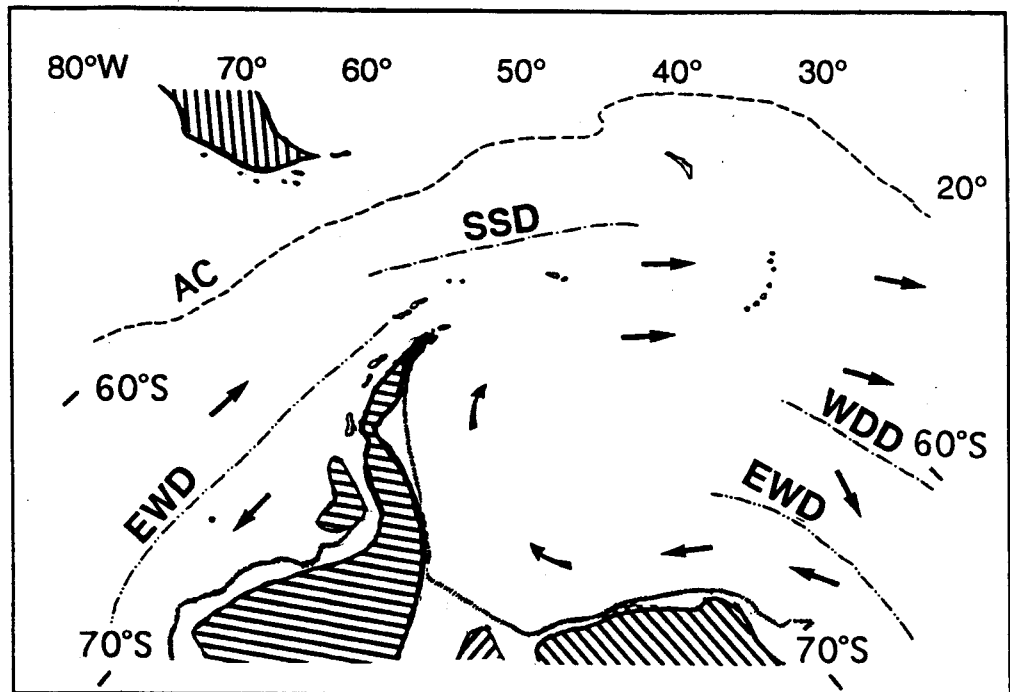


Figure 2: Major circulation pattern of surface water in the Weddell sector of the Southern Ocean (after Macintosh, 1972 in Everson, 1976). AC: Antarctic Convergence, EWD: northern limit of East Wind Drift, WDD: Weddell drift divergence, SSD: Scotia Sea divergence.

2.4 Results

2.4.1 Hydrological characteristics and sea ice conditions

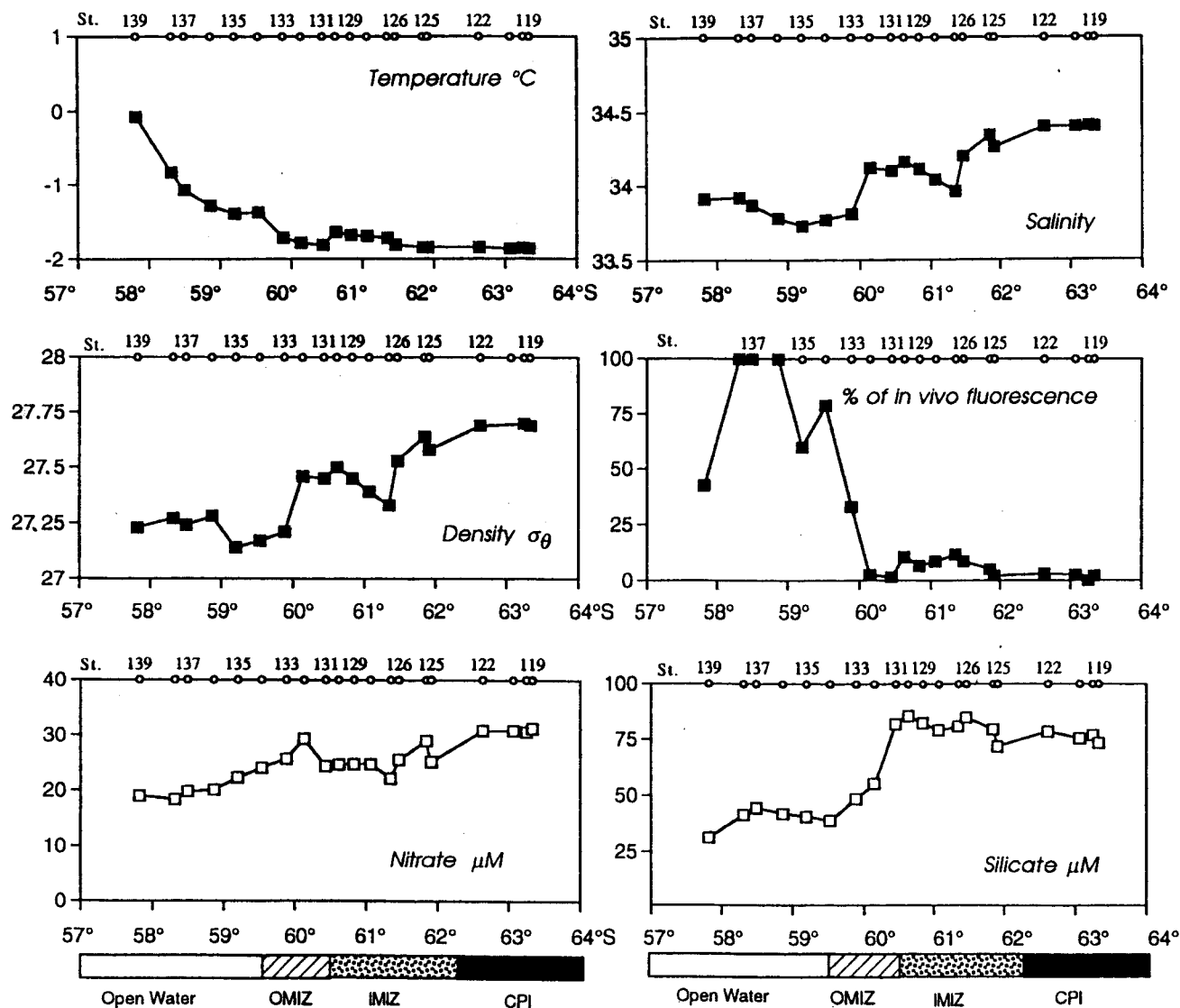
a. Horizontal pattern of water masses.

The latitudinal distribution of temperature, salinity and density in surface waters between $63^{\circ}21'S$ $47^{\circ}40'W$ (station 119) and $57^{\circ}50'S$ $46^{\circ}29'W$ (station 139) is presented at figure 3. The transect, carried out at the end of the austral winter 1988, from November 3 (station 119) to 13 (station 139), includes the closed pack-ice, the marginal ice zone and the open water.

The Outer Marginal Ice Zone, characterized by 50% of open water and with ice consisting of brash and old floes, extended from approximately $60^{\circ}30'S$ (station 131) to $59^{\circ}50'S$ (station 133). North of $58^{\circ}30'S$ (station 137), only occasional bits of brash ice were encountered (Eicken and Lange, 1989).

In the superficial layer, the Weddell Sea Winter Water, very cold (temperature $< -1.80^{\circ}C$) and with salinities between 34.2 and 34.5, was identified from station 119 to station 126. North of station 126, the Antarctic Surface Water was found. This is a water mass with higher

temperature and lower salinity than the Weddell Sea Winter Water (Larsson *et al.*, 1989). The northernmost stations were located in the southern part of the Weddell-Scotia Confluence, with warmer water at the surface.



ANTAR
II/06

Figure 3: Subsurface distribution of temperature ($^{\circ}\text{C}$), salinity (PSU), density (σ_θ), *in vivo* fluorescence (%), nitrate (μM) and silicate (μM) in the Northern Weddell Sea, between $63^{\circ}21'\text{S}$ $47^{\circ}40'\text{W}$ (station 119, 03/11/88) and $57^{\circ}50'\text{S}$ $46^{\circ}29'\text{W}$ (station 139, 13/11/88). OMIZ: Outer Marginal Ice zone; IMIZ: Inner Marginal Ice zone; CPI: Closed Pack-ice Temperature, salinity and density data from Larsson and Sehlstedt in Larsson (1990). Nutrients from Bianchi *et al.* in Larsson (1990).

b. Vertical structure of water column

In the pack-ice area (station 122, figure 4), the water column was completely homogeneous until 100 meters and the water temperature very low (-1.84 $^{\circ}\text{C}$ at the surface). Below 100 meters, a progressive increase in temperature and salinity was observed.

In the outer marginal ice zone (station 131, figure 5), the vertical structure of the water column was very similar to that of the pack-ice area and the surface temperature remained very low (-1.81°C at the surface).

At the northern limit of the marginal ice zone (station 133) and in the open water (station 135, figure 6), the water column exhibited a homogeneous mixed layer restricted to the 50 upper meters, due mainly to the presence of a less saline core.

2.4.2 Latitudinal distribution of nutrients and phytoplankton

a. Horizontal distribution

The superficial distribution of *in vivo* fluorescence along the transect between the consolidated pack-ice and the open water (figure 3) shows that in all the area covered by the pack and in the southern part of the marginal ice zone, the phytoplankton biomasses were very low (0 and 10% of relative *in vivo* fluorescence) and corresponds to 0 to $0.2\ \mu\text{g chl } a/l$ measured by HPLC. From the northern part of the marginal ice zone, the phytoplankton biomass increased sharply, reaching maximum values of $1.8\ \mu\text{g chl } a/l$ ($> 100\%$ of fluorescence on the figure) in the open water, at station 138. Concurrently, nitrate and silicate showed distinct minima coincident with the highest biomass values (figure 3).

b. Vertical distribution

Below the pack (station 122, figure 4) and in the marginal ice zone (station 131, figure 5), no vertical structure in the phytoplankton distribution was observed and fluorescence values remained very low along the whole water column. High nitrate and silicate levels (figures 4 and 5) were observed.

In the open water, north of the ice gradient, elevated phytoplankton biomasses ($> 1\ \mu\text{g chl } a/l$) occurred in the surface mixed layer. At station 135 (figure 6), chlorophyll *a* exhibited a strong subsuperficial maximum (around $1.7\ \mu\text{g chl } a/l$) at the pycnocline. Parallel to the increases in phytoplankton concentration, nitrate and silicate were depleted in the surface layer (figure 6).

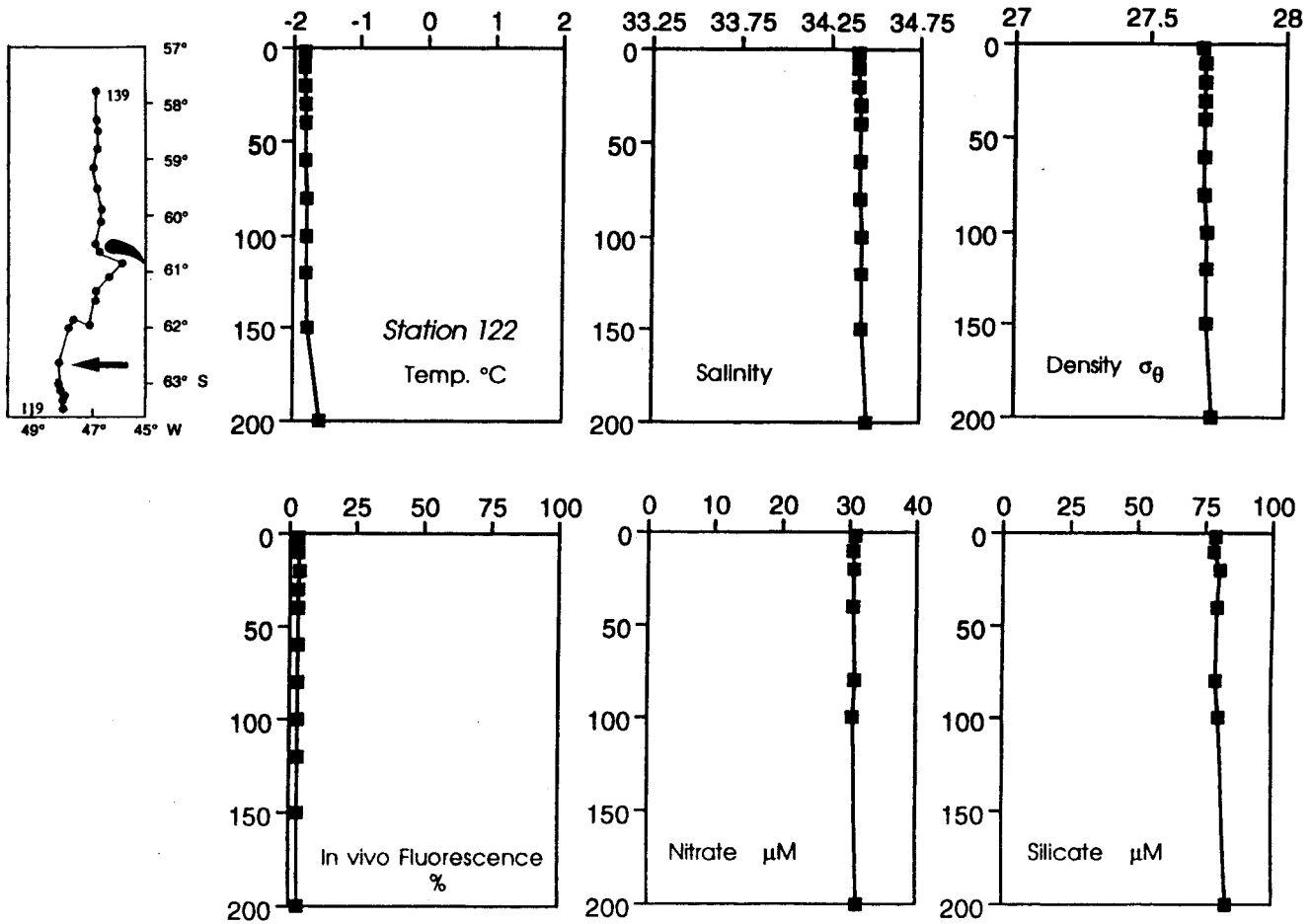


Figure 4: Vertical distribution of temperature ($^{\circ}\text{C}$), salinity (PSU), density (σ_θ), in vivo fluorescence (%), nitrate (μM) and silicate (μM) in the closed pack ice area (station 122). Temperature, salinity and density data from Larsson and Sehlstedt in Larsson (1990). Nutrients from Bianchi *et al.*, in Larsson (1990).

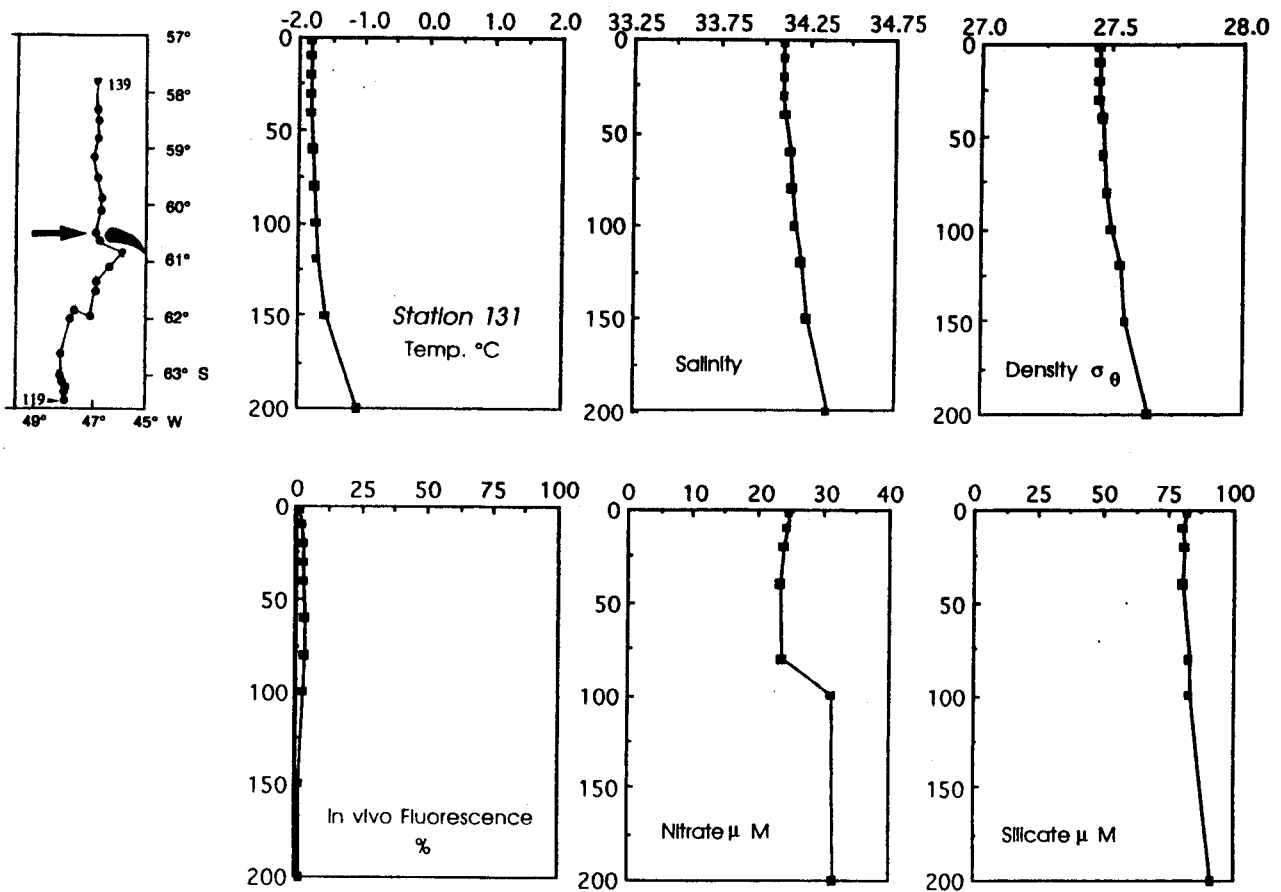


Figure 5: Vertical distribution of temperature ($^{\circ}\text{C}$), salinity (PSU), density (σ_θ), in vivo fluorescence (%), nitrate (μM) and silicate (μM) at the outer marginal ice zone (station 131). *Temperature, salinity and density data from Larsson and Sehlstedt in Larsson (1990). Nutrients from Bianchi et al., in Larsson (1990).*

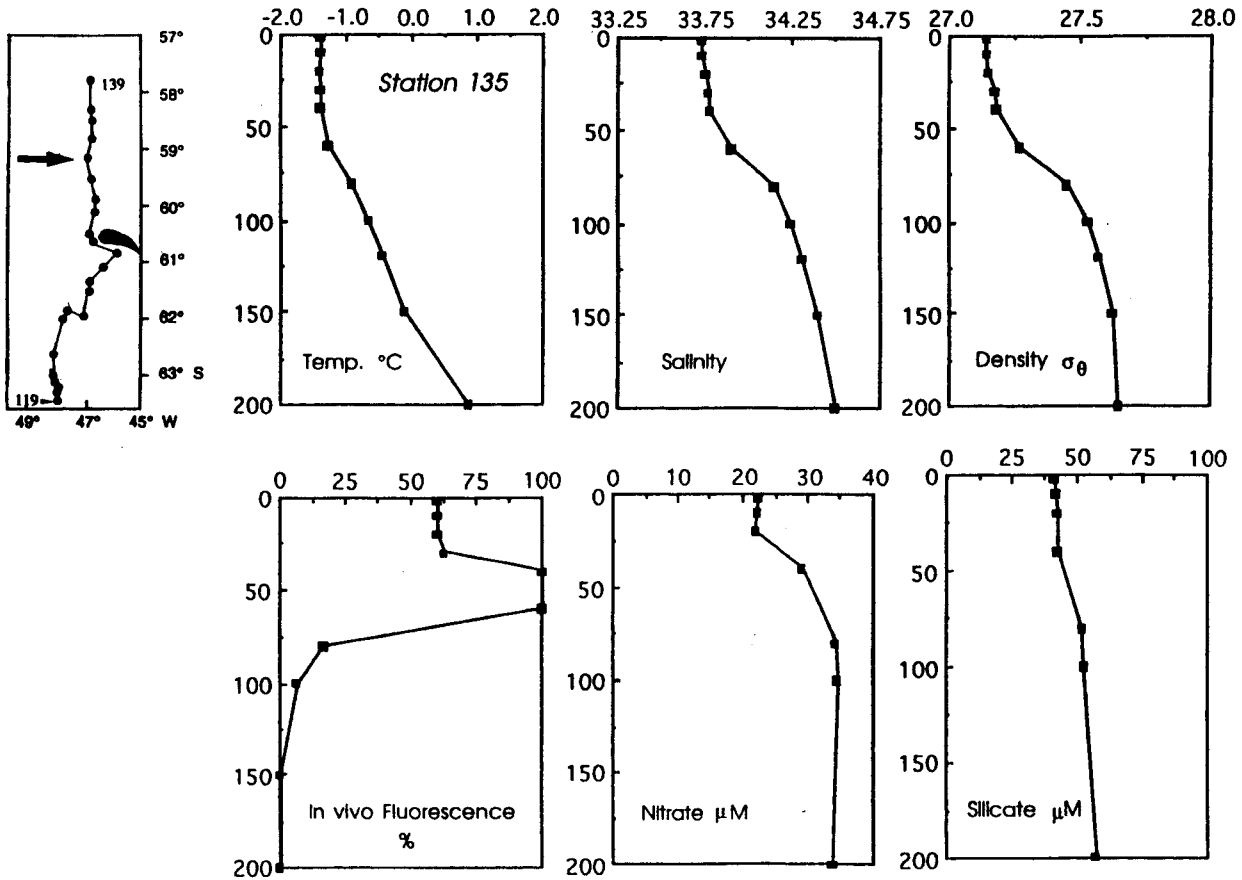


Figure 6: Vertical distribution of temperature ($^{\circ}\text{C}$), salinity (PSU), density (σ_θ), in vivo fluorescence (%), nitrate (μM) and silicate (μM) in the open water (station 135). *Temperature, salinity and density data from Larsson and Sehlstedt in Larsson (1990). Nutrients from Bianchi et al. in Larsson (1990).*

2.4.3 Latitudinal distribution of zooplankton

Latitudinal distribution of total zooplanktonic biomass (standardized fishing depth from 300 meters to the surface, mesh size 300 μm) between stations 199 and 139 is presented at figure 7. Biomasses varied between 2 and 4 mg of dry weight/ m^3 , except in the southernmost stations, under the consolidated pack-ice, where it increased slightly (7 mg of d.w./ m^3). On the other hand, the specific composition of zooplankton populations was very diverse, with larval or juvenile stages of molluscs and echinoderms. In the same samples, Polychaetes, ctenophores, pteropods, different species of ostracodes and chaetognaths were also regularly found (Battaglia *et al.*, 1989). In the southernmost stations, the increase of the total biomass was mainly due to the presence of two typical Antarctic copepods, *Calanus propinquus* and *Calanoïdes acutus*. Under the ice, *Euphausia superba* was one of the most dominant species of the megazooplankton community. Stations where krill was collected are mentioned.

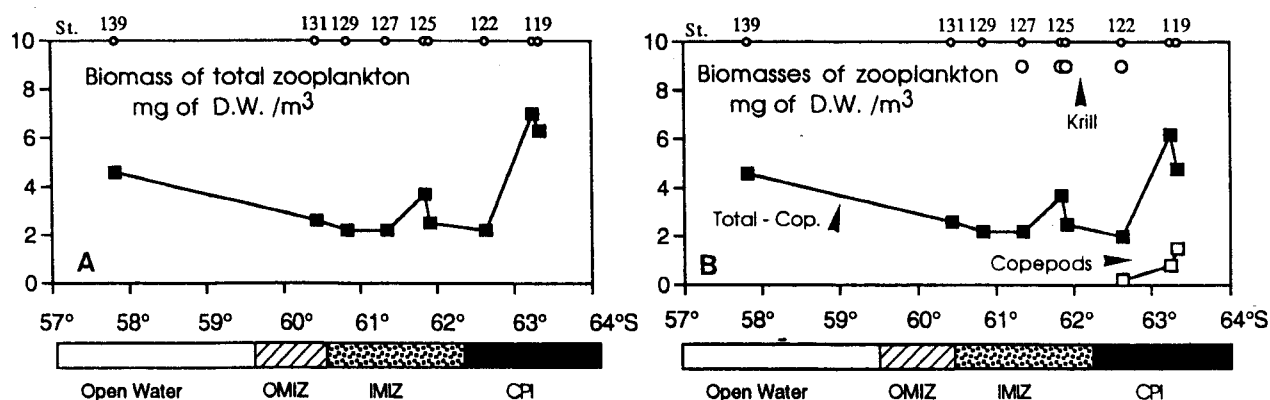


Figure 7: Latitudinal variation of zooplanktonic biomass hauled between 0 and 300 meters (mg of dry weight/ m^3) along the same transect as in figure 3. **A:** Total biomass **B:** Biomasses of adult *Calanus propinquus* and *Calanoïdes acutus* -Copepods- and of total plankton without adult copepods -Total-Cop.-. Stations where *Euphausia superba* was caught are mentioned for their qualitative interest. OMIZ: Outer Marginal Ice zone; IMIZ: Inner Marginal Ice zone; CPI: Closed Pack-ice.

2.4.4 Lipid contents and fatty acids composition of zooplankton

Total lipids and fatty acids analyses have been performed on *Euphausia superba*, on sorted *Calanus propinquus* and *Calanoïdes acutus* and on total zooplankton without these adult copepods (figure 8).

In the total zooplankton without adult copepods, total lipid concentration was uniformly very low (5 % of the dry weight) along each

transect, except in the southernmost stations where it reached 10% of the dry weight. In the adult copepods *Calanus propinquus* and *Calanoïdes acutus*, the lipid concentration was much higher, with a mean value of 18.6 % of the dry weight for the 3 stations where these species were caught. In *Euphausia superba*, the variability of the lipid contents between the different stations was very high (5 - 21 % of the dry weight).

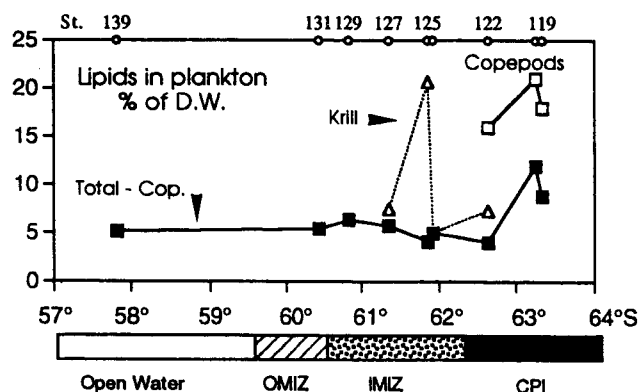


Figure 8: Latitudinal variation of lipid contents (% of dry weight) of the adult *Calanus propinquus* and *Calanoïdes acutus* -Copepods-, of the total plankton without adult copepods -Total-Cop.- and of *Euphausia superba*. Each value on the figure is the mean of 5 samples. OMIZ: Outer Marginal Ice zone; IMIZ: Inner Marginal Ice zone; CPI: Closed Pack-ice.

ANTAR
II/06

In the total zooplankton without adult copepods, in the copepods and in the krill, the distribution of the fatty acids saturated in C14 (myristic acid), C16 (palmitic acid) and C18 (stearic acid) presents irregular fluctuations that are not correlated with the position of the marginal ice zone or the phytoplankton abundance (figure 9). Percentages of myristic acid are presented in table 1.

The percentages of monoinsaturated fatty acids in C16 (C16:1 ω 7, palmitoleic acid) and C18 (C18:1 ω 9, oleic acid) show the predominance of the oleic acid in each of the sorted fraction (figure 10). Concentrations in oleic acid were the highest in the total zooplankton without adult copepods, with values between 15.6 (station 139) and 29.6 % (station 119) of the total fatty acids. Neither does it seem that monoinsaturated fatty acids fluctuate clearly with any measured parameters.

Changes in polyinsaturated fatty acids distribution (C20:5 ω 3, eicosapentaenoic acid and C22:6 ω 3, docosahexaenoic acid) are difficult to link with environmental parameters. Moreover, in *Euphausia superba*, eicosapentaenoic acid is quasi absent while it is proportionally important

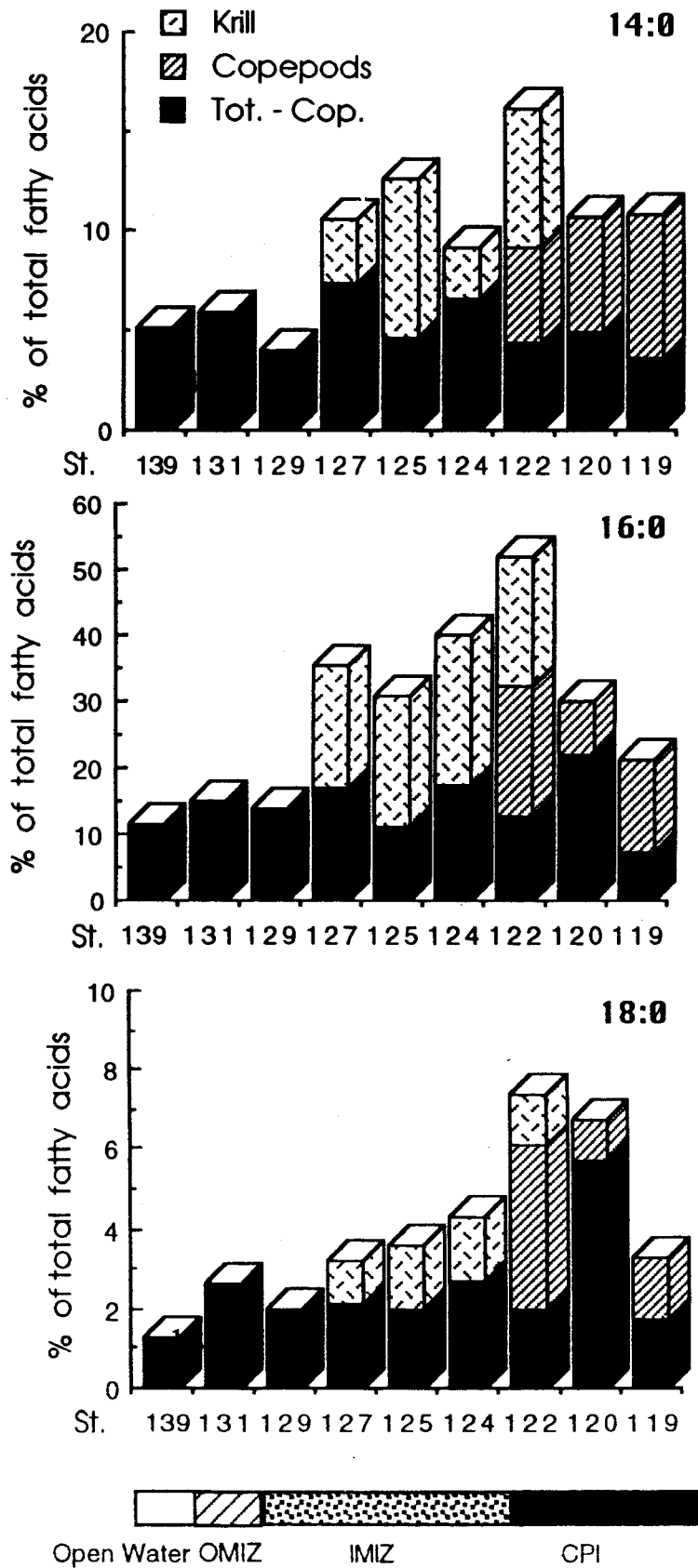


Figure 9: Latitudinal distribution of percentages in myristic (C14:0), palmitic (C16:0) and stearic (C18:0) acids in the adult *Calanus propinquus* and *Calanoides acutus* -Copepods-, in the total plankton without adult copepods -Tot.-Cop.- and in *Euphausia superba* -Krill-. OMIZ: Outer Marginal Ice zone; IMIZ: Inner Marginal Ice zone; CPI: Closed Pack-ice

in adult *Calanus propinquus* and *Calanoïdes acutus* (figure 11). The total polyunsaturated fatty acids percentages (PUFA) are presented at table 1.










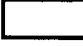



| | St. 139 | St. 131 | St. 129 | St. 127 | St. 125 | St. 124 | St.122 | St.120 | St.119 |
|----------------------|--|--|--|--|--|--|---|--|--|
| Tot.-Cop. (a) % 14:0 | 5.1 | 5.9 | 4.0 | 7.3 | 4.6 | 6.5 | 4.3 | 4.9 | 3.6 |
| Tot.-Cop. (a) % PUFA | 8.9 | 9.7 | 19.6 | 11.5 | 13.5 | 12.0 | 13.9 | 3.6 | 5.4 |
| Copepods (b) % 14:0 | | | | | | | 4.8 | 5.8 | 7.2 |
| Copepods (b) % PUFA | | | | | | | 8.2 | 11.1 | 12.0 |
| Krill (c) % 14:0 | | | | 3.2 | 7.9 | 2.6 | 7.1 | | |
| Krill (c) % PUFA | | | | 15.4 | 8.8 | 19.5 | 13.8 | | |
| |  |  |  |  |  |  |  |  |  |

Table 1: Percentages of C14:0 and PUFA (C20:5 ω 3 + C22:6 ω 3) in total fatty acids at the different stations of the transect. Each value is the mean of 5 samples. a: Total zooplankton without adult copepods. b: *Calanus propinquus* and *Calanoïdes acutus*. c: *Euphausia superba*.

| | |
|--|-------------------------|
|  | Open water |
|  | Outer Marginal ice Zone |
|  | Inner Marginal Ice zone |
|  | Closed pack-ice |

ANTAR
II/06

2.4.5 Discussion

Intense phytoplankton blooms near the edge of seasonally retreating pack-ice are quite common in the Southern Ocean (El Sayed *et al.*, 1983; Nelson *et al.*, 1987; Fryxell and Kendrick, 1988). They can support the base of the food web and in this way are essential in the functioning of the Antarctic ecosystem. However, most data presently available from such blooms have been obtained in spring and summer. During the EPOS leg 1 cruise, we were able to study the early spring characteristics of phyto- and zooplankton communities in relation with the ice distribution. Neither before that cruise, the inner part of the seasonal ice zone nor the heavy pack-ice of the Weddell Sea have ever been studied during winter/early spring conditions (Hempel, 1989).

From a physical point of view, only the northernmost stations (North of 58°30'S), situated on the Weddell-Scotia Confluence, were completely

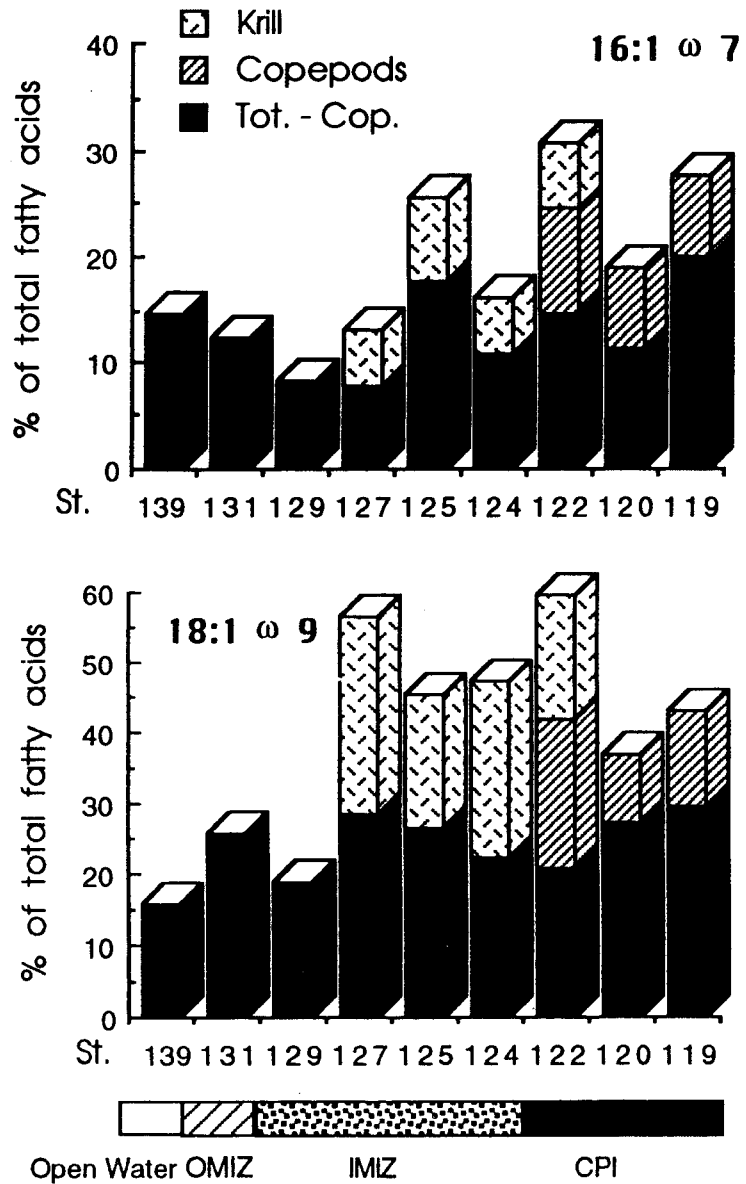


Figure 10: Latitudinal distribution of percentages in palmitoleic (C16:1 ω 7) and oleic (C18:1 ω 9) acids in the adult *Calanus propinquus* and *Calanoides acutus* -Copepod-, in the total plankton without adult copepods -Tot.-Cop.- and in *Euphausia superba* -Krill-. OMIZ: Outer Marginal Ice zone; IMIZ: Inner Marginal Ice zone; CPI: Close Pack-ice.

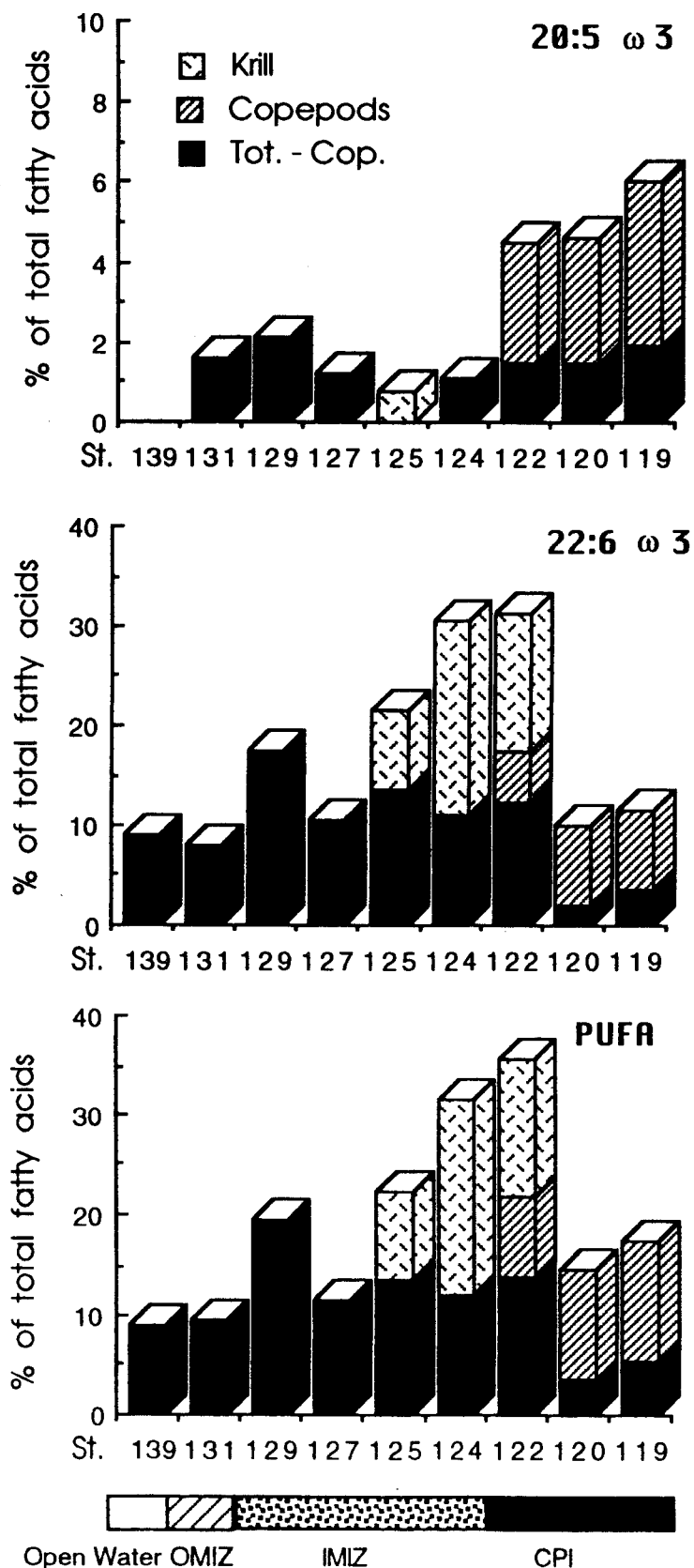
ANTAR
II/06

Figure 11: Latitudinal distribution of percentages in eicosapentaenoic (C20:5 ω 3) and docosahexaenoic (C22:6 ω 3) acids and in total polyunsaturated fatty acids (PUFA) in the adult *Calanus propinquus* and *Calanoïdes acutus* -Copepods-, in the total plankton without adult copepods -Tot.-Cop.- and in *Euphausia superba* -Krill-. OMIZ: Outer Marginal Ice zone; IMIZ: Inner Marginal Ice zone; CPI: Closed Pack-ice

ice-free. In the same general area, in 1983, Nelson *et al.* (1987) indicate that the sea ice retreating began from its maximum northward extent in mid-September, with a mean rate of southward retreat of 5.2 km/day.

In all the area of heavy ice cover, no vertical stability within the upper 100 meters was observed and chlorophyll *a* concentrations in the water column were very low, with levels inferior to 0.2 $\mu\text{g chl } a/l$.

Relatively high phytoplankton biomass ($> 1 \mu\text{g chl } a/l$) was associated exclusively with the northernmost part of the marginal ice zone and with the adjacent open water, coincident with the Weddell-Scotia Confluence. Nitrate and silicate show local minima correlated with the biomass maxima. The bloom had a North-South extent of at least 185 km (stations 134 to 139) and the highest surface phytoplankton concentrations (1.8 $\mu\text{g chl } a/l$ at stations 138) were approximately 165 km north from the ice edge. The bloom developed only in the stations showing a vertical stratification with a homogeneous mixed layer restricted to the upper 50 meters. In this case, the stabilization of the water column seems to be due both to the early melting of the ice edge and to the presence of the Weddell-Scotia Confluence, dominated by sharp temperature gradients.

As shown by Nelson *et al.* (1987), it seems that the hydrographic conditions near the ice edge in early November were sufficient to initiate a phytoplankton bloom, but had not been in place long enough for high biomass to develop. On the basis of a maximum net growth rate of 0.3 day^{-1} , Nelson *et al.* (1987) computed that it takes two weeks or more for Southern Oceans phytoplankton to grow from the very low biomass levels typical of the ice-covered winter water column ($< 0.3 \mu\text{g chl } a/l$) to those that characterize ice edge blooms in Antarctic waters ($> 7 \mu\text{g chl } a/l$), even in the absence of losses due to grazing and sinking. In the Weddell Sea, in November, they calculated a net growth rate of 0.13 day^{-1} , leading to a very slow increase in phytoplankton biomass.

As a general rule, during EPOS leg 1, we found an inverse phytoplankton and zooplankton correlation, as El-Sayed and Mandelli (1965) showed in their southern Weddell Sea study. Moreover, zooplankton abundance was very poor. Lipid contents were generally much lower than values reported in the literature for other seasons, both for total zooplankton and for adult copepods. For instance, in the Western Weddell Sea, in January, Hagen (1988) gives lipid contents of respectively 25.3 and 46.9 % of the dry weight for adult *Calanus propinquus* and *Calanoides acutus*, considered herbivorous (Conover and Huntley, 1991), while we get a mean value of 18.6 % for these two species. As showed by our results, distribution of fatty acids presents irregular fluctuations that are not correlated with the position of the marginal ice zone or the phytoplankton abundance. PUFA concentrations, a good tracer of the food

web because animals are unable to elaborate them, and C14:0 values, considered as a prominent constituent of phytoplanktonic lipid, and especially in diatoms (Bottino, 1974), are much lower than values obtained at the end of the austral summer by Goffart and Hecq (1989) in the Indian sector of the Southern Ocean.

All these observations and the spatial splitting between the maxima of phyto- and zooplankton biomasses suggest that the overwintering zooplankton of the Western Weddell Sea were just surviving after exhausting their lipid storage and had not began to graze on new phytoplankton in the marginal ice zone. Recently, Conover and Huntley (1991) have emphasized the importance of sea-ice algae, which may be of considerable importance as a food source for the resident copepods populations. They suggest that herbivores, as krill, do not depend exclusively on the spring and summer period of phytoplankton abundance in the water column. So, more and more, it appears that lipid storage by herbivorous zooplankton is the result of very complex behavioural and physiological strategies and that the idea of general lipid richness in Antarctic zooplankton is not always supported, as confirmed by Hagen (1988).

3. ROSS SEA

3.1 Vth ITALIANTARTIDE expedition: general objectives and work at sea

The general objective of the Vth ITALIANTARTIDE oceanographic expedition, carried out on board of the R.V. "Cariboo", was an interdisciplinary study of the Antarctic pelagic ecosystem, related to hydrodynamical constraints, like macroscale water masses distribution associated with frontal systems, ice coverage and establishment of the vertical structure of the water column during the spring time. The cruise took place in the Pacific sector of the Southern Ocean and in the Ross Sea, from 50°S to Balleny Islands and from Balleny Islands to the Italian base of Terra Nova (75°S) in the Ross Sea, from November 23, 1989 to February 2, 1990 (figure 12).

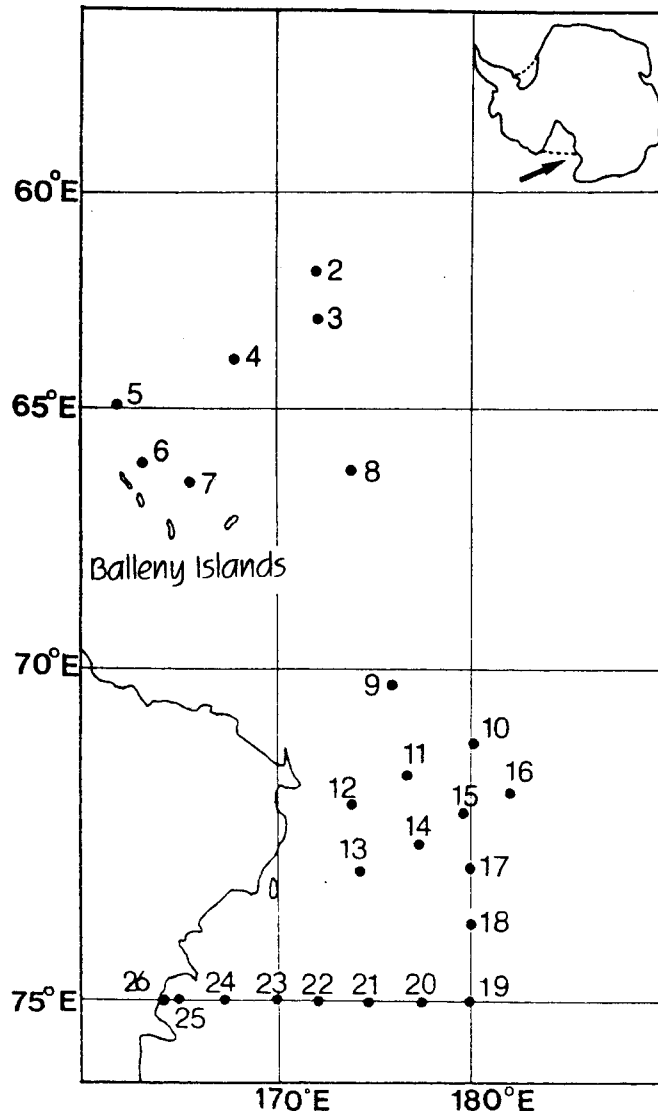


Figure 12: Position of the stations of the 1989-1990 ITALIANTARTIDE cruise.

Hydrological, chemical and biological data are presented according to following transects:

- a macroscale latitudinal view, from 61°55'S to 74°57'S (stations 2, 3, 8, 9, 10, 15, 17, 18, 19)
- a continental slope section in the Ross Sea (stations 13 to 16)
- an East to West, offshore to inshore transect along 75°S, from central Ross Sea to Terra Nova Bay (stations 19 to 25).

3.2 Materials and methods

Ice coverage changes during the cruise have been recorded on the base of remote sensing. Data are taken from satellite images published weekly by NAVY-NOAA Jont ICE Center. The sampling network was adapted to vertical stations and subsurface horizontal profiles. At 25 stations, a 12 bottles rosette and a Neil Brown Mark III CTD have been used by Artegiani *et al.* (Italy) from the surface to the bottom. NO₃, NO₂, SiOH₄ and PO₄ were determined according to Hansen and Grasshoff (1983) and NH₄⁺ according to a modified method of Folkard (1978).

Along the cruise track, the subsurface (2.5 meters) *in vivo* chlorophyll *a* fluorescence was recorded by L. Lazzara and C. Nuccio (Italy).

Phytopigments analysis were carried out on board by High Performance Liquid Chromatography (HPLC) on samples from the continuous surface profiles and from the stations. The HPLC technique, described in Hecq *et al.* (1992), allows to quantify the primary producers stocks, using the chlorophyll *a* as an universal indicator of phytoplankton biomass but also gives informations on the grazing pressure by measuring specific chlorophyll *a* degradation products, mainly phaeophorbids (Bidigare *et al.* 1986; Klein and Sournia, 1987). According to Jeffrey (1974) and Welschmeyer and Lorenzen (1985), phaeophorbids *a* are the major degradation products found in fecal pellets and result from the breakdown of chlorophyll *a* (loss of Mg⁺⁺ and phytol chain) by enzymatic activity of zooplankton digestive system. They apparently are not assimilated and can be used as conservative tag for ingested phytoplankton in feeding conditions.

After filtration of 4 liters of sea water on GF/C filters, phytoplankton fatty acids analysis were performed by Gas Liquid Chromatography, according to Hecq and Goffart (1984).

Zooplankton sampling was carried out by L. Guglielmo's research team (Italy) with an Eznet-Bioness, a multitude opening-and-closing net system with ten 500 µm mesh nets, each one with a mouth opening of 0.25 m². Hauling speed was less than three knots and samples were collected between the surface and a maximum depth of 1000 meters. Two internal

and external ME-SM 11H flowmeters provided measurements of the volume of filtered water. A KMS multiparametric probe and a Back-Scat fluorometer supplied data on temperature, salinity, oxygen, pH, light attenuation and chlorophyll fluorescence. Zooplanktonic components were counted after the cruise. Krill was detected by echosurvey by Azzali's group. Krill aggregations, were classified according to BIOMASS recommendations (Kalinowski and Witek, 1985).

3.3 General hydrology

The physical oceanography of the Pacific sector of the Southern Ocean has been investigated during numerous cruises (i.e. Deacon, 1937; Jacobs *et al.*, 1970). The areas of Antarctic Convergence and Antarctic Divergence, characterized by the presence of thermal fronts at the surface and in the deep layers, have been well described (Gordon, 1971a; Gordon, 1971b). Still the mechanisms involved in the formation of the polar fronts are not well understood. Some investigations have been also carried out on the Antarctic continental shelf of the Ross Sea (Dunbar *et al.*, 1985; Jacobs and Comiso, 1989) and in the Ross Sea itself (Jacobs *et al.*, 1970).

3.4 Results

3.4.1 Sea ice conditions

During the cruise, as a typical characteristic of the Ross Sea, the ice-free surface was propagating from South to North (figure 13). At the stations on the two transects across the continental slope (stations 10 to 12 and stations 13 to 16), the area was ice free for only approximately two weeks. On the contrary, the area encompassing the East-West section from stations 19 to 25 was ice free since almost one month (Guglielmo *et al.*, 1992).

3.4.2 Hydrological characteristics

a. Latitudinal transect (stations 2 to 19)

In the northern part of the section (figure 14), the Antarctic Convergence (or Antarctic Polar Front) has been identified between stations 2 and 3 and is characterized by a strong thermal gradient separating the Subantarctic Surface Water at North and the Antarctic Surface Water southwards. It corresponds to the structure described at around 62°S by Deacon (1982).

Between stations 15 and 18, close to the continental shelf, the thermal characteristics of divergences are recognized. In the northern part of the section, the Pacific Ocean Deep Water, characterized by a maximum of temperature and a minimum of dissolved oxygen, is observed in the 200-

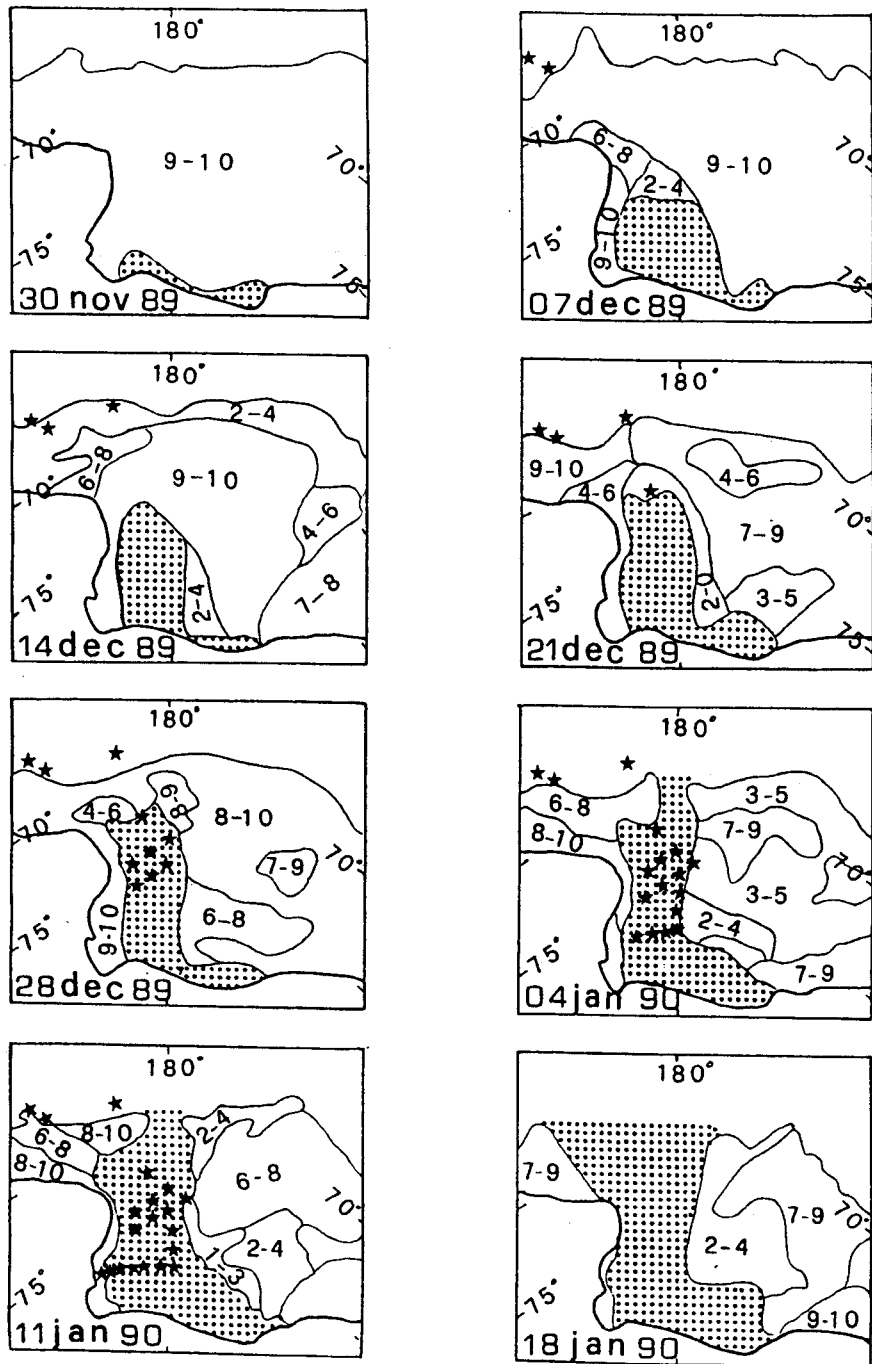
ANTAR
II/06

Figure 13: Ice cover ice temporal evolution in the southern part of the studied area during the cruise period. Numbers (like 7-9) represent the cover ice of the sea-surface in tenth. Data are taken from satellite images published weekly by NAVY-NOAA Joint ICE Center. Stars represent the location of the hydrological stations executed until the date of the image. The dotted area is the ice free area (after Guglielmo *et al.*, 1992).

2,000 meters. Proceeding southwards, it is identified in a more and more surface layer, almost reaching the surface at station 17. In its upper part, the Pacific Ocean Deep Water meets the colder, but less dense Antarctic Surface Water, with a resulting increase of the thermal stratification in the upper layer of the water column. South of station 17, a second frontal zone is determined by the sinking of Antarctic Bottom Water flowing out of the

Ross Sea Shelf along the continental slope, and by the rising to the surface of the Circumpolar and Pacific Ocean Deep Waters (Guglielmo *et al.*, 1992).

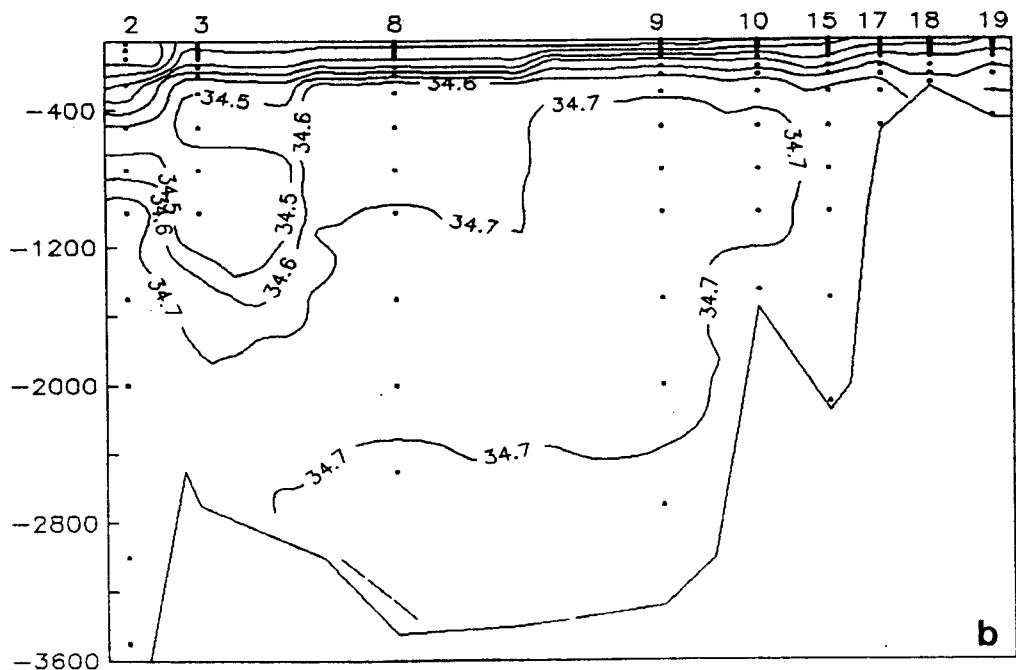
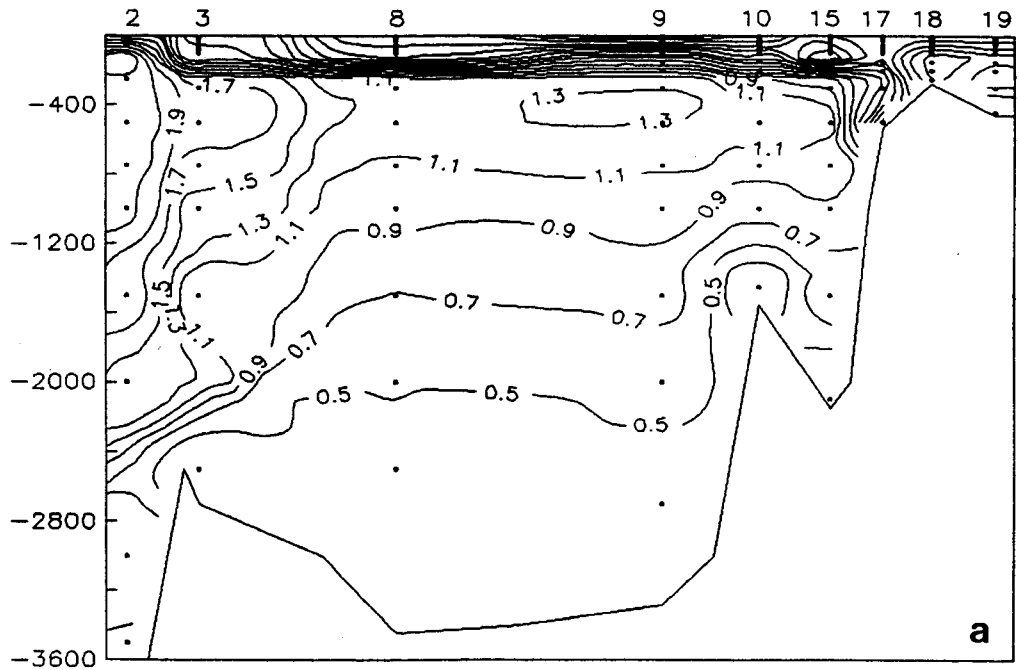
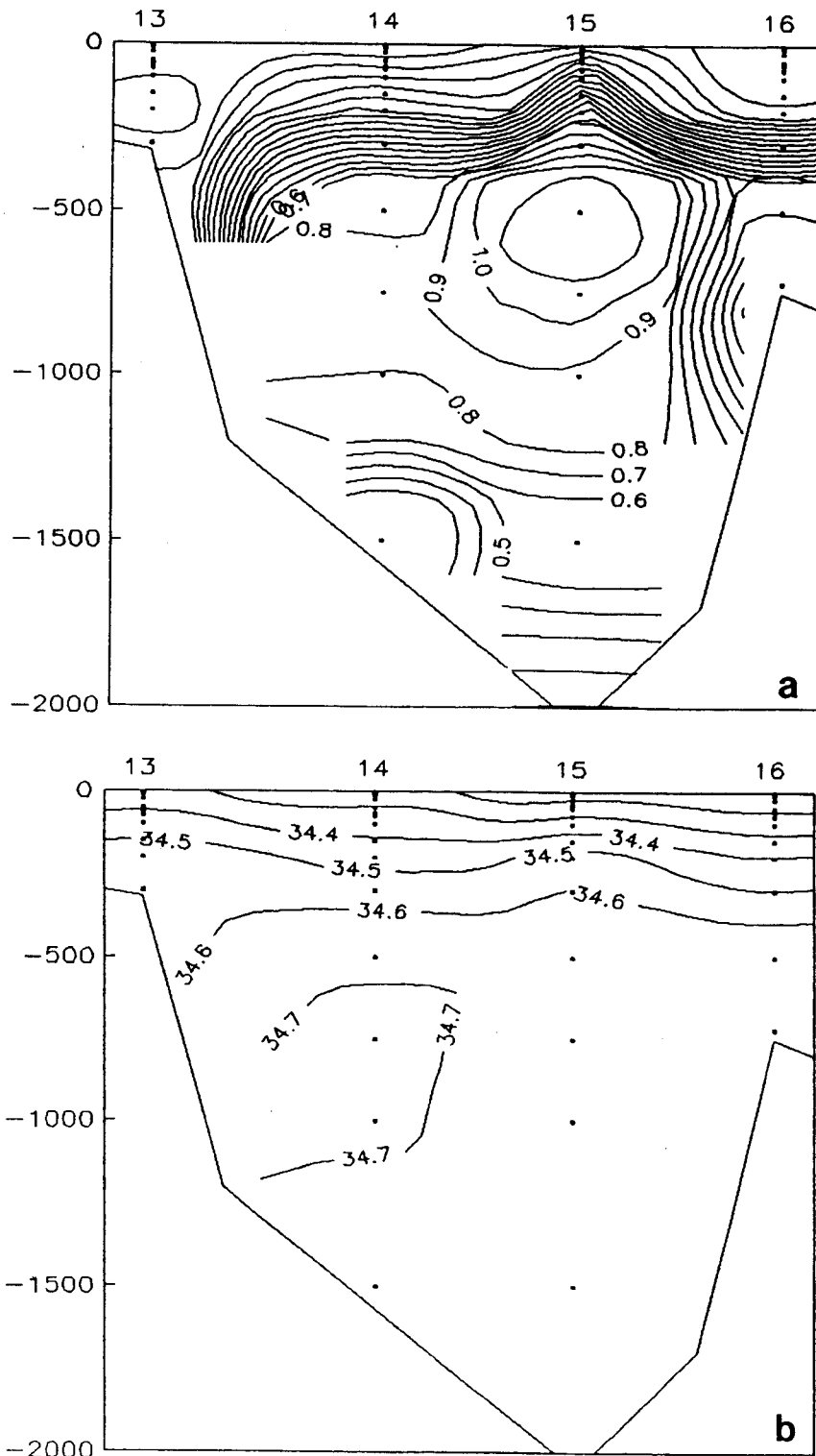


Figure 14: Temperature in °C (A) and salinity in PSU (B) distributions along the North-South section from station 2 (61°55'S 172°26'E) to station 19 (74°59'S, 179°55'E) (after Guglielmo *et al.*, 1992).

b. Ross Sea continental slope section (stations 13 to 16)

The Antarctic Bottom Water, flowing northwards out of the Ross Sea Shelf and characterized by a low temperature, close to 0°C, is observed at the bottom (figure 15). A water core around 800 meters, warmer than the



ANTAR
II/06

Figure 15: Temperature in °C (A) and salinity in PSU (B) distributions from the continental slope (station 13, 73° 08'S 174° 25'E) to the Iselin Bank (station 16, 71° 58'S 177° 50'W) (from Guglielmo *et al.*, 1992).

Antarctic Bottom Water and with a maximum salinity, has been identified as the Circumpolar Deep Water described by Lutjerharms *et al.* (1985). The Pacific Ocean Deep Water, warmer than the surrounding waters, is centered on 500 meters at station 15, below the Antarctic Surface Water (Guglielmo *et al.*, 1992). In the upper 200 meters, a thermohaline front separates the salty coastal waters (station 13) from the less saline offshore waters (figure 16).

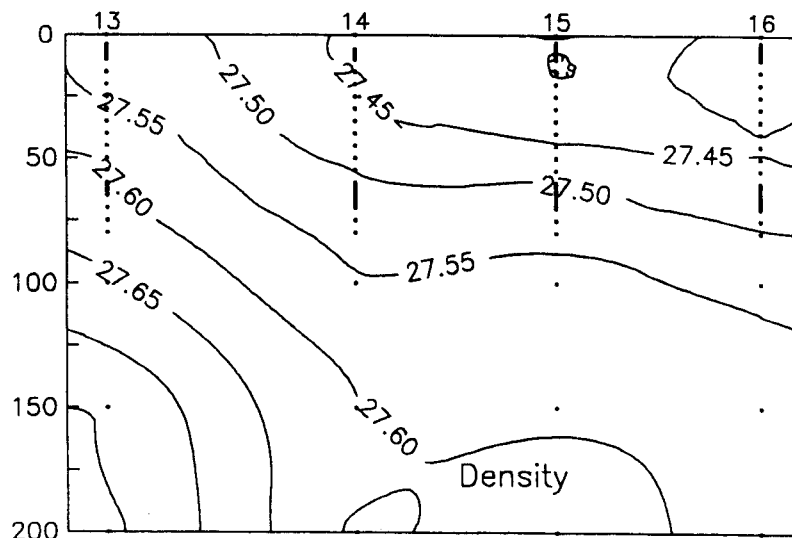


Figure 16: Upper 200 meters distribution of density between stations 13 ($73^{\circ} 08'S$ $174^{\circ} 25'E$) and 16 ($71^{\circ} 58'S$ $177^{\circ} 50'W$).

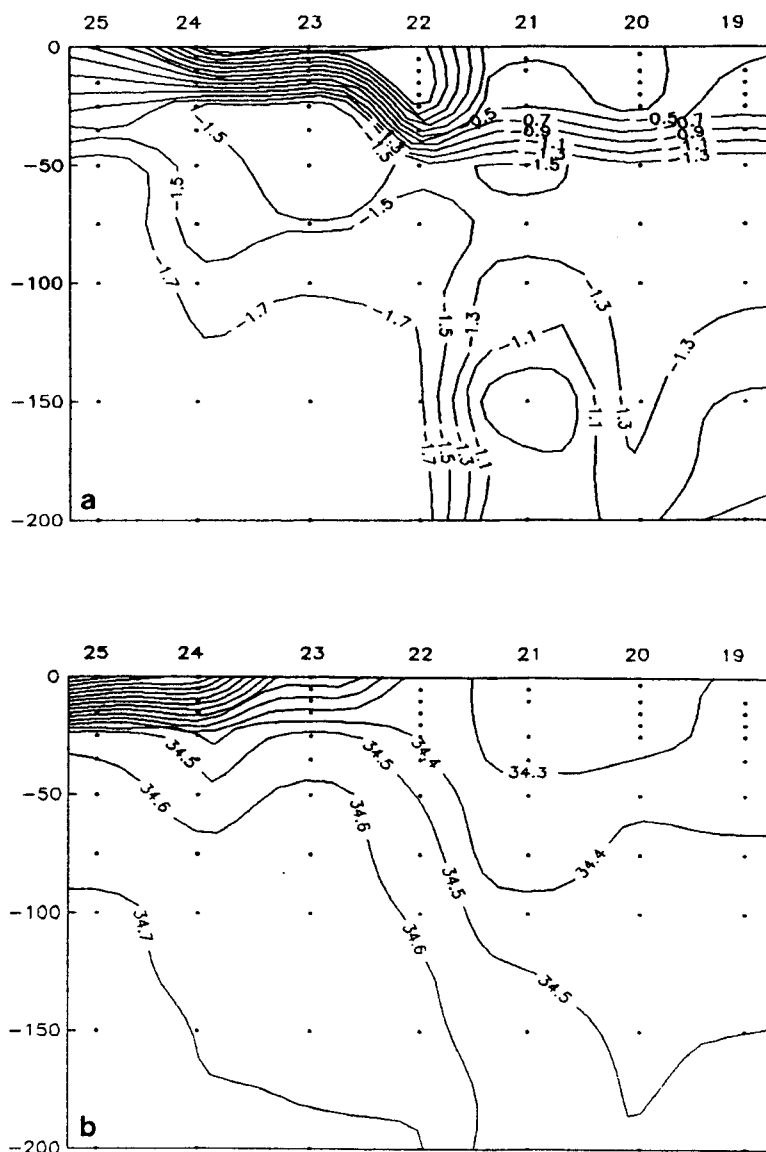
c. Offshore - inshore transect at $75^{\circ}S$ (stations 19 to 25)

On the offshore - inshore transect across the Ross Sea continental shelf (stations 19 to 25), the temperature and salinity fields allow to distinguish two different areas (figure 17).

The first area, close to the Ross ice shelf (stations 25, 24, 23 and partially station 22) is characterized by a very cold and high saline water lying between 50 meters and the bottom, with a temperature range from -1.8 to $-1.9^{\circ}C$ and a maximum salinity of 34.91 PSU. This water mass corresponds to the water flowing out from beneath the Ross Ice Shelf during summer. From station 25 to station 23, the upper 30 meters are dominated by a very strong thermohaline gradient, with temperatures varying from $>1^{\circ}C$ at the surface to $<-1.6^{\circ}C$ at 30 meters. At the same time, the salinity increased from low values at the surface (< 33.4 PSU) to values > 34.5 PSU at 30 meters. This upper 30 meters water layer, warm and less saline, appears as a consequence of the heating by solar energy and the

melting of the sea ice. A very thin and well mixed surface layer is followed by a sharp pycnocline.

East, stations 21, 20 and 19 exhibit different thermohaline characteristics. The surface mixed layer is deeper (50 meters) and shows a lower temperature (-0.5°C) and higher salinity (34.3 PSU). From 50 meters to the bottom, the water column is much less homogeneous than in the onshore part, with temperature higher than -1.6°C and salinity increasing slowly and continuously up to a maximum value of 34.6 PSU. This probably indicates a stratification of the water column existing since a long period.



ANTAR
II/06

Figure 17: Upper 200 meters distributions of temperature in $^{\circ}\text{C}$ (A) and salinity in PSU (B) along the latitude 75°S , between stations 19 ($179^{\circ} 55'\text{E}$) and 25 (Terra Nova Bay, 165°E) (after Guglielmo et al., 1992).

The thermohaline coastal front, detected between stations 22 and 21 and situated between 50 meters and the bottom delineates the cold and salty water mass coming out from beneath the Ross Ice Shelf (Guglielmo *et al.*, 1992).

3.4.3 Distribution of nutrients

a. Latitudinal section (stations 2 to 19)

Distributions of nitrate and silicate in the upper layer (0-200 meters) of the latitudinal section (figure 18) show strong horizontal gradients between stations 2 and 3. Nitrate and silicate concentrations increase respectively from 25.8 to 29.2 μM and from 18.6 to 52.9 μM . These gradients correspond to the Antarctic Convergence, well known for its sharp increase in silica concentrations (Deacon, 1982; El Corre et Minas, 1983; Le Jehan and Treguer, 1985; Lutjerharms *et al.*, 1985; Goffart and Hecq, 1989). At the Antarctic Polar Front, the phosphate gradient is not so marked, the concentrations being relatively high at the front. For phosphate, the most important increase occurs further to the north, at the Subtropical Convergence (Goffart and Hecq, 1989).

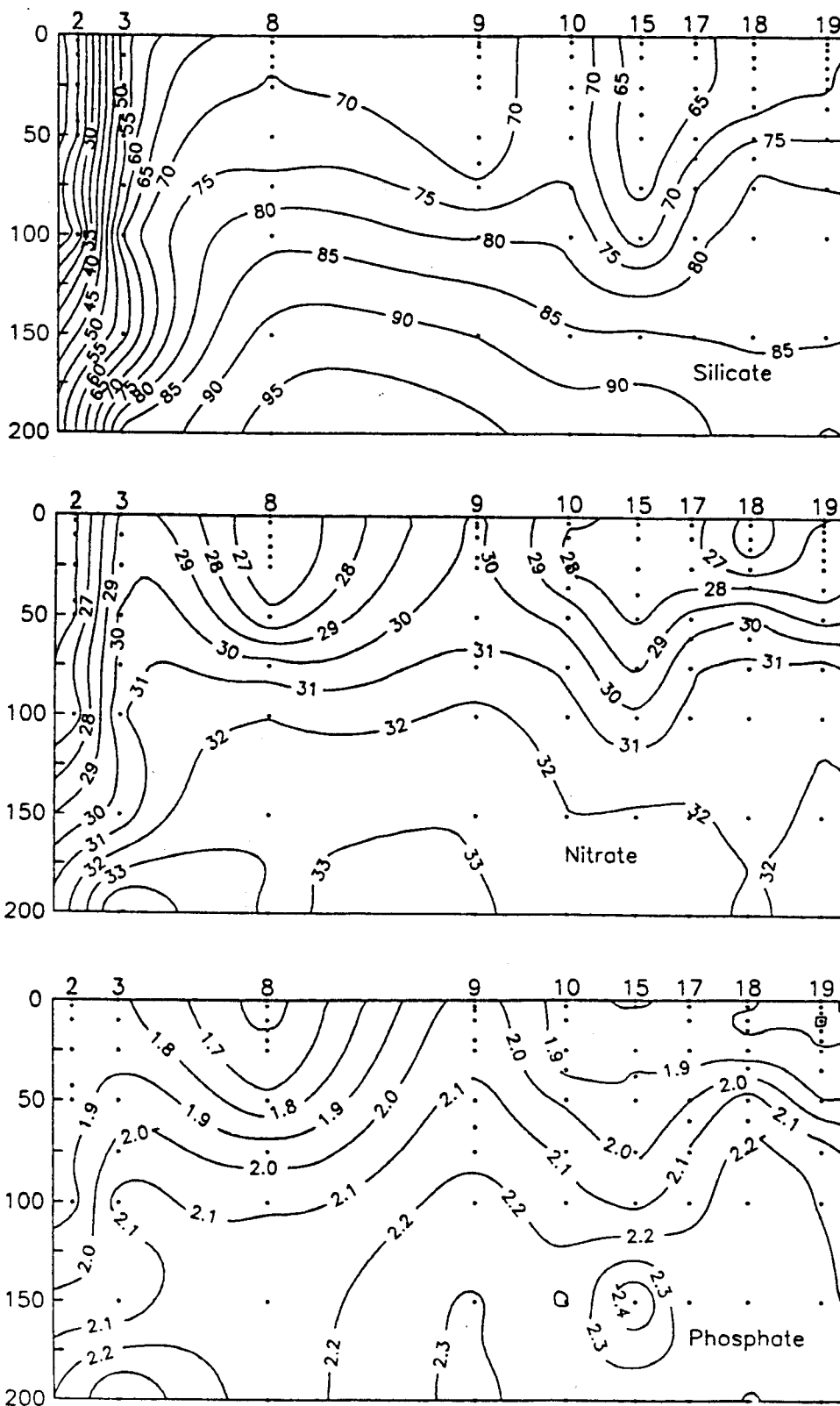
South of the Antarctic Polar Front, NO_3 and PO_4 reach their surface minimum values (respectively 26.4 and 1.6 μM at station 8).

Further South, at station 9 ($70^\circ 12' \text{S}$), surface maxima of nitrate and phosphate occur, with respective concentrations of 30.1 and 2.04 μM . The highest surface concentration in silicate has been measured at station 10 ($71^\circ 12' \text{S}$) with a value of 74.1 μM . While Gordon *et al.* (1978) and Deacon (1982) identified the Antarctic Divergence around 70°S on the basis of coupled surface maxima of silicate and salinity, we observed rather low values of salinity (33.99) associated with silicate maximum and did not get a clear surface signature of the Antarctic Divergence along this latitudinal section (Guglielmo *et al.*, 1992).

Still farther South, at stations 17 and 18, nitrate and phosphate (respectively 25.7 and 1.8 μM at 3 meters at the station 18) present superficial low values, probably resulting from biological activity. The increased stratification, due to the frontal zone, can be one of the factors promoting the nutrients utilization by phytoplankton (Hecq *et al.*, 1992).

b. Ross Sea continental slope section (stations 13 to 16)

In the upper 200 meters, the distribution of silicate, nitrate and phosphate is strongly influenced by the presence of the thermohaline front (figure 19). The East-West gradient is especially notable for silicate, reaching the highest values at station 13 (76.5 μM at the surface).



ANTAR
II/06

Figure 18: Silicate, nitrate and phosphate distributions (μM) along the North-South section from station 2 ($61^{\circ}55'\text{S } 172^{\circ}26'\text{E}$) to station 19 ($74^{\circ}59'\text{S } 179^{\circ}55'\text{E}$) between 0 and 200 meters (silicate and nitrate from Guglielmo *et al.*, 1992).

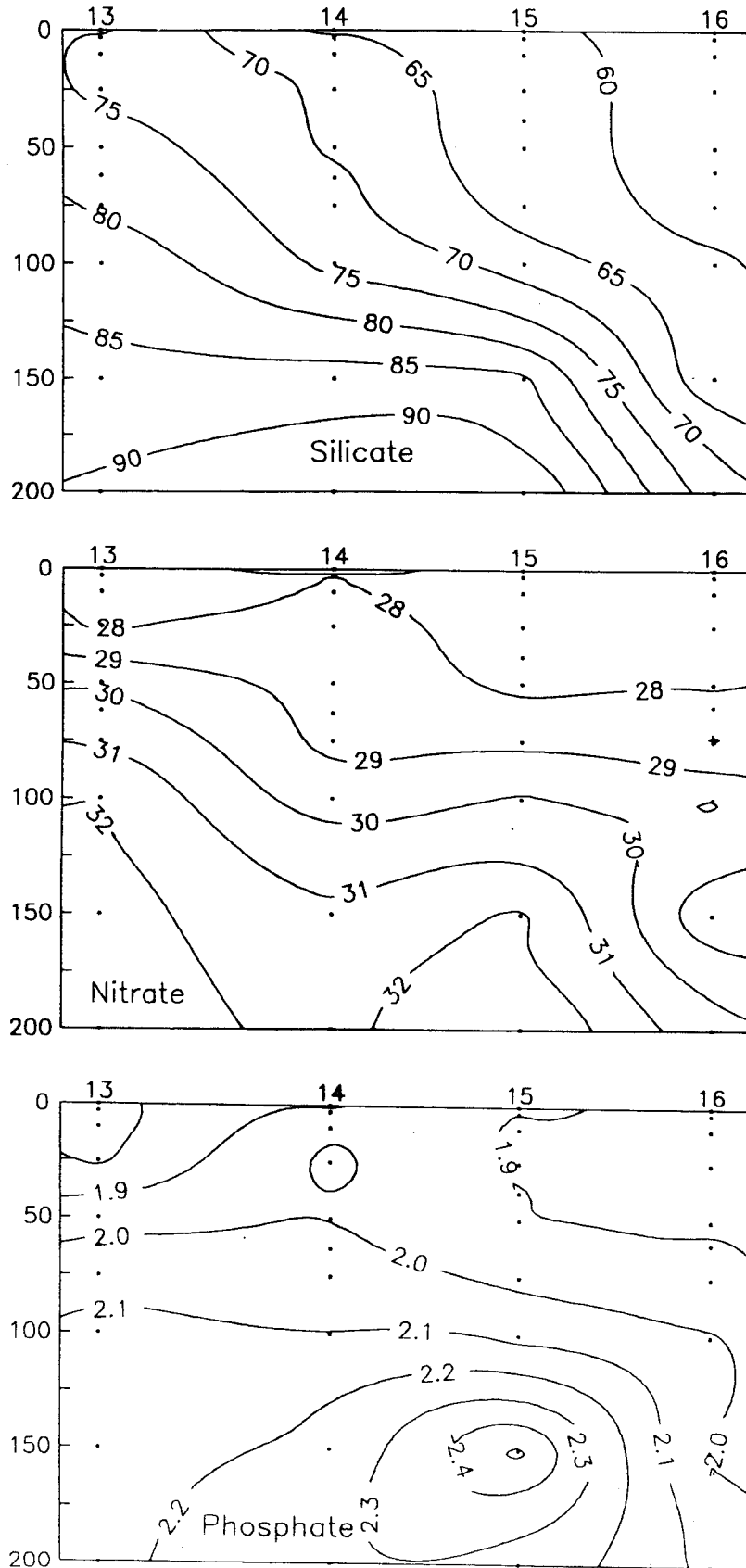


Figure 19: Upper 200 meters distributions of silicate, nitrate and phosphate (μM) from the continental slope (station 13, $73^{\circ} 08'S$ $174^{\circ} 25'E$) to the Iselin Bank (station 16, $71^{\circ} 58'S$ $177^{\circ} 50'W$).

c. Offshore - inshore transect at 75°S (stations 19 to 25)

Distributions of nitrate, silicate and phosphate in the upper 200 meters layer are shown at figure 20. They exhibit strong differences between the western part of the section (stations 22 to 25) and the eastern one (stations 19, 20 and 21). At the surface, nitrate, silicate and phosphate concentrations are respectively of 8.7 μM , 18.7 and 0.34 μM at station 25 and of 26.9, 69.5 and 1.81 μM at station 21. Surface nutrients depletion is strictly correlated with the low density meltwater and in the inshore part, below 50 meters, relatively low nitrate and high silicate (respectively 31.4 and 83.9 μM at 100 meters at station 25) seem to be characteristic of the water mass flowing out from beneath the Ross ice shelf.

Highest concentrations of ammonium ($\geq 1 \mu\text{M}$) occurred near the coast (station 25) and at station 22, below the chlorophyll maxima (figure 23).

3.4.4 Surface distribution of phytoplankton

As a contribution to the improvement of the knowledge of phytoplankton biomass in the Southern Ocean, the horizontal distribution of phytoplankton has been studied from 45°S to the Ross Sea (Terra Nova Bay).

From 45°S to Terra Nova Bay, the chlorophyll *a* fluorescence showed very low values until 62-63°S and from 70 to 75°S (figure 21). The first increase appears around station 3 which corresponds to the Antarctic Polar Front. Two other very wide regions (hundred miles) with exceptionally high fluorescence values (100 to 130 UF) occur between stations 5 to 7 and between stations 8 and 9. These two maxima of fluorescence are located in areas between heavy (just broken) pack-ice, and ice-free waters. At the stations 5 to 7, the samples showed chlorophyll maxima in the upper 15 meters (Guglielmo *et al.*, 1992).

In the Ross Sea, the horizontal subsurface profile of chlorophyll *a* fluorescence corresponds to the transect east-west from station 19 to station 25. Three zones of fluorescence maxima are found. They correspond to the highest subsurface chlorophyll concentrations measured at the stations (5.5 $\mu\text{g chl a /l}$). It can be noted that along this transect, there is an evident decline of surface salinity by more than 1.5 PSU, probably due to the progressive melting of sea and land ice that determines lower surface salinity than in the two zones of stations 5-7 and 8-9, where a lower variability, around 34 PSU is noted (Guglielmo *et al.*, 1992).

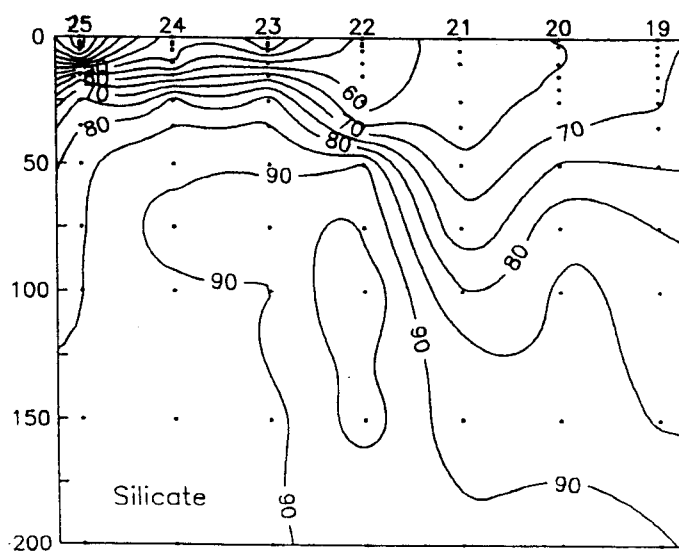
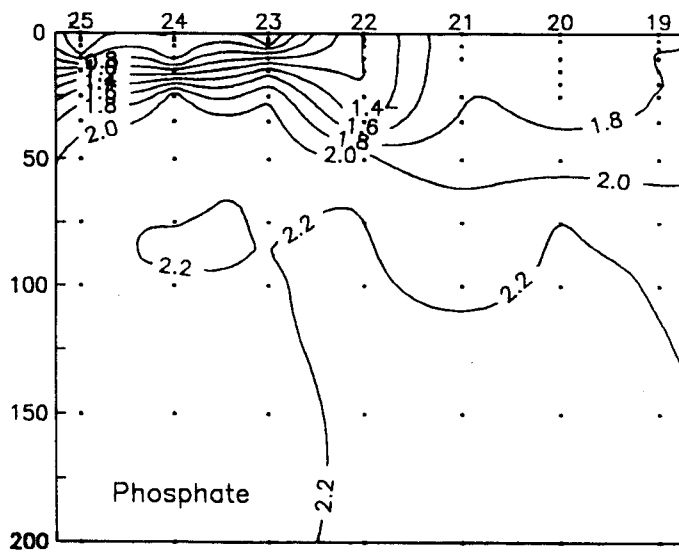
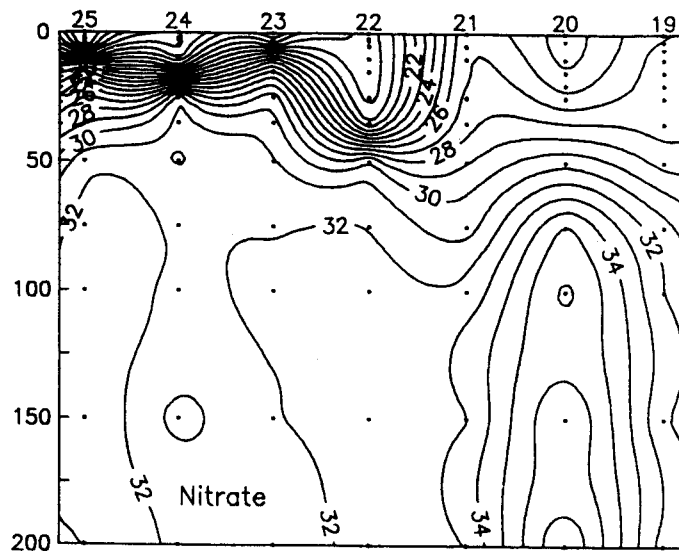


Figure 20: Upper 200 meters distributions of silicate, nitrate and phosphate (μM) along the latitude 75°S , between stations 19 ($179^\circ 55'\text{E}$) and 25 (Terra Nova Bay, 165°E) (nitrate from Guglielmo *et al.*, 1992).

Regarding phytoplankton taxonomic composition, some preliminary observations reveal that at station 25, the population was strongly dominated by two forms of *Nitzschia* (*Fragilaropsis* group), the same species observed, as near exclusive, in coloured ice samples, while station 6, situated in the marginal ice zone near the Balleny Islands, has more differentiated population of diatoms (Guglielmo *et al.*, 1992).

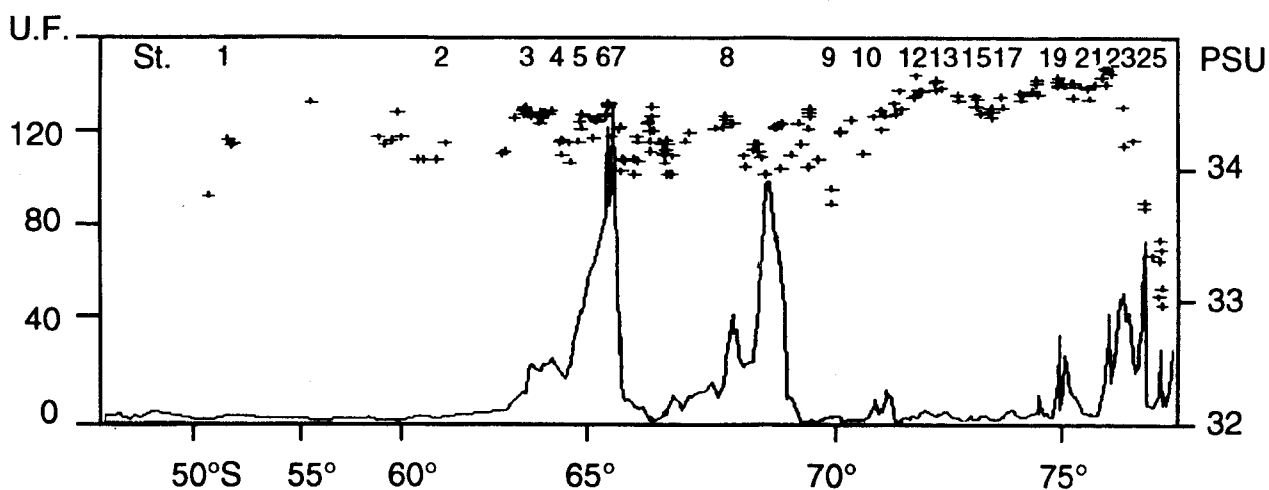


Figure 21: Subsurface continuous profiles of "in vivo" fluorescence and salinity from 45°S to 75°S. Fluorescence in units of fluorescence (UF), salinity in PSU (after Guglielmo *et al.*, 1992).

ANTAR
II/06

3.4.5 HPLC characterization of phytoplankton

From the point of view of pigments, diverse regions can be distinguished along the latitudinal transect from the North to the South and in the Ross Sea (figures 22 and 24):

- North of the Antarctic Polar Front (stations 1 and 2), phytoplanktonic pigments are scarce (less than 0.2 μg of chl *a/l*). The composition of xanthophylls is diversified, showing the presence of many species of diatoms but also dinoflagellates and prymnesiophytes. The dominance of hexanoyloxyfucoxanthin, the presence of phaeophytin *a* and the low concentrations in phaeophorbids indicate aged and diversified phytoplankton, with poor grazing activity.

- South of the Polar Front, pigments concentration increase strongly, reaching 1.4 μg of chl *a/l* at 50 meters at station 3. The vertical distribution of all pigments shows a maximum between 50 and 75 meters while a second phytoplanktonic peak (1.09 μg of chl *a/l*) is detected at 150 meters. The diversity of pigments is lower than northern and the high

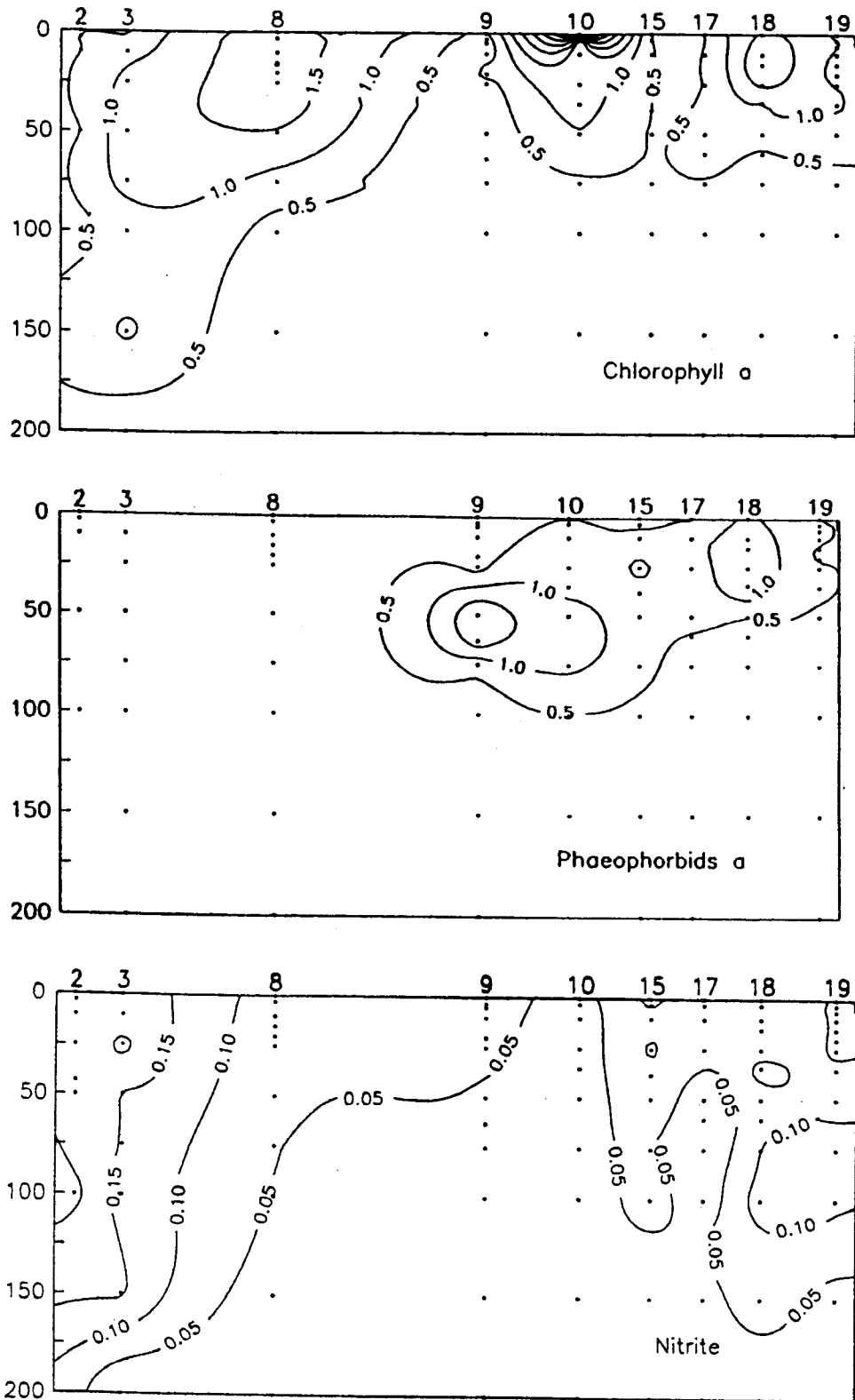


Figure 22: Vertical distribution (0-200 meters) of HPLC chlorophyll a ($\mu\text{g/l}$), phaeophorbids a ($\mu\text{g/l}$) and nitrite (μM) along the North-South section from station 2 ($61^{\circ}55'S$ $172^{\circ}26'E$) to station 19 ($74^{\circ}59'S$ $179^{\circ}55'E$) (chlorophyll and phaeophorbids after Hecq *et al.*, 1992).

values of fucoxanthin, diadinoxanthin and diatoxanthin indicate young diatoms growing populations.

- In the vicinity of the Balleny Islands (stations 5 to 7) and in the northern Ross Sea (stations 8 and 10), phytopigments concentrations show strong maxima (2 - 6 $\mu\text{g chl } a/l$) along the ice edge and in the area of freshly broken pack-ice. Fucoxanthin, diadinoxanthin and diatoxanthin are the only quantitatively important carotenoids.

- Farther south in the Ross Sea (stations 9, 15, 17, 18 and 19), the total chloropigments concentration is quite the same as in the northern part. However, chlorophyll a is often replaced by high concentrations of phaeophorbids a (2 to 3 μg of phaeophorbids a/l). At station 9, the maximum of phaeophorbids is situated between 40 and 70 meters. Proceeding southwards, it is identified in a more and more superficial layer, reaching the surface at station 18. Pigments patterns show significant amounts of fucoxanthin, diadinoxanthin and hexanoyloxyfucoxanthin, a typical pigment of Prymnesiophyceae (Williams and Claustre, 1991). Vertical distributions of chlorophyll and phaeophorbids a between stations 13 and 16 (figure 23) are presented with the distribution of ammonium and will be discussed later in relation with zooplankton distribution.

- Along the East to West transect (stations 19 to 25), the highest chlorophyll a concentrations (maximum of 6.7 $\mu\text{g chl } a/l$ at 15 meters at station 25) occur in the shallow mixed layer of the western part of the section (stations 22 to 25) and are correlated with the lowest salinities and the surface nutrients depleted waters. Moreover, a good correlation between the location of the chlorophyll and phaeophorbids maxima is observed. Phytopigments composition of surface water is mainly typical of young diatoms in the inshore part of the section (stations 25 to 21) while a more diversified phytoplankton community accounts at stations 20 and 19, as shown by the high values of hexanoyloxyfucoxanthin.

These results have been confirmed by data acquired during the subsurface return transect, but with phytopigments patterns generally indicating less active populations (Hecq *et al.*, 1992).

3.4.6 Fatty acids composition of phytoplankton

Phytoplanktonic fatty acids distribution along the east to west transect (stations 19 to 26) is presented at figures 25, 26 and 27.

Percentage of myristic acid (C14) is quite constant along the section while other saturated fatty acids in C15, C16 and C18 present more irregular fluctuations. Palmitoleic acid (C16:1 ω 7) appears to be the

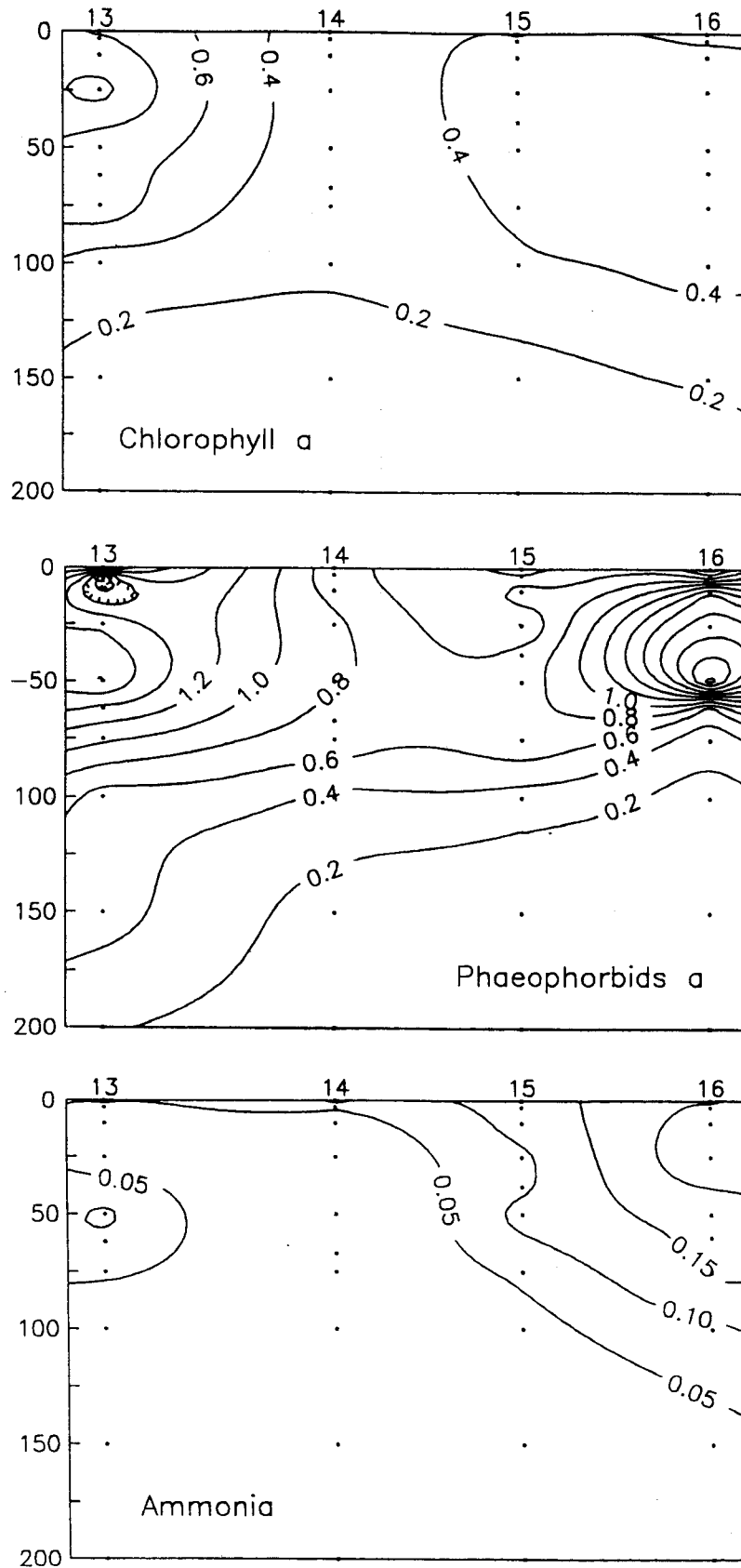
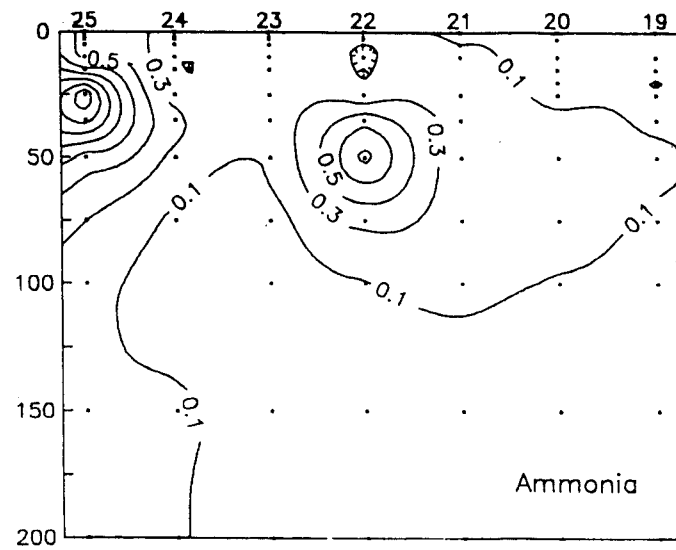
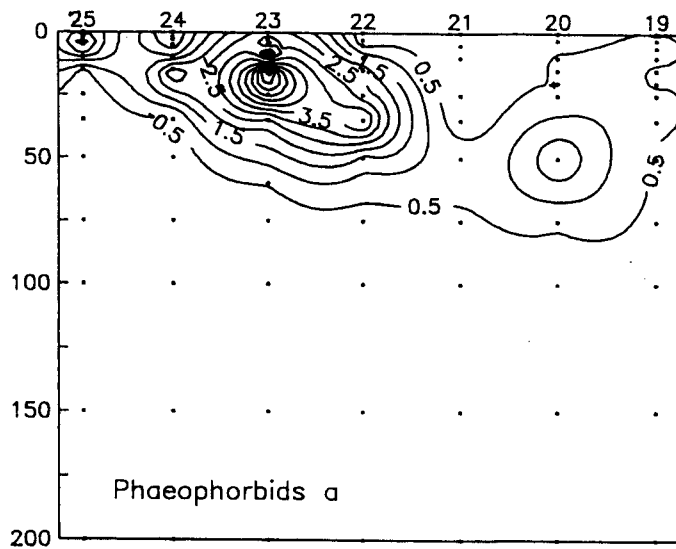
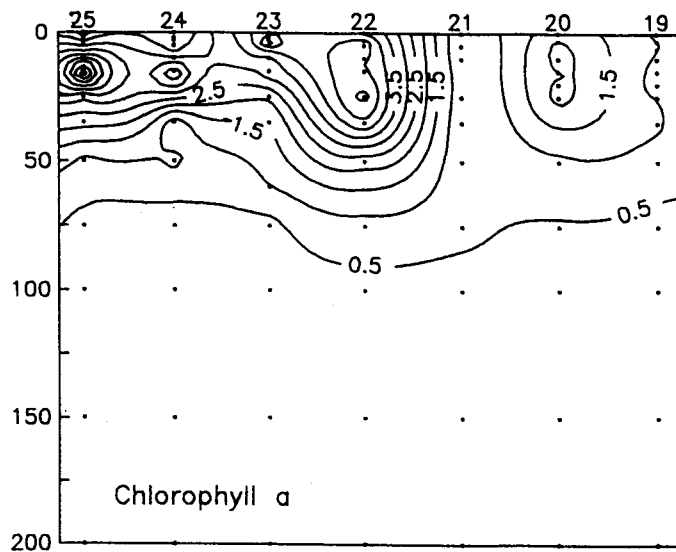


Figure 23: Vertical distribution (0-200 meters) of HPLC chlorophyll a ($\mu\text{g/l}$), phaeophorbids a ($\mu\text{g/l}$) and ammonium (μM) from the continental slope (station 13, $73^{\circ}08'S$ $174^{\circ}25'E$) to the Iselin Bank (station 16, $71^{\circ}58'S$ $177^{\circ}50'W$) (after Hecq *et al.*, 1992).



ANTAR
II/06

Figure 24: Vertical distribution (0-200 meters) of HPLC chlorophyll a ($\mu\text{g/l}$), phaeophorbids a ($\mu\text{g/l}$) and ammonium (μM) between stations 19 ($179^\circ 55'\text{E}$) to 25 (Terra Nova Bay, 165°E) (chlorophyll and phaeophorbids after Hecq *et al.*, 1992).

dominant monounsaturated fatty acid and its distribution shows only small variations between stations 19 and 26. Changes in polyunsaturated fatty acids distribution (C20:5 ω 3, eicosapentaenoic acid and C22:6 ω 3, docosahexaenoic acid) are proportionally very important and difficult to link with any environmental parameters or phytopigments characteristics.

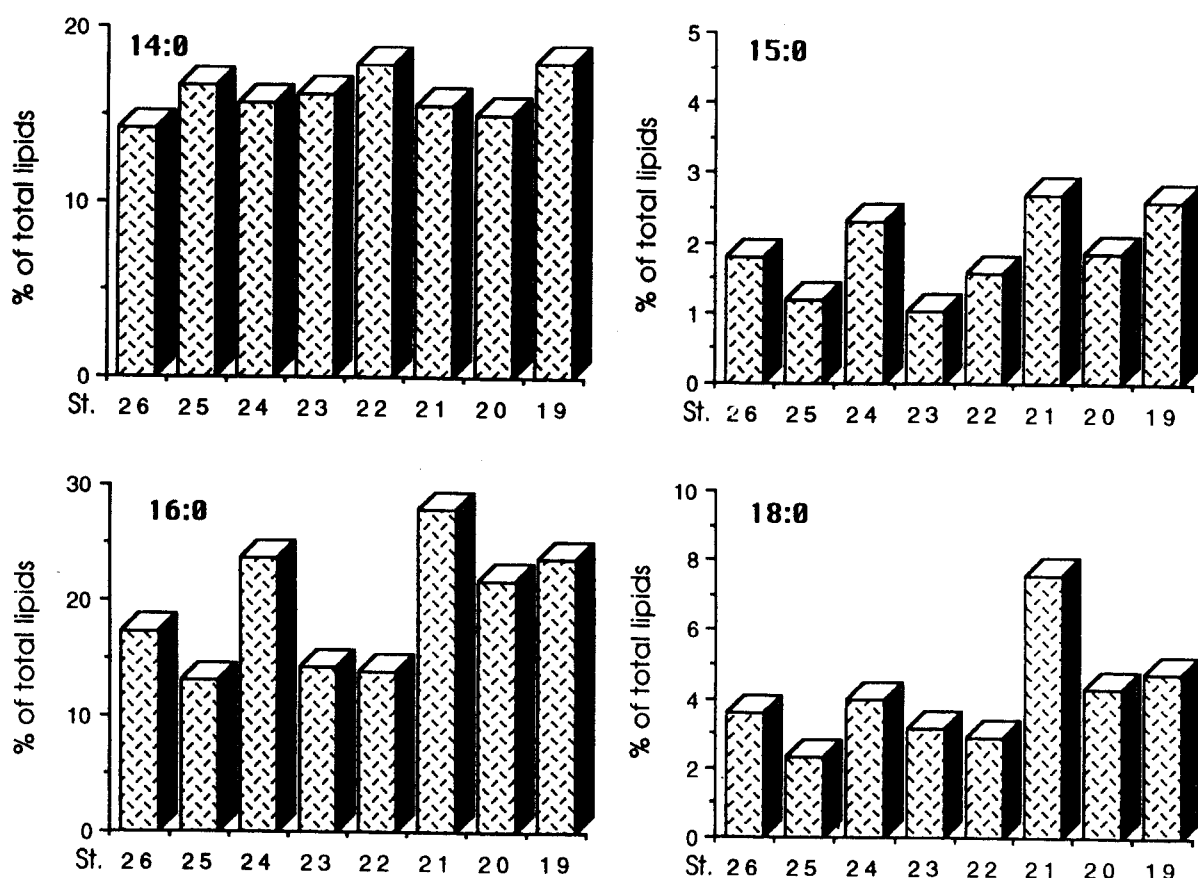


Figure 25: Percentages in saturated fatty acids (C14:0, C15:0, C16:0 and C18:0) in surface phytoplankton of the southern Ross Sea (stations 19 to 26).

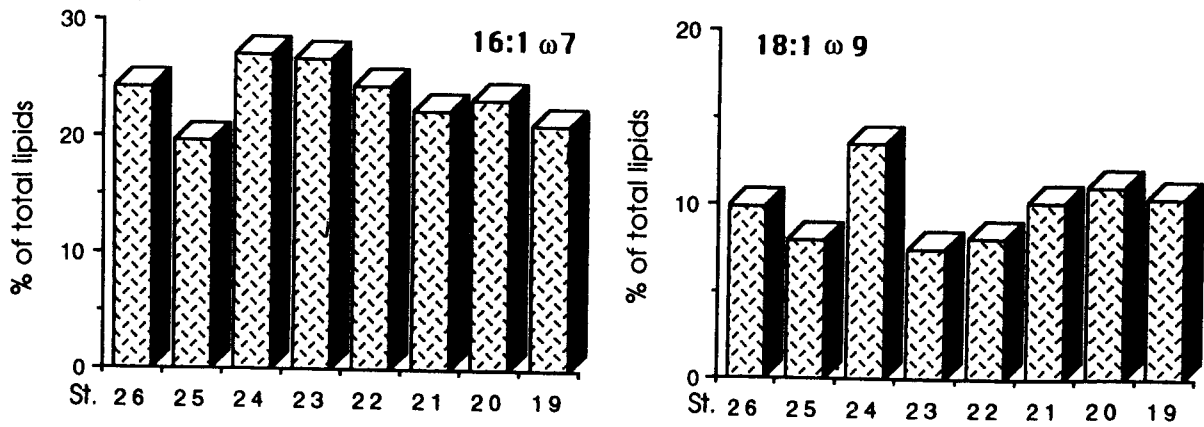
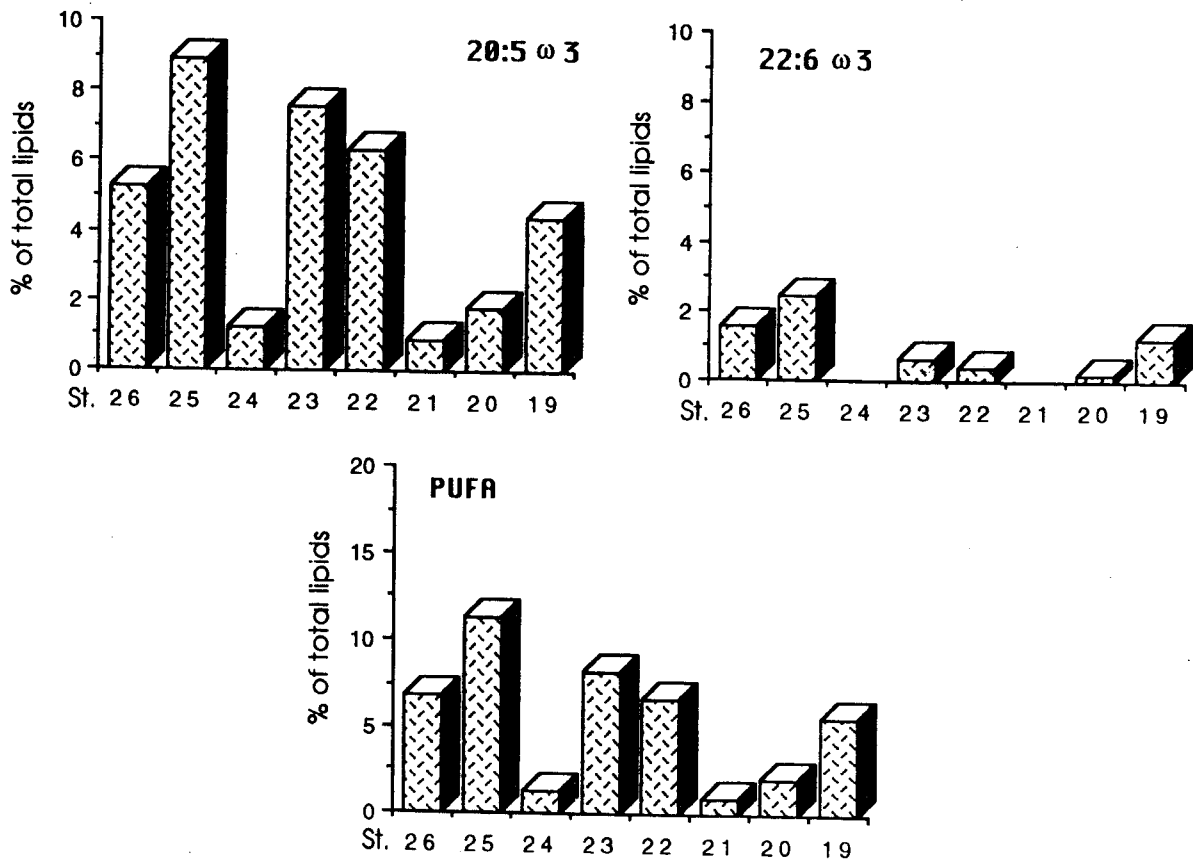


Figure 26: Percentages in palmitoleic (C16:1 ω 7) and oleic (C18:1 ω 9) acids in surface phytoplankton of the southern Ross Sea (stations 19 to 26).



ANTAR
II/06

Figure 27: Percentages in eicosapentaenoic (C20:5 ω 3) and docosahexaenoic (C22:6 ω 3) acids and in total polyunsaturated fatty acids (PUFA) in surface phytoplankton of the southern Ross Sea (stations 19 to 26).

3.4.7 Zooplankton distribution

a. Area of the Antarctic Convergence

Vertical distribution (0-1000 meters) of total and specific zooplankton in the area of the Antarctic Convergence is presented at figures 28 (station 2) and 29 (station 3 bis).

North of the Antarctic Convergence (station 2), total zooplankton abundance ranges from 26 to 10,235 ind./100 m³. The highest concentrations were found between the surface and 200 meters. Below 300 meters, the abundance decreased uniformly. In the upper 200 meters, copepods (8,231 ind./100 m³), furcilia stages of euphausiids (2,333 ind./100 m³), pteropods (926 ind./100 m³), ostracods (747 ind./100 m³), chaetognaths (222 ind./100 m³), polychaetes (128 ind./100 m³) and amphipods (81 ind./100 m³) constituted the most important groups. The maximum of adult euphausiids (24 ind./100 m³) was recorded between 200 and 300 meters (Guglielmo *et al.*, 1992).

South of the Polar Front (station 3 bis), total zooplankton density was higher than northern and very high concentrations were observed in the phytoplankton rich layer, between the surface and 20 meters (105,665 ind./100 m³). These concentrations correspond to the values found at the Antarctic Convergence by Foxton (1956) and Voronina (1966). Adult copepods (66,718 ind./100 m³) with their nauplii stages (20,280 ind./100 m³) dominated the community, while calyptopis (4,071 ind./100 m³) and furcilia (4,571 ind./100 m³) stages of euphausiids contributed also to the total density. The presence of abundant herbivorous *Salpa fusiformis* (6,712 ind./100 m³) between 140 and 160 meters enhances the hypothesis of Longhurst (1967), associating the presence of salps with upwelling areas. Copepods (1,548 ind./100 m³), chaetognaths (25 ind./100 m³), salps (25 ind./100 m³) and ostracods (123 ind./100 m³) show an other maximum density at 700 meters (Guglielmo *et al.*, 1992).

b. Ross Sea continental slope section (stations 13 to 16)

In the Ross Sea area, the horizontal and vertical distributions of zooplankton have been studied in the upper 200 meters, along the transect across Victoria Land shelf (stations 13 to 16, figure 30).

The coastal station (station 13) was characterized by a very low density of organisms (39 to 143 ind./100 m³). *Limacina* and *Clionida* were the dominant groups in the 20-30 meters layer depth (48 and 89 ind./100 m³), while copepods were scarce. Pteropods constituted the first herbivorous group in the surface layer, while amphipods were abundant between 70 and 100 meters (Guglielmo *et al.*, 1992; Hecq *et al.*, 1992).

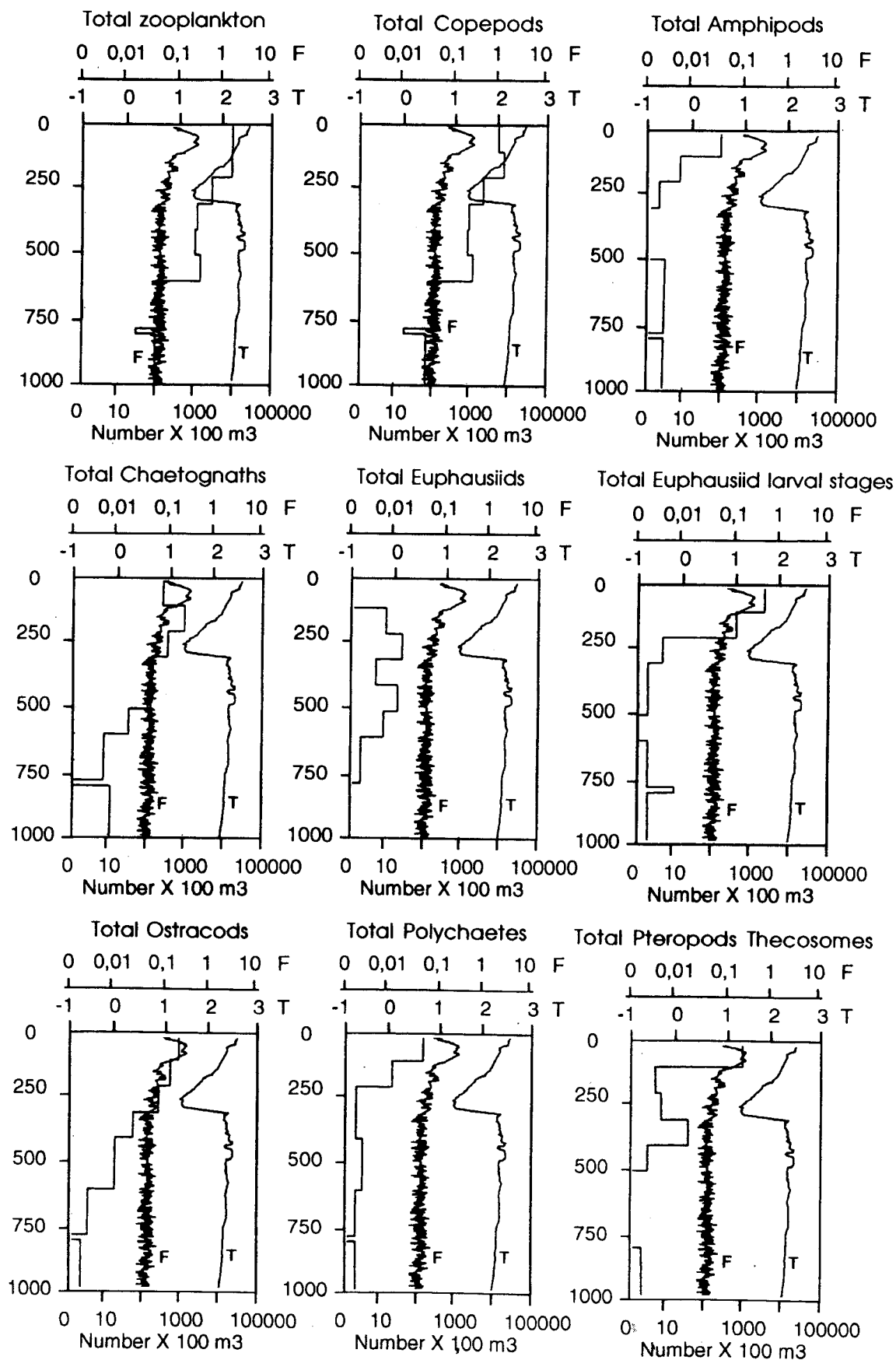
ANTAR
II/06

Figure 28: Vertical distribution of total and specific zooplankton (number/100 m³) at station 2 (61°55'S 172°26'E) from 0 to 1,000 meters deep. Temperature (°C) and salinity are indicated (after Guglielmo *et al.*, 1992 and Hecq *et al.*, 1992).

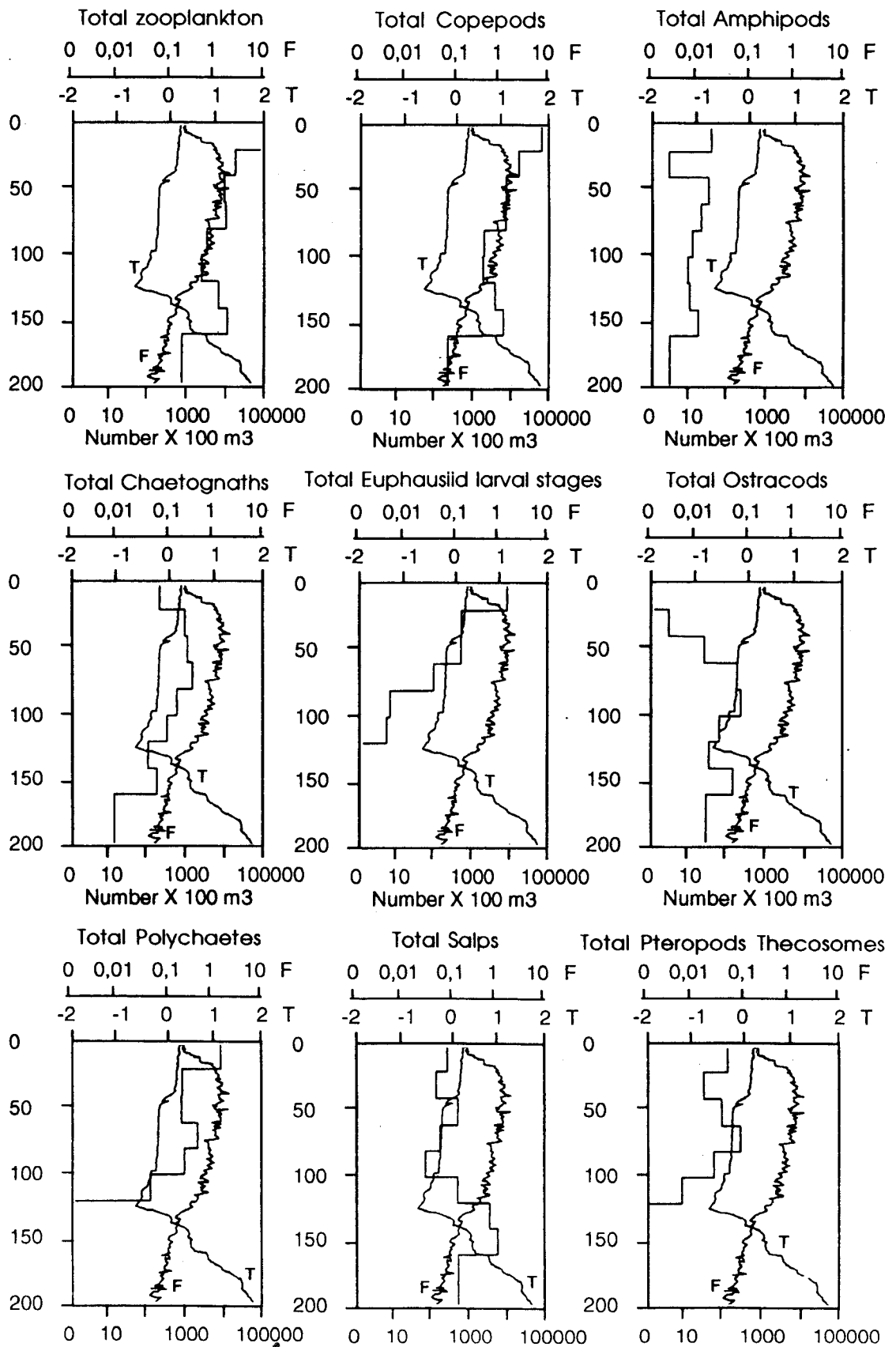


Figure 29: Vertical distribution of total and specific zooplankton (number/100 m³) at station 3 Bis (63°01' S 172°12' E) from 0 to 200 meters deep. Temperature (°C) and fluorescence are indicated (after Guglielmo *et al.*, 1992 and Hecq *et al.*, 1992).

At the more central stations 14 and 15, much higher densities of copepods were recorded. The maximum of biomass was observed between 60 and 80 meters at station 14 (19,336 ind./100 m³) and between 40 to 60 meters at station 15 (17,794 ind./100 m³).

In the pelagic zone (station 16), zooplankton density reached 55,808 ind./100 m³ in the 0-20 meters layer. The total biomass of the pelagic zone was represented almost entirely by copepods and chaetognaths which constitute the two trophic levels of herbivorous and carnivores, while ostracods were important in deeper layers. High densities of chaetognaths were always found below the copepods maximum (Guglielmo et al., 1992; Hecq et al., 1992).

Position of the maxima of chlorophyll a, phaeophorbids a and ammonium along the same section (figure 23) display a good correlation with the maxima of amphipods in the coastal waters and with the maxima of copepods and chaetognaths in the easternmost stations.

3.4.8 General distribution of Krill

The Antarctic krill, *Euphausia superba*, is one of the dominant components of the Antarctic pelagic ecosystem and provides an important link in the food web between lower and higher trophic levels, including squids, fishes, marine mammals and birds (Laws, 1985).

During the expedition, large patches (layers, superswarms) and concentrations of krill were not detected. Mainly swarms and sometimes irregular forms were observed. Irregular forms appeared on the echogram in a variety of shapes, among which it was possible to distinguish, but not to separate, small clouds, layers, swarms. It is interesting that it was not seen typical, scattered forms, as has often reported in numerous papers from Atlantic and Indian sectors. Probably it was result of absence of night during our observations. Only once, in the northern part of the investigated area (70°30'S, 20/01/1990 at local time 02h30), when light was not intensive, quasiscattered forms appeared. This confirms the important role of visual contact among the individuals for cohesive forms formation and suggests nonmechanical mode of it (Hecq et al., 1992).

In the region between 61° and 64°30'S, other species besides krill occurred, mainly salps. Irregular forms dominated ones.

In the northern and central parts of the Ross Sea, krill population were as abundant as those of the Atlantic and Indian sectors (Hecq et al., 1992). In the central and southern parts of the Ross Sea, completely surrounded by pack ice, numerous swarms were detected near the regions of planktonic bloom and near the ice edge. They were typically some hundreds

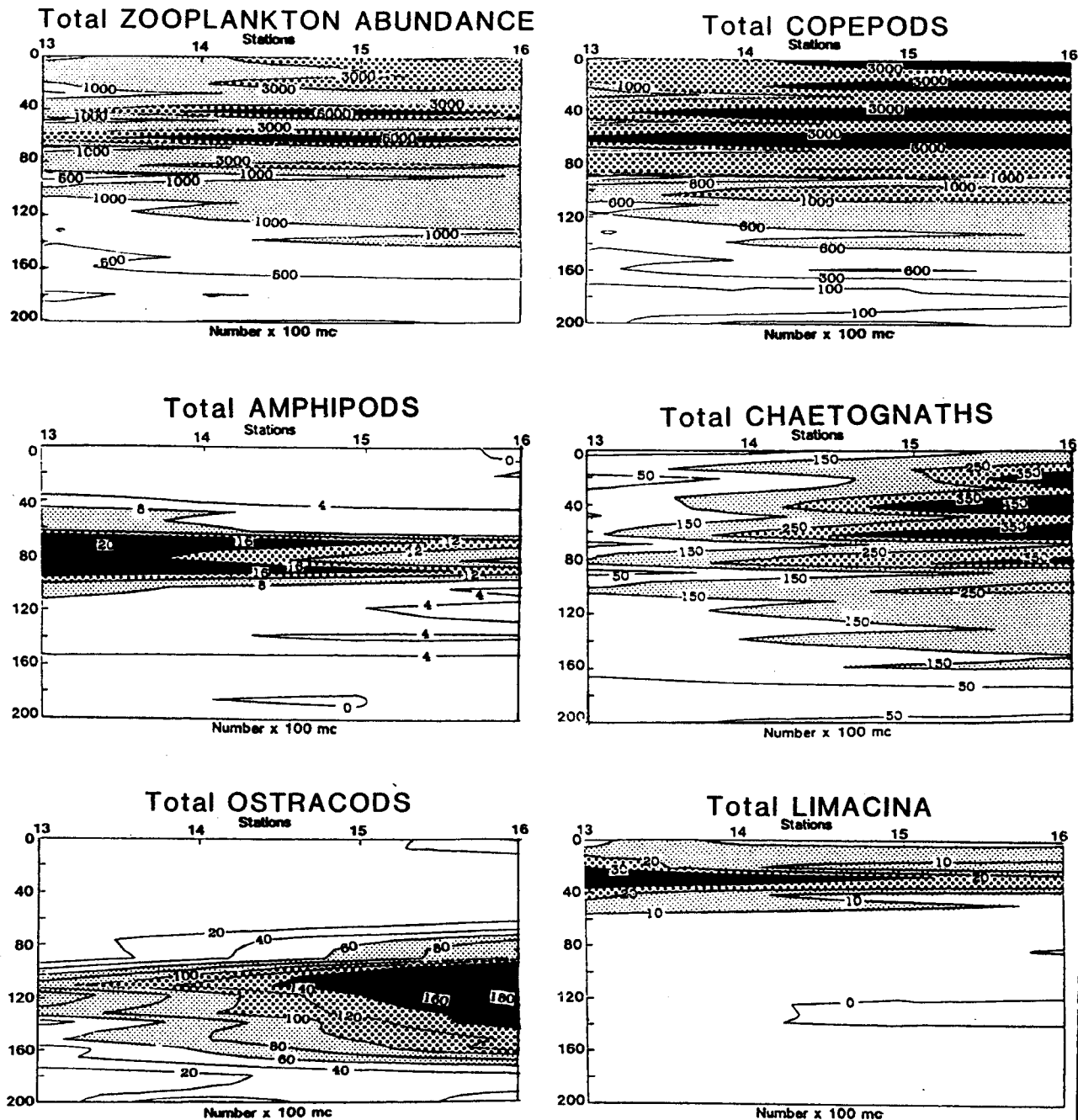


Figure 30: Spatial distribution of total and specific zooplankton between stations 13 (73°08'S 174°25'E) and station 16 (71°58'S 177°50'W) and between 0 and 200 meters deep (after Hecq *et al.*, 1992a).

of meters long, some tens of meters deep and densities varied up to 200 g/m³. Visual observations of predators indicated that abundant groups of birds were presented above the places where krill aggregations were

were detected as reported by Croxall et al. (1984). Among swarmed distribution, frequently, irregulars forms were found. They were some tens meters deep and much longer than swarms. Density of theirs varied from 1 to 100 g/m³ (Hecq et al., 1992).

3.4.9 Discussion

On the basis of hydrological, chemical and biological data, different areas have been recognized in the Pacific sector of the Southern Ocean and in the Ross Sea (Hecq et al., 1992).

1. North of the Antarctic Convergence (Polar Front), phytoplankton populations are scarce but diversified, and grazing activity is poor.

2. South of the Polar Front, phytoplankton concentrations increase strongly. Young growing diatoms prevail and exhibit a subsuperficial maximum, between 50 and 75 meters. Moreover, high living chlorophyll *a* standing crops are observed until 150 meters, suggesting a downwards transport of phytoplankton along the strongly sloping isopycnals in relation with vertical currents associated with the frontal hydrodynamics.

3. In the vicinity of the Balleney Islands and in the northern part of the Ross Sea, phytoplankton concentrations showed intense maxima (2 - 6 µg chl *a*/l) along the ice edge and in the area of recently broken pack-ice. These very high biomasses, associated with high primary production, can be attributed to the liberation of ice algae by the melting of ice. Moreover, in that area, analysis performed on ice algae from the ice-snow interface revealed phytopigments concentrations varying from 80 to 250 µg of chl *a*/l.

ANTAR
II/06

These observations emphasize previous studies (El-Sayed and Taguchi, 1981; Smith and Nelson, 1985; Nelson and Smith, 1986; Nelson et al., 1987) showing that waters adjacent to receding ice edges develop extensive phytoplankton blooms and play a major role in the production and regeneration of organic matter. However, at the ice-edge of the Balleney Islands and of the northern Ross Sea, mesozooplankton density was scarce on the whole water column. Probably because of the recent history of phytoplankton populations, herbivorous zooplankton had not yet developed. On the other hand, many individuals of *Euphausia superba*, measuring between 25 and 32 mm in total length, were caught. Their stomach content, rich in microalgae with a characteristic esmerald green colour, showed that they were actively grazing on the ice algae through a series of channels spotted in the ice pack.

4. In the southern part of the Ross Sea, the total chloropigments concentrations are quite the same as in the northern part. However,

phaeophorbids *a* comprised a high and quite constant part of the total pigments ($\approx 50\%$), indicating a tight coupling between phytoplankton abundance and zooplankton and/or krill grazing. Because waters are ice-free for a longer time than northern, the phytoplanktonic bloom began early and zooplanktonic communities had time to develop. The phytoplanktonic communities are probably in steady state with mesozooplanktonic grazing and their turnover is probably higher than in the northernmost areas (Hecq *et al.*, 1992).

Regarding krill distribution, the general opinion that the Pacific sector of the Southern Ocean is poor with *Euphausia superba* has not been confirmed. The occurrence of numerous and dense aggregations of krill in the areas covered by the pack ice some weeks before suggests that krill aggregations occur both in the open water and below the ice. The fundamental role of *Euphausia superba* in the functioning of the southern Ross Sea has been emphasized by the spatial superposition of phaeophorbids patches and krill swarms detected by acoustic surveys and by the abundance of birds above the places where krill aggregations were detected (Hecq *et al.*, 1992).

If phytoplankton abundance is one of the main factor controlling zooplankton development, the edge of the shelf, and the associated thermohaline front, may act also as a boundary, separating continental populations and offshore communities. For example, along a Ross Sea continental slope section (stations 13 to 16), two groups of herbivorous macrozooplankton were found, following their position on the shelf. Amphipods were restricted to the coastal waters while copepods and krill were abundant in deep waters, outside the shelf (Hecq *et al.*, 1992). Because both communities have different vertical distribution in the water column and thereby are not accessible to the same predators (fishes, squids and whales or birds), the thermohaline front, due to the circulation of water on and off the continental shelf appears to orientate the switch zooplankton \rightarrow fishes or zooplankton \rightarrow birds and to influence the distribution of higher trophic levels. Moreover, following migrations of zooplankton and sedimentation rates of fecal pellets, recycling will occur in the euphotic zone or in the deeper layers.

5. In the southernmost investigated area, the local circulation and the summer continuous melting of the Ross ice shelf lead to the formation of a thermohaline coastal front and to further increasing of water column stability near the coast. In these conditions, waters diluted by the melting of the Ross ice shelf develop an extensive diatoms bloom, as observed also by Smith and Nelson (1985a, 1985b) and Nelson and Smith (1986). The chlorophyll distribution section shows clearly that the extent of the bloom was ca. 150 km. In the bloom, chlorophyll levels were very high, reaching the maximum values of 187.64 mg/m^2 at station 25 when integrated from

the surface to 150 meters. In comparison, for the same area of the Ross Sea and in January-February 1983, Smith and Nelson (1985b) obtained chlorophyll levels averaging 128.2 ± 91.7 mg chl *a*/m² (0-150 m.). Therefore, it appears that phytoplankton biomasses observed near the Ross ice shelf are greater than most of those observed in other studies of the Southern Ocean which have investigated the marginal ice-zone.

Within the high biomass core, surface nitrate, silicate and phosphate depleted to < 10.0 , < 20.0 and < 0.4 μ M, indicating a long and intense period of production. Such bloom, because its relatively long duration at one location, is actively exploited by grazers, as shown by phaeophorbids distribution, and might be expected to contribute substantially to the global productivity of the Ross Sea. Most southern in the Ross Sea (77°S), the exceptional observation of Nelson and Smith (1986), reporting that, at one station during the austral summer 1983, nitrate and phosphate were undetectable throughout the surface mixed layer, emphasizes the importance of the Ross ice shelf in the production of organic matter.

Stations where phytoplankton is actively grazed by zooplankton, as shown by high phaeophorbids, are also characterized by high ammonium concentrations. This correlation could indicate that zooplanktonic excretion is a major source of NH_4^+ in the investigated part of the Ross Sea. However, on the water column, the maximum of ammonium occurs below the chlorophyll maximum, probably because NH_4^+ , when available, is taken up as a preferred nutrient by Southern Ocean phytoplankton (Biggs *et al.*, 1985).

As a general rule, fatty acids analysis in phytoplankton do not provide additional informations on the dynamics of the food web. The dominance of myristic and palmitoleic acids, two important constituents of diatoms (Ackman *et al.*, 1966; Bottino, 1974) confirm the importance of this group. However, fatty acids do not allow to distinguish the coastal and offshore communities, as done on the basis of phytopigments and do not seem to be direct reliable tracers of the ecosystem complexity.

4. GENERAL CONCLUSIONS

The approach used in our ecohydrodynamical study of phytoplankton communities of the Southern Ocean has enabled us to identify the major mechanisms controlling the distribution of phytoplankton standing crops, their biochemical speciation and their utilization by higher trophic levels.

Mesoscale study of the ice edge and of the adjacent open water in the Weddell Sea and in the Ross Sea confirms that, in the Southern Ocean, phytoplankton biomass and productivity are sharply discontinuous in space and time, with restricted periods of high biomass and productivity in a general environment of low productivity. The spatial patchiness of high chlorophyll *a* concentrations is bound up with the main frontal systems and with the areas of increased stability. These areas of increased stability may occur in the open water but much more often, are imputable to the stabilization of the upper layers of the water column due to the retreat of the constantly melting ice-edge.

In the western Weddell Sea, during early spring, relatively high phytoplankton biomass ($> 1 \mu\text{g chl } a/l$) was associated exclusively with the northernmost part of the marginal ice zone and with the adjacent open water, coincident with the Weddell-Scotia Confluence. The bloom had a north-south extent of at least 185 km and the highest surface phytoplankton concentrations ($1.8 \mu\text{g chl } a/l$) were approximately 165 km north from the ice edge. The bloom developed only in the stations showing a vertical stratification with a homogeneous mixed layer restricted to the upper 50 meters. In this case, the stabilization of the water column seems to be due both to the early melting of the ice edge and to the presence of the Weddell-Scotia Confluence, dominated by sharp temperature gradients.

As a general rule, we found an inverse phytoplankton and zooplankton relationship and a spatial splitting between the maxima of phyto- and zooplankton biomasses, suggesting that the overwintering animals of the Western Weddell Sea were just surviving after exhausting their lipid storage and had not begun to graze on new phytoplankton in the marginal ice zone. The paucity of zooplankton abundance and its minimal lipids contents, probably due to the overwintering, do not support the idea of general lipid richness in Antarctic zooplankton.

During spring in the Ross Sea, the most interesting results are that biomass, composition and productivity of phytoplankton seem to depend essentially on the time after the waters become ice-free. The following pattern could be proposed (Hecq *et al.*, 1992): Ice algae (mainly diatoms) are liberated by melting ice, sink in the water column and grow in the

stable surface layer. After about 2 weeks, phytoplankton communities are actively grazed by zooplankton, inducing both transformation of chlorophyll in phaeophorbids and ammonium excretion. Because NH_4^+ is taken up as a preferred nutrient by Southern Ocean phytoplankton, it is used immediately and favours a nanophytoplanktonic regenerated production, prymnesiophytes dominated.

In the southernmost investigated area, waters diluted by the melting of the Ross ice shelf develop an extensive diatoms bloom, characterized by a spatial extent of ca. 150 km and very high chlorophyll levels, reaching the maximum values of 187.64 mg/m^2 when integrated from the surface to 150 meters. Because nutrients depletion indicates a long and intense period of production, such bloom might be expected to contribute substantially to the global productivity of the Ross Sea.

If phytoplankton abundance is one of the main factor controlling herbivorous zooplankton development, the edge of the shelf, and the associated thermohaline front, affect also the horizontal and vertical patchiness of zooplankton and its specific composition. Amphipods dominated populations were restricted to the coastal waters while copepods and krill dominated in deep waters. Because both communities have different vertical distribution in the water column and thereby are not accessible to the same predators (fishes, squids and whales or birds), the thermohaline front appears to orientate the switch zooplankton → fishes or zooplankton → birds and to influence the distribution of higher trophic levels.

ANTAR
II/06

The distribution and the biochemical speciation of the lipid content of plankton as a function of environmental parameters have been studied, but, on a general way, fatty acids and lipids composition do not seem to be direct reliable tracers of the ecosystem complexity.

5. ACKNOWLEDGEMENTS

This work was supported by the Belgian Scientific Research Programme on Antarctica, funded by the Science Policy Office (Brussels, Belgium), under contract ANTAR II/06. The authors are also grateful to the "Programma Nazionale di Ricerche in Antartide" (Italy) that supported an important part of the research in the Ross Sea. The exchange of opinions with Italian experts allowed the elaboration of all presented results.

6. BIBLIOGRAPHY

- Ackman R.G., Tocker C.S. and McLachlan J.M. (1968). Marine phytoplankter fatty acids. *J. Fish. Res. Bd. Canada*, **25**: 1603-1620.
- Barnes H. and Blackstock J. (1973). Estimation of lipids in marine animals and tissues: detailed investigation of the sulfophosphovanillin method for "total" lipids. *J. Exp. Mar. Biol. Ecol.*, **12**: 103-118.
- Battaglia B., Goffart A., Hempel I. and Siegel V. (1989). Zooplankton distribution, biochemistry and genetics. In "The expedition Antarktis VII/1 and 2 (EPOS 1) of RV "Polarstern" in 1988/89". *Berichte zur Polarforschung*, **62**: 143-147.
- Bidigare R.R., Frank J.T., Zastrow C. and Brooks J.M. (1986). The distribution of algal chlorophylls and their degradation products in the Southern Ocean. *Deep-Sea Research*, **33**: 923-937.
- Biggs D.C., Amos A.F. and Holm-Hansen O. (1985). Oceanographic Studies of Epi-Pelagic Ammonium distribution: The Ross Sea NH₄⁺ Flux Experiment. In W.R. Siegfried, P.R. Condy and R.M. Laws Eds., *Antarctic Nutrient Cycles and Food Webs*. Springer Verlag, Berlin Heidelberg, 93-103.
- Bottino N.R. (1974). The fatty acids of Antarctic phytoplankton and euphausiids. Fatty acid exchange among trophic levels of the Ross Sea. *Marine Biology*, **27**, 197-204.
- Cederlöf U., Ober S., Schmidt R., Svansson A. and Veth K. (1989). Hydrography. In "The expedition Antarktis VII/3 (EPOS Leg 2) of RV "Polarstern" in 1988-89". *Berichte zur Polarforschung*, **65**: 14-19.
- Conover R.J. and Huntley M. (1991). Copepods in ice-covered seas - Distribution, adaptations to seasonally limited food, metabolism, growth patterns and life cycle strategies in polar seas. *Journal of Marine Systems*, **2**: 1-41.
- Croxall J.P., RicKetts C.R. and Princee P.A. (1984). Impact of sea birds on marine resources, especially krill, of South Georgia waters. In G.C. Whittow and H. Rahn Eds., *Seabirds Energetics*. Plenum publish, 285-317.
- Deacon G.E.R. (1937). The hydrology of the Southern Ocean. *Discovery Reports*, **15**: 1-124.

- Deacon G.E.R. (1982). Physical and biological zonation in the southern Ocean. *Deep-Sea Research*, **29**: 1-15.
- Dunbar R.B., Anderson J.B., Domack E.W. and Jacobs S.S. (1985). Oceanographic influences on sedimentation along the antarctic continental shelf. *Oceanology of the Antarctic Continental Shelf, Antarctic Research Series*, **13**: 291-312.
- Eicken H. and Lange M.A. (1989). Sea ice conditions. In "The expedition Antarktis VII/1 and 2 (EPOS 1) of RV "Polarstern" in 1988/89". *Berichte zur Polarforschung*, **62**: 55-63.
- El-Sayed S.Z. (1987). Biological productivity of Antarctic waters: present paradoxes and emerging paradigms. In: "*Antarctic Aquatic Biology*", BIOMASS Scientific Series, **7**: 1-21.
- El-Sayed S.Z. and Mandelli E.F. (1965). Primary production and standing crop of phytoplankton in the Weddell Sea and Drake Passage. In "*Biology of the Antarctic Seas II*", G.A. Llano ed., *Antarctic Research Series*, **5**: 87-406.
- El-Sayed S.Z. and Taguchi S. (1981). Primary production and standing crop of phytoplankton along the ice-edge in the Weddell Sea. *Deep-Sea Research*, **28**, 1017-1032.
- El-Sayed S.Z., Biggs D.C. and Holm-Hansen O. (1983). Phytoplankton standing crop, primary productivity, and near-surface nitrogenous nutrient fields in the Ross Sea, Antarctica. *Deep-Sea Research*, **30**: 871-886.
- Everson I. (1976). Antarctic krill: a reappraisal of its distribution. *Polar Record*, **18**: 15-23.
- Falk-Petersen S. (1990). Life strategy in Arctic zooplankton and pelagic fish in relation to lipid chemistry. *Abstracts of the 22nd International Liège Colloquium on Ocean Hydrodynamics*, 19.
- Folkard A.R. (1978). Automatic analysis of seawater nutrients. *Fish. Res. Tech. Rep. Dir. Fish Res., MAFF, Lowestoft (UK)*, **46**:1-23.
- Foxton P. (1956). The distribution of the standing crop of zooplankton in the Southern Ocean. *Discovery Reports*, **28**: 191-236.

- Fryxell G.A. and Kendrick G.A. (1988). Austral spring microalgae across the Weddell Sea ice edge: spatial relationships found along a northward transect during AMERIEZ 83. *Deep-Sea Research*, **35**: 1-20.
- Goffart A. and Hecq J.H. (1989). Zooplankton Biochemistry and Ecodynamics. In S. Caschetto editor, *Belgian Scientific Research Programme on Antarctica, Scientific Results of phase 1 (Oct.85 - Jan.89)*. Prime Minister's Services - Science Policy Office.
- Gordon A.L. (1971a). Oceanography of Antarctic Water. Antarctic Oceanology. I. *Antarctic Research Series*, **15**: 169-203.
- Gordon A.L. (1971b). Antarctic Polar Front Zone. Antarctic Oceanology. I. *Antarctic Research Series*, **15**: 169-203.
- Gordon A.L., Molinelli E. and Baker, T. (1978). Large-scale dynamic topography of the Southern Ocean. *Journal of Geophysical Research*, **87**: 3023-3032.
- Gordon A.L., Molinelli E.J. and Baker T.N. (1982). *Southern Ocean Atlas*. Columbia, University Press, New York 11 pp. 233 plates.
- Guglielmo L., Hecq J.H., Artegiani A., Azzolini R., Benedetti F., Catalano G., Goffart A., Innamorati M., Lazzara L., Nuccio C., Paschini, E. Povero P. and Vanucci S. (1992). Ecohydrodynamical approach of the planktonic ecosystem during the Vth Italian Antarctic expedition in the Pacific sector of the Southern Ocean (1989-1990). I. Oceanographic data. Submitted at *Journal of Marine Systems*.
- Hagen W. (1988). On the significance of Lipids in Antarctic Zooplankton. *Berichte zur Polarforschung*, **49**: 129 pp.
- Hansen H.P. and Grasshoff K. (1983). Automated chemical analysis. In K. Grasshoff, M. Ehrhardt and K. Kremling Eds., "*Methods of seawater analysis*", 2nd Ed. Verlag Chemie, Weinheim, 347-379.
- Hecq J.H, Gaspar A. et Dauby P. (1981). Caractéristiques écologiques et biochimiques de l'écosystème planctonique en baie de Calvi (Corse). *Bulletin de la Société Royale des Sciences de Liège*, **11-12**: 440-445.
- Hecq J.H. and Goffart A. (1984). Analyse des classes de lipides et des acides gras de *Leptomysis lingvura* (Sars), crustacé Mysidacé. Influences des conditions nutritionnelles. *Bulletin de la Société Royale des Sciences de Liège*, **53**: 69-80.

- Hecq J.H., Azzali M., Catalano G., Decembrini F., Fabiano M., Goffart A., Guglielmo L., Kalinowski J., Magazzù G. (1992). Ecohydrodynamical approach of the planktonic ecosystem during the Vth Italian Antarctic expedition in the Pacific sector of the Southern Ocean (1989-1990). II. Structure and functioning of the ecosystem. Submitted at *Journal of Marine Systems*.
- Hecq J.H., Magazzù G., Goffart A., Catalano G., Vanucci S. and Guglielmo L. (1992b). Distribution of planktonic components related to vertical structure of water masses in the Ross Sea and the Pacific sector of the Southern Ocean. *Atti del IX Congresso dell' Associazione Italiana di Oceanologia e Limnologia, Santa Margherita Ligure, 20-23/11/1990*, 665-678.
- Hempel G. (1989). Introduction to EPOS1. In "The expedition Antarktis VII/1 and 2 (EPOS 1) of RV "Polarstern" in 1988/89". *Berichte zur Polarforschung*, 62: 37-41.
- Jacobs S.S., Amos A.F. and Bruchhausen P.M. (1970). Ross Sea oceanography and Antarctic Bottom Water formation. *Deep-Sea Research*, 17: 935-962.
- Jacobs S.S. and Comiso J.C. (1989). Sea ice and oceanic processes on the Ross Sea continental shelf. *Journal of Geophysical Research*, 94: 18195-18211.
- Jeffrey, S.W. (1974). Profiles of photosynthetic pigments in the ocean using thin-layer chromatography. *Marine Biology*, 26: 101-110.
- Kalinowski J. and Witek Z. (1985). Scheme for classifying aggregations of Antarctic krill. *BIOMASS Handbook*, 27, 11 pp.
- Klein B. and Sournia A. (1987). A daily study of the diatom spring bloom at Roscoff (France) in 1985. II. Phytoplankton pigments composition studied by HPLC analysis. *Marine Ecology Progress Series*, 37: 265-275.
- Larsson A.M. (ed.) (1990). Data report on hydrological, chemical and biological observations during the European Polarstern study -EPOS leg 1-. University of Gothenburg, Sweden, 91 pp.
- Larsson A.M., Sehlstedt P.I., Ljungek G. and Paviglione A. (1989). Physical oceanography. In "The expedition Antarktis VII/1 and 2 (EPOS 1) of RV "Polarstern" in 1988/89". *Berichte zur Polarforschung*, 62: 69-71.

- Laws R.M. (1985). The Ecology of Southern Ocean. *American Scientist*, **73**: 26-44.
- Le Corre P. et Minas H.J. (1983). Distribution et évolution des éléments nutritifs dans le secteur indien de l'Océan Antarctique en fin de période estivale. *Oceanologica Acta*, **6**: 365-381.
- Le Jehan S. and Treguer P. (1985). The distribution of inorganic nitrogen, phosphorus, silicon and dissolved organic matter in surface and deep waters of the Southern Ocean. In W.R. Siegfried, P.R. Condy and R.M. Laws Eds., *Antarctic Nutrient Cycles and Food Webs*. Springer Verlag, Berlin Heidelberg, 22-29.
- Longhurst A.R. (1967). Vertical distribution of zooplankton in relation to the Pacific oxygen minimum. *Deep-Sea Research*, **14**: 51-63.
- Lutjeharms J., Walters N. and Allanson B. (1985). Oceanic frontal systems and biological enhancement. In W.R. Siegfried, P.R. Condy and R.M. Laws Eds., *Antarctic Nutrient Cycles and Food Webs*. Springer Verlag, Berlin Heidelberg, 11-21
- Mackintosh N.A. (1972). Life cycle of Antarctic krill in relation to ice and water conditions. *Discovery reports*; **36**: 1-14.
- Nelson D.M. and Smith W.O.J. (1986). Phytoplankton bloom dynamics of the western Ross Sea ice edge - II Mesoscale cycling of nitrogen and silicon. *Deep-Sea Research*, **33**: 1389-1412.
- Nelson D.A., Smith W., Gordon L. and Huber B. (1987). Spring Distributions of Density, Nutrients and phytoplankton biomass in the Ice Edge Zone of the Weddell-Scotia Sea. *Journal of Geophysical Research*, **92**: 7181-7190.
- Smith W.O.J. and Nelson D.M. (1985a). Phytoplankton bloom produced by a receding ice edge in the Ross Sea: spatial coherence with the density field. *Science*, **227**:163-166.
- Smith W.O.J. and Nelson D.M. (1985b). Phytoplankton Biomass near a receding Ice-Edge in the Ross Sea. In W.R. Siegfried, P.R. Condy and R.M. Laws Eds., *Antarctic Nutrient Cycles and Food Webs*. Springer Verlag, Berlin Heidelberg, 70-77.
- Voronina N.M. (1966). The zooplankton of the Southern Ocean; some study results. *Oceanology*, **6**: 557-563.

- Welschmeyer N.A. and Lorenzen C.J. (1985) Chlorophyll budgets: zooplankton grazing and phytoplankton growth in a temperate fjord and the Central Pacific Gyres. *Limnology and Oceanography*, **30**: 1-21.
- Williams R. and Claustre H. (1991). Photosynthetic pigments as biomarkers of phytoplankton populations and processes involved in the transformation of particulate organic matter at the Biotrans site (47°N, 20°W). *Deep-Sea Research*, **38**: 347-355.



BELGIAN SCIENCE POLICY OFFICE
Rue de la Science 8
B - 1040 Brussels
Belgium
tel (+32-2) 238 34 11 fax (+32-2) 230 59 12